NEW INSIGHTS INTO AND INTERVENTIONS OF THE PERSISTENT IMMUNE RESPONSES IN CHRONIC GRAFT REJECTION,
2nd Edition

EDITED BY: Hao Wang and Caigan Du
PUBLISHED IN: Frontiers in Immunology

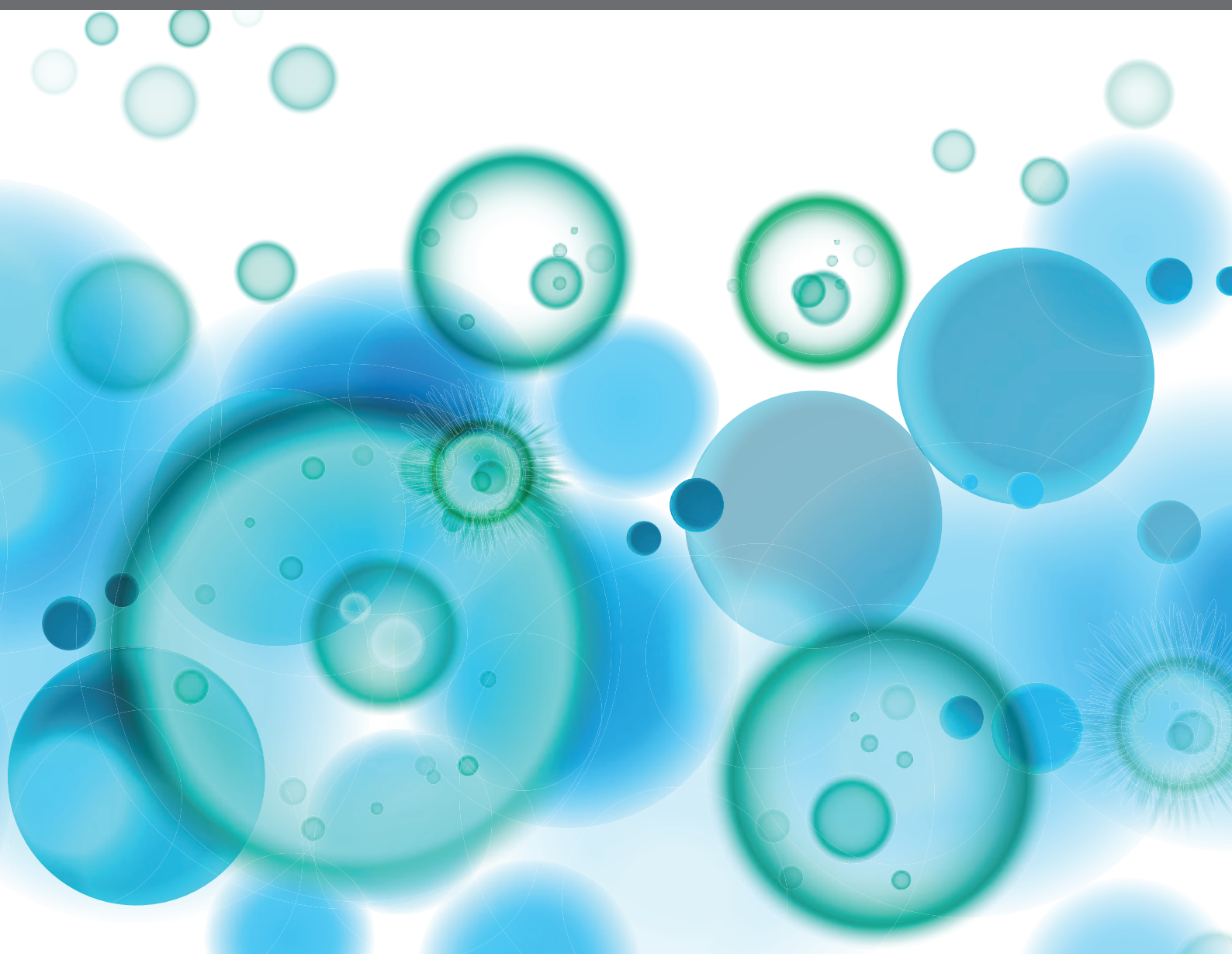

frontiers Research Topics

frontiers

ISSN 1664-8714
ISBN 978-2-88974-408-4
DOI 10.3389/978-2-88974-408-4

About Frontiers

Frontiers is more than just an open-access publisher of scholarly articles: it is a pioneering approach to the world of academia, radically improving the way scholarly research is managed. The grand vision of Frontiers is a world where all people have an equal opportunity to seek, share and generate knowledge. Frontiers provides immediate and permanent online open access to all its publications, but this alone is not enough to realize our grand goals.

Frontiers Journal Series

The Frontiers Journal Series is a multi-tier and interdisciplinary set of open-access, online journals, promising a paradigm shift from the current review, selection and dissemination processes in academic publishing. All Frontiers journals are driven by researchers for researchers; therefore, they constitute a service to the scholarly community. At the same time, the Frontiers Journal Series operates on a revolutionary invention, the tiered publishing system, initially addressing specific communities of scholars, and gradually climbing up to broader public understanding, thus serving the interests of the lay society, too.

Dedication to Quality

Each Frontiers article is a landmark of the highest quality, thanks to genuinely collaborative interactions between authors and review editors, who include some of the world's best academicians. Research must be certified by peers before entering a stream of knowledge that may eventually reach the public - and shape society; therefore, Frontiers only applies the most rigorous and unbiased reviews.
Frontiers revolutionizes research publishing by freely delivering the most outstanding research, evaluated with no bias from both the academic and social point of view. By applying the most advanced information technologies, Frontiers is catapulting scholarly publishing into a new generation.

What are Frontiers Research Topics?

Frontiers Research Topics are very popular trademarks of the Frontiers Journals Series: they are collections of at least ten articles, all centered on a particular subject. With their unique mix of varied contributions from Original Research to Review Articles, Frontiers Research Topics unify the most influential researchers, the latest key findings and historical advances in a hot research area! Find out more on how to host your own Frontiers Research Topic or contribute to one as an author by contacting the Frontiers Editorial Office: frontiersin.org/about/contact

NEW INSIGHTS INTO AND INTERVENTIONS OF THE PERSISTENT IMMUNE RESPONSES IN CHRONIC GRAFT REJECTION,
2nd Edition

Topic Editors:
Hao Wang, Tianjin Medical University General Hospital, China
Caigan Du, University of British Columbia, Canada

Publisher's note: This is a 2nd edition due to an article retraction.

Citation: Wang, H., Du, C., eds. (2022). New Insights into and Interventions of the Persistent Immune Responses in Chronic Graft Rejection, 2nd Edition. Lausanne: Frontiers Media SA. doi: 10.3389/978-2-88974-408-4

Table of Contents

05 ***Editorial: New Insights Into and Interventions of the Persistent Immune Responses in Chronic Graft Rejection***
Dejun Kong, Caigan Du and Hao Wang

08 ***Hydrogen in Patients With Corticosteroid-Refractory/Dependent Chronic Graft-Versus-Host-Disease: A Single-Arm, Multicenter, Open-Label, Phase 2 Trial***
Liren Qian, Miao Liu, Jianliang Shen, Jian Cen and Defeng Zhao

16 ***Elevated Circulating IL-10 Producing Breg, but Not Regulatory B Cell Levels, Restrain Antibody-Mediated Rejection After Kidney Transplantation***
Yongsheng Luo, Feifei Luo, Kuanxin Zhang, Shilei Wang, Haojie Zhang, Xianlei Yang, Wenjun Shang, Junxiang Wang, Zhigang Wang, Xinlu Pang, Yonghua Feng, Lei Liu, Hongchang Xie, Guiwen Feng and Jinfeng Li

26 ***Prevention of Chronic Rejection of Marginal Kidney Graft by Using a Hydrogen Gas-Containing Preservation Solution and Adequate Immunosuppression in a Miniature Pig Model***
Kotaro Nishi, Satomi Iwai, Kazuki Tajima, Shozo Okano, Motoaki Sano and Eiji Kobayashi

39 ***Artemisinin Attenuates Transplant Rejection by Inhibiting Multiple Lymphocytes and Prolongs Cardiac Allograft Survival***
Zhe Yang, Fei Han, Tao Liao, Haofeng Zheng, Zihuan Luo, Maolin Ma, Jiannan He, Lei Li, Yongrong Ye, Rui Zhang, Zhengyu Huang, Yannan Zhang and Qiquan Sun

50 ***M2 Macrophages Serve as Critical Executor of Innate Immunity in Chronic Allograft Rejection***
Hanwen Zhang, Zhuonan Li and Wei Li

58 ***Allograft or Recipient ST2 Deficiency Oppositely Affected Cardiac Allograft Vasculopathy* via *Differentially Altering Immune Cells Infiltration***
Zhenggang Zhang, Na Zhang, Junyu Shi, Chan Dai, Suo Wu, Mengya Jiao, Xuhuan Tang, Yunfei Liu, Xiaoxiao Li, Yong Xu, Zheng Tan, Feili Gong and Fang Zheng

67 ***The Unique Immunomodulatory Properties of MSC-Derived Exosomes in Organ Transplantation***
Qingyuan Zheng, Shuijun Zhang, Wen-Zhi Guo and Xiao-Kang Li

81 ***IL-21 Receptor Blockade Shifts the Follicular T Cell Balance and Reduces* De Novo *Donor-Specific Antibody Generation***
Yeqi Nian, Zhilei Xiong, Panpan Zhan, Zhen Wang, Yang Xu, Jianghao Wei, Jie Zhao and Yingxin Fu

89 ***The mTOR Deficiency in Monocytic Myeloid-Derived Suppressor Cells Protects Mouse Cardiac Allografts by Inducing Allograft Tolerance***
Jiawei Li, Juntao Chen, Mingnan Zhang, Chao Zhang, Renyan Wu, Tianying Yang, Yue Qiu, Jingjing Liu, Tongyu Zhu, Yi Zhang and Ruiming Rong

99 ***PSMP Is Discriminative for Chronic Active Antibody-Mediated Rejection and Associate With Intimal Arteritis in Kidney Transplantation***
Panpan Zhan, Haizheng Li, Mingzhe Han, Zhen Wang, Jie Zhao, Jinpeng Tu, Xiaofeng Shi and Yingxin Fu

110 ***Impaired ATG16L-Dependent Autophagy Promotes Renal Interstitial Fibrosis in Chronic Renal Graft Dysfunction Through Inducing EndMT by NF-κB Signal Pathway***
Zeping Gui, Chuanjian Suo, Zijie Wang, Ming Zheng, Shuang Fei, Hao Chen, Li Sun, Zhijian Han, Jun Tao, Xiaobin Ju, Haiwei Yang, Min Gu and Ruoyun Tan

126 ***Case Report: Splenic Irradiation for the Treatment of Chronic Active Antibody-Mediated Rejection in Kidney Allograft Recipients With* De Novo *Donor-Specific Antibodies***
Lan Zhu, Zhiliang Guo, Rula Sa, Hui Guo, Junhua Li and Gang Chen

134 ***Melatonin Synergizes With Mesenchymal Stromal Cells Attenuates Chronic Allograft Vasculopathy***
Ya-fei Qin, De-jun Kong, Hong Qin, Yang-lin Zhu, Guang-ming Li, Cheng-lu Sun, Yi-ming Zhao, Hong-da Wang, Jing-peng Hao and Hao Wang

152 ***Tackling Chronic Kidney Transplant Rejection: Challenges and Promises***
Xingqiang Lai, Xin Zheng, James M. Mathew, Lorenzo Gallon, Joseph R. Leventhal and Zheng Jenny Zhang

165 ***Connective Tissue Growth Factor is Overexpressed in Explant Lung Tissue and Broncho-Alveolar Lavage in Transplant-Related Pulmonary Fibrosis***
Arno Vanstapel, Roel Goldschmeding, Roel Broekhuizen, Tri Nguyen, Annelore Sacreas, Janne Kaes, Tobias Heigl, Stijn E. Verleden, Alexandra De Zutter, Geert Verleden, Birgit Weynand, Erik Verbeken, Laurens J. Ceulemans, Dirk E. Van Raemdonck, Arne P. Neyrinck, Helene M. Schoemans, Bart M. Vanaudenaerde and Robin Vos

179 ***Efficacy and Safety of Bone Marrow-Derived Mesenchymal Stem Cells for Chronic Antibody-Mediated Rejection After Kidney Transplantation- A Single-Arm, Two-Dosing-Regimen, Phase I/II Study***
Yongcheng Wei, Xiaoyong Chen, Huanxi Zhang, Qun Su, Yanwen Peng, Qian Fu, Jun Li, Yifang Gao, Xirui Li, Shicong Yang, Qianyu Ye, Huiting Huang, Ronghai Deng, Gang Li, Bowen Xu, Chenglin Wu, Jiali Wang, Xiaoran Zhang, Xiaojun Su, Longshan Liu, Andy Peng Xiang and Changxi Wang

frontiers in Immunology

EDITORIAL
published: 03 September 2021
doi: 10.3389/fimmu.2021.759189

Editorial: New Insights Into and Interventions of the Persistent Immune Responses in Chronic Graft Rejection

Dejun Kong[1,2,3,4], *Caigan Du*[5,6] *and Hao Wang*[1,2*]

[1] Department of General Surgery, Tianjin Medical University General Hospital, Tianjin, China, [2] Tianjin General Surgery Institute, Tianjin, China, [3] Organ Transplantation Center, Tianjin First Central Hospital, Tianjin, China, [4] School of Medicine, Nankai University, Tianjin, China, [5] Department of Urologic Sciences, the University of British Columbia, Vancouver, BC, Canada, [6] Immunity and Infection Research Centre, Vancouver Coastal Health Research Institute, Vancouver, BC, Canada

Keywords: transplantation, chronic graft rejection, innate immunity, organ preservation, treatment

Editorial on the Research Topic

New Insights Into and Interventions of the Persistent Immune Responses in Chronic Graft Rejection

OPEN ACCESS

Edited and reviewed by:
Antoine Toubert, Université Paris Diderot, France

***Correspondence:**
Hao Wang
hwangca272@hotmail.com; hwang1@tmu.edu.cn

Specialty section:
This article was submitted to Alloimmunity and Transplantation, a section of the journal Frontiers in Immunology

Received: *16 August 2021*
Accepted: *19 August 2021*
Published: *03 September 2021*

Citation:
Kong D, Du C and Wang H (2021) Editorial: New Insights Into and Interventions of the Persistent Immune Responses in Chronic Graft Rejection. Front. Immunol. 12:759189. doi: 10.3389/fimmu.2021.759189

INTRODUCTION

Solid organ transplantation is the best therapeutic option for the patients who are suffered from end-stage organ failure. In practice, the organ transplantation is mainly used as either a form of life-saving or life-enhancing. However, due to the donor organ shortage crisis, not every patient on the waiting list can receive a donor organ. During the past few decades, with the great development of surgical skills, post-operative monitoring and care, and immunosuppressive agents, the short-term graft survival has been significantly improved after organ transplantation, indicated by as high as 95% of survival rate (1). Nevertheless, the incidence of long-term graft insufficiency or dysfunction remains very high (49.7% from the marginal donors and 34.1% from living donors) (2), which becomes one of the biggest obstacles to achieving the long-term function of a transplanted organ. There are several immune and non-immune factors involving in the pathogenesis of chronic allograft rejection (CAR), including donor's individual circumstances, ischemia reperfusion injury (IRI), innate and adaptive immunity and so on. This Research Topic gathers different contributions highlighting the recent pre-clinical and clinical researches regarding the new insights into the CAR.

INNATE IMMUNITY, MACROPHAGE AND CAR

A diversity of innate immune cells has received much attention towards the understanding of CAR. Increasing evidence focuses on the profound roles of innate immune cells, such as NK cells, macrophages, and neutrophils, in the late phase change of the allografts. Emerging attention has been paid to the intragraft macrophage infiltration in the immunopathological characteristics of CAR. It has been well established that M1-like macrophages are inclined to produce pro-inflammatory cytokines TNF-α, IL-6, and IL-1β, mediating IRI in the early stage after

transplantation. As pro-/anti- inflammatory activation and tissue repair co-exist, grafts may undergo dynamic change. Failing to control or prevent acute inflammation may result in chronic inflammation, attributing to establishment of allograft inflammatory fibrosis and gradual deterioration in functions.

Zhang et al. have reviewed the roles of macrophages as a pivotal part of innate immunity in CAR. In their review, the diverse functions of M1 and/or M2 macrophages that drive different pathophysiological mechanisms in the acute or CAR are elaborated. Importantly, despite the fact that the predominated effects of adaptive antibody-mediated rejection on the loss of the grafts, the innate-immune-mediated fibrotic rejection triggered by the macrophages should not be neglected. The pathogenesis of the tissue fibrosis is a shared and central part of numerous pathologies, including autoimmunity, metabolic disorders, and graft rejection. The M2 macrophages not only contribute to anti-inflammation in the very early stage of graft survival, but also promote fibrotic processes *via* producing TGF-β1 and VEGF. This review provides us with better insights into the crosstalk between the macrophages and CAR.

BIOMARKERS FOR CAR

As described above, there is an emerging pivotal role of the macrophages in the pathogenesis of CAR (3). Macrophage infiltration after one year post-transplantation has been demonstrated to be significantly associated with graft dysfunction and fibrosis. Furthermore, $CD68^{+}CD163^{+}$ macrophages (M2 macrophage) tend to increase in grafts with chronic antibody-mediated rejection as compared those with acute antibody-mediated rejection and T cell-mediated rejection, suggesting that these macrophages could promote the chronic progressive injury (4).

Zhan et al. have reported that PC3-secreted microprotein (PSMP) functions as a newly identified chemokine that could interact with C-C motif chemokine receptor 2 so as to mediate macrophage infiltration in local tissue, which may recruit the macrophages and promote the intimal arteritis, resulting in allograft lost in cABMR. This study may indicate PSMP may be a potential histopathological diagnostic biomarker and therapeutic target for kidney transplant rejection. However, whether PSMP plays the same role as in other organ transplants is not clear.

IMPROPER ORGAN PRESERVATION LEADS TO ALLOGRAFT REJECTION

At present, the organ donors for organ transplantation around the world are mainly from Donation after Cardiac Death (DCD) donors (5). However, the DCD marginal organs are at a high risk of short-term or long-term graft loss, depending on the donor's individual circumstances and organ preservation post-harvest. It has been known that in both humans and animal models, transplants from DCD with a longer ischemia time are less likely to survive long-term and undergo chronic rejection as compared with those from living donors, which remains an obstacle to using organ transplantation as a common therapy around the world. Nishi et al. for the first time have reported that hydrogen benefits long-term prognosis of kidney transplants in a minipig model of the ischemic kidney transplantation and can inhibit chronic rejection response under a strict multi-immunosuppressant protocol.

NOVEL STRATEGIES TO PREVENT CAR

Potential Therapeutic Targets Against CAR

Autophagy is a cellular physiological process responsible for protein and organelle degradation as a mechanism of cytoprotection against stress (6). Endothelial-to-mesenchymal transition (EndMT) plays an important role in the development of the fibrosis following kidney transplantation. Gui et al. have shown that the autophagic activity temporarily increases at the early stages of allograft transplantation, and it gradually decreases as ATG16L declines. ATG16L-dependent autophagy, as a cytoprotective process, could attenuate the transplanted kidney interstitial fibrosis *via* the regulation of the EndMT induced by IL-1β, IL-6 and TNF-α.

Zhang et al. have reported an interesting phenomenon indicating that ST2 deficiency in either allografts or recipients oppositely affects the cardiac allograft vasculopathy/fibrosis *via* differentially altering immune cells infiltration, suggesting that interrupting IL-33/ST2 signaling locally or systematically in heart transplantation may benefit the prevention of cardiac allograft vasculopathy. Nian et al. have also demonstrated that treatment with αIL-21R shifts the Tfh/Tfr balance toward DSA inhibition, which means that αIL-21R may be a potential therapeutic agent to prevent the chronic antibody-mediated rejection in organ transplantation. Finally, Li et al. have reported that mTOR deficiency enhances the immunosuppressive function of M-MDSCs and prolongs mouse cardiac allograft survival.

Traditional Chinese Medicine and CAR

To suppress the host immune response to the graft and to improve the recipient's tolerance to the transplant remain a primary focus in organ transplantation. Traditional Chinese medicine is an indispensable part in the health care in China. During the past decades, the extracts of Chinese medical herbs and their derivatives have been used in the treatment of immune- and non-immune-mediated diseases. Yang et al. have reported that artemisinin, a well-known anti-malaria agent, can effectively inhibit multiple lymphocytes, resulting in prolongation of cardiac allograft survival in a rat model of cardiac allotransplantation, and Zhou et al. have showed that curcumin, a natural polyphenol compound extracted from turmeric alleviates IL-6–dependent EndMT by promoting autophagy *in vitro* and *in vivo* in a rat model of kidney transplantation.

Mesenchymal Stromal Cells and CAR

Mesenchymal stromal cell (MSC)-based therapy emerges as an effective method for immunomodulation after transplantation (7). MSCs are adult multipotent stem cells with potent immune regulation and tissue regeneration potential. Numerous studies have demonstrated that MSCs could induce long-term allograft tolerance *via* releasing cytokines, chemokines, and extracellular vesicles and so on (8).

Qin et al. have demonstrated that melatonin can synergize with MSCs in the inhibition of chronic allograft vasculopathy in a mouse model of heterotopic aortic transplantation *via* strengthening immunomodulatory effects of MSCs. Zheng et al. review the recent development of MSCs-derived exosomes in preventing the organ transplant rejection, which may provide new strategies for improving the long-term prognosis of organ transplantation patients. Surprisingly, Wei et al. have conducted a clinical trial to confirm the clinical efficacy of MSCs. In their clinical trial, kidney recipients with biopsy-proven chronic active antibody-mediated rejection (cABMR) are divided into Regimen 1 (n = 8, a dose of 1.0×10^6 cells/kg monthly for four consecutive months) and Regimen 2 (n = 15, a dose of 1.0×10^6 cells/kg weekly during four consecutive weeks). Contemporaneous cABMR patients who did not receive Bone marrow-derived-MSCs are retrospectively used as a control group (n = 30). Kidney allograft recipients with cABMR are tolerable to BM-MSCs, and the immunosuppressive drugs combined with intravenous BM-MSCs can delay the deterioration of allograft function, probably by decreasing DSA level and reducing DSA-induced injury.

CONCLUSION

We hope that this Research Topic could provide a different perspective towards a further understanding of CAR and novel therapeutic strategies for the prevention of the CAR in the post-transplant care in the near future.

AUTHOR CONTRIBUTIONS

DK: first draft of manuscript writing. CD: manuscript editing. HW: financial support, administrative support, manuscript writing, final revision and approval of manuscript. All authors contributed to the article and approved the submitted version.

FUNDING

This work was supported by grants to HW from National Natural Science Foundation of China (No. 82071802), Li Jieshou Intestinal Barrier Research Special Fund (No. LJS_201412), and Natural Science Foundation of Tianjin (No. 18JCZDJC35800)

REFERENCES

1. Poggio ED, Augustine JJ, Arrigain S, Brennan DC, Schold JD. Long-Term Kidney Transplant Graft Survival-Making Progress When Most Needed. *Am J Transplant* (2021) 21(8):2824–32. doi: 10.1111/ajt.16463
2. Hart A, Smith JM, Skeans MA, Gustafson SK, Wilk AR, Castro S, et al. OPTN/SRTR 2017 Annual Data Report: Kidney. *Am J Transplant* (2019) 19 Suppl 2:19–123. doi: 10.1111/ajt.15274
3. Blériot C, Chakarov S, Ginhoux F. Determinants of Resident Tissue Macrophage Identity and Function. *Immunity* (2020) 52(6):957–70. doi: 10.1016/j.immuni.2020.05.014
4. van den Bosch TPP, Hilbrands LB, Kraaijeveld R, Litjens NHR, Rezaee F, Nieboer D, et al. Pretransplant Numbers of CD16(+) Monocytes as a Novel Biomarker to Predict Acute Rejection After Kidney Transplantation: A Pilot Study. *Am J Transplant* (2017) 17(10):2659–67. doi: 10.1111/ajt.14280
5. Quintini C, Muiesan P, Detry O, Gastaca M, de Jonge J, Clavien PA, et al. Early Allograft Dysfunction and Complications in DCD Liver Transplantation: Expert Consensus Statements From the International Liver Transplantation Society. *Transplantation* (2021) 105(8):1643–52. doi: 10.1097/TP.0000000000003877
6. Mizushima N, Komatsu M. Autophagy: Renovation of Cells and Tissues. *Cell* (2011) 147(4):728–41. doi: 10.1016/j.cell.2011.10.026
7. Casiraghi F, Perico N, Cortinovis M, Remuzzi G. Mesenchymal Stromal Cells in Renal Transplantation: Opportunities and Challenges. *Nat Rev Nephrol* (2016) 12(4):241–53. doi: 10.1038/nrneph.2016.7
8. Huang Y, Yang L. Mesenchymal Stem Cell-Derived Extracellular Vesicles in Therapy Against Fibrotic Diseases. *Stem Cell Res Ther* (2021) 12(1):435. doi: 10.1186/s13287-021-02524-1

Conflict of Interest: The authors declare that the research was conducted in the absence of any commercial or financial relationships that could be construed as a potential conflict of interest.

frontiers in Immunology

ORIGINAL RESEARCH
published: 25 November 2020
doi: 10.3389/fimmu.2020.598359

Hydrogen in Patients With Corticosteroid-Refractory/Dependent Chronic Graft-Versus-Host-Disease: A Single-Arm, Multicenter, Open-Label, Phase 2 Trial

Liren Qian[1†], Miao Liu[2†], Jianliang Shen[1], Jian Cen[1] and Defeng Zhao[3]*

[1] Department of Hematology, The Sixth Medical Center, Chinese PLA General Hospital, Beijing, China, [2] Department of Statistics and Epidemiology, Graduate School of Medical School of Chinese PLA General Hospital, Beijing, China, [3] Department of Hematology, Boren Hospital, Beijing, China

OPEN ACCESS

Edited by:
Hao Wang,
Tianjin Medical University General Hospital, China

Reviewed by:
Ying-Jun Chang,
Peking University People's Hospital, China
Thomas Luft,
Heidelberg University Hospital, Germany

***Correspondence:**
Liren Qian
qlr2007@126.com

[†]*These authors have contributed equally to this work*

Specialty section:
This article was submitted to Alloimmunity and Transplantation, a section of the journal Frontiers in Immunology

Received: *24 August 2020*
Accepted: *02 November 2020*
Published: *25 November 2020*

Citation:
Qian L, Liu M, Shen J, Cen J and Zhao D (2020) Hydrogen in Patients With Corticosteroid-Refractory/Dependent Chronic Graft-Versus-Host-Disease: A Single-Arm, Multicenter, Open-Label, Phase 2 Trial. Front. Immunol. 11:598359. doi: 10.3389/fimmu.2020.598359

Chronic graft-versus-host-disease (cGVHD) is the leading cause of late non-relapse mortality after allogeneic hematopoietic stem cell transplantation(HSCT). There is no standard therapy for patients refractory or dependent to corticosteroid treatment. We hypothesized that hydrogen may exert therapeutic effects on cGVHD patients with few side effects. A prospective open-label phase 2 study of hydrogen was conducted. Patients received hydrogen-rich water 4ml/kg orally three times a day. Responses were graded in the skin, mouth, Gastrointestinal(GI), liver, eyes, lungs and joints and fascia every 3 months. A total of 24 patients (median age 27) were enrolled. Of the 24 patients, 18 (75%; 95% CI, 55.1% to 88%) had an objective response. No significant toxicity was observed. The estimated 4-year overall survival rate was 74.7%(95% CI, 54.9%–94.5%). The survival time was significantly prolonged in the response group. The survival rate at 4 years in the response group is significantly higher than the nonresponse group (86.6% vs 0%; p= 0.000132). Hydrogen showed great efficacy on cGVHD patients and long-term administration of hydrogen was not associated with significant toxic effects. The trial was registered at www.ClinicalTrials.Gov, NCT02918188.

Keywords: corticosteroid, hydrogen, graft-versus-host-disease, refractory, chronic graft-versus-host-disease

INTRODUCTION

Allogeneic hematopoietic stem cell transplantation (allo-HSCT) has been widely used in the treatment of benign and malignant hematopoietic diseases. Chronic graft-versus-host disease (cGVHD) is a very common complication of allo-HSCT and has become the main cause of non-transplant-related death after transplantation (1). Among patients who received allo-HSCT, the cumulative incidence of cGVHD requiring treatment within 2 years after transplantation reaches 30%–40%. With the increased use of allo-HSCT in elderly patients, the widespread use of peripheral blood stem cells as sources and the improvement of the initial survival rate after transplantation, the incidence of cGVHD is increasing year by year (2). However, in the past three decades, the first-line treatment of cGVHD still mainly

depends on corticosteroids (such as prednisone, methylprednisolone, dexamethasone, etc.). Clinical initial treatment of cGVHD often uses prednisone with or without cyclosporine or tacrolimus. The initial dose of prednisone is usually 0.5–1 mg/kg/day, which will be gradually reduced after the disease is controlled (3, 4). In the process of glucocorticoid reduction, the symptoms of patients with cGVHD are often aggravated or even relapsed, which leads to the cessation of glucocorticoid reduction or even increase. The duration of treatment of cGVHD with glucocorticoids often reaches 3 months or even longer (5). However, long-term use of glucocorticoids can lead to serious toxic side effects. In order to minimize the toxic side effects of long-term use of glucocorticoids, clinicians often use glucocorticoids in combination with other immunosuppressive agents to treat cGVHD (6), mainly including calmodulin inhibitors (such as cyclosporine, tacrolimus), azathioprine, mycophenolate mofetil (MMF), hydroxychloroquine, etc. However, a number of clinical trials have confirmed that combining azathioprine (7), mycophenolate mofetil (5), hydroxychloroquine (8), thalidomide, etc (9) on the basis of initial treatment did not bring benefits. Fifty percent to 60% of cGVHD patients treated with first-line treatment still need to receive second-line treatment (10). At present, a number of clinical trials on the second-line treatment of cGVHD has been carried out internationally, but the results are often not convincing due to flaws in trial design (6). Clearly, there is an urgent need to find a better treatment for cGVHD (11). In 2007, Ohsawa et al. systematically reported the biological effects of molecular hydrogen (H_2) for the first time (12). Their study found that H_2 has a good antioxidant effect. Compared with tacrolimus, H_2 has the same therapeutic effect on cerebral ischemia-reperfusion injury in rats. The researchers also found that, similar to tacrolimus, H_2 has a strong anti-inflammatory effect in addition to its antioxidant effect. Tacrolimus has already become a first-line treatment for rejection of solid organ transplantation and cGVHD after allo-HSCT. In addition, H_2 has also been proven to have a good anti-fibrotic effect. Terasaki Y et al. found in the mouse models of pulmonary fibrosis post radiation that breathing air containing 4% H_2 has a significant therapeutic effect on chronic pulmonary fibrosis, and can significantly delay the progress of pulmonary fibrosis (13). Although the current mechanism of cGVHD is not very clear, in the currently recognized pathogenesis of cGVHD, inflammatory factors imbalance and fibrosis occupy a dominant position (4, 14). Since H_2 has anti-inflammatory and anti-fibrosis effects, we speculate that H_2 may have potential therapeutic effects for cGVHD after allo-HSCT. We have proved the its therapeutic effects in a mouse model preliminary (15). To further verify the hypothesis, we conducted a multiple center study of hydrogen in patients with corticosteroid-refractory/dependent cGVHD to look at response rate and to detect any unique toxicities.

SUBJECT AND METHODS

Patient Eligibility

This investigator-initiated study was approved by the ethics committee of the Sixth Medical Center, Chinese People's Liberation Army (PLA) General Hospital, China. All of the patients or their legal guardians signed informed consent forms in accordance with the Declaration of Helsinki. This trial has been registered as NCT02918188 (www.clinicaltrials.gov).

Patients who underwent allogeneic stem cell transplantation were enrolled. Eligible patients met the following criteria: patients younger than 65 years diagnosis of steroid-refractory cGVHD (no response after prednisone at least 1 mg/kg or equivalent dose of another steroid or another immunosuppressive regimen) or steroid-dependent cGVHD (had an initial response followed by a cGVHD flare upon steroid taper). A tissue biopsy before entering the study with histology consistent with cGVHD was required unless there was a medical contraindication such as concern for poor wound healing after the biopsy. Exclusion criteria were: patients with other stable diseases(not chronic GVHD), not well controlled by the current treatment; pregnancy; HIV positive; severe liver or renal impairment: serum creatinine >2.5 mg/dl, serum bilirubin>2.5 mg/dl (without evidence of hepatic cGVHD); uncontrolled malignancies including the persistence of the underlying malignancy before the allogeneic transplantation and the relapse of hematopoietic malignancy; any other investigational agents administered within last four weeks; cardiac insufficiency (>grade II, New York Heart Association classification); inability to comply with medical therapy or follow-up.

Therapy

Patients included in this study received hydrogen-rich water as their only new intervention. Hydrogen-rich water (0.8 ppm H_2) was administered orally three times a day at 4 ml/kg. The hydrogen-rich water (0.8 ppm H_2) was supplied by Beijing Huoliqingyuan Beverage Co., Ltd. (Beijing, China) as previously described (16). All patients received 12 months of therapy unless they required earlier removal from the study. It was recommended that a corticosteroid taper be started between 8 and 12 weeks after initiating hydrogen-rich water. A reduction of 25% of the initial dose every 2 weeks was the recommended corticosteroid taper. It was also recommended that if subjects were receiving a calcineurin inhibitor at the time of study initiation that they remain on it through the duration of the study unless there was drug toxicity. All other immunosuppressants were to be tapered on an individual basis.

Evaluation of Response and Toxicity

Subjects were evaluated at baseline and then every 3 months using the form according to National Institutes of Health (NIH) Consensus for cGVHD (17). In each subjects, seven domains were assessed: mouth, gastrointestinal, lungs, liver, joint, skin, and ocular. Each domain's therapeutic response was measured according to the NIH consensus on response criteria (17). No response was defined as disease progression, no change, mixed response (response in 1 or more domains, progress in 1 or more domains) or initial response followed by disease progression. Therapeutic response for each subject was followed 12 months until the completion of the study. Toxicity was assessed every 3 months using Common Toxicity Criteria Version 3.0 according to the National Cancer Institute Common Toxicity Criteria.

Removal From Protocol

Patients were removed from the study if cGVHD progressed after 12 or more weeks of treatment. Patients were also removed if they were lost to follow-up or if the family withdrew consent. For subjects that were removed from the study, the last assessment before removal was used to determine response. Subjects that were removed are counted as nonresponders. Two patients were removed from this study both due to loss of follow-up.

Statistics

The primary statistical endpoint was overall response rate (defined as complete or partial response). Subjects were evaluated at baseline and then every 3 months using the form according to National Institutes of Health (NIH) Consensus for cGVHD (17). Overall response was measured according to the NIH consensus on response criteria (17). No response was defined as disease progression, no change, mixed response (response in 1 or more domains, progress in 1 or more domains) or initial response followed by disease progression. A sample size of 17 was calculated according to have 80% power to detect a response rate of at least 50% (11), compared with a control response rate of 20%, with 80% power and a type I error rate of 5%. Although this design required 17 patients, the final sample size was 24.

A secondary outcome was response rate in each domain measured in subjects that had had initial involvement in that domain. In each subjects, seven domains were assessed: mouth, gastrointestinal, lungs, liver, joint, skin, and ocular. Each domain's therapeutic response was measured according to the NIH consensus on response criteria (17). Response rates were calculated together with 95% exact binomial confidence intervals. Descriptive characteristics are shown with percentages or with medians and ranges, as appropriate. Logistic Regression analysis was used to determine significance of certain factors such as history of acute GVHD and severity stage of chronic GVHD on final response. Time to initial response was analyzed using cumulative incidence (18). Survival percentages and confidence intervals were calculated using Kaplan-Meier curves. Curves were compared using the log-rank test. All analyses were performed with SAS (SAS Institute) and SPSS.

RESULTS

Patient Characteristics

Twenty-four patients from four different institutions were enrolled. Two patients were removed from the study because of loss of follow-up. Patient characteristics at the entry were given in **Table 1**. Median age of the patients was 27 years old. Patients were diagnosed as acute myeloid leukemia/myelodysplasia (n=12), acute lymphoblastic leukemia(n=10), systemic lupus erythematosus (n=1) and hemophagocytic lymphohistiocytosis (n=1). All patients received myeloablative hematopoietic stem cell transplantation. Subjects had received different donor stem cell sources: haploidentical bone marrow plus peripheral blood stem cell (PBSC) (n=13), human leukocyte antigen (HLA)-identical sibling bone marrow plus PBSC (n=5), HLA-identical sibling PBSC (n=3), unrelated donor PBSC (n=1), unrelated cord blood (n=1), and haploidentical PBSC (n=1).

The chronic GVHD characteristics of the subjects at study entry are given in **Table 2**. Median beginning platelet count was 168, and 33.3% of the subjects are with platelet count less than 100×10^9/L. 79.2% of the subjects at study entry are on corticosteroids and median beginning prednisone dose was 0.21 mg/kg/day. 66.7% of the subjects had a history of acute GVHD. 79.2% had severe chronic GVHD according to the NIH global severity stage (17). The Karnofsky performance scale (KPS) of 10 subjects is no greater than 80.

Response

At the entry of the study, skin was the most involved (75.0%), followed by the gastrointestinal tract (70.8%), while liver is the least involved organ(8.3%). 66.7% of patients had clinical manifestations of cGVHD in mouth, 63% of patients manifestated in the eyes, 33.3% in lungs, and 29.2% in joints and fascia. Overall, of the 24 patients, 18 (75.0%; 95% CI, 55.1% to 88%) had an objective response to hydrogen therapy at the last evaluation. Eight patients had complete response, 10 had partial response, five had disease progression, and one had stable disease. Of the 18 patients who responded to treatment, 15 had a response at 30 days of treatment, two at 90 days, one at 180

TABLE 1 | Patient characteristics at study entry (N=24).

	Values	Responders	Non-responders
Median Age, y(range)*	27(9–54)	27(9–54)	32.5(21–37)
Gender*			
Male, n (%)	12 (50.0)	10(55.6)	2(33.3)
Female, n (%)	12 (50.0)	8(44.4)	4(66.7)
Diagnoses*			
Acute myeloid leukemia/ myelodysplasia, n (%)	12 (50.0)	9(50.0)	3(50.0)
Acute lymphoblastic leukemia, n (%)	10 (41.7)	7(38.9)	3(50.0)
Systemic lupus erythematosus, n (%)	1 (4.2)	1(5.6)	0
Hemophagocytic lymphohistiocytosis, n (%)	1 (4.2)	1(5.6)	0
Transplantation regimen*			
Myeloablative, n (%)	24 (100)	18(100)	6 (100)
Stem cell Source*			
Haploidentical bone marrow + PBSC, n (%)	13 (54.2)	10(55.6)	3(50.0)
HLA-identical sibling bone marrow + PBSC, n(%)	5 (20.8)	3(16.7)	2(33.3)
HLA-identical sibling PBSC, n(%)	3 (12.5)	2(11.1)	1(16.7)
Unrelated donor PBSC, n(%)	1 (4.2)	1(5.6)	0
Unrelated cord blood, n(%)	1 (4.2)	1(5.6)	0
Haploidentical PBSC, n(%)	1 (4.2)	1(5.6)	0

*HLA, human leukocyte antigen; PBSC, peripheral blood stem cell. The responders compared with non-responders *P > 0.05.*

TABLE 2 | Chronic GVHD characteristics at study entry.

	Values	Responders	Non-responders
Median beginning platelet count, 10^9/L (range) *	168(31–428)	182.5(31–428)	142.5 (33–175)
Median beginning prednisone dose, mg/kg/d (range) *	0.21(0–0.81)	0.185(0–0.81)	0.27(0–0.48)
Subjects on corticosteroids at study entry, n (%)*	19(79.2)	14(77.8)	5(83.3)
Subjects with platelet count less than 100×10^9/L, n (%)*	8(33.3)	6(33.3)	2(33.3)
Performance score no greater than 80, n (%)	10(41.7)	7(38.9)	3(50.0)
History of acute GVHD, n (%)*	16 (66.7)	11(61.1)	5(83.3)
Severe chronic GVHD (NIH global severity stage), n (%)*	19 (79.2)	14(77.8)	5(83.3)

*GVHD, graft-versus-host disease; NIH, National Institutes of Health. The responders compared with non-responders *P > 0.05.*

days. All these 18 patients had sustained response at last evaluation. The median time to response was 30 days (range, 30 to 180 days).

Of the 24 patients enrolled, 18 patients received therapy for 12 months. Two patients were removed from the study both due to loss of follow-up. Four patients died within 12 months. Of the 18 patients who received therapy for 12 months, eight had complete response, nine had partial response, and one had disease progression. The percentage of patients who received 12 months of therapy and had a response was 17/24 (70.8%; 95% CI, 50.8% to 85.1%).

Among the 16 patients with cGVHD affecting the oral cavity, 10 patients had complete remission and three patients had partial remission. The response rate was 81.25% (95% CI, 57.0%–93.4%). Of the 17 patients with cGVHD affecting gastrointestinal tract, 13 had complete remission and one had partial remission. The response rate was 82.35% (95% CI, 59.0%–93.8%). The detailed response rates in the various organs are listed in **Table 3**. Among them, the response rate of lung is the lowest, 50% (95% CI, 21.5%–78.5%), and the response rate of liver is the highest, 100% (34.2%-100%). Detailed grades of the cGVHD per organ at study entry and one year after or last assessment for each patient is showed in **Table 4**. We also used the Karnofsky performance scale (KPS) as an indicator of the patient's quality of life. Our study found that among patients who continued to drink hydrogen-rich water for more than 12 months, KPS has been improved (p=0.034).

We also evaluated whether hydrogen therapy had a corticosteroid sparing effect in patients who responded. The median beginning prednisone dose in the response group was 0.185 mg/kg/day (0–0.81 mg/kg/day) while the median end prednisone dose was 0 mg/kg/day (0–0.59 mg/kg/day; P=0.004) (**Figure 1**). In the six patients who did not respond to hydrogen therapy, the median beginning prednisone dose in the non-response group was 0.27mg/kg/day (0–0.48 mg/kg/day) while the median end prednisone dose was 0.05 mg/kg/day (0–0.27 mg/kg/day). The change in non-response group was not statistically significant (P =0.115). Besides, as shown in **Table 5**, there were 13 patients taking immunosuppressive drugs at the entry and one year after study entry among the 18 patients who reached this time point.

Toxicity and Mortality

None of the enrolled patients were removed from the study due to toxicity. No obvious toxicity and side effects were seen in 24 enrolled patients. Only three patients had transient hiccups. Three patients died during treatment, one case was due to a serious fungal infection. One-year survival rate of the entire cohort was 81.5% (95% CI, 65.0%–98.0%). The 4-year projected survival rate of the entire cohort was 74.7% (95% CI, 54.9%–94.5%).The 4-year projected survival rate was 86.6%(95% CI, 69.0%–100%) among patients who responded to treatment, which was significantly higher than that in the group did not respond to treatment(p= 0.000132), as shown in **Figure 2**. The median follow-up time was 38.5 months (range, 3–51 months).

DISCUSSION

In this study, we evaluated the response rate and toxicity of molecular hydrogen on patients with chronic GVHD who are corticosteroid-refractory/dependent. The study found a greater than 50% response rate, which reached its primary endpoint.

Results of the study are encouraging, mainly due to the following points: Firstly. It has been confirmed that molecular hydrogen has a good response rate in chronic graft-versus-host patients, and the overall response rate can reach 74.7%. However, the response rate reported in the previous literature fluctuated between 40% and 60% (11, 19). Secondly, Hydrogen is not toxic.

TABLE 3 | Response by domain (N=24).

	Involved, n (%)	Complete Response, n (%)	Partial Response, n (%)	Stable, n (%)	Progression, n (%)	Response rate, % (95% CI)*
Mouth	16 (66.7)	10(62.5)	3(18.8)	1(6.3)	2(12.5)	81.25(57.0–93.4)
Gastrointestinal	17 (70.8)	13(76.5)	1(5.9)	0(0)	3(17.6)	82.4(59.0–93.8)
Lung	8 (33.3)	4(50.0)	0(0)	2(25.0)	2(25.0)	50.0(21.5–78.5)
Liver	2 (8.3)	1(50)	1(50)	0(0)	0(0)	100(34.2–100)
Skin	18 (75.0)	11(61.1)	1(5.6)	2(11.1)	4(22.2)	66.7(43.8–83.7)
Ocular	17 (63.0)	9(52.9)	2(11.8)	3(17.6)	3(17.6)	64.7(41.3–82.7)
Joints and fascia	7 (29.2)	5(71.4)	0(0)	1(14.3)	1(14.3)	71.4(35.9–91.8)

*CI, confidence interval. *Response rate included CR + PR.*

TABLE 4 | Severity score of chronic graft-versus-host-disease (cGVHD) per organ at study entry and one year after or last assessment.

Patient number	Mouth at the entry	Mouth at one year or last assessment	Gastrointestinal at the entry	Gastrointestinal at one year or last assessment	Lung at the entry	Lung at one year or last assessment	Liver at the entry	Liver at one year or last assessment	Skin at the entry	Skin at one year or last assessment	Ocular at the entry	Ocular at one year or last assessment	Joints and fascia at the entry	Joints and fascia at one year or last assessment
1	3	2	2	0	0	0	0	0	2	0	1	0	0	0
2	0	0	0	0	0	0	0	0	3	0	0	0	0	0
3	0	0	0	0	2	2	0	0	0	0	2	0	0	0
4	2	2	3	0	2	0	0	0	0	0	0	0	1	0
5	3	2	2	0	0	0	0	0	0	0	1	0	2	0
6	2	0	1	0	2	0	0	0	3	0	3	3	0	0
7	1	0	1	0	0	0	0	0	2	0	1	0	0	0
8	1	0	1	0	0	0	0	0	3	0	3	0	0	0
9	1	0	1	2	0	0	0	0	2	1	0	0	1	1
10	3	2	1	0	0	0	0	0	0	2	2	2	0	0
11	3	0	3	0	0	3	0	0	3	0	1	0	0	0
12	2	0	0	0	0	0	0	0	3	0	1	0	0	0
13	0	0	1	0	0	0	0	0	1	0	0	0	0	0
14	3	0	2	0	1	0	0	0	3	0	3	2	1	0
15	3	0	1	0	0	0	0	0	0	0	1	0	0	0
16	0	0	1	0	0	0	0	0	2	0	0	0	1	0
17	0	0	3	2	0	0	3	0	0	0	0	0	0	0
18	2	0	0	0	2	3	0	0	1	1	2	2	0	0
19	0	0	0	0	2	0	2	1	0	0	0	0	0	0
20	2	0	0	0	0	0	0	0	3	3	3	1	0	0
21	0	0	1	0	1	1	0	0	1	0	2	0	1	0
22	3	3	2	3	0	0	0	0	3	3	3	3	1	3
23	2	3	1	3	0	0	0	0	3	3	1	3	0	0
24	0	0	0	0	0	0	0	0	3	3	3	3	0	0

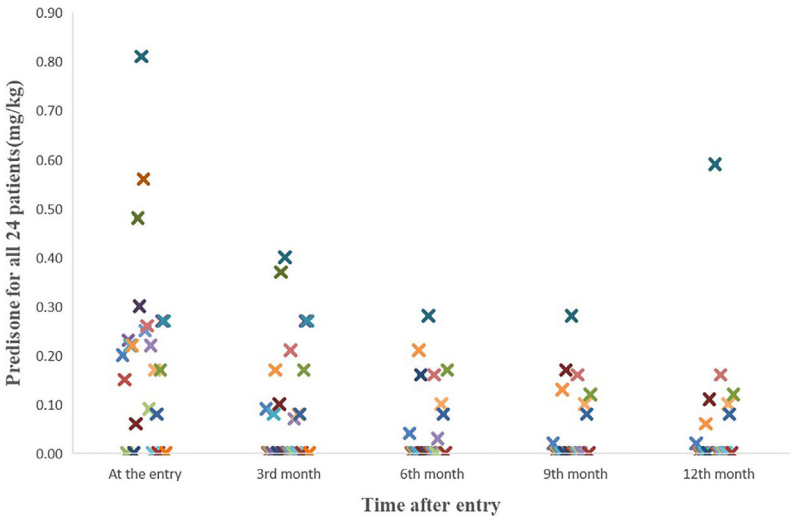

FIGURE 1 | The course of the prednisone doses for all 24 patients. The median beginning prednisone dose in the response group was 0.185 mg/kg/d (0-0.81mg/kg/d) while the median end prednisone dose was 0 mg/kg/d (0-0.59mg/kg/d; P=0.004).

TABLE 5 | Immunosuppressive drugs taken at the entry and one year after study entry for subjects reached this time point.

Patients	At entry	One year after study entry
1	Prednisone	Prednisone
2	Prednisone + CSA	FK506
3	None	None
4	Prednisone + CSA	MMF
5	Prednisone + CSA	CSA
6	Prednisone + FK506	Prednisone + FK506
7	FK506	FK506
8	Prednisone + CSA	Prednisone
9	Prednisone + FK506	\
10	Prednisone + FK506	\
11	Prednisone + CSA	Prednisone + FK506
12	Prednisone + FK506	None
13	Prednisone + FK506	MMF + FK506
14	Prednisone + FK506	Prednisone
15	Prednisone + CSA	None
16	Prednisone	None
17	None	\
18	Prednisone + FK506	Prednisone + FK506
19	Prednisone + FK506	Prednisone + FK506
20	Azathioprine + MTX + MMF	None
21	Prednisone + FK506	Prednisone + FK506
22	Prednisone + CSA + MMF	\
23	Prednisone + CSA + MMF	\
24	None	\

FK506, Tacrolimus; MMF, Mycophenolate Mofetil; CSA, Cyclosporine A

Treating chronic GVHD with immunosuppressive agents can increase the risk of infection. However, in polymicrobial sepsis models, molecular hydrogen has been proved to have anti-infective effects but not increasing the risk of infection (20–22), which is different from immunosuppressive agents. In our study, only three patients experienced transient hiccups and no other side effects. Hydrogen and helium mixed gas has been used in diving for a long time, and divers have no obvious adverse reactions even when breathing high-pressure hydrogen (23). Besides, bacteria in the colon of humans and animals can also produce a certain level of H_2 (12). These all indicate that H_2 has no toxic side effects on the human body. Moreover, H_2 in the body can be discharged through the respiratory system without any residue. This characteristic determines that H_2 can be used for a long time, and this characteristic can precisely target the long-term, repeated and protracted disease characteristics of cGVHD. It was found in the study that the median response time is 30 days, and the response rate gradually increases with the extension of the treatment time. The study was designed to administer hydrogen continuously for 1 year. We believe that if the administration time is extended, the overall response rate will still rise. Thirdly, the hydrogen molecule is very small, has a strong penetration ability, can quickly penetrate the biofilm, and reach a higher concentration in the cell to play a therapeutic role (24). Finally, H_2 is cheap and easy to obtain. H_2 is widely distributed in nature, and the industrial preparation technology is very mature and the price is very low. A considerable part of the existing cGVHD drugs (such as tacrolimus, Ixazomib (25), ibutinib (26, 27), ruxolitinib (28), etc.) are very expensive, making many families poorer due to illness.

In our study, we can see that the response rate of the digestive system is higher, the response rate of the oral cavity can reach 81.25%, and the response rate of the gastrointestinal tract can reach 82.4%. Both patients with liver involvement have obtained a response. We considered that the overall repoonse rate is higher because the hydrogen-rich water can directly act on the digestive system due to the higher hydrogen concentration in the digestive system. Therefore, we speculate that patients with lung involvement can use the method of breathing hydrogen, patients

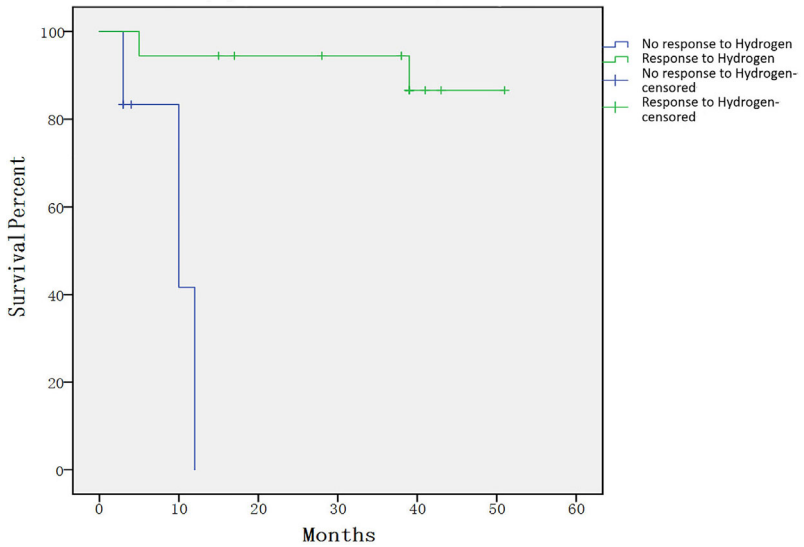

FIGURE 2 | Individual survival curves shown for subjects that had response compared with those that did not. The 4-year projected survival rate was 86.6% (95% CI, 69.0%–100%) among patients who responded to treatment, which was significantly higher than that in the group did not respond to treatment (p= 0.000132).

with eye involvement can use hydrogen-rich eye drops, and patients with skin involvement can use hydrogen-rich water to wash, which may achieve better treatment results.

Although the long-term outcome is not a primary endpoint of the study, our research indicates that the 4-year projected overall survival rate of 74.7% is encouraging. Recently, the number of studies on chronic GVHD have gradually increased (19, 25, 29, 30), but few publications report the long-term survival rate of corticosteroid-refractory/dependent cGVHD. In a newly diagnosed children study, the 3-year survival rate is approximately 70% (31). In a corticosteroid-refractory cGVHD study, the 3-year survival rate is approximately 60% (11). Therefore, in our study, the four-year survival rate of 74.7% is very exciting. Compared with the group that did not respond to H_2, the survival rate of patients who responded to hydrogen treatment was significantly improved. Therefore, we can use the response to hydrogen therapy as a potential prognostic indicator. In our study, all patients in the group that did not respond to hydrogen therapy died within 1 year, which may be due to the seriousness of the conditions of the enrolled patients, because patients with severe cGVHD accounted for nearly 80% at entry of study.

In conclusion, this study for the first time suggested effectiveness of hydrogen therapy in patients with corticosteroid-refractory/dependent cGVHD compared to historical controls. The overall response rate can reach 75%, with almost no toxic side effects, which can precisely target the disease characteristics of cGVHD. Its long-term survival rate is encouraging. We strongly support the future multi-institutional research in the world. Whether molecular hydrogen can be used as the first-line treatment of cGVHD still requires further clinical trials.

DATA AVAILABILITY STATEMENT

The original contributions presented in the study are included in the article/supplementary material. Further inquiries can be directed to the corresponding author.

ETHICS STATEMENT

The studies involving human participants were reviewed and approved by the ethics committee of the Sixth Medical Center, Chinese PLA General Hospital, China. Written informed consent to participate in this study was provided by the participants' legal guardian/next of kin.

AUTHOR CONTRIBUTIONS

LQ and ML designed the experiment, analyzed data, and wrote the paper. JS, JC, and DZ performed the experiments and analyzed data. All authors contributed to the article and approved the submitted version.

FUNDING

This work was supported by a grant from the National Natural Science Foundation of China (Grant No. 81800180).

ACKNOWLEDGMENTS

We thank Beijing Huoliqingyuan Beverage Co., Ltd for providing hydrogen-rich water.

REFERENCES

1. Martin PJ, Counts GWJr., Appelbaum FR, Lee SJ, Sanders JE, Deeg HJ, et al. Life expectancy in patients surviving more than 5 years after hematopoietic cell transplantation. *J Clin Oncol* (2010) 28:1011–6. doi: 10.1200/JCO.2009.25.6693
2. Anasetti C, Logan BR, Lee SJ, Waller EK, Weisdorf DJ, Wingard JR, et al. Peripheral-blood stem cells versus bone marrow from unrelated donors. *N Engl J Med* (2012) 367:1487–96. doi: 10.1056/NEJMoa1203517
3. Flowers ME, Martin PJ. How we treat chronic graft-versus-host disease. *Blood* (2015) 125:606–15. doi: 10.1182/blood-2014-08-551994
4. Xu KL. [How I treat chronic graft-versus-host disease]. *Zhonghua Xue Ye Xue Za Zhi* (2018) 39:89–93. doi: 10.3760/cma.j.issn.0253-2727.2018.02.001
5. Martin PJ, Storer BE, Rowley SD, Flowers ME, Lee SJ, Carpenter PA, et al. Evaluation of mycophenolate mofetil for initial treatment of chronic graft-versus-host disease. *Blood* (2009) 113:5074–82. doi: 10.1182/blood-2009-02-202937
6. Martin PJ, Inamoto Y, Carpenter PA, Lee SJ, Flowers ME. Treatment of chronic graft-versus-host disease: Past, present and future. *Korean J Hematol* (2011) 46:153–63. doi: 10.5045/kjh.2011.46.3.153
7. Sullivan KM, Witherspoon RP, Storb R, Weiden P, Flournoy N, Dahlberg S, et al. Prednisone and azathioprine compared with prednisone and placebo for treatment of chronic graft-v-host disease: prognostic influence of prolonged thrombocytopenia after allogeneic marrow transplantation. *Blood* (1988) 72:546–54. doi: 10.1182/blood.V72.2.546.bloodjournal722546
8. Gilman AL, Schultz KR, Goldman FD, Sale GE, Krailo MD, Chen Z, et al. Randomized trial of hydroxychloroquine for newly diagnosed chronic graft-versus-host disease in children: a Children's Oncology Group study. *Biol Blood Marrow Transplant* (2012) 18:84–91. doi: 10.1016/j.bbmt.2011.05.016
9. Flowers ME, Martin PJ. Evaluation of thalidomide for treatment or prevention of chronic graft-versus-host disease. *Leuk Lymphoma* (2003) 44:1141–6. doi: 10.1080/1042819031000079096
10. Inamoto Y, Flowers ME, Sandmaier BM, Aki SZ, Carpenter PA, Lee SJ, et al. Failure-free survival after initial systemic treatment of chronic graft-versus-host disease. *Blood* (2014) 124:1363–71. doi: 10.1182/blood-2014-03-563544
11. Jacobsohn DA, Gilman AL, Rademaker A, Browning B, Grimley M, Lehmann L, et al. Evaluation of pentostatin in corticosteroid-refractory chronic graft-versus-host disease in children: a Pediatric Blood and Marrow Transplant Consortium study. *Blood* (2009) 114:4354–60. doi: 10.1182/blood-2009-05-224840
12. Ohsawa I, Ishikawa M, Takahashi K, Watanabe M, Nishimaki K, Yamagata K, et al. Hydrogen acts as a therapeutic antioxidant by selectively reducing cytotoxic oxygen radicals. *Nat Med* (2007) 13:688–94. doi: 10.1038/nm1577
13. Terasaki Y, Ohsawa I, Terasaki M, Takahashi M, Kunugi S, Dedong K, et al. Hydrogen therapy attenuates irradiation-induced lung damage by reducing oxidative stress. *Am J Physiol Lung Cell Mol Physiol* (2011) 301:L415–26. doi: 10.1152/ajplung.00008.2011
14. Sarantopoulos S, Cardones AR, Sullivan KM. How I treat refractory chronic graft-versus-host disease. *Blood* (2019) 133:1191–200. doi: 10.1182/blood-2018-04-785899
15. Qian L, Liu X, Shen J, Zhao D, Yin W. Therapeutic effects of hydrogen on chronic graft-versus-host disease. *J Cell Mol Med* (2017) 21:2627–30. doi: 10.1111/jcmm.13155
16. Zhang Y, Su WJ, Chen Y, Wu TY, Gong H, Shen XL, et al. Effects of hydrogen-rich water on depressive-like behavior in mice. *Sci Rep* (2016) 6:23742. doi: 10.1038/srep23742
17. Lee SJ, Wolff D, Kitko C, Koreth J, Inamoto Y, Jagasia M, et al. Measuring therapeutic response in chronic graft-versus-host disease. National Institutes of Health consensus development project on criteria for clinical trials in chronic graft-versus-host disease: IV. The 2014 Response Criteria Working Group report. *Biol Blood Marrow Transplant* (2015) 21:984–99. doi: 10.1016/j.bbmt.2015.02.025
18. Gooley TA, Leisenring W, Crowley J, Storer BE. Estimation of failure probabilities in the presence of competing risks: new representations of old estimators. *Stat Med* (1999) 18:695–706. doi: 10.1002/(SICI)1097-0258(19990330)18:6<695::AID-SIM60>3.0.CO;2-O
19. Shapiro RM, Antin JH. Therapeutic options for steroid-refractory acute and chronic GVHD: an evolving landscape. *Expert Rev Hematol* (2020) 13:519–32. doi: 10.1080/17474086.2020.1752175
20. Li GM, Ji MH, Sun XJ, Zeng QT, Tian M, Fan YX, et al. Effects of hydrogen-rich saline treatment on polymicrobial sepsis. *J Surg Res* (2013) 181:279–86. doi: 10.1016/j.jss.2012.06.058
21. Yao W, Guo A, Han X, Wu S, Chen C, Luo C, et al. Aerosol inhalation of a hydrogen-rich solution restored septic renal function. *Aging (Albany NY)* (2019) 11:12097–113. doi: 10.18632/aging.102542
22. Qiu P, Liu Y, Zhang J. Recent Advances in Studies of Molecular Hydrogen against Sepsis. *Int J Biol Sci* (2019) 15:1261–75. doi: 10.7150/ijbs.30741
23. Abraini JH, Gardette-Chauffour MC, Martinez E, Rostain JC, Lemaire C. Psychophysiological reactions in humans during an open sea dive to 500 m with a hydrogen-helium-oxygen mixture. *J Appl Physiol* (1994) 76:1113–8. doi: 10.1152/jappl.1994.76.3.1113
24. Qian L, Wu Z, Cen J, Pasca S, Tomuleasa C. Medical Application of Hydrogen in Hematological Diseases. *Oxid Med Cell Longev* (2019) 2019:3917393. doi: 10.1155/2019/3917393
25. Pidala J, Bhatt VR, Hamilton B, Pusic I, Wood WA, Onstad L, et al. Ixazomib for Treatment of Refractory Chronic Graft- versus-Host Disease: A Chronic GVHD Consortium Phase II Trial. *Biol Blood Marrow Transplant* (2020) 26(9):1612–9. doi: 10.1016/j.bbmt.2020.05.015
26. Waller EK, Miklos D, Cutler C, Arora M, Jagasia MH, Pusic I, et al. Ibrutinib for Chronic Graft-versus-Host Disease After Failure of Prior Therapy: 1-Year Update of a Phase 1b/2 Study. *Biol Blood Marrow Transplant* (2019) 25:2002–7. doi: 10.1016/j.bbmt.2019.06.023
27. Miklos D, Cutler CS, Arora M, Waller EK, Jagasia M, Pusic I, et al. Ibrutinib for chronic graft-versus-host disease after failure of prior therapy. *Blood* (2017) 130:2243–50. doi: 10.1182/blood-2017-07-793786
28. Schoettler M, Duncan C, Lehmann L, Furutani E, Subramaniam M, Margossian S. Ruxolitinib is an effective steroid sparing agent in children with steroid refractory/dependent bronchiolitis obliterans syndrome after allogenic hematopoietic cell transplantation. *Bone Marrow Transplant* (2019) 54:1158–60. doi: 10.1038/s41409-019-0450-3
29. Pidala J, Jaglowski S, Im A, Chen G, Onstad L, Storer B, et al. Carfilzomib for Treatment of Refractory Chronic Graft-versus-Host Disease: A Chronic GVHD Consortium Pilot Phase II Trial. *Biol Blood Marrow Transplant* (2020) 26:278–84. doi: 10.1016/j.bbmt.2019.09.002
30. Boberg E, von Bahr L, Afram G, Lindstrom C, Ljungman P, Heldring N, et al. Treatment of chronic GvHD with mesenchymal stromal cells induces durable responses: A phase II study. *Stem Cells Trans Med* (2020) 9(10):1190–202. doi: 10.1002/sctm.20-0099
31. Zecca M, Prete A, Rondelli R, Lanino E, Balduzzi A, Messina C, et al. Chronic graft-versus-host disease in children: incidence, risk factors, and impact on outcome. *Blood* (2002) 100:1192–200. doi: 10.1182/blood-2001-11-0059

Conflict of Interest: The authors declare that the research was conducted in the absence of any commercial or financial relationships that could be construed as a potential conflict of interest.

frontiers in Immunology

ORIGINAL RESEARCH
published: 28 January 2021
doi: 10.3389/fimmu.2020.627496

Elevated Circulating IL-10 Producing Breg, but Not Regulatory B Cell Levels, Restrain Antibody-Mediated Rejection After Kidney Transplantation

Yongsheng Luo[1†], Feifei Luo[2,3†], Kuanxin Zhang[4†], Shilei Wang[1], Haojie Zhang[1], Xianlei Yang[1], Wenjun Shang[1], Junxiang Wang[1], Zhigang Wang[1], Xinlu Pang[1], Yonghua Feng[1], Lei Liu[1], Hongchang Xie[1], Guiwen Feng[1] and Jinfeng Li[1*]*

[1] Kidney Transplantation Unit, The First Affiliated Hospital of Zhengzhou University, Zhengzhou, China, [2] Biotherapy Research Center, Fudan University, Shanghai, China, [3] Department of Digestive Diseases, Huashan Hospital, Fudan University, Shanghai, China, [4] Department of Colorectal Surgery, The First Affiliated Hospital of Zhengzhou University, Zhengzhou, China

OPEN ACCESS

Edited by:
Hao Wang,
Tianjin Medical University General Hospital, China

Reviewed by:
Helong Dai,
Central South University, China
Cheng Yang,
Fudan University, China

***Correspondence:**
Jinfeng Li
jinfenglis512@126.com
Guiwen Feng
feng_guiwen123@163.com

†These authors have contributed equally to this work

Specialty section:
This article was submitted to Alloimmunity and Transplantation, a section of the journal Frontiers in Immunology

Received: 09 November 2020
Accepted: 07 December 2020
Published: 28 January 2021

Citation:
Luo Y, Luo F, Zhang K, Wang S, Zhang H, Yang X, Shang W, Wang J, Wang Z, Pang X, Feng Y, Liu L, Xie H, Feng G and Li J (2021) Elevated Circulating IL-10 Producing Breg, but Not Regulatory B Cell Levels, Restrain Antibody-Mediated Rejection After Kidney Transplantation. Front. Immunol. 11:627496. doi: 10.3389/fimmu.2020.627496

Background: Antibody-mediated rejection (AMR) occupies a major position for chronic rejection after kidney transplantation. Regulatory B cell (Breg) has been reported to have an inhibitory immune function, which contributes to the resistance for AMR.

Methods: A nested case–control study for nine healthy donors, 25 stable (ST) patients, and 18 AMR patients was performed to determine the type of Breg in maintaining immune tolerance and preventing AMR.

Results: Compared to the ST group, circulating interleukin (IL)-10^+ Bregs, but not Bregs, significantly decreased. The receiver operating characteristic (ROC) curve analysis revealed that rather than the circulating Bregs, decreased circulating IL-10^+ Breg levels were positively associated with AMR. However, kidney B cell and IL-10 infiltration was significantly increased in the AMR group with high expression of C-X-C motif chemokine 13 (CXCL13). In addition, circulating IL-10^+ Bregs, rather than Bregs, remained higher than those at pre-operation, during the 90-day post-operation in immune homeostasis.

Conclusion: The circulating IL-10^+ Breg levels are more appropriate measures for assessing the resistance of AMR after kidney transplantation.

Keywords: Breg phenotyping, kidney transplantation, antibody-mediated rejection, homeostasis, dynamic

INTRODUCTION

Kidney transplantation is the best choice for the end-stage treatment of chronic kidney disease. At present, antibody-mediated rejection (AMR), which is characterized by the presence of a donor-specific antibody (DSA) directed to human leukocyte antigen (HLA), has emerged as the leading cause of chronic damage to the kidney graft, which largely limits the long-term survival of the graft. (1, 2). However, existing schemes have failed to achieve promising results in the clinical

treatment of AMR (1, 3, 4). Thus, there is an urgent need to identify potential biomarkers and risk factors for AMR after kidney transplantation, which is critical for treatment and patient outcomes.

Accumulating evidence suggests that under inflammatory circumstances, B cells can differentiate into antibody-secreting plasmablasts and regulatory B cells (Bregs), which are a special B cell subset that secretes immunosuppressive cytokines, particularly interleukin (IL)-10. (1, 5–7). Thus, plasmablasts produce alloantibodies, resulting in AMR, while Bregs exhibit immunoregulatory functions and help induce immune homeostasis. Thus, Bregs have been reported to be closely associated with the resistance to AMR after kidney transplantation (1, 8, 9).

Although the distinct surface markers of Breg subsets have not yet been identified in humans (1), previous studies have reported four common subpopulations of Bregs: memory Bregs (mBregs) defined with the $CD19^+CD24^+CD27^+$ (10), transitional Bregs (tBregs) defined with $CD19^+CD24^+CD38^+$ (10, 11), IL-10-producing memory Bregs (IL-10^+ mBregs) defined with $CD19^+CD24^+CD27^+$IL-10^+ (12), and IL-10-producing transitional Bregs (IL-10^+ tBregs) defined with $CD19^+CD24^+$ $CD38^+$IL-10^+ (13). Laguna-Goya et al. reported that the reduction in tBregs and IL-10^+ tBregs is positively associated with acute rejection after kidney transplantation (14). However, Zhou et al. reported that mBregs, rather than tBregs, significantly decreased in five patients with acute rejection at post-liver transplantation (10). Furthermore, Shabir et al. reported that tBregs were not associated with kidney allograft rejection in three AMR patients (15). In light of these inconsistent results, there is a need to further clarify which Breg subpopulation plays a vital role in AMR patients after kidney transplantation.

In the present study, the proportions of four subpopulations of circulating Bregs were compared among the healthy, stable (ST), and AMR groups. Then, the biodistribution of B cell, IL-10, and chemokines in the kidney grafts of healthy, ST, and AMR patients were determined. Furthermore, the dynamics of the four subpopulations of circulating Bregs in ST patients for 90 days after surgery were investigated. These present results, together those reported by previous studies (1), suggest that circulating IL-10^+ mBregs and IL-10^+ tBregs are the leading Breg subpopulations that contribute to the resistance of AMR.

MATERIALS AND METHODS

Patients and Groups

All patients provided a signed informed consent prior to the study. The present study was approved by the Ethics Committee of the First Affiliated Hospital of Zhengzhou University (2018-KY-72). The clinical trial registration number is ChiCTR1900022501.

These patients were divided into three groups: (1) healthy control group (healthy, n = 9): healthy kidney donors within 18–55 years old (free of disease), consisting of the siblings and spouses of the recipients; (2) recipients with stable graft function group (ST, n = 25): patients within 18–55 years old, whose kidney function was stable (free of infection or rejection before and after kidney transplantation) during the follow-up period (≥6 months); (3) recipients with AMR group (AMR, n = 18): patients within 18–55 years old, who were diagnosed with AMR. The kidney grafts of recipients with ST and AMR were obtained from healthy kidney donors. The differential diagnosis between the ST and AMR groups was confirmed by two kidney pathologists, according to the Banff 2017 consensus (3, 16).

Peripheral Blood, Kidney Tissues, and Cell Samples

The peripheral blood samples from the healthy group were collected at pre-operation, and at 1, 7 and 14 days post-operation. Samples obtained from the ST group were collected at pre-operation, and at 1, 7, 14, 30, and 90 days post-operation. Samples obtained from the AMR group were collected when rejection occurred (before the anti-rejection therapy for AMR). Peripheral blood mononuclear cells (PBMCs) were isolated from 5 ml of blood by Ficoll-Paque gradient centrifugation and preserved with 10% dimethyl sulfoxide (Solarbio Inc., Beijing, China) in liquid nitrogen.

The core needle renal biopsy specimens obtained from the healthy group were collected before surgery for time-zero donor kidney biopsies. The core needle renal biopsy specimens obtained from the ST group were collected at 90 days post-operation after their kidney function stabilized due to the protocol biopsy. In light of the second puncture impairment of kidney function, all AMR patients refused the core needle renal biopsy after anti-rejection therapy for AMR. Thus, core needle renal biopsy specimens from the AMR group were only collected when rejection occurred (before the anti-rejection therapy for AMR). A total of three healthy donors, nine ST patients, and nine AMR patients provided a signed informed consent before the core needle renal biopsy. The remaining six healthy donors, 16 ST patients, and nine AMR patients refused the core needle renal biopsy due to fear of major bleeding in association with the biopsy. Single cells were isolated from the core needle renal biopsy specimens of three healthy donors, three ST patients, and three AMR patients, by combining mechanical dissociation with the enzymatic degradation of the extracellular matrix, which maintains the structural integrity of tissues (Multi Tissue Dissociation Kit 1; Miltenyi Biotec, Bergisch Gladbach, Germany). The kidney cells were preserved with 10% dimethyl sulfoxide (Solarbio Inc., Beijing, China) in liquid nitrogen, and the remaining core needle renal biopsy specimens were embedded in paraffin at 4°C.

Flow Cytometry

Cells stored in liquid nitrogen were quickly thawed in a water bath set at 37°C for 3 min. A total of 2–3 × 10^6 PBMCs were incubated with the Roswell Park Memorial Institute 1640 dilution-cell stimulation cocktail (500×), which comprised of the PMA (Phorbol 12-Myristate 13-Acetate), a calcium ionophore (Ionomycin), and protein transport inhibitors Brefeldin A and Monensin, (eBioscience, San Diego, CA), at 37°C with 5% CO_2 for 5 h. Dead cells were excluded by staining

with 7-Aminoactinomycin D (Thermo Fisher Scientific, Pittsburgh, PA, USA), and the surface markers of Bregs were stained with fluorochrome-labeled antibodies (Brilliant Violet 421™ anti-human CD19, phycoerythrin (PE)/Cy7 anti-human CD24, Alexa FluorR647 anti-human CD27, Alexa FluorR488 anti-human CD38, and Brilliant Violet 510™ anti-human CD45; the appropriate isotype controls: Brilliant Violet 421™ Mouse IgG1 κ Isotype Control, PE/Cy7 Mouse IgG2a κ Isotype Control, Alexa FluorR647 Mouse IgG1 κ Isotype Control, Alexa FluorR488 Mouse IgG1 κ Isotype Control, and Brilliant Violet 510™ Mouse IgG1 κ Isotype Control; Biolegend, San Diego, CA, USA) for 30 min at 4°C, with protection from light. For the intracellular staining, cells were stained with antibodies targeting the intracellular cytokines of Bregs (PE anti-human IL-10; the appropriate isotype controls: PE Rat IgG1 κ Isotype Control; Biolegend, San Diego, CA, USA) for 30 minutes at room temperature, with protection from light. The labeled cells were analyzed using the BD Biosciences Canto II instrument (BD Biosciences, USA). A total of 100,000 events were acquired in the lymphocyte gate. The data analysis was performed using FlowJo software (Tree Star, San Carlos, CA, USA).

Immunohistochemistry

Immunohistochemistry staining of CD19, IL-10, and C-X-C motif chemokine 13 (CXCL13) in kidney tissues was performed, respectively. Briefly, 4 μm sections obtained from formalin-fixed, paraffin-embedded kidney tissue samples were incubated with 1:500-diluted anti-CD19, 1:1000-diluted anti-CXCL13 (rabbit anti-human; Abcam, Cambridge, UK), and 1:500-diluted anti-IL-10 (rabbit anti-human; Absin, Shanghai, China) primary antibodies overnight at 4°C, followed by Horseradish Peroxidase-conjugated 1:20,000-diluted goat anti-rabbit secondary antibody (Abcam, Cambridge, UK) for 1 h at room temperature and then 3,3′-diaminobenzidine for another 10 min. DAPI appears in blue. Immunohistochemistry images were acquired with an Aperio ScanScope AT Turbo (Aperio, Vista, CA). Numbers of CD19, IL-10, and CXCL13 positivities were scored as follows: 0 positivity, score = zero; 1–5 positivities, score = one; 6–10 positivities, score = two; 11–20 positivities, score = three; >20 positivities, score = four.

Statistical Analysis

In the nested case–control study, receiver operating characteristic (ROC) curve analysis was performed by MedCalc v18.11.3. The remaining statistical analyses were performed using IBM SPSS 21.0. Normally distributed measurement data with a homogeneity of variance were expressed as mean ± standard deviation ($\bar{x}$ ± s) and analyzed by independent-sample t-test (between-group comparisons) or one-way analysis of variance (among-group comparisons). Measurement data that did not have a normal distribution or homogeneity of variance were expressed in median with interquartile range (IQR) and analyzed by Mann–Whitney U test (between-group comparisons) or the Kruskal–Wallis test (among-group comparisons). Count data were analyzed by χ^2 test, a corrected χ^2 test, or Fisher's exact test, as needed. One-way repeated measures analysis of variance was used at various time points. *P*-values <0.05 were considered statistically significant.

RESULTS

Baseline Characteristics of the Patients

A total of nine healthy donors, 25 ST patients, and 18 AMR patients were included in the present study. As shown in **Table 1**, the gender of the recipients, age, body mass index (BMI), initial nephropathy, HLA mismatch, CNIs, warm-ischemia time, and cold-ischemia time did not differ among groups, or between groups ($P > 0.05$, for all). However, the incidence of both anti-class I and anti-class II DSA-positivity in the AMR group was significantly higher, when compared to those in the ST group ($P < 0.001$ for anti-class I DSA, $P < 0.001$; $P = 0.001$ for anti-class II DSA). Furthermore, compared with ST patients, AMR patients had significantly higher scores in tubulitis (t), interstitial inflammation (i), and peritubular capillaritis (ptc) ($P = 0.012$ for t; $P < 0.001$ for i and ptc), according to the Banff classification (normal, score = 0; mild, score = 1; moderate, score = 2; severe, score = 3) (3, 16) (**Supplemental Tables 1** and **2**).

Antibody-Mediated Rejection Patients Exhibited Decreased Circulating Interleukin-10$^+$ Regulatory B Cell Levels

In order to determine which Breg subpopulation could contribute to the resistance of AMR, four subpopulations of

TABLE 1 | Characteristics of patients in the healthy, stable (ST) and antibody-mediated rejection (AMR) groups.

	Healthy	ST	AMR	P-value*
Total number (n)	9	25	18	–
Female/Male (n)	5/4	5/20	8/10	0.088
Age	42.11 ± 11.22	38.52 ± 9.17	33.44 ± 8.80	0.065
BMI (kg/m^2)	23.25 ± 2.84	20.95 ± 2.57	20.94 ± 2.51	0.063
Initial nephropathy (n)†	–	13/5/3/4	8/2/0/8	0.120
Glomerulonephritis	–	13	8	–
IgA nephropathy	–	5	2	–
Hypertensive nephropathy	–	3	0	–
Other	–	4	8	–
HLA mismatch (n)†	–	3 (3, 3)	3 (3, 3)	0.749
Warm ischemic time (min)†	–	5 (4, 6)	6 (5, 8)	0.082
Cold ischemic time (h)†	–	7 (6, 8)	8 (7, 9)	0.116
CNIs (n)†	–	17/8	11/7	0.640
Tacrolimus	–	17	11	–
Cyclosporine A	–	8	7	–

*ST, stable; AMR, antibody-mediated rejection; BMI, body mass index; HLA, human leukocyte antigen; CNIs, calcineurin inhibitors; Normally distributed measurement data with homogeneity of variance were expressed as the mean ± standard deviation and analyzed by one-way analysis of variance (among-group comparisons). Measurement data that did not have a normal distribution or homogeneity of variance were expressed as the median with interquartile range and analyzed by the Mann–Whitney U test (between-group comparisons). Count data were analyzed by the χ^2 test. † The comparison between the ST and AMR groups. *P-values <0.05 were considered statistically significant.*

circulating Bregs were analyzed, from the healthy group before surgery, from the ST group at 90 days post-operation, and from the AMR group before the anti-rejection therapy. The mBreg, tBreg, IL-10$^+$ mBreg, and IL-10$^+$ tBreg were distinguished by flow cytometry (**Figure 1A**).

As shown in **Figure 1B**, the percentage of B cells (CD19$^+$) in PBMCs were similar in the healthy, ST, and AMR groups (P = 0.095). The percentage of both mBregs and tBregs in B cells did not differ among groups (P = 0.949 for mBregs; P = 0.506 for tBregs) (**Figure 1C**). Additionally, it was found that compared with the

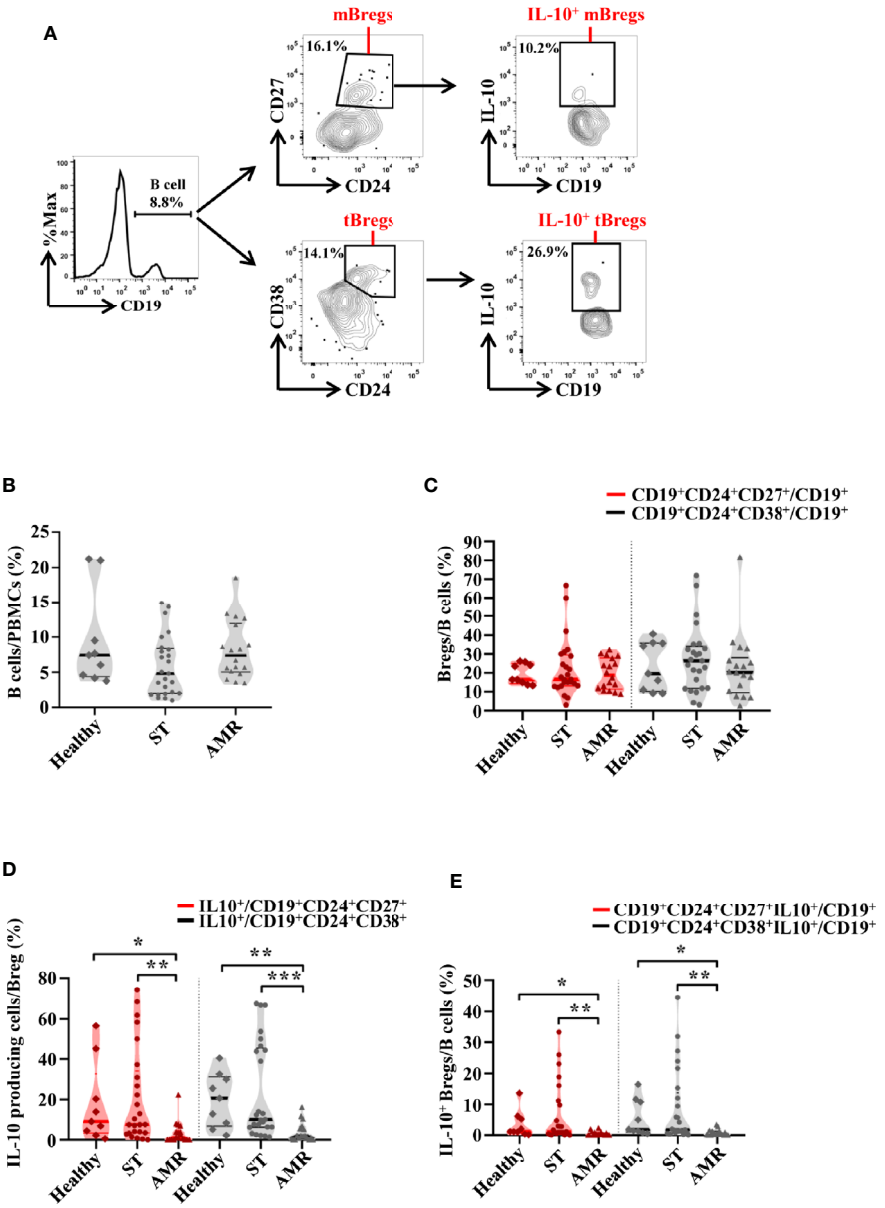

FIGURE 1 | The percentages of four subpopulations of circulating Bregs among the healthy, stable (ST) and antibody-mediated rejection (AMR) groups. Flow cytometry analysis of peripheral blood mononuclear cells (PBMCs) isolated from healthy donors (n = 9) at pre-operation, the ST group (n = 25) at day 90 post-operation, and the AMR group (n = 18) at day 1 before anti-rejection therapy. **(A)** Representative dot plots depict the gating strategy to determine B cell subsets in PBMC. CD19$^+$ B cells were identified based on high expression of CD19. Memory Bregs (mBregs) were identified from CD19$^+$ B cells based on the high expression of CD24 and positivity of CD27. IL-10-producing memory Bregs (IL-10$^+$ mBregs) were further gated based on the high expression of IL-10. Transitional Bregs (tBregs) were identified based on high expression of CD38 and CD24. IL-10-producing transitional Bregs (IL-10$^+$ tBregs) were further gated based on the high expression of IL-10. **(B–D)** The statistical summary for the percentages of CD19$^+$ B cells in PBMCs **(B)**, CD19$^+$CD24$^+$CD27$^+$ mBregs or CD19$^+$CD24$^+$CD38$^+$ tBregs in CD19$^+$ B cells **(C)**, CD19$^+$CD24$^+$CD27$^+$IL-10$^+$ or CD19$^+$CD24$^+$CD38$^+$IL-10$^+$ Bregs (IL-10$^+$ mBregs or IL-10$^+$ tBregs) in CD19$^+$ B cells **(D)**. Differences were evaluated by Kruskal–Wallis one-way analysis of variance (k samples) and *post-hoc* tests with all pairwise. *P < 0.05; **P < 0.01; ***P < 0.001.

AMR group, the percentages of the IL-10-producing cells in either mBregs or tBregs were significantly increased in the ST group [P = 0.001 for mBregs; P < 0.001 for tBregs] and the healthy group [P = 0.029 for mBregs; P = 0.004 for tBregs] (**Figure 1D**). In line with these results, it was found that the IL-10$^+$ mBreg or IL-10$^+$ tBreg ratios in B cells were significantly lower in the AMR group, when compared to the ST group (P = 0.002 for IL-10$^+$ mBregs; P = 0.001 for IL-10$^+$ tBregs) and healthy group (P = 0.017 for IL-10$^+$ mBregs; P = 0.013 for IL-10$^+$ tBregs) (**Figure 1E**).

Decreased Circulating IL-10$^+$ Regulatory B Cell Levels Were Positively Associated With Antibody-Mediated Rejection

The diagnostic capacity of four subpopulations of circulating Bregs was compared between the ST (at day 90 post-operation) and AMR (before the anti-rejection therapy) groups by ROC curve analysis (**Figure 2A**). The diagnostic indicators are shown in **Table 2**. According to the criteria of Swets (18), although the mBreg or tBreg ratios in B cells had a low diagnostic accuracy,

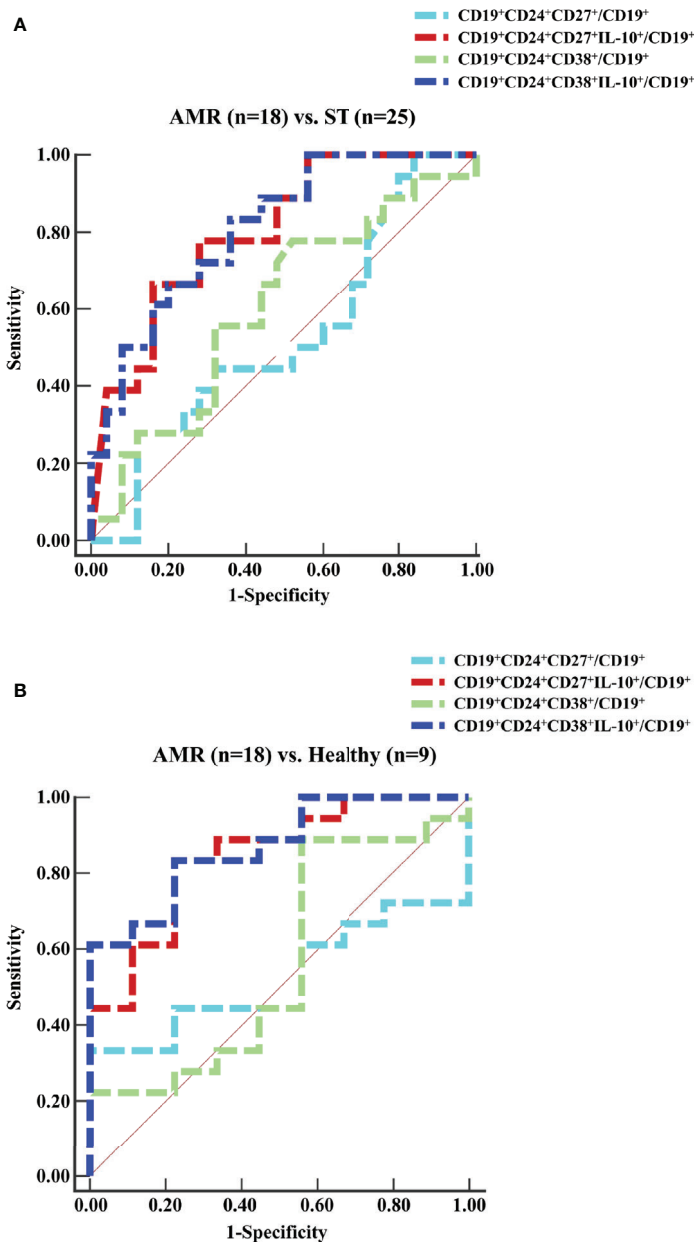

FIGURE 2 | ROC curves for the ratios of four subpopulations of circulating Bregs. Peripheral blood mononuclear cells (PBMCs) were isolated from the ST group (n = 25) at day 90 post-operation, the healthy group (n = 9) before surgery, and the AMR group (n = 18) at day 1 before anti-rejection therapy. **(A, B)** The percentages of four subpopulations of circulating Bregs in B cells were analyzed by the ROC assay.

TABLE 2 | Comparison of different Breg subpopulations as a distinction between stable (ST) (n = 25) and antibody-mediated rejection (AMR) (n = 18) patients.

Factor	AUC (95% CI)	Threshold	Sensitivity (95% CI)	Specificity (95% CI)	PPV (95% CI)	NPV (95% CI)	LR+ (95% CI)	LR– (95% CI)	DOR	*P*-values*
$CD19^+CD24^+CD27^+$ /$CD19^+$ (%)	52.8 (37.0–68.2)	11.8	27.8 (9.7–53.5)	88.0 (68.8–97.5)	62.5 (31.3–85.9)	62.9 (55.1–70.0)	2.3 (0.6–8.5)	0.8 (0.6–1.1)	2.8	0.004
$CD19^+CD24^+CD27^+IL\text{-}10^+$ /$CD19^+$ (%)	80.3 (65.4–90.9)	0.5	66.7 (41.0–86.7)	84.0 (63.9–95.5)	75.0 (53.6–88.6)	77.8 (64.0–87.3)	4.2 (1.6–10.8)	0.4 (0.2–0.8)	10.4	
$CD19^+CD24^+CD38^+$ /$CD19^+$ (%)	60.6 (44.5–75.1)	20.5	55.6 (30.8–78.5)	68.0 (46.5–85.1)	55.6 (38.2–71.7)	68 (54.3–79.2)	1.7 (0.9–3.5)	0.7 (0.4–1.2)	2.7	0.008
$CD19^+CD24^+CD38^+IL\text{-}10^+$ /$CD19^+$ (%)	81.1 (66.3–91.4)	0.2	50.0 (26.0–74.0)	92.0 (74.0–99.0)	81.8 (52.4–94.8)	71.9 (61.4–80.4)	6.3 (1.5–25.5)	0.5 (0.3–0.9)	11.6	

*PBMCs, peripheral blood mononuclear cells; AUC, area under curve; CI, confidence interval; PPV, positive predictive value; NPV, negative predictive value; LR+, positive likelihood ratio; LR–, negative likelihood ratio; DOR, diagnostic odds ratio; *P-values: DeLong et al. (17) for comparison of different receiver operating characteristic (ROC) curves. Obtained from ROC curves in ST vs. AMR patient samples.*

the $IL\text{-}10^+$ mBreg or $IL\text{-}10^+$ tBreg ratios in B cells exhibited a good sensitivity and area under the ROC curve (AUC) in diagnosing patients with AMR. Meanwhile, compared to the mBreg or tBreg ratios, the $IL\text{-}10^+$ mBreg or $IL\text{-}10^+$ tBreg ratios in B cells exhibited a statistically significant superior ability to discriminate between ST and AMR patients ($P < 0.05$ for all). Furthermore, similar results appeared between the healthy (before surgery) and AMR (before the anti-rejection therapy) groups (**Figure 2B** and **Table 3**).

Circulating $IL\text{-}10^+$ Bregs Were Recruited to the Graft in Antibody-Mediated Rejection Patients

The biodistribution of CD19, IL-10, and CXCL13 in grafted kidney tissues was analyzed through the immunohistochemistry staining in six ST and six AMR biopsy samples (**Figure 3A**). The mean count scores in B cells were significantly higher in the AMR group than in the ST group ($P = 0.020$). Then, it was found that the mean count scores in IL-10 positivity were significantly higher in the AMR group than in the ST group ($P = 0.008$). Additionally, compared with ST patients, AMR patients had significantly higher scores in CXCL13, which is a B cell specific chemokine (19) ($P = 0.007$) (**Figure 3B**).

Kidney cells were further collected from three healthy donors, three ST patients, and three AMR patients, respectively. After gating on $CD45^+$ leukocytes (20, 21), the $IL\text{-}10^+$ mBregs and $IL\text{-}10^+$ tBregs were analyzed (**Figure 3C**). The percentages of $IL\text{-}10^+$ mBregs or $IL\text{-}10^+$ tBregs in $CD45^+$ leukocytes were significantly higher in the AMR group than in the ST group ($P = 0.044$ for $IL\text{-}10^+$ mBregs; $P = 0.013$ for $IL\text{-}10^+$ tBregs) and healthy group ($P = 0.035$ for $IL\text{-}10^+$ mBregs; $P = 0.041$ for $IL\text{-}10^+$ tBregs) (**Figure 3D**).

The Circulating Interleukin-10^+ Regulatory B Cell Levels Remained High During Transplantation Homeostasis

The dynamic variation of four subpopulations of circulating Bregs in 25 ST patients was analyzed at 0, 1, 7, 14, 30, and 90 days post-operation. These four subpopulations of circulating Bregs were distinguished by flow cytometry (**Figure 1A**). Samples obtained from nine healthy donors were only collected at 0, 1, 7, and 14 days post-operation, respectively, due to shorter hospital stay. The mean percentage ± standard deviation and median with IQR at each time point in the ST group and healthy group are shown in **Supplemental Tables 3** and **4**.

In the healthy group, except that the mBreg ratios in B cells were lower at day one post-operation than those at pre-operation ($P < 0.05$), the four subpopulations of circulating Bregs had no significant differences between pre-operation and post-operation ($P > 0.05$) (**Figure 4A**). However, in the ST group, except that the mBreg ratios in B cells were non-significantly high at day one post-operation, compared to those at pre-operation ($P > 0.05$), the four subpopulations of circulating Bregs remained higher

TABLE 3 | Comparison of different Breg subpopulations as a distinction between healthy (n = 9) and antibody-mediated rejection (AMR) (n = 18) patients.

Factor	AUC (95% CI)	Threshold	Sensitivity (95% CI)	Specificity (95% CI)	PPV (95% CI)	NPV (95% CI)	LR+ (95% CI)	LR– (95% CI)	DOR	*P*-values*
$CD19^+CD24^+CD27^+$ /$CD19^+$ (%)	52.5 (32.5–71.9)	13.3	33.3 (13.3–59.0)	88.9 (51.8–99.7)	85.7 (45.8–97.7)	40.0 (30.9–49.9)	3.0 (0.9–21.3)	0.8 (0.5–1.1)	4.0	0.029
$CD19^+CD24^+CD27^+IL\text{-}10^+$ /$CD19^+$ (%)	84.6 (65.5–95.5)	1.0	83.3 (58.6–96.4)	77.8 (40.0–97.2)	88.2 (68.5–96.3)	70.0 (44.0–87.4)	3.8 (1.1–13.0)	0.2 (0.1–0.6)	17.9	
$CD19^+CD24^+CD38^+$ /$CD19^+$ (%)	56.8 (36.5–75.6)	33.5	88.9 (65.3–98.6)	44.4 (13.7–78.8)	76.2 (63.6–85.4)	66.7 (30.9–89.9)	1.6 (0.9–2.9)	0.3 (0.1–1.1)	6.4	0.014
$CD19^+CD24^+CD38^+IL\text{-}10^+$ /$CD19^+$ (%)	87.0 (68.5–96.8)	1.3	83.3 (58.6–96.4)	77.8 (40.0–97.2)	88.2 (68.5–96.3)	70.0 (44.0–87.4)	3.8 (1.1–13.0)	0.2 (0.1–0.6)	17.9	

*PBMCs, peripheral blood mononuclear cells; AUC, area under curve; CI, confidence interval; PPV, positive predictive value; NPV, negative predictive value; LR+, positive likelihood ratio; LR–, negative likelihood ratio; DOR, diagnostic odds ratio; *P-values: DeLong et al. (17) for comparison of different receiver operating characteristic (ROC) curves. Obtained from ROC curves in ST vs. AMR patient samples.*

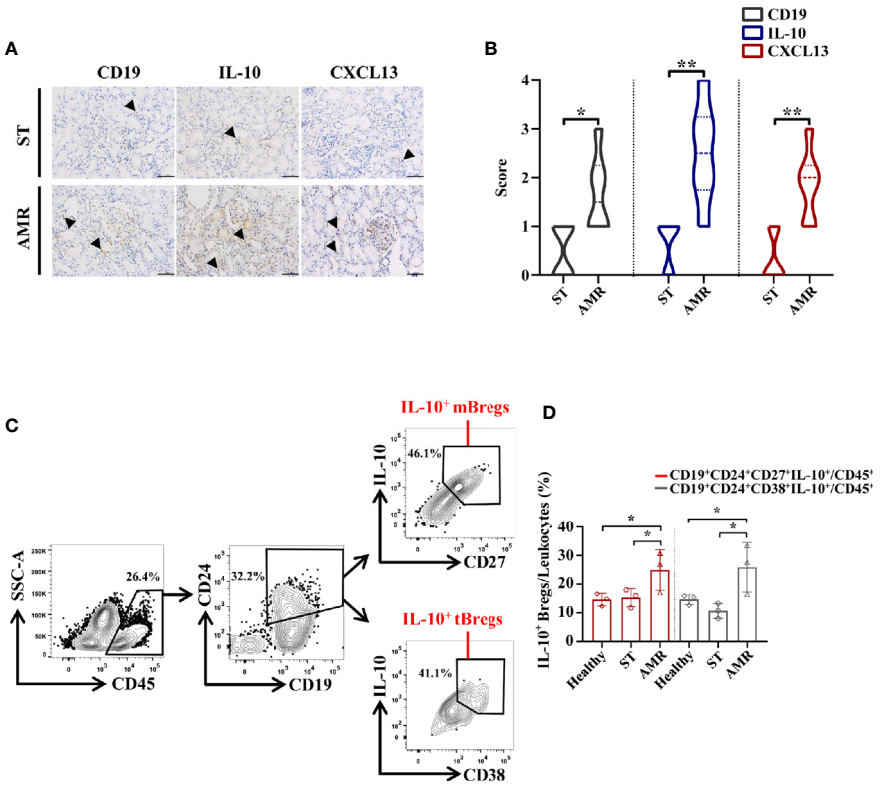

FIGURE 3 | Analysis of IL-10$^+$ Bregs in kidney tissue and cells from healthy, stable (ST) and antibody-mediated rejection (AMR) groups. **(A)** Immunohistochemistry was performed on kidney tissues from six ST patients and six AMR patients to detect CD19, IL-10, and CXCL13 (brown). DAPI staining (blue) was performed to visualize the nuclei. Scale bars, 100 μm. **(B)** The statistical summary for the scores according to the counts of CD19, IL-10, and CXCL13. **(C)** Kidney cells from three healthy donors, three ST patients, and three AMR patients were measured by flow cytometry. Representative dot plots depict the gating strategy to determine B cell subsets in kidney. CD45$^+$ leukocytes were identified based on high expression of CD45. CD19$^+$CD24$^+$ cells were gated based on the high expression of CD24 and CD19. IL-10-producing memory Bregs (IL-10$^+$ mBregs) were further gated based on the high expression of IL-10 and CD27 while IL-10-producing transitional Bregs (IL-10$^+$ tBregs) were identified based on high expression of IL-10 and CD28. **(D)** The statistical summary for the percentages of CD19$^+$CD24$^+$CD27$^+$IL-10$^+$ or CD19$^+$CD24$^+$CD38$^+$IL-10$^+$ Bregs (IL-10$^+$ mBregs or IL-10$^+$ tBregs) in CD45$^+$ leukocytes. The score differences were evaluated by Mann–Whitney U-test. The percentage differences were evaluated by one-way analysis of variance, and multiple comparisons were made with the least significant difference test. *$P < 0.05$; **$P < 0.01$.

than those at pre-operation during the three months following transplantation ($P < 0.05$) (**Figure 4B**). Additionally, it was found that the mBreg or tBreg ratios in B cells had no significant differences at each time point between the healthy and ST groups ($P > 0.05$, for all). However, the percentage for both IL-10$^+$ mBregs and IL-10$^+$ tBregs in B cells were significantly higher at days 1, 7, and 14, post-operation, in the ST group, when compared to those in the healthy group ($P < 0.05$, for all) (**Figure 4C**). In line with these results, it was inferred that compared with the mBreg and tBreg ratios, the IL-10$^+$ mBreg and IL-10$^+$ tBreg ratios in B cells were more pivotal during the transplantation homeostasis.

DISCUSSION

Several studies have reported that Bregs can attenuate inflammation and contribute to the resistance of AMR (22–26). However, there is presently no comprehensive clinical research on the effect of the four subpopulations of Bregs in AMR patients after kidney transplantation. Thus, in the first step, the relationship between these cells and AMR occurrence was verified. The present flow cytometric analysis revealed that rather than the circulating mBregs and tBregs, the circulating IL-10$^+$ mBregs and IL-10$^+$ tBregs decreased in AMR patients, indicating that circulating IL-10$^+$ Bregs are closely associated with AMR occurrence. The ROC curve analysis further demonstrated that compared with the circulating mBreg and tBreg levels, decreased circulating IL-10$^+$ mBreg and IL-10$^+$ tBreg levels were more suitable to use as a diagnostic tool for AMR. These results imply that IL-10$^+$ mBregs and IL-10$^+$ tBregs may play a vital role in AMR patients at post-kidney transplantation.

Subsequently, the immunohistochemistry assay revealed that the kidney B cell and IL-10 infiltration increased in AMR patients, when compared with ST patients. It was inferred that the increased B cells exhibit immunoregulatory functions in kidney grafts of AMR patients. Then, the flow cytometric analysis of kidney cells demonstrated that the kidney IL-10$^+$ Breg ratios in leukocytes increased in AMR patients. In light of

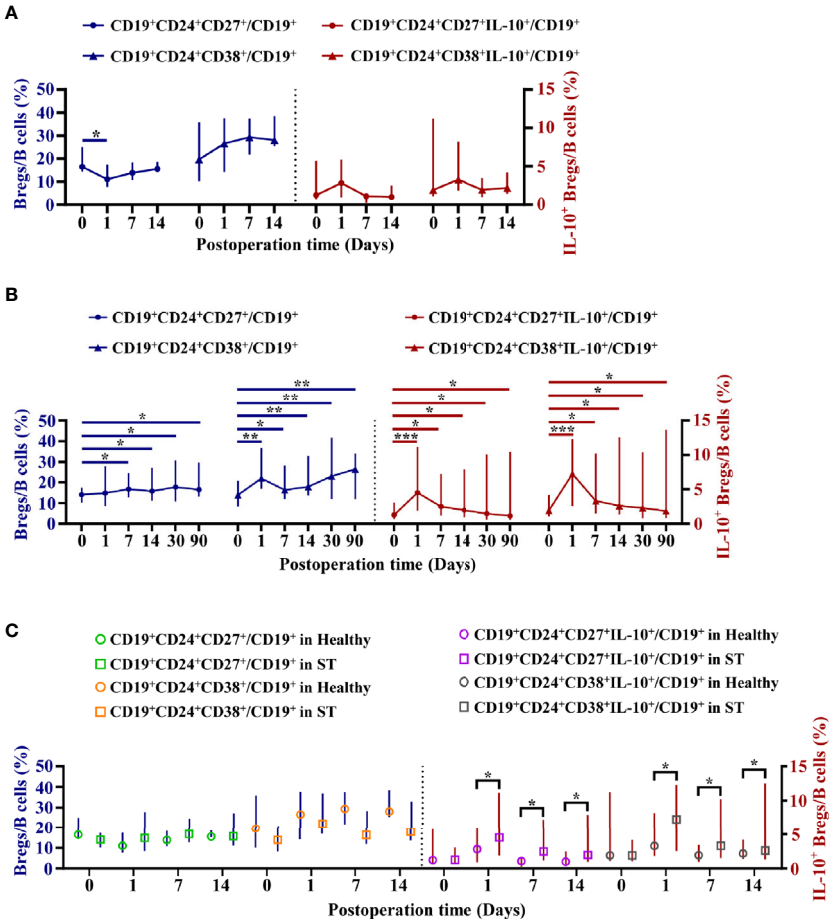

FIGURE 4 | Dynamic variation of four subpopulations of circulating Bregs in healthy donors or stable (ST) patients. Flow cytometry analysis of peripheral blood mononuclear cells (PBMCs) isolated from nine healthy donors at 0, 1, 7, and 14 days post-operation and 25 ST patients at 0, 1, 7, 14, 30, and 90 days post-operation. **(A, B)** Dynamic variation of four subpopulations of circulating Breg ratios in Bcells in healthy donors **(A)** and ST patients **(B)**. **(C)** The differences of four subpopulations of circulating Breg ratios in Bcells between the healthy group and the ST group at the same time point. Comparisons between the healthy group and the ST group at the same time point were analyzed using independent-samples T test. Comparisons at different time points in healthy donors or ST patients were analyzed using one-way repeated measures analysis of variance, and multiple comparisons were made with the least significant difference test. $^{*}P < 0.05$; $^{**}P < 0.01$; $^{***}P < 0.001$.

the contradictory results between peripheral blood and kidney grafts, a logical explanation was the recruitment of circulating IL-10^{+} Bregs to the graft. At present, the putative mechanisms leading to IL-10^{+} Breg infiltration in kidney tissues was largely attributable to chemokines, which has been generally considered to be the main mediators in leukocyte trafficking under inflammatory conditions (19, 27, 28). Indeed, it was also found that compared with ST patients, the expression of CXCL13 in kidney grafts was higher in AMR patients. These results were consistent with a previous report, in which CXCL13 and its receptor established distinct B cell rich compartments at the site of kidney tissue inflammation (19). Additionally, the present data revealed that compared with ST patients, both the IL-10 secreted by Bregs and the DSA sourced from plasmablasts increased in AMR patients with greater severity of interstitial and vascular rejection in kidney grafts. This was also in accordance with the report, in which there was a high prevalence of B cells in the interstitial rejection processes (19). Thus, it could be inferred that during AMR occurrence, the CXCL13 mediates the circulating IL-10^{+} Breg influx into kidney grafts, which leads to a large number of IL-10 production, subsequently contributing to the resistance of antibody-mediated interstitial and vascular rejection. On the contrary, since immune homeostasis has already been established, ST patients had less IL-10^{+} Breg influx into the kidney grafts. However, due to clinical technical problems that involve the tracing of IL-10^{+} Breg influx into kidney grafts, the inference needs to be further proven through experimental animal studies.

From another perspective, in order to further determine whether circulating Bregs also help in the maintenance of immune homeostasis, the dynamic variation of circulating Bregs in ST patients was analyzed. The present data revealed that only circulating IL10^{+} mBregs and IL10^{+} tBregs in the ST group at post-operation remained at a higher level, when

compared to those in the healthy group, which had a higher level, when compared to those at pre-operation. Therefore, it was inferred that the high level of $IL10^+$ Bregs may be a reserve force of anti-rejection, which can be mobilized to attenuate inflammation and resist rejection during AMR occurrence. Additionally, existing research has shown that the transfer of IL-10^+ Bregs is obviously effective during AMR initiation (29, 30). Importantly, these findings provide an innovative perspective that the promotion of the circulating IL-10^+ Bregs, such as the autologous transfer of IL-10^+ Bregs during the early phase after kidney transplantation, may restrain the incidence of AMR.

One of the strengths of the present study is that this is a comprehensive kidney transplant cohort to prospectively measure four subpopulations of circulating Bregs to identify potential biomarkers and risk factors for AMR. Further studies using the circulating IL-10^+ Bregs found in AMR, combined with other immunologic features, such as T cell phenotyping, observed in this state, will help to identify specific and sensitive parameters to evaluate the progression to AMR. The results of the present study are biologically plausible and extend the present literature, which supports efforts to further clarify IL-10^+ Breg role in kidney transplantation, either as biomarkers of AMR risk, or in potential cell-based therapies. Certainly, the present study was limited by its small sample size, which impaired the ability to draw a definitive conclusion on the role of IL-10^+ Bregs in AMR after kidney transplantation. Additionally, PBMCs from the AMR group should also be collected after the anti-rejection therapy.

DATA AVAILABILITY STATEMENT

The raw data supporting the conclusions of this article will be made available by the authors, without undue reservation.

ETHICS STATEMENT

The studies involving human participants were reviewed and approved by the Ethics Committee of the First Affiliated Hospital of Zhengzhou University (2018-KY-72). The clinical trial registration number is ChiCTR1900022501. The patients/participants provided their written informed consent to participate in this study.

AUTHOR CONTRIBUTIONS

YL, FL, and KZ performed the experiments, analyzed the data, and wrote the manuscript. SW and HZ participated in the study design, material support, and coordination. XY, WS, JW, ZW, XP, YF, LL, and HX carried out parts of the experiments. JL and GF conceived the study and performed critical revisions of the manuscript. All authors contributed to the article and approved the submitted version.

FUNDING

This work was supported by the National Natural Science Foundation of China (No. 82070771) and Foundation of Henan Provincial Health Bureau (SBGJ2018022).

ACKNOWLEDGMENTS

The authors would like to thank the invaluable assistance of Zhiguang Ping (Zhengzhou University) in performing the statistical analyses and of Yuqiong Liu (The First Affiliated Hospital of Zhengzhou University) in interpreting the graft histology.

SUPPLEMENTARY MATERIAL

The Supplementary Material for this article can be found online at: https://www.frontiersin.org/articles/10.3389/fimmu.2020.627496/full#supplementary-material

REFERENCES

1. Li J, Luo Y, Wang X, Feng G. Regulatory B cells and advances in transplantation. *J Leukoc Biol* (2019) 105(4):657–68. doi: 10.1002/JLB.5RU0518-199R
2. Sellares J, de Freitas DG, Mengel M, Reeve J, Einecke G, Sis B, et al. Understanding the causes of kidney transplant failure: the dominant role of antibody-mediated rejection and nonadherence. *Am J Transplant* (2012) 12 (2):388–99. doi: 10.1111/j.1600-6143.2011.03840.x
3. Haas M, Loupy A, Lefaucheur C, Roufosse C, Glotz D, Seron D, et al. The Banff 2017 Kidney Meeting Report: Revised diagnostic criteria for chronic active T cell-mediated rejection, antibody-mediated rejection, and prospects for integrative endpoints for next-generation clinical trials. *Am J Transplant* (2018) 18(2):293–307. doi: 10.1111/ajt.14625
4. Lachmann N, Duerr M, Schonemann C, Pruss A, Budde K, Waiser J, et al. Treatment of Antibody-Mediated Renal Allograft Rejection: Improving Step by Step. *J Immunol Res* (2017) 2017:6872046. doi: 10.1155/2017/6872046
5. Cascalho MII, Chen BJ, Kain M, Platt JL. The paradoxical functions of B cells and antibodies in transplantation. *J Immunol* (2013) 190(3):875–9. doi: 10.4049/jimmunol.1100120
6. Dominguez-Pantoja M, Lopez-Herrera G, Romero-Ramirez H, Santos-Argumedo L, Chavez-Rueda AK, Hernandez-Cueto A, et al. CD38 protein deficiency induces autoimmune characteristics and its activation enhances IL-10 production by regulatory B cells. *Scand J Immunol* (2018) 87(6):e12664. doi: 10.1111/sji.12664
7. Ran Z, Yue-Bei L, Qiu-Ming Z, Huan Y. Regulatory B Cells and Its Role in Central Nervous System Inflammatory Demyelinating Diseases. *Front Immunol* (2020) 11:1884. doi: 10.3389/fimmu.2020.01884
8. Chesneau M, Pallier A, Braza F, Lacombe G, Le Gallou S, Baron D, et al. Unique B cell differentiation profile in tolerant kidney transplant patients. *Am J Transplant* (2014) 14(1):144–55. doi: 10.1111/ajt.12508
9. Salehi S, Shahi A, Afzali S, Keshtkar AA, Farashi BS, Soleymanian T, et al. Transitional immature regulatory B cells and regulatory cytokines can discriminate chronic antibody-mediated rejection from stable graft function. *Int Immunopharmacol* (2020) 86:106750. doi: 10.1016/j.intimp.2020.106750
10. Zhou H, Zhan F, Zhang H, Gu J, Mu X, Gao J, et al. The proportion of CD19 (+)CD24(hi)CD27(+) regulatory B cells predicts the occurrence of acute allograft rejection in liver transplantation. *Ann Transl Med* (2010) 7 (18):465. doi: 10.21037/atm.2019.08.05

11. Silva HM, Takenaka MC, Moraes-Vieira PM, Monteiro SM, Hernandez MO, Chaara W, et al. Preserving the B-cell compartment favors operational tolerance in human renal transplantation. *Mol Med* (2012) 18:733–43. doi: 10.2119/molmed.2011.00281
12. Stozek K, Grubczak K, Marolda V, Eljaszewicz A, Moniuszko M, Bossowski A. Lower proportion of CD19(+)IL-10(+) and CD19(+)CD24(+)CD27(+) but not CD1d(+)CD5(+)CD19(+)CD24(+)CD27(+) IL-10(+) B cells in children with autoimmune thyroid diseases. *Autoimmunity* (2020) 53(1):46–55. doi: 10.1080/08916934.2019.1697690
13. Song J, Xiao L, Du G, Gao Y, Chen W, Yang S, et al. The role of regulatory B cells (Bregs) in the Tregs-amplifying effect of Sirolimus. *Int Immunopharmacol* (2016) 38:90–6. doi: 10.1016/j.intimp.2016.05.014
14. Laguna-Goya R, Utrero-Rico A, Cano-Romero FL, Gomez-Massa E, Gonzalez E, Andres A, et al. Imbalance favoring follicular helper T cells over IL10(+) regulatory B cells is detrimental for the kidney allograft. *Kidney Int* (2020) 98 (3):732–43. doi: 10.1016/j.kint.2020.02.039
15. Shabir S, Girdlestone J, Briggs D, Kaul B, Smith H, Daga S, et al. Transitional B lymphocytes are associated with protection from kidney allograft rejection: a prospective study. *Am J Transplant* (2015) 15(5):1384–91. doi: 10.1111/ajt.13122
16. Haas M, Sis B, Racusen LC, Solez K, Glotz D, Colvin RB, et al. Banff 2013 meeting report: inclusion of c4d-negative antibody-mediated rejection and antibody-associated arterial lesions. *Am J Transplant* (2014) 14(2):272–83. doi: 10.1111/ajt.12590
17. DeLong DM, Clarke-Pearson DL. Comparing the areas under two or more correlated receiver operating characteristic curves: a nonparametric approach. *Biometrics* (1988) 44(3):837–45.
18. Swets JA. Measuring the accuracy of diagnostic systems. *Science* (1988) 240 (4857):1285–93. doi: 10.1126/science.3287615
19. Steinmetz OM, Panzer U, Kneissler U, Harendza S, Lipp M, Helmchen U, et al. BCA-1/CXCL13 expression is associated with CXCR5-positive B-cell cluster formation in acute renal transplant rejection. *Kidney Int* (2005) 67 (4):1616–21. doi: 10.1111/j.1523-1755.2005.00244.x
20. Itani HA, McMaster WJ, Saleh MA, Nazarewicz RR, Mikolajczyk TP, Kaszuba AM, et al. Activation of Human T Cells in Hypertension: Studies of Humanized Mice and Hypertensive Humans. *Hypertension* (2016) 68 (1):123–32. doi: 10.1161/HYPERTENSIONAHA.116.07237
21. Rheinlander A, Schraven B, Bommhardt U. CD45 in human physiology and clinical medicine. *Immunol Lett* (2018) 196:22–32. doi: 10.1016/j.imlet.2018.01.009
22. Nouel A, Segalen I, Jamin C, Doucet L, Caillard S, Renaudineau Y, et al. B cells display an abnormal distribution and an impaired suppressive function in patients with chronic antibody-mediated rejection. *Kidney Int* (2014) 85 (3):590–9. doi: 10.1038/ki.2013.457
23. Newell KA, Asare A, Kirk AD, Gisler TD, Bourcier K, Suthanthiran M, et al. Identification of a B cell signature associated with renal transplant tolerance in humans. *J Clin Invest* (2010) 120(6):1836–47. doi: 10.1172/JCI39933
24. Yoshizaki A, Miyagaki T, DiLillo DJ, Matsushita T, Horikawa M, Kountikov E II, et al. Regulatory B cells control T-cell autoimmunity through IL-21-dependent cognate interactions. *Nature* (2012) 491(7423):264–8. doi: 10.1038/nature11501
25. Peng B, Ming Y, Yang C. Regulatory B cells: the cutting edge of immune tolerance in kidney transplantation. *Cell Death Dis* (2018) 9(2):109. doi: 10.1038/s41419-017-0152-y
26. Chong AS, Khiew SH. Transplantation tolerance: don't forget about the B cells. *Clin Exp Immunol* (2017) 189(2):171–80. doi: 10.1111/cei.12927
27. Moser B, Wolf M, Walz A, Loetscher P. Chemokines: multiple levels of leukocyte migration control. *Trends Immunol* (2004) 25(2):75–84. doi: 10.1016/j.it.2003.12.005
28. Steinmetz OM, Stahl RA, Panzer U. Chemokines and B cells in renal inflammation and allograft rejection. *Front Biosci (Schol Ed)* (2009) 1:13–22. doi: 10.2741/s2
29. Matsushita T, Yanaba K, Bouaziz JD, Fujimoto M, Tedder TF. Regulatory B cells inhibit EAE initiation in mice while other B cells promote disease progression. *J Clin Invest* (2008) 118(10):3420–30. doi: 10.1172/JCI36030
30. Hamaguchi Y, Xiu Y, Komura K, Nimmerjahn F, Tedder TF. Antibody isotype-specific engagement of Fcgamma receptors regulates B lymphocyte depletion during CD20 immunotherapy. *J Exp Med* (2006) 203(3):743–53. doi: 10.1084/jem.20052283

Conflict of Interest: The authors declare that the research was conducted in the absence of any commercial or financial relationships that could be construed as a potential conflict of interest.

The reviewer CY declared a shared affiliation, though no other collaboration, with one of the authors FL to the handling editor.

frontiers in Immunology

ORIGINAL RESEARCH
published: 17 February 2021
doi: 10.3389/fimmu.2020.626295

Prevention of Chronic Rejection of Marginal Kidney Graft by Using a Hydrogen Gas-Containing Preservation Solution and Adequate Immunosuppression in a Miniature Pig Model

Kotaro Nishi[1†], *Satomi Iwai*[1†], *Kazuki Tajima*[2,3], *Shozo Okano*[1], *Motoaki Sano*[4] *and Eiji Kobayashi*[5*]

[1] Laboratory of Small Animal Surgery 2, School of Veterinary Medicine, Kitasato University, Towada, Japan, [2] Laboratory of Small Animal Internal Medicine 2, School of Veterinary Medicine, Kitasato University, Towada, Japan, [3] Department of Surgery, Keio University School of Medicine, Tokyo, Japan, [4] Department of Cardiology, Keio University School of Medicine, Tokyo, Japan, [5] Department of Organ Fabrication, Keio University School of Medicine, Tokyo, Japan

OPEN ACCESS

Edited by:
Hao Wang,
Tianjin Medical University General Hospital, China

Reviewed by:
Alexandra R. Lucas,
Arizona State University, United States
Zheng Jenny Zhang,
Northwestern University, United States

***Correspondence:**
Eiji Kobayashi
organfabri@a2.keio.jp

[†]These authors have contributed equally to this work and share first authorship

Specialty section:
This article was submitted to Alloimmunity and Transplantation, a section of the journal Frontiers in Immunology

Received: 05 November 2020
Accepted: 29 December 2020
Published: 17 February 2021

Citation:
Nishi K, Iwai S, Tajima K, Okano S, Sano M and Kobayashi E (2021) Prevention of Chronic Rejection of Marginal Kidney Graft by Using a Hydrogen Gas-Containing Preservation Solution and Adequate Immunosuppression in a Miniature Pig Model. Front. Immunol. 11:626295. doi: 10.3389/fimmu.2020.626295

In clinical kidney transplantation, the marginal kidney donors are known to develop chronic allograft rejection more frequently than living kidney donors. In our previous study, we have reported that the hydrogen gas-containing organ preservation solution prevented the development of acute injuries in the kidney of the donor after cardiac death by using preclinical miniature pig model. In the present study, we verified the impact of hydrogen gas treatment in transplantation with the optimal immunosuppressive protocol based on human clinical setting by using the miniature pig model. Marginal kidney processed by hydrogen gas-containing preservation solution has been engrafted for long-term (longer than 100 days). A few cases showed chronic rejection reaction; however, most were found to be free of chronic rejection such as graft tissue fibrosis or renal vasculitis. We concluded that marginal kidney graft from donor after cardiac death is an acceptable model for chronic rejection and that if the transplantation is carried out using a strict immunosuppressive protocol, chronic rejection may be alleviated even with the marginal kidney.

Keywords: kidney transplantation, hydrogen-containing organ preservation solution, chronic allograft nephropathy, chronic rejection, marginal donor, mature minipig model, multi-immunosuppressant

INTRODUCTION

The number of patients with end-stage chronic kidney disease is high worldwide; this is a crucial issue because of the substantial cost of medical treatment (1). A considerable number of patients with end-stage chronic kidney disease are awaiting kidney transplantation because of a chronic shortage of living donors. As a result, dialysis is required for these patients. Although the survival of grafts in living kidney transplantation has been greatly improved by the emergence of effective

calcineurin inhibitors and antimetabolites (2, 3), it is critical to secure organs from a wide range of donors to solve the problem of living donor shortage. Moreover, effective utilization of marginal organs from donors after cardiac death (DCD) is required.

Marginal kidneys from DCD carry a high risk of short-term or long-term graft loss, depending on the donor's individual circumstances (including age, sex, blood pressure, and medical history) (4). In particular, ischemia-reperfusion injury (IRI) due to prolongation of warm ischemic time in the transplanted kidney causes strong expression of cytokines and oxidants such as IL-1, IL-6, and TNF-α, resulting in primary nonfunction and delayed graft function (4–7). In addition, T cell- and antibody-mediated rejection of kidney tissues is factors that exacerbate acute rejection (8, 9). The presence of acute rejection may trigger and lead to chronic allograft rejection. Thus, IRI increases the risk of developing a chronic allograft rejection over the long-term post-transplantation period, and outcomes have not improved despite appropriate immunosuppressant therapy after surgery (3, 10). It is known not only in humans but also in animal models that ischemic kidney transplantation from DCD is less likely to survive long-term and undergo chronic rejection than transplantation from living donors (11, 12). It has been reported that chronic allograft rejection involves immunological factors such as HLA histocompatibility and acute rejection and non-immunological factors such as nephrotoxicity by calcineurin inhibitor and ischemia-reperfusion (13, 14). However, only about 60% of chronic graft damage can be explained by these risk factors (15). To date, several studies have been conducted on mechanical perfusion and the inclusion of oxygen and carbon monoxide in organ preservation fluids to reduce acute and chronic damage, some of which are used clinically (16–18). However, despite the benefits, chronic allograft nephropathy remains a highlight. Therefore, it is thought that the mechanism of chronic allograft rejection involves a combination of several of these factors.

Currently, there have been several studies that attempted to alleviate acute and chronic allograft rejection by improving IRI during transplantation at an early stage, using animal models such as rodents, rabbits, dogs, and pigs (1, 19). In particular, the rat model was used in several studies owing to its advantages of low cost, easy maintenance, and established techniques for blood vessel and ureteral anastomosis. Furthermore, in humans, chronic changes such as thickening of the blood vessel wall and atrophy of the kidney tubules develop over several years to decades, whereas in rat models, these results, as well as chronic tissue changes, can be observed within several months (20). Nevertheless, these rats are typically young and male, with mild ischemic injury and an observation period of <3 months, and does not show clinical manifestations of chronic allograft rejection. Furthermore, most rat strains used have been allogeneic transplants when the rat MHC antigen subtypes such as F344 and LEW were the same or were a combination of strains with low rejection (20–23). There have been few papers describing control of ischemic kidney transplantation using a combination of multiple immunosuppressants in a system with strong rejection, assuming actual clinical practice (13, 24, 25). In a rat study, allograft tolerance occurred by administering a single immunosuppressant for several weeks to several months after surgery. From the viewpoint of chronic allograft nephropathy, this also makes it difficult to extrapolate to human transplant recipients who are maintained using several immunosuppressants.

In a previous study, we reported that hydrogen-containing organ preservation solution for rinsing and preservation of grafts reduced acute phase IRI in kidneys of adult minipigs (26). The anti-inflammatory effects of hydrogen, such as inhibiting inflammatory cytokines, inducing HO-1, and activating NF-E2-related factor, have been reported in transplanted organs (27, 28). This solution has been shown to be effective in suppressing IRI in transplanted organs such as the heart, lung, and kidney (29–34). In the present study, we aimed to verify the impact of hydrogen gas treatment in the prevention of chronic rejection of marginal kidney graft with an optimal immunosuppressive protocol based on human clinical setting by using the miniature pig model.

MATERIALS AND METHODS

The pigs used in this study were micro-miniature pigs (Fujimicra Ltd., Shizuoka, Japan) with body weights not exceeding 30 kg even when mature, as previously described (26, 35, 36). We used four males and eight females, with mean age of 25.8 ± 5.5 months (range, 14.8–37.7 months; median, 25.4 months) and mean weight at 20.9 ± 2.4 kg (range, 17.4–26.8 kg; median, 20.3 kg). The pigs were randomly selected donors and recipients and had different swine leukocyte antigen (SLA) suitability. The pigs were housed in cages under temperature- and light-controlled conditions (12-h light/dark cycle) and were provided with food and water *ad libitum*. The breeding room was clean and maintained by washing twice daily. These experiments were conducted with the approval of the Research Council and Animal Care and Use Committee of Kitasato University (approval number, 18-133, 19-086). The animal experiments were performed according to the ARRIVE (Animal Research: Reporting of *In Vivo* Experiments) guidelines 2.0 as a guideline for animal experiments, and all necessary checklist criteria were met.

Pre-Operative Examination and Treatment

Blood and urine tests were performed at screening before surgery to confirm absence of health-related abnormalities, and blood compatibility testing was completed to determine the matching donor and recipient settings in all cases. The recipients began receiving tacrolimus (0.15 mg/kg, PO, BID) and mycophenolate mofetil (500 mg/head, PO, BID) for the induction of immunosuppression 2 days before kidney transplantation.

Preparation for Hydrogenation

The organ preservation solution used for rinsing and preservation of organs was extracellular-type trehalose-containing Kyoto (ETK), which has been shown to have a renal-preservation

effect in previous studies (37). The hydrogen addition method to ETK was performed using a hydrogen storage alloy canister as described (26). The hydrogen was fed from a rubber stopper into a bag of ETK cooled to 4°C and mixed when the internal pressure of the container reached 0.06 ppm. The hydrogen concentration decreased slowly when stored at 4°C under normal pressure, and dissolved hydrogen concentration of 1 ppm or more could be secured for 4 h. Therefore, the pressure reduction was similar to that reported previously and the product was stored at 4°C (26). These operations were performed immediately before ischemic nephrectomy of the donor.

Anesthesia Methods

The donor and the recipient at the time of transplantation were sedated by intramuscular administration of a mixed solution of medetomidine (20 μg/kg), midazolam (0.2 mg/kg), and butorphanol (0.2 mg/kg) to the gluteal muscle. After sufficient sedation was induced, mask inhalation was performed with isoflurane of 3.0%, and anesthesia was induced until the pharyngeal reflex disappeared. The 24-G catheter indwelling needle was inserted into the central ear vein, and lactated Ringer's solution was started at 5 ml/kg/h. The infusion volume was changed appropriately by monitoring anesthesia during surgery. Then, a 5.5-Fr tracheal tube was introduced, and anesthesia was maintained with isoflurane 2.0%. An 8-Fr balloon catheter was placed in the bladder of the recipient to secure visuals of the surgical field and confirm urination during surgery. The catheter was removed after surgery. All pigs were administered with enrofloxacin [5 mg/kg, SC (subcutaneously), BID (bis in die/twice daily)] and cefazolin sodium hydrate (30 mg/kg, IV, BID) as antibiotics and buprenorphine (20 μg/kg, IV, BID) as an analgesic from the preoperative period.

Kidney Transplantation Procedure

Two kidneys obtained from one donor were transplanted to two recipients, and both kidneys of the recipients were excised. The group using hydrogenated ETK was classified as H-DCD20 (n = 4) and the normal ETK group as NH-DCD20 (n = 3). The living kidney-transplanted individual (DCD 0, n = 1) was treated with the same protocol as the other groups except for ischemic manipulation.

The donor was anesthetized and held in a supine position. The chest and abdomen were shaved and disinfected. A midline incision was made in the abdomen with an electric scalpel. Blood flow to the aorta and posterior vena cava was blocked on the cranial and caudal sides of the kidney arteries and veins to induce kidney ischemic time for 20 min. An anticoagulant was not used in blocking the blood flow of the donor. Twenty minutes later, the abdominal aorta and posterior vena cava, left and right kidneys, and ureter were separated and excised. The excised kidney was immediately cannulated from the kidney artery and rinsed with cooling hydrogenated ETK or normal cooled ETK from a height of 1 m by natural dropping for 10 min (**Figure 1A**). Further, it was immersed in a cooled storage solution similar to the rinse liquid. Excessive soft tissue around the kidney hilum was trimmed in the preservation solution, and anastomosis of the blood vessel was formed. The kidneys were stored for 60 or 240 min in the same preservation solution as the rinse solution and allowed to stand until transplantation.

The recipient underwent anesthesia as per the donor protocol. A midline incision was made in the abdomen, and we incised the retroperitoneum to separate the kidney and renal artery and vein on the side to be transplanted. The vascular anastomosis method was determined by the confirmed shape of the blood vessel of the transplanted kidney. The blood flow of the abdominal aorta or renal artery, posterior vena cava, or renal vein was blocked with a vascular clamp, after which the recipient-kidney was removed, and then, the anastomosed blood vessel was formed. Heparin (1,000 units/head) was administered intravenously and was administered again 2 h after the first administration. The donor-kidneys were taken out from the preservation solution and placed in the abdominal cavity of the recipient after the preservation time of the donor-kidney was finished. Subsequently, the kidney artery was sutured for end-to-side or end-to-end anastomosis with 5–0 monofilament non-absorbable thread and the kidney vein with 6-0 monofilament non-absorbable thread. In the case of anastomosis to the abdominal aorta, the ischemic time of the recipient was set to within 30 min from clamping of the abdominal aorta. After the arterial anastomosis was competed, the blood vessel clamp was moved to the renal artery, and the blood flow in the abdominal aorta was restarted. Following kidney arteriovenous anastomosis, the blood flow block was released, and blood flow into the kidney and normal pulsation of the kidney artery were confirmed (**Figures 1B, C**). The ureter was anastomosed with 6-0 monofilament non-absorbable thread and the retroperitoneum was sutured. The abdominal wall was sutured using 1-0 and 3-0 synthetic multifilament absorbent threads. Furthermore, the skin was routinely sutured using 2-0 nylon thread. An access port for sampling blood and drug administration was installed in the jugular vein using a central vein (CV) catheter kit. The CV catheter in the surviving pig was removed 1 month after surgery.

Perioperative Management and Long-Term Observation

The pigs receiving kidney transplantation were provided with food and water *ad libitum* from the first day after surgery. Antibiotics and analgesics were administered postoperatively, and tacrolimus [0.1 mg/kg/day, IV (intravenously)] was intravenously administered continuously until ingestion was observed if the animal had no appetite. Tacrolimus (0.15–0.6 mg/kg, p.o., BID), mycophenolate mofetil (250–500 mg/head, po, BID), and methylprednisolone (0.5–2 mg/kg, IV or PO, BID) were administered during the follow-up period. Tacrolimus and mycophenolate mofetil doses were set based on previous reports (38). Tacrolimus trough levels were measured routinely and the dose adjusted to maintain trough levels of 5–15 ng/ml. When a decrease in the trough level of tacrolimus was observed, the dose of tacrolimus was gradually increased to adjust the dose. In situations considered to represent acute rejection, the dose of prednisolone was increased for 3 days (2 mg/kg, BID) and gradually decreased over 1 week. As an analgesic, buprenorphine (20 μg/kg, IV, BID) was administered. As appropriate, famotidine (0.5 mg/kg, PO or IV BID) was orally or intravenously administered, as well as

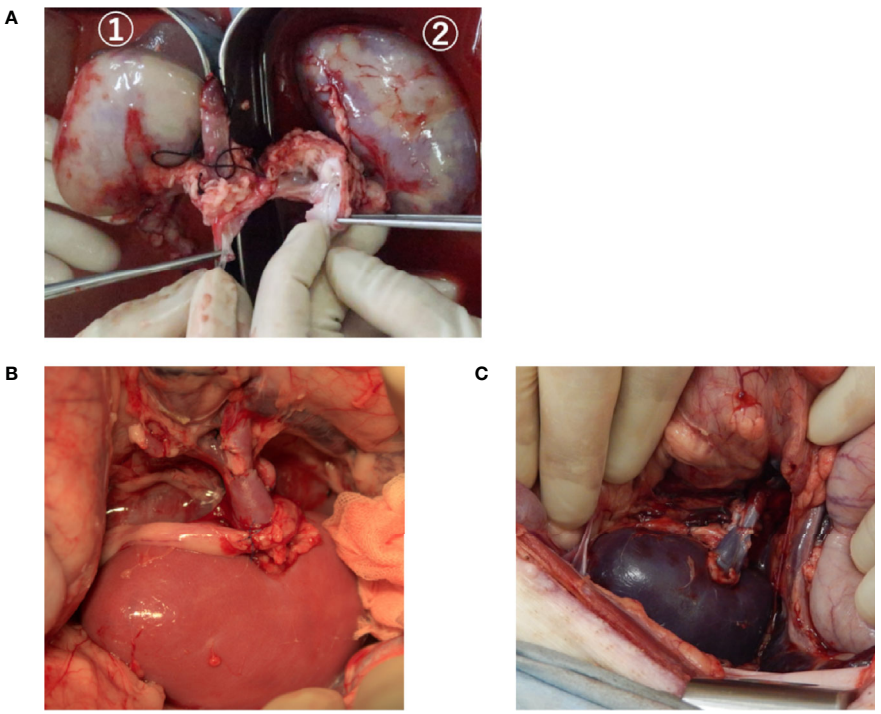

FIGURE 1 | The kidneys during rinse and after reperfusion of blood. **(A)** A typical image showing the kidney being rinsed by the organ preservation solution. The kidney of ① is rinsed with a hydrogenated organ preservation solution. ② is rinsed with a non-hydrogenated organ preservation solution. The whole area of ① is flushed compared to ②. **(B, C)** The transplanted kidney immediately after reperfusion after rinsing and storage with an organ preservation solution. B, hydrogenated kidney; C, non-hydrogenated kidney.

darbepoetin (30 μg/head, SC, once a week) and iron which was administered orally.

Blood sampling from the CV catheter was performed until the kidney function stabilized. Blood was collected every day until the first week after the operation and at 2 weeks, 1 month, 2 months, and 100 days postoperatively. We recorded the complete blood count (CBC), blood urea nitrogen (BUN), and creatinine levels. In addition, syndecan-1 levels were measured using plasma before surgery and 4 h after transplantation using an ELISA kit (MBS101321, MyBioSource, CA, USA), because the increase in syndecan-1 levels due to angiopathy occurs at approximately 2–4 h postoperatively, according to a previous report (39). Urine was collected at the same time as blood sampling, and the urine was evaluated for specific gravity, pH, and sediment.

The observation period was 100 days after the operation, and individuals surviving 100 days or more were sacrificed to remove the transplanted kidney. In addition, individuals with postoperatively elevated creatinine levels, anuria for 6 days or more, and exacerbated clinical symptoms (frequent vomiting, diarrhea, inability to stand, loss of appetite) were sacrificed. The method of sacrifice was the same method as for anesthesia during surgery, followed by rapid administration of pentobarbital (100 mg/kg, IV) and potassium chloride (25 ml/head, IV). Ten minutes later, we confirmed cardiopulmonary arrest. At the time of sacrifice, blood was collected and ultrasonography and contrast-enhanced computed tomography (CT) were performed to evaluate the kidneys.

Ultrasonography and Contrast-Enhanced CT Examination

Ultrasonography was performed under sedation to confirm blood flow and for morphological evaluation of the transplanted kidney. The pig was placed in the supine position. The vascular resistance coefficient (RI) was measured by the calculated systolic and diastolic blood flow rates using the pulsed Doppler method. RI is known to be high in rejection and kidney artery stenosis and has been shown to be associated with antibody-related rejection and acute tubular necrosis (40). In order to avoid variations in results due to differences in flow velocity depending on the measurement position, RI measurements were performed uniformly on the interlobar artery in all individuals. The RI was measured three times consecutively, and the average value was calculated. In contrast-enhanced CT examination, blood flow to the renal arteries and veins under sedation was observed. The pig was in the supine position, and iohexol (1 ml/kg) was rapidly administered intravenously for imaging.

Histopathological Examination

The removed kidney, renal artery and vein, and ureter were immersed in 4% paraformaldehyde-phosphate buffer (4% PFA) and fixed at 4°C for 24–48 h. The kidneys were sectioned longitudinally to include the papilla centering on the cortex. The artery, vein, and ureter were divided along the lumen to a longitudinal section and were embedded. After embedding, thin-layer slices (3 μm) were prepared using a conventional method. Thin sections were stained with hematoxylin and eosin, Masson's trichrome stain, and Elastica van Gieson stain. Histological examination was performed by blinded pathologists, and kidney graft pathology was assessed according to the Banff classification (41, 42).

RESULTS

Recipient Information and Survival Days

Table 1 shows the survival days, preservation time, and warm ischemic time in all groups. The warm ischemic time was the time from the placement of the transplanted kidney in the recipient to the reperfusion. Ischemia was slightly prolonged in the three individuals of H-DCD20 due to blood vessel site injury and bleeding. DCD0 was able to survive for 100 days. The day after the operation, appetite improved and urination was observed. Three H-DCD20 survivors (3/4 heads) survived for 100 days, whereas the remaining survivor had a nephrostomy tube under anesthesia 28 days after surgery due to severe ureteral obstruction. The general condition improved and was maintained. The surviving animals gradually recovered their appetite from postoperative days 2–3, and urinary excretion and normal feces were observed. NH-DCD20 was sacrificed 3–7 days after surgery due to exacerbation of clinical symptoms including anuria, vomiting, and deterioration of kidney function. Taken together, these findings suggest H-DCD20 enabled long-term survival despite of the more severe ischemic conditions than NH-DCD20.

Blood and Urinary Tests

The BUN and creatinine of Nos. 2, 3, and 8 peaked on postoperative days 2–4 and gradually decreased; following that, the value remained stable (**Figure 2A**). No. 4 showed increased BUN and creatinine due to ureteral obstruction; however, BUN and creatinine improved with percutaneous nephrostomy tube placement and medical management under anesthesia. The BUN and creatinine of non-surviving individuals in H-DCD20 and all the individuals in NH-DCD20 continued to increase and did not improve (**Figure 2B**). Syndecan-1 levels are displayed in **Table 2**. The concentration in NH-DCD20 was higher than in DCD0 and H-DCD20 before and after surgery. Only the H-DCD20 (3/4) and DCD0 were able to provide urine after surgery. One individual in H-DCD20 and all the individuals in NH-DCD20 did show urine in the bladder by ultrasonography; however, urine could not be collected. The result of urinary testing 2 weeks after surgery showed that H-DCD20 (1.016 ± 0.004) had a lower specific gravity than DCD0 (1.029). In summary, the renal function in H-DCD20 could be earlier recovered than that of NH-DCD20 and remain stable.

TABLE 2 | Concentration of Syndecan-1.

No.	H-DCD 20 (n = 2)		NH-DCD 20 (n = 2)		DCD 0 (n = 1)
	3	4	5	6	8
Pre (μg/ml)	5.08	2.48	10.32	10.99	5.24
Post (μg/ml)	9.06	5.46	16.46	15.13	7.34
Rate of variability (%)	40.0	78.3	120.3	59.4	37.7

ND, under than the limited value of measurement.

Imaging Findings

Ultrasonography showed clear blood flow in the kidneys of the segmental arteries in the surviving DCD0 and H-DCD20 individuals from postoperative day 1 to follow-up (**Figure 3**). One individual in the NH-DCD20 and H-DCD20 who died less than 7 days after transplantation had little or no kidney blood flow from the early postoperative period. In addition, the entire kidney was hypoechoic, making anatomical evaluation of the kidney difficult (**Figure 3**). The measured RI was higher for H-DCD20 than for DCD0 after surgery; however, it gradually decreased and became stable (**Table 3**). Only No. 5 could be measured in the NH-DCD20, and RI was higher than that of the other groups from the first day after surgery. All surviving individuals had clear contrast-enhanced images within the renal parenchyma using contrast-enhanced CT examination on day 100 (**Figure 3**). The renal arteries and veins were clearly visualized. The individuals who died within 7 days after operation did not show contrast medium influx into the renal parenchyma. Collectively, data indicate that clear blood flow in the surviving H-DCD20 individuals could be observed by ultrasonography and contrast-enhanced CT examination from postoperative day 1 to follow-up.

TABLE 1 | Information of groups.

	H-DCD 20 (n = 4)				NH-DCD 20 (n = 3)			DCD 0 (n = 1)
	No. 1	No. 2	No. 3	No. 4	No. 5	No. 6	No. 7	No. 8
Survival days	1	100	100	100	3	6	7	100
Warm ischemic time (min)	60	79	64	69	60	60	60	60
Preservation time (min)	240	60	240	240	60	60	60	17

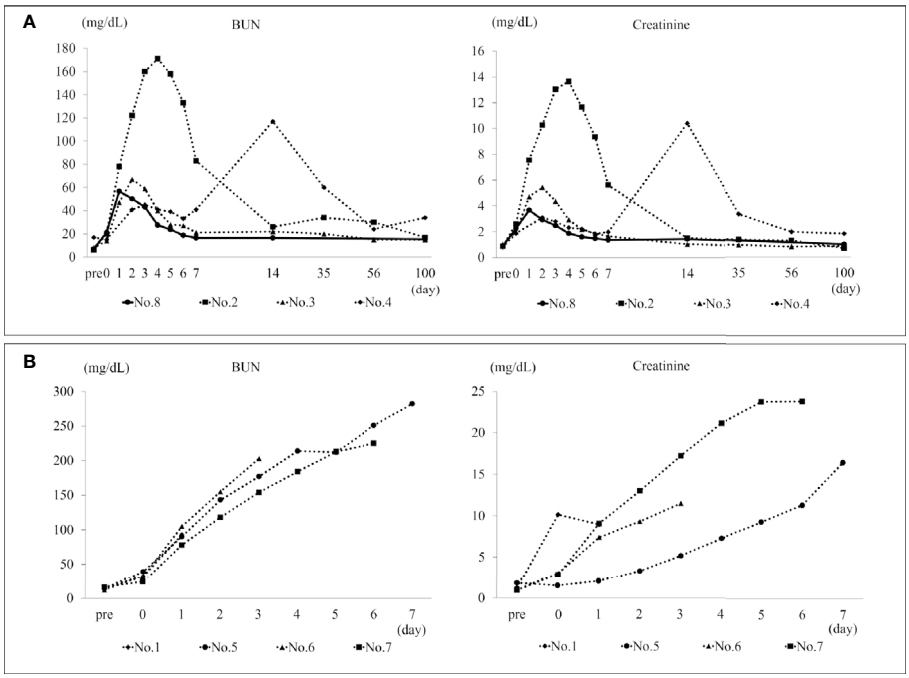

FIGURE 2 | BUN and creatinine in the survival span. **(A)** The transition of BUN and creatinine in H-DCD20 individuals who were able to survive up to 100 days after surgery. The solid line shows DCD0. No. 4 has a temporary increase in BUN and creatinine due to ureteral obstruction. In other individuals, BUN and creatinine peaks within 5 days after surgery, and kidney function is stable until 100 days. **(B)** The transition of BUN and creatinine in individuals who died early after surgery. These continue to rise after the operation, and no improvement is observed. BUN, blood urea nitrogen. *H-DCD20: n=4, NH-DCD20: n=3, DCD0: n=1.

Pathology Anatomy

No renal arteriovenous thrombus was observed in any individual who survived for 100 days (**Table 4**). In addition, individuals who survived for 100 days with H-DCD20 had ureteral anastomosis stenosis or adhesion to surrounding tissues, as well as dilated renal pelvis and ureters. The individuals who died within 1 week after surgery had thrombus in the kidney arteries (**Table 4**). In individuals whose blood flow could not be confirmed before dissection using ultrasound images, thrombus was confirmed in the renal arteries and in some of the segmental arteries and veins. In summary, individuals in H-DCD20 had no thrombus formation in the renal artery and vein; however, the individuals in NH-DCD20 had thrombus in the kidney arteries.

Histopathological Findings

The histopathological images are shown in **Figure 4**. DCD0 (No. 8) and the surviving individuals (Nos. 2, 3, and 4) showed chronic tissue changes. The kidney of No. 2 showed moderate tubular inflammation and glomerulitis and mild mononuclear cell infiltration into the stroma. Histological images showed mild chronic allograft nephropathy such as tubular atrophy and interstitial fibrosis. Stenosis of the arterial lumen, necrosis of the intima, edema of the media, and cell infiltration into the adventitia were observed (**Figures 4A–C**). These were comprehensively evaluated and found to be type I chronic allograft nephropathy, according to the Banff classification (**Table 5**). In No. 3, the glomerulitis was moderate; however, there was no cell infiltration into the stroma. Additionally, the tubular atrophy and tubular inflammation were mild (**Figures 4D, E**). Therefore, No. 3 was identified to have no chronic allograft nephropathy. In No. 4, mild interstitial fibrosis and atrophy of renal tubules were observed, and cellular infiltration, arterial intima, and venous infarction were noted in some areas (**Figures 4F, G**). Thus, we concluded that this was a type I chronic rejection, according to the Banff classification (**Table 5**). Three of the four individuals who died within 7 days showed severe tubular necrosis over the entire area, and cellular proliferation and hemorrhage from the intima to the adventitia of the renal arteries and veins were detected (**Figure 4H**). In Nos. 1 and 7, there were infarcts due to thrombus in the renal arteries (**Figure 4I**).

The supplementary table shows the number of drops in the infusion line when rinsing with ETK. As in previous reports, H-ETK (n = 3) has a higher number of drops per minute than NH-ETK (n = 3). The supplementary figure is the result of histopathological examination. This result was examined after the graft was treated by the same procedure as in this study and immediately fixed. As a result, the hydrogen-treated graft (hydrogen; n = 1) tended to have a mild tubular degeneration to necrosis with dilatation score compared to the non-hydrogenized graft (control; n = 1).

Collectively, data indicate that the surviving individuals in H-DCD20 showed no to mild chronic allograft nephropathy since there was a possibility that the hydrogen improved an acute

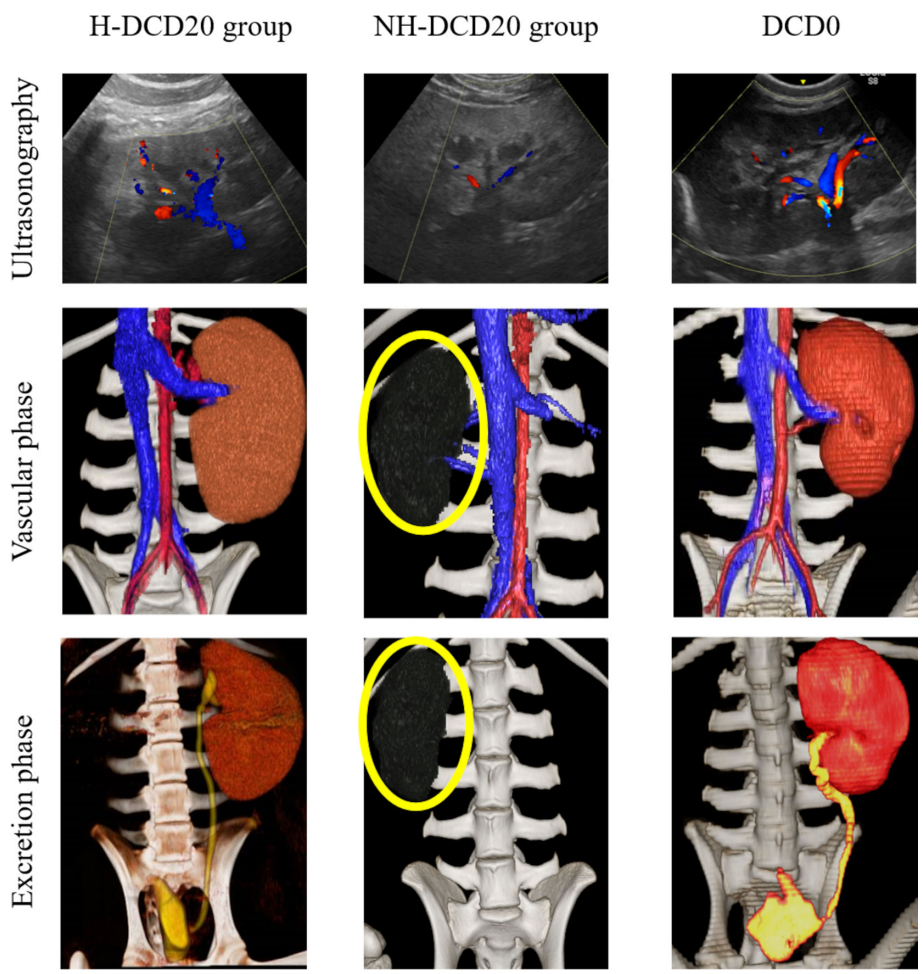

FIGURE 3 | Ultrasonographic and contrast CT images. Upper row: Ultrasound images on the first day after the operation are shown. Renal blood flow in H-DCD20 individuals is clearly confirmed; however, some areas are difficult to see with a Doppler. Almost no renal blood flow is observed in NH-DCD20 individuals, and the renal parenchyma shows a hypoechoic image similar to that of surrounding tissues. Kidney blood flow in DCD0 is clearly confirmed, and branching of interlobar arteries and veins is observed from segmental arteries and veins. Middle/lower row: contrast-enhanced CT is used to demonstrate the vascular and excretory phases, and 3D stereoscopic images are shown. In H-DCD20 and DCD0, inflow of contrast medium into the kidney is observed, and the ureter and bladder are imaged. However, in individuals of NH-DCD20 and H-DCD20 without blood flow, the renal arteries are not imaged, and the ureter and bladder are not imaged during the excretory phase (yellow circle, transplanted kidney). CT, computed tomography; 3D, three-dimensional. *H-DCD20, n = 4; NH-DCD20, n = 3; DCD0, n = 1.

TABLE 3 | RI value by ultrasonography.

		Day after operation							
		Day 1	**Day 3**	**Day 5**	**1 week**	**2 weeks**	**1 month**	**2 months**	**Day 100**
H-DCD20	No. 1	NT	Dead	–	–	–	–	–	–
(n = 4)	No. 2	0.61	0.68	0.72	0.53	0.54	0.51	0.55	0.55
	No. 3	0.63	0.59	0.64	0.59	0.51	0.72	0.60	0.46
	No. 4	NT	NT	0.64	0.64	NT	0.63	0.75	0.71
NH-DCD20	No. 5	0.71	0.78	0.63	0.82	Dead	–	–	–
(n = 3)	No. 6	NT	NT	Dead	–	–	–	–	–
	No. 7	NT	NT	NT	Dead	–	–	–	–
DCD0	No. 8	0.50	0.51	0.53	NT	0.47	NT	0.51	0.66
(n = 1)									

NT, not tested (no blood flow or difficult to measure).

TABLE 4 | Ultrasonographic and anatomical findings in the last day.

		H-DCD20 (n = 4)	NH-DCD20 (n = 3)	DCD 0 (n = 1)
Ultrasonographic findings	Renal artery flow	3/4	3/3	1/1
	Renal venous flow	3/4	3/3	1/1
	Ureteral dilation	3/4	0/3	0/1
	Pelvis dilation	3/4	0/3	0/1
Anatomical findings	Arterial thrombus	1/4	1/3	0/1
	Venous thrombus	1/4	0/3	0/1
	Ureteral dilation	3/4	0/3	0/1
	Pelvis dilation	3/4	0/3	0/1

tubular degeneration and necrosis compared to the non-hydrogen-treated kidney.

DISCUSSION

To the best of our knowledge, this is the first study to observe long-term prognosis after transplantation using hydrogen in the ischemic kidney of mature minipigs and to inhibit chronic rejection response using a strict multi-immunosuppressant protocol.

NH-DCD20 showed severe kidney damage in the acute phase and was sacrificed, whereas H-DCD20 quickly recovered from IRI in the acute phase and all survived for long periods except for one individual. Kidney transplant dysfunction can lead to 6-day survival. Therefore, we believe that the cause of an early death of the individual in H-DCD20 was not transplanted kidney dysfunction; rather, there were other causative factors. We speculate that hydrogen improved microcirculation and that this was one of the factors that caused the difference in the long-term survival between the two groups.

In human studies, kidney allograft thrombosis accounts for 2%–7% of graft loss (43). The causes include technical factors, vascular endothelial damage, decreased cardiac output, acute tubular necrosis, and acute rejection. In the case of ischemic organ transplantation, rejection is strongly associated with microcirculatory changes induced by inflammatory cytokines due to IRI (44, 45). Hydrogen has been shown to suppress the production of the major inflammatory cytokines IL-1β, IL-6, and TNF-α, and it has anti-inflammatory effects that reduce tissue damage (29, 34). Saito et al. reported that using hydrogenated preservatives for lung transplantation reduced the expression of IL-1β and 8-hydroxyguanosine and reduced the number of neutrophils attached to the vascular wall and hydrogen-inhibited vascular endothelial damage (29). In addition, ETK potentially contributes to improving microcirculation. In actual human clinical cases, its clinical application in lung transplantation has been reported (46). Although its application in kidney transplantation as a clinical example has not been reported, in experimental animals, we has previously shown prolongation of individual survival by ETK preservation in ischemic kidney transplant rat models compared to the University of Wisconsin solution and lactated Ringer's solution (37). The high-sodium/low-potassium composition of ETK and the trehalose contained in it are thought to suppress vasoconstriction due to high potassium concentration and cell edema, reduce reperfusion injury, and inhibit further ischemia. Chronic tissue changes can be expected to suppress inflammatory cytokines and reactive oxygen species and improve ischemia. Therefore, the combination of H and ETK may be one of the leading protocols for ischemic kidney transplantation.

The glycocalyx present in vascular endothelial cells is an extremely fragile structure, consisting of proteoglycan, glycoprotein, and glycan; it is responsible for maintaining microcirculation and barrier function of blood vessels and easily disintegrates upon stimuli such as IRI and cytokines (7, 34, 47, 48). The glycocalyx is present on the surface of glomerular capillaries and podocytes in the kidney and has been shown to be exfoliated by exposure to lipopolysaccharides. Hydrogen is thought to protect the glycocalyx (49). There were decreased expression levels of syndecan-1 in the glycocalyx when hydrogen was inhaled in a non-traumatic hemorrhagic shock rat model, showing that hydrogen contributed to the prolongation of survival (49). One study showed that an increase in syndecan-1 levels in tubular epithelial cells was associated with improved graft function and prolonged engraftment (50). Furthermore, syndecan-1 knockout mice were often affected by renal IRI and were prone to fibrosis. Although measured syndecan-1 levels increased postoperatively in all groups, the fluctuating rate was lower in NH-DCD 20 than in H-DCD 20. The reason may be as follows: NH-DCD 20 did not effectively rinse out cytokines and oxidants, thereby inducing thrombus formation immediately after reperfusion. Systemic circulation of syndecan-1 did not occur during reperfusion. This can further be determined by the appearance of the kidney after reperfusion (**Figures 2B, C**). This suggests that the increasing serum levels of syndecan-1 may have been underestimated. In contrast, in H-DCD 20, the rate of change of syndecan-1 expression was relatively high because hydrogen removed microthrombi and blood entered the systemic circulation from the graft.

No chronic rejection was observed in the transplanted kidney with long-term engraftment of H-DCD 20, and there were individuals with the same histopathological image as DCD 0. In previous studies, it has been shown that ischemic kidney transplantation is likely to induce chronic rejection. The ischemic state of the transplanted kidney contributes to non-immune chronic rejection, and the induction of acute inflammation and rejection by IRI results in chronic organic changes in tissue, including thickening of the arterial wall. We evaluated the rate of decrease during ETK flow within the kidney and confirmed that rapid flow of ETK decreased in the line, similar to previous reports (**Supplementary Table**). Furthermore, we confirmed that the histopathological findings of the kidney immediately after rinsing with ETK showed no difference; however, tubule degeneration associated with dilation was mild in the kidney using ETK containing hydrogen (**Supplemental Figure**). Currently, most studies on chronic rejection have been using rats with low-responder combinations, and immunosuppressants have often been used alone for short periods of time. In the present study, we did not confirm the haplotypes of SLA. Most MHC haplotypes of the microminiature pigs used have been identified; however,

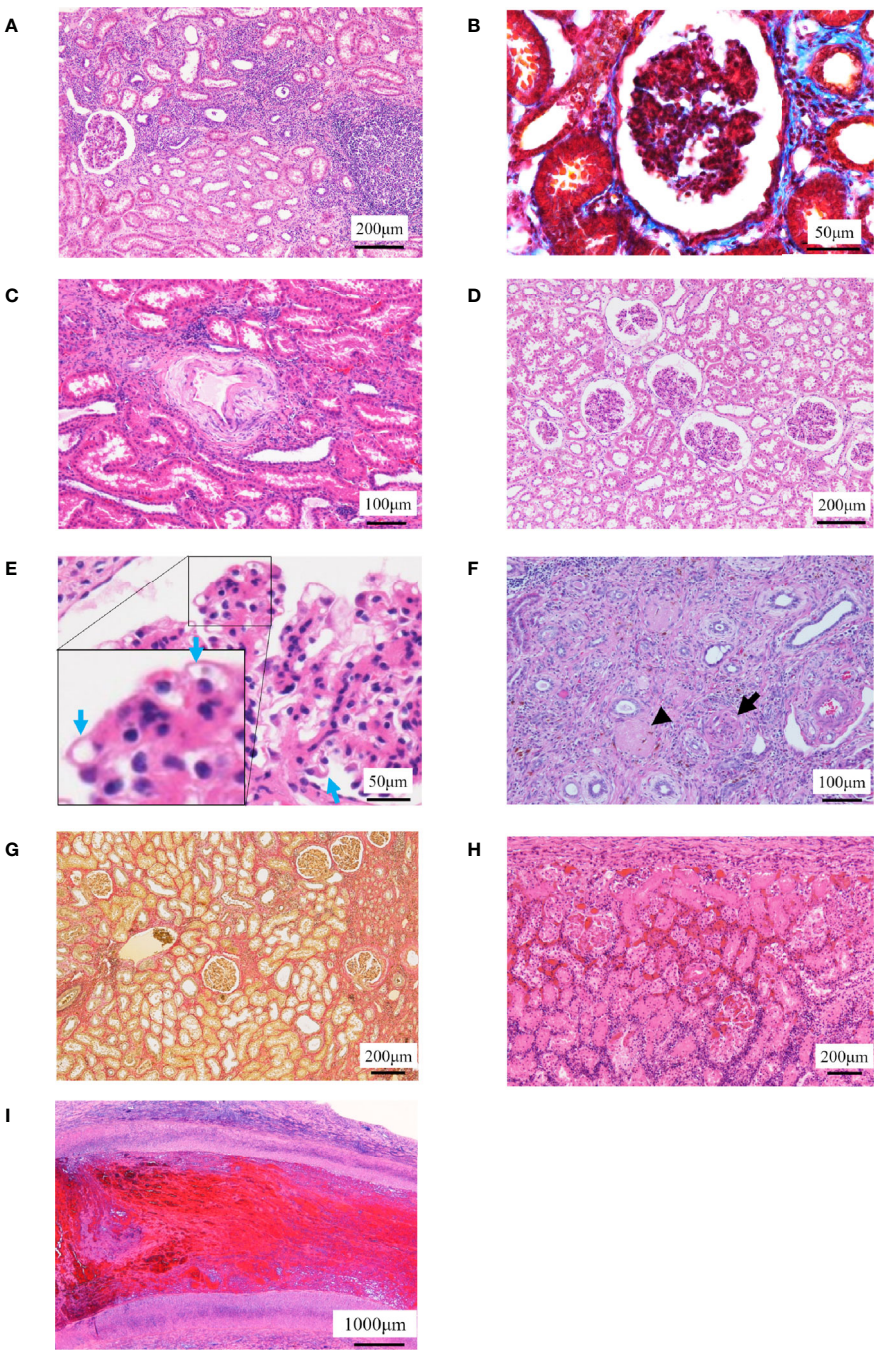

FIGURE 4 | Histopathological examinations. **(A–C)** The histopathological images in No. 2 are shown. **(A)** Localized cell infiltration is observed, and cell infiltration is observed around the epithelial edema. **(B)** Mild fibrosis is observed (Masson's trichrome staining). **(C)** Stenosis of the lumen in the kidney artery, necrosis of the intima and edema of the media, and cell infiltration in the adventitia are observed. **(D, E)** The histopathological images in No. 3 are shown. **(D)** Borderline change is observed to the extent that localized cell infiltration is observed. **(E)** Chronic glomerulosis due to thickening of the vascular loop (blue arrow) is shown with an increase in mesangial substrate. **(F, G)** The histopathological images in No. 4 are shown. **(F)** Arterial infarction (arrow) and venous infarction (arrowhead) are observed. **(G)** Fibrosis was mild but more extensive than No. 2 (Elastica van Gieson staining). **(H, I)** Representative histopathological images of individuals who died early after operation are shown. **(H)** Tubular necrosis is observed throughout the whole kidney. Infiltration of mononucleosis is observed near the capsule. **(I)** Thrombus formation is observed in the renal artery.

TABLE 5 | Histopathological findings for kidney allograft.

No.	H-DCD 20 (n = 4)				NH-DCD 20 (n = 3)			DCD 0 (n = 1)
	1	2	3	4	5	6	7	8
Glomerulitis	/	2	2	2	3	/	/	2
Interstitial mononuclear cell infiltration	0	1	0	1	3	/	/	0
Tubulitis	0	2	1	3	3	1	2	0
Intimal arteritis	0	1	0	1	1	0	0	0
Chronic allograft nephropathy type/grade	0	I	0	I	I	0	0	0
Chronic transplant glomerulopathy	/	3	1	3	2	/	/	0
Interstitial fibrosis	0	1	0	1	2	0	0	0
Tubular atrophy	0	1	1	1	3	0	0	1
Mesangial matrix	/	3	3	3	3	/	/	1
Vascular fibrous intimal thickening	0	1	1	2	0	0	0	0

Grade 0, no change; 1, mild; 2, moderate; 3, severe;/, no examination.
Chronic allograft nephropathy type/grade.
I. Mild interstitial fibrosis and tubular atrophy (<25% of cortical area).
II. Moderate interstitial fibrosis and tubular atrophy (26%–50% of cortical area).
III. Severe interstitial fibrosis and tubular atrophy/loss (>50% of cortical area).

this is currently under study (36). SLA has multiple haplotypes, as in humans. This suggests the requirement for multi-immunosuppressant protocols similar to actual clinical practice. Furthermore, recently, a mechanism called IL-6 amplifier has been considered for MHC class II-related inflammatory reactions. This indicates that CD4+ T cell-derived cytokines such as IL-17A may lead to sustained activation of IL-6 due to T-cell activation and local accumulation that are not related to antigen specificity (51). To support this, it is shown that synaptotagmin-17, a type of urinary exosome, is increased in association with IL-6 amplifiers in patients with chronic active antibody-mediated rejection in kidney transplantation (52). These were considered that may be relating the suppression of cytokines by hydrogen and may affect the results of mild fibrosis and tubular atrophy in the H-DCD20 (29, 34).

Hydroxyl radical (OH^-) and reactive oxygen species cause oxidative damage to kidney tissue, producing cytokines such as TGF-β1 and tubular cells, causing epithelial-mesenchymal transition (EMT). EMT causes fibrosis by filling the tubular interstitial with fibrotic substances such as vimentin and α-smooth muscle actin, causing arterial ischemia and atrophy of glomeruli and kidney tubules. Therefore, it was suggested that the hydrogen-dissolved organ preservation solution suppresses the upper cascade of fibrosis by removing hydroxyl radicals, reactive oxygen species, and inflammatory cytokines, and may contribute to the reduction of chronic rejection.

The ischemic time affected long-term survival in the ischemic kidney transplant model of miniature pigs used in this study. In humans, it has been shown that the retention and survival rate of transplanted organs decreased when the ischemic time was 30 min or more (53), and the ischemic time compatible with survival after transplantation differs depending on the animal species. Previous studies in miniature pigs showed ischemic times of 30 min and observation periods of less than 1 week (26). In addition, we noted that survival after kidney transplantation in miniature pigs with an ischemia time of 30 min was difficult for all (n = 9, unpublished data). Autologous transplantation using general domestic pigs and miniature pigs involve young pigs and there is no use of immunosuppressants; hence, the ischemic time is 30–60 min (54, 55). Therefore, it was speculated that the maturity of microminiature pigs was one of the factors giving rise to the difference in viability despite using the same animal species. As mentioned previously, pigs generally used in transplantation experiments are young, typically less than 6 months old. It cannot be denied that this acts as a kidney protective effect because many factors such as immune response and growth hormone can be confounded during the growth period (56), and this precludes extrapolation to humans. The ischemic kidney transplantation model of mature miniature pigs created in this study is expected to contribute significantly to preclinical studies in humans.

The limitations of this study were the small number of individuals included and the limited data obtained, unknown detail SLA types, and the lack of complete elucidation of the mechanism by which the improvement tendency of chronic rejection occurred. Regarding this point, we are considering experiments considering the combination of SLAs in the future. The purpose of this study was to confirm long-term survival and the accompanying changes in chronic tissue response; IHC, PCR, ELISA, and flow cytometry were not performed on tissue sections. However, Abe et al. reported that dissolving hydrogen in the UW organ preservation solution during renal transplantation in rats suppressed tubular apoptosis and reduced interstitial macrophage infiltration (57). We think this can be observed in miniature pigs as well. In addition, we plan to analyze the inflammatory cytokine cascade and its associated cell-mediated immune response. Nevertheless, it is clear that hydrogen improves the blood flow environment in the ischemic kidney in ischemic kidney transplantation in mature pigs. Hydrogen enables rapid recovery of kidney function and long-term survival in the context of administration of multidrug immunosuppressive therapy. Furthermore, the fact that chronic rejection was not observed or was mild in ischemic kidney transplantation of pigs, we can infer that this was mediated by hydrogen. This factor can contribute significantly in explaining the chronic rejection mechanism.

In conclusion, hydrogen induced a positive effect on IRI, possibly suppressing thrombus formation and microcirculation

for lethal ischemic kidney transplantation in miniature pigs. Furthermore, findings suggested suppression of chronic rejection in long-term engrafted kidney tissue and showed a relationship between inflammation and rejection in the acute phase and chronic tissue changes. This is a significant preclinical model, and we believe that this model will provide further insight into the mechanism of chronic rejection.

DATA AVAILABILITY STATEMENT

The original contributions presented in the study are included in the article/**Supplementary Material**. Further inquiries can be directed to the corresponding author.

ETHICS STATEMENT

The animal study was reviewed and approved by The Research Council and Animal Care and Use Committee of Kitasato University (approval number: 18-133, 19-086).

AUTHOR CONTRIBUTIONS

KN, SI, and EK contributed substantially to the conception and design of the work. SI made the same contribution as KN in this research. KN, SI, KT, SO, MS, and EK contributed to the acquisition, statistics, analysis, and interpretation of data. EK supervised and confirmed all the data and supervised the opinions of all the co-authors. All co-authors reviewed the final version of this paper and agreed to submit it. The authors agreed to be accountable for all aspects of the work in ensuring that questions related to the accuracy or integrity of any part of the work are appropriately investigated and resolved. All authors contributed to the article and approved the submitted version.

FUNDING

This work was supported by grants from Doctors Man Co., who had no role in study design, data collection and analysis, decision to publish, or preparation of the manuscript (Grant number: 2225-7257, 2225-7265).

ACKNOWLEDGMENTS

This work was supported by grants from Doctors Man Co., Ltd. Sou Hashimoto from this company assisted with devising the system for infusing hydrogen gas into organs as preservation solution.

SUPPLEMENTARY MATERIAL

The Supplementary Material for this article can be found online at: https://www.frontiersin.org/articles/10.3389/fimmu.2020.626295/full#supplementary-material

REFERENCES

1. Nieuwenhuijs-Moeke GJ, Pischke SE, Berger SP, Sanders JSF, Pol RA, Struys MMRF, et al. Ischemia and Reperfusion Injury in Kidney Transplantation: Relevant Mechanisms in Injury and Repair. *J Clin Med* (2020) 9(1):253. doi: 10.3390/jcm9010253
2. Hariharan S, Johnson CP, Bresnahan BA, Taranto SE, McIntosh MJ, Stablein D. Improved graft survival after renal transplantation in the United States, 1988 to 1996. *N Engl J Med* (2000) 342(9):605–12. doi: 10.1056/NEJM200003023420901
3. Yilmaz S. Chronic Allograft Nephropathy (Chronic Allograft Damage): Can It Be Avoided? *Curr Transplant Rep* (2014) 1:91–9. doi: 10.1007/s40472-014-0009-6
4. Singh RP, Farney AC, Rogers J, Zuckerman J, Reeves-Daniel A, Hartmann E, et al. Kidney transplantation from donation after cardiac death donors: lack of impact of delayed graft function on post-transplant outcomes. *Clin Transplant* (2011) 25(2):255–64. doi: 10.1111/j.1399-0012.2010.01241.x
5. Ledinh H, Bonvoisin C, Weekers L, de Roover A, Honoré P, Squifflet JP, et al. Results of kidney transplantation from donors after cardiac death. *Transplant Proc* (2010) 42(7):2407–14. doi: 10.1016/j.transproceed.2010.07.055
6. Tomita Y, Iwadoh K, Hoshino A, Ogawa Y, Sannomiya A, Nakajima I, et al. Primary Nonfunction on Kidney Transplant Recipients From Donation After Circulatory Death Donors. *Transplant Proc* (2019) 51(8):2523–6. doi: 10.1016/j.transproceed.2019.01.201
7. Chappell D, Hofmann-Kiefer K, Jacob M, Rehm M, Briegel J, Welsch U, et al. TNF-alpha Induced Shedding of the Endothelial Glycocalyx Is Prevented by Hydrocortisone and Antithrombin. *Basic Res Cardiol* (2009) 104(1):78–89. doi: 10.1007/s00395-008-0749-5
8. Erpicum P, Detry O, Weekers L, Bonvoisin C, Lechanteur C, Briquet A, et al. Mesenchymal stromal cell therapy in conditions of renal ischaemia/reperfusion. *Nephrol Dial Transplant* (2014) 29(8):1487–93. doi: 10.1093/ndt/gft538
9. Denecke C, Tullius SG. Innate and adaptive immune responses subsequent to ischemia-reperfusion injury in the kidney. *Prog Urol* (2014) 24(Suppl 1): S13–19. doi: 10.1016/S1166-7087(14)70058-2
10. Timsit MO, Yuan X, Floerchinger B, Ge X, Tullius SG. Consequences of transplant quality on chronic allograft nephropathy. *Kidney Int Suppl* (2010) 119:S54–58. doi: 10.1038/ki.2010.424
11. Matas AJ, Gillingham KJ, Payne WD, Najarian JS. The impact of an acute rejection episode on long-term renal allograft survival (t1/2). *Transplantation* (1994) 57(6):857–9. doi: 10.1097/00007890-199403270-00015
12. Orosz CG, Bergese SD, Wakely E, Xia D, Gordillo GM, VanBuskirk AM. Acute versus chronic graft rejection: Related manifestations of allosensitization in graft recipients. *Transplant Rev* (1997) 11(1):38–50. doi: 10.1016/S0955-470X(97)80036-5
13. Fujishiro J, Kudou S, Iwai S, Takahashi M, Hakamata Y, Kinoshita M, et al. Use of sphingosine-1-phosphate 1 receptor agonist, KRP-203, in combination with a subtherapeutic dose of cyclosporine A for rat renal transplantation. *Transplantation* (2006) 82(6):804–12. doi: 10.1097/01.tp.0000232687.78242.cd
14. Liptak P, Eva Kemeny E, Ivanyi B. Primer: histopathology of polyomavirus-associated nephropathy in renal allografts. *Nat Clin Pract Nephrol* (2006) 2 (11):631–6. doi: 10.1038/ncpneph0319
15. Yilmaz S, Isik I, Afrouzian M, Monroy M, Sar A, Benediktsson H, et al. Evaluating the accuracy of functional biomarkers for detecting histological changes in chronic allograft nephropathy. *Transpl Int* (2007) 20(7):608–15. doi: 10.1111/j.1432-2277.2007.00494.x
16. Vaziri N, Thuillier R, Favreau FD, Eugene M, Milin S, Chatauret NP, et al. Analysis of machine perfusion benefits in kidney grafts: a preclinical study. *J Transl Med* (2011) 9:15. doi: 10.1186/1479-5876-9-15
17. Kasil A, Giraud S, Couturier P, Amiri A, Danion J, Donatini G, et al. Individual and Combined Impact of Oxygen and Oxygen Transporter

Supplementation during Kidney Machine Preservation in a Porcine Preclinical Kidney Transplantation Model. *Int J Mol Sci* (2019) 20(8):1992. doi: 10.3390/ijms20081992
18. Nakao A, Faleo G, Shimizu H, Nakahira K, Kohmoto J, Sugimoto R, et al. Ex vivo carbon monoxide prevents cytochrome P450 degradation and ischemia/reperfusion injury of kidney grafts. *Kidney Int* (2008) 74(8):1009–16. doi: 10.1038/ki.2008.342
19. Cavaillé-Coll M, Bala S, Velidedeoglu E, Hernandez A, Archdeacon P, Gonzalez G, et al. Summary of FDA Workshop on Ischemia Reperfusion Injury in Kidney Transplantation. *Am J Transplant* (2013) 13(5):1134–48. doi: 10.1111/ajt.12210
20. Shrestha B, Haylor J. Experimental rat models of chronic allograft nephropathy: a review. *Int J Nephrol Renovasc Dis* (2014) 7:315–22. doi: 10.2147/IJNRD.S65604. eCollection 2014.
21. Li J, Basler M, Alvarez G, Brunner T, Kirk CJ, Groettrup M. Immunoproteasome inhibition prevents chronic antibody-mediated allograft rejection in renal transplantation. *Kidney Int* (2018) 93(3):670–80. doi: 10.1016/j.kint.2017.09.023
22. Zhang Y, Yang Y, Li X, Chen D, Tang G, Men T. Thalidomide ameliorate graft chronic rejection in an allogenic kidney transplant model. *Int Immunopharmacol* (2019) 71:32–9. doi: 10.1016/j.intimp.2018.12.035
23. Deng J, Xia Y, Zhou Q, Wang X, Xiong C, Shao X, et al. Protective effect of rosiglitazone on chronic renal allograft dysfunction in rats. *Transpl Immunol* (2019) 54:20–8. doi: 10.1016/j.trim.2019.01.002
24. Luo L, Sun Z, Wu W, Luo G. Mycophenolate mofetil and FK506 have different effects on kidney allograft fibrosis in rats that underwent chronic allograft nephropathy. *BMC Nephrol* (2012) 13:53. doi: 10.1186/1471-2369-13-53
25. Nakamura K, Kawato Y, Kaneko Y, Hanaoka K, Kubo K, Nakanishi T, et al. Prevention of chronic renal allograft rejection by AS2553627, a novel JAK inhibitor, in a rat transplantation model. *Transpl Immunol* (2018) 46:14–20. doi: 10.1016/j.trim.2017.10.001
26. Kobayashi E, Sano M. Organ preservation solution containing dissolved hydrogen gas from a hydrogen-absorbing alloy canister improves function of transplanted ischemic kidneys in miniature pigs. *PloS One* (2019) 14(10): e0222863. doi: 10.1371/journal.pone.0222863
27. Nakao A, Noda K, Kawamura T, Kohama K, Yamada T, Kokubo K, et al. A new hydrogen administration method for cardiac graft preservation. *Organ Biol* (2014) 21(2):150–8. doi: 10.11378/organbio.21.150
28. Kawamura T, Momozane T, Funaki S, Funaki S, Bessho T, Shintani Y, et al. Relieving effect of hydrogen inhalation to donor lung on posttransplantational ischemia-reperfusion injury. *Organ Biol* (2015) 22(2):117–20. doi: 10.11378/organbio.22.117
29. Saito M, Chen-Yoshikawa TF, Takahashi M, Kayawake H, Yokoyama Y, Kurokawa R, et al. Protective effects of a hydrogen-rich solution during cold ischemia in rat lung transplantation. *J Thorac Cardiovasc Surg* (2020) 159 (5):2110–8. doi: 10.1016/j.jtcvs.2019.09.175
30. Meng C, Ma L, Niu L, Cui X, Liu J, Kang J, et al. Protection of donor lung inflation in the setting of cold ischemia against ischemia-reperfusion injury with carbon monoxide, hydrogen, or both in rats. *Life Sci* (2016) 151:199–206. doi: 10.1016/j.lfs.2016.03.015
31. Haam S, Lee JG, Paik HC, Park MS, Limet BJ. Hydrogen gas inhalation during ex vivo lung perfusion of donor lungs recovered after cardiac death. *J Heart Lung Transplant* (2018) 37(10):1271–8. doi: 10.1016/j.healun.2018.06.007
32. Tan M, Sun X, Guo L, Su C, Sun X, Xuet Z, et al. Hydrogen as additive of HTK solution fortifies myocardial preservation in grafts with prolonged cold ischemia. *Int J Cardiol* (2013) 167(2):383–90. doi: 10.1016/j.ijcard.2011.12.109
33. Noda K, Shigemura N, Tanaka Y, Kawamura T, Lim SH, Kokubo K, et al. A novel method of preserving cardiac grafts using a hydrogen-rich water bath. *J Heart Lung Transplant* (2013) 32(2):241–50. doi: 10.1016/j.healun.2012.11.004
34. Sekijima M, Sahara H, Miki K, Villani V, Ariyoshi Y, Iwanaga T, et al. Hydrogen Sulfide Prevents Renal Ischemia-Reperfusion Injury in CLAWN Miniature Swine. *J Surg Res* (2017) 219:165–72. doi: 10.1016/j.jss.2017.05.123
35. Kaneko N, Itoh K, Sugiyama A, Izumi Y. Microminipig, a Non-rodent Experimental Animal Optimized for Life Science Research: Preface. *J Pharmacol Sci* (2011) 115(2):112–4. doi: 10.1254/jphs.10r16fm
36. Ando A, Imaeda N, Matsubara T, Takasu M, Miyamoto A, Oshima S, et al. Genetic Association between Swine Leukocyte Antigen Class II Haplotypes and Reproduction Traits in Microminipigs. *Cells* (2019) 8(8):783. doi: 10.3390/cells8080783
37. Iwai S, Kikuchi T, Kasahara N, Teratani T, Yokoo T, Sakonju I, et al. Impact of normothermic preservation with extracellular type solution containing trehalose on rat kidney grafting from a cardiac death donor. *PloS One* (2012) 7(3):e33157. doi: 10.1371/journal.pone.0033157
38. Enosawa S, Kobayashi E. Controllable Immunosuppression in Pigs as a Basis for Preclinical Studies on Human Cell Therapy. In: S Miyagawa, editor. *Xenotransplantation - Comprehensive Study*. London: InTech Open Limited (2020). p. 113–121. doi: 10.5772/intechopen.89521
39. Cruz MV, Carney BC, Luker JN, Monger KW, Vazquez JS, Moffatt LT, et al. Plasma Ameliorates Endothelial Dysfunction in Burn Injury. *J Surg Res* (2019) 233:459–66. doi: 10.1016/j.jss.2018.08.027
40. Naesens M, Heylen L, Lerut E, Claes K, De Wever L, Claus F, et al. Intrarenal Resistive Index after Renal Transplantation. *N Engl J Med* (2013) 369 (19):1797–806. doi: 10.1056/NEJMoa1301064
41. Loupy A, Haas M, Solez K, Racusen L, Glotz D, Seron D, et al. The Banff 2015 Kidney Meeting Report: Current challenges in rejection classification and prospects for adopting molecular pathology. *Am J Transplant* (2017) 17 (1):28–41. doi: 10.1111/ajt.14107
42. Solez K, Axelsen RA, Benediktsson H, Burdick JF, Cohen AH, Colvin RB, et al. International standardization of criteria for the histologic diagnosis of renal allograft rejection: the Banff working classification of kidney transplant pathology. *Kidney Int* (1993) 44(2):411–22. doi: 10.1038/ki.1993.259
43. Ponticelli C, Moia M, Montagnino G. Renal allograft thrombosis. *Nephrol Dialysis Transplant* (2009) 24(5):1388–93. doi: 10.1093/ndt/gfp003
44. Dong Y, Zhang Q, Wen J, Chen T, He L, Wang Y, et al. Ischemic Duration and Frequency Determines AKI-to-CKD Progression Monitored by Dynamic Changes of Tubular Biomarkers in IRI Mice. *Front Physiol* (2019) 10:153. doi: 10.3389/fphys.2019.00153
45. Ponticelli C. Ischaemia-reperfusion injury: a major protagonist in kidney transplantation. *Nephrol Dial Transplant* (2014) 29(6):1134–40. doi: 10.1093/ndt/gft488
46. Ikeda M, Bando T, Yamada T, Sato M, Menjyu T, Aoyama A, et al. Clinical application of ET-Kyoto solution for lung transplantation. *Surg Today* (2015) 45(4):439–43. doi: 10.1007/s00595-014-0918-0
47. Song JW, Zullo J, Lipphardt M, Dragovich M, Zhang FX, Fu B, et al. Endothelial Glycocalyx-The Battleground for Complications of Sepsis and Kidney Injury. *Nephrol Dial Transplant* (2018) 33(2):203–11. doi: 10.1093/ndt/gfx076
48. Okada H, Takemura G, Suzuki K, Oda K, Takada C, Hotta Y, et al. Three-dimensional ultrastructure of capillary endothelial glycocalyx under normal and experimental endotoxemic conditions. *Crit Care* (2017) 21(1):261. doi: 10.1186/s13054-017-1841-8
49. Sato T, Mimuro S, Katoh T, Kurita T, Truong SK, Kobayashi K, et al. 1.2% Hydrogen Gas Inhalation Protects the Endothelial Glycocalyx During Hemorrhagic Shock: A Prospective Laboratory Study in Rats. *J Anesth* (2020) 34(2):268–75. doi: 10.1007/s00540-020-02737-3
50. Celie JW, Katta KK, Adepu S, Melenhorst WB, Reijmers RM, Slot EM, et al. Tubular epithelial syndecan-1 maintains renal function in murine ischemia/reperfusion and human transplantation. *Kidney Int* (2012) 81(7):651–61. doi: 10.1038/ki.2011.425
51. Murakami M, Hirano T. A four-step model for the IL-6 amplifier, a regulator of chronic inflammations in tissue-specific MHC class II-associated autoimmune diseases. *Front Immunol* (2011) 2:22. doi: 10.3389/fimmu.2011.00022
52. Takada Y, Kamimura D, Jiang JJ, Higuchi H, Iwami D, Hotta K, et al. Increased urinary exosomal SYT17 levels in chronic active antibody-mediated rejection after kidney transplantation via the IL-6 amplifier. *Int Immunol* (2020) 32(10):653–62. doi: 10.1093/intimm/dxaa032
53. Guo N, Su M, Xie Z, Wang K, Yuan H, Li M, et al. Characterization and comparative analysis of immunoglobulin lambda chain diversity in a neonatal porcine model. *Vet Immunol Immunopathol* (2018) 195:84–91. doi: 10.1016/j.vetimm.2017.12.002
54. Damasceno-Ferreira JA, Bechara GR, Costa WS, Pereira-Sampaio MA, Sampaio FJB, Souza DB, et al. The relationship between renal warm ischemia time and

glomerular loss. An experimental study in a pig model. *Acta Cir Bras* (2017) 32 (5):334–41. doi: 10.1590/s0102-865020170050000002

55. Tillet S, Giraud S, Kerforne T, Saint-Yves T, Joffrion S, Goujon JM, et al. Inhibition of coagulation proteases Xa and IIa decreases ischemia-reperfusion injuries in a preclinical renal transplantation model. *Transl Res* (2016) 178:95–106.e1. doi: 10.1016/j.trsl.2016.07.014
56. Tohyama S, Kobayashi E. Age-Appropriateness of Porcine Models Used for Cell Transplantation. *Cell Transplant* (2018) 28(2):224–8. doi: 10.1177/0963689718817477
57. Abe T, Li XK, Yazawa K, Hatayama N, Xie L, Sato B, et al. Transplantation. Hydrogen-rich University of Wisconsin solution attenuates renal cold ischemia-reperfusion injury. *Transplantation* (2012) 94: (1):14–21. doi: 10.1097/TP.0b013e318255f8be

Conflict of Interest: Co-authors of this manuscript, EK and MS, are medical advisors to Doctors Man Co., Ltd.

The remaining authors declare that the research was conducted in the absence of any commercial or financial relationships that could be construed as a potential conflict of interest.

frontiers in Immunology

ORIGINAL RESEARCH
published: 24 February 2021
doi: 10.3389/fimmu.2021.634368

Artemisinin Attenuates Transplant Rejection by Inhibiting Multiple Lymphocytes and Prolongs Cardiac Allograft Survival

Zhe Yang†, Fei Han†, Tao Liao†, Haofeng Zheng, Zihuan Luo, Maolin Ma, Jiannan He, Lei Li, Yongrong Ye, Rui Zhang, Zhengyu Huang, Yannan Zhang* and Qiquan Sun**

Research Institute of Organ Transplantation, The Third Affiliated Hospital of Sun Yat-sen University, Guangzhou, China

OPEN ACCESS

Edited by:
Hao Wang,
Tianjin Medical University General Hospital, China

Reviewed by:
Xiaopeng Hu,
Capital Medical University, China
Helong Dai,
Central South University, China

***Correspondence:**
Qiquan Sun
sunqiq@mail.sysu.edu.cn
Yannan Zhang
zhangyannanyn@163.com
Zhengyu Huang
h_zhengyu@163.com

†These authors have contributed equally to this work

Specialty section:
This article was submitted to Alloimmunity and Transplantation, a section of the journal Frontiers in Immunology

Received: *27 November 2020*
Accepted: *07 January 2021*
Published: *24 February 2021*

Citation:
Yang Z, Han F, Liao T, Zheng H, Luo Z, Ma M, He J, Li L, Ye Y, Zhang R, Huang Z, Zhang Y and Sun Q (2021) Artemisinin Attenuates Transplant Rejection by Inhibiting Multiple Lymphocytes and Prolongs Cardiac Allograft Survival. Front. Immunol. 12:634368. doi: 10.3389/fimmu.2021.634368

Immunological rejection is an important factor resulting in allograft dysfunction, and more valid therapeutic methods need to be explored to improve allograft outcomes. Many researches have indicated that artemisinin and its derivative exhibits immunosuppressive functions, apart from serving as a traditional anti-malarial drug. In this assay, we further explored the therapeutic effects of artemisinin for transplant rejection in a rat cardiac transplantation model. We found that it markedly attenuated allograft rejection and histological injury and significantly prolonged the survival of allograft. Upon further exploring the mechanism, we demonstrated that artemisinin not only attenuated T cell-mediated rejection (TCMR) by reducing effector T cell infiltration and inflammatory cytokine secretion and increasing regulatory T cell infiltration and immunoregulatory cytokine levels, but also attenuated antibody-mediated rejection (ABMR) through inhibition of B cells activation and antibody production. Furthermore, artemisinin also reduced macrophage infiltration in allografts, which was determined to be important for TCMR and ABMR. Moreover, we demonstrated that artemisinin significantly inhibited the function of pure T cells, B cells, and macrophages *in vitro*. All in all, this study provide evidence that artemisinin significantly attenuates TCMR and ABMR by targeting multiple effectors. Therefore, this agent might have potential for use in clinical settings to protect against transplant rejection.

Keywords: artemisinin, cardiac transplantation, transplant rejection, T cell-mediated rejection, antibody-mediated rejection

INTRODUCTION

Cardiac transplantation has become the gold-standard long-term medical treatment for end-stage heart failure and has achieved remarkable success (1). However, its biggest challenge is concomitant rejection, resulting from interactions between the recipient immune system and allograft. Immune responses could result in the rejection to cardiac allografts, which including chronic rejection (CR) and acute rejection (AR). And AR is a leading cause to the development of CR (2). Furthermore, transplant rejection mainly consists of T cell-mediated rejection (TCMR) and antibody-mediated

rejection (ABMR) (3). Although immunosuppression has achieved good results for TCMR therapy, side effects such as infection and graft toxicities are likely to be a significant impact on patient prognosis (4). Moreover, ABMR, caused by donor-specific antibodies (DSAs), has emerged as an important immunological barrier to successful transplantation (5, 6). Current therapeutic strategies for ABMR focus on removing the generated antibodies in the peripheral blood, or eliminating B cells to inhibit the generation of antibodies, but these strategies are not as effective as expected (7). Therefore, more effective and safe strategies must be explored to improve transplant outcomes.

Artemisinin ($C_{15}H_{22}O_5$, ART), derived from sweet wormwood (Artemisia annua L), has been used to treat malaria in China for a long time. Taking the high safety without noticeable side effects and adverse reactions into consideration, ART has been used to treat millions patients in the world (8). Recently, ART and its derivatives were found to have other properties, including immunosuppressive and anti-inflammatory effects (9).

ART and its derivatives exhibit immunosuppressive and against inflammation *via* regulation of the immune system, inhibiting T lymphocyte proliferation, enhancing Treg differentiation, and increasing the proliferation of Treg (10–12). Dihydroartemisinin (derivative of ART) treatment also decreases autoantibodies in lupus model (13). However, as ART could obviously inhibit the activation and proliferation of T cells, the decrease of antibody level was considered as a secondary effect on the inhibition of T cells. and the direct effects of these drugs on B cells (especially for DSAs) are unclear. Moreover, ART can to regulate innate immune cells. Studies have indicated that ART significantly reduces peritoneal macrophage phagocytosis and the phagocytic index *in vivo* and can also inhibit monocyte/macrophage adhesion to HUVECs to protect against the development of early atherosclerotic lesions (14, 15). To date, the anti-inflammatory and immunosuppressive properties of ART have been discussed, but their effect on immunological rejection has not been reported.

Therefore, here, we investigated the therapeutic effects of ART on rejection, including TCMR and ABMR, using a rat cardiac transplantation model, providing a novel therapy choice for the patients undergoing transplant rejection.

MATERIALS AND METHODS

Reagents

ART (purity: 99.83%, Selleck Chemicals, California, USA) was dissolved in DMSO at 100 mM for storage and use. Antibodies used for immunohistochemical staining included anti-CD3 (ab16669,1:800), anti-CD8 (ab217344,1:400), anti-CD68 (ab31630, 1:1600), anti-Foxp3 (ab22510, 1:400; all from Abcam, Cambridge, England), anti-CD4 (Cell Signaling Technology, Shanghai, China; D7D2Z, 1:800), and anti-rat C4d (Hycult Biotech, Uden, Netherlands; HP8034, 1:400). Anti-rat antibodies for flow cytometry were from BioLegend, including CD45-Pacific Blue, CD3-FITC, CD4-APC/Cy7, CD8a-PerCP, and CD11b- PE/Cy7. B220-PE was purchased from Thermo Fisher.

Experimental Protocol and Groups

The model of cardiac allograft transplant rejection was established by transplanting Brown Norway (BN) hearts into Lewis recipient rats. Recipients were random assigned to two groups as follows: (a) ART (n=6), ART was diluted in peanut oil (100 g/L) and administered intragastrically daily at 22 mg/kg/day from day 0 until cardiac graft rejection; (b) control (n=6), an equal volume of peanut oil was applied to vehicle-treated recipients. Cardiac Lewis-to-Lewis rat transplantation served as the isograft control (n=5), and these animals all received a daily equal volume of peanut oil administered intragastrically. For rats only undergoing skin transplantation, animals were divided into two groups as follows: (1) ART, ART was fed intragastrically (22 mg/kg/day) from day 0 to day 36 post skin transplantation; (2) control, an equal volume of peanut oil was applied to control group animals every day.

Subjects and Animals

Peripheral blood was obtained from healthy volunteers between the ages of 18 and 26 years who were acquired from Sun Yat-sen University. All subjects signed informed consent forms and our study was approved by the Ethical Committee of Sun Yat-sen University.

Male rats weighing 200–250 g were obtained from Vital River Laboratory Animal Technology Co., Ltd. Animals used in this assay were proved by the Sun Yat-sen University Institutional Ethical Guidelines and consistent with the Guide for the Care and Use of Laboratory Animals.

Rat Skin Transplantation

For skin transplantation, the donor rat was anesthetized with isoflurane, the tail was excised, and full-thickness tail skin was obtained. The recipient was anesthetized, and full-thickness skin grafts (1–2.0 × 2 cm^2) were acquired from BN donors. The grafts were then transplanted onto the dorsal area of Lewis rats with an 8–0 nylon suture.

Rat Heterotopic Cardiac Transplantation

Detailed processes of cardiac transplantation were described previously (16, 17). Briefly, the pulmonary artery and ascending aorta of the heart were anastomosed end-to-end to the vena cava and abdominal aorta, respectively. Survival of cardiac graft function was judged everyday by abdominal palpation. Rejection was defined as total cessation of contractions.

Detection of Circulating Donor-Specific Antibodies

Graft recipient sera were obtained at the indicated time points. Circulating DSA (IgM and IgG) was evaluated using flow cytometry. Briefly, donor splenocytes were incubated with recipient sera for 30 min at 37°C, washed, and then incubated with anti-rat IgM and IgG (Bio Legend) for 1 h at 4°C. The mean fluorescence intensity was used to reflect individual DSAs.

Histology and Immunohistochemistry

Five days post cardiac transplantation, cardiac grafts were fixed and embedded. Hematoxylin and eosin (H&E), anti-CD3, anti-CD4, anti-CD8, anti-CD68, and anti-Foxp3 were used for further assessment. Sections were examined by light microscopy to evaluate the pathologic features of cardiac allografts. For TUNEL staining, the one-step TUNEL apoptosis assay kit (Roche TMR-RED; 12156792910) was used and strict limited to the protocol. Sections were counterstained with DAPI to label nuclei. Fields containing both the rejection area and the normal zone were scanned.

Flow Cytometry

Fresh recipient cardiac grafts or spleens were digested in RPMI 1640 with collagenase 1 and DNAse for 60 min at 37°C. Thereafter, cells were stained using antibodies for CD45, CD11b, B220, CD3, CD8a, and CD4, results were analyzed using a CytoFLEX flow cytometer (Beckman Coulter).

Quantitative Real-Time Polymerase Chain Reaction

mRNA levels were determined using RT-qPCR. RNA was acquired from fresh tissues or cells using TRIzol reagent (Invitrogen, USA). PrimeScript RT master mix (TAKARA, Japan) was used for reversing transcribed. SYBR Green I master mix (Roche, Switzerland) was used for RT-qPCR in a LightCycler480 system (Roche), with *GAPDH* as an internal control. Detailed Primers used could be found in **Table 1**.

Isolation and *In Vitro* Culture of T Cells, B Cells, and Macrophages

Corresponding microbeads (Miltenyi Biotec, Germany) were used for cells isolation from peripheral blood mononuclear cells (PBMCs). Flow cytometry was used for determining purity of the cells, and the purity was consistently >95%.

In the presence or absence of ART, purified T-cells ($CD3^+$ cells) were incubated for 48 h with anti-CD3 plus anti-CD28, purified B-cells ($CD19^+$ cells) were incubated for 9 days with anti-CD40L plus anti-IgM, and purified macrophages ($CD14^+$ cells) were incubated for 48 h with LPS (lipopolysaccharide). PBMCs and isolated cells were cultured in RPMI-1640 (100 U/ml penicillin,10% FBS, and 100 mg/ml streptomycin) at 37°C with 5% CO_2.

TABLE 1 | List of primers used for qPCR.

Gene	Forward primer	Reverse primer
CD3	TTCAAGATAGAAGTGGTTGAATATG	CACCTCCTTCGCCAGCTCC
CD4	TGTGTCAGGTGCCGGCACCAACAG	GTGGGGCCCAGGCCTCATATG
CD8	AGGGAATGGGATTGGGCTTCGC	CTCTGAAGGTCTGGGCTTGAC
CD19	CACCCATGGTTCATTGCCCA	GCACAACATTGTCTCCCTCTTC
Foxp3	TGCAGCTCCGGCAACTTTTC	TGTCTGAGGCAGGCTGGATA
IL-1β	CAGCTTTCGACAGTGAGGAGA	TTGTCGAGATGCTGCTGTGA
IL-2	GCAGGCCACAGAATTGAAAC	CCAGCGTCTTCCAAGTGAA
IL-6	CTTCCAGCCAGTTGCCTTCT	GACAGCATTGGAAGTTGGGG
IL-10	TGCTATGTTGCCTGCTCTTACTG	TCAAATGCTCCTTGATTTCTGG
IL-17	GGAGAATTCCATCCATGTGCC	GGCGTTTGGACACACTGAAC
IFN-γ	ATCCATGAGTGCTACACGCC	TCGTGTTACCGTCCTTTTGC
TGF-β	TTGCTTCAGCTCCACAGAGA	TGGTTGTAGAGGGCAAGGAC
GAPDH	CATCAACGACCCCTTCATTGA	ACTCCACGACATACTCAGCACC

Assessment of Apoptosis

An annexin V apoptosis detection kit (R&D Systems) was used for apoptosis detection according to the manufacturer's instructions using flow cytometry (BD, San Diego, CA).

Enzyme-Linked Immunosorbent Assay

Commercially available ELISA kits used to measure IFN-γ, IL-1β, or Ig levels in *in vitro* culture system supernatants as follows: IFN-γ, IL-1β, IgG, and IgM ELISA kits from Thermo Fisher (San Diego, CA, USA, catalog:88-7316-88, 88-7261-88, 88-50550, and 88-50620).

Statistical Analysis

The KS normality test was first used to test if the data were normally distributed; all data met this criterion. The Student's t tests were used for analysis of significant differences. The log-rank test was used for graft survival. Data are expressed as the mean ± standard deviation (SD). Statistical analyses were performed using Prism (GraphPad). $^*P < 0.05$ was considered significant.

RESULTS

ART Reduces Rejection and Prolongs Cardiac Allograft Survival

Recipients treated with ART had longer graft survival than controls (17.33 ± 4.89 vs 6.83 ± 0.75 days); approximately 66% of grafts in the ART group survived over 2 weeks, while survival time of grafts were less than 8 day in the control group (**Figure 1A**). Subsequently, allografts were harvested on day 5 after cardiac transplantation. As shown by representative H&E photomicrographs, the rejection area of the ART group was noticeably thinner than that of the control group. Interstitial vasculitis, hemorrhage, and edema were evident in the control group, which were significantly diminished by ART treatment (**Figure 1B**). Moreover, TUNEL staining revealed apoptotic cells (red) in the ART group were significantly less than that in the control group, especially in the rejection area. DAPI staining (blue) indicated that nuclei in the control group were deformed and broken, which indicated that more cells were in a state of apoptosis. Together, these data indicate that ART reduced rejection and protected cardiomyocytes (**Figure 1C**).

ART Attenuates T Cell-Mediated Rejection, and Increasing Regulatory T Cell Infiltration in Allografts

Five days after transplantation, inflammatory cell ($CD45^+$) frequencies and numbers were significantly lower in the cardiac grafts obtained from the ART group compared with the control group (**Figures 2A–C**). As shown in **Figures 2D–K**, infiltrative $CD3^+$, $CD3^+$ $CD4^+$, and $CD3^+$ $CD8^+$ cell numbers were significantly less in cardiac grafts of the ART group than in

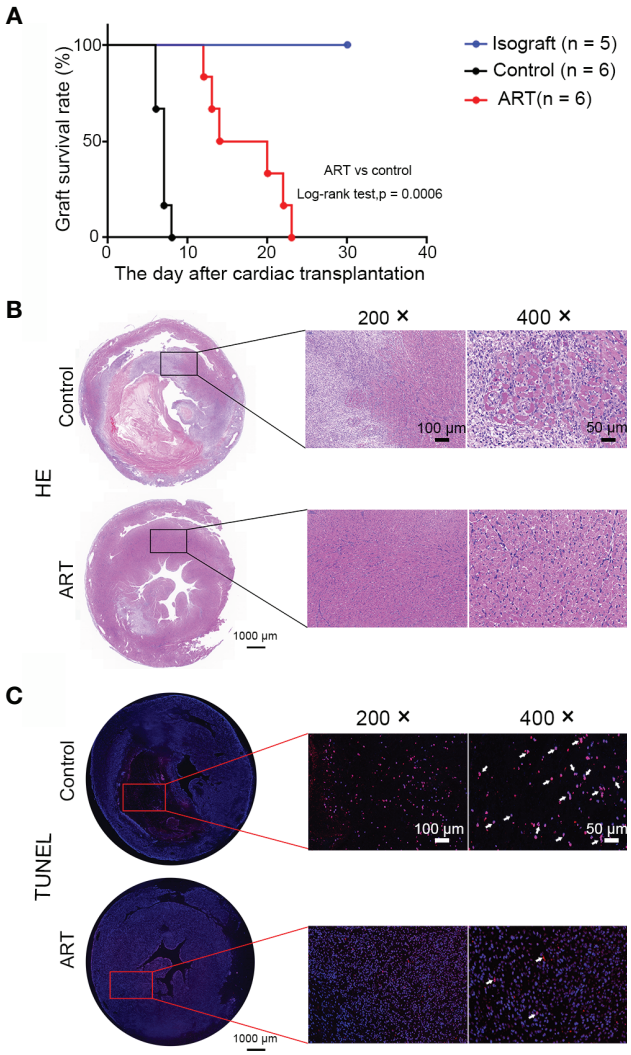

FIGURE 1 | Artemisinin (ART) reduces inflammatory infiltration, myocyte damage, and apoptosis of cells to prolong cardiac allograft survival. **(A)** ART significantly prolonged allograft survival compared to that in controls. **(B)** Histologic evaluation of cardiac allografts post-transplant. Hematoxylin and eosin staining showing interstitial vasculitis, hemorrhage, edema, and myocyte damage. **(C)** Representative images of heart sections showing TUNEL-positive cells (red, arrowheads indicated) in the rejection area; nuclei are stained with DAPI (blue). TUNEL, (TdT)-mediated nick end-labeling; DAPI, 4',6-diamidino-2-phenylindole.

those of the control group, although the percentages of these cells did not change significantly. As shown by representative IHC stains, ART treatment significantly decreased the infiltration of T cells (**Figures 2L–N**), and the results showed the same trend as flow cytometry results. Intriguingly, ART treatment also dramatically enhanced Treg cell (Foxp3$^+$) expansion based on IHC results (**Figure 2O**). Additionally, mRNA levels of the T cell-associated genes *IL-2*, *IFN-γ*, *CD3*, *CD8*, *CD4*, and *IL-17* were significantly reduced following ART treatment (**Figures 3A–F**). Furthermore, those of Treg cell-associated genes, *Foxp3*, *IL-10*, and *TGF-β*, were significantly elevated (**Figures 3G–I**).

ART Inhibits B Cells Activation and Donor-Specific Antibodies Production and Attenuates Allograft Antibody-Mediated Rejection

ABMR, caused by B cell activation and DSA production, is an important factor in allograft dysfunction. By flow cytometry, we examined B cell (B220$^+$) populations in spleens and allografts of recipients obtained 5 days after transplantation and quantitatively analyzed frequencies and cell numbers. Although there was no effect on B cell frequencies, ART treatment decreased the number of B cells in the spleens and cardiac grafts compared with the control group (**Figures 4A–F**). Furthermore, changes in DSA levels (IgG and IgM) at 0 and 5 days after cardiac transplantation were detected; ART treatment conspicuously inhibited this upward trend (**Figure 4G**). No significantly difference was found regarding the levels of IgM between the ART -treated and control groups (**Figure 4H**). To further explore the influence of ART on DSAs, we established a rat skin transplant model. Levels of IgG increased at day 8 post skin transplantation gradually, whereas ART significantly inhibited the upward trend, with 16.1%, 22.3%, 22.8%, 30.8%, 35.5%, 43.9%, 47.7%, and 51.2% reductions at days 8, 12, 16, 20, 24, 28, 32, and 36, respectively (**Figure 4I**). On the contrary, limited response was found regrading IgM levels post skin allograft transplantation (**Figure 4J**). Moreover, ART treatment significantly reduces diffuse C4d and IgG deposition in capillaries (**Figure 4K**).

ART Reduces Macrophage Infiltration Into Allografts

According to the diagnosis of heart rejection, interstitial mononuclear and macrophage cell infiltration is the typical feature of AR, and macrophage is of vital importance in the development of TCMR and ABMR (18, 19). Therefore, macrophage infiltration in the allografts were detected. Less frequencies of macrophages (CD11b$^+$) were found in the ART -treated group than the control group (49.34 ± 5.77% vs. 60.16 ± 7.76%, $P < 0.05$), and macrophage numbers were reduced more clearly (**Figures 5A–C**). Representative histological analysis also revealed ART treatment inhibited infiltration of CD68 cells (**Figures 5D, E**). Moreover, levels of pro-inflammatory cytokines (*IL-6* and*IL-1β*) were decreased in the ART group when compared with the control group, indicating that macrophage function was inhibited by ART treatment (**Figures 5F, G**).

Artemisinin Significantly Suppresses T Cell, B Cell, and Macrophage Function *In Vitro*

To further explore mechanisms underlying the suppression of lymphocyte function by ART, we performed *in vitro* assays using PBMCs. Because ART can induce apoptosis, to exclude the potential confounding effects of reduced cytokine secretion, which might result from apoptosis, we independently assessed the proapoptotic effect of ART on total lymphocytes. Specifically, PBMCs were cultured with ART at concentrations ranging from

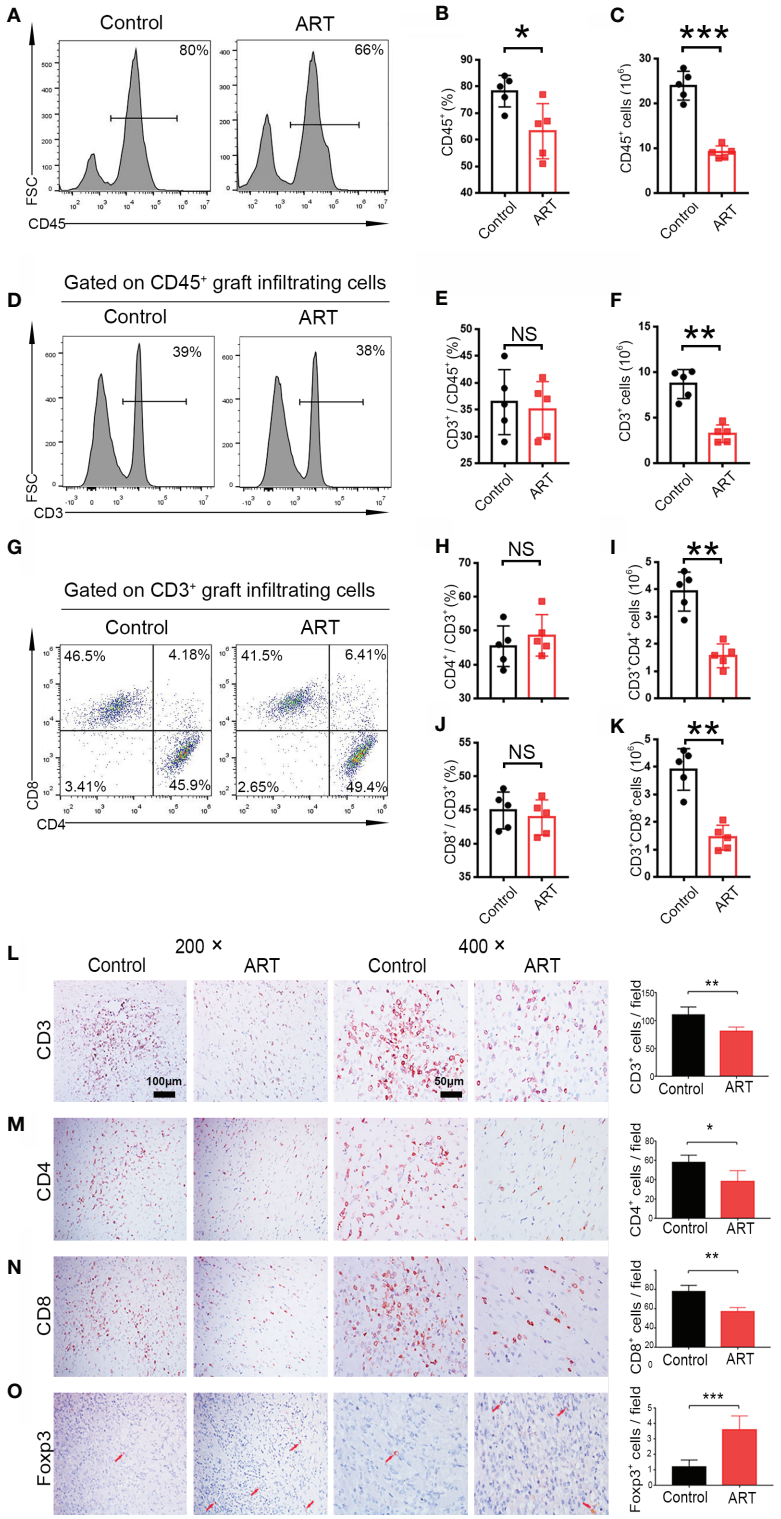

FIGURE 2 | Artemisinin (ART) reduces T cell infiltration in cardiac allografts. Lymphocytes ($CD45^+$), T cells ($CD3^+$), $CD4^+$ T cells ($CD3^+CD4^+$), and $CD8^+$ T cells ($CD3^+CD8^+$) in cardiac allografts were detected by flow cytometry. Representative histograms and quantitative analysis of frequencies and counts of lymphocyte cells **(A–C)**, T cells **(D–F)**, $CD4^+$ T cells and $CD8^+$ T cells in allografts **(G–K)** (n = 5/group). **(L–O)** Representative immunohistochemistry staining images and results of quantitative analysis of cell numbers/view based on CD3, CD4, CD8, and Foxp3 in the Control and ART groups (n = 5/group). Magnification: 200× and 400×. *$P < 0.05$; ** $P < 0.01$; *** $P < 0.001$. NS, no significance.

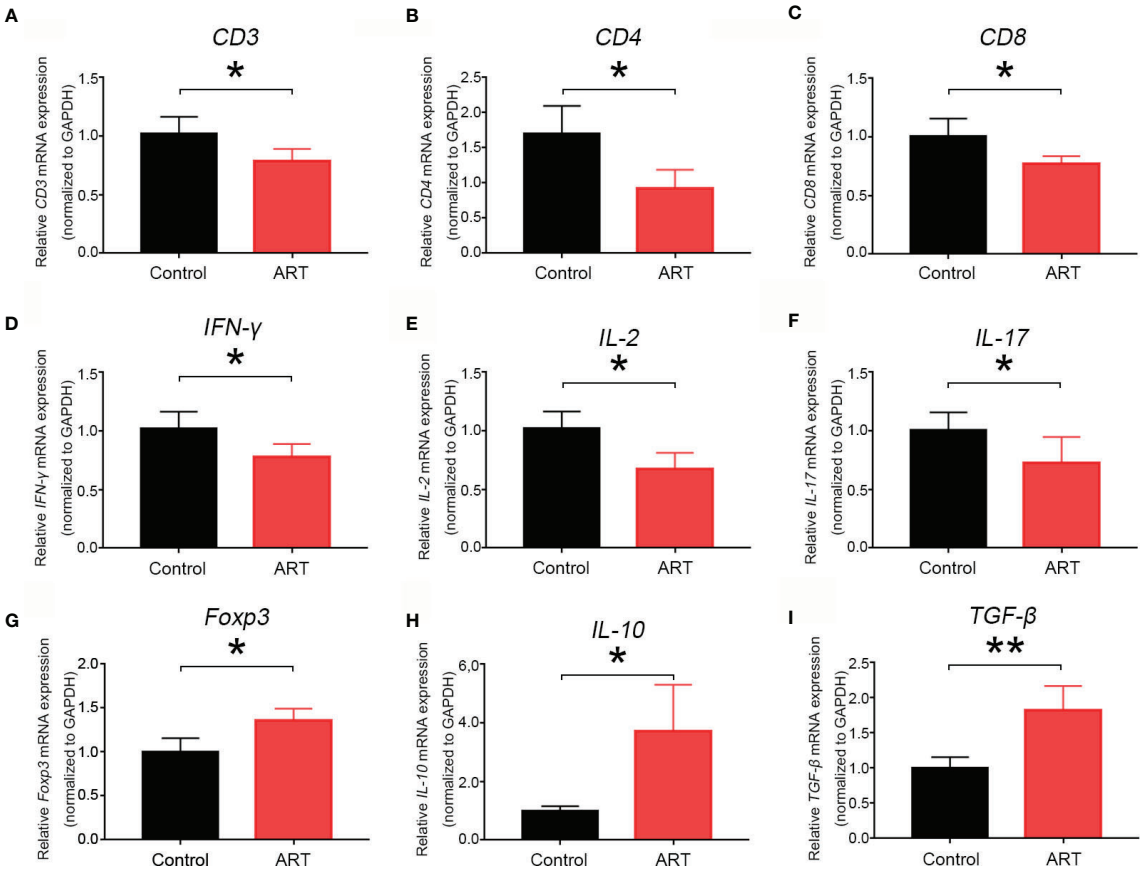

FIGURE 3 | Artemisinin (ART) inhibits mRNA expression levels of T cell-associated markers and pro-inflammatory cytokines and promotes mRNA expression of Treg- associated cytokines. The mRNA expression of T cell-associated markers **(A–C)**, T-cell-associated pro-inflammatory cytokines **(D–F)**, and Treg-associated cytokines **(G–I)** were determined by qPCR. The mRNA levels were normalized to those of *GAPDH*. Three independent experiments were performed showing similar results. * $P < 0.05$; ** $P < 0.01$.

2 to 500 μM for 24 h, and PI-Annexin V staining was performed to evaluate cell survival. ART promoted apoptosis in a dose-dependent manner (**Figure 6A**). Finally, our results showed that at 20 μM, the pro-apoptotic effect of ART was mild, while apoptosis occurred when cells were cultured over 20 μM ART (**Figure 6B**). Moreover, measurements of ART (20 μM)-induced cell death overtime revealed the rapid accumulation of annexin V^+PI^- cells at the early stage of culture, which transitioned to annexin V^+PI^+ cells over time (**Figure 6C**). Therefore, subsequent *in vitro* experiments were performed with a range of ART centered around 20 μM.

Next, we purified specify cells, including B cells ($CD19^+$), T cells ($CD3^+$), and monocytes ($CD14^+$) from human peripheral mononuclear leukocytes and cultured them with different ART concentrations to evaluate cytokine secretion *in vitro*. As shown in **Figure 6D**, purified $CD3^+$ T cells from PBMCs produced high levels of IFN-γ following stimulation of anti-CD3 plus anti-CD28. Further, cytokine productions were inhibited by ART in a dose-dependent manner. A significant inhibitory effect was observed at 10 μM, and a decrease in cytokines was induced at higher concentrations (~100 μM). B cells ($CD19^+$) purified from PBMCs were stimulated with CD40L and anti-IgM for 9 days with or without ART at different concentrations and supernatant IgG and IgM levels were evaluated by ELISA. ART also inhibited IgG production in a dose-dependent manner at 10 μM. Except for with 100 μM ART, IgM levels were not significantly changed (**Figures 6E, F**). As mentioned, purified $CD14^+$ cells produced high levels of IL-1β following LPS stimulation. However, ART, from 10 to 100 μM, significantly inhibited this in a dose-dependent manner (**Figure 6G**).

DISCUSSION

ART and its derivatives are associated with potent immunosuppressive function and have been involved in some clinical trials dealing with autoimmune diseases (20, 21). Here, we provide the first evidence demonstrating the effect of ART on transplant immunity using a rat cardiac transplantation model. Specifically, it significantly inhibited rejection by targeting multiple effectors, attenuated allograft injury, and thus prolonged cardiac allograft survival.

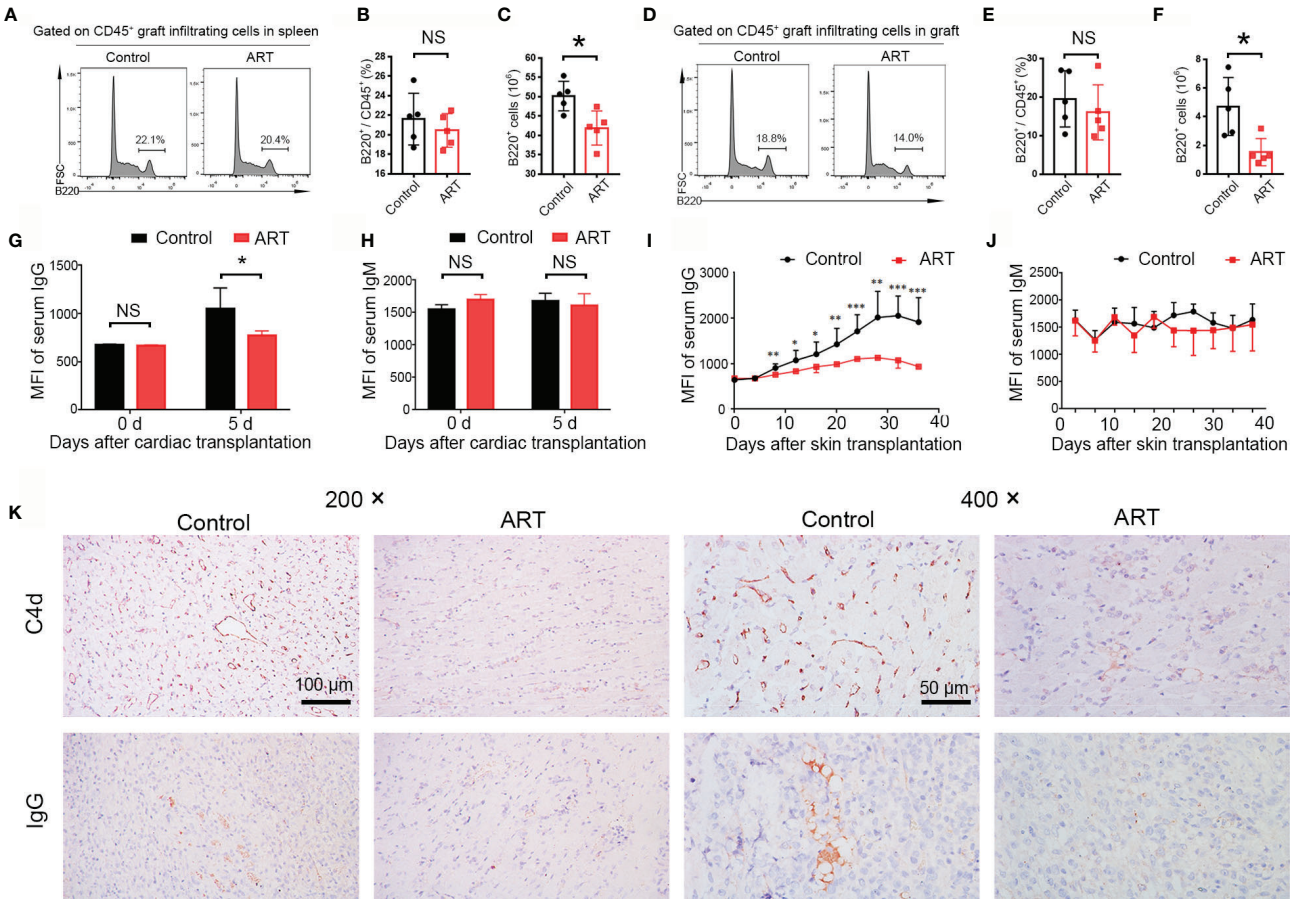

FIGURE 4 | Artemisinin (ART) attenuates antibody-mediated rejection *via* the inhibition of B cell and donor specific antibody (DSA) production. **(A–F)** B cells ($B220^+$) were detected by flow cytometry in fresh spleens and allografts on day 5 after cardiac transplantation. Representative histograms showing the frequencies and counts of B cells in host spleens **(A–C)** and cardiac grafts **(D–F)** are presented. **(G, H)** Changes in DSA levels (IgG and IgM) on day 0 and 5 after cardiac transplantation (n = 5). **(I, J)** Changes in DSA levels (IgG and IgM) after Lewis rats that received skin allografts from BN donors were treated with (ART group) or without ART (control group) for 36 days. **(K)** Representative immunohistochemistry stained images showing the deposition of C4d and IgG. Magnification: 200× and 400×. * $P < 0.05$; ** $P < 0.01$; *** $P < 0.001$. NS, no significance.

Currently, transplant rejection is recognized as a dangerous factor for allograft loss (22). Thus, sustainable treatment of rejection remains critical for long-term graft function. Although immunosuppressive therapy has dramatically prolonged the lives of patients, the notable problems associated with these drugs remain. First of all, significant toxicities which affect allograft survival should be taken into consideration. Second, their long-term use inevitably increases infection risks and it might lead to death, especially in the first year post-transplantation (23). Therefore, safe and effective immunosuppression in clinical practice is expected.

Fully MHC-mismatched cardiac transplantation was used to establish a rat transplant rejection model. Rejection diagnosis and classification were based on histological changes, which occur with allograft injury, and inflammatory cell infiltration, and experiments have indicated that rejection is a mix of humoral and cellular rejection (24). In this assay, macrophages and T cells were the major subsets of immune cells infiltrating into the grafts, in accordance with previous results (25). We also observed B cell infiltration and C4d and IgG deposition in the allografts, suggesting that ABMR was involved in rejection in this model. Further, ART significantly attenuated TCMR and ABMR by inhibiting T cell, B cell, and macrophage activation and infiltration. More importantly, approximately 66% of recipients administered ART survived beyond 14 days without combinations with any other drugs or strategies, this is unprecedented.

T cell is of vital importance in rejection post allogeneic transplantation. Recognize allo-antigens by T cell is the primary basis for allograft rejection (23). ART and its derivative were shown to inhibit T lymphocytes. Wang et al. demonstrated that artemether (an ART derivative) has direct inhibitory effects on T cells, suppressing T cell proliferation and activation *via* the Ras–Raf1–ERK1/2 (11). Another study found that SM934 (an ART derivative) inhibits the accumulation and differentiation of Th1 and Th17 cells and induces the differentiation and expansion of Treg cells (26). In our study, all cardiac grafts were rejected within

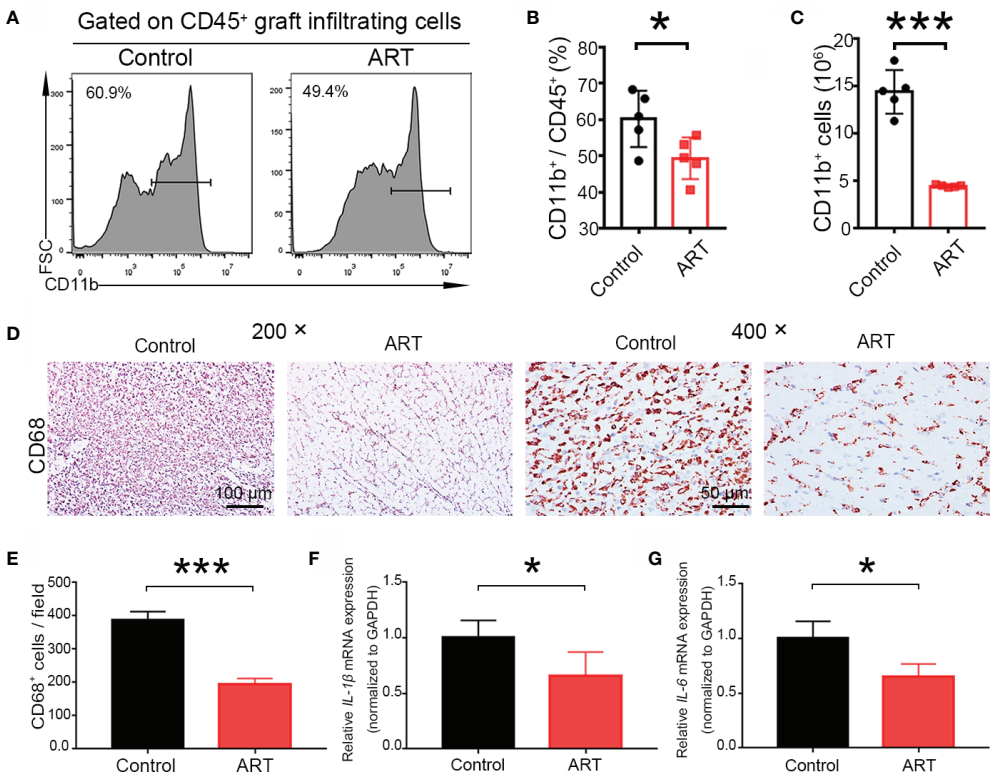

FIGURE 5 | Artemisinin (ART) suppresses the number and function of macrophages *in vivo*. **(A–C)** Macrophages ($CD11b^+$) were detected by flow cytometry in allografts on day 5 after cardiac transplantation, and the representative histograms for frequencies and counts of macrophages in cardiac grafts **(D, E)** are shown. Representative immunohistochemistry staining images and quantitative analysis of cell number/view, based on CD68, in the control and ART groups (n = 5/group). **(F, G)** ART inhibited the mRNA expression of *IL-1β* and *IL-6*. The mRNA levels were normalized to those of *GAPDH*. Three independent experiments were performed showing similar results. Data were expressed as the mean ± SD. * $P < 0.05$; *** $P < 0.001$. Magnification: 200× and 400×.

8 days post transplantation when no other interventions were applied. Flow cytometric and histological analysis showed that ART treatment significantly inhibited infiltration of lymphocytes, especially effector T cells, in allografts and reduced inflammatory cytokine secretion. Moreover, functions of pure T cells were inhibited by ART *in vitro* in a dose-dependent manner. These results indicated that ART could significantly inhibit the occurrence of TCMR. Intriguingly, ART treatment also dramatically enhanced the expansion of Treg cells, which play a central role in transplant tolerance. This is consistent with other assays and our previously published data showing that Treg cell therapy could significantly alleviate renal allograft injury and induce immune tolerance in animal and clinical trials (27, 28). Our data thus showed that ART could effectively inhibit TCMR and induce Treg cell expansion.

ABMR occurs when recipients are presensitized to donor antigens before surgery or due to *de novo* DSA production post-operatively. B cells are the main effectors of ABMR. To explore the changes in B cells, we first observed that ART decreased these cell numbers in recipient spleens and allografts. Although function of infiltration B cell in grafts is a mystery, Hippen et al. demonstrated that B cells might be involved in the deterioration of allograft function and anti-donor antibody production (29). These data provided evidence that infiltration of B cell as a critical parameter of ABMR. Therefore, ART treatment could reduce B cell infiltration in the recipient spleen and allografts.

Although some studies have demonstrated that ART family drugs reduce antibodies in a model of systemic lupus erythematosus, it was not known if ART could decrease DSAs with organ transplantation (13, 30). We generated a new animal model of BN skin transplantation into Lewis recipients to detect changes in DSAs in the circulation of different treatment groups. This study, for the first time, demonstrated that ART dramatically reduces circulating DSA-IgG levels in this model. Moreover, the changes in DSA-IgG levels at 0 and 5 days after cardiac transplantation were similar. Histological changes, including IgG and C4d were decreased in ART-treated group. Current therapeutic strategies to control DSAs are focused on antibody removal with plasma exchange, intravenous immunoglobulin, and monoclonal antibodies (31, 32). However, these strategies also have some limitations, although a combination of multiple strategies could contribute to a synergistic effect (33, 34). Owing to its excellent suppressive effects on production of DSAs, ART might be an economical and effective choice for therapy of AMR in clinical settings.

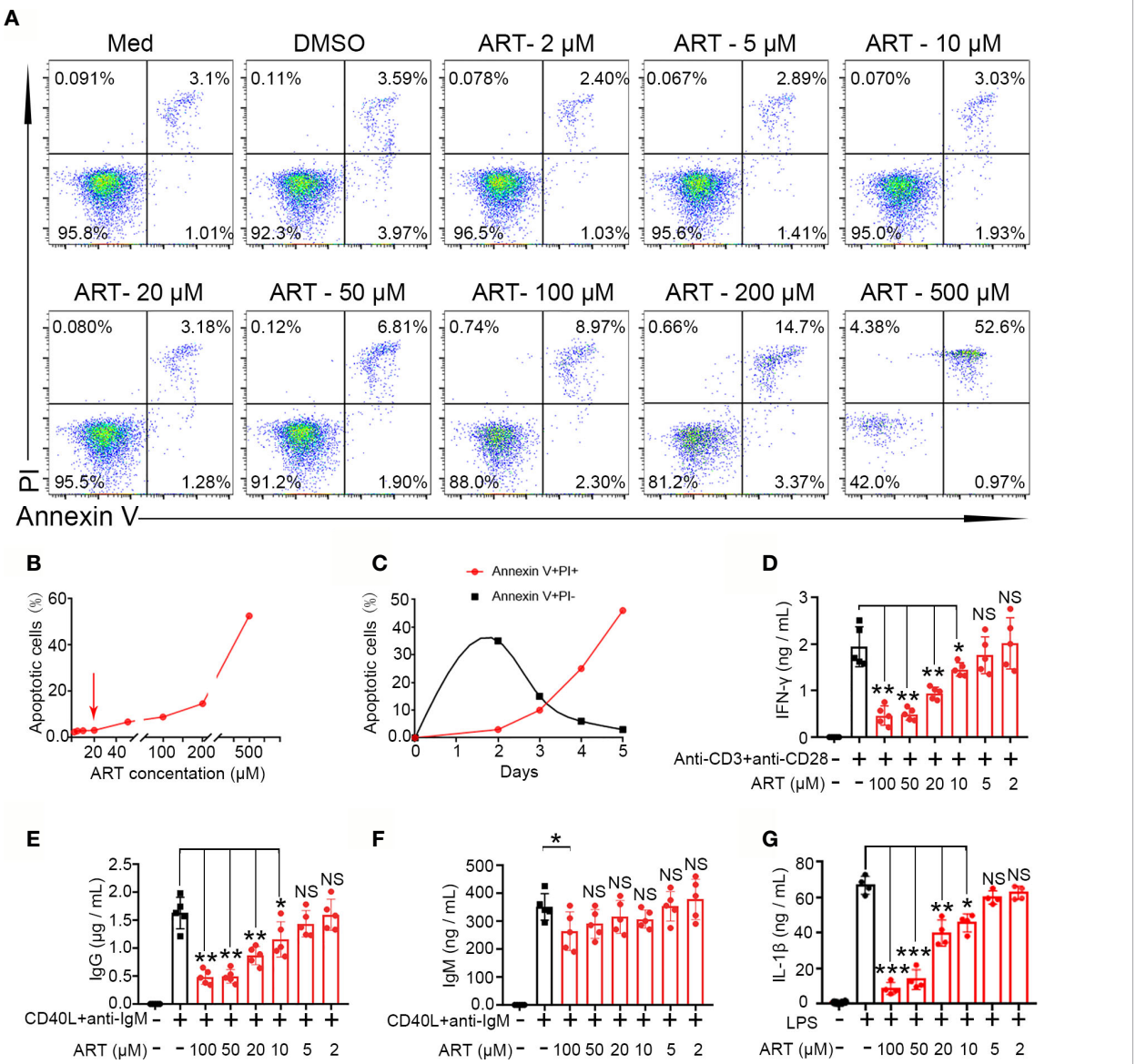

FIGURE 6 | Artemisinin (ART) inhibits T cell, B cell, and macrophage differentiation and reduces cytokines secretion *in vitro*. **(A, B)** Effect of ART on cell apoptosis was assessed by PI staining. **(C)** The dynamics of cell death induced by ART (20 μM) were measured by PI and annexin V staining. **(D)** Purified $CD3^+$ T cells from PBMCs were stimulated with or without anti-CD3 plus anti-CD28 (1 μg/ml) in the presence or absence of various concentrations (2 to 100 μM) of ART. The cell culture supernatants were collected at 48 h and the level of IFN-γ was measured by ELISA (n = 5). **(E, F)** Purified $CD19^+$ cells from PBMCs were stimulated with or without CD40L (1 μg/ml) plus anti-IgM (5 μg/ml) in the presence or absence of various concentrations (2 to 100 μM) of ART. The cell culture supernatants were collected at 9 days and the levels of IgG and IgM were measured by ELISA (n = 5). **(G)** Purified $CD14^+$ T cells from PBMCs were stimulated with or without LPS (1 μg/ml) in the presence or absence of various concentrations (1 to 20 μM) of ART. The cell culture supernatants were collected at 48 h and the levels of IL-1β were measured by ELISA (n = 5). Statistical results are shown as the mean ± SD. *$P < 0.05$; **$P < 0.01$, ***$P < 0.001$. PI, propidium iodide; PBMC, peripheral blood mononuclear cell; ELISA, enzyme linked immunosorbent assay. NS, no significance.

Apart from adaptive immune cells, other innate immune cells including macrophages, monocytes, and NK cells infiltrate allografts during rejection and were proven to aggravate allograft injuries (18, 35, 36). Moreover, macrophages are important innate immune cells; in human cardiac transplants, the infiltrates associated with rejection are predominantly composed of mononuclear cells and macrophages with macrophages outnumbering T cells, especially in the prophase of rejection (37, 38). Moreover, recent studies have found that innate myeloid immune cells, such as macrophages and monocytes, can form antigen-specific immune memory and thus serve as an central component in immune rejection (39). All of these results indicate that macrophage is of vital importance during transplantation immune response. Accordingly, our results showed that

macrophages were outnumbered T cells, and ART treatment could significantly reduce the frequency and number of macrophages compared to those in the control group. Pro-inflammatory cytokine *IL-1β* were also decreased in the ART group. These results also proved that ART treatment can not only inhibit the number of infiltrating macrophages but also reduce their function.

Although our results indicated that ART could significantly attenuate rejection by inhibiting multiple pathways, several limitations should be noted. First, effects of ART are wide, and we did not conduct studies on such mechanisms in depth. Second, the research on immune cell function was not thorough, and especially, the subtype analysis of cytokines was not sufficient. Finally, the concentration of ART *in vivo* was determined based on our experience and references, and thus, the side effects of ART should be further explored.

In summary, we established a transplant rejection model and demonstrated that ART can suppress TCMR, ABMR, and macrophage infiltration *in vivo* and provided evidence that ART attenuates allograft injury and rejection after rat cardiac transplantation. Subsequently, we demonstrated the inhibitory effect of ART on the function of various purified lymphocytes *in vitro*. Although this was a pilot study of the suppressive effects of ART on rejection, this study provides novel evidence for the therapy of rejection in patients who suffer transplantation.

DATA AVAILABILITY STATEMENT

The original contributions presented in the study are included in the article/supplementary material. Further inquiries can be directed to the corresponding authors.

ETHICS STATEMENT

The animal study was reviewed and approved by Sun Yat-sen University Institutional Ethical Guidelines for animal experiments.

AUTHOR CONTRIBUTIONS

ZY: study design and drafting of the manuscript. FH: performed the model. TL: performed the model and helped write the manuscript. HZ: performed the experiments. ZL: performed the experiments. MM: performed the transplantation model. JH: performed the transplantation model. LL: generated the immune- histochemistry data. YY: labeled the image and statistical analysis. RZ: labeled the image and statistical analysis. ZH: critical revision of the manuscript. YZ: conceived the study and performed the experiments. QS: conceived the study and critical revision of the manuscript. All authors contributed to the article and approved the submitted version.

FUNDING

This study was supported by the National Natural Science Foundation of China (No. 81970649, 81970650, 81770753, 81800662, and 81800663); the National Key R&D Program of China (2018YFA0108804); Guangdong Basic and Applied Basic Research Foundation (2019A1515011942); and the PhD Start-up Fund of Natural Science Foundation of Guangdong Province, China (2018A030310324); the China Postdoctoral Science Foundation (2020M683083).

REFERENCES

1. Dhital KK, Iyer A, Connellan M, Chew HC, Gao L, Doyle A, et al. Adult heart transplantation with distant procurement and ex-vivo preservation of donor hearts after circulatory death: a case series. *Lancet* (2015) 385(9987):2585–91. doi: 10.1016/S0140-6736(15)60038-1
2. Meier-Kriesche HU, Ojo AO, Hanson JA, Cibrik DM, Punch JD, Leichtman AB, et al. Increased impact of acute rejection on chronic allograft failure in recent era. *Transplantation* (2000) 70(7):1098–100. doi: 10.1097/00007890-200010150-00018
3. Bhagra SK, Pettit S, Parameshwar J. Cardiac transplantation: indications, eligibility and current outcomes. *Heart* (2019) 105(3):252–60. doi: 10.1136/heartjnl-2018-313103
4. Lund LH, Edwards LB, Kucheryavaya AY, Benden C, Christie JD, Dipchand AI, et al. The registry of the International Society for Heart and Lung Transplantation: thirty-first official adult heart transplant report–2014; focus theme: retransplantation. *J Heart Lung Transpl* (2014) 33(10):996–1008. doi: 10.1016/j.healun.2014.08.003
5. Lefaucheur C, Loupy A, Vernerey D, Duong-Van-Huyen JP, Suberbielle C, Anglicheau D, et al. Antibody-mediated vascular rejection of kidney allografts: a population-based study. *Lancet* (2013) 381(9863):313–9. doi: 10.1016/S0140-6736(12)61265-3
6. Loupy A, Toquet C, Rouvier P, Beuscart T, Bories MC, Varnous S, et al. Late Failing Heart Allografts: Pathology of Cardiac Allograft Vasculopathy and Association With Antibody-Mediated Rejection. *Am J Transpl* (2016) 16 (1):111–20. doi: 10.1111/ajt.13529
7. Colvin MM, Cook JL, Chang P, Francis G, Hsu DT, Kiernan MS, et al. Antibody-mediated rejection in cardiac transplantation: emerging knowledge in diagnosis and management: a scientific statement from the American Heart Association. *Circulation* (2015) 131(18):1608–39. doi: 10.1161/CIR.0000000000000093
8. Klayman DL. Qinghaosu (artemisinin): an antimalarial drug from China. *Science* (1985) 228(4703):1049–55. doi: 10.1126/science.3887571
9. Ho WE, Peh HY, Chan TK, Wong WS. Artemisinins: pharmacological actions beyond anti-malarial. *Pharmacol Ther* (2014) 142(1):126–39. doi: 10.1016/j.pharmthera.2013.12.001
10. Li T, Chen H, Yang Z, Liu XG, Zhang LM, Wang H. Evaluation of the immunosuppressive activity of artesunate in vitro and in vivo. *Int Immunopharmacol* (2013) 16(2):306–12. doi: 10.1016/j.intimp.2013.03.011
11. Wang JX, Tang W, Shi LP, Wan J, Zhou R, Ni J, et al. Investigation of the immunosuppressive activity of artemether on T-cell activation and proliferation. *Br J Pharmacol* (2007) 150(5):652–61. doi: 10.1038/sj.bjp.0707137
12. Zhao YG, Wang Y, Guo Z, Gu AD, Dan HC, Baldwin AS, et al. Dihydroartemisinin ameliorates inflammatory disease by its reciprocal effects on Th and regulatory T cell function via modulating the mammalian target of rapamycin pathway. *J Immunol* (2012) 189(9):4417–25. doi: 10.4049/jimmunol.1200919
13. Dong YJ, Li WD, Tu YY. [Effect of dihydro-qinghaosu on auto-antibody production, TNF alpha secretion and pathologic change of lupus nephritis in BXSB mice]. *Zhongguo Zhong Xi Yi Jie He Za Zhi* (2003) 23(9):676–9.
14. Wang Y, Cao J, Fan Y, Xie Y, Xu Z, Yin Z, et al. Artemisinin inhibits monocyte adhesion to HUVECs through the NF-kappaB and MAPK pathways in vitro. *Int J Mol Med* (2016) 37(6):1567–75. doi: 10.3892/ijmm.2016.2579
15. Yang Z, Ding J, Yang C, Gao Y, Li X, Chen X, et al. Immunomodulatory and anti-inflammatory properties of artesunate in experimental colitis. *Curr Med Chem* (2012) 19(26):4541–51. doi: 10.2174/092986712803251575

16. Liao T, Li Q, Zhang Y, Yang Z, Huang Z, Han F, et al. Precise treatment of acute antibody-mediated cardiac allograft rejection in rats using C4d-targeted microbubbles loaded with nitric oxide. *J Heart Lung Transplant* (2020) 39 (5):481–90. doi: 10.1016/j.healun.2020.02.002
17. Liao T, Liu X, Ren J, Zhang H, Zheng H, Li X, et al. Noninvasive and quantitative measurement of C4d deposition for the diagnosis of antibody-mediated cardiac allograft rejection. *EBioMedicine* (2018) 37:236–45. doi: 10.1016/j.ebiom.2018.10.061
18. Ko JH, Lee HJ, Jeong HJ, Kim MK, Wee WR, Yoon SO, et al. Mesenchymal stem/stromal cells precondition lung monocytes/macrophages to produce tolerance against allo- and autoimmunity in the eye. *Proc Natl Acad Sci U S A* (2016) 113(1):158–63. doi: 10.1073/pnas.1522905113
19. Stewart S, Winters GL, Fishbein MC, Tazelaar HD, Kobashigawa J, Abrams J, et al. Revision of the 1990 working formulation for the standardization of nomenclature in the diagnosis of heart rejection. *J Heart Lung Transpl* (2005) 24(11):1710–20. doi: 10.1016/j.healun.2005.03.019
20. Jin O, Zhang H, Gu Z, Zhao S, Xu T, Zhou K, et al. A pilot study of the therapeutic efficacy and mechanism of artesunate in the MRL/lpr murine model of systemic lupus erythematosus. *Cell Mol Immunol* (2009) 6(6):461–7. doi: 10.1038/cmi.2009.58
21. Li Y, Wang S, Wang Y, Zhou C, Chen G, Shen W, et al. Inhibitory effect of the antimalarial agent artesunate on collagen-induced arthritis in rats through nuclear factor kappa B and mitogen-activated protein kinase signaling pathway. *Transl Res* (2013) 161(2):89–98. doi: 10.1016/j.trsl.2012.06.001
22. Lund LH, Khush KK, Cherikh WS, Goldfarb S, Kucheryavaya AY, Levvey BJ, et al. The Registry of the International Society for Heart and Lung Transplantation: Thirty-fourth Adult Heart Transplantation Report-2017; Focus Theme: Allograft ischemic time. *J Heart Lung Transpl* (2017) 36 (10):1037–46. doi: 10.1016/j.healun.2017.07.019
23. Lechler RI, Sykes M, Thomson AW, Turka LA. Organ transplantation–how much of the promise has been realized? *Nat Med* (2005) 11(6):605–13. doi: 10.1038/nm1251
24. Kfoury AG, Miller DV, Snow GL, Afshar K, Stehlik J, Drakos SG, et al. Mixed cellular and antibody-mediated rejection in heart transplantation: In-depth pathologic and clinical observations. *J Heart Lung Transpl* (2016) 35(3):335–41. doi: 10.1016/j.healun.2015.10.016
25. Gupta SK, Itagaki R, Zheng X, Batkai S, Thum S, Ahmad F, et al. miR-21 promotes fibrosis in an acute cardiac allograft transplantation model. *Cardiovasc Res* (2016) 110(2):215–26. doi: 10.1093/cvr/cvw030
26. Hou LF, He SJ, Li X, Yang Y, He PL, Zhou Y, et al. Oral administration of artemisinin analog SM934 ameliorates lupus syndromes in MRL/lpr mice by inhibiting Th1 and Th17 cell responses. *Arthritis Rheumatol* (2011) 63 (8):2445–55. doi: 10.1002/art.30392
27. Liao T, Xue Y, Zhao D, Li S, Liu M, Chen J, et al. In Vivo Attenuation of Antibody-Mediated Acute Renal Allograft Rejection by Ex Vivo TGF-beta-Induced CD4(+)Foxp3(+) Regulatory T Cells. *Front Immunol* (2017) 8:1334. doi: 10.3389/fimmu.2017.01334
28. Roemhild A, Otto NM, Moll G, Abou-El-Enein M, Kaiser D, Bold G, et al. Regulatory T cells for minimising immune suppression in kidney transplantation: phase I/IIa clinical trial. *BMJ* (2020) 371:m3734. doi: 10.1136/bmj.m3734
29. Hippen BE, DeMattos A, Cook WJ, Kew CE,2, Gaston RS. Association of CD20+ infiltrates with poorer clinical outcomes in acute cellular rejection of renal allografts. *Am J Transpl* (2005) 5(9):2248–52. doi: 10.1111/j.1600-6143.2005.01009.x
30. Wu Y, He S, Bai B, Zhang L, Xue L, Lin Z, et al. Therapeutic effects of the artemisinin analog SM934 on lupus-prone MRL/lpr mice via inhibition of TLR-triggered B-cell activation and plasma cell formation. *Cell Mol Immunol* (2016) 13(3):379–90. doi: 10.1038/cmi.2015.13
31. Abe T, Ishii D, Gorbacheva V, Kohei N, Tsuda H, Tanaka T, et al. Anti-huCD20 antibody therapy for antibody-mediated rejection of renal allografts in a mouse model. *Am J Transpl* (2015) 15(5):1192–204. doi: 10.1111/ajt.13150
32. Djamali A, Kaufman DB, Ellis TM, Zhong W, Matas A, Samaniego M. Diagnosis and management of antibody-mediated rejection: current status and novel approaches. *Am J Transpl* (2014) 14(2):255–71. doi: 10.1111/ajt.12589
33. Gupta G, Abu Jawdeh BG, Racusen LC, Bhasin B, Arend LJ, Trollinger B, et al. Late antibody-mediated rejection in renal allografts: outcome after conventional and novel therapies. *Transplantation* (2014) 97(12):1240–6. doi: 10.1097/01.TP.0000442503.85766.91
34. Immenschuh S, Zilian E, Dammrich ME, Schwarz A, Gwinner W, Becker JU, et al. Indicators of treatment responsiveness to rituximab and plasmapheresis in antibody-mediated rejection after kidney transplantation. *Transplantation* (2015) 99(1):56–62. doi: 10.1097/TP.0000000000000244
35. Fabritius C, Ritschl PV, Resch T, Roth M, Ebner S, Gunther J, et al. Deletion of the activating NK cell receptor NKG2D accelerates rejection of cardiac allografts. *Am J Transpl* (2017) 17(12):3199–209. doi: 10.1111/ajt.14467
36. Halloran PF, Venner JM, Madill-Thomsen KS, Einecke G, Parkes MD, Hidalgo LG, et al. Review: The transcripts associated with organ allograft rejection. *Am J Transpl* (2018) 18(4):785–95. doi: 10.1111/ajt.14600
37. Sun Q, Zhang M, Xie K, Li X, Zeng C, Zhou M, et al. Endothelial injury in transplant glomerulopathy is correlated with transcription factor T-bet expression. *Kidney Int* (2012) 82(3):321–9. doi: 10.1038/ki.2012.112
38. Li T, Zhang Z, Bartolacci JG, Dwyer GK, Liu Q, Mathews LR, et al. Graft IL-33 regulates infiltrating macrophages to protect against chronic rejection. *J Clin Invest* (2020) 130(10):5397–412. doi: 10.1172/JCI133008
39. Dai H, Lan P, Zhao D, Abou-Daya K, Liu W, Chen W, et al. PIRs mediate innate myeloid cell memory to nonself MHC molecules. *Science* (2020) 368 (6495):1122–7. doi: 10.1126/science.aax4040

Conflict of Interest: The authors declare that the research was conducted in the absence of any commercial or financial relationships that could be construed as a potential conflict of interest.

frontiers in Immunology

REVIEW
published: 17 March 2021
doi: 10.3389/fimmu.2021.648539

M2 Macrophages Serve as Critical Executor of Innate Immunity in Chronic Allograft Rejection

Hanwen Zhang[1], *Zhuonan Li*[2] *and Wei Li*[1]*

[1] Department of Hepatobiliary-Pancreatic Surgery, China-Japan Union Hospital of Jilin University, Changchun, China, [2] Plastic Surgery, China-Japan Union Hospital of Jilin University, Changchun, China

Allograft functional failure due to acute or chronic rejection has long been a major concern in the area of solid organ transplantation for decades. As critical component of innate immune system, the macrophages are unlikely to be exclusive for driving acute or chronic sterile inflammation against allografts. Traditionally, macrophages are classified into two types, M1 and M2 like macrophages, based on their functions. M1 macrophages are involved in acute rejection for triggering sterile inflammation thus lead to tissue damage and poor allograft survival, while M2 macrophages represent contradictory features, playing pivotal roles in both anti-inflammation and development of graft fibrosis and resulting in chronic rejection. Macrophages also contribute to allograft vasculopathy, but the phenotypes remain to be identified. Moreover, increasing evidences are challenging traditional identification and classification of macrophage in various diseases. Better understanding the role of macrophage in chronic rejection is fundamental to developing innovative strategies for preventing late graft loss. In this review, we will update the recent progress in our understanding of diversity of macrophage-dominated innate immune response, and reveal the roles of M2 macrophages in chronic allograft rejection as well.

Keywords: solid organ transplantation, chronic allograft rejection, macrophage, IRI, inflammation, ECM, fibrosis, vasculopathy

OPEN ACCESS

Edited by:
Hao Wang,
Tianjin Medical University General Hospital, China

Reviewed by:
Shintaro Yagi,
Kanazawa University, Japan
Yong Zhao,
Chinese Academy of Sciences (CAS), China

***Correspondence:**
Wei Li
weili888@jlu.edu.cn

Specialty section:
This article was submitted to Alloimmunity and Transplantation, a section of the journal Frontiers in Immunology

Received: *31 December 2020*
Accepted: *10 February 2021*
Published: *17 March 2021*

Citation:
Zhang H, Li Z and Li W (2021) M2 Macrophages Serve as Critical Executor of Innate Immunity in Chronic Allograft Rejection. Front. Immunol. 12:648539. doi: 10.3389/fimmu.2021.648539

INTRODUCTION

Organ transplantation appears to be the best treatment method for patients who suffered from the end-stage diseases. However, chronic allograft rejection following transplantation remains to be a major challenge to long term allograft survival and functions. Organ allografts are susceptible to ischemia reperfusion injury (IRI) and recipient alloimmunity, suffering from acute and chronic rejection inevitably (1). Much attention has once focused on acute rejection, but nowaday it is no longer the common cause of late graft loss due to the application of systemic immunosuppressants (2). Increasing evidences are focusing on the profound meaning of innate immune cells, such as NK cells, macrophages, and neutrophils, in the late phase change of allografts.

Diversity of innate immune cells is drawing much attention. Neutrophils have been characterized as a major component in driving inflammation for a long time. They are known to be recruited into stressed solid organ and contribute to tissue injury, while recent data have demonstrated their contradictory function in tissue repair (3, 4). Identically, distinctive functional features between two different populations of macrophages are considered as a hot spot to study in varies diseases models. Despite the fact that macrophages are recognized as a

key participant in triggering both graft acute inflammatory damage and inflammation resolution in organ transplantation (5). The role of macrophage-mediated late phase graft rejection and corresponding therapies to mitigate allograft dysfunction or loss still remain largely unknown.

Monocyte-derived macrophages infiltrate into allografts after transplantation and then mainly differentiate into two phenotypes: pro-inflammatory M1-like macrophages and anti-inflammatory M2-like type (6), thus represent opposite functions during acute phase in organ transplant. However, M2-like macrophages also show potentials for enabling fibrosis, resulting in poor long-term graft survival. Moreover, macrophages are reported to be related with graft vasculopathy (7), but the data on their heterogeneity are limited. Tissue-resident macrophages are displaying differential features compared with their infiltrating counterpart. Although it has been proved that the replenishment of local macrophage niche in organ under unsteady state, increasing data have shown the differential characteristics and features between embryonic and monocyte-derived populations (8). Diverse macrophages dynamically represent various functions in local immune environment in response to stimuli, stress and tissue injury, while a great deal of work is yet to be done in the area of chronic allograft rejection. An improved understanding of macrophage related cellular immune events which trigger the late phase rejection and ultimately responsible for allograft dysfunction and loss, is fundamental for the development of innovative strategies for the treatment of organ allograft recipients. In this review, we will update the recent progresse of diversity of macrophage dominated innate immune responses and reveal the roles of M2 macrophages in chronic allograft rejection as well.

IDENTIFICATION OF MACROPHAGES

Distinct Origins and Functions of Macrophages

As we all know so far, both innate and adaptive immune responses are involved in chronic allograft rejection. The key effective innate immune cells, macrophages, play important roles in variety of physiologic and pathologic processes, for instance, host defense, acute and chronic inflammation and tissue repair (9). Macrophages are derived from monocytes in the circulation and then represent resident features in lymphoid and non-lymphoid tissues, including solid organs, involved in tissue homeostasis (10). They were characterized by plasticity and diverse functions. The activated macrophages polarize and exhibit classical M1-like or alternative M2-like phenotypes. M1 macrophages tend to produce reactive oxygen species (ROS), nitric oxide (NO) and pro-inflammatory cytokines such as IL-6, IL-12, and TNF-α that play crucial roles in defense against dead cells, microbial infection and cancer. On the contrary, M2 macrophages tend to express scavenging receptors and produce various anti-inflammatory mediators including IL-10 and TGF-β to promote the inflammation resolution, tissue repair, wound healing and fibrosis (11).

Traditionally, the polarization of macrophage may be defined by M1/M2 markers including Nitric Oxide Synthases (NOSs), arginase family (Arg1/2), CD206 and CD163. In spite of that, macrophages are likely to represent distinctive polarization and differentiation under various circumstances in complex organism. Understanding dynamic reprogramming landscapes of macrophage is important for exploiting the mechanisms of transplant immune responses (**Figure 1**). Of note, a unique macrophage subset driven by IL-23 has been recently discussed. IL-23, a heterodimeric cytokine essential for expression of IL-17, shares p40 subunit with IL-12 that induces the production of IFN-γ (12). It was reported that IL-23 involved in IL-17 and IFN-γ related tissue inflammatory response by innate lymphoid cells, including macrophages (13, 14). Treated with recombinant IL-23, unpolarized mouse peritoneal macrophages represent significantly increased production of IL-17A and IFN-γ via STAT3-RORγ T pathways, but not M1/M2 related cytokines, and neither polarized M1 nor M2-like macrophages can convert to such an IL-17/IFN-γ high-producing subset: M(IL-23) (15). Thus, M(IL-23) is likely to be defined as a new macrophage subpopulation and is worth discussing since alloreactive production of IL-17/IFN-γ is closely related to allograft rejection (16).

Dynamic Change Among Resident Macrophage Niche in Allograft Rejection

Tissue resident macrophages are crucial participants in organ homeostasis and are likely to exhibit a M2-like phenotype (17). However, M2-like macrophages could also display pro-fibrogenic feature. In other word, tissue-resident macrophages are double-edged swords that have potential to either alleviate IRI and inflammation, or result in fibrotic rejection. Recently, many studies are focusing on postnatal development of tissue resident macrophages and their functions in metabolism, immune activation and regulation. Unlike primitive tissue-resident macrophages such as Kupffer cells (KCs) in the liver, microglia in brain and renal resident macrophages that arise from yolk sac (18–20), macrophages originate from bone marrow-derived monocytes and then reside in solid organs, serving as executors of innate immunity. Identical to liver parenchyma cells, non-parenchyma cells (NPCs) in the liver suffer from hypoxia, leading to ischemia-induced necrotic activation (21). Although it has been widely acknowledged that immigrant macrophages and tissue-resident macrophages display distinct features and properties in some aspects, niche-specific reprogramming of recruited macrophages with the help of "KC-enhancers" expressed by liver sinusoidal endothelial cells and hepatocytes have been recently discovered on the basis of "resident like" marker V-set immunoglobulin-domain-containing 4 (VSIG4) (22, 23). Tissue resident macrophages are susceptible to endo-/exogenous stimulation and contribute to necrotic or apoptotic depletion. Tremendous findings have demonstrated that the potentials on the transformation of the immigrant populations into the resident are not only compensating impaired resident macrophage pool, but also representing resident-like features and functions that "newcome"

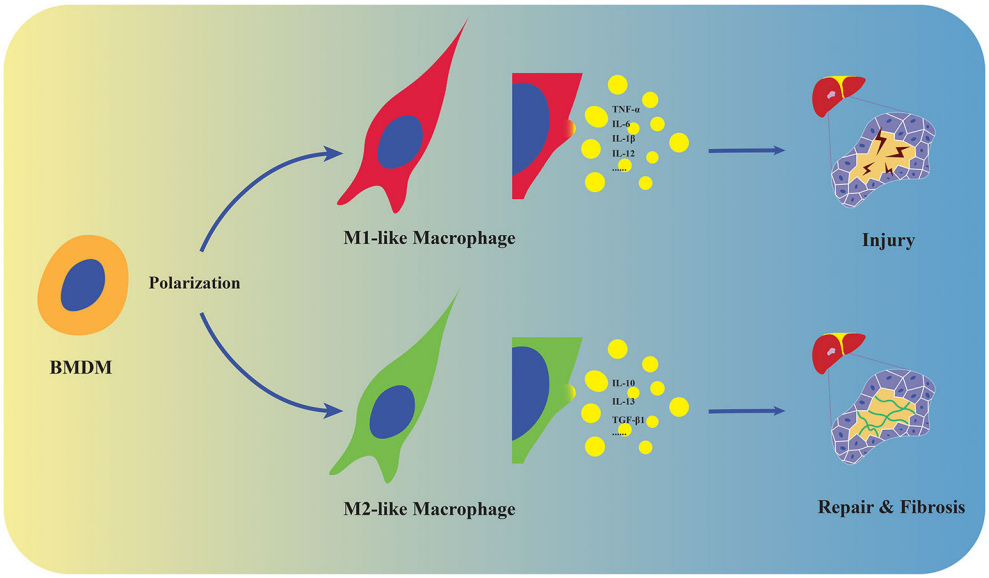

FIGURE 1 | Polarization and distinct functions of macrophages. Macrophages derive from monocytes in the circulation and polarize into M1/M2-like phenotypes. M1-like macrophages promote tissue injury by producing pro-inflammatory cytokines including TNF-α, IL-6, IL-1β, and IL-12, while M2 represent tissue repair and fibrosis by expressing anti-inflammatory and fibrogenic mediators such as IL-10, IL-13, and TGF-β1 in stressed liver.

macrophages lack in response to stress including surgery-induced IRI, infection and chronic inflammation (17, 22, 24). Despite the fact that limited works have focused on macrophage reprogramming in organ transplantation, progress pertaining to the aforementioned factors suggest the innovative possibility in alleviating macrophage-mediated chronic allograft rejection.

MACROPHAGES, INFLAMMATION AND CHRONIC ALLOGRAFT REJECTION

Innate Immunity Dominated IRI in Transplantation

IRI which triggered by activation of innate immune receptors, not only play a key role in graft failure at the early stage, but also result in chronic rejection at the late stage of transplantation (25). This inevitable complication initiates tissue damage by promoting release of danger-associated molecular pattern (DAMP) such as high mobility group box-1 (HMGB1) which derived from necrotic or stressed cells to activate sentinel pattern recognition receptor Toll-like receptor 4 (TLR4), thus mediating sterile inflammation (26, 27). As the major innate immune cells responding to DAMPs, monocyte-derived macrophage are activated and infiltrate into IR-stressed organs, which is closely associated with inflammation and tissue injury. However, the functions of macrophage are different in their population and may represent distinct roles in response to IRI stress. It has been revealed based on the biological phenotype of macrophage that M1-like macrophages are responsible for inducing neutrophil-mediated tissue injury, while M2-like phenotype monocyte-derived macrophages and kupffer cells are likely to represent anti-inflammatory and wound-healing features during liver IRI (28, 29).

Macrophages in Inflammation and Allograft Rejection

Compared with monocyte-derived macrophages originated from bone-marrow progenitor cells and take time to be recruited from circulation, tissue-resident macrophages represent rapid response. They sense neighboring cells death and react to DAMPs as soon as they are released by dead organ parenchymal cells, directly function on cellular debris degradation and cytokines secretion against injury (25). More notably, they are stimulated and activated during ischemic stage before the recruitment of monocyte-derived macrophages into stressed organ. Thus, diverse macrophage subsets and complex innate immune activation demonstrate a complicated scenario, converting immunologically quiescent milieu into an inflammatory activation vs. resolution condition and resulting in tissue damage, injury repair and fibrosis.

M1-like macrophage-dominated innate immune response is one of the major sources of acute neutrophil-mediated inflammation in transplant recipients. Indeed, study using transgenic cre-inducible diphtheria toxin receptor (DTR) system that specifically targets $CD11b^{+}$ (a surface marker expressed on macrophages) cells *in vivo* to deplete infiltrating macrophages demonstrated the alleviative effect on liver IRI in mice (30, 31). At early stage of post-transplant, overwhelming innate immune response dominates acute rejection, while T-cell mediated adaptive allograft rejection

has not yet been established. M1-like macrophages are inclined to produce pro-inflammatory cytokines TNF-α, IL-6, and IL-1β, mediating injury. As pro-/anti- inflammatory activation and tissue repair co-exist, implants undergo dynamic change. Failing to resolve acute inflammation may result in chronic inflammation, attributing to establishment of allograft inflammatory fibrosis and gradual deterioration in functions (32).

MACROPHAGES, FIBROSIS, AND CHRONIC ALLOGRAFT REJECTION

Fibrosis and Solid Organ Diseases

Upon injuries or diseases, there is an impressive repertoire of machinery in place for self-preservation and healing. One of the most important protective mechanisms for wound healing and tissue regeneration is the formation of extracellular matrix (ECM). As a highly dynamic construction, ECM undergoes an independent remodeling process, contributes to restructuring of tissue architecture in regarding to maintenance of stable organ structure and function (33, 34). ECM unbalance caused by endo-/exogenous risk factors is likely to result in disorganization or dysfunction. Fibroblasts, one of the most abundant cell types are widely distributed in the connective tissue throughout the body. They are acknowledged to compose the basic framework for tissues and organs by producing, maintaining and reabsorption of ECM, but act as circumstantial effectors that unfrequently function expression and remodeling of ECM (35). Under homeostasis, fibroblasts remain relatively quiescent, while in response to stress and stimuli, they adapt to microenvironment and are activated in coordination with inflammation related cytokines, especially TGF-β1, by differentiating into their apex stage, myofibroblasts (36). In response to tissue injury or chronic inflammation, myofibroblasts with a terminally differentiated phenotype not only extensively produce ECM, but also inherit a contractile apparatus in order to manipulate ECM fibers physically that fill the wounds and attribute to acute or chronic inflammatory damage (37).

Fibrosis is a shared and central part of numerous pathologies including autoimmunity, metabolic disorders and graft rejection (38–40). Tissue fibrosis is a dangerous condition and pathological manifestations characterized by an excessive accumulation of ECM in response to acute/chronic injuries. In addition, interstitial fibrosis and tubular atrophy (IF/TA) of kidney cortex is best known as its paramount importance in development of poorer renal function and outcome in chronic kidney disease (CKD) and kidney transplantation (41, 42). In spite of the fact that emphasizing the predominated effects of adaptive antibody-mediated rejection (AMR) in loss of implants, innate-immune-dominated fibrotic rejection triggered by macrophages should not be neglected (43). Diverse populations of macrophage represent functionally distinction during early and late phases post-transplantation. When it comes to fibrosis, they controversially drive spectrum of phenotypes that display both pro- and anti-fibrotic functions.

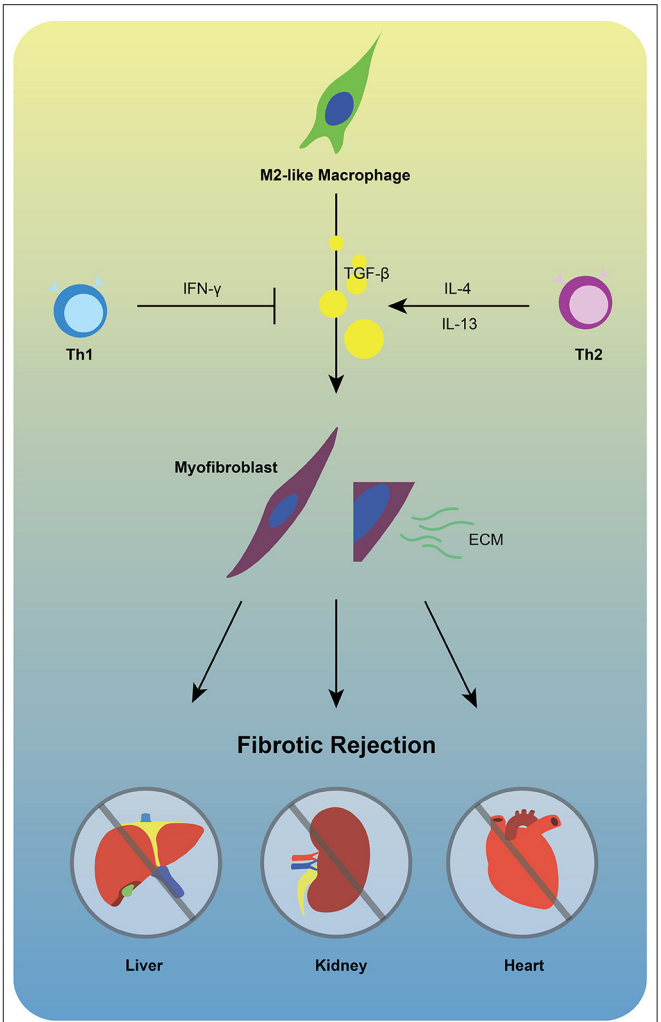

FIGURE 2 | M2-like macrophages are unlikely to be exclusive for fibrotic rejection. TGF-β1 produced by M2-like macrophages facilitates differentiation of fibroblasts into myofibroblasts that extensively produce ECM, promoting chronic fibrotic allograft rejection. During this process, Th1 cells may inhibit the activation of TGF-β by producing IFN-γ, while Th2 cells represent opposite feature via secretion of IL-4/IL-13.

M2-like Macrophages Are Responsible for Driving Fibrogenesis

In the process of chronic rejection, imbalance between pro- and anti-fibrosis play an important role. Wound healing M2-like macrophages not only play critical roles in anti-inflammation in the very early stage of IRI, but also regulate tissue inflammation resolution and promote fibrotic processes via producing TGF-β1 and VEGF (44). Infiltrating macrophages differentiate into M2-like feature is likely to produce IL-10, which is crucial for suppressing pro-inflammatory gene programs. A clinical study obtained renal allograft biopsies from 12 month post-transplant, demonstrating the strong relationship between area

of fibrosis and numbers of $CD206^+$ M2-like macrophages (45). Smad-3 is an intracellular molecule facilitates transmit chemical signals from plasma membrane to the nucleus, operating downstream of growth/differentiation factors including TGF-β, activin, and myostatin (46). In the development of chronic kidney allograft rejection, Smad-3-dependent macrophage-myofibroblast transition (MMT) process, which occurs predominantly within M2-like macrophages, resulting in renal interstitial fibrosis (47, 48). Moreover, a novel adenosine triphosphate (ATP)-gated ion channel protein P2X7, initially reported to function in fast synaptic transmission and lysis of antigen-presenting cells (APCs), is recently found to play important roles in neutrophil adhesion, contributes to acute/chronic inflammation and M2-like macrophages-mediated chronic heart fibrotic rejection (33, 49–51). During the progression of fibrotic rejection, macrophages derived TGF-β undoubtedly play a pivotal role in differentiation of fibroblasts into myofibroblasts, but whether and how adaptive immune system affect this process remain worth studying. T helper type 1 cells (Th1 cells), defined by their secretion of IFN-γ, have potential to disrupt TGF-β/Smad3 signaling pathway-mediated fibrosis (52, 53). On the contrary, T helper type 2 cells (Th2 cells) is likely to promote the TGF-βmediated fibrosis via the production of IL-4 and IL-13 (54). Thus, further investigating the interaction between innate and adaptive immune systems in fibrotic rejection might be of great benefits (**Figure 2**).

MACROPHAGES, VASCULOPATHY AND CHRONIC ALLOGRAFT REJECTION

Vasculopathy Is a Hallmark of Chronic Allograft Rejection

In spite of progresses in immunosuppressive therapy, long-term success of allogeneic organ transplantation is limited by the establishment of allograft vasculopathy. Vasculopathy is another dangerous risk factor and hallmark of chronic allograft rejection triggered by multifactorial immunologic events, characterized by endothelial injury and dysfunction, myointimal hyperplasia and extracellular matrix synthesis (55, 56). Transplant vasculopathy inevitably occurs in ∼90% of allografts, developing severe intimal hyperplastic lesions that eventually result in luminal flow restriction and graft failure during long-term follow-up (57). In line with this scenario, cellular and antibody-mediated rejection processes and anti-HLA antibodies against implant play crucial roles in mediating inflammation that drive the development of vasculopathy-induced chronic allograft failure (58). Transplant vasculopathy has long been considered to consequent to chronic allograft rejection, especially kidney and heart (59, 60). Nearly one-third of patients developed cardiac allograft vasculopathy (CAV) by 5 years post-transplant, leading to 12.5% CAV-induced death rate (61). Moreover, it is demonstrated that the renal vasculopathy characterized by perivascular leukocyte infiltration and neointimal hyperplasia is unlikely to be exclusive for affecting the intrarenal blood vessels (62).

Macrophages Are Unlikely to Be Exclusive for Vasculopathy-Related Rejection

It has been reported by Croker et al. (63) that infiltrating macrophage-based post-transplant inflammation played a crucial role in chronic allograft nephropathy and dysfunction. Transplant vasculopathy is referred to as an accelerated pathologically fibroproliferative process characterized by smooth muscle proliferation and lipid deposition-induced circumferential intimal thickening (61, 64). Studies define macrophage as predominant cell type in the intimal of renal allograft arteries and demonstrate their unfavorably effects on graft survival in both acute and chronic rejection (65, 66). Depleting or inhibiting infiltrating macrophages by using λ-carrageenan type IV or a small molecule β2 integrin agonist leukadherin-1 (LA1) significantly suppressed cardiac and renal vasculopathy, alleviated chronic tissue injury and dysfunction (67, 68). Although increasing evidence suggest that macrophage-mediated vasculopathy is an integral part of the chronic allograft rejection process, the underlying mechanisms have not been well-defined. Distinct macrophage populations and functions in the process of allograft vasculopathy still remain to be further studied.

MACROPHAGES, ADAPTIVE IMMUNE SYSTEM AND CHRONIC ALLOGRAFT REJECTION

It has been widely recognized that adaptive immune response mediated by T and B lymphocytes, and donor-specific antibodies (DSA) are all involved in culminating chronic allograft rejection (69). In consideration of important roles of macrophages in the development of transplant rejection, questions concerning the link between macrophages and adaptive immune system need to be addressed. Despite the potential effects of CD4+ T cells in macrophage-mediated fibrotic rejection, which we have mentioned above, interestingly, recent arguments are challenging the traditional perspective on macrophage as innate immune cells. Chu et al. have advocated the concept that macrophage is potential to represent adaptive immune feature in allograft rejection, stating that $CD4^+$T cells facilitate the acquisition of long-term specific memory of macrophages against skin allograft (70, 71). Moreover, another study demonstrates that macrophages can produce B-cell activating factor (BAFF), resulting in graft damage during antibody mediated rejection (72). Thus, in spite of the innate immune features of macrophages, mechanistic appreciation of their roles in connecting with adaptive immune system will be of interest in the future.

CONCLUSION AND FUTURE REMARK

Lots of efforts have been made to dissect the mechanisms of both innate and adaptive immune response so as to prevent chronic rejection and improve allograft survival

(73). At present, a remarkable progress has been made in the study of macrophage-related immunoregulation and immunosuppression for the treatment of organ transplant rejection. Inhibiting infiltration or activation of monocytes/macrophages by mycophenolate mofetil (MMF) seems to be a promising therapeutic strategy (74). Indeed, depletion of monocytes/macrophages attenuate neutrophils-related tissue damage at the early stage of transplant (75–77), while it may also prevent tissue repair and induction of tolerance at late stage due to loss of reprogrammed macrophages that participate in reconstitution of homeostasis (17, 78). Moreover, chronic rejection mediated by M2-like macrophages is also an ineligible issue. Manipulating macrophage activities and polarization will be of significant challenge in against chronic allograft rejection.

AUTHOR CONTRIBUTIONS

HZ initially collected literatures and primarily drafted the article. ZL performed an intensive revision of the manuscript. WL contributed to the conceptual design and carried out critical revision and finalization of the manuscript. All authors contributed to the article and approved the submitted version.

ACKNOWLEDGMENTS

The authors acknowledged the Nature Science Foundation of the Science and Technology Bureau of Jilin Province (Li 20190201227JC), the innovation capacity building fund of The Development and Reform Commission of Jilin Province (Li 2019C015), and NSFC regional innovation and Development Fund (U20A20360).

REFERENCES

1. Hirao H, Dery KJ, Kageyama S, Nakamura K, Kupiec-Weglinski JW. Heme oxygenase-1 in liver transplant ischemia-reperfusion injury: from bench-to-bedside. *Free Radic Biol Med.* (2020) 157:75–82. doi: 10.1016/j.freeradbiomed.2020.02.012
2. Loupy A, Lefaucheur C. Antibody-mediated rejection of solid-organ allografts. *N Engl J Med.* (2018) 379:1150–60. doi: 10.1056/NEJMra1802677
3. Schofield ZV, Woodruff TM, Halai R, Wu MC, Cooper MA. Neutrophils–a key component of ischemia-reperfusion injury. *Shock.* (2013) 40:463–70. doi: 10.1097/SHK.0000000000000044
4. Yang W, Tao Y, Wu Y, Zhao X, Ye W, Zhao D, et al. Neutrophils promote the development of reparative macrophages mediated by ROS to orchestrate liver repair. *Nat Commun.* (2019) 10:1076. doi: 10.1038/s41467-019-09046-8
5. Zhai Y, Busuttil RW, Kupiec-Weglinski JW. Liver ischemia and reperfusion injury: new insights into mechanisms of innate-adaptive immune-mediated tissue inflammation. *Am J Transplant.* (2011) 11:1563–9. doi: 10.1111/j.1600-6143.2011.03579.x
6. Yue S, Rao J, Zhu J, Busuttil RW, Kupiec-Weglinski JW, Lu L, et al. Myeloid PTEN deficiency protects livers from ischemia reperfusion injury by facilitating M2 macrophage differentiation. *J Immunol.* (2014) 192:5343–53. doi: 10.4049/jimmunol.1400280
7. Khan SQ, Guo L, Cimbaluk DJ, Elshabrawy H, Faridi MH, Jolly M, et al. A small molecule β2 integrin agonist improves chronic kidney allograft survival by reducing leukocyte recruitment and accompanying vasculopathy. *Front Med.* (2014) 1:45. doi: 10.3389/fmed.2014.00045
8. Blériot C, Chakarov S, Ginhoux F. Determinants of resident tissue macrophage identity and function. *Immunity.* (2020) 52:957–70. doi: 10.1016/j.immuni.2020.05.014
9. Martinez FO, Sica A, Mantovani A, Locati M. Macrophage activation and polarization. *Front Biosci.* (2008) 13:453–61. doi: 10.2741/2692
10. Geissmann F, Manz MG, Jung S, Sieweke MH, Merad M, Ley K. Development of monocytes, macrophages, and dendritic cells. *Science.* (2010) 327:656–61. doi: 10.1126/science.1178331
11. Luo Y, Shao L, Chang J, Feng W, Liu YL, Cottler-Fox MH, et al. M1 and M2 macrophages differentially regulate hematopoietic stem cell self-renewal and *ex vivo* expansion. *Blood Adv.* (2018) 2:859–70. doi: 10.1182/bloodadvances.2018015685
12. Husted TL, Blanchard J, Schuster R, Shen H, Lentsch AB. Potential role for IL-23 in hepatic ischemia/reperfusion injury. *Inflamm Res.* (2006) 177-178. doi: 10.1007/s00011-006-0073-1
13. Li L, Huang L, Vergis AL, Ye H, Bajwa A, Narayan V, et al. IL-17 produced by neutrophils regulates IFN-gamma-mediated neutrophil migration in mouse kidney ischemia-reperfusion injury. *J Clin Invest.* (2010) 120:331–42. doi: 10.1172/JCI38702
14. Jing X, Korchagina AA, Shein SA, Muraoka WT, Koroleva E, Tumanov AV. IL-23 contributes to *Campylobacter jejuni*-induced intestinal pathology via promoting IL-17 and IFNγ responses by innate lymphoid cells. *Front Immunol.* (2021) 11:579615. doi: 10.3389/fimmu.2020.579615
15. Hou Y, Zhu L, Tian H, Sun HX, Wang R, Zhang L, et al. IL-23-induced macrophage polarization and its pathological roles in mice with imiquimod-induced psoriasis. *Protein Cell.* (2018) 9:1027–38. doi: 10.1007/s13238-018-0505-z
16. Chen X, Huang Y, Wang D, Dong N, Du X. PJ34, a PARP1 inhibitor, attenuates acute allograft rejection after murine heart transplantation via regulating the CD4+ T lymphocyte response. *Transpl Int.* (2020) doi: 10.1111/tri.13809
17. Blériot C, Dupuis T, Jouvion G, Eberl G, Disson O, Lecuit M. Liver-resident macrophage necroptosis orchestrates type 1 microbicidal inflammation and type-2-mediated tissue repair during bacterial infection. *Immunity.* (2015) 42:145–58. doi: 10.1016/j.immuni.2014.12.020
18. Kierdorf K, Prinz M, Geissmann F, Gomez Perdiguero E. Development and function of tissue resident macrophages in mice. *Semin Immunol.* (2015) 27:369–78. doi: 10.1016/j.smim.2016.03.017
19. Cole AP, Hoffmeyer E, Chetty SL, Cruz-Cruz J, Hamrick F, Youssef O, et al. Microglia in the brain tumor microenvironment. *Adv Exp Med Biol.* (2020) 1273:197–208. doi: 10.1007/978-3-030-49270-0_11
20. Hoeffel G, Chen J, Lavin Y, Low D, Almeida FF, See P, et al. C-Myb(+) erythro-myeloid progenitor-derived fetal monocytes give rise to adult tissue-resident macrophages. *Immunity.* (2015) 42:665–78. doi: 10.1016/j.immuni.2015.03.011
21. Yue S, Zhou H, Wang X, Busuttil RW, Kupiec-Weglinski JW, Zhai Y. Prolonged ischemia triggers necrotic depletion of tissue-resident macrophages to facilitate inflammatory immune activation in liver ischemia reperfusion injury. *J Immunol.* (2017) 198:3588–95. doi: 10.4049/jimmunol.1601428
22. Sakai M, Troutman TD, Seidman JS, Ouyang Z, Spann NJ, Abe Y, et al. Liver-derived signals sequentially reprogram myeloid enhancers to initiate and maintain Kupffer cell identity. *Immunity.* (2019) 51:655–70.e8. doi: 10.1016/j.immuni.2019.09.002
23. Tran S, Baba I, Poupel L, Dussaud S, Moreau M, Gélineau A, et al. Impaired Kupffer cell self-renewal alters the liver response to lipid overload during non-alcoholic steatohepatitis. *Immunity.* (2020) 53:627–40.e5. doi: 10.1016/j.immuni.2020.06.003
24. Devisscher L, Scott CL, Lefere S, Raevens S, Bogaerts E, Paridaens A, et al. Non-alcoholic steatohepatitis induces transient changes within the liver macrophage pool. *Cell Immunol.* (2017) 322:74–83. doi: 10.1016/j.cellimm.2017.10.006
25. Rao J, Yue S, Fu Y, Zhu J, Wang X, Busuttil RW, et al. ATF6 mediates a pro-inflammatory synergy between ER stress and TLR activation in the pathogenesis of liver ischemia-reperfusion injury. *Am J Transplant.* (2014) 14:1552–61. doi: 10.1111/ajt.12711

26. Sosa RA, Terry AQ, Kaldas FM, Jin YP, Rossetti M, Ito T, et al. Disulfide high-mobility group box 1 drives ischemia-reperfusion injury in human liver transplantation. *Hepatology*. (2020) doi: 10.1002/hep.31324. [Epub ahead of print].
27. Gill R, Tsung A, Billiar T. Linking oxidative stress to inflammation: toll-like receptors. *Free Radic Biol Med.* (2010) 48:1121–32. doi: 10.1016/j.freeradbiomed.2010.01.006
28. Yona S, Kim KW, Wolf Y, Mildner A, Varol D, Breker M, et al. Fate mapping reveals origins and dynamics of monocytes and tissue macrophages under homeostasis. *Immunity.* (2013) 38:79–91 doi: 10.1016/j.immuni.2012.12.001
29. Jin D, Lu T, Ni M, Wang H, Zhang J, Zhong C, et al. Farnesoid X receptor activation protects liver from ischemia/reperfusion injury by up-regulating small heterodimer partner in Kupffer cells. *Hepatol Commun.* (2020) 4:540–54. doi: 10.1002/hep4.1478
30. Buch T, Heppner FL, Tertilt C, Heinen TJ, Kremer M, Wunderlich FT, et al. A Cre-inducible diphtheria toxin receptor mediates cell lineage ablation after toxin administration. *Nat Methods.* (2005) 2:419–26. doi: 10.1038/nmeth762
31. Devey L, Ferenbach D, Mohr E, Sangster K, Bellamy CO, Hughes J, et al. Tissue-resident macrophages protect the liver from ischemia reperfusion injury via a heme oxygenase-1-dependent mechanism. *Mol Ther.* (2009) 17:65–72. doi: 10.1038/mt.2008.237
32. Khan F, Sar A, Gonul I, Benediktsson H, Doulla J, Yilmaz S, et al. Graft inflammation and histologic indicators of kidney chronic allograft failure: low-expressing interleukin-10 genotypes cannot be ignored. *Transplantation.* (2010) 90:630–8. doi: 10.1097/TP.0b013e3181ea391e
33. Nakamura K, Kageyama S, Kupiec-Weglinski JW. The evolving role of neutrophils in liver transplant ischemia-reperfusion injury. *Curr Transplant Rep.* (2019) 6:78–89. doi: 10.1007/s40472-019-0230-4
34. Lu P, Takai K, Weaver VM, Werb Z. Extracellular matrix degradation and remodeling in development and disease. *Cold Spring Harb Perspect Biol.* (2011) 3:a005058. doi: 10.1101/cshperspect.a005058
35. Dick MK, Miao JH, Limaiem F. *Histology, Fibroblast*. Treasure Island, FL: StatPearls Publishing. (2020). Available online at: https://www.ncbi.nlm.nih.gov/books/NBK541065/
36. Feghali CA, Wright TM. Cytokines in acute and chronic inflammation. *Front Biosci.* (1997) 2:d12–26. doi: 10.2741/A171
37. Kendall RT, Feghali-Bostwick CA. Fibroblasts in fibrosis: novel roles and mediators. *Front Pharmacol.* (2014) 5:123. doi: 10.3389/fphar.2014.00123
38. Janik MK, Kruk B, Szczepankiewicz B, Kostrzewa K, Raszeja-Wyszomirska J, Górnicka B, et al. Measurement of liver and spleen stiffness as complementary methods for assessment liver fibrosis in autoimmune hepatitis. *Liver Int.* (2020) 41:348–56. doi: 10.1016/S0168-8278(20)31449-5
39. Iritani S, Akuta N, Kawamura Y, Kajiwara A, Kasuya K, Fujiyama S, et al. Non-invasive predictors of prognosis of Asian patients with histopathologically-confirmed lean nonalcoholic fatty liver disease. *BMC Gastroenterol.* (2020) 20:368. doi: 10.1186/s12876-020-01509-3
40. Helgeson ES, Mannon R, Grande J, Gaston RS, Cecka MJ, Kasiske BL, et al. i-IFTA and chronic active T cell-mediated rejection: a tale of 2 (DeKAF) cohorts. *Am J Transplant*. (2020) doi: 10.1111/ajt.16352. [Epub ahead of print].
41. Coelho S, Ortíz F, Gelpi R, Koskinen P, Porta N, Bestard O, et al. Sterile leukocyturia is associated with interstitial fibrosis and tubular atrophy in kidney allograft protocol biopsies. *Am J Transplant.* (2014) 14:908–15. doi: 10.1111/ajt.12639
42. Denic A, Elsherbiny H, Mullan AF, Leibovich BC, Thompson RH, Ricaurte Archila L, et al. Larger nephron size and nephrosclerosis predict progressive CKD and mortality after radical nephrectomy for tumor and independent of kidney function. *J Am Soc Nephrol.* (2020) 31:2642–52. doi: 10.1681/ASN.2020040449
43. Clotet-Freixas S, McEvoy CM, Batruch I, Pastrello C, Kotlyar M, Van JAD, et al. Extracellular matrix injury of kidney allografts in antibody-mediated rejection: a proteomics study. *J Am Soc Nephrol.* (2020) 31:2705–24. doi: 10.1681/ASN.2020030286
44. Kaul AM, Goparaju S, Dvorina N, Iida S, Keslar KS, de la Motte CA, et al. Acute and chronic rejection: compartmentalization and kinetics of counterbalancing signals in cardiac transplants. *Am J Transplant*. (2015) 15:333–45. doi: 10.1111/ajt.13014
45. Toki D, Zhang W, Hor KL, Liuwantara D, Alexander SI, Yi Z, et al. The role of macrophages in the development of human renal allograft fibrosis in the first year after transplantation. *Am J Transplant*. (2014) 14:2126–36. doi: 10.1111/ajt.12803
46. Itoh Y, Saitoh M, Miyazawa K. Smad3-STAT3 crosstalk in pathophysiological contexts. *Acta Biochim Biophys Sin.* (2018) 50:82–90. doi: 10.1093/abbs/gmx118
47. Wang S, Meng XM, Ng YY, Ma FY, Zhou S, Zhang Y, et al. TGF-β/Smad3 signalling regulates the transition of bone marrow-derived macrophages into myofibroblasts during tissue fibrosis. *Oncotarget.* (2016) 7:8809–22. doi: 10.18632/oncotarget.6604
48. Wang YY, Jiang H, Pan J, Huang X-R, Wang Y-C, Huang H-F, et al. Macrophage-to-myofibroblast transition contributes to interstitial fibrosis in chronic renal allograft injury. *J Am Soc Nephrol.* (2017) 28:2053–67. doi: 10.1681/ASN.2016050573
49. Surprenant A, Rassendren F, Kawashima E, North RA, Buell G. The cytolytic P2Z receptor for extracellular ATP identified as a P2X receptor (P2X7). *Science.* (1996) 272:735–8. doi: 10.1126/science.272.5262.735
50. Kubes P, Mehal WZ. Sterile inflammation in the liver. *Gastroenterology.* (2012) 143:1158–72. doi: 10.1053/j.gastro.2012.09.008
51. Wu C, Zhao Y, Xiao X, Fan Y, Kloc M, Liu W, et al. Graft-infiltrating macrophages adopt an M2 phenotype and are inhibited by purinergic receptor P2X7 antagonist in chronic rejection. *Am J Transplant.* (2016) 16:2563–73. doi: 10.1111/ajt.13808
52. Wynn TA, Ramalingam TR. Mechanisms of fibrosis: therapeutic translation for fibrotic disease. *Nat Med.* (2012) 18:1028–40. doi: 10.1038/nm.2807
53. Ulloa L, Doody J, Massagué J. Inhibition of transforming growth factor-beta/SMAD signalling by the interferon-gamma/STAT pathway. *Nature.* (1999) 397:710–3. doi: 10.1038/17826
54. Chiaramonte MG, Donaldson DD, Cheever AW, Wynn TA. An IL-13 inhibitor blocks the development of hepatic fibrosis during a T-helper type 2-dominated inflammatory response. *J Clin Invest.* (1999) 104:777–85. doi: 10.1172/JCI7325
55. Rahmani M, Cruz RP, Granville DJ, McManus BM. Allograft vasculopathy versus atherosclerosis. *Circ Res.* (2006) 99:801–15. doi: 10.1161/01.RES.0000246086.93555.f3
56. Luo Z, Liao T, Zhang Y, Zheng H, Sun Q, Han F, et al. Triptolide attenuates transplant vasculopathy through multiple pathways. *Front Immunol.* (2020) 11:612. doi: 10.3389/fimmu.2020.00612
57. Mitchell RN, Libby P. Vascular remodeling in transplant vasculopathy. *Circ Res.* (2007) 100:967–78. doi: 10.1161/01.RES.0000261982.76892.09
58. Shetty M, Chowdhury YS. *Heart Transplantation Allograft Vasculopathy*. Treasure Island, FL: StatPearls Publishing (2020).
59. Lin FY, Shih CM, Huang CY, Tsai YT, Loh SH, Li CY, et al. Dipeptidyl peptidase-4 inhibitor decreases allograft vasculopathy via regulating the functions of endothelial progenitor cells in normoglycemic rats. *Cardiovasc Drugs Ther.* (2020) doi: 10.1007/s10557-020-07013-w. [Epub ahead of print].
60. Merola J, Jane-Wit DD, Pober JS. Recent advances in allograft vasculopathy. *Curr Opin Organ Transplant.* (2017) 22:1–7. doi: 10.1097/MOT.0000000000000370
61. Chih S, Chong AY, Mielniczuk LM, Bhatt DL, Beanlands RS. Allograft vasculopathy: the Achilles' heel of heart transplantation. *J Am Coll Cardiol.* (2016) 68:80–91. doi: 10.1016/j.jacc.2016.04.033
62. Zarjou A, Guo L, Sanders PW, Mannon RB, Agarwal A, George JF. A reproducible mouse model of chronic allograft nephropathy with vasculopathy. *Kidney Int.* (2012) 82:1231–5. doi: 10.1038/ki.2012.277
63. Croker BP, Clapp WL, Abu Shamat AR, Kone BC, Peterson JC. Macrophages and chronic renal allograft nephropathy. *Kidney Int Suppl.* (1996) 57:S42–9.
64. Valantine HA. Cardiac allograft vasculopathy: central role of endothelial injury leading to transplant "atheroma". *Transplantation.* (2003) 76:891–9. doi: 10.1097/01.TP.0000080981.90718.EB
65. Sun HJ, Zhou T, Wang Y, Fu YW, Jiang YP, Zhang LH, et al. Macrophages and T lymphocytes are the predominant cells in intimal arteritis of resected renal allografts undergoing acute rejection. *Transpl Immunol.* (2011) 25:42–8. doi: 10.1016/j.trim.2011.04.002
66. Matheson PJ, Dittmer ID, Beaumont BW, Merrilees MJ, Pilmore HL. The macrophage is the predominant inflammatory cell in

renal allograft intimal arteritis. *Transplantation.* (2005) 79:1658–62. doi: 10.1097/01.TP.0000167099.51275.EC
67. Kozakowski N, Böhmig GA, Exner M, Soleiman A, Huttary N, Nagy-Bojarszky K, et al. Monocytes/macrophages in kidney allograft intimal arteritis: no association with markers of humoral rejection or with inferior outcome. *Nephrol Dial Transplant.* (2009) 24:1979–86. doi: 10.1093/ndt/gfp045
68. Kitchens WH, Chase CM, Uehara S, Cornell LD, Colvin RB, Russell PS, et al. Macrophage depletion suppresses cardiac allograft vasculopathy in mice. *Am J Transplant.* (2007) 7:2675–82. doi: 10.1111/j.1600-6143.2007.01997.x
69. Haas M, Loupy A, Lefaucheur C Mengel M et al. The Banff 2017 Kidney Meeting Report: revised diagnostic criteria for chronic active T cell-mediated rejection, antibody-mediated rejection, and prospects for integrative endpoints for next-generation clinical trials. *Am J Transplant.* (2018) 18:293–307. doi: 10.1111/ajt.14625
70. Chu Z, Sun C, Sun L, Feng C, Yang F, Xu Y, et al. Primed macrophages directly and specifically reject allografts. *Cell Mol Immunol.* (2020) 17:237–46. doi: 10.1038/s41423-019-0226-0
71. Chu Z, Feng C, Sun C, Xu Y, Zhao Y. Primed macrophages gain long-term specific memory to reject allogeneic tissues in mice. *Cell Mol Immunol.* (2020) doi: 10.1038/s41423-020-00521-7. [Epub ahead of print].
72. Peng X, Yong Z, Xiaoyan W, Yuanshan C, Guangzhu W, Xuehuan L. Mechanism of graft damage caused by NTPDase1-activated Macrophages in acute antibody-mediated rejection. *Transplant Proc.* (2021) 53:436–42. doi: 10.1016/j.transproceed.2020.06.033
73. Moreau A, Varey E, Anegon I, Cuturi MC. Effector mechanisms of rejection. *Cold Spring Harb Perspect Med.* (2013) 3:a015461. doi: 10.1101/cshperspect.a015461
74. Allison AC, Eugui EM. Mechanisms of action of mycophenolate mofetil in preventing acute and chronic allograft rejection. *Transplantation.* (2005) 80(Suppl. 2):S181–90. doi: 10.1097/01.tp.0000186390.10150.66
75. Kolaczkowska E, Kubes P. Neutrophil recruitment and function in health and inflammation. *Nat Rev Immunol.* (2013) 13:159–75. doi: 10.1038/nri3399
76. Broichhausen C, Riquelme P, Geissler EK, Hutchinson JA. Regulatory macrophages as therapeutic targets and therapeutic agents in solid organ transplantation. *Curr Opin Organ Transplant.* (2012) 17:332–42. doi: 10.1097/MOT.0b013e328355a979
77. Jose MD, Ikezumi Y, van Rooijen N, Atkins RC, Chadban SJ. Macrophages act as effectors of tissue damage in acute renal allograft rejection. *Transplantation.* (2003) 76:1015–22. doi: 10.1097/01.TP.0000083507.67995.13
78. Ordikhani F, Pothula V, Sanchez-Tarjuelo R, Jordan S, Ochando J. Macrophages in organ transplantation. *Front Immunol.* (2020) 11:582939. doi: 10.3389/fimmu.2020.582939

Conflict of Interest: The authors declare that the research was conducted in the absence of any commercial or financial relationships that could be construed as a potential conflict of interest.

frontiers in Immunology

ORIGINAL RESEARCH
published: 18 March 2021
doi: 10.3389/fimmu.2021.657803

Allograft or Recipient ST2 Deficiency Oppositely Affected Cardiac Allograft Vasculopathy *via* Differentially Altering Immune Cells Infiltration

Zhenggang Zhang[1†], *Na Zhang*[1†], *Junyu Shi*[1], *Chan Dai*[1], *Suo Wu*[1], *Mengya Jiao*[1], *Xuhuan Tang*[1], *Yunfei Liu*[1], *Xiaoxiao Li*[1], *Yong Xu*[1], *Zheng Tan*[1,2], *Feili Gong*[1] *and Fang Zheng*[1,2*]

[1] Department of Immunology, School of Basic Medicine, Tongji Medical College, Huazhong University of Science and Technology, Wuhan, China, [2] Key Laboratory of Organ Transplantation, Ministry of Education, NHC Key Laboratory of Organ Transplantation, Key Laboratory of Organ Transplantation, Chinese Academy of Medical Sciences, Wuhan, China

OPEN ACCESS

Edited by:
Hao Wang,
Tianjin Medical University General Hospital, China

Reviewed by:
Hong Zhou,
Anhui Medical University, China
Yingxin Fu,
Tianjin First Central Hospital, China

***Correspondence:**
Fang Zheng
zhengfangtj@hust.edu.cn

[†]*These authors have contributed equally to this work*

Specialty section:
This article was submitted to Alloimmunity and Transplantation, a section of the journal Frontiers in Immunology

Received: *24 January 2021*
Accepted: *05 March 2021*
Published: *18 March 2021*

Citation:
Zhang Z, Zhang N, Shi J, Dai C, Wu S, Jiao M, Tang X, Liu Y, Li X, Xu Y, Tan Z, Gong F and Zheng F (2021) Allograft or Recipient ST2 Deficiency Oppositely Affected Cardiac Allograft Vasculopathy via Differentially Altering Immune Cells Infiltration. Front. Immunol. 12:657803. doi: 10.3389/fimmu.2021.657803

The role of IL-33/ST2 signaling in cardiac allograft vasculopathy (CAV) is not fully addressed. Here, we investigated the role of IL-33/ST2 signaling in allograft or recipient in CAV respectively using MHC-mismatch murine chronic cardiac allograft rejection model. We found that recipients ST2 deficiency significantly exacerbated allograft vascular occlusion and fibrosis, accompanied by increased F4/80$^+$ macrophages and CD3$^+$ T cells infiltration in allografts. In contrast, allografts ST2 deficiency resulted in decreased infiltration of F4/80$^+$ macrophages, CD3$^+$ T cells and CD20$^+$ B cells and thus alleviated vascular occlusion and fibrosis of allografts. These findings indicated that allografts or recipients ST2 deficiency oppositely affected cardiac allograft vasculopathy/fibrosis *via* differentially altering immune cells infiltration, which suggest that interrupting IL-33/ST2 signaling locally or systematically after heart transplantation leads different outcome.

Keywords: IL-33, ST2, heart transplantation, cardiac allograft vasculopathy, chronic rejection

INTRODUCTION

Despite improvement in short-term patient survival after heart transplantation (HTx), long-term survival rates have not improved much, mainly because of Cardiac Allograft Vasculopathy (CAV) (1). CAV is a major cause of graft failure in cardiac transplant recipients who survives more than 1 year after transplantation, with the morbidity of CAV exceeding 50% at 5 years (2). CAV is primarily characterized as an immune-mediated pan-arterial disease with intimal hyperplasia and narrowing of the allograft artery (3). Recent insights have underscored the fact that innate and specific immune responses are involved in the pathogenesis of CAV (4, 5). Because individual responses to an allograft change over time, assays to monitor the recipient's immune response and individualized methods for therapeutic immune modulation are clearly needed. Nevertheless, past extensive studies, the molecular mechanisms underlying cardiac allograft vasculopathy are not yet to be fully elucidated (6). Up to now, there have been no enough strategies to effectively prevent CAV (7). IL-33 is a member of the IL-1 family (8). IL-33 has been identified to be the special ligand

for the unique receptor ST2 (9). The IL-33/ST2 signaling has emerged as a pathway with a central role in processes of the immune response and homeostasis (10). At present, some studies have demonstrated that IL-33 as a novel alarmin in heart transplantation that limits CAV *via* restraining the local activation of macrophages (11, 12). IL-33 expression has been reported in the coronary artery (8, 13). How IL-33/ST2 signaling pathway is modulated in CAV and the functional effects of IL-33/ST2 is remained unknown. Based on these findings, we examined the role and functional significance of IL-33/ST2 signaling in cardiac allogeneic transplantation in mice. Our data indicated that grafts or recipients IL-33/ST2 signaling oppositely affected CAV *via* differentially altering immune cells infiltration.

MATERIALS AND METHODS

Animals

C57BL/6 (B6, H-2^b) mice, males, aged 7-9 weeks, were purchased from Shanghai SLAC Laboratory Animal Center, Chinese Academy of Sciences (Shanghai, China). B6.C-H-2bm12KhEg (bm12, H-2^{bm12}) males, strains of mice B6 arose through a spontaneous mutation in the MHC-II I-A^b molecule (14), were purchased from the Jackson Laboratory (Bar Harbor, ME). ST2 knockout C57BL/6 mice were custom-made by Cyagen (Guangzhou) Bioscience Inc. All experimental mice were maintained in micro-isolator cages under humidity free conditions in the animal facility. All experiments were performed in compliance with the guidelines of Tongji Medical College Animal Care and Use Committee.

Heterotopic Cardiac Transplantation

Heterotopic heart transplantation was performed by a microsurgical technique. Donor hearts were transplanted into recipients through end-to-side anastomosis of the donor ascending aorta and pulmonary artery to the recipient abdominal aorta and inferior vena cava as described before (15). For cardiac transplantation models, C57BL/6 and bm12 mice were used both as donors and recipients, respectively. In single MHC-II mismatched models, bm12 mice were used as donors and B6 mice were used as recipients. Meanwhile, the *ST2*$^{-/-}$ mice received bm12 donors' hearts as the experimental group. Donors and recipients switch roles in turning. This is an established mice cardiac transplantation model of chronic allograft rejection without immunosuppressive treatment. After cardiac transplantation, allograft impulse was assessed by daily abdominal palpation.

General Histology and Immunohistochemical Staining

The heart allografts were resected from the recipient mouse in weeks 2, 4 and 8 weeks post transplantation. The heart specimens were fixed in 4% formaldehyde and then embedded in paraffin, sections were cut into 4μm thickness. The heart sections were stained with haematoxylin and eosin (H&E) staining to access the general histology. In addition, immunohistochemical staining was performed to determine the infiltration of inflammatory situation. In brief, the deparaffinized sections were quenched in 3% H_2O_2 for 30 minutes followed by antigen retrieval in sodium citrate (pH6.0) at 98°C for 20 minutes. Subsequently, sections were incubated with antibodies against CD3 (1:200, #PB9093, Boster Ltd., Wuhan, China), CD20 (1:500, #GB11540, Servicebio, Wuhan, China), and F4/80 (1:200, #70076, Cell Signaling Technology, Inc., Danvers, MA, USA) over night at 4°C to detect the infiltration of T cell, B cell and macrophage into heart, respectively. Next, 3,3'-diaminobenziding (DAB) were used as a chromogenic substrate. Statistical analysis of the histological sections was performed to quantitatively determine the amount of inflammatory cells at 2, 4, and 8 weeks. Graft rejection was graded on the extent of infiltration and the anatomical localization of inflammatory cells according to the International Society of Heart and Lung Transplantation (ISHLT) standard (16). In addition, the heart sections were also stained with Masson trichrome (#G1006, Servicebio, Wuhan, China) which differentially stains the nucleus, muscle tissue, and collagen. After H&E staining, immunohistochemical staining or Masson trichrome staining, each section was observed under light microscope at 200× and 400× magnifications, and at least 2 arteries were obtained in the same section. Quantitative analysis was performed by using the image analytical software ImageJ (Media Cybernetics, Rockville, MD, USA) to determine the histological changes after the heart transplantation for 2, 4, and 8 weeks.

Statistical Analysis

Experimental data are expressed as the mean ± standard error of the mean (SEM). Statistical analysis was performed using Prism 6.0 (GraphPad Software, San Diego, CA) and statistical tested use indicated in the figure legends. A value of $P<0.05$ was considered statistically significant.

RESULTS

Recipients ST2 Deficiency Exacerbated and Allograft ST2 Deficiency Alleviated Allograft Vasculopathy

To ascertain the potential impact of ST2 deficiency on CAV, we used the chronic heart transplantation rejection mice model (heart transplantation in between bm12 mouse and C57 mouse). As shown in **Supplementary Figure 1A**, the pathological features of the left and right ventricle of the cardiac allograft after transplantation were different. In addition, the coronary artery is composed of intima which comprises endothelial cells, the media consisting of smooth muscle cells, and adventitia which contains fibroblasts and other cell types. In this study, we mainly observed the allograft artery in the outer tissue of left ventricle free wall (**Supplementary Figure 1B**). In the syngeneic groups (bm12→bm12 or C57→C57) (**Figure 1A**, left panel), there were no intimal hyperplasia and stenosis and no inflammatory

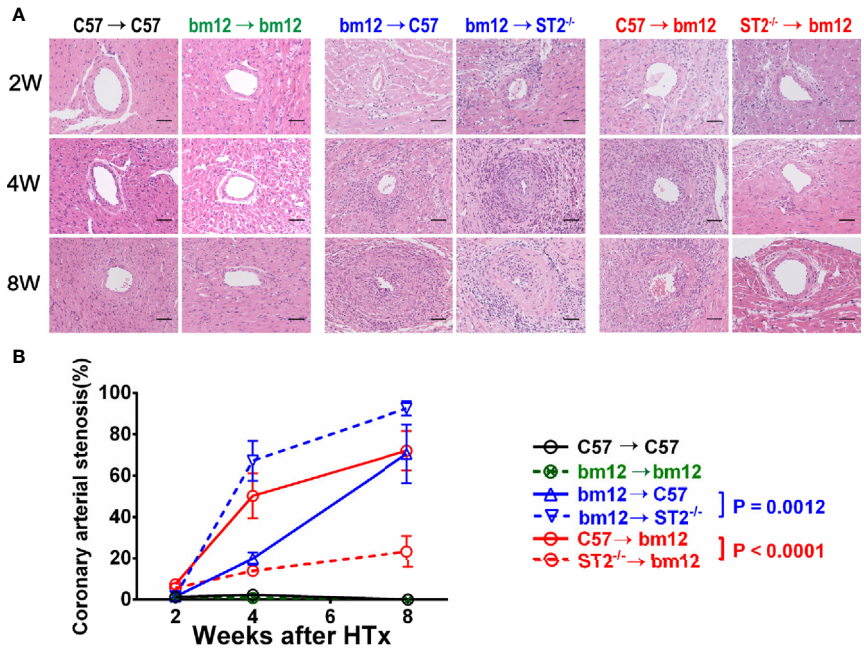

FIGURE 1 | The effects of ST2 absence in cardiac graft or recipients on cardiac allograft vasculopathy. bm12 cardiac grafts were transplanted into wild type (WT) or *ST2*$^{-/-}$ C57 recipients. Cardiac grafts from WT or *ST2*$^{-/-}$ C57 mice were transplanted into bm12 recipients (n=3-6 per group). **(A)** H&E staining of allograft artery harvested on week 2,4 and 8. **(B)** Quantification of vasculopathy luminal occlusion (n = 3-6 per group) in the allografts. The percentage of vascular occlusion area was quantified by Image J. Coronary arterial stenosis (%) = (Area of internal lamina – Area of lamina)/Area of internal lamina×100% (17). Data are shown as mean ± SEM. Scale bars 50 μm. *P* values were established by 2-way ANOVA.

cells infiltration in the intima and adventitia of cardiac allograft arteries. The intimal cells of cardiac allograft arteries were monolayer and neatly glabrate. After bm12 hearts were transplanted into C57 recipients (bm12→C57 group), the intima of allograft artery had no significant variation and the adventitia was infiltrated a few of inflammatory cells at week 2 (**Figure 1A**, middle panel, up). At week 4, the intima of the allograft artery significantly thickened, complicating vascular stenosis and the infiltration of inflammatory cells (**Figure 1A**, middle panel, middle). At week 8, the vascular stenosis, the infiltration of inflammatory cells in the intima and adventitia, as well as the intimal hyperplasia further aggravated. The allograft artery was almost totally occluded (**Figure 1A**, middle panel, down). Compared with bm12→C57 group, ST2 deficiency in recipients (bm12→ST2$^{-/-}$ group) markedly aggravated intimal hyperplasia, vascular stenosis and immune cells infiltration of allograft artery at both week 4 and 8 (**Figures 1A**, middle panel, **B**, blue line). The pathological features of coronary artery in the transplanted heart of group C57→bm12 were similar with that in group bm12→C57 (**Figure 1A**, right panel). There was no statistically significant difference between the two groups at 2 weeks, 4 weeks and 8 weeks (*P* value was 0.9505, 0.1449 and 0.4570). However, compared with C57→bm12 group, deficiency of ST2 in cardiac allografts (ST2$^{-/-}$→bm12 group) markedly alleviated the coronary arterial stenosis at week 4 and 8 (**Figures 1A**, right panel, B red line). These results suggested that the ST2 signaling in the recipient prevents, and in the transplanted heart enhance, the cardiac allograft vasculopathy.

Recipients ST2 Deficiency Exacerbated and Allograft ST2 Deficiency Alleviated Allograft Vasculopathy Fibrosis

To further confirm the effects of ST2 deficiency on CAV, the quantitative Masson staining was used to detect the vasculopathy fibrosis. In the syngeneic groups, the fibrosis of the allograft artery was not obvious (**Figure 2A**, left panel). In bm12→C57 group, the fibrosis of the allograft artery gradually increased and arrived the peak at week 8 (**Figure 2A**, left panel). Compared with bm12→C57 group, ST2 deficiency in recipients (bm12→ST2$^{-/-}$ group) markedly aggravated the fibrosis of the allograft artery, especially at week 4 and 8. (**Figures 2A**, middle panel, **B**). The fibrosis of allograft artery C57→bm12 group were similar with that in group bm12→C57 at each time point (**Figure 2A**, right panel). There was no statistically significant difference between the two groups at 2 weeks, 4 weeks and 8 weeks (*P* value was 0.0832, 0.1779 and 0.0958). ST2 deficiency in cardiac allograft (ST2$^{-/-}$→bm12) decreased the fibrosis of allograft artery significantly (**Figures 2A**, right panel, **B**). Next, we further observed the characteristics of the fibrosis of vasculopathy in detail. As illustrated in **Supplementary Figure 2A**, in bm12→C57 group, the fibrosis of allograft arteries major existed in adventitia at week 2. Accompanying the development

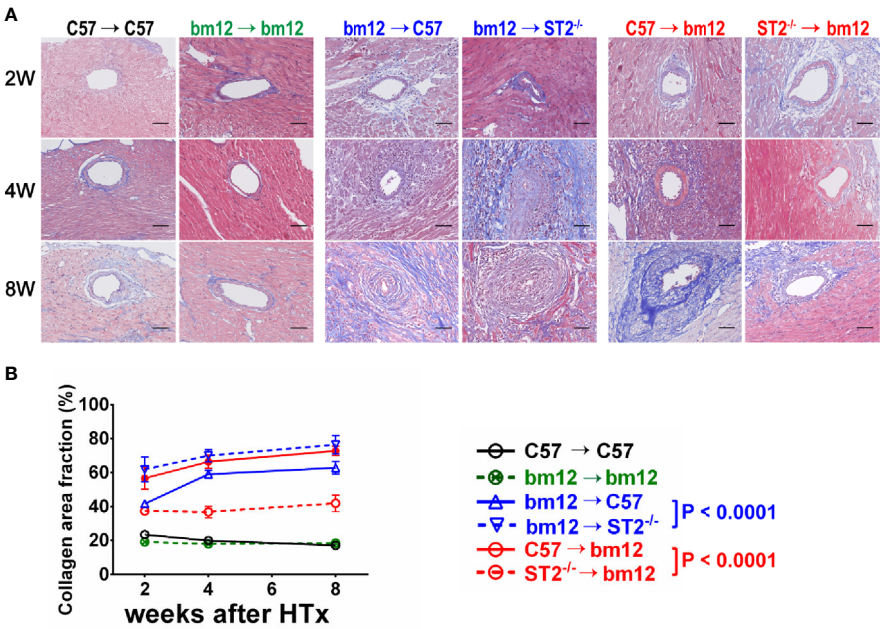

FIGURE 2 | The effects of recipient or allograft ST2 deficiency on the fibrosis of vasculopathy. **(A)** Masson staining of allografts artery harvested on week 2, 4 and 8. **(B)** Quantification of collagen area fraction in vasculopathy (n = 3-6 per group) using Image (J) The cardiac allograft vasculopathy collagen area fraction (%) = Area of artery collagen volume/Area of artery cross sections×100%. Data are shown as mean ± SEM. Scale bars are 50 μm. *P* values were established by 2-way ANOVA.

of CAV, the fibrosis in intima increased gradually. Recipients ST2 deficiency significantly enhanced the percentage of intima fibrosis in the total fibrosis of vasculopathy, while an opposite tendency was displayed when allograft ST2 was deleted. These results suggested that recipient-derived ST2 signaling inhibited and graft-derived ST2 signaling accelerated the fibrosis of vasculopathy.

Recipients ST2 Deficiency Increased and Allograft ST2 Deficiency Decreased Macrophage Infiltration in Allografts

To investigate whether the immune cells infiltration was associated with the influence of ST2 deficiency on cardiac allograft vasculopathy, the impact of ST2 deficiency on macrophage infiltration was detected *via* immunohistochemistry. As shown in **Figure 3**, there were no obvious macrophage ($F4/80^+$ cells) infiltration in the arterial wall of allograft in syngeneic groups (**Figures 3A**, left panel, **B**, black line and green line). In the control group (bm12→C57), there was a few of $F4/80^+$ macrophages infiltration in the arterial wall of the allograft at week 2 (**Figure 3A**, middle panel). Subsequently, at week 4 and 8, the infiltrated macrophages increased. Deficiency of ST2 in recipients markedly increased $F4/80^+$ macrophages infiltration to the maximum at week 4 (**Figures 3A**, middle panel, **B**, blue lines). In C57→bm12 group, there was the maximum infiltration of $F4/80^+$ macrophages in the arterial wall at week 4 (**Figures 3A**, right panel, **B**). The $F4/80^+$ macrophages infiltration in the arterial wall of the allograft C57→bm12 group were similar with that in group bm12→C57 at each time point (**Figures 3A**, right panel, **B**). There was no statistically significant difference between the two groups at 2 weeks, 4 weeks and 8 weeks (*P* value was 0.2260, 0.9271 and 0.2906). However, at week 8, the number of infiltrated macrophages no obvious changed compared with that at week 4 (**Figures 3A**, right panel, **B**, red solid line). ST2 deficiency in cardiac allograft markedly diminished the infiltration $F4/80^+$ macrophages in the coronary arterial wall at week 2, 4 and 8 (**Figures 3A**, right panel, **B**, red dotted line).

Next, we further observed the macrophages infiltration in the arterial intima and adventitia respectively. Recipients ST2 deficiency increased the macrophages infiltration either in the arterial intima or adventitia (**Supplementary Figures 3A, B**). Allograft ST2 deficiency decreased macrophages infiltration in both arterial intima and adventitia (**Supplementary Figures 3C, D**). These results suggested that the CAV and fibrosis degree alteration induced by ST2 deficiency is positively associated with the number of infiltrated macrophages.

Recipients ST2 Deficiency Increased and Allograft ST2 Deficiency Decreased $CD3^+$ T Cells Infiltration in Allografts

To confirm whether the specific immune cells infiltration was associated with the influence of ST2 deficiency on cardiac allograft vasculopathy, the impact of ST2 deficiency on T cells infiltration was detected *via* immunohistochemistry. As shown in **Figure 4**, there were no obvious T cells ($CD3^+$ cells) infiltration in the arterial wall of allograft in syngeneic groups

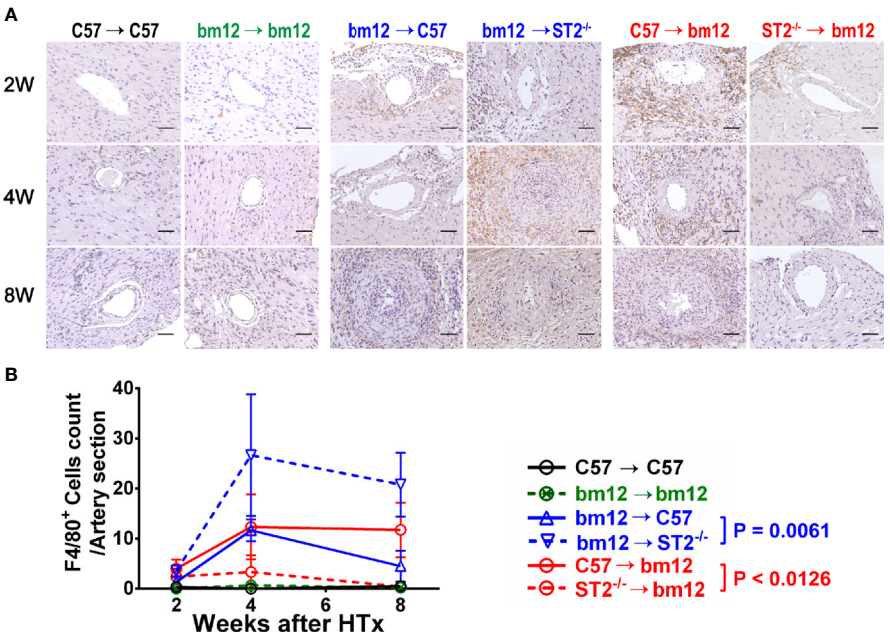

FIGURE 3 | The effects of recipient or graft ST2 deficiency on F4/80$^+$ macrophages infiltration in cardiac allograft. **(A)** The allograft infiltrated F4/80$^+$ macrophages identified using IHC. **(B)** Quantification of infiltrated F4/80$^+$ macrophages (n = 4-6 per group) in the arterial wall of allografts with Image (J) HTx: heart transplantation. Data are presented as mean ± SEM. Scale bars are 50 μm. *P* values were established by 2-way ANOVA.

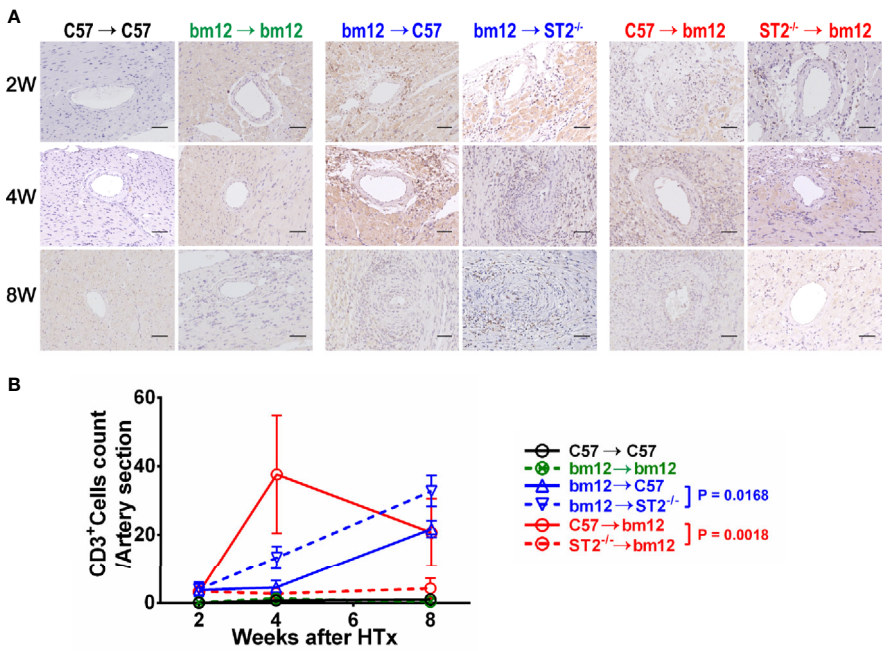

FIGURE 4 | The effects of recipient or graft ST2 deficiency on CD3$^+$ T cells infiltration in cardiac allograft. **(A)** The allograft infiltrated CD3$^+$ T cells identified using IHC. **(B)** Quantification of infiltrated CD3$^+$ T cells (n = 4-6 per group) in the arterial wall of allografts with Image J. HTx: heart transplantation. Data are presented as mean ± SEM. Scale bars are 50 μm. *P* values were established by 2-way ANOVA.

(**Figures 4A**, left panel, **B**, black line and green line). In the control group (bm12→C57), there was a few of $CD3^+$ T cells infiltration in the arterial wall of the graft at week 2 (**Figure 4A**, middle panel). Subsequently, at week 4 and 8, the infiltrated $CD3^+$ T cells increased. Deficiency of ST2 in recipients markedly increased $CD3^+$ T cells infiltration to the maximum at week 8 (**Figures 4A**, middle panel, **B**, blue lines). In C57→bm12 group, there was the maximum infiltration of $CD3^+$ T cells in the arterial wall at week 4 (**Figures 4A**, right panel, **B**). The $CD3^+$ T cells infiltration in the arterial wall of the allograft C57→bm12 group were similar with that in group bm12→C57 at each time point (**Figures 4A**, right panel, **B**). There was no statistically significant difference between the two groups at 2 weeks, 4 weeks and 8 weeks (*P* value was 0.7389, 0.0724 and 0.8444). However, at week 8, the number of infiltrated $CD3^+$ T cells significantly decreased compared with that at week 4 (**Figures 4A**, right panel, **B** red solid line). ST2 deficiency in cardiac allograft markedly diminished the infiltration $CD3^+$ T cells in the coronary arterial wall at week 2, 4 and 8 (**Figures 4A**, right panel, **B**, red dotted line).

Next, we further observed the $CD3^+$ T cells infiltration in the arterial intima and adventitia respectively. Recipients ST2 deficiency increased the $CD3^+$ T cells infiltration either in the arterial intimae or adventitia (**Supplementary Figures 4A, B**). Allograft ST2 deficiency decreased $CD3^+$ T cells infiltration in both arterial intimae and adventitia (**Supplementary Figures 4C, D**). These results suggested that the CAV and fibrosis degree alteration induced by ST2 deficiency is positively associated with the number of infiltrated $CD3^+$ T cells.

Recipients ST2 Deficiency Had No Impact on and Allograft ST2 Deficiency Decreased $CD20^+$ B Cells Infiltration in Allografts

We further investigated whether the B cells infiltration was associated with the influence of ST2 deficiency on cardiac allograft vasculopathy. As shown in **Figure 5**, there were no obvious B cells ($CD20^+$ B cells) infiltration in the arterial wall of allograft in syngeneic groups (**Figures 5A**, left panel, **B**, black line and green line). In the control group (bm12→C57), there was few of $CD20^+$ B cells infiltration in the arterial wall of the graft at the week 2 (**Figure 5A**, middle panel). Subsequently, at week 4 and 8, the infiltrated $CD20^+$ B cells slightly increased. Deficiency of ST2 in recipients slightly mitigated $CD20^+$ B cells infiltration at week 4 and 8, but no statistical significance (**Figures 5A**, middle panel, **B**, blue lines). In C57→bm12 group, the number of infiltrated $CD20^+$ B cells in the arterial wall gradually increased to the maximum at week 8. The $CD20^+$ T cells infiltration in the arterial wall of the allograft C57→bm12 group were similar with that in group bm12→C57 at each time point (**Figures 5A**, right panel, **B**). There was no statistically significant difference between the two groups at 2 weeks, 4 weeks and 8 weeks (*P* value was 0.3466, 0.1167 and 0.2712). ST2 deficiency in cardiac allograft markedly diminished the infiltration of $CD20^+$ B cells in the arterial wall at week 4 and 8 (**Figures 5A**, right panel, **B**, red lines).

Next, we further observed the $CD20^+$ B cells infiltration in the arterial intimae and adventitia respectively. Recipients

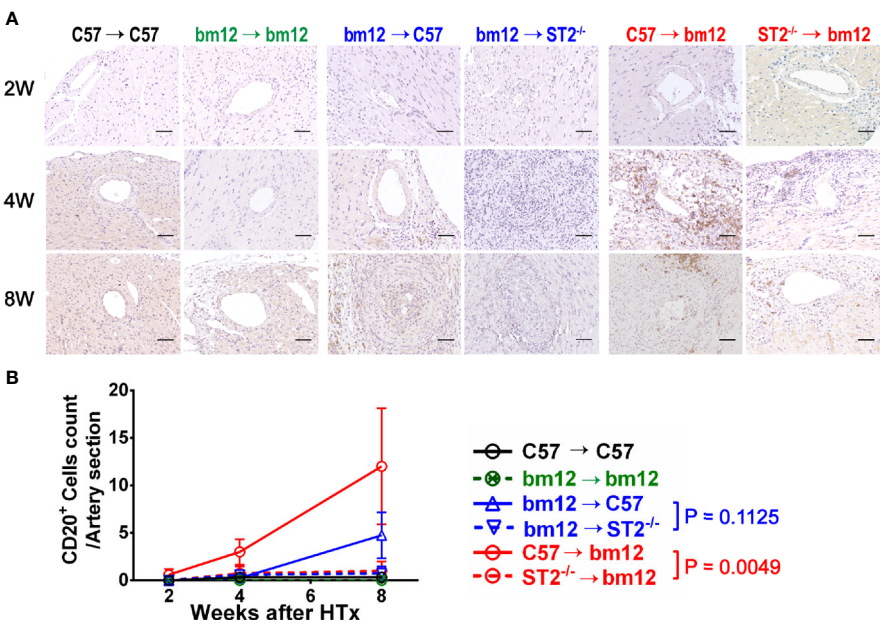

FIGURE 5 | The effects of recipient or graft ST2 deficiency on $CD20^+$ B cells infiltration in cardiac allograft. **(A)** The allograft infiltrated $CD20^+$ B cells identified using IHC and quantified with Image J. **(B)** Quantification of vasculopathy infiltrated $CD20^+$ B cells (n = 4-6 per group) in the wall of the allograft artery. Data are shown as mean ± SEM. Scale bars are 50 μm. *P* values were established by 2-way ANOVA.

ST2 deficiency significantly influence the $CD20^+$ B cells infiltration neither in the arterial intima nor in the adventitia **(Supplementary Figures 5A, B)**. Allograft ST2 deficiency decreased $CD20^+$ B cells infiltration in both arterial intimae and adventitia **(Supplementary Figures 5C, D)**. These results suggested that the CAV and fibrosis degree alteration induced by allograft ST2 deficiency is positively associated with the number of infiltrated $CD20^+$ B cells.

DISCUSSION

While great improvement has been achieved in the precaution of acute rejection, CAV is still primarily resistant to therapy. The immunopathology of CAV is not well understood (18). The aim of this study was to accurately address the role of IL-33/ST2 signaling in cardiac allograft vasculopathy *via* deleting ST2 in allograft or recipient respectively. The ST2 deficiency of the recipient mainly reflects the effects of IL-33/ST2 signaling on immune cells, and the ST2 deficiency of the donor reflects the effects on allograft resident cells. This research method is more conducive to analyze the precise role of IL-33/ST2 signaling in the allograft and recipient. In clinical practice, although the immunosuppressive drugs effectively inhibit immune rejection, they have several side effects and increase the risk of infection. Therefore, it is another choice to intervene regional immunity happened in allograft with relatively few side effects and better curative outcome. Our results suggest that the allograft IL-33/ST2 signal plays obvious roles in the development of CAV, and intervention of the allograft IL-33/ST2 signal may have a better effect. We further observed the local characteristics of CAV. The pathological characteristics of the graft artery were analyzed by dividing it into intima and media. The aim is to more accurately describe the pathological characteristics of each layer of allograft artery tissue and to provide a precise therapeutic target. The tissue sections selected for immunohistochemistry were continuous and similar in structure, which could reflect the spatial location of infiltrated immune cells in CAV and supply the clues communication between different subsets. Immunohistochemistry was an important method to explore the details of the development of CAV.

Our results demonstrate that recipients ST2 deficiency exacerbated fibrosis of vasculopathy. The fibrosis is the major characteristic of the CAV development. In the process of chronic rejection after heart transplantation, specific immune cells infiltrated into the heart graft vessels *via* blood or lymph circulation. Recent studies addressed that ST2 is expressed on many immune cells, including macrophages, and T cells, in particular Th2 cells (10). Our data revealed that the local vascular fibrosis in the allografts of ST2-deficiency recipients accompanied with immune cells, and clear majority of infiltrated immune cells were $CD3^+$ T cells and $F4/80^+$ macrophages. The enhanced local inflammatory response may be related to the increased collagen deposition. Consequently, it can be inferred that the IL-33/ST2 signal of the recipient may influence local fibrosis by impacting the inflammatory cells infiltration. By contrast, allograft ST2 deficiency alleviated allograft vasculopathy fibrosis, especially the intima. It may be related to the decrease of IL-33/ST2 signal-related inflammatory chemokines and pro-inflammatory cytokine that determine the immune cells infiltration in the allograft artery. Li et al. reported that the absence of graft IL-33 resulted in increased chronic allograft vasculopathy and fibrosis (12) which was consistent with our results. In our study, the expression of IL-33 in the heart grafts were not affected in the ST2 knockout donors, and the expression of ST2 in immune cells from the recipients were normal as well. Consequently, the IL-33/ST2 signal could play a protective role normally. However, IL-33 effects, although mostly cardioprotective, vary depending on the disease state and cell type. ST2L is constitutively expressed on cells of the cardiovascular system, in particular endothelial cells (19). Several studies have reported direct activation and pro-inflammatory effects of IL-33 on endothelial cells which is the main cause of CAV (20, 21). Therefore, it can be speculated that the activation endothelial cells were reduced when ST2 deficiency in the transplanted heart, and then the CAV was relieved. This is also the focus of the mechanism we want to explore next. In the same way, it can be inferred that in ST2 knockout recipient mice, the expression of ST2 in the heart grafts endothelial cells were normal, there may be some factors that can promote the development of CAV. In addition, the deficiency of ST2 in the recipient may affect the number and function of immune cells infiltrating the transplanted heart. And this speculation needs further verification. In summary, Li's results are similar to us in exploring the role of IL-33/ST2 signaling in CAV. Besides, our study focused on the role of ST2 in cardiac resident cells and immune cells, which could further explain the mechanism during the development of CAV.

In a word, we provide the evidences that the bioactivities of IL-33/ST2 signaling in CAV are pleiotropy. IL-33/ST2 signaling may inhibit the development of CAV *via* acting on immune cells and facilitate the CAV *via* acting on allograft resident cells. The clinical significance of these findings is that blockade of IL-33/ST2 signal in cardiac allograft may offer new strategy to delay the development of CAV.

DATA AVAILABILITY STATEMENT

The original contributions presented in the study are included in the article/**Supplementary Material**. Further inquiries can be directed to the corresponding author.

ETHICS STATEMENT

The animal study was reviewed and approved by Tongji Medical College Animal Care and Use Committee.

AUTHOR CONTRIBUTIONS

FZ worked on conception and design. Acquisition of data and analysis was conducted by ZZ and NZ. ZZ performed the majority of the experiments, and JS, CD, SW, MJ, XT, YL, XL, YX, ZT, and FG contributed to the experimentation. All authors contributed to the article and approved the submitted version.

FUNDING

This work was supported by the National Natural Science Foundation of China (Grant No. 31670876) and (Grant No. 31470852).

SUPPLEMENTARY MATERIAL

The Supplementary Material for this article can be found online at: https://www.frontiersin.org/articles/10.3389/fimmu.2021.657803/full#supplementary-material

Supplementary Figure 1 | The pathological features of cardiac allograft in chronic transplantation rejection mice model. C57BL/6 cardiac allografts were transplanted into bm12 recipients (n=3 per group). **(A)** Grafts harvested at week 4 were assessed by H&E staining and percentage of vascular occlusion area was quantified by Image J. Quantification of vasculopathy luminal area (n=3 per group) in the allografts. Abbreviations used in this figure: RV: right ventricular; LV: left ventricular; I, Intima; M, Media; A, Adventitia. **(B)** The representative allograft coronary artery section image post transplantation 4 weeks. The dotted area represents the part we sampled arteries which diameters were greater than 50μm. Data were shown as mean ± SEM. Scale bars= 50μm. *P* values established by unpaired Student's t-test. ***P*<0.01.

Supplementary Figure 2 | The Masson staining of coronary artery in cardiac allograft. **(A)** bm12 grafts were transplanted into C57BL/6 or ST2-deficient (*ST2*$^{-/-}$) C57BL/6 recipients (n≥3 per group). The graft collagen volume fraction identified using Masson staining (n = 4-6 per group) in the allografts. The green dotted line represents the elastic layer. The black dotted line indicates the media layer. The red dotted bordered stands for artery lumen. The thickening intima of artery is between the red and green dotted line. Between the green dotted line and the black dotted line are the medial and media parts of the artery. **(B)** Quantification of vasculopathy collagen volume fraction (n = 4-6 per group) in the allografts. **(C)** C57BL/6 or ST2-deficient (*ST2*$^{-/-}$) C57BL/6 grafts were transplanted into bm12 recipients (n ≥ 3 per group). **(D)** Quantification of vasculopathy collagen volume fraction (n = 4-6 per group) in the allografts. In the diagram, the red dotted line indicates the intima layer. Data were shown as mean ± SEM. Scale bars = 50μm. *P* values were established by 2-way ANOVA.

Supplementary Figure 3 | F4/80^{+} macrophages infiltration in allografts in ST2 deficiency recipients or just graft ST2 deficiency recipients. **(A, C)** The graft infiltrating F4/80^{+} macrophages identified using IHC and quantified with Image J. In the diagram, the red dotted line indicates the intima layer. The green dotted line represents the elastic layer. The black dotted line indicates the media layer. The red dotted bordered stands for artery lumen. The thickening intima of artery is between the red and green dotted line. Between the green dotted line and the black dotted line are the medial and media parts of the artery. **(B, D)** Quantification of vasculopathy infiltrating F4/80^{+} macrophages (n = 4-6 per group) in the allografts. Data were shown as mean ± SEM. Scale bars 50μm. *P* values were established by 2-way ANOVA.

Supplementary Figure 4 | The effects of recipient or graft ST2 deficiency on CD3^{+} T cells infiltration in cardiac allograft. **(A, C)** The graft infiltrated CD3^{+} T cells were identified using IHC and quantified with Image J. The red dotted circle indicates the intimae layer and bordered artery lumen. The green dotted circle represents the elastic layer. The black dotted circle indicates the media layer. The thickening intimae of artery is between the red and green dotted circle. Between the green dotted circle and the black dotted circle is the medial layer of the artery. **(B, D)** Quantification of vasculopathy infiltrating CD3^{+} cells (n = 4-6 per group) in the allografts. Data were shown as mean ± SEM. Scale bars = 50μm. *P* values were established by 2-way ANOVA.

Supplementary Figure 5 | The effect of recipient or graft ST2 deficiency on CD20^{+} B cells infiltration in allograft artery. **(A, C)** The infiltrated CD20^{+} B cells were identified using IHC and quantified with Image J. In A and C, the red dotted circle indicates the intimae layer. The green dotted circle represents the elastic layer. The black dotted circle indicates the media layer. The red dotted circle bordered artery lumen. The thickening intimae of artery is between the red and green dotted circle. Between the green dotted circle and the black dotted circle, it is the medial layer of the artery. **(B, D)** Quantification of vasculopathy infiltrating CD20^{+} cells (n = 4-6 per group) in the allografts. Data were shown as mean ± SEM. Scale bars = 50μm. n = 4-6 per group. *P* values were established by 2-way ANOVA.

REFERENCES

1. Patel CB, Holley CL. Cardiac Allograft Vasculopathy: A Formidable Foe. *J Am Coll Cardiol* (2019) 74(1):52–3. doi: 10.1016/j.jacc.2019.05.028
2. Kimura N, Itoh S, Nakae S, Axtell RC, Velotta JB, Bos EJ, et al. Interleukin-16 deficiency suppresses the development of chronic rejection in murine cardiac transplantation model. *J Heart Lung Transplant* (2011) 30(12):1409–17. doi: 10.1016/j.healun.2011.08.017
3. Kim IC, Youn JC, Kobashigawa JA. The Past, Present and Future of Heart Transplantation. *Korean Circ J* (2018) 48(7):565–90. doi: 10.4070/kcj.2018.0189
4. SPARTALIS ES M, TZATZAKI E. Cardiac allograft vasculopathy after heart transplantation current prevention and treatment strategies. *Eur Rev Med Pharmacol Sci* (2019) 23:303–11. doi: 10.26355/eurrev_201901_16777
5. Nandi D, Chin C, Schumacher KR, Fenton M, Singh RK, Lin KY, et al. Surveillance for cardiac allograft vasculopathy: Practice variations among 50 pediatric heart transplant centers. *J Heart Lung Transplant* (2020). doi: 10.1016/j.healun.2020.08.003
6. Shi X, Zhang M, Liu F, Wang Z, Zhang L, Cheng H, et al. Tim-1-Fc suppresses chronic cardiac allograft rejection. *Int J Clin Exp Pathol* (2014) 7(2):509–20.
7. Franz M, Neria D, Berndt A. Chronic cardiac allograft rejection: critical role of ED-A+ fibronectin and implications for targeted therapy strategies. *J Pathol* (2012) 226(4):557–61. doi: 10.1002/path.3968
8. Jin Y, Kong D, Liu C, Gong W. Role of IL-33 in transplant biology. *Eur Cytokine Netw* (2019) 30(2):39–42. doi: 10.1684/ecn.2019.0429
9. Yin H, Li XY, Jin XB, Zhang BB, Gong Q, Yang H, et al. IL-33 prolongs murine cardiac allograft survival through induction of TH2-type immune deviation. *Transplantation* (2010) 89(10):1189–97. doi: 10.1097/TP.0b013e3181d720af
10. Cayrol C, Girard JP. Interleukin-33 (IL-33): A nuclear cytokine from the IL-1 family. *Immunol Rev* (2018) 281(1):154–68. doi: 10.1111/imr.12619
11. Brunner SM, Schiechl G, Falk W, Schlitt HJ, Geissler EK, Fichtner-Feigl S. Interleukin-33 prolongs allograft survival during chronic cardiac rejection. *Transpl Int* (2011) 24(10):1027–39. doi: 10.1111/j.1432-2277.2011.01306.x
12. Li T, Zhang Z, Bartolacci JG, Dwyer GK, Liu Q, Mathews L, et al. Graft IL-33 regulates infiltrating macrophages to protect against chronic rejection. *J Clin Invest* (2020). doi: 10.1172/JCI133008
13. Garbern JC, Williams J, Kristl AC, Malick A, Rachmin I, Gaeta B, et al. Dysregulation of IL-33/ST2 signaling and myocardial periarteriolar fibrosis. *J Mol Cell Cardiol* (2019) 128:179–86. doi: 10.1016/j.yjmcc.2019.01.018
14. Zou H, Yang Y, Gao M, Zhang B, Ming B, Sun Y, et al. HMGB1 Is Involved in Chronic Rejection of Cardiac Allograft via Promoting Inflammatory-Like mDCs. *Am J Transplant* (2014) 14(8):1765–77. doi: 10.1111/ajt.12781
15. Hasegawa T, Visovatti SH, Hyman MC, Hayasaki T, Pinsky DJ. Heterotopic vascularized murine cardiac transplantation to study graft arteriopathy. *Nat Protoc* (2007) 2(3):471–80. doi: 10.1038/nprot.2007.48

16. Dai C, Lu FN, Jin N, Yang B, Gao C, Zhao B, et al. Recombinant IL-33 prolongs leflunomide-mediated graft survival by reducing IFN-gamma and expanding CD4(+)Foxp3(+) T cells in concordant heart transplantation. *Lab Invest* (2016) 96(8):820–9. doi: 10.1038/labinvest.2016.54
17. Khattar M, Baum CE, Schroder P, Breidenbach JD, Haller ST, Chen W, et al. Interleukin 21 (IL-21) regulates chronic allograft vasculopathy (CAV) in murine heart allograft rejection. *PloS One* (2019) 14(11):e0225624. doi: 10.1371/journal.pone.0225624
18. Lee F, Nair V, Chih S. Cardiac Allograft Vasculopathy: Insights on pathogenesis and therapy. *Clin Transpl* (2020), e13794. doi: 10.1111/ctr.13794
19. Altara R, Ghali R, Mallat Z, Cataliotti A, Booz GW, Zouein FA. Conflicting vascular and metabolic impact of the IL-33/sST2 axis. *Cardiovasc Res* (2018) 114(12):1578–94. doi: 10.1093/cvr/cvy166
20. Cao K, Liao X, Lu J, Yao S, Wu F, Zhu X, et al. IL-33/ST2 plays a critical role in endothelial cell activation and microglia-mediated neuroinflammation modulation. *J Neuroinflamm* (2018) 15(1):136. doi: 10.1186/s12974-018-1169-6
21. Yamamoto M, Umebashi K, Tokito A, Imamura J, Jougasaki M. Interleukin-33 induces growth-regulated oncogene-α expression and secretion in human umbilical vein endothelial cells. *Am J Physiol Regulatory Integr Comp Physiol* (2017) 313(3):R272–r9. doi: 10.1152/ajpregu.00435.2016

Conflict of Interest: The authors declare that the research was conducted in the absence of any commercial or financial relationships that could be construed as a potential conflict of interest.

frontiers in Immunology

REVIEW
published: 06 April 2021
doi: 10.3389/fimmu.2021.659621

The Unique Immunomodulatory Properties of MSC-Derived Exosomes in Organ Transplantation

Qingyuan Zheng[1], *Shuijun Zhang*[1], *Wen-Zhi Guo*[1]* *and Xiao-Kang Li*[1,2]*

[1] Department of Hepatobiliary and Pancreatic Surgery, The First Affiliated Hospital of Zhengzhou University, Zhengzhou, China, [2] Division of Transplantation Immunology, National Research Institute for Child Health and Development, Tokyo, Japan

Methods for suppressing the host immune system over the long term and improving transplantation tolerance remain a primary issue in organ transplantation. Cell therapy is an emerging therapeutic strategy for immunomodulation after transplantation. Mesenchymal stem cells (MSCs) are adult multipotent stem cells with wide differentiation potential and immunosuppressive properties, which are mostly used in regenerative medicine and immunomodulation. In addition, emerging research suggests that MSC-derived exosomes have the same therapeutic effects as MSCs in many diseases, while avoiding many of the risks associated with cell transplantation. Their unique immunomodulatory properties are particularly important in the immune system-overactive graft environment. In this paper, we review the effects of MSC-derived exosomes in the immune regulation mechanism after organ transplantation and graft-versus-host disease (GvHD) from various perspectives, including immunosuppression, influencing factors, anti-inflammatory properties, mediation of tissue repair and regeneration, and the induction of immune tolerance. At present, the great potential of MSC-derived exosomes in immunotherapy has attracted a great deal of attention. Furthermore, we discuss the latest insights on MSC-derived exosomes in organ transplantation and GvHD, especially its commercial production concepts, which aim to provide new strategies for improving the prognosis of organ transplantation patients.

Keywords: immunomodulation, MSC-derived exosomes, immune tolerance, transplantation, GvHD

OPEN ACCESS

Edited by:
Hao Wang,
Tianjin Medical University General Hospital, China

Reviewed by:
Lin Zhong,
Shanghai General Hospital, China
Bin Li,
Shanghai Jiao Tong University School of Medicine, China

***Correspondence:**
Xiao-Kang Li
ri-k@ncchd.go.jp
Wen-Zhi Guo
fccguowz@zzu.edu.cn

Specialty section:
This article was submitted to Alloimmunity and Transplantation, a section of the journal Frontiers in Immunology

Received: *28 January 2021*
Accepted: *22 February 2021*
Published: *06 April 2021*

Citation:
Zheng Q, Zhang S, Guo W-Z and Li X-K (2021) The Unique Immunomodulatory Properties of MSC-Derived Exosomes in Organ Transplantation. Front. Immunol. 12:659621. doi: 10.3389/fimmu.2021.659621

INTRODUCTION

Organ transplantation is the most effective treatment for patients with end-stage disease, and it is one of the most noticeable and important achievements in the development of medicine in the 20th century (1). Although the short-term survival rate of allogeneic organ transplantation has been greatly improved, the development of methods to increase the long-term survival of transplanted organs remains a major challenge in clinical medicine. Currently, the combined application of immunosuppressant is the main method to prevent anti-rejection reaction after organ transplantation, but it is not sensitive to chronic rejection (2). Thus, the potential application of cell therapy in improving recipient tolerance to transplantation has attracted widespread interest.

Mesenchymal stem cells (MSCs) are a group of self-renewing stem cells with broad differentiation potential, implantation and homing capabilities, and immunomodulatory effects; thus, they have been increasingly applied in clinical studies (3–5). MSCs derived from the development of early mesoderm and ectoderm, showed the expression of major histocompatibility complex I (MHC-I), CD90, CD105, and CD73, but did not express CD45, CD34, CD14, or CD11b (6). Under certain circumstances, they can be induced to differentiate into connective tissue, bone, cartilage, fat and bone marrow stromal cells. Some studies have confirmed that MSCs had an immunosuppressive effect, which can play an immunomodulatory role by inhibiting T cell proliferation, preventing B cell activation, affecting the differentiation, maturation, and function of dendritic cells (DCs) and interfering with the activation and maturation of antigen-presenting cells (APCs) (7–10). Besides, a study found that MSCs may inhibit IL-2-induced NK cell activity *in vitro* (11). Studies have shown that the paracrine function of MSCs is the key mechanism for the immune function. Exosomes are important molecules that play a role in the transmission of information and biological functions. This review systematically summarizes the mechanism, influencing factors and clinical applications of MSC immunosuppression, especially the research and prospects of MSC-derived exosomes in the field of organ transplantation and graft-versus-host disease (GvHD).

THE IMMUNOSUPPRESSIVE EFFECT OF MSCs AND ITS MECHANISM

MSCs have an immunomodulatory effect that influences all cells involved in the immune response (**Figure 1**). MSCs inhibit T cell activity, induce regulatory T cell activation, trigger cell apoptosis and arrest the cell cycle in the G0/G1 phase. Glennie et al. (12) found that the potential for the inhibition of B cell proliferation by MSCs is similar to that of T cells. It has been confirmed that MSCs can inhibit the proliferation of natural killer (NK) cells and interferon IFN-γ stimulated by IL-2 or IL-15(13). In summary, the MSCs inhibit the immune responses and effector cells of the memory cell, thereby modulating innate immunity and adaptive immunity. Furthermore, MSCs can increase the amounts of regulatory T cells (Tregs), regulatory B cells (Bregs), and regulatory DCs (DCregs)—resulting in the loss of function of T cells—to regulate the immune function (14). BM-MSCs have also been proven to inhibit the proliferation and cytotoxicity of NK cells by changing the phenotype of NK cells and cell-to-cell contact (15, 16). In general, MSCs produce resistant cytokines, which directly inhibit the ongoing immune response and inhibit the proliferation of lymphocytes. Circulating hematopoietic cells actively home into the wall across the vascular endothelium of different organs and bone marrow; this is important for the host defense and repair functions (17). This depends on multiple molecular signals, including growth factors, chemical factors, and adhesion factors. The plastic adhesion properties of MSCs may have chemotactic functions (18). Similarly to other immune cells at sites of injury and inflammation, with the help of the homing ability, MSCs chemotactically transport to target organs, mediating anti-inflammatory response and tissue repair and regeneration. These functions represent a key feature that plays a role in regenerative medicine.

MSCs have effective immunomodulatory properties and anti-inflammatory abilities, which produce extracellular vesicles, including exosomes, and a large number of cytokines and growth factors. The inhibition of the proliferation of T and B cells and the maturation of monocytes promotes the production of Tregs and M2 macrophages. Studies have shown that when the paracrine mechanism of MSCs is activated, they can directly secrete anti-inflammatory cytokines, such as indolamine 2,3-dioxygenase (IDO), prostaglandin E2 (PGE2), nitric oxide (NO), HLA-G, transforming growth factor-β (TGF-β), and vascular endothelial growth factor (VEGF) (19, 20). These cytokines affect the number of immune cells and achieve the effect of suppressing the immune response. Among them, PGE2 and IDO have a synergistic effect (21). Research by Cho et al. (22) showed that BM-MSCs can convert bone marrow-derived macrophages from M1 to M2, promote the proliferation of M2 macrophages, enhance the ability of macrophages to inhibit inflammation, and weaken their pro-inflammatory ability. The study by Vasandan et al. (23) was consistent with the above findings. MSCs produce soluble factors in response to inflammatory stimuli to induce the activation of the Treg, DCreg, and M2 populations in a variety of inflammatory diseases. Thus, even if the MSCs soon disappear *in vivo*, these cytokines can still suppress the immune level of the body for a long time (24).

According to several *in vivo* and *in vitro* studies, the immunosuppressive effect of MSCs is affected by many factors, such as different cell sources, administration methods and dosages, and the microenvironment created by the interaction with fibroblasts, endothelial cells, epithelial cells, and macrophages. For MSCs from different sources, although their proliferation and differentiation abilities are similar, they may show different specific phenotypes and immunomodulatory properties, resulting in differences in efficacy. Harman et al. (25) performed single-cell RNA sequencing (scRNA-seq) on primary equine MSCs that were collected from adipose tissue, bone marrow, and peripheral blood. They observed that transcriptional differences corresponded with phenotypic variance in cellular motility and the immune regulatory function (25). Meanwhile, the timing of administration, dosage and state of activation of MSCs has a great influence on the *in vivo* efficacy. In general, the dose of MSCs that is intravenously injected in mice is 5×10^7/kg, while the clinical dose for humans is usually $1–2 \times 10^6$/kg (26). When BM-MSCs were intravenously administered preoperatively at doses of 0.5×10^6/kg and 1.0×10^6/kg, combined with mycophenolate mofetil (MMF), to a mouse model of allogenic heart transplantation, the graft survival rates were different. Taken together, only the MSC-MMF combination of three different MSC—drug combinations led to a super-additive immunosuppressive effect. And the survival time of grafts in the low-dose group of BM-MSCs was higher (27). A great deal of further experimentation is needed to investigate the dose-dependent effects. The

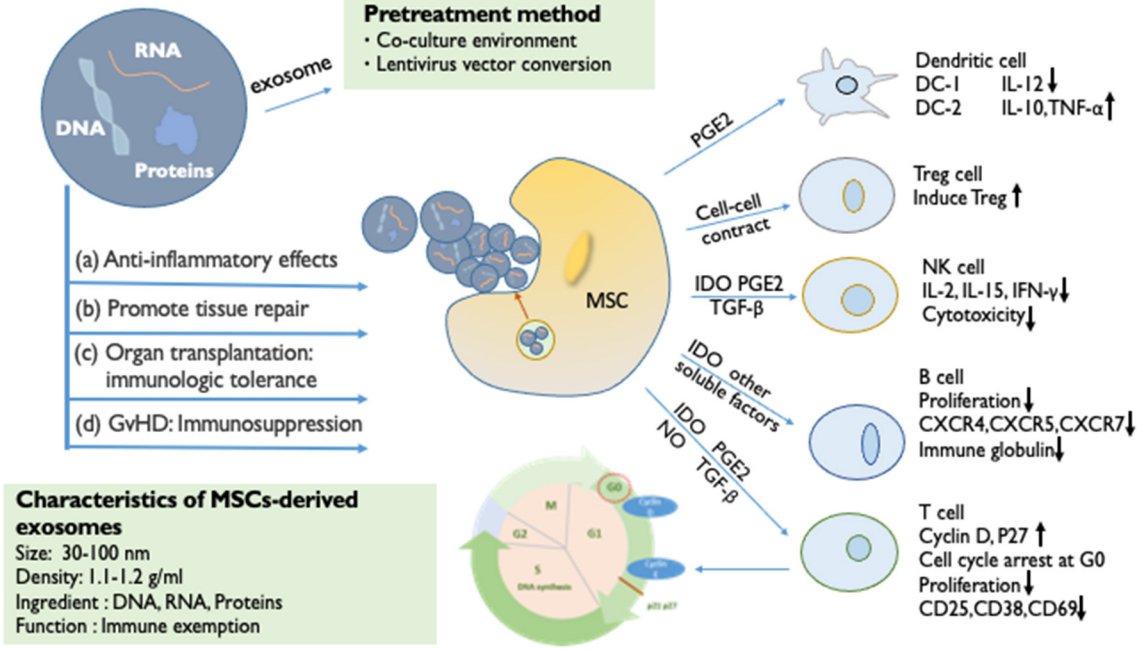

FIGURE 1 | The immunosuppressive effect of MSCs and MSC-derived exosomes. The immunomodulatory effects of MSCs can be largely attributed to paracrine factors (IDO, PGE2, NO, TGF-β, and exosome). By secreting soluble factors, the proliferation of T cells is inhibited (cell cycle arrest at G0), B cell activation is prevented (reduced proliferative capacity), NK cells are influenced (reduced cytotoxicity), and the differentiation and maturation of DC is affected. Through cell-to-cell contact, it can Tregs can be induced. MSC-derived exosomes are small vesicles of 30–100 nm in diameter, which are rich in important biomolecules such as DNA, RNA, and proteins. MSC-derived exosomes have the same immunosuppressive effect as MSCs. (a) Anti-inflammatory effects. (b) Promotion of tissue repair. (c) Organ transplantation: immunologic tolerance. (d) Immunosuppression in GvHD. The targeted pretreatment of exosomes is an important means of current biological treatment. The method of changing the co-culture environment, and the lentiviral vector transferring functional proteins or mRNA into exosomes, can pre-enhance the activity of exosomes to enhance efficacy.

immunosuppressive effects and mechanisms of MSCs derived from different tissues of the same species are also different. With the responder T lymphocyte population in mixed lymphocyte culture (MLC), the allogeneic and autologous MSCs induced a significant differentiation of $CD4^+$ T-cell subsets co-expressing CD25. However, only allogeneic MSCs favored an increase in cytotoxic T lymphocyte antigen-4+ populations. With respect to autologous MSCs, allogeneic MSCs may play a more effective suppressive activity (28). In particular, the positioning and migration of MSCs after *in vivo* injection are involved in the long-term tolerance of the graft by secreting soluble factors in close contact with the target site. At present, the combined use of multiple immunosuppressive agents causes different degrees of immunodeficiency, causing side effects, such as infection and malignant tumors, which are major problems after organ transplantation. However, whether MSCs can be used in combination with immunosuppressive agents remains to be verified. Will MSCs permanently alter the body's immune response mechanisms? We hypothesize that in a complex *in vivo* microenvironment, MSCs promote long-term tolerance of the graft and will also induce rejection. Therefore, an in-depth understanding of the interaction between MSCs and other cells is particularly important for the improvement of stem cell therapy in the future.

MSC-DERIVED EXOSOMES

Exosomes were first discovered in 1983 in the reticulocyte network. They are considered to be a physiological cystic structure of waste from the process of red blood cell development. They remove specific proteins during the maturation of reticulocytes. Exosomes includes DNA, mRNA, miRNA, and proteins and other important molecules. Active exosomes are secreted by a variety of cells of 30–100 nm in diameter, which have a lipid bilayer structure, and the distribution of Four transmembrane protein superfamilies; they carry and transport proteins, nucleic acids, lipids and other biologically active molecules (**Figure 1**) (29–32). In the process of transportation, exosomes not only maintain their biological activity but also can distribution of the transmembrane protein modify and process molecules, which plays an important role in the transduction of intercellular material and information (33). MSCs can tend to the injured site and perform the functions of tissue repair, wound healing, and immune regulation. Immunization exemptions are one reason for their high-profile in the field of organ transplantation (34). The paracrine effect is one of the important mechanisms for MSCs (35, 36). Bruno et al. (37) revealed that exosomes play an important role in the paracrine effect of MSCs. MSC-derived exosomes with cytokines and growth factors, lipid

signals, mRNA, and miRNA regulatory biomolecules have a biological function or information transfer function (38, 39). They have similar functions to MSCs, including the promotion of tissue repair, immunosuppression, and neuroprotection. As a medium component of cell-to-cell communication, exosomes spread biological information between cells in the form of paracrine and remote secretion, and play an important regulatory role in physiological and pathological conditions.

More and more studies have shown that MSC-derived exosomes have the ability to affect the activity of immune cells, including T cells, B cells, NK cells, and macrophages. Studies have suggested that the therapeutic effect of exosomes is mediated by mRNA delivery. Many of these are involved in transcription regulation, proliferation, and immune regulation, indicating that they contribute to the induction of tissue regeneration (40). In addition, the function of exosomes is also affected by other molecules (such as proteins, lipids, enzymes, signal molecules) to exert their functional activities. These proteins are mainly involved in cell adhesion, membrane fusion and signal transduction (41). Those most common proteins are tetraspanin and integrin proteins (CD63, CD9, CD81, and CD82), which is crucial for cell adhesion. They are located on the surface of exosomes as markers (42, 43). Furthermore, the proteins involved in membrane fusion are Rab GTPases, annexins, and heat shock protein (HSP70 and HSP90) (43). Exosomes can interact with recipient cells by ligand-receptor binding or direct endocytosis. Exosome uptake by recipient cells is cell-specific. The interaction of surface molecules of exosomes is important for recipient cell targeting (44, 45). However, the complex microenvironment between different molecules or different cells causes the exosomes derived from MSC to be not equivalent. Exosomes of the same cell express different epitopes, indicating that there may be different subtypes of exosomes. Compared with BMSC-derived exosomes, AD-MSC contain up to 4-fold higher levels of enzymatically active neprilysin (24, 46). The molecules that synthesize exosomes actually depend on the cell type. MSCs are a major component of the tumor microenvironment (TME). MSC-derived exosomes will be altered when MSCs are cultured in TME. MSCs remodel the extracellular matrix, and tumor-derived small vesicles may exert profound effects on tumor growth (47, 48). Hypoxia injury is one of the main causes of apoptosis and decreased β-cell function in islet grafts. In organ transplantation, a study found that huMSC-derived exosomes played an important role in hypoxic resistance, which could protect neonatal porcine islet cell clusters from hypoxia-induced dysfunction (49). The functions of different microenvironments are complex and changeable. In conclusion, we should further explore the interaction between different molecules on the surface or within exosomes.

ANTI-INFLAMMATORY AND TISSUE REPAIR PROMOTING EFFECTS OF MSC-DERIVED EXOSOMES

Recent studies have shown that MSCs will not directly implant and replace damaged tissues, and the exosomes secreted by MSCs are considered to be key cytokines with strong anti-inflammatory potential. A clinical study showed that MSC-derived exosomes may reduce the ability of peripheral blood mononuclear cells (PBMCs) to release proinflammatory cytokines *in vivo*. MSC-derived exosomes upregulated IL-10 and TGF-β1 from PBMCs, thereby promoting the proliferation and immunosuppression capacity of Tregs (50). Another study found that MSC-derived exosomes can reduce the neuroinflammation of autoimmune encephalomyelitis in mice and increase the number of Tregs to generate innate immunity (51). MSCs have been used for treating the inflammatory storm caused by severe pneumonia in COVID-19 patients, MSC-derived exosomes are more convenient and superior, and are recommended for alternative treatments (52).

The exosomes obtained after IFN-γ stimulation reduce the proliferation of PBMCs *in vitro*, reduce the pro-inflammatory factors and increase the immunosuppressive factor IDO (53, 54). In a study involving traumatic brain injury, Long et al. found that MSC-derived exosomes reduce the level of pro-inflammatory cytokines (55). Exosomes have been used as a treatment to reduce neuroinflammation after brain injury (56). Besides, MSC-derived exosomes have a special effect on the treatment of necrotizing enterocolitis (57–59) and bronchopulmonary dysplasia (60, 61). In a mouse model of bronchoalveolar dysplasia, MSC-derived exosomes can regulate the changes in the M1/M2 phenotype of macrophages to reduce the inflammatory damage caused by hyperoxia (62). Studies have found that Human Wharton's jelly mesenchymal stem cell (hWJ-MSC)-derived exosomes have anti-inflammatory effects in perinatal brain injury (63). We therefore hope to explore the anti-inflammatory potential of exosomes derived from hWJ-MSCs in the treatment of brain injury. *In vitro*, exosomes affected microglia and reduced the LPS-stimulated release of pro-inflammatory cytokines. *In vivo*, the intranasal administration of hWJ-MSC-derived exosomes is an effective method for reducing neuroinflammation.

MSC-derived exosomes are small in size, and among the non-coding RNAs (miRNA and LncRNA) involved in immunosuppressive effects, the shorter miRNA is mostly involved in mRNA post-transcriptional regulation of gene expression levels, and thereby controls the key pathways of cell development and differentiation (64). Studies have found that in the brain damage caused by stroke, the increase of miR-133b in exosomes released by bone marrow mesenchymal stem cells may be realized by the transfer of exosomes from MSCs to the parenchyma (65, 66). miR-133b transferred through the exosomes from MSCs into astrocytes may downregulate the expression of connective tissue growth factor (CTGF), reduce glial scarring, and facilitate axonal growth. Meanwhile, miR-133 downregulates the expression of RhoA protein, while inhibiting RhoA promotes the regeneration of the corticospinal tract after spinal cord injury (67). These studies have shown that MSC-derived exosomes secrete mRNA to induce the regeneration of damaged tissues.

In an animal study of acute myocardial infarction, ligation of the left anterior descending artery (LAD) in rats induced cardiomyocyte apoptosis, and the immediate intravenous injection of human umbilical cord mesenchymal stem cells (hucMSC)-derived exosomes (400 μg of protein) could

significantly improve cardiac contractility and reduce heart fibrosis. They hypothesized that hucMSC-derived exosomes may protect cardiomyocytes from apoptosis by regulating the expression of the Bcl-2 family and promote the tube formation and migration of vascular endothelial cells (68). Exosomes secreted by hucMSCs protect cardiomyocytes from anoxia-reoxygenation injury (69). Similar studies are equally effective in mouse ischemia/reperfusion injury models (70). hucMSC-derived exosomes can alleviate CCl_4-induced liver fibrosis, prevent cisplatin-induced renal oxidative stress and cell apoptosis, and enhance skin wound healing.

RESEARCH AND EXPLORATION OF MSC-DERIVED EXOSOMES IN THE FIELD OF ORGAN TRANSPLANTATION

Pre-infusion of different regulatory cells (including MSCs, Tregs and DCs) is currently a viable alternative therapy for transplant recipients. At present, the clinical application of MSCs in organ transplantation used to improve the prognosis of transplant recipients has broad prospects. However, efficiency is still the biggest concern in clinical research. Most clinical-stage MSC therapies have been unable to meet primary efficacy endpoints. This creates issues with practicality and feasibility (71). Although MSC-derived exosomes have similar functions to MSCs, the direct application of MSC-derived exosomes is not yet mature. Studies have proven the alloantigen presentation and immune regulation abilities of exosomes, which induced immune tolerance in a rat allograft model (72).

In allotransplantation, MHC antigen is the main foreign antigen that induces transplant rejection (73). The allograft survival rate mainly depends on the degree of human leukocyte antigen (HLA) type matching between the recipient and donor. Exosomes are MHC-bearing vesicles that are secreted by various cells. A study from the Institute of Transplantation of the University of Nantes in France found that exosomes express MHC-I and MHC-II (74, 75). The researchers found that injecting donor DC-derived exosomes both prolonged the survival time of rat heart allografts before and after transplantation. Interestingly, two injections of donor DC-derived exosomes at 2 and 1 week, respectively, prior to heart allotransplantation did not induce tolerance to long-term graft survival. Thus, the researchers used LF15-0195 (a new type of immunosuppressant) with exosomes for short-term combination therapy, and found that it effectively prevented the maturation of DCs. Exosome/LF treatment prevented or significantly delayed the appearance of chronic rejection. MHC antigens from donor exosomes strongly suppressed the anti-donor proliferation response. Coincidentally, combined with rapamycin, donor exosomes from immature dendritic cells (imDex) can prolong the survival of cardiac allografts and induce specific allograft tolerance (76). These results suggest that the presentation of donor MHC antigens (from exosomes) in combination with immunosuppressive therapy induces a regulatory response that modulates allograft rejection and induces donor-specific allograft tolerance. It is noteworthy that data showed that the number of damaged blood vessels was significantly reduced in 60% of transplanted rats and that exosomes completely prevented chronic rejection in 40% of cases at 200 days after transplantation (74).

Immunosuppressants are the main treatment for avoiding immune rejection after organ transplantation. Exosomes combined with suboptimal doses of immunosuppressants may achieve specific allograft tolerance and long-term transplant survival (72). It is worth noting that it is difficult to achieve tolerance or long-term survival without the use of immunosuppressants. In a rat intestinal transplantation model, the intravenous infusion of exosomes from imDex (20 μg) before transplantation could reduce the host's anti-donor cell response, induce the production of Tregs, and prolong the survival of allografts (77). The long-term use of immunosuppressants can increase the risk of infection, and it is important to determine the optimal dose or find alternative therapy. Tregs can protect allografts from immune rejection. Ma et al. (78) found that imDex combined with Tregs could induce immune tolerance in a rat liver transplantation model. Post-transplant liver samples were obtained for HE staining by researchers at 0, 10, 35, and 100 days after transplantation. Interestingly, the imDex and Tregs treatment groups, respectively, showed a high number of inflammatory infiltrates and symptoms of chronic rejection (e.g., biliary atresia and cholestasis). However, there were no symptoms of chronic rejection in the co-processing group. At 100 days, the co-processing group of grafts showed regenerated hepatic fibrous tissue. Although the structure of the hepatic lobules is disordered, mononuclear cell infiltration is reduced. After liver transplantation, chronic rejection leads to structural disorder of hepatic lobules and tissue fibrosis. The immunomodulatory effects of MSC-derived exosomes and their promotion of angiogenesis and tissue repair effectively alleviated the progress of the pathological process. Thus, we confirm that MSC-derived exosomes can be an important foundation for the treatment of chronic rejection of the field of liver transplantation. Co-treatment reduced rejection and helped the recipient liver regenerate after undergoing slight acute rejection (78).

During transplantation, graft injury caused by cold ischemia, organ preservation, and reperfusion has always been a matter of concern. After ischemic injury, the graft will undergo a second blow of reperfusion injury as blood flow opens up. In an experiment using a rat model of kidney donation after circulatory death, the researchers used Belzer solution (BS) and BS supplemented with MSC-derived exosomes to compare renal perfusion injury. During cold organ perfusion (4 h), the signs of kidney damage were significantly less severe in DCD kidneys treated with MSC-derived exosomes (79). Ischemia reperfusion injury (IRI) is an important cause of liver failure after liver resection and early non-immunological inactivation after liver transplantation. It also increases the chance of acute and chronic rejection of the transplanted organ and leads to late immunological inactivation (80). Preconditioning of graft perfusion with MSCs and MSC-derived exosomes before transplantation may be an effective method for limiting ischemia-reperfusion injury. Using a normothermic hypoxic rat liver perfusion model, Rigo et al. (81) perfused the graft for 4 h and

delivered extracellular vesicles derived from human hepatic stem-like cells (HLSCs), and found that the levels of hepatocyte damage and hepatocyte lysis markers in the lavage fluid were reduced. This effect has also been verified in the lung (82) and heart (83). Although they did not use MSC-derived exosomes, we could also observe that using exosomes would be very likely to limit the graft damage caused by ischemia-reperfusion before and after transplantation (84–87).

In addition, in heart transplantation, a study found a new biomarker method in which donor heart exosomal signals are monitored to understand the intensity of immune rejection after transplantation. We can use exosomes from the recipient's blood or urine for functional monitoring of allograft dysfunction and rejection. This is an effective way to reduce the pain of invasive biopsies (88). Studies have confirmed that exosomes can be used as biomarkers for tolerance monitoring in kidney (89), heart (90), liver (91), islet (92), and lung (93) transplantation. Furthermore, in post-myocardial infarction inflammation, hucMSC-derived exosomes increased the density of infarct myofibroblasts, reduced inflammation, and promoted the differentiation of fibroblasts into myofibroblasts inflammation *in vitro*. Researchers hypothesize that human MSC-derived exosomes may have a cardioprotective effect. MSCs-secretions improve the donor heart function following *ex vivo* cold storage (94). In a porcine model of myocardial infarction subjected to intravenous bolus injection, myocardial infarction measured at 7 and 28 days significantly reduced the infarct size (30–40%) (95). This opens up new ideas for fibrosis caused by chronic rejection after organ transplantation. Jiang et al. (70) also found MSC-derived exosomes can reduce oxidative stress, the inhibition of hepatic apoptosis, and reduced CCl_4-induced liver fibrosis. In engrafted liver mouse models, a single systemic administration of human MSC-derived exosomes (16 mg/kg) effectively rescued the recipient mice from CCl_4-induced liver failure (96). IDO-BMSC-derived exosomes can be used to improve immune tolerance and prolong survival of heart allotransplantation (97). Given the few existing studies on MSC-derived exosomes in the transplantation field, this will be a new research direction. Combined with the previous statement, MSC-derived exosomes are beneficial for tolerance induction in organ transplantation. Considering its characteristics as a drug carrier, the use of exosomes will undoubtedly become a direction of scientific and technological development in the field of organ transplantation (98).

Furthermore, in numerous studies exploring the roles of exosomes in tumor immunity, exosomes have a dual function of adjustment on tumor cell proliferation (99, 100). Following the injection of MSC-derived exosomes into a mouse model of liver cancer, the anti-tumor miR-122 and other secreted biological molecules not only effectively inhibited tumor growth, but also significantly increased the antitumor efficacy of sorafenib against hepatocellular carcinoma (101). Another study found that MiR-199a-modified exosomes from AD-MSCs improved hepatocellular carcinoma chemosensitivity through the mTOR pathway (102). Multiple studies have shown that exosomes combined with immunosuppressants or targeted chemotherapeutic agents are effective in the treatment of chronic rejection or cancer. However, the effect of direct infusion of miRNA is easy to degrade. The author believes that MSC-derived exosomes can be used as carriers for drug and molecular delivery, and that pretreatment of target effect miRNA can become a consensus for disease treatment. If pretreated exosomes are used to enhance the sensitivity of chemotherapeutic agents in reduced-time treatment before liver transplantation for patients with liver cancer, it will effectively reduce the perioperative time and improve the patient prognosis. These studies have provided new ideas for the adjuvant treatment of liver cancer patients with liver transplantation (101, 102).

After reviewing the literature, we retrieved 93 studies of exosomes on www.clinicaltrials.gov, including 3 MSC-derived exosomes clinical trials involving acute ischemic stroke and ophthalmic diseases (103). They have also been reported to have therapeutic effects on acute and chronic kidney disease in animal models. Many efforts have been made to prove that MSC and MSC-derived exosomes can produce similar therapeutic benefits in various disease models (24). Clinical application showed the feasibility of exosomes. Current research focuses on preconditioning the graft before transplantation and preventing ischemia/reperfusion injury to improve the viability of transplanted organs (104, 105). In large animal experiments, we can better understand the biological and functional characteristics of MSC-derived exosomes and define the acceptance in allotransplantation. However, there is no studies have been conducted on the application of MSC-derived exosomes in large animal transplantation models. In pig models of traumatic brain injury and hemorrhagic shock, early treatment with a single dose of exosomes provided neuroprotective effects and improved Blood brain barrier integrity (106–108). In fact, using large animals (pigs or monkeys) is more convincing than small animal models. The advantages of large animal experiments include the complexity of the disease, effective cell dose, cell survival rate after transplantation, and tissue inflammation and immune response associated with transplantation (109, 110). Therefore, we need to invest a lot of energy to study the role of MSC-derived exosomes in large animal transplantation models before clinical application. Xenotransplantation is the development direction of organ transplantation (111). However, there is no application of MSC-derived exosomes in xenotransplantation. If MSC-derived exosomes can reduce the risk of rejection of xenotransplantation, it will be a milestone breakthrough. We boldly speculate that with the continuous development of research, the application of MSC-derived exosomes in organ transplantation will produce better and better results.

MSC-DERIVED EXOSOMES AND GvHD

MSCs were introduced as a treatment strategy for acute GvHD by Le Blanc et al. (112). The application of MSCs in the treatment of GvHD is summarized in **Table 1** (118). As described above, MSC-derived exosomes play the same role as MSCs. In GvHD, a study published in 2014, which describes the first human case in which MSC-derived exosomes were successfully used to treat

TABLE 1 | The application of MSCs in GvHD.

Clinical research	Source of MSCs	Injection-method	Injection dose	Type of Study	Research results	References
CBT combined MSCs (MSC-CBT)	BM-MSCs	Intramedullary injection	/	Phase I trial	Co-transplantation of MSCs may prevent GvHD with no inhibition of engraftment	(113)
CBT combined MSCs (MSC-CBT)	BM-MSCs	Intramedullary injection	0.5×10^6/kg	Phase I trial	The safety of CBT combined with intrabone marrow injection of MSCs	(114)
GvHD after HSC transplantation	AT-MSCs	/	1×10^6/kg, 3×10^6/kg	Phase I/II trial	AT-MSCs, in combination with immunosuppressive therapy, may be considered feasible and safe	(115)
Akt1-MSCs Ameliorates Acute Liver GVHD.	BM-MSCs	/	/	Prospective controlled study	BM-MSCs genetically modified with Akt1 have a survival advantage and an enhanced immunomodulatory function	(116)
Steroid-refractory GvHD after HSC transplantation	BM-MSCs	Intravenous injection	6.81×10^6/kg (range, 0.98–29.78 $\times 10^6$/kg)	Multi-center retrospective study	This therapeutic modality is safe and should be considered for steroid-refractory aGvHD	(117)

CBT, cord blood transplantation; MSCs-CBT, CBT combined MSCs; HSC, haploid hematopoietic stem cell; AT-MSCs, adipose tissue-derived mesenchymal stromal cells; Akt1-MSCs, BM-MSCs genetically modified with AKT1; aGvHD, acute graft-versus-host disease.

graft-versus-host disease, seems to indicate that it is feasible to use MSCs as a therapeutic agent for the alternative therapy of various diseases (119). Lai et al. (120) injected MSC-derived exosomes into a GvHD model; this significantly inhibited the activity of Th17 and Treg cells, and reduced immune rejection and pathological damage. MSC-derived exosomes effectively prolonged the survival of chronic GvHD mice and diminished the clinical and pathological scores of chronic GvHD (120). In the same study, in a GvHD model induced by the injection of human peripheral blood mononuclear cells into irradiated mice, MSC-derived exosomes could alleviate the symptoms of GvHD and improve the survival rate. MSC-derived exosomes promoted the production of Tregs *in vivo* and *in vitro* through APC-mediated pathways (121). Interestingly, in the mouse GvHD model, human BM-MSCs were injected intravenously into the mouse 3 days after the operation. When the BM-MSCs undergo macrophage phagocytosis, inflammatory M1 macrophages were functionally attenuated with a concomitant shift toward alternatively activated M2 state. The effector mechanisms of immunosuppression are activated in BM-MSCs, increasing the metabolic conversion efficiency of macrophages and resulting in a large reduction in IDO spleen and lung inflammatory infiltration (23). MSC paracrine factors can cause immunosuppression for a long time. Extracellular vesicles derived from mesenchymal stem cells (MSC-EVs) prevented fibrosis in a sclerodermatous chronic GvHD mouse model by suppressing the activation of macrophages and the B cell immune response (122). The application of MSC-derived exosomes in GvHD and transplantation is summarized in **Table 2**.

GENE EDITING OF MSC-DERIVED EXOSOMES

MSC-derived exosomes have been confirmed to play a therapeutic role in a variety of disease models. If a method can be found for enhancing the efficacy of exosomes before infusion therapy, for example (e.g., gene-editing, tumor targeted delivery), it may expand the numbers of patients in a good prognosis (**Figure 1**) (124, 125). Different sources of MSCs affect the characteristics of the secreted exosomes; however, the MSCs are changed by changes in the external microenvironment. Can pretreatment with MSCs enhance the activity of exosomes to increase their efficacy? Studies have found that under a hypoxic environment, and after some cytokines and chemicals change the state of MSCs, their immune regulation function, including immune suppression and the ability to promote tissue and blood vessel regeneration, change (126). Under a hypoxic environment, the proliferation ability of BM-MSCs decreases, while adipose mesenchymal stem cells (AD-MSCs) increase. The gene and cell surface of MSCs can also be modified to enhance the therapeutic effect of exosomes. It has been reported that directly or indirectly increasing the activity of exosome pretreatment may be used to maximize the therapeutic potential of MSC-derived exosomes. For example, Ma et al. found that exosomes released by Akt-overexpressing MSCs showed beneficial effects in cardioprotection and angiogenesis, and the cardiac function of animals treated with Akt-Exo was significantly improved. The expression of platelet-derived growth factor D (PDGF-D) in Akt-Exo was significantly upregulated. In addition, Akt-Exo also significantly promotes the proliferation and migration of vascular endothelial cells for the formation of the tubular structure of blood vessels, tube-like structure formation *in vitro* and blood vessel formation *in vivo* (67). Regarding the application in the field of organ transplantation, Wen et al. modified human bone marrow mesenchymal stem cells so that their overexpression could inhibit the expression of fatty acid synthetase (Fas) interfering RNA and inhibit the expression of miR-375 RNA. The source and culture conditions of MSCs affected the function of exosomes. Exosomes co-cultured with PBMCs were transferred into an rat model of islet transplantation, downregulated Fas and miR-375 of islets. Then, by inhibiting the proliferation of PBMCs and enhancing Treg cell function, it exhibits an immunoregulatory function that

TABLE 2 | The application of MSC-derived exosomes in GvHD and transplantation.

Clinical research	Source of exo	Injection-methods	Injection dose	Type of Study	Research results	References
An cGVHD mouse model	MSCs-exo/Fib-exo	Tail vein injection	Once a week for 6 weeks	Preclinical studies	MSCs-exo could improve the survival and ameliorate the pathologic damage of cGVHD by suppressing Th17 cells and inducing Treg	(120)
MSC-ex secreted by MSCs stimulated by different cytokines	huc-MSCs	/	/	Preclinical studies	TGF-β combined with IFN-γ exosome more effectively promoted the transformation of mononuclear cells to Tregs, IDO may play an important role	(54)
An aGVHD mouse model	BM-MSCs	Intravenous injection	/	Preclinical studies	The amelioration of aGVHD by therapeutic infusion of BM-MSC-derived EVs is associated with the preservation of circulating naive T cells	(123)
The lethal chimeric human-SCID mouse model of GvHD	MSCs-exo were incubated with mouse spleen $CD4^+$ T cells	/	/	Preclinical studies	MSC exosome enhanced Treg production *in vitro* and *in vivo* through an APC-mediated pathway.	(121)
aGVHD	MSCs-exo	Intravenous injection	4×10^7 MSCs was calculated as 1 unit, administered every 2–3 days until 4 units	Preclinical studies	MSC-derived exosomes may provide a potential new and safe tool to treat therapy-refractory GvHD	(119)
A mouse hepatic I/R model	MSCs-Heps-exo	Tail vein injection	100 μg	Preclinical studies	*In vivo*, MSC-Heps-Exo effectively relieve hepatic I/R damage, reduce hepatocyte apoptosis	(86)
A mouse hepatic I/R model	UC-MSCs	Tail vein injection	/	Preclinical studies	MiR-20a-containing exosomes from umbilical cord mesenchymal stem cells alleviates liver ischemia/reperfusion injury	(85)
Mouse models of CCl_4-induced ALI/CLI	hucMSCs-exo	Tail vein injection	6×10^{10} particles/kg, 1.2×10^{11} particles/kg, 2.4×10^{11} particles/kg	Preclinical studies	hucMSC-Ex alleviated CCl4-induced acute liver injury and liver fibrosis and restrained the growth of liver tumors	(70)
Myocardial I/R model	MSCs-exo	Intramyocardial injection	50 μg	Preclinical studies	MSCs-exo attenuated myocardial I/R injury in mice via shuttling miR-182, which modified the polarization status of macrophages	(83)
Rats heart transplants model	IDO-BMSCs	Intravenous injection	800 mg/ml	Preclinical studies	Exosomes derived from IDO-BMSCs can be used to promote immunotolerance and prolong the survival of cardiac allografts	(97)
An rat IRI model	BMSCs-exo/Fib-exo	Intravenous injection	/	Preclinical studies	Rat BM-MSC-derived exosome protects against ischemia reperfusion injury with decreased inflammatory response and apoptosis in rats.	(84)
An IRR-induced ALL model	BMSCs-exo	Intravenous injection	5–10 μg	Preclinical studies	MSC-derived exosomes provide protection similar to that of MSCs against IIR-induced ALI via inhibition of TLR4/NF-κB signaling	(87)

exo, exosome; cGVHD, chronic Graft-Versus-Host Disease; Fib-exo, exosomes from human dermal fibroblasts; huc-MSCs, human umbilical cord-derived MSCs; aGvHD, acute graft-versus-host Disease; SCID, severe combined immunodeficiency disease; I/R, Ischemia/Reperfusion injury; MSC-Heps-exo, mesenchymal stem cell-derived hepatocyte-like cell exosomes; CCl_4, carbon tetrachloride; ALI, acute liver injury; CLI, chronic liver injury; IDO, indoleamine 2;3-dioxygenase; ALI, acute lung injury; IIR, intestinal ischemia-reperfusion.

significantly improves immune tolerance after pancreatic islet transplantation (127, 128).

Given the ability of MSCs to return to the nest site of injury, they may serve as a good carrier for MSC-derived exosomes. In order to increase the effect of exosomes, we aim to explore the exosomes synthesis/secretion pathway of MSCs. By gene editing or changing the microenvironment of MSCs, we hope to increase the number and purity of exosomes after pretreatment of MSCs, which can deliver accurate and large amounts of MSC-derived exosomes to target tissues effect. For example, we can preserve

the original function of anti-inflammatory and tissue repair of exosomes. At the same time, we edit and introduce shRNA or miRNA with disease treatment effects into MSC-derived exosomes, so that exosomes could increase the gene therapy effect of specific nucleic acids. The author believes that in future clinical applications, especially for chronic rejection after organ transplantation, it will be possible to use MSC-derived exosomes to induce transplant tolerance. The edited pretreatment of MSC-derived exosomes plays an immunomodulatory role, which is expected to become a new direction in regenerative medicine and transplantation.

DOSE ISSUES AND COMMERCIAL PRODUCTION OF MSC-DERIVED EXOSOMES

The dose dependence of MSCs and its exosomes is a difficult problem in clinical applications. At this stage, the main route of administration is intravenous injection, and most pre-clinical studies and clinical trials have used different doses. For example, one study showed that the intravenous administration of 1–3 $\times$ 10^6/kg units of MSCs may reverse GvHD. In malignant tumors, 4 $\times$ 10^8/kg could inhibit tumor growth, while low doses accelerated tumor proliferation (129). In a clinical study in novel coronavirus patients with pneumonia, 15 mL of exosomes derived from allogeneic bone marrow mesenchymal stem cells was added to 100 ml of normal saline, and administered intravenously 60 min. After a single intravenous injection of exogenous bone marrow exosomes, hypoxia, cytokines and immune reconstitution storms were profound reversal, and no patients developed adverse reactions in association with the treatment (130). However, the biological role of exosomes is not yet fully understood, and we still need to pay close attention to their side effects. It is certain that MSC-derived exosomes play an immunomodulatory role, and we are confident that the research of MSC-derived exosomes will make a major breakthrough in the future.

For clinical safety, the production of MSCs for therapeutic purposes must comply with good manufacturing practices to ensure the provision of safe, repeatable and efficient products. The production of safe and reliable clinical MSCs includes multiple requirements, including tissue sources, culture methods, and quality control standards. It is now believed that exosomes have low immunogenicity and tumorigenicity. In comparison to simple MSCs, MSC-derived exosomes are well-tolerated. And they are more convenient and practical to be applied *in vivo*. Thus, MSC-derived exosomes have broad prospects as a therapeutic agent. It is worth noting that although MSC exosomes avoid the risks of immunogenicity and tumorigenicity that are associated with cell transplantation, there are still many problems associated with application in the clinical setting, including production standards (e.g., culture separation, cell phenotype, quantification, and positioning tracking after infusion) and the monitoring of efficacy (131). The determination of clinical indications for different diseases, especially the production of standard dosage in the field of organ transplantation, is a problem that needs to be solved urgently.

Studies have suggested that for the actual production of therapeutic exosomes, some lentiviral vectors that are currently being tested in clinical trials should be used to transform cells.

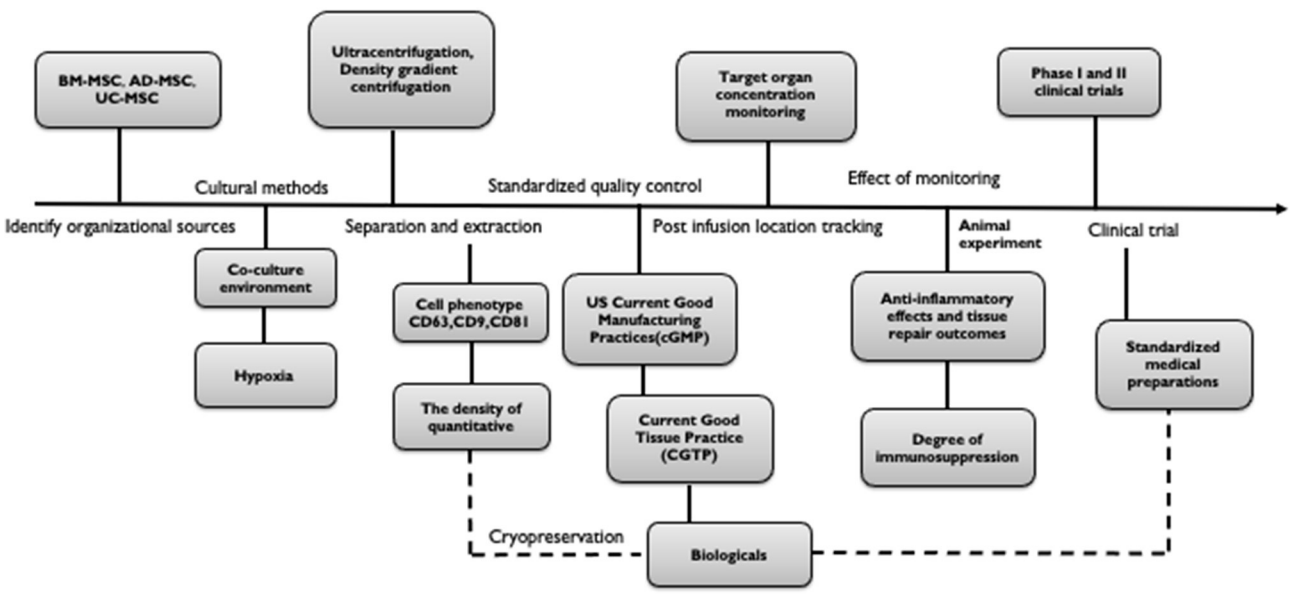

FIGURE 2 | Standardization process for the preparation of exosomes for medical biologics. The process is as follows: (a) Identify organizational sources (BM-MSC, AD-MSC, UC-MSC, etc.). (b) Culture and separation (condition, environment, segregation pattern). (c) Test confirmation (cell phenotype, quantity, purity). (d) Standardized quality control (cGMP, CGTP). (e) Post-infusion location tracking (target organ concentration monitoring, efficacy monitoring). (f) Clinical trial (Phase I and II).

It is extremely important to establish methods that MSC-derived exosomes can be stably supplied. We not only aim to expand cell phenotypes of MSC-derived exosomes but also to pay attention to not damage the original roles of the MSC at the same time of increasing the production of exosomes. Thus, the optimization of cryopreservation strategies for the long-term storage of functional MSC-derived exosomes may be helpful for the development of off-the-shelf biologics (132). Current methods that are important for the extraction of exosomes are ultracentrifugation and density gradient centrifugation. However, methods for obtaining exosomes with high- quantity and high-purity remain a focus of research. Cytokine priming upregulated RAB27B siRNA in AD-MSCs, increasing their secretion of exosomes, which is a useful strategy for harvesting anti-inflammatory MSC-EVs for clinical applications (39). As mentioned earlier, gene editing is used to overexpress therapeutically effective molecules (such as mRNA, miRNA, and proteins) in MSCs to produce characteristic MSC-derived exosomes for different diseases. Alternatively, the therapeutic efficacy may be increased by targeting organ-targeted MSC-derived exosomes. In addition to the production standards in biomedical engineering, it is equally important to verify the safety and feasibility through a large number of pre-clinical studies and clinical trials. The specific phenotype and function and the degree of conversion should be verified by quality control methods and should adhere to quality standards. In this section, we summarized the preparation of a standardization process for the medical application of exosomes as biologic agents (**Figure 2**). However, the standard has not yet reached a consensus. Although we have put forward some points, we still need a multi-center study to determine a feasible solution.

CONCLUDING REMARKS

We hope that MSC-derived exosomes research will open up new medical and pharmaceutical fields while focusing on safety, the standardization of production steps, and determination of therapeutic doses, providing new viable commercial products for the treatment of organ transplantation and GvHD, and other diseases.

AUTHOR CONTRIBUTIONS

QYZ, SJZ, W-ZG, and X-KL conceived and designed the manuscript. QYZ and X-KL wrote the paper. All authors listed have made a substantial, direct and intellectual contribution to the work, and approved it for publication.

FUNDING

This work was supported in part by Science and Technology Innovation Talents in Henan Universities (No. 19HASTIT003) and research grants from the National Center for Child Health and Development (30–20), the Ministry of Education, Culture, Sports, Science and Technology of Japan (17H04277, 18F17794, and 19K18045).

REFERENCES

1. Primc D, Rački S, Arnol M, Marinović M, Fućak-Primc A, Muzur A, et al. The beginnings of kidney transplantation in south-east europe. *Acta Clin Croat.* (2020) 59:135–40. doi: 10.20471/acc.2020.59.01.16
2. Fang YH, Wang SPH, Chang HY, Yang PJ, Liu PY, Liu YW. Immunogenicity in stem cell therapy for cardiac regeneration. *Acta Cardiol Sin.* (2020) 36:588–94. doi: 10.6515/ACS.202011_36(6).20200811A
3. Takayama Y, Kusamori K, Tsukimori C, Shimizu Y, Hayashi M, Kiyama I, et al. Anticancer drug-loaded mesenchymal stem cells for targeted cancer therapy. *J Control Release.* (2020) 329:1090–101. doi: 10.1016/j.jconrel.2020.10.037
4. Sordi V. Mesenchymal stem cell homing capacity. *Transplantation.* (2009) 87(Suppl. 9):S42–5. doi: 10.1097/TP.0b013e3181a28533
5. Meng QS, Liu J, Wei L, Fan HM, Zhou XH, Liang XT. Senescent mesenchymal stem/stromal cells and restoring their cellular functions. *World J Stem Cells.* (2020) 12:966–85. doi: 10.4252/wjsc.v12.i9.966
6. Dominici M, Le Blanc K, Mueller I, Slaper-Cortenbach I, Marini F, Krause D, et al. Minimal criteria for defining multipotent mesenchymal stromal cells. The international society for cellular therapy position statement. *Cytotherapy.* (2006) 8:315–7. doi: 10.1080/14653240600855905
7. van Megen KM, van 't Wout ET, Lages Motta J, Dekker B, Nikolic T, Roep BO. Activated mesenchymal stromal cells process and present antigens regulating adaptive immunity. *Front Immunol.* (2019) 10:694. doi: 10.3389/fimmu.2019.00694
8. Fathollahi A, Hashemi SM, Haji Molla Hoseini M, Tavakoli S, Farahani E, Yeganeh F. Intranasal administration of small extracellular vesicles derived from mesenchymal stem cells ameliorated the experimental autoimmune encephalomyelitis. *Int Immunopharmacol.* (2020) 90:107207. doi: 10.1016/j.intimp.2020.107207
9. Carreras-Planella L, Monguió-Tortajada M, Borràs F E, Franquesa M. Immunomodulatory effect of MSC on B cells is independent of secreted extracellular vesicles. *Front Immunol.* (2019) 10:1288. doi: 10.3389/fimmu.2019.02413
10. Mittal SK, Foulsham W, Shukla S, Elbasiony E, Omoto M, Chauhan SK. Mesenchymal stromal cells modulate corneal alloimmunity via secretion of hepatocyte growth factor. *Stem Cells Transl Med.* (2019) 8:1030–40. doi: 10.1002/sctm.19-0004
11. Spaggiari GM, Capobianco A, Abdelrazik H, Becchetti F, Mingari MC, Moretta L. Mesenchymal stem cells inhibit natural killer-cell proliferation, cytotoxicity, and cytokine production: role of indoleamine 2,3-dioxygenase and prostaglandin E2. *Blood.* (2008) 111:1327–33. doi: 10.1182/blood-2007-02-074997
12. Glennie S, Soeiro I, Dyson PJ, Lam EW, Dazzi F. Bone marrow mesenchymal stem cells induce division arrest anergy of activated T cells. *Blood.* (2005) 105:2821–7. doi: 10.1182/blood-2004-09-3696
13. Chen J, Ji T, Wu D, Jiang S, Zhao J, Lin H, et al. Human mesenchymal stem cells promote tumor growth via MAPK pathway and metastasis by epithelial mesenchymal transition and integrin α5 in hepatocellular carcinoma. *Cell Death Dis.* (2019) 10:425. doi: 10.1038/s41419-019-1622-1
14. Hoogduijn MJ, Lombardo E. Mesenchymal stromal cells anno 2019: dawn of the therapeutic era? Concise Review. *Stem Cells Transl Med.* (2019) 8:1126–34. doi: 10.1002/sctm.19-0073
15. Valencia J, Blanco B, Yáñez R, Vázquez M, Herrero Sánchez C, Fernández-García M, et al. Comparative analysis of the immunomodulatory capacities of human bone marrow- and adipose tissue-derived mesenchymal stromal cells from the same donor. *Cytotherapy.* (2016) 18:1297–311. doi: 10.1016/j.jcyt.2016.07.006

16. Pelizzo G, Veschi V, Mantelli M, Croce S, Di Benedetto V, D'Angelo P, et al. Microenvironment in neuroblastoma: isolation and characterization of tumor-derived mesenchymal stromal cells. *BMC Cancer.* (2018) 18:1176. doi: 10.1186/s12885-018-5082-2
17. Qiu X, Liu J, Zheng C, Su Y, Bao L, Zhu B, et al. Exosomes released from educated mesenchymal stem cells accelerate cutaneous wound healing via promoting angiogenesis. *Cell Prolif.* (2020) 53:e12830. doi: 10.1111/cpr.12830
18. Molchanova EA, Bueverova EI, Starostin VI, Domaratskaia EI. [The sensitivity of mesenchymal stromal cell subpopulations with different times of adhesion property manifestation and derived from hemopoietic organs to growth factors EGF, bFGF, and PDGF]. *Izv Akad Nauk Ser Biol.* (2011) 133–44.
19. Torres Crigna A, Uhlig S, Elvers-Hornung S, Klüter H, Bieback K. Human adipose tissue-derived stromal cells suppress human, but not murine lymphocyte proliferation, via indoleamine 2,3-dioxygenase activity. *Cells.* (2020) 9:2419. doi: 10.3390/cells9112419
20. Yang H, Sun J, Li Y, Duan WM, Bi J, Qu T. Human umbilical cord-derived mesenchymal stem cells suppress proliferation of PHA-activated lymphocytes *in vitro* by inducing CD4(+)CD25(high)CD45RA(+) regulatory T cell production and modulating cytokine secretion. *Cell Immunol.* (2016) 302:26–31. doi: 10.1016/j.cellimm.2016.01.002
21. Liang C, Chen SL, Wang M, Zhai WJ, Zhou Z, Pang AM, et al. [Synergistic immunomodulatory effects of interferon-gamma and bone marrow mesenchymal stem cells]. *Zhonghua Xue Ye Xue Za Zhi.* (2013) 34:213–6. doi: 10.3892/mmr.2017.6330
22. Cho DI, Kim MR, Jeong HY, Jeong HC, Jeong MH, Yoon SH, et al. Mesenchymal stem cells reciprocally regulate the M1/M2 balance in mouse bone marrow-derived macrophages. *Exp Mol Med.* (2014) 46:e70. doi: 10.1038/emm.2013.135
23. Vasandan AB, Jahnavi S, Shashank C, Prasad P, Kumar A, Prasanna SJ. Human Mesenchymal stem cells program macrophage plasticity by altering their metabolic status via a PGE(2)-dependent mechanism. *Sci Rep.* (2016) 6:38308. doi: 10.1038/srep38308
24. Phinney DG, Pittenger MF. Concise review: MSC-derived exosomes for cell-free therapy. *Stem Cells.* (2017) 35:851–8. doi: 10.1002/stem.2575
25. Harman RM, Patel RS, Fan JC, Park JE, Rosenberg BR, Van de Walle GR. Single-cell RNA sequencing of equine mesenchymal stromal cells from primary donor-matched tissue sources reveals functional heterogeneity in immune modulation and cell motility. *Stem Cell Res Ther.* (2020) 11:524. doi: 10.1186/s13287-020-02043-5
26. Galipeau J, Sensébé L. Mesenchymal stromal cells: clinical challenges and therapeutic opportunities. *Cell Stem Cell.* (2018) 22:824–33. doi: 10.1016/j.stem.2018.05.004
27. Eggenhofer E, Renner P, Soeder Y, Popp FC, Hoogduijn MJ, Geissler EK, et al. Features of synergism between mesenchymal stem cells and immunosuppressive drugs in a murine heart transplantation model. *Transpl Immunol.* (2011) 25:141–7. doi: 10.1016/j.trim.2011.06.002
28. Maccario R, Podestà M, Moretta A, Cometa A, Comoli P, Montagna D, et al. Interaction of human mesenchymal stem cells with cells involved in alloantigen-specific immune response favors the differentiation of $CD4^+$ T-cell subsets expressing a regulatory/suppressive phenotype. *Haematologica.* (2005) 90:516–25.
29. Roefs MT, Sluijter JPG, Vader P. Extracellular vesicle-associated proteins in tissue repair. *Trends Cell Biol.* (2020) 30:990–1013. doi: 10.1016/j.tcb.2020.09.009
30. Théry C, Ostrowski M, Segura E. Membrane vesicles as conveyors of immune responses. *Nat Rev Immunol.* (2009) 9:581–93. doi: 10.1038/nri2567
31. Zhang P, Wu X, Gardashova G, Yang Y, Zhang Y, Xu L, et al. Molecular and functional extracellular vesicle analysis using nanopatterned microchips monitors tumor progression and metastasis. *Sci Transl Med.* (2020) 12:eaaz2878. doi: 10.1126/scitranslmed.aaz2878
32. van der Pol E, Böing AN, Harrison P, Sturk A, Nieuwland R. Classification, functions, and clinical relevance of extracellular vesicles. *Pharmacol Rev.* (2012) 64:676–705. doi: 10.1124/pr.112.005983
33. Pegtel DM, Gould SJ. Exosomes. *Annu Rev Biochem.* (2019) 88:487–514. doi: 10.1146/annurev-biochem-013118-111902
34. Barker CF, Billingham RE. The lymphatic status of hamster cheek pouch tissue in relation to its properties as a graft and as a graft site. *J Exp Med.* (1971) 133:620–39. doi: 10.1084/jem.133.3.620
35. Asare-Werehene M, Nakka K, Reunov A, Chiu CT, Lee WT, Abedini MR, et al. The exosome-mediated autocrine and paracrine actions of plasma gelsolin in ovarian cancer chemoresistance. *Oncogene.* (2020) 39:1600–16. doi: 10.1038/s41388-019-1087-9
36. Spees JL, Lee RH, Gregory CA. Mechanisms of mesenchymal stem/stromal cell function. *Stem Cell Res Ther.* (2016) 7:125. doi: 10.1186/s13287-016-0363-7
37. Bruno S, Kholia S, Deregibus MC, Camussi G. The role of extracellular vesicles as paracrine effectors in stem cell-based therapies. *Adv Exp Med Biol.* (2019) 1201:175–93. doi: 10.1007/978-3-030-31206-0_9
38. Wu K, Xing F, Wu SY, Watabe K. Extracellular vesicles as emerging targets in cancer: recent development from bench to bedside. *Biochim Biophys Acta Rev Cancer.* (2017) 1868:538–63. doi: 10.1016/j.bbcan.2017.10.001
39. Cheng A, Choi D, Lora M, Shum-Tim D, Rak J, Colmegna I. Human multipotent mesenchymal stromal cells cytokine priming promotes RAB27B-regulated secretion of small extracellular vesicles with immunomodulatory cargo. *Stem Cell Res Ther.* (2020) 11:539. doi: 10.1186/s13287-020-02050-6
40. Mead B, Tomarev S. Bone marrow-derived mesenchymal stem cells-derived exosomes promote survival of retinal ganglion cells through miRNA-dependent mechanisms. *Stem Cells Transl Med.* (2017) 6:1273–85. doi: 10.1002/sctm.16-0428
41. Simpson RJ, Lim JW, Moritz RL, Mathivanan S. Exosomes: proteomic insights and diagnostic potential. *Expert Rev Proteomics.* (2009) 6:267–83. doi: 10.1586/epr.09.17
42. Andreu Z, Yáñez-Mó M. Tetraspanins in extracellular vesicle formation and function. *Front Immunol.* (2014) 5:442. doi: 10.3389/fimmu.2014.00442
43. He C, Zheng S, Luo Y, Wang B. Exosome theranostics: biology and translational medicine. *Theranostics.* (2018) 8:237–55. doi: 10.7150/thno.21945
44. Kahroba H, Hejazi M S, Samadi N. Exosomes: from carcinogenesis and metastasis to diagnosis and treatment of gastric cancer. *Cell Mol Life Sci.* (2019) 76:1747–58. doi: 10.1007/s00018-019-03035-2
45. Min BH, Shin JS, Kim JM, Kang SJ, Kim HJ, Yoon IH, et al. Delayed revascularization of islets after transplantation by IL-6 blockade in pig to non-human primate islet xenotransplantation model. *Xenotransplantation.* (2018) 25. doi: 10.1111/xen.12374
46. Katsuda T, Tsuchiya R, Kosaka N, Yoshioka Y, Takagaki K, Oki K, et al. Human adipose tissue-derived mesenchymal stem cells secrete functional neprilysin-bound exosomes. *Sci Rep.* (2013) 3:1197. doi: 10.1038/srep01197
47. Dostert G, Mesure B, Menu P, Velot É. How do mesenchymal stem cells influence or are influenced by microenvironment through extracellular vesicles communication? *Front Cell Dev Biol.* (2017) 5:6. doi: 10.3389/fcell.2017.00006
48. Whiteside TL. Exosome and mesenchymal stem cell cross-talk in the tumor microenvironment. *Semin Immunol.* (2018) 35:69–79. doi: 10.1016/j.smim.2017.12.003
49. Nie W, Ma X, Yang C, Chen Z, Rong P, Wu M, et al. Human mesenchymal-stem-cells-derived exosomes are important in enhancing porcine islet resistance to hypoxia. *Xenotransplantation.* (2018) 25:e12405. doi: 10.1111/xen.12405
50. Du YM, Zhuansun YX, Chen R, Lin L, Lin Y, Li JG. Mesenchymal stem cell exosomes promote immunosuppression of regulatory T cells in asthma. *Exp Cell Res.* (2018) 363:114–20. doi: 10.1016/j.yexcr.2017.12.021
51. Riazifar M, Mohammadi MR, Pone EJ, Yeri A, Lässer C, Segaliny AI, et al. Stem cell-derived exosomes as nanotherapeutics for autoimmune and neurodegenerative disorders. *ACS Nano.* (2019) 13:6670–88. doi: 10.1021/acsnano.9b01004
52. Askenase PW. COVID-19 therapy with mesenchymal stromal cells (MSC) and convalescent plasma must consider exosome involvement: do the exosomes in convalescent plasma antagonize the weak immune antibodies? *J Extracell Vesicles.* (2020) 10:e12004. doi: 10.1002/jev2.12004
53. Bulati M, Miceli V, Gallo A, Amico G, Carcione C, Pampalone M, et al. The immunomodulatory properties of the human amnion-derived mesenchymal stromal/stem cells are induced by INF-γ produced by activated

lymphomonocytes and are mediated by cell-to-cell contact and soluble factors. *Front Immunol.* (2020) 11:54. doi: 10.3389/fimmu.2020.00054
54. Zhang Q, Fu L, Liang Y, Guo Z, Wang L, Ma C, et al. Exosomes originating from MSCs stimulated with TGF-β and IFN-γ promote Treg differentiation. *J Cell Physiol.* (2018) 233:6832–40. doi: 10.1002/jcp.26436
55. Long X, Yao X, Jiang Q, Yang Y, He X, Tian W, et al. Astrocyte-derived exosomes enriched with miR-873a-5p inhibit neuroinflammation via microglia phenotype modulation after traumatic brain injury. *J Neuroinflammation.* (2020) 17:89. doi: 10.1186/s12974-020-01761-0
56. Wang X, Yan X, Zhang L, Cai J, Zhou Y, Liu H, et al. Identification and peptidomic profiling of exosomes in preterm human milk: insights into necrotizing enterocolitis prevention. *Mol Nutr Food Res.* (2019) e1801247. doi: 10.1002/mnfr.201801247. [Epub ahead of print].
57. Li B, Hock A, Wu RY, Minich A, Botts SR, Lee C, et al. Bovine milk-derived exosomes enhance goblet cell activity and prevent the development of experimental necrotizing enterocolitis. *PLoS ONE.* (2019) 14:e0211431. doi: 10.1371/journal.pone.0211431
58. Chen W, Wang X, Yan X, Yu Z, Zhang J, Han S. The emerging role of exosomes in the pathogenesis, prognosis and treatment of necrotizing enterocolitis. *Am J Transl Res.* (2020) 12:7020–33.
59. Porzionato A, Zaramella P, Dedja A, Guidolin D, Van Wemmel K, Macchi V, et al. Intratracheal administration of clinical-grade mesenchymal stem cell-derived extracellular vesicles reduces lung injury in a rat model of bronchopulmonary dysplasia. *Am J Physiol Lung Cell Mol Physiol.* (2019) 316:L6–19. doi: 10.1152/ajplung.00109.2018
60. Braun R K, Chetty C, Balasubramaniam V, Centanni R, Haraldsdottir K, Hematti P, et al. Intraperitoneal injection of MSC-derived exosomes prevent experimental bronchopulmonary dysplasia. *Biochem Biophys Res Commun.* (2018) 503:2653–8. doi: 10.1016/j.bbrc.2018.08.019
61. Willis GR, Fernandez-Gonzalez A, Anastas J, Vitali SH, Liu X, Ericsson M, et al. Mesenchymal stromal cell exosomes ameliorate experimental bronchopulmonary dysplasia and restore lung function through macrophage immunomodulation. *Am J Respir Crit Care Med.* (2018) 197:104–16. doi: 10.1164/rccm.201705-0925OC
62. Thomi G, Surbek D, Haesler V, Joerger-Messerli M, Schoeberlein A. Exosomes derived from umbilical cord mesenchymal stem cells reduce microglia-mediated neuroinflammation in perinatal brain injury. *Stem Cell Res Ther.* (2019) 10:105. doi: 10.1186/s13287-019-1207-z
63. Xing L, Tang X, Wu K, Huang X, Yi Y, Huan J. LncRNA HAND2-AS1 suppressed the growth of triple negative breast cancer via reducing secretion of MSCs derived exosomal miR-106a-5p. *Aging.* (2020) 13:424–36. doi: 10.18632/aging.202148
64. Xin H, Li Y, Buller B, Katakowski M, Zhang Y, Wang X, et al. Exosome-mediated transfer of miR-133b from multipotent mesenchymal stromal cells to neural cells contributes to neurite outgrowth. *Stem Cells.* (2012) 30:1556–64. doi: 10.1002/stem.1129
65. Shen H, Yao X, Li H, Li X, Zhang T, Sun Q, et al. Role of exosomes derived from miR-133b modified MSCs in an experimental rat model of intracerebral hemorrhage. *J Mol Neurosci.* (2018) 64:421–30. doi: 10.1007/s12031-018-1041-2
66. Li D, Zhang P, Yao X, Li H, Shen H, Li X, et al. Exosomes derived from miR-133b-modified mesenchymal stem cells promote recovery after spinal cord injury. *Front Neurosci.* (2018) 12:845. doi: 10.3389/fnins.2018.00845
67. Ma J, Zhao Y, Sun L, Sun X, Zhao X, Sun X, et al. Exosomes derived from akt-modified human umbilical cord mesenchymal stem cells improve cardiac regeneration and promote angiogenesis via activating platelet-derived growth factor D. *Stem Cells Transl Med.* (2017) 6:51–9. doi: 10.5966/sctm.2016-0038
68. Huang L, Yang L, Ding Y, Jiang X, Xia Z, You Z. Human umbilical cord mesenchymal stem cells-derived exosomes transfers microRNA-19a to protect cardiomyocytes from acute myocardial infarction by targeting SOX6. *Cell Cycle.* (2020) 19:339–53. doi: 10.1080/15384101.2019.1711305
69. Tang J, Jin L, Liu Y, Li L, Ma Y, Lu L, et al. Exosomes derived from mesenchymal stem cells protect the myocardium against ischemia/reperfusion injury through inhibiting pyroptosis. *Drug Des Devel Ther.* (2020) 14:3765–75. doi: 10.2147/DDDT.S239546
70. Jiang W, Tan Y, Cai M, Zhao T, Mao F, Zhang X, et al. Human umbilical cord MSC-derived exosomes suppress the development of CCl(4)-induced liver injury through antioxidant effect. *Stem Cells Int.* (2018) 2018:6079642. doi: 10.1155/2018/6079642
71. Levy O, Kuai R, Siren EMJ, Bhere D, Milton Y, Nissar N, et al. Shattering barriers toward clinically meaningful MSC therapies. *Sci Adv.* (2020) 6:eaba6884. doi: 10.1126/sciadv.aba6884
72. Monguió-Tortajada M, Lauzurica-Valdemoros R, Borràs FE. Tolerance in organ transplantation: from conventional immunosuppression to extracellular vesicles. *Front Immunol.* (2014) 5:416. doi: 10.3389/fimmu.2014.00416
73. Stepkowski SM, Raza-Ahmad A, Duncan WR. The role of class I and class II MHC antigens in the rejection of vascularized heart allografts in mice. *Transplantation.* (1987) 44:753–9. doi: 10.1097/00007890-198712000-00006
74. Pêche H, Renaudin K, Beriou G, Merieau E, Amigorena S, Cuturi MC. Induction of tolerance by exosomes and short-term immunosuppression in a fully MHC-mismatched rat cardiac allograft model. *Am J Transplant.* (2006) 6:1541–50. doi: 10.1111/j.1600-6143.2006.01344.x
75. Pêche H, Heslan M, Usal C, Amigorena S, Cuturi M C. Presentation of donor major histocompatibility complex antigens by bone marrow dendritic cell-derived exosomes modulates allograft rejection. *Transplantation.* (2003) 76:1503–10. doi: 10.1097/01.TP.0000092494.75313.38
76. Li X, Li JJ, Yang JY, Wang DS, Zhao W, Song WJ, et al. Tolerance induction by exosomes from immature dendritic cells and rapamycin in a mouse cardiac allograft model. *PLoS ONE.* (2012) 7:e44045. doi: 10.1371/journal.pone.0044045
77. Yang X, Meng S, Jiang H, Zhu C, Wu W. Exosomes derived from immature bone marrow dendritic cells induce tolerogenicity of intestinal transplantation in rats. *J Surg Res.* (2011) 171:826–32. doi: 10.1016/j.jss.2010.05.021
78. Ma B, Yang JY, Song WJ, Ding R, Zhang ZC, Ji HC, et al. Combining exosomes derived from immature dcs with donor antigen-specific Treg cells induces tolerance in a rat liver allograft model. *Sci Rep.* (2016) 6:32971. doi: 10.1038/srep32971
79. Gregorini M, Corradetti V, Pattonieri EF, Rocca C, Milanesi S, Peloso A, et al. Perfusion of isolated rat kidney with mesenchymal stromal cells/extracellular vesicles prevents ischaemic injury. *J Cell Mol Med.* (2017) 21:3381–93. doi: 10.1111/jcmm.13249
80. Chouchani ET, Pell VR, Gaude E, Aksentijević D, Sundier SY, Robb EL, et al. Ischaemic accumulation of succinate controls reperfusion injury through mitochondrial ROS. *Nature.* (2014) 515:431–5. doi: 10.1038/nature13909
81. Rigo F, De Stefano N, Navarro-Tableros V, David E, Rizza G, Catalano G, et al. Extracellular vesicles from human liver stem cells reduce injury in an *ex vivo* normothermic hypoxic rat liver perfusion model. *Transplantation.* (2018) 102:e205–10. doi: 10.1097/TP.0000000000002123
82. Stone ML, Zhao Y, Robert Smith J, Weiss ML, Kron I L, Laubach VE, et al. Mesenchymal stromal cell-derived extracellular vesicles attenuate lung ischemia-reperfusion injury and enhance reconditioning of donor lungs after circulatory death. *Respir Res.* (2017) 18:212. doi: 10.1186/s12931-017-0704-9
83. Zhao J, Li X, Hu J, Chen F, Qiao S, Sun X, et al. Mesenchymal stromal cell-derived exosomes attenuate myocardial ischaemia-reperfusion injury through miR-182-regulated macrophage polarization. *Cardiovasc Res.* (2019) 115:1205–16. doi: 10.1093/cvr/cvz040
84. Wang R, Lin M, Li L, Li L, Qi G, Rong R, et al. [Bone marrow mesenchymal stem cell-derived exosome protects kidney against ischemia reperfusion injury in rats]. *Zhonghua Yi Xue Za Zhi.* (2014) 94:3298–303.
85. Zhang L, Song Y, Chen L, Li D, Feng H, Lu Z, et al. MiR-20a-containing exosomes from umbilical cord mesenchymal stem cells alleviates liver ischemia/reperfusion injury. *J Cell Physiol.* (2020) 235:3698–710. doi: 10.1002/jcp.29264
86. Yang B, Duan W, Wei L, Zhao Y, Han Z, Wang J, et al. Bone marrow mesenchymal stem cell-derived hepatocyte-like cell exosomes reduce hepatic ischemia/reperfusion injury by enhancing autophagy. *Stem Cells Dev.* (2020) 29:372–9. doi: 10.1089/scd.2019.0194
87. Liu J, Chen T, Lei P, Tang X, Huang P. Exosomes released by bone marrow mesenchymal stem cells attenuate lung injury induced by intestinal ischemia reperfusion via the TLR4/NF-κB pathway. *Int J Med Sci.* (2019) 16:1238–44. doi: 10.7150/ijms.35369

88. Benichou G, Wang M, Ahrens K, Madsen JC. Extracellular vesicles in allograft rejection and tolerance. *Cell Immunol.* (2020) 349:104063. doi: 10.1016/j.cellimm.2020.104063
89. Schröppel B, Legendre C. Delayed kidney graft function: from mechanism to translation. *Kidney Int.* (2014) 86:251–8. doi: 10.1038/ki.2014.18
90. Kennel PJ, Saha A, Maldonado DA, Givens R, Brunjes DL, Castillero E, et al. Serum exosomal protein profiling for the non-invasive detection of cardiac allograft rejection. *J Heart Lung Transplant.* (2018) 37:409–17. doi: 10.1016/j.healun.2017.07.012
91. Ono Y, Perez-Gutierrez A, Nakao T, Dai H, Camirand G, Yoshida O, et al. Graft-infiltrating PD-L1(hi) cross-dressed dendritic cells regulate antidonor T cell responses in mouse liver transplant tolerance. *Hepatology.* (2018) 67:1499–515. doi: 10.1002/hep.29529
92. Vallabhajosyula P, Korutla L, Habertheuer A, Yu M, Rostami S, Yuan CX, et al. Tissue-specific exosome biomarkers for noninvasively monitoring immunologic rejection of transplanted tissue. *J Clin Invest.* (2017) 127:1375–91. doi: 10.1172/JCI87993
93. Gunasekaran M, Sharma M, Hachem R, Bremner R, Smith MA, Mohanakumar T. Circulating exosomes with distinct properties during chronic lung allograft rejection. *J Immunol.* (2018) 200:2535–41. doi: 10.4049/jimmunol.1701587
94. Wang M, Yan L, Li Q, Yang Y, Turrentine M, March K, et al. Mesenchymal stem cell secretions improve donor heart function following *ex vivo* cold storage. *J Thorac Cardiovasc Surg.* (2020) S0022-5223(20)32487–9. doi: 10.1016/j.jtcvs.2020.08.095
95. Charles CJ, Li RR, Yeung T, Mazlan SMI, Lai RC, de Kleijn DPV, et al. Systemic mesenchymal stem cell-derived exosomes reduce myocardial infarct size: characterization with MRI in a porcine model. *Front Cardiovasc Med.* (2020) 7:601990. doi: 10.3389/fcvm.2020.601990
96. Yan Y, Jiang W, Tan Y, Zou S, Zhang H, Mao F, et al. hucMSC exosome-derived GPX1 is required for the recovery of hepatic oxidant injury. *Mol Ther.* (2017) 25:465–79. doi: 10.1016/j.ymthe.2016.11.019
97. He JG, Xie Q L, Li BB, Zhou L, Yan D. Exosomes derived from IDO1-overexpressing rat bone marrow mesenchymal stem cells promote immunotolerance of cardiac allografts. *Cell Transplant.* (2018) 27:1657–83. doi: 10.1177/0963689718805375
98. Baek G, Choi H, Kim Y, Lee HC, Choi C. Mesenchymal stem cell-derived extracellular vesicles as therapeutics and as a drug delivery platform. *Stem Cells Transl Med.* (2019) 8:880–6. doi: 10.1002/sctm.18-0226
99. Khalife J, Sanchez JF, Pichiorri F. Extracellular vesicles in hematological malignancies: from biomarkers to therapeutic tools. *Diagnostics.* (2020) 10:1065. doi: 10.3390/diagnostics10121065
100. Ganji A, Farahani I, Shojapour M, Ghazavi A, Mosayebi G. *In vivo* therapeutic effects of colorectal cancer cell-derived exosomes. *Iran J Basic Med Sci.* (2020) 23:1439–44. doi: 10.22038/ijbms.2020.46465.10730
101. Lou G, Song X, Yang F, Wu S, Wang J, Chen Z, et al. Exosomes derived from miR-122-modified adipose tissue-derived MSCs increase chemosensitivity of hepatocellular carcinoma. *J Hematol Oncol.* (2015) 8:122. doi: 10.1186/s13045-015-0220-7
102. Lou G, Chen L, Xia C, Wang W, Qi J, Li A, et al. MiR-199a-modified exosomes from adipose tissue-derived mesenchymal stem cells improve hepatocellular carcinoma chemosensitivity through mTOR pathway. *J Exp Clin Cancer Res.* (2020) 39:4. doi: 10.1186/s13046-019-1512-5
103. Mendt M, Rezvani K, Shpall E. Mesenchymal stem cell-derived exosomes for clinical use. *Bone Marrow Transplant.* (2019) 54(Suppl. 2):789–92. doi: 10.1038/s41409-019-0616-z
104. Grange C, Bellucci L, Bussolati B, Ranghino A. Potential applications of extracellular vesicles in solid organ transplantation. *Cells.* (2020) 9:369. doi: 10.3390/cells9020369
105. Massa M, Croce S, Campanelli R, Abbà C, Lenta E, Valsecchi C, et al. Clinical applications of mesenchymal stem/stromal cell derived extracellular vesicles: therapeutic potential of an acellular product. *Diagnostics.* (2020) 10:999. doi: 10.3390/diagnostics10120999
106. Williams AM, Dennahy IS, Bhatti UF, Halaweish I, Xiong Y, Chang P, et al. Mesenchymal stem cell-derived exosomes provide neuroprotection and improve long-term neurologic outcomes in a swine model of traumatic brain injury and hemorrhagic shock. *J Neurotrauma.* (2019) 36:54–60. doi: 10.1089/neu.2018.5711
107. Williams AM, Bhatti UF, Brown JF, Biesterveld BE, Kathawate RG, Graham NJ, et al. Early single-dose treatment with exosomes provides neuroprotection and improves blood-brain barrier integrity in swine model of traumatic brain injury and hemorrhagic shock. *J Trauma Acute Care Surg.* (2020) 88:207–18. doi: 10.1097/TA.0000000000002563
108. Williams AM, Wu Z, Bhatti UF, Biesterveld BE, Kemp MT, Wakam GK, et al. Early single-dose exosome treatment improves neurologic outcomes in a 7-day swine model of traumatic brain injury and hemorrhagic shock. *J Trauma Acute Care Surg.* (2020) 89:388–96. doi: 10.1097/TA.0000000000002698
109. Poncelet AJ, Vercruysse J, Saliez A, Gianello P. Although pig allogeneic mesenchymal stem cells are not immunogenic *in vitro*, intracardiac injection elicits an immune response *in vivo*. *Transplantation.* (2007) 83:783–90. doi: 10.1097/01.tp.0000258649.23081.a3
110. Kuo YR, Goto S, Shih HS, Wang FS, Lin CC, Wang CT, et al. Mesenchymal stem cells prolong composite tissue allotransplant survival in a swine model. *Transplantation.* (2009) 87:1769–77. doi: 10.1097/TP.0b013e3181a664f1
111. Cooper DKC, Gaston R, Eckhoff D, Ladowski J, Yamamoto T, Wang L, et al. Xenotransplantation-the current status and prospects. *Br Med Bull.* (2018) 125:5–14. doi: 10.1093/bmb/ldx043
112. Le Blanc K, Rasmusson I, Sundberg B, Götherström C, Hassan M, Uzunel M, et al. Treatment of severe acute graft-versus-host disease with third party haploidentical mesenchymal stem cells. *Lancet.* (2004) 363:1439–41. doi: 10.1016/S0140-6736(04)16104-7
113. Goto T, Murata M, Nishida T, Terakura S, Kamoshita S, Ishikawa Y, et al. Phase I clinical trial of intra-bone marrow cotransplantation of mesenchymal stem cells in cord blood transplantation. *Stem Cells Transl Med.* (2020). doi: 10.1002/sctm.20-0381. [Epub ahead of print].
114. Goto T, Murata M, Terakura S, Nishida T, Adachi Y, Ushijima Y, et al. Phase I study of cord blood transplantation with intrabone marrow injection of mesenchymal stem cells: a clinical study protocol. *Medicine.* (2018) 97:e0449. doi: 10.1097/MD.0000000000010449
115. Jurado M, De La Mata C, Ruiz-García A, López-Fernández E, Espinosa O, Remigia MJ, et al. Adipose tissue-derived mesenchymal stromal cells as part of therapy for chronic graft-versus-host disease: a phase I/II study. *Cytotherapy.* (2017) 19:927–36. doi: 10.1016/j.jcyt.2017.05.002
116. Zhou L, Liu S, Wang Z, Yao J, Cao W, Chen S, et al. Bone marrow-derived mesenchymal stem cells modified with Akt1 ameliorates acute liver GVHD. *Biol Proced Online.* (2019) 21:24. doi: 10.1186/s12575-019-0112-2
117. Dotoli GM, De Santis GC, Orellana MD, de Lima Prata K, Caruso SR, Fernandes TR, et al. Mesenchymal stromal cell infusion to treat steroid-refractory acute GvHD III/IV after hematopoietic stem cell transplantation. *Bone Marrow Transplant.* (2017) 52:859–62. doi: 10.1038/bmt.2017.35
118. Zhao L, Chen S, Yang P, Cao H, Li L. The role of mesenchymal stem cells in hematopoietic stem cell transplantation: prevention and treatment of graft-versus-host disease. *Stem Cell Res Ther.* (2019) 10:182. doi: 10.1186/s13287-019-1287-9
119. Kordelas L, Rebmann V, Ludwig AK, Radtke S, Ruesing J, Doeppner TR, et al. MSC-derived exosomes: a novel tool to treat therapy-refractory graft-versus-host disease. *Leukemia.* (2014) 28:970–3. doi: 10.1038/leu.2014.41
120. Lai P, Chen X, Guo L, Wang Y, Liu X, Liu Y, et al. A potent immunomodulatory role of exosomes derived from mesenchymal stromal cells in preventing cGVHD. *J Hematol Oncol.* (2018) 11:135. doi: 10.1186/s13045-018-0680-7
121. Zhang B, Yeo RWY, Lai RC, Sim EWK, Chin KC, Lim SK. Mesenchymal stromal cell exosome-enhanced regulatory T-cell production through an antigen-presenting cell-mediated pathway. *Cytotherapy.* (2018) 20:687–96. doi: 10.1016/j.jcyt.2018.02.372
122. Guo L, Lai P, Wang Y, Huang T, Chen X, Geng S, et al. Extracellular vesicles derived from mesenchymal stem cells prevent skin fibrosis in the cGVHD mouse model by suppressing the activation of macrophages and B cells immune response. *Int Immunopharmacol.* (2020) 84:106541. doi: 10.1016/j.intimp.2020.106541
123. Fujii S, Miura Y, Fujishiro A, Shindo T, Shimazu Y, Hirai H, et al. Graft-versus-host disease amelioration by human bone marrow mesenchymal stromal/stem cell-derived extracellular vesicles is associated with peripheral preservation of naive T cell populations. *Stem Cells.* (2018) 36:434–45. doi: 10.1002/stem.2759

124. Shao J, Zaro J, Shen Y. Advances in exosome-based drug delivery and tumor targeting: from tissue distribution to intracellular fate. *Int J Nanomedicine.* (2020) 15:9355–71. doi: 10.2147/IJN.S281890
125. Xu L, Faruqu FN, Liam-Or R, Abu Abed O, Li D, Venner K, et al. Design of experiment (DoE)-driven *in vitro* and *in vivo* uptake studies of exosomes for pancreatic cancer delivery enabled by copper-free click chemistry-based labelling. *J Extracell Vesicles.* (2020) 9:1779458. doi: 10.1080/20013078.2020.1779458
126. Kadle RL, Abdou SA, Villarreal-Ponce AP, Soares MA, Sultan DL, David JA, et al. Microenvironmental cues enhance mesenchymal stem cell-mediated immunomodulation and regulatory T-cell expansion. *PLoS ONE.* (2018) 13:e0193178. doi: 10.1371/journal.pone.0193178
127. Wen D, Peng Y, Liu D, Weizmann Y, Mahato RI. Mesenchymal stem cell and derived exosome as small RNA carrier and immunomodulator to improve islet transplantation. *J Control Release.* (2016) 238:166–75. doi: 10.1016/j.jconrel.2016.07.044
128. Marote A, Teixeira FG, Mendes-Pinheiro B, Salgado AJ. MSCs-derived exosomes: cell-secreted nanovesicles with regenerative potential. *Front Pharmacol.* (2016) 7:231. doi: 10.3389/fphar.2016.00231
129. Ra JC, Shin IS, Kim SH, Kang SK, Kang BC, Lee HY, et al. Safety of intravenous infusion of human adipose tissue-derived mesenchymal stem cells in animals and humans. *Stem Cells Dev.* (2011) 20:1297–308. doi: 10.1089/scd.2010.0466
130. Sengupta V, Sengupta S, Lazo A, Woods P, Nolan A, Bremer N. Exosomes derived from bone marrow mesenchymal stem cells as treatment for severe COVID-19. *Stem Cells Dev.* (2020) 29:747–54. doi: 10.1089/scd.2020.0080
131. Hettich BF, Ben-Yehuda Greenwald M, Werner S, Leroux JC. Exosomes for wound healing: purification optimization and identification of bioactive components. *Adv Sci.* (2020) 7:2002596. doi: 10.1002/advs.202002596
132. Budgude P, Kale V, Vaidya A. Cryopreservation of mesenchymal stromal cell-derived extracellular vesicles using trehalose maintains their ability to expand hematopoietic stem cells *in vitro*. *Cryobiology.* (2020) 98:152–63. doi: 10.1016/j.cryobiol.2020.11.009

Conflict of Interest: The authors declare that the research was conducted in the absence of any commercial or financial relationships that could be construed as a potential conflict of interest.

frontiers in Immunology

ORIGINAL RESEARCH
published: 09 April 2021
doi: 10.3389/fimmu.2021.661580

IL-21 Receptor Blockade Shifts the Follicular T Cell Balance and Reduces *De Novo* Donor-Specific Antibody Generation

Yeqi Nian[1,2,3,4], *Zhilei Xiong*[1], *Panpan Zhan*[2,3,4], *Zhen Wang*[1], *Yang Xu*[1], *Jianghao Wei*[1], *Jie Zhao*[1,2,3,4*†] *and Yingxin Fu*[1,2,3,4*†]

[1] Department of Kidney Transplantation, Tianjin First Central Hospital, School of Medicine, Nankai University, Tianjin, China, [2] Kidney Transplantation Research Laboratory, Tianjin First Central Hospital, Tianjin, China, [3] Key Laboratory of Transplantation, Chinese Academy of Medical Sciences, Tianjin, China, [4] Tianjin Key Laboratory for Organ Transplantation, Tianjin First Central Hospital, Tianjin, China

OPEN ACCESS

Edited by:
Hao Wang,
Tianjin Medical University General Hospital, China

Reviewed by:
Zhaoli Sun,
Johns Hopkins University, United States
Ruiming Rong,
Fudan University, China

***Correspondence:**
Yingxin Fu
fuyingxintj@163.com
Jie Zhao
zjsecond@aliyun.com

†These authors share last authorship

Specialty section:
This article was submitted to Alloimmunity and Transplantation, a section of the journal Frontiers in Immunology

Received: 31 January 2021
Accepted: 17 March 2021
Published: 09 April 2021

Citation:
Nian Y, Xiong Z, Zhan P, Wang Z, Xu Y, Wei J, Zhao J and Fu Y (2021) IL-21 Receptor Blockade Shifts the Follicular T Cell Balance and Reduces De Novo Donor-Specific Antibody Generation. Front. Immunol. 12:661580. doi: 10.3389/fimmu.2021.661580

Donor-specific antibodies (DSAs) play a key role in chronic kidney allograft injury. Follicular T helper (Tfh) cells trigger the humoral alloimmune response and promote DSA generation, while T-follicular regulatory (Tfr) cells inhibit antibody production by suppressing Tfh and B cells. Interleukin (IL)-21 exerts a distinct effect on Tfh and Tfr. Here, we studied whether blocking IL-21R with anti-IL-21R monoclonal antibody (αIL-21R) changes the Tfh/Tfr balance and inhibits DSA generation. First, we investigated the impact of αIL-21R on $CD4^+$ T cell proliferation and apoptosis. The results showed that αIL-21R did not have cytotoxic effects on $CD4^+$ T cells. Next, we examined Tfh and regulatory T cells (Tregs) in an *in vitro* conditioned culture model. Naïve $CD4^+$ T cells were isolated from 3-month-old C57BL/6 mice and cultured in Tfh differentiation inducing conditions in presence of αIL-21R or isotype IgG and differentiation was evaluated by CXCR5 expression, a key Tfh marker. αIL-21R significantly inhibited Tfh differentiation. In contrast, under Treg differentiation conditions, FOXP3 expression was inhibited by IL-21. Notably, αIL-21R rescued IL-21-inhibited Treg differentiation. For *in vivo* investigation, a fully mismatched skin transplantation model was utilized to trigger the humoral alloimmune response. Consistently, flow cytometry revealed a reduced Tfh/Tfr ratio in recipients treated with αIL-21R. Germinal center response was evaluated by flow cytometry and lectin histochemistry. We observed that αIL-21R significantly inhibited germinal center reaction. Most importantly, DSA levels after transplantation were significantly inhibited by αIL-21R at different time points. In summary, our results demonstrate that αIL-21R shifts the Tfh/Tfr balance toward DSA inhibition. Therefore, αIL-21R may be a useful therapeutic agent to prevent chronic antibody mediated rejection after organ transplantation.

Keywords: follicular T helper cells, T-follicular regulatory cells, IL-21, donor specific antibodies, antibody mediated rejection, chronic rejection

INTRODUCTION

The clinical success of Tacrolimus-based immunosuppression, surgical techniques, and patient management has largely reduced short-term graft loss caused by acute rejection. However, improving long-term organ survival remains a challenge (1). The latest reports from the United States and Europe have shown almost no improvement in long-term kidney allograft survival during the last two decades (2, 3). Antibody-mediated rejection and the development of *de novo* donor-specific antibodies (dnDSAs) are recognized as distinct and common causes of late allograft injury and are responsible for one-third of failed allografts (4, 5). However, dnDSA generation is refractory to treatment with conventional immunosuppression, thus highlighting the need for a more comprehensive understanding of the underlying mechanism and the development of novel therapeutic strategies (6, 7).

T follicular helper (Tfh) cells are a distinct lineage of $CD4^+$ T cells. Tfh cells are essential for mounting humoral immune response in secondary lymphoid organs, where they present help to B cells, form germinal centers (GCs), regulate affinity maturation, generate memory B cells, and activate long-lived plasma cells (8, 9). The function and presence of Tfh are linked to *de novo* DSA generation and chronic rejection (10). In contrast, T follicular regulatory (Tfr) cells, another $CD4^+$ T cell type that express Forkhead Box P3 (FOXP3), suppress Tfh cell function, reduce GC reactions, and inhibit antibody responses (11). Notably, clinical data demonstrate that an increased Tfh/Tfr ratio is associated with antibody-mediated rejection and chronic renal allograft dysfunction (12, 13). Therefore, tilting the Tfh/Tfr balance toward inhibiting antibody production is a potential way to prevent chronic allograft injury.

Interleukin (IL)-21 is a critical cytokine in the humoral immune response and is primarily produced by Tfh cells. By binding to the IL-21 receptor (IL-21R), IL-21 promotes Tfh cell differentiation in an autocrine manner and induces its own expression (14). Notably, Tfh cell-mediated IL-21 functions are required for efficient antibody responses (15). Indeed, IL-21R-deficient patients showed compromised Tfh cell differentiation, reduced serum IgG levels, and poor antibody responses following vaccination with T cell-dependent antigens (16). Intriguingly, IL-21R exerts different effects in Tfr cells than in Tfh cells (17). In a mouse model, IL-21 reduced FOXP3 expression and influenced regulatory T (Treg) cell homeostasis (18). Moreover, Treg expansion was observed in patients with a loss-of-function IL-21R mutation (17). This demonstrates the distinct effect of IL-21 on Tfh and Tfr cells and suggests its potential as a target to modulate Tfh/Tfr balance.

In this study, we aimed to modulate the Tfh/Tfr balance using a monoclonal antibody against IL-21R (αIL-21R) and evaluated effects of αIL-21R on dnDSA generation. Our results show that αIL-21R shifts the Tfh/Tfr ratio to inhibit the humoral alloimmune response, thereby providing a novel way to prevent dnDSA generation.

METHOD

Animals

Wide-type male C57BL/6 (H2b, 8–12 weeks) and BALB/c (H2d, 8-12 weeks) mice were purchased from Vital River Laboratories (Beijing, China). Animals were allowed free access to water and standard chow. Animal experiments were approved by the Institutional Ethics committee for Research on Animals. The use and care of animals were in accordance with the Institutional Animal Care and Use Committee guidelines.

αIL-21R

Monoclonal αIL-21R was obtained from BioXcell (Lebanon, NH, USA), diluted with PBS, and added to the cell culture medium at 10 μg/mL. For *in vivo* experiments, mice were treated with intraperitoneal injections of 1 mg/kg αIL-21R or isotype starting on the day of transplantation and three times per week for three weeks.

Cell Isolation and T Cell Differentiation

Single cell suspensions were prepared from the spleens of C57BL/6 mice. Naive $CD4^+$ T cells were isolated by negative selection, using biotinylated antibodies directed against markers of non-naive $CD4^+$ T cells (CD8, CD11b, CD11c, CD19, CD24, CD25, CD44, CD45R, CD49b, TCRγ/δ, and TER119) and streptavidin-coated magnetic particles (Stemcell Technologies, Vancouver, BC, Canada). Cells were used at a purity of > 95%.

Naive $CD4^+$ T cells were cultured in 96-well flat-bottom plates (2.0×10^5 per well) suspended in 0.5 mL RPMI 1640 media supplemented with 10% fetal calf serum, 200 mM L-glutamine, 100 U/mL penicillin/streptomycin and 5×10^{-5} M 2-mercaptoethanol at 37°C in a 95%/5% air/CO_2 atmosphere with saturating humidity. The wells were coated with 8 μg/mL anti-mouse α-CD3, and 2 μg/mL soluble anti-mouse α-CD28 was added to the media. The Tfh cell differentiation procedure was modified from Gao et al. (19) T cell-depleted splenocytes were stimulated with lipopolysaccharide (LPS) for 24 h and co-cultured with naive $CD4^+$ T cells (1:10) to stimulate Tfh cell differentiation. IL-6 (100ng/mL) and IL-21 (50ng/mL) were added to the cell culture. For Treg differentiation, a cocktail containing IL-2, TGF-β, and all-trans retinoic acid (Immunocult; Stemcell Technologies, Vancouver, BC, Canada) was added to cell culture. After 5 days, the cells were collected, and analyzed by flow cytometry. To determine the absolute number of viable lymphocytes, Trypan blue staining was performed and live cells were counted using a hemocytometer.

Flow Cytometry

Single cell suspensions were prepared from the spleens of recipient mice. Cells were labeled for surface and intracellular markers using fluorescence-labeled anti-mouse α-CD4, α-CXCR5, α-ICOS, α-PD1, α-FOXP3, α-GL7, and α-Fas antibodies (eBioscience, CA, USA). Intracellular FOXP3

staining was performed using a commercially available staining kit that included permeabilization solution and buffer (eBioscience). Flow cytometric measurements were performed on a FACSAria III (BD Bioscience, CA, USA) and data were analyzed using FlowJo (FlowJo Software, OR, USA). For proper gating, apoptotic cells were excluded, and the samples were compared with isotype controls, fluorescence minus one (FMO)-stained, permeabilized, and unpermeabilized unstained cells. For the carboxyfluorescein diacetate succinimidyl ester (CFSE; Invitrogen, CA, USA) cell proliferation assay, cells were labeled with 1 μM CFSE. The CFSE dilution was measured by flow cytometry.

Skin Transplantation

Fully mismatched skin transplants were performed as described previously (20). In detail, full-thickness skin grafts (1 cm^2) were obtained from the tails of BALB/c mice and engrafted onto the dorsolateral thoracic walls of C57BL/6 mice. Graft rejection was monitored daily and necrosis > 90% indicated graft rejection.

Lectin Histochemistry

To analysis the germinal center, paraffin sections of spleen were deparaffinized, microwaved, immersed in 0.01 M citrate buffer (pH 6.0) for 20 min, washed with PBS, and incubated at room temperature for 30 minutes with biotinylated peanut agglutinin (PNA). After washing, tissues were incubated with peroxidase for 30 minutes. Reaction signals were developed using 3, 3' diaminobenzidine (DAB; Dako, Denmark).

Donor-Specific Antibody (DSA) Assay

For DSA detection, serum was diluted (1:18) and incubated with 10^6 BALB/c splenocytes for 1 h at 4°C. Next, the cells were washed and incubated with anti-IgG and anti-IgM antibodies (Jackson immunoResearch, PA, USA) for 30 min. The mean fluorescence intensity of the cells was measured by flow cytometry.

Statistical Analysis

Differences between groups were analyzed using unpaired Student's *t*-tests. Graft survival was compared using log-rank tests. Results with $p < 0.05$ were considered statistically significant (*p<0.05; **p<0.01; ***p<0.001).

RESULTS

αIL-21R Does Not Alter $CD4^+$ T Cell Proliferation and Apoptosis Under Th0 Conditions

To test the overall effect of αIL-21R on $CD4^+$ T cells, we first investigated whether this monoclonal antibody induced proliferation or apoptosis in the unspecific Th0 condition. As

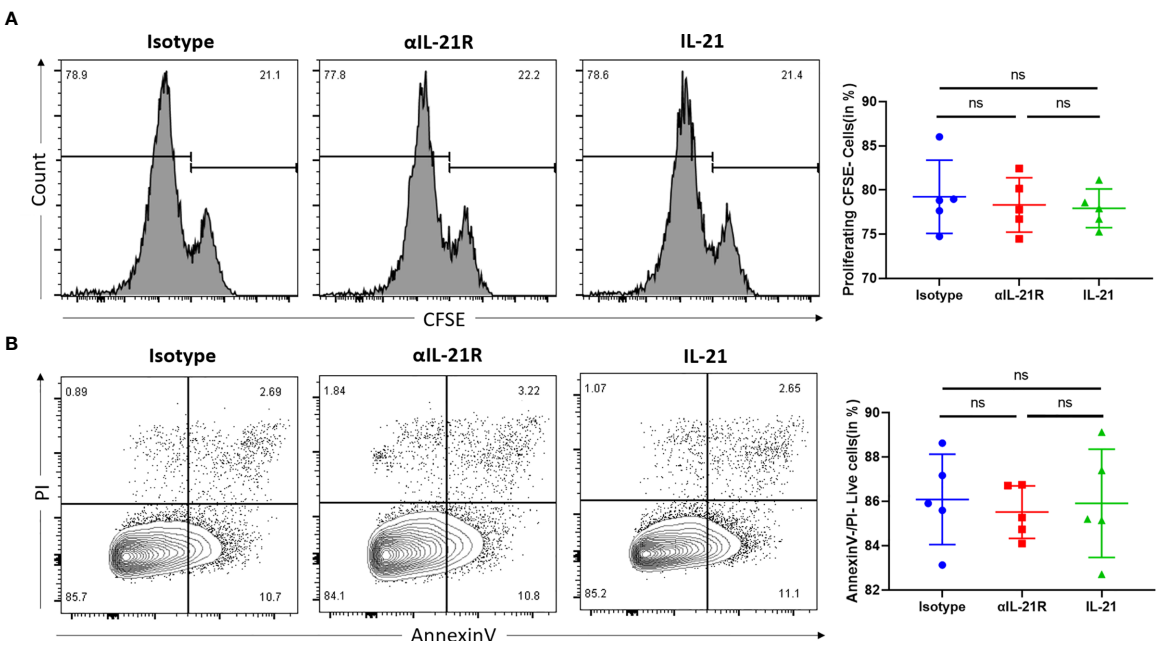

FIGURE 1 | αIL-21R does not alter CD4+ T cell proliferation and apoptosis under Th0 conditions. **(A)** Naïve CD4+ T cells were isolated from C57BL/6 mice and labeled with 1μM CFSE. Naïve CD4+ T cells were activated with anti-CD3/anti-CD28 to induce proliferation. Proliferation of naïve CD4+ T cells was measured by the dilution of CFSE, in the presence of 10μg/ml αIL-21R or Isotype control. **(B)** Naïve CD4+ T cells from C57BL/6 mice were activated with anti-CD3/anti-CD28 under the condition of 10μg/ml αIL-21R or Isotype control. Lived cell was measured by the frequency of Annexin V^-PI^- cells. Column plots display individual data points and mean ± SD, n = 5/group. ns, not significant.

shown by the CFSE proliferation assay, $CD4^+$ T cells treated with αIL-21R or isotype control showed comparable proliferating cell rates (**Figure 1A**). Moreover, there was no significant difference the number of in live cells, dead cells, or apoptotic cells between the groups. These results indicate that αIL-21R is not cytotoxic and is not expected to kill a large number of cells or inhibit cell proliferation (**Figure 1B**).

αIL-21R Inhibits Tfh Cell Differentiation and Rescues the IL-21 Induced Inhibition in Treg Cells

Both Tfh and Tfr cells expressed IL-21R. However, IL-21 promoted Tfh differentiation and inhibited the expression of FOXP3, the signature transcription factor of Tfr and Treg cells. Furthermore, αIL-21R decreased the Tfh/Tfr ratio by inhibiting Tfh differentiation while blocking the IL-21 induced inhibition of Tfr cells. To assess the effect of αIL-21R on Tfh/Tfr ratio, we individually examined the impact of αIL-21R on Tfh and Treg differentiation. Under Tfh differentiation conditions, the frequency of Tfh cells reduced significantly by αIL-21R treatment (**Figure 2A**). Since a well-established method for Tfr differentiation is lacking, we observed the effect of αIL-21R on Tregs. As shown in **Figure 2B**, IL-21 reduced the frequency of Treg cells, and this effect was reversed by αIL-21R treatment (**Figure 2B**). Notably, αIL-21R treatment alone did not alter Treg differentiation (data not shown). Taken together, these data suggest that αIL-21R treatment can modify the Tfh/Tfr balance.

αIL-21R Decreases the Tfh/Tfr Ratio in Transplant Recipient Mice

A skin transplantation model was used to investigate the effect of αIL-21R treatment on the Tfh/Tfr ratio in the context of alloimmune responses. Mice that received fully mismatched skin allografts were treated with αIL-21R or isotype control for 14 days after surgery and their splenocytes were analyzed. We observed that αIL-21R treatment did not reduce the frequency of $CD4^+CXCR5^+$ T cells (**Figure 3A**). However, a significant decrease was observed in the frequency of $CD4^+CXCR5^+ ICOS^+PD^+$ Tfh cells (**Figure 3B**). Meanwhile, αIL-21R increased the frequency of $CD4^+CXCR5^+FOXP3^+$ Tfr cells (**Figure 3C**). The Tfh/Tfr ratio was calculated as the absolute number of $CD4^+CXCR5^+PD1^+ICOS^+$ and $CD4^+CXCR5^+ FOXP3^+$ cells. The results showed that αIL-21R significantly decreased the Tfh/Tfr ratio (**Figure 3D**). Notably, the absolute number of Tfh cells was lower in the group treated with αIL-21R, although the results was statistically insignificant (**Figure 3D**).

GC Reaction and dnDSA Generation Are Blocked by αIL-21R

To assess whether the *in vivo* decrease in Tfh/Tfr ratio mediated by αIL-21R inhibited the antibody response, we treated skin

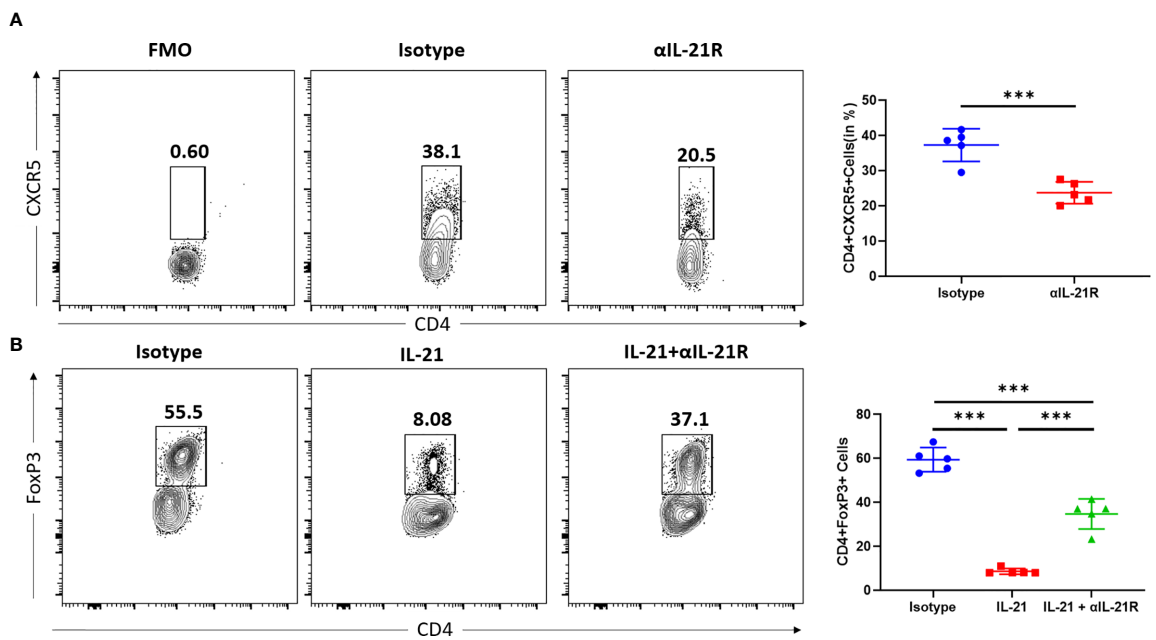

FIGURE 2 | αIL-21R inhibits Tfh cell differentiation and rescues the IL-21 induced inhibition in Treg cells. **(A)** Naïve CD4+ T cells were isolated from C57BL/6 mouse and cultured under Tfh condition in the presence of 10μg/ml αIL-21R or Isotype control. Frequencies of $CD4^+CXCR5^+$ Tfh cells were analyzed by flow cytometry. **(B)** Naïve $CD4^+$ T cells were isolated from C57BL/6 mouse and cultured under Treg condition, in the presence of 10ug/ml IL21, with αIL-21R or Isotype control. Frequencies of $CD4^+FOXP3^+$ Treg cells were analyzed by flow cytometry. Column plots display individual data points and mean ± SD, n = 5/group. Fluorescence minus one (FMO) controls are the experimental cells stained with all the fluorophores minus the fluorophore of target. FMO controls were used to properly interpret flow cytometry data. ***p<0.001.

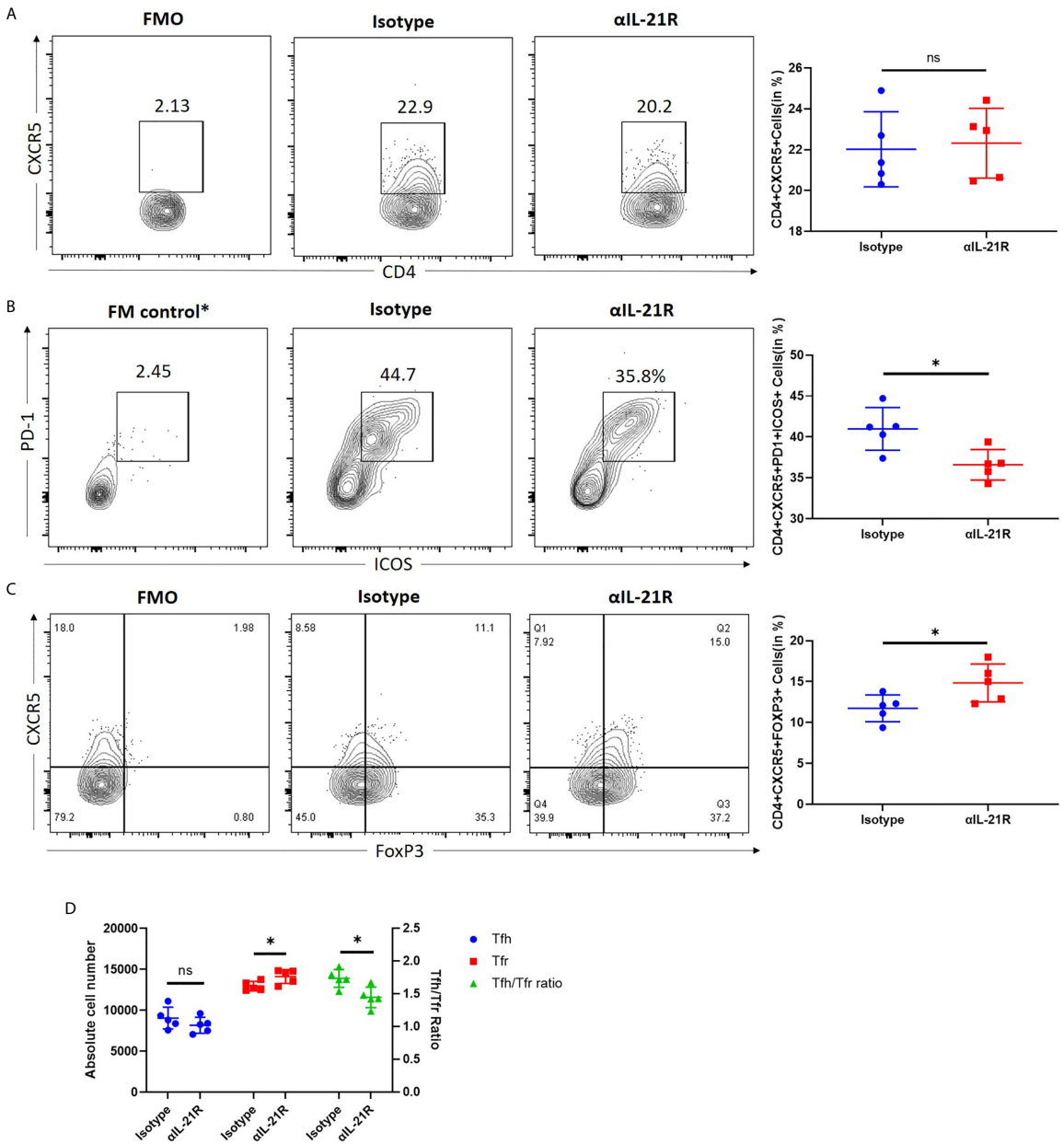

FIGURE 3 | αIL-21R decreases the Tfh/Tfr ratio in transplant recipient mice. Skin allografts from BALB/c mice were transplanted onto C57BL/6 mice. Recipients were treated with 1 mg/kg αIL-21R three times every week or Isotype starting on the day of transplantation. **(A)** Frequencies of $CD4^+CXCR5^+$ T cells and **(B)** frequencies of $CD4^+CXCR5^+ICOS^+PD1^+$ Tfh cells and **(C)** frequencies of $CD4^+CXCR5^+FOXP3^+$ Tfr cells in the spleen were assessed after 14 days by flow cytometry gating on single cells. **(D)** Absolute number of Tfh, Tfr cells and Tfh/Tfr ratio were calculated based on the results of flow cytometry by multiplication total number per sample and percentage of interested cells. Column plots display individual data points and mean ± SD, n = 5/group. *p<0.05.

transplantation recipients with αIL-21R or control IgG and analyzed the GC response after 14 days. Flow cytometry analysis revealed a significant decrease in the frequency of GC B cells ($B220^+GL7^+Fas^+$ cells) in mice treated with αIL-21R (**Figure 4A**). In line with this finding, PNA staining confirmed that αIL-21R inhibited GC formation (**Figure 4B**). Finally, we investigated the effect of αIL-21R on dnDSA generation by monitoring the levels of donor-specific IgG and IgM for 5-weeks (**Figure 4C**). As previously reported, IgG levels in the control group continued to increase and peaked at 3-weeks post-surgery, after which, the IgG level decreased, and remained at a stable level. No significant difference was observed between the treatment and control groups during the first 2-weeks. However, the difference appeared at 2-weeks as αIL-21R treatment blocked increasing IgG levels, and even caused them to decrease. At 3-weeks after surgery, IgG levels in the αIL-21R treatment group

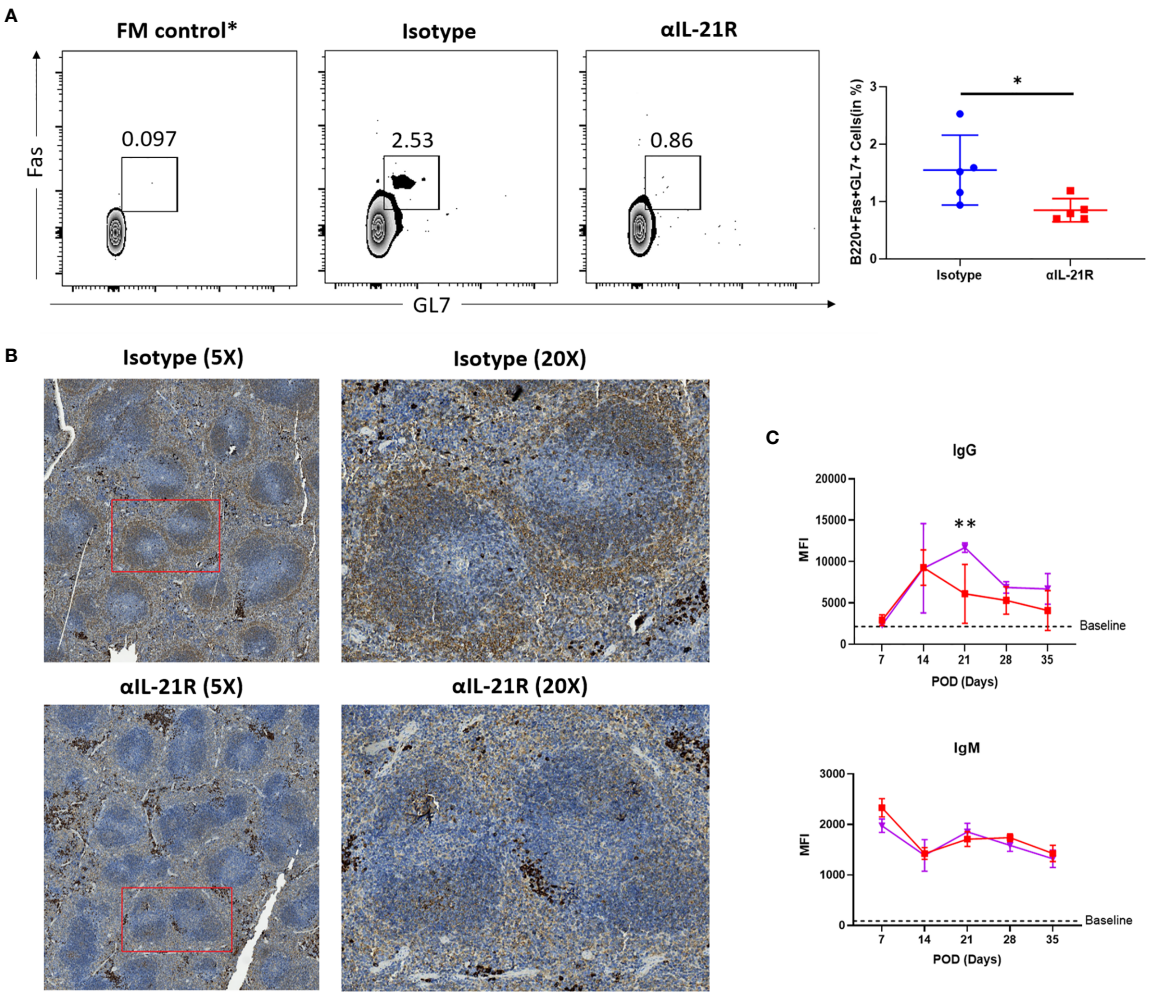

FIGURE 4 | GC reaction and dnDSA generation are blocked by αIL-21R. Skin allografts from BALB/c mice were transplanted onto C57BL/6 mice. Recipients were treated with 1 mg/kg αIL-21R three times every week or Isotype starting on the day of transplantation. **(A)** Frequencies of $B220^{+}GL7^{+}Fas^{+}$ GC B cells were assessed after 14 days by flow cytometry. **(B)** Spleens were harvest from recipients after 14 days of transplantation and stained with PNA. GC was identified as brown area in while pulp. **(C)** Serum was collected from recipients every week after transplantation. IgG and IgM level were detected with flow cytometry. Column plots display individual data points and mean ± SD, n = 5/group. *p<0.05, **p<0.01.

were significantly lower than in the control group. Although no significant difference was observed afterward, the αIL-21R group showed an overall lower IgG level compared to the control group; no significant difference was observed in IgM levels between the groups (**Figure 4C**).

DISCUSSION

In this study, we evaluated the ability of αIL-21R to modulate the Tfh/Tfr balance and evaluated its effects on dnDSA generation. Our main finding from this study is that αIL-21R shifts the Tfh/Tfr ratio toward inhibition of humoral immune response and reduces dnDSA generation against a fully mismatched allograft. Furthermore, the IgG kinetics observed in the control group were consistent with the natural course of allosensitization (21). The IgG level continued to increase after transplantation and peaked at 3-weeks, after which it decreased, and remained at a stable level; however, this level was still higher than the baseline level. In contrast, αIL-21R treatment significantly altered the IgG generation kinetics. Indeed, the time of IgG increase was shorter and peak was lower. Given that earlier clinical data demonstrated the association between dnDSA and chronic allograft injury, our results provide new evidence to support the use of αIL-21R in organ transplantation to improve long-term outcomes (4, 5).

Notably, the kinetics observed in this study are in line with the Tfh/Tfr dynamic balance observed in the humoral response. Tfr cells control antigen-specific Tfh cell expansion and terminate the GC reaction (22). In the B cell follicle, Tfh and Tfr cells are present in an equal proportion (23). Upon antigen challenge, both Tfh and Tfr cells begin to expand (24) but they do not proliferate at a similar rate.

Tfh cells proliferate faster and shift the Tfh/Tfr ratio in favor of helper T cell generation. Indeed, the Tfh cell response reached its peak at postoperative day 7, while Tfr cells represented a far lower proportion of the follicular $CD4^+$ T cell population. GCs begin to form at this time point and start to generate antibodies. By day 10, the Tfh numbers started to decrease, while Tfr cells continued to proliferate. Thus, the Tfh/Tfr ratio shifted toward inducing termination of the GC reaction. The mean Tfh/Tfr ratio was 1.44 and the DSA continued to increase until day 21. In contrast, the mean Tfh/Tfr ratio was 1.73 in the αIL-21R treatment group and DSA began to decrease on day 14. Thus, modulating the Tfr/Tfr ratio with αIL-21R is a potential strategy to limit dnDSA generation and may have applications in clinical settings in the future.

The mechanism underlying the αIL-21R effect is to modulate the differential effect of IL-21 on Tfh and Tfr cells. Antigen-stimulated Tfh cells proliferate rapidly and produce IL-21 as a major effector cytokine. IL-21R is broadly expressed on T, B, natural killer, and dendritic cells. Further, IL-21 signaling, *via* Jak-Stat and other pathways, promotes their proliferation, differentiation, and effector function (25). However, in our study, IL-21 reduced the expression of FOXP3, the key transcription factor in Tfr cells. IL-2 is an essential cytokine for the expression of FOXP3. Webster et al. reported that IL-21 inhibits Tfr differentiation by inhibiting their response to IL-2 in a Bcl6-dependent mechanism (17). At the molecular level, Jak-STAT3 signaling is activated by IL-21 and leads to STAT1 and STAT3 phosphorylation, whereas IL-2 strongly activates STAT5. Thus, the ability of different STAT molecules to compete for STAT binding sites and affect gene transcription may underlie the differential effects of IL-21 on Tfh and Tfr (26, 27). In addition, Foxp3+ regulatory T cells suppress the emergence of long-lived splenic plasma cells, thus increased Foxp3 expression by blocking IL-21 receptor may diminish the DSA production (28).

In summary, this study reports αIL-21R mediated modulation of the Tfh/Tfr ratio and subsequent reduction in dnDSA generation. Given that IL-21R is broadly expressed, targeting IL-21 signaling may have multiple-target effects on the humoral immune response. Indeed, IL-21R antagonists inhibit the B cell differentiation toward plasmablasts when exposed to alloantigens (29). Despite the fact that dnDSA plays a central role in antibody-mediated chronic graft rejection, the lack of graft survival data is a major limitation of our study. However, our study provides a novel strategy to control chronic allograft injury. In further studies, IL-21R transgenic mice and a minor-mismatch heart transplantation model will be used to provide direct evidence that targeting IL-21R protects against chronic allograft injury.

DATA AVAILABILITY STATEMENT

The raw data supporting the conclusions of this article will be made available by the authors, without undue reservation.

ETHICS STATEMENT

The animal study was reviewed and approved by Tianjin First Central Hospital, Nankai University.

AUTHOR CONTRIBUTIONS

YN and ZX performed experiments, analyzed data, and wrote the manuscript. PZ, YX, and JW supported experiments and edited the manuscript. JZ and YF designed experiments, supervised the work, and wrote the manuscript. All authors contributed to the article and approved the submitted version.

FUNDING

This work was supported by a grant (81970654) from National Natural Science Foundation of China to YF and a grant (CM201812) from Tianjin First Center Hospital to JZ.

ACKNOWLEDGMENTS

We would like to thank Editage (www.editage.cn) for English language editing.

REFERENCES

1. Gaston RS, Fieberg A, Hunsicker L, Kasiske BL, Leduc R, Cosio FG, et al. Late graft failure after kidney transplantation as the consequence of late versus early events. *Am J Transplant* (2018) 18(5):1158–67. doi: 10.1111/ajt.14590
2. Lamb KE, Lodhi S, Meier-Kriesche HU. Long-term renal allograft survival in the United States: a critical reappraisal. *Am J Transplant* (2011) 11(3):450–62. doi: 10.1111/j.1600-6143.2010.03283.x
3. Coemans M, Süsal C, Döhler B, Anglicheau D, Giral M, Bestard O, et al. Analyses of the short- and long-term graft survival after kidney transplantation in Europe between 1986 and 2015. *Kidney Int* (2018) 94 (5):964–73. doi: 10.1016/j.kint.2018.05.018
4. Einecke G, Sis B, Reeve J, Mengel M, Campbell PM, Hidalgo LG, et al. Antibody-mediated microcirculation injury is the major cause of late kidney transplant failure. *Am J Transplant* (2009) 9(11):2520–31. doi: 10.1111/j.1600-6143.2009.02799.x
5. Sellarés J, de Freitas DG, Mengel M, Reeve J, Einecke G, Sis B, et al. Understanding the causes of kidney transplant failure: the dominant role of antibody-mediated rejection and nonadherence. *Am J Transplant* (2012) 12 (2):388–99. doi: 10.1111/j.1600-6143.2011.03840.x
6. Loupy A, Lefaucheur C. Antibody-Mediated Rejection of Solid-Organ Allografts. *N Engl J Med* (2018) 379(12):1150–60. doi: 10.1056/NEJMra1802677
7. Eskandary F, Regele H, Baumann L, Bond G, Kozakowski N, Wahrmann M, et al. A Randomized Trial of Bortezomib in Late Antibody-Mediated Kidney Transplant Rejection. *J Am Soc Nephrol* (2018) 29(2):591–605. doi: 10.1681/ASN.2017070818
8. Tangye SG, Ma CS, Brink R, Deenick EK. The good, the bad and the ugly - TFH cells in human health and disease. *Nat Rev Immunol* (2013) 13(6):412–26. doi: 10.1038/nri3447
9. Badell IR, Ford ML. T follicular helper cells in the generation of alloantibody and graft rejection. *Curr Opin Organ Transplant* (2016) 21(1):1–6. doi: 10.1097/MOT.0000000000000260
10. Niu Q, Kraaijeveld R, Li Y, Mendoza Rojas A, Shi Y, Wang L, et al. An overview of T follicular cells in transplantation: spotlight on their clinical significance. *Expert Rev Clin Immunol* (2019) 15(12):1249–62. doi: 10.1080/1744666X.2020.1693262

11. Lopez-Ocasio M, Buszko M, Blain M, Wang K, Shevach EM. T Follicular Regulatory Cell Suppression of T Follicular Helper Cell Function Is Context-Dependent in vitro. *Front Immunol* (2020) 11:637. doi: 10.3389/fimmu.2020.00637
12. Chen W, Bai J, Huang H, Bi L, Kong X, Gao Y, et al. Low proportion of follicular regulatory T cell in renal transplant patients with chronic antibody-mediated rejection. *Sci Rep* (2017) 7(1):1322. doi: 10.1038/s41598-017-01625-3
13. Yan L, Li Y, Li Y, Wu X, Wang X, Wang L, et al. Increased circulating Tfh to Tfr ratio in chronic renal allograft dysfunction: a pilot study. *BMC Immunol* (2019) 20(1):26. doi: 10.1186/s12865-019-0308-x
14. Vogelzang A, McGuire HM, Yu D, Sprent J, Mackay CR, King C. A fundamental role for interleukin-21 in the generation of T follicular helper cells. *Immunity* (2008) 29(1):127–37. doi: 10.1016/j.immuni.2008.06.001
15. Wu Y, van Besouw NM, Shi Y, Hoogduijn MJ, Wang L, Baan CC. The Biological Effects of IL-21 Signaling on B-Cell-Mediated Responses in Organ Transplantation. *Front Immunol* (2016) 7:319. doi: 10.3389/fimmu.2016.00319
16. Tangye SG, Ma CS. Regulation of the germinal center and humoral immunity by interleukin-21. *J Exp Med* (2020) 217(1):e20191638. doi: 10.1084/jem.20191638
17. Jandl C, Liu SM, Cañete PF, Warren J, Hughes WE, Vogelzang A, et al. IL-21 restricts T follicular regulatory T cell proliferation through Bcl-6 mediated inhibition of responsiveness to IL-2. *Nat Commun* (2017) 8:14647. doi: 10.1038/ncomms14647
18. Oestreich KJ, Mohn SE, Weinmann AS. Molecular mechanisms that control the expression and activity of Bcl-6 in TH1 cells to regulate flexibility with a TFH-like gene profile. *Nat Immunol* (2012) 13(4):405–11. doi: 10.1038/ni.2242
19. Gao X, Wang H, Chen Z, Zhou P, Yu D. An optimized method to differentiate mouse follicular helper T cells in vitro. *Cell Mol Immunol* (2020) 17(7):779–81. doi: 10.1038/s41423-019-0329-7
20. Nian Y, Iske J, Maenosono R, Minami K, Heinbokel T, Quante M, et al. Targeting age-specific changes in CD4(+) T cell metabolism ameliorates alloimmune responses and prolongs graft survival. *Aging Cell* (2021) 20(2):e13299. doi: 10.1111/acel.13299
21. Yang J, Chen J, Young JS, Wang Q, Yin D, Sciammas R, et al. Tracing Donor-MHC Class II Reactive B cells in Mouse Cardiac Transplantation: Delayed CTLA4-Ig Treatment Prevents Memory Alloreactive B-Cell Generation. *Transplantation* (2016) 100(8):1683–91. doi: 10.1097/TP.0000000000001253
22. Wing JB, Ise W, Kurosaki T, Sakaguchi S. Regulatory T cells control antigen-specific expansion of Tfh cell number and humoral immune responses via the coreceptor CTLA-4. *Immunity* (2014) 41(6):1013–25. doi: 10.1016/j.immuni.2014.12.006
23. Sage PT, Sharpe AH. In vitro assay to sensitively measure T(FR) suppressive capacity and T(FH) stimulation of B cell responses. *Methods Mol Biol (Clifton NJ)* (2015) 1291:151–60. doi: 10.1007/978-1-4939-2498-1_13
24. Shulman Z, Gitlin AD, Targ S, Jankovic M, Pasqual G, Nussenzweig MC, et al. T follicular helper cell dynamics in germinal centers. *Science (New York NY)* (2013) 341(6146):673–7. doi: 10.1126/science.1241680
25. Xie A, Buras ED, Xia J, Chen W. The Emerging Role of Interleukin-21 in Transplantation. *J Clin Cell Immunol* (2012) Suppl 9(2):1–7. doi: 10.4172/2155-9899.S9-002
26. Sage PT, Alvarez D, Godec J, von Andrian UH, Sharpe AH. Circulating T follicular regulatory and helper cells have memory-like properties. *J Clin Invest* (2014) 124(12):5191–204. doi: 10.1172/JCI76861
27. Johnston RJ, Choi YS, Diamond JA, Yang JA, Crotty S. STAT5 is a potent negative regulator of TFH cell differentiation. *J Exp Med* (2012) 209(2):243–50. doi: 10.1084/jem.20111174
28. Jang E, Cho WS, Cho ML, Park HJ, Oh HJ, Kang SM, et al. Foxp3+ regulatory T cells control humoral autoimmunity by suppressing the development of long-lived plasma cells. *J Immunol (Baltimore Md 1950)* (2011) 186(3):1546–53. doi: 10.4049/jimmunol.1002942
29. de Leur K, Dor FJ, Dieterich M, van der Laan LJ, Hendriks RW, Baan CC. IL-21 Receptor Antagonist Inhibits Differentiation of B Cells toward Plasmablasts upon Alloantigen Stimulation. *Front Immunol* (2017) 8:306. doi: 10.3389/fimmu.2017.00306

Conflict of Interest: The authors declare that the research was conducted in the absence of any commercial or financial relationships that could be construed as a potential conflict of interest.

frontiers in Immunology

ORIGINAL RESEARCH
published: 09 April 2021
doi: 10.3389/fimmu.2021.661338

The mTOR Deficiency in Monocytic Myeloid-Derived Suppressor Cells Protects Mouse Cardiac Allografts by Inducing Allograft Tolerance

Jiawei Li[1,2†], Juntao Chen[1,2†], Mingnan Zhang[3†], Chao Zhang[1,2], Renyan Wu[3], Tianying Yang[1,2], Yue Qiu[4], Jingjing Liu[2,5], Tongyu Zhu[1,2], Yi Zhang[2,5*] and Ruiming Rong[1,2*]*

[1] Department of Urology, Zhongshan Hospital, Fudan University, Shanghai, China, [2] Shanghai Key Laboratory of Organ Transplantation, Shanghai, China, [3] Department of Immunology and Microbiology, Shanghai Institute of Immunology, Shanghai Jiao Tong University School of Medicine, Shanghai, China, [4] Department of Critical Care Medicine, Zhongshan Hospital, Fudan University, Shanghai, China, [5] Biomedical Research Center, Institute for Clinical Sciences, Zhongshan Hospital, Fudan University, Shanghai, China

OPEN ACCESS

Edited by:
Hao Wang,
Tianjin Medical University General Hospital, China

Reviewed by:
Jinfeng Li,
First Affiliated Hospital of Zhengzhou University, China
Xiaoyi Zheng,
Stanford University, United States

***Correspondence:**
Ruiming Rong
rong.ruiming@zs-hospital.sh.cn
Yi Zhang
yzhang_med@fudan.edu.cn
Tongyu Zhu
zhu.tongyu@zs-hospital.sh.cn

[†]These authors have contributed equally to this work

Specialty section:
This article was submitted to Alloimmunity and Transplantation, a section of the journal Frontiers in Immunology

Received: 30 January 2021
Accepted: 12 March 2021
Published: 09 April 2021

Citation:
Li J, Chen J, Zhang M, Zhang C, Wu R, Yang T, Qiu Y, Liu J, Zhu T, Zhang Y and Rong R (2021) The mTOR Deficiency in Monocytic Myeloid-Derived Suppressor Cells Protects Mouse Cardiac Allografts by Inducing Allograft Tolerance. Front. Immunol. 12:661338. doi: 10.3389/fimmu.2021.661338

Background: Myeloid-derived suppressor cells (MDSCs) can prevent allograft rejection and induce immune tolerance in transplantation models. Previous studies have demonstrated that inhibition of mTOR signaling can enhance the MDSC protective effect in heart transplantation (HTx) by promoting MDSC expansion. In addition, mTOR inhibition is related to autophagy. The present study investigated the protective mechanism of mTOR-deficient monocytic MDSCs (M-MDSCs) in mouse HTx.

Methods: Myeloid-specific mTOR conditional knockout mice were generated to obtain $mTOR^{-/-}$ M-MDSCs. The proliferation and immunosuppressive function of $mTOR^{-/-}$ M-MDSCs were determined by flow cytometry and T cell proliferation assays. The $mTOR^{-/-}$ M-MDSC intracellular autophagy levels were determined using western blotting and electron microscopy. RNAseq analysis was performed for wild-type (WT) and $mTOR^{-/-}$ M-MDSCs. Allogeneic HTx mouse model was established and treated with WT or $mTOR^{-/-}$ M-MDSCs. Enzyme-linked immunosorbent assay, flow cytometry, and immunohistochemistry assays were performed to determine WT and $mTOR^{-/-}$ M-MDSC-induced immune tolerance.

Results: The mTOR deficiency promoted M-MDSC differentiation and enhanced intracellular autophagy levels *in vivo* and *in vitro*. mTOR deficiency also enhanced the immunosuppressive function of M-MDSCs. In addition, infusing with WT and $mTOR^{-/-}$ M-MDSCs prolonged cardiac allograft survival and established immune tolerance in recipient mice by inhibiting T cell activation and inducing regulatory T cells.

Conclusion: mTOR deficiency enhances the immunosuppressive function of M-MDSCs and prolongs mouse cardiac allograft survival.

Keywords: MDSC (myeloid-derived suppressor cell), cardiac transplantation, mTOR, autophagy, immune tolerance

INTRODUCTION

Myeloid-derived suppressor cells (MDSCs) were first discovered in tumorigenesis, but were later found to be involved in other pathological conditions, such as obesity, sepsis, and organ transplantation (1). MDSCs are heterogeneous progenitor and immature myeloid cells. Based on the different cell surface markers, MDSCs can be classified into granulocytic MDSCs (G-MDSCs and CD11b^{+}Ly6G^{+}Ly6C^{low}) and monocytic MDSCs (M-MDSCs and CD11b^{+}Ly6G^{-}Ly6C^{high}) (1, 2). MDSCs are components of tumor microenvironment (TME) and support tumor progression, invasion, and metastases (3, 4). In TME, MDSCs suppress T cell activation, regulate inflammatory cytokines, and promote immune tolerance to enhance tumor growth (5). The function of T cell inhibition by MDSCs is correlated with the induction and recruitment of regulatory T cells (Tregs) (2, 6, 7).

Some recent studies have found that infusing with *in vitro*-induced MDSCs can prevent rejection in cardiac transplantation and recruitment for chimerism and tolerance (8). Preclinical studies have demonstrated that murine MDSCs, derived from either embryonic stem cells or adult bone marrow (BM), potently inhibit graft-versus-host disease without aborting graft-versus-leukemia response (9). MDSCs treated with drugs or cytokines, or edited using genetic technology *in vitro*, showed directional differentiation potential or enhanced function in inducing tolerance. In mouse skin transplantation models, M-CSF plus TNF-α-induced M-MDSCs have a stronger immunosuppressive function and promote immune tolerance against donor antigens (10), as well as CsA-induced MDSCs (11). In addition, prolonged mouse cardiac allograft survival was demonstrated after treatment with mammalian target of rapamycin (mTOR) inhibitor rapamycin, which induced MDSC expansion in recipient hearts (12). Our previous study demonstrated that blocking the mTOR signaling pathways ameliorated acute kidney injury (AKI) by promoting the induction, recruitment, and immunosuppressive activity of MDSCs (13).

The inhibition of mTOR is related to autophagy (14). Autophagy is initiated when mTOR is downregulated, resulting in the release of the transcription factor Unc-51-like autophagy-activating kinase 1, which, in turn, induces vacuole formation by activating PI3KC3, Beclin1 (Atg6), and the Atg12, -5, and -16 complex (15). The influence of mTOR inhibition on MDSC proliferation/function has been recently elucidated by Wu et al. in alloskin-grafted and tumor-bearing mouse models. They demonstrated that rapamycin treatment or using mTOR knockout (KO) mice decreased the percentages and number of M-MDSCs and reduced their immunosuppressive activity (16). Autophagy inhibition also increased the quantity of apoptotic MDSCs, demonstrating that autophagy extends the survival and increases the viability of MDSCs (17). Whether mTOR deficiency may affect MDSC differentiation in cardiac transplantation remains unknown.

The present study found that mTOR deficiency can promote M-MDSC differentiation and enhance intracellular autophagy levels, which leads to the upregulated immunosuppressive function of M-MDSCs. In addition, infusing with mTOR-deficient M-MDSCs can prolong cardiac allograft survival and establish immune tolerance in recipient mice by inhibiting T cell activation and inducing Tregs. These findings can potentially be used in the future for preventing graft rejection and immune tolerance induction in transplantation.

MATERIALS AND METHODS

Mice

Wild-type (WT) C57BL/6 and BALB/c mice were purchased from the SLAC Laboratory Animal Co., Ltd (Shanghai, China). Lyz-Cre and mTOR$^{flox/flox}$ mice were generously provided by Professor Yong Zhao at the Institute of Zoology, Chinese Academy of Sciences (Beijing, China). Myeloid-specific mTOR conditional knockout (KO) mice (mTOR$^{-/-}$, Lyz-Cre) were generated by mating mTOR$^{flox/flox}$ mice with Lyz-Cre mice. Mouse genotypes were determined using PCR with the following primers: Lyz-common, Lyz-WT, Lyz-mutant, mTOR-common, mTOR-WT, and mTOR-mutant. Primer sequences are listed in **Table 1**. All animal experiments were performed according to the guidelines of the Care and Use of Laboratory Animals of the Laboratory Animal Ethical Commission of Fudan University and were approved by the Animal Ethical Committee of Zhongshan Hospital, Fudan University, Shanghai, China.

Cervical Cardiac Transplantation Model

Allogeneic heterotopic heart transplantation (HTx) was performed as previously described (18). Briefly, cardiac grafts from BALB/c donor mice were perfused with cold heparinized normal saline (4°C) and stored at 4°C for 10–15 min. The common carotid artery and the external jugular vein of C57BL/6 recipient mice were ligated. Then, the two vessels were everted onto two cuffs. Donor ascending aorta and pulmonary artery were anastomosed end-to-end to the recipient's common carotid artery and external jugular vein. The graft function was evaluated daily by observation of donor heartbeat palpitation. Graft rejection was defined as complete cessation of the heartbeat.

Recipient mice were divided into four groups (1): syngeneic control group, mice transplanted with isografts (C57BL/6 to C57BL/6); (2) allogeneic HTx group, mice transplanted with allografts (BALB/c to C57BL/6); (3) WT M-MDSC

TABLE 1 | Genotyping primer list.

Primers' name	Primers' sequence
Lyz-common	CTTGGGCTGCCAGAATTTCTC
Lyz-mutant	CCCAGAAATGCCAGATTACG
Lyz-wt	TTACAGTCGGCCAGGCTGAC
mTOR mutant	TCGTGGTATCGTTATGCGCC
mTOR common	CAGCCCCTTGGTTCTCTGTC
mTOR wt	ACAAGGCTCATGCCCATTTC

For genotyping mTOR-flox mouse, we used mTOR-common as forward primer, and both mTOR-wt and mTOR-mutant as reversed primers. If mTOR was not knocked out, the primer pair mTOR-common and mTOR-wt will work and amplifying DNA band at desired size, while the primer pair mTOR-common and mTOR-mutant did not work. If mTOR was knocked out, the primer pair mTOR-common and mTOR-mutant will work and amplifying DNA band at desired size, while the primer pair mTOR-common and mTOR-wt did not work. The genotyping Lyz-Cre mouse was constructed by using the same way.

group,allogeneic HTx mice treated with WT MDSCs; and (4) mTOR$^{-/-}$ M-MDSC group, allogeneic HTx mice treated with mTOR$^{-/-}$ MDSCs. Recipient mice from MDSC treatment groups were intravenously treated with 5×10^5 of MDSCs through the tail vein 1 day prior to HTx.

Primary MDSC Culture

The generation of BM-derived MDSCs was performed as previously described (13). Briefly, BM was flushed from femurs and tibias with phosphate-buffered saline (PBS). Red blood cells were lysed with lysis buffer (BD Biosciences, Franklin Lakes, NJ, USA). Then, cells were incubated in dishes for 2 h and non-adherent cells were collected and cultured with 50 ng/ml of GM-CSF and 50 ng/ml of IL-6 in RPMI 1640 medium with 10% fetal bovine serum, 1% MEM non-essential amino acid solution, 1% sodium pyruvate, 1% penicillin–streptomycin–glutamine (all from Gibco, NY, USA), and 2 μl of 2-mercaptoethanol (Sigma-Aldrich, St. Louis, MO, USA) for 7 days at 37°C and 5% CO_2.

Flow Cytometry and Cell Sorting

To analyze MDSCs, single-cell suspensions were prepared from peripheral blood, spleens, and hearts. Collected cells were labeled with CD11b (PerCp-cy5.5), Ly6C (FITC), and Ly6G (all from eBioscience, San Diego, CA, USA) and analyzed on BD FACSAria™ II (BD Biosciences). Cell sorting was performed on BD FACSAria™ III Cell Sorter (BD Biosciences).

CFSE T Cell Proliferation Assays

$CD4^+$ T cells were magnetically purified from spleens of WT C57BL/6 mice in accordance with the manufacturer recommendations (Miltenyi Biotec, Auburn, CA, USA). Then, $CD4^+$ T cells were stimulated with concanavalin A (ConA; 50 μg/ml; Sigma-Aldrich) and labeled with CFSE (2.5 μM; Invitrogen, USA). A total of 1×10^5 CFSE-labeled $CD4^+$ T cells were co-cultured with G-MDSCs or M-MDSCs at a ratio of 1:1, 2:1, or 4:1 in 96-well round bottom plates. After 3 days, the CFSE signal of gated $CD4^+$ T cells was analyzed by flow cytometry on BD FACSAria™ II (BD Biosciences).

Histological and Immunohistochemical Analysis

Heart specimens were fixed in 10% formalin, embedded in paraffin, and cut into 5-μm sections. Then, sections were deparaffinized and stained with hematoxylin and eosin (H&E) at room temperature. For immunohistochemical staining, sections from heart specimens were incubated with the primary antibody against mTOR and then labeled with fluorescence-conjugated secondary antibodies. Sections were then washed, dried, sealed, and examined under a microscope (Leica, Wetzlar, Germany).

Quantitative Real-Time PCR

Total RNA was extracted from cells and was subsequently reverse-transcribed using Superscript II reverse transcriptase and random primer oligonucleotides (Vazyme Biotech Co., Ltd., Nanjing, China). Quantitative real-time PCR was performed using HieffTM qPCR SYBR Green Master Mix (Yeasen, Shanghai, China) on an ABI Prism 7900HT (Applied Biosystems, Foster City, CA, USA). The thermocycler conditions included a 2-min incubation at 50°C, followed by an incubation at 95°C for 10 min. This was followed by a two-step PCR program as follows: 15 s at 95°C and 60 s at 60°C for 40 cycles. GAPDH was used as an internal control to normalize the differences in the amount of total RNA in each sample. The primers for the genes of interest were as follows (5′–3′): mTOR, CAG TTC GCC AGT GGA CTG AAG and GCT GGT CAT AGA AGC GAG TAG AC; GAPDH, AGG TCG GTG TGA ACG GAT TTG and TGT AGA CCA TGT AGT TGA GGT CA.

Western Blotting

For western blotting analyses, MDSCs sorted using flow cytometry were washed with cold PBS and lysed in RIPA buffer (Sigma-Aldrich) on ice for 30 min. Lysates were centrifuged at 15,000×*g* for 10 min at 4°C. A total of 40 μg of cell protein were separated by sodium dodecyl sulfate-10% polyacrylamide gel electrophoresis and transferred to a nitrocellulose membrane (Millipore, Tullagreen, Ireland). After blocking with TBS and 2% milk for 1 h at room temperature, membranes were incubated overnight at 4°C with the following diluted primary antibodies: Beclin1, Atg5, Atg7, LC3I/II, and β-actin (all from CST, Danvers, MA, USA; dilution: 1:1,000). After extensive washing, membranes were incubated for 1 h at room temperature with the corresponding HRP-coupled secondary antibodies. Immunoreactive proteins were visualized using an ECL reagent.

Enzyme-Linked Immunosorbent Assay (ELISA)

Serum samples were isolated by centrifuging blood at 1,000×*g* for 10 min at 4°C. The samples were diluted nine times with PBS (pH 7.4). A total of 40 μl of diluted serum sample were placed in each well of the 96-well plate coated with the following antibodies: IL-1β, IFN-γ, TNF-α, and IL-1β. The plate was then incubated with 100 μl of HRP-labeled antibodies for 60 min at 37°C. The reactions were then stopped and the OD values at 450 nm were recorded.

Electron Microscopy

For electron microscopy analyses, MDSCs were fixed in 2% PFA and 2.5% glutaraldehyde in 0.1 M sodium cacodylate buffer (Sigma-Aldrich; pH 7.4) for 2 h on ice. After three washes with 0.1 M PBS at pH 7.4, the cells were fixed with 1% osmium tetroxide in 0.1 M PBS at pH 7.4 for 2 h. The cells were then dehydrated and embedded in Epon resin following a standard procedure as previously described. Subsequently, 70-nm sections were obtained using an UC7 ultramicrotome (Leica) and stained with uranyl acetate and lead citrate. Cell sections were analyzed using an electron microscope.

RNA Sequencing and Bioinformatics Analysis

WT and mTOR$^{-/-}$ M-MDSCs were obtained from WT and Lyz-mTOR mice (n = 3). Total RNA samples were isolated using TRIzol

(Sigma-Aldrich). RNA quality was determined using the ratios of A260/A280 with a Nanodrop 2000 spectrophotometer (Thermo Fisher Scientific, Waltham, MA, USA). RNA samples were further tested using an Agilent 2100 Bioanalyzer (Agilent Technologies, USA). Samples with RIN>7 were selected for sequencing library construction using the (Illumina, USA). The final library was sequenced using an Illumina Novaseq 6000 sequencer. On average, about 20 million 150-bp paired end reads were generated per sample. The raw reads were aligned to the mouse reference genome (version mm10) using Bowtie2 RNASeq alignment software. Then, HTSeq was used to generate read counts for every gene. The read counts were normalized using DESeq2. Subsequently, the normalized read counts were centered and scaled for each gene, generating z-scores (**Table 2**). A Benjamini–Hochberg corrected p-value of <0.05 and fold-change of at least 2 were considered significant. Gene ontology (GO) and Kyoto Encyclopedia of Genes and Genomes (KEGG) analyses were performed using OmicsBean software.

Statistical Analysis

Data were analyzed using GraphPad Software (GraphPad Holdings, San Diego, CA, USA). Student's *t*-test was used to analyze the differences between two groups. One-way ANOVA was used to analyze whether an overall statistically significant change existed using a two-tailed paired or unpaired Student's *t* test. All analyses were performed at least three times independently and results were expressed as the mean ± SD. A p-value of <0.05 was considered statistically significant.

RESULTS

The mTOR Deficiency Enhances Endogenous MDSC Differentiation and the Immunosuppressive Function

After verifying the depletion of mTOR in MDSCs (**Supplementary Figure 1**), we investigated whether mTOR deficiency had an effect on MDSC differentiation and function, spleen- and heart-derived MDSC populations were detected in WT and Lyz-mTOR mice. Flow cytometry analysis showed that heart and spleen CD11b$^+$ cell populations from Lyz-mTOR mice were significantly increased (**Figure 1A**). The mTOR deficiency also increased the percentage of M-MDSCs, but decreased the G-MDSC ratio (**Figure 1B**). Moreover, M-MDSCs from Lyz-mTOR mice showed a stronger immunosuppressive function in inhibiting CD4$^+$ T cell proliferation than M-MDSCs from WT mice (**Figures 1C, D**). These results suggested that mTOR deficiency enhanced M-MDSC proliferation and the immunosuppressive function *in vivo*.

TABLE 2 | Raw data size.

Libraries' name	Raw bases (G)	Raw reads (M)
L-M1	5.74	19.13
L-M2	6.02	20.07
L-M3	6.40	21.33
WT1	6.43	21.43
WT2	6.76	22.53
WT3	6.30	21.00

1 M raw reads = 0.3 G raw bases.

The mTOR Deficiency Promotes M-MDSC Proliferation and Immunosuppressive Function *In Vitro*

To confirm whether mTOR deficiency has an influence on BM-induced MDSC differentiation and immunosuppressive function *in vitro*, BM samples from WT and Lyz-mTOR mice were harvested for MDSC induction. Flow cytometry analysis indicated that mTOR deficiency dramatically increased the percentage of CD11b$^+$ cells (**Figure 2A**) and M-MDSCs, but decreased the G-MDSC ratio (**Figure 2B**) in BM from Lyz-mTOR mice. To determine the role of mTOR in immunosuppressive function of MDSCs, T cell proliferation was elicited using ConA with or without BM-derived MDSC*** from WT and Lyz-mTOR mice. Both mTOR$^{-/-}$ G-MDSCs and M-MDSCs markedly inhibited the proliferative response of CD4$^+$ T cells in a dose-dependent manner (**Figures 2C, D**). According to these results, mTOR deficiency shifted the differentiation from G-MDSCs towards M-MDSCs and significantly enhanced the immunosuppressive function of BM-derived G-MDSCs and M-MDSCs *in vitro*.

The mTOR Deficiency Enhances Intracellular M-MDSC Autophagy Levels

Next, autophagy levels in endogenous and BM-induced M-MDSCs were detected. M-MDSCs from the spleens of WT and Lyz-mTOR mice were harvested and intracellular autophagy-related proteins were examined. Western blot analysis showed that the expression of Beclin1, Atg5, Atg7, and LC3I/II was significantly increased in mTOR$^{-/-}$ M-MDSCs (**Figure 3A**). Accordingly, similar results for the expression of intracellular autophagy-related proteins in BM-induced M-MDSCs with mTOR deficiency (**Figure 3B**) were obtained. Furthermore, electron microscopy was used to investigate the intracellular autophagy levels. More autophagic vacuoles were present in mTOR$^{-/-}$ M-MDSCs than in WT M-MDSCs (**Figure 3C**). This finding demonstrated that mTOR deficiency enhanced intracellular M-MDSC autophagy levels.

The mTOR$^{-/-}$ M-MDSCs Have the Potential to Reduce Allograft Rejection

RNA sequencing (RNAseq) was employed to investigate differentially expressed genes (DEGs) between WT and mTOR$^{-/-}$ M-MDSCs. Down-regulated genes were colored blue and up-regulated genes were colored red (**Figure 4A**). The volcano plot showed DEGs up- or down-regulated by mTOR deficiency (**Figure 4B**). GO enrichment analysis identified the main DEG functions, including T cell receptor binding (**Figure 4C**). Furthermore, DEG KEGG pathways showed that allograft rejection is involved in the KEGG pathways (**Figure 4D**), implying that mTOR$^{-/-}$ M-MDSCs might have a role in suppressing T cell activation and reducing rejection in organ transplantation.

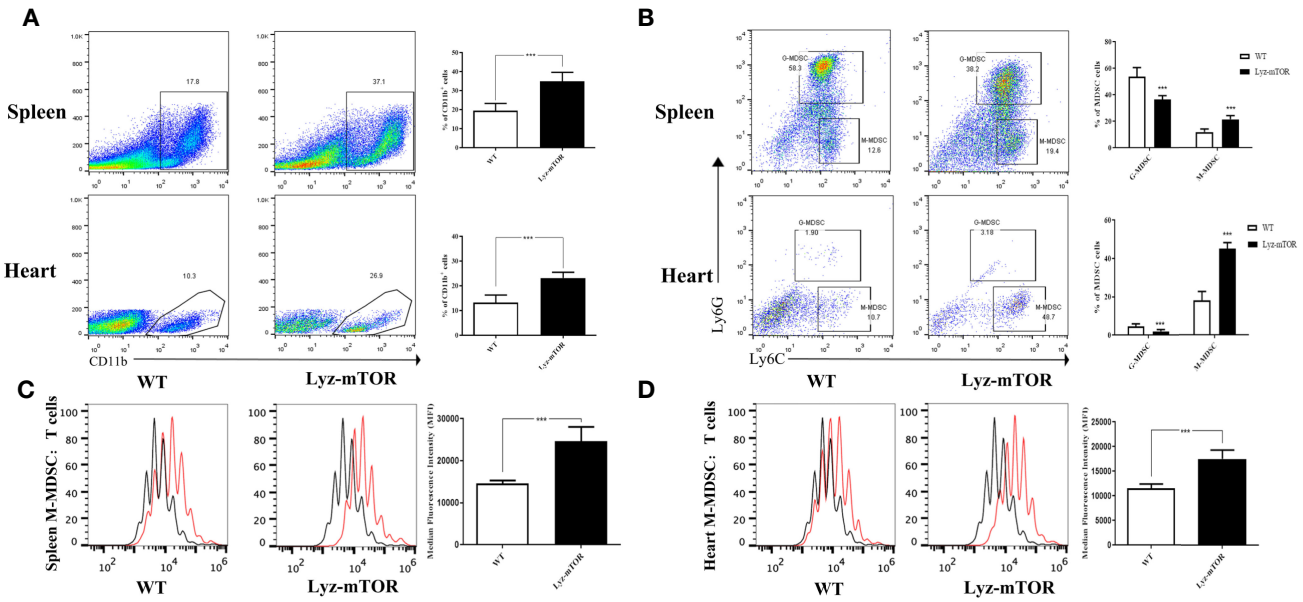

FIGURE 1 | Enhanced M-MDSC differentiation and immunosuppressive function in Lyz-mTOR mice. **(A)** Percentages of CD11b$^+$ cells in spleens and hearts from WT and Lyz-mTOR mice. **(B)** Percentages of G-MDSCs and M-MDSCs in spleens and hearts from WT and Lyz-mTOR mice. **(C, D)** CFSE-labeled T cell proliferation pattern was examined using flow cytometry analysis of CFSE dilution in gated CD4$^+$ T cells. CFSE MFI represents T cell proliferation, which reflects the immunosuppressive function of G-MDSCs and M-MDSCs in spleens and hearts from WT and Lyz-mTOR mice (n = 5 mice per group, ***P < 0.001).

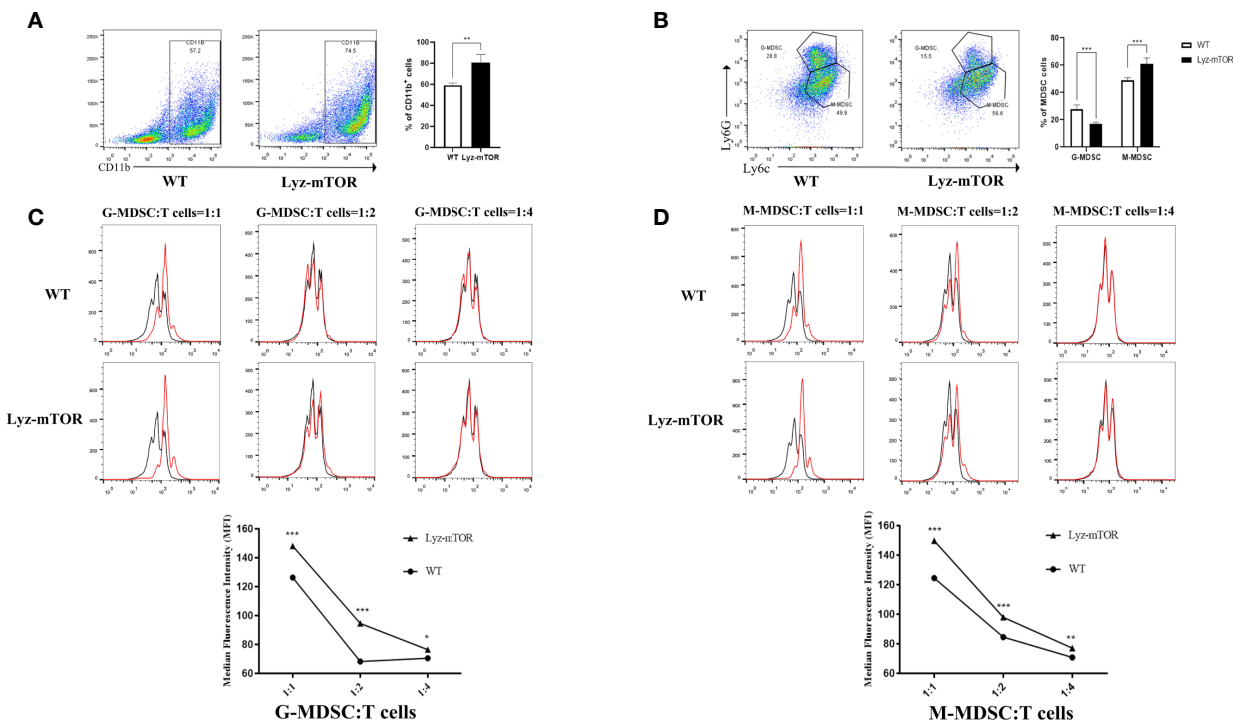

FIGURE 2 | Increased induced M-MDSC ratios and immunosuppressive functions in Lyz-mTOR mice. **(A)** Percentages of CD11b$^+$ cells from WT and Lyz-mTOR mouse BM. **(B)** Percentages of G-MDSCs and M-MDSCs from WT and Lyz-mTOR mice. **(C, D)** Induced G-MDSCs and M-MDSCs were co-cultured with T cells stimulated by ConA (G/M-MDSCs: T cells = 1:1, 1:2, and 1:4). CFSE-labeled T cell proliferation pattern was examined using flow cytometry analysis of CFSE dilution in gated CD4$^+$ T cells. G/M-MDSCs inhibitory curves were generated (n = 5, *P < 0.05, **P < 0.01, and ***P < 0.001).

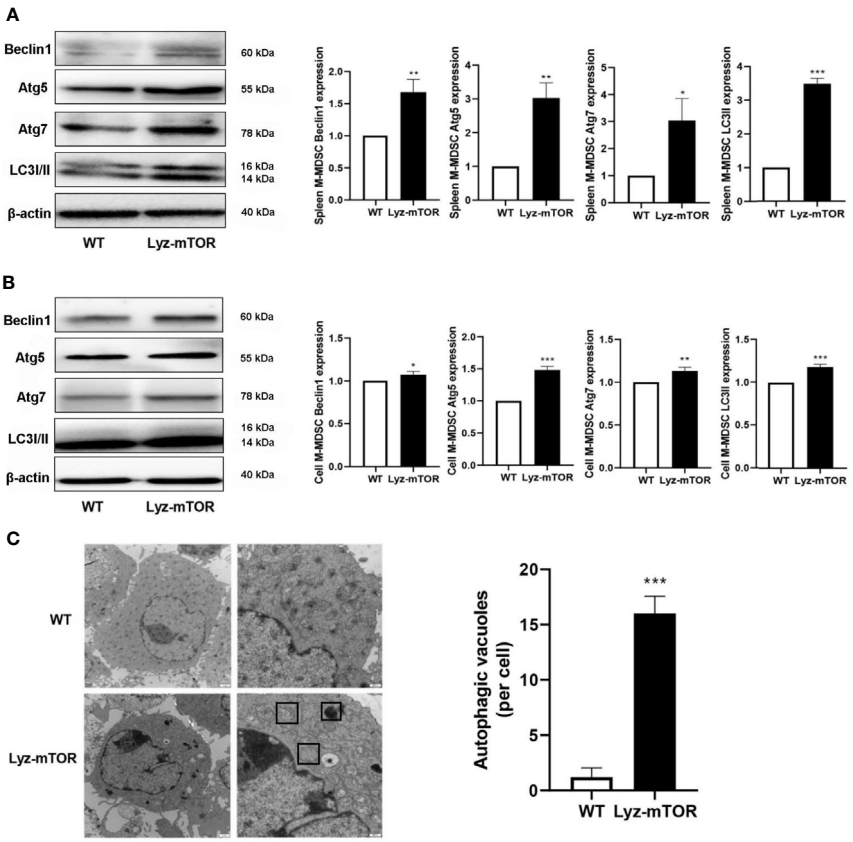

FIGURE 3 | Enhanced autophagy levels in M-MDSCs. **(A, B)** Spleen/induced M-MDSC intracellular autophagy-related proteins, such as Beclin1, Atg5, Atg7, and LC3I/II, were detected by western blot and normalized to β-actin. **(C)** Autophagic vacuoles were evaluated by electron microscopy (n = 5, *P < 0.05, **P < 0.01, and ***P < 0.001).

The mTOR$^{-/-}$ M-MDSC Significantly Prolongs Cardiac Allograft Survival

To verify the RNAseq results, BALB/c to B6 cervical cardiac transplantation mouse models were established with the infusion of WT or mTOR$^{-/-}$ M-MDSCs into the recipient mice. mTOR$^{-/-}$ M-MDSC treatment significantly extended cardiac allograft survival compared to WT M-MDSCs (**Figure 5A**). ELISA was then employed to examine the inflammatory cytokines in the recipient serum samples and found that IFN-γ, TNF-α, IL-6, and IL-1β levels were all markedly downregulated in allogeneic HTx mice treated with mTOR$^{-/-}$ M-MDSCs compared to the WT M-MDSC treatment (**Figure 5B**). In addition, H&E staining showed that mTOR$^{-/-}$ M-MDSCs improved inflammatory cell infiltration and tissue damage in the hearts of allogeneic HTx mice (**Figure 5C**). These results indicated that mTOR$^{-/-}$ M-MDSCs had a better potency in extending allograft survival, reducing inflammatory cytokines, and protecting tissues.

The mTOR$^{-/-}$ M-MDSC-Induced Immune Tolerance in HTx Mice

Recipient mouse T cell status was then measured to investigate the protective function of mTOR$^{-/-}$ M-MDSCs. Flow cytometry analysis demonstrated that the proportions of CD4$^+$ and CD8$^+$ T were decreased, while Treg populations were greatly increased in the peripheral blood, spleens, and hearts of mTOR$^{-/-}$ M-MDSC-treated HTx mice (**Figures 6A–C**). Similar results were observed by immunohistochemistry analysis (**Figure 6D**). Together, these results suggested that infusion of mTOR$^{-/-}$ M-MDSCs ameliorated T cell response and favor Tregs.

DISCUSSION

The mTOR is an evolutionary conserved serine-threonine kinase that senses various environmental stimuli in most cells primarily to control cell growth, cellular proliferation, and immunosuppressive function (19). In TME, mTOR activity in a subset of cells within the tumor mass can mediate MDSC accumulation (20). Welte et al. have found that oncogenic mTOR signaling recruits MDSCs to promote tumor initiation (21). Our previous study indicated that using rapamycin to inhibit the mTOR signaling pathway in MDSCs increases cell immunosuppressive function in AKI mouse models (13). However, whether mTOR regulates MDSCs in organ transplantations remains unclear. Thus, cervical cardiac transplantation models were used to investigate the

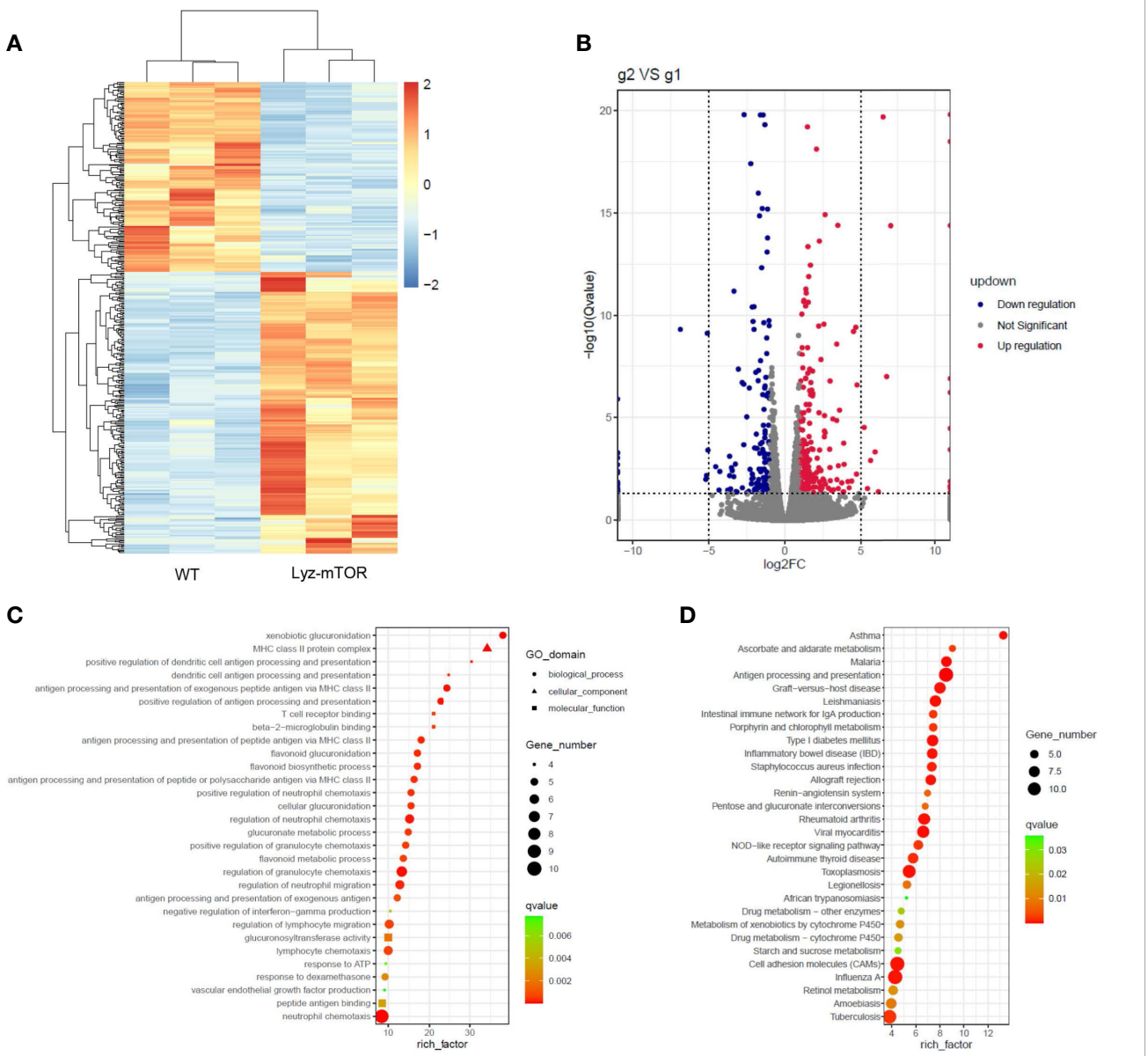

FIGURE 4 | RNAseq analysis of WT and mTOR$^{-/-}$ M-MDSCs: DEGS, GO enrichment, and KEGG pathway. **(A)** DEG heat map. **(B)** DEG volcano plot. **(C)** DEG GO enrichment analysis, including biological process, cellular component, and molecular function. **(D)** Main KEGG pathways (n = 3 per group).

function of mTOR-deficient M-MDSCs and to analyze mTOR regulation in MDSC proliferation and differentiation.

The present study used lyz-Cre-mTOR-flox mice to reveal the function of mTOR deficiency in myeloid cells, in which cells from other sources could still synthesize mTOR. The mTOR deficiency increased the proportion of endogenous M-MDSCs, while decreasing G-MDSCs in the spleens and hearts of Lyz-mTOR mice. Because G-MDSCs are considered to be immature MDSCs (1), it seems that mTOR deletion may have a role in promoting G-MDSC differentiation to M-MDSCs. Research also indicates that mTOR deficiency may result in more recruitment of myeloid-derived cells into organs. Results were similar to those in the present study in rapamycin-treated mice, as the total MDSC population in spleens was increased (12). In addition, spleen and heart M-MDSCs were isolated from WT and Lyz-mTOR mice and co-cultured with CFSE-labeled T cells to evaluate the immunosuppressive function of endogenous mTOR$^{-/-}$ M-MDSCs. Both M-MDSC sources had a stronger suppressive function in inhibiting T cell proliferation, indicating that mTOR deficiency enhanced the immunosuppressive function of M-MDSCs. Our results are consistent with another study, which demonstrated the increased number of M-MDSCs from spleens of rapamycin-treated HTx mice and enhanced immunosuppressive ability to inhibit CD4^{+} T cell proliferation (12). However, Wu et al.

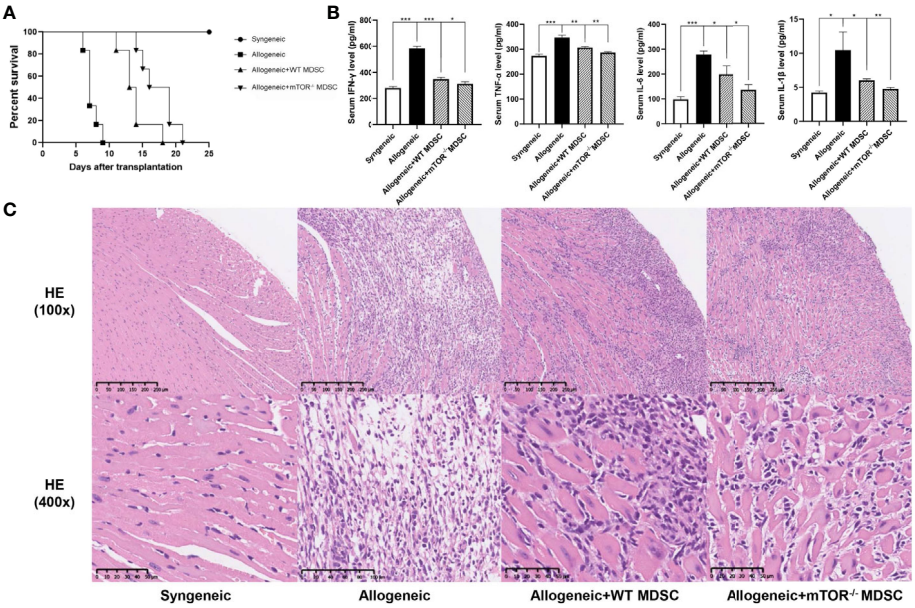

FIGURE 5 | Infusion of mTOR$^{-/-}$ M-MDSCs protected cardiac transplantation allografts. **(A)** Cardiac transplantation allograft survival rates. **(B)** ELISA analysis of IFN-γ, TNF-α, IL-6, and IL-1β in different groups. **(C)** H&E heart staining (n = 5, *P < 0.05, **P < 0.01, and ***P < 0.001).

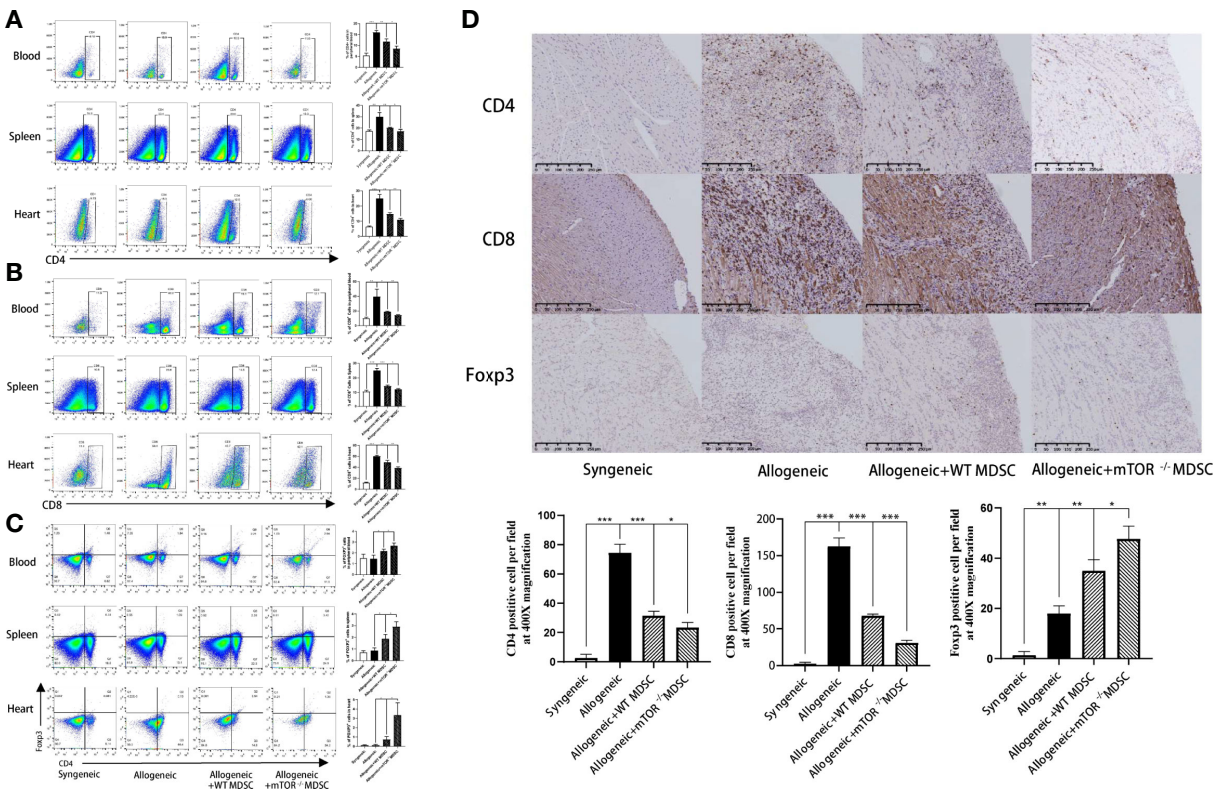

FIGURE 6 | Infusion of mTOR$^{-/-}$ M-MDSCs reduced CD4$^+$ and CD8$^+$ T cells and increased Tregs in blood, spleen, and heart. **(A)** Proportion of CD4$^+$, CD8$^+$ T cells, and Foxp3$^+$ Tregs in blood. **(B)** Proportion of CD4$^+$, CD8$^+$ T cells, and Foxp3$^+$ Tregs in spleen. **(C)** Proportion of CD4$^+$, CD8$^+$ T cells, and Foxp3$^+$ Tregs in heart. **(D)** CD4, CD8, and Foxp3 immunohistochemistry staining in cardiac allograft with semi-quantification analysis (400×; n = 5, *P < 0.05, **P < 0.01, and ***P < 0.001).

have reported a contradictory conclusion that inhibition of mTOR by rapamycin inhibited the number and function of M-MDSCs in the spleen of alloskin-grafted mice, although the proportion of M-MDSCs in alloskin was not investigated (16). The discrepancy in mTOR inhibition in M-MDSCs may depend on microenvironment specificity in different disease models. Sun et al. have demonstrated that M-MDSCs with a high expression of CCR9 became the predominant type after MDSCs accumulated in the endometrium, resulting in the inhibition of autologous T cell activity in an immunoinflammatory microenvironment (22). This study suggested that immune cell migration from lymphoid organs to target tissues may largely rely on the expression of surface chemokine receptors, which can be recruited by their chemokine ligand secreted in the microenvironment. Nevertheless, further study on MDSC function is still needed.

Inhibition of the amino acid-responsive mTOR kinase complex is a key signal for autophagosome biogenesis, primarily through activation of the ULK kinase complex that occurs in conjunction with that of the PIK3C3-BECN1-Atg14 complex (23). Tumor-infiltrating autophagy-deficient M-MDSCs demonstrated impaired suppressive activity *in vitro* and *in vivo*, whereas M-MDSCs exhibited impaired lysosomal degradation, thereby enhancing surface expression of MHC class II molecules and resulting in efficient activation of tumor-specific $CD4^+$ T cells (17). In addition, degradation of cytoplasmic components through starvation-induced autophagy regenerates amino acids that are used in the tricarboxylic acid cycle to produce energy that the cells need to survive, thus allowing them to avoid death (24). The present study found that the intracellular autophagy levels were up-regulated in mTOR-deficient M-MDSCs, which explained the enhanced cell differentiation and immunosuppressive function.

A previous study has demonstrated that using rapamycin in mouse cardiac transplantation models enhanced the proliferation of MDSCs, which prolonged allograft survival (12). However, the rapamycin action mechanism remains unclear. Thus, RNAseq was used to investigate the potential function of mTOR-deficient M-MDSCs. KEGG pathway analysis showed that induced M-MDSCs from Lyz-mTOR mice might have a role in preventing allograft rejection. Based on these analysis results, Lyz-mTOR mouse BM was used to induce $mTOR^{-/-}$ M-MDSCs, which were then infused into cardiac transplantation recipient mice. The results showed that $mTOR^{-/-}$ M-MDSCs did not only prolong allograft survival, but also reduced T cell infiltration and increased Treg populations in the allografts. However, the molecular mechanism involved in the prone differentiation of M-MDSCs with mTOR deficiency genetically remains unclear. Recently, Yo et al. have shown that a combined inhibition of glutamine metabolism and mTOR significantly suppressed $CD4^+$ T cell activation-mediated arthritis in mice better than each monotherapy, implying the essential role of cellular metabolism in immune cell mTOR signaling (25). Another study reported that inhibition of mTOR activity by SIRT1- and HIF-1α-associated metabolism participated in regulating the differentiation and function of Th9 cells (26). Both studies focusing on cellular metabolism are concordant with our data analyzed by RNAseq to some extent, showing that retinol, ascorbate, and aldarate metabolism might be involved in mTOR-mediated MDSC differentiation. The exact mechanism requires further verification and study.

In conclusion, the present study found that mTOR deficiency enhanced the immunosuppressive function of M-MDSCs both *in vitro* and *in vivo*, which might be correlated with the increased levels of intracellular autophagy. In addition, mTOR-deficient M-MDSCs prolonged cardiac allograft survival and induced immune tolerance by increasing Treg population. These findings explained the function of mTOR in MDSCs, demonstrated that $mTOR^{-/-}$ M-MDSCs had a stronger immunosuppressive ability, and suggested that infusing with $mTOR^{-/-}$ M-MDSCs reduced allograft rejection and induce immune tolerance. These results might be of benefit for clinical translation of cell therapy in organ transplantation.

DATA AVAILABILITY STATEMENT

The datasets presented in this study can be found in online repositories. The name of the repository and accession number can be found below: National Center for Biotechnology Information (NCBI) Gene Expression Omnibus (GEO), https://www.ncbi.nlm.nih.gov/geo/, GSE167594.

ETHICS STATEMENT

The animal study was reviewed and approved by Animal Ethical Committee of Zhongshan Hospital, Fudan University.

AUTHOR CONTRIBUTIONS

YZ and RR conceived the project, designed the project and approved the final manuscript. JWL drafted the manuscript. JWL, JC, MZ, CZ, YQ and JJL conducted the experiments. RW and TY analyzed RNAseq data. All authors contributed to the article and approved the submitted version.

FUNDING

This work was supported by the National Key R&D Program of China (2018YFA0107501 to RR), National Natural Science Foundation of China (81400688 to YZ, 81770747 and 81970646 to RR).

SUPPLEMENTARY MATERIAL

The Supplementary Material for this article can be found online at: https://www.frontiersin.org/articles/10.3389/fimmu.2021.661338/full#supplementary-material

Supplementary Figure 1 | The expression of mTOR in M-MDSCs induced from BM of WT and Lyz-mTOR mice in mRNA level.

REFERENCES

1. Veglia F, Perego M, Gabrilovich D. Myeloid-derived suppressor cells coming of age. *Nat Immunol* (2018) 19(2):108–19. doi: 10.1038/s41590-017-0022-x
2. Gabrilovich DI. Myeloid-derived suppressor cells. *Cancer Immunol Res* (2017) 5(1):3–8. doi: 10.1158/2326-6066.CIR-16-0297
3. Kumar V, Patel S, Tcyganov E, Gabrilovich DI. The nature of myeloid-derived suppressor cells in the tumor microenvironment. *Trends Immunol* (2016) 37 (3):208–20. doi: 10.1016/j.it.2016.01.004
4. Condamine T, Ramachandran I, Youn JI, Gabrilovich DI. Regulation of tumor metastasis by myeloid-derived suppressor cells. *Annu Rev Med* (2015) 66:97–110. doi: 10.1146/annurev-med-051013-052304
5. Parker KH, Beury DW, Ostrand-Rosenberg S. Myeloid-derived suppressor cells: Critical cells driving immune suppression in the tumor microenvironment. *Adv Cancer Res* (2015) 128:95–139. doi: 10.1016/bs.acr.2015.04.002
6. Li J, Li L, Wang S, Zhang C, Zheng L, Jia Y, et al. Resveratrol alleviates inflammatory responses and oxidative stress in rat kidney ischemia-reperfusion injury and H2O2-induced NRK-52E cells via the Nrf2/TLR4/NF-kappaB pathway. *Cell Physiol Biochem Int J Exp Cell Physiol Biochem Pharmacol* (2018) 45(4):1677–89. doi: 10.1159/000487735
7. Yang Y, Li C, Liu T, Dai X, Bazhin AV. Myeloid-derived suppressor cells in tumors: From mechanisms to antigen specificity and microenvironmental regulation. *Front Immunol* (2020) 11:1371. doi: 10.3389/fimmu.2020.01371
8. Zhao Y, Shen XF, Cao K, Ding J, Kang X, Guan WX, et al. Dexamethasone-induced myeloid-derived suppressor cells prolong allo cardiac graft survival through iNOS- and glucocorticoid receptor-dependent mechanism. *Front Immunol* (2018) 9:282. doi: 10.3389/fimmu.2018.00282
9. Blazar BR, MacDonald KPA, Hill GR. Immune regulatory cell infusion for graft-versus-host disease prevention and therapy. *Blood* (2018) 131(24):2651–60. doi: 10.1182/blood-2017-11-785865
10. Yang F, Li Y, Wu T, Na N, Zhao Y, Li W, et al. TNFalpha-induced M-MDSCs promote transplant immune tolerance via nitric oxide. *J Mol Med (Berl)* (2016) 94(8):911–20. doi: 10.1007/s00109-016-1398-z
11. Han C, Wu T, Na N, Zhao Y, Li W, Zhao Y. The effect of immunosuppressive drug cyclosporine A on myeloid-derived suppressor cells in transplanted mice. *Inflammation Res* (2016) 65(9):679–88. doi: 10.1007/s00011-016-0949-7
12. Nakamura T, Nakao T, Yoshimura N, Ashihara E. Rapamycin prolongs cardiac allograft survival in a mouse model by inducing myeloid-derived suppressor cells. *Am J Transplant* (2015) 15(9):2364–77. doi: 10.1111/ajt.13276
13. Zhang C, Wang S, Li J, Zhang W, Zheng L, Yang C, et al. The mTOR signal regulates myeloid-derived suppressor cells differentiation and immunosuppressive function in acute kidney injury. *Cell Death Dis* (2017) 8(3):e2695. doi: 10.1038/cddis.2017.86
14. Klionsky DJ, Abdelmohsen K, Abe A, Abedin MJ, Abeliovich H, Acevedo Arozena A, et al. Guidelines for the use and interpretation of assays for monitoring autophagy (3rd edition). *Autophagy* (2016) 12(1):1–222. doi: 10.1080/15548627.2015.1100356
15. Parker KH, Horn LA, Ostrand-Rosenberg S. High-mobility group box protein 1 promotes the survival of myeloid-derived suppressor cells by inducing autophagy. *J Leukoc Biol* (2016) 100(3):463–70. doi: 10.1189/jlb.3HI0715-305R
16. Wu T, Zhao Y, Wang H, Li Y, Shao L, Wang R, et al. mTOR masters monocytic myeloid-derived suppressor cells in mice with allografts or tumors. *Sci Rep* (2016) 6:20250. doi: 10.1038/srep20250
17. Alissafi T, Hatzioannou A, Mintzas K, Barouni RM, Banos A, Sormendi S, et al. Autophagy orchestrates the regulatory program of tumor-associated myeloid-derived suppressor cells. *J Clin Invest* (2018) 128(9):3840–52. doi: 10.1172/JCI120888
18. Chen J, Miao X, Liu C, Liu B, Wu X, Kong D, et al. BET protein inhibition prolongs cardiac transplant survival via enhanced myocardial autophagy. *Transplantation* (2020) 104(11):2317–26. doi: 10.1097/TP.0000000000003319
19. Saemann MD, Haidinger M, Hecking M, Horl WH, Weichhart T. The multifunctional role of mTOR in innate immunity: implications for transplant immunity. *Am J Transplant* (2009) 9(12):2655–61. doi: 10.1111/j.1600-6143.2009.02832.x
20. Guri Y, Nordmann TM, Roszik J. mTOR at the transmitting and receiving ends in tumor immunity. *Front Immunol* (2018) 9:578:578. doi: 10.3389/fimmu.2018.00578
21. Welte T, Kim IS, Tian L, Gao X, Wang H, Li J, et al. Oncogenic mTOR signalling recruits myeloid-derived suppressor cells to promote tumour initiation. *Nat Cell Biol* (2016) 18(6):632–44. doi: 10.1038/ncb3355
22. Sun Y, Shao J, Jiang F, Wang Y, Yan Q, Yu N, et al. CD33(+) CD14(+) CD11b (+) HLA-DR(-) monocytic myeloid-derived suppressor cells recruited and activated by CCR9/CCL25 are crucial for the pathogenic progression of endometriosis. *Am J Reprod Immunol* (2019) 81(1):e13067. doi: 10.1111/aji.13067
23. Munson MJ, Ganley IG. MTOR, PIK3C3, and autophagy: Signaling the beginning from the end. *Autophagy* (2015) 11(12):2375–6. doi: 10.1080/15548627.2015.1106668
24. Lum JJ, Bauer DE, Kong M, Harris MH, Li C, Lindsten T, et al. Growth factor regulation of autophagy and cell survival in the absence of apoptosis. *Cell* (2005) 120(2):237–48. doi: 10.1016/j.cell.2004.11.046
25. Ueda Y, Saegusa J, Okano T, Sendo S, Yamada H, Nishimura K, et al. Additive effects of inhibiting both mTOR and glutamine metabolism on the arthritis in SKG mice. *Sci Rep* (2019) 9(1):6374. doi: 10.1038/s41598-019-42932-1
26. Yu Q, Dong L, Li Y, Liu G. SIRT1 and HIF1alpha signaling in metabolism and immune responses. *Cancer Lett* (2018) 418:20–6. doi: 10.1016/j.canlet.2017.12.035

Conflict of Interest: The authors declare that the research was conducted in the absence of any commercial or financial relationships that could be construed as a potential conflict of interest.

frontiers in Immunology

ORIGINAL RESEARCH
published: 09 April 2021
doi: 10.3389/fimmu.2021.661911

PSMP Is Discriminative for Chronic Active Antibody-Mediated Rejection and Associate With Intimal Arteritis in Kidney Transplantation

*Panpan Zhan[1,2,3], Haizheng Li[4], Mingzhe Han[5], Zhen Wang[1], Jie Zhao[1], Jinpeng Tu[1], Xiaofeng Shi[1] and Yingxin Fu[1,2,3]**

[1] Department of Kidney Transplantation, Tianjin First Central Hospital, School of Medicine, Nankai University, Tianjin, China, [2] Department of Kidney Transplantation and Kidney Transplantation Research Laboratory, Tianjin First Central Hospital, Tianjin, China, [3] Key Laboratory of Transplantation, Chinese Academy of Medical Sciences, Tianjin, China, [4] First Central Clinical College of Tianjin Medical University, Tianjin, China, [5] Institute of Hematology & Blood Diseases Hospital, State Key Laboratory of Experimental Hematology, National Clinical Research Center for Blood Diseases, Chinese Academy of Medical Sciences & Peking Union Medical College, Tianjin, China

OPEN ACCESS

Edited by:
Hao Wang,
Tianjin Medical University General Hospital, China

Reviewed by:
Xiaopeng Hu,
Capital Medical University, China
Qiquan Sun,
Third Affiliated Hospital of Sun Yat-sen University, China

***Correspondence:**
Yingxin Fu
fuyingxintj@163.com

Specialty section:
This article was submitted to Alloimmunity and Transplantation, a section of the journal Frontiers in Immunology

Received: 31 January 2021
Accepted: 08 March 2021
Published: 09 April 2021

Citation:
Zhan P, Li H, Han M, Wang Z, Zhao J, Tu J, Shi X and Fu Y (2021) PSMP Is Discriminative for Chronic Active Antibody-Mediated Rejection and Associate With Intimal Arteritis in Kidney Transplantation. Front. Immunol. 12:661911. doi: 10.3389/fimmu.2021.661911

Chronic active antibody-mediated rejection (CAAMR) is an intermediate process that occurs during the development of chronic antibody-mediated rejection (CAMR), which is a key problem associated with the long-term kidney grafts survival. This study investigated the role played by PC3-secreted microprotein (PSMP) in the progression of CAAMR and CAMR. We showed that CAAMR and CAMR patients' allografts dysfunction with declined survival rate, which suggested that earlier diagnosis and treatment of CAAMR might be important to prevent irreversible chronic injury of CAMR progression. We found PSMP was an important factor in the development of chronic antibody-mediated rejection. The PSMP expression increased significantly in CAAMR biopsy samples but not in CAMR and control patients, which distinguished CAAMR patients from CAMR and non-rejection patients. Moreover, our results showed that infiltration of $CD68^+$ macrophages in CAAMR increased, and the correlation between $CD68^+$ macrophages and PSMP expression in CAAMR patients was significant. Additionally, our data also revealed that intimal arteritis (v-lesion) accompanied by increased macrophage infiltration might have contributed to more graft loss in CAAMR, and PSMP expression was significantly associated with the v-lesion score. These results indicated that PSMP played an important role in the recruitment of macrophages and promote intimal arteritis inducing allograft lost in CAAMR progression. In future study PSMP could be a potential histopathological diagnostic biomarker and treatment target for CAAMR in kidney transplantation.

Keywords: kidney transplantation, chronic active antibody-mediated rejection, PC3-secreted microprotein, macrophages, intimal arteritis

INTRODUCTION

Chronic active antibody-mediated rejection (CAAMR) is an intermediate process that occurs during the development of chronic antibody-mediated rejection (CAMR), which has been recognized recently. CAAMR leads to the gradual loss of allograft, becoming an obstacle to the long-term survival of renal allografts (1). Significant improvements in short-term renal graft survival have been achieved in recent decades due to the continuous updating of immunosuppressive agents, such as calcineurin inhibitors, which greatly reduce the occurrence of T cell-mediated rejection (TCMR) (2). However, long-term renal allograft loss caused by CAAMR has no significant improvements without effective therapeutic drugs (3, 4). Although the diagnostic criteria for CAAMR were defined in the revised Banff 2017 criteria (5, 6), many morphological lesions associated with CAAMR and CAMR appear similar and it's difficult to distinguish this two phases in clinic clearly. Moreover, it's lacking specific molecular pathological biomarkers available for expressing the intermediate injury from CAAMR progress to CAMR (7).

Increasing attention has been paid to macrophage graft infiltration in the immunopathological characteristics of chronic allotransplantation rejection (8). Macrophages are a type of innate immune cell that participate in adaptive immunity through antigen presentation, co-stimulation, tissue repair, and the production of pro-inflammatory cytokines. Macrophages may be recruited to the rejection site, augmenting the immune response and promoting the renal glomeruli and tubules injury. The persistent inflammation mediated by macrophages may lead to fibrosis and chronic rejection in renal allograft (9). Macrophage infiltration one year after transplantation has been demonstrated to be associated with graft dysfunction and fibrosis (10). The evidence shows that $CD68^+CD163^+$ macrophages tend to increase in CAAMR compared with acute antibody-mediated rejection (ABMR) and TCMR (11, 12), which may promote the chronic progressive injury. Macrophages found in renal allografts can include resident macrophages from donor tissues and blood-derived macrophages from recipients. However, recent studies have shown that macrophages associated with chronic rejection are primarily derived from renal transplant recipients (13). Peripheral circulating macrophages can be recruited into grafts by a variety of chemokines. PC3-secreted microprotein (PSMP) is a newly identified chemokine found in the PC3 cell line and malignant prostate tumors (13). PSMP has a similar affinity for C-C motif chemokine receptor 2 (CCR2) as that of C-C motif chemokine ligand 2 (CCL2). PSMP can recruit monocytes from the peripheral blood through interactions with CCR2, mediating macrophage infiltration in tissue. Recent studies have shown that PSMP plays an important role in liver fibrosis in humans and mice. PSMP promotes the infiltration and polarization of inflammatory macrophages which cause liver fibrosis through interactions with CCR2. The administration of a PSMP neutralizing antibody can significantly improve liver fibrosis in mice (14), indicating that PSMP plays a key role in the pathogenesis of inflammation-related diseases.

In this study, we explored the roles played by PSMP in the progression of CAAMR and CAMR. We showed that the expression of PSMP was significantly increased in CAAMR patients but not in CAMR patients, suggesting that PSMP represent a significant discriminative marker between CAAMR and CAMR patients. A significant correlation was found between PSMP expression and $CD68^+$ macrophages infiltration in CAAMR patients, and PSMP expression levels were significantly associated with intimal arteritis, which indicated that PSMP might play an important role in CAAMR.

MATERIALS AND METHODS

Study Population and Samples

We retrospective studied 312 patients who underwent kidney biopsy between July 2017 and October 2020 in Tianjin First Central Hospital. We selected 198 biopsies with an original diagnose of rejection, 20 biopsies were re-evaluated and defined as CAAMR, 8 biopsies were defined as CAMR according to the 2017 revised Banff criteria (15). In 114 subjects without rejection, 12 patients diagnosed with non-specific lesions or mild drug-induced injuries were defined as Control. We excluded 1 subject with incomplete formalin-fixed paraffin-embedded (FFPE) slides and 5 subjects with incomplete central pathology data, resulting in the inclusion of 34 subjects (10 Control, 17 CAAMR, 7 CAMR) in the final analysis (**Figure 1**). The sample size was set to 6 for feasibility reasons in each group. Assuming an effect size of about 1.6 and provide 80% power using Tukey's test, two-sided significance level of 0.05. Urine and blood samples were collected at the time of the biopsy. All patients underwent ABO-compatible renal transplantations, and biopsies were obtained from all patients for clinical surveillance due to elevated creatinine or proteinuria. The collection of human samples was approved by the Ethics Committee of Tianjin First Central Hospital and was performed according to the Declaration of Helsinki guidelines.

The diagnostic criteria of CAAMR follow the 2017 revised Banff criteria as follows (1): At least 1 AMR chronicity histologic features: – Banff Lesion Score cg > 0. – 7 or more layers in 1 cortical peritubular capillary (ptc) and 5 or more in 2 additional capillaries. – Arterial intimal fibrosis of new onset (2). At least 1 criterion of antibody interaction with tissue. –At least moderate MVI (g + ptc > 1) in the absence of glomerulonephritis. If suspicious (Borderline) for acute T cell-mediated rejection (TCMR), acute TCMR, or infection is present, Banff Lesion Score g>1 is required (3). At least 1 criterion of DSA or equivalents: – DSA positive (anti-HLA or other specificity). – Banff Lesion Score C4d > 1 (IF on fresh frozen tissue) or C4d > 0 (IHC on FPE tissue).

Immunohistochemistry

We used a PSMP polyclonal antibody [3D5, purified and provided by the Institute of Hematology and Blood Diseases Hospital, Chinese Academy of Medical Science, Beijing, China (16)] to detect the expression of PSMP in renal biopsies. In brief,

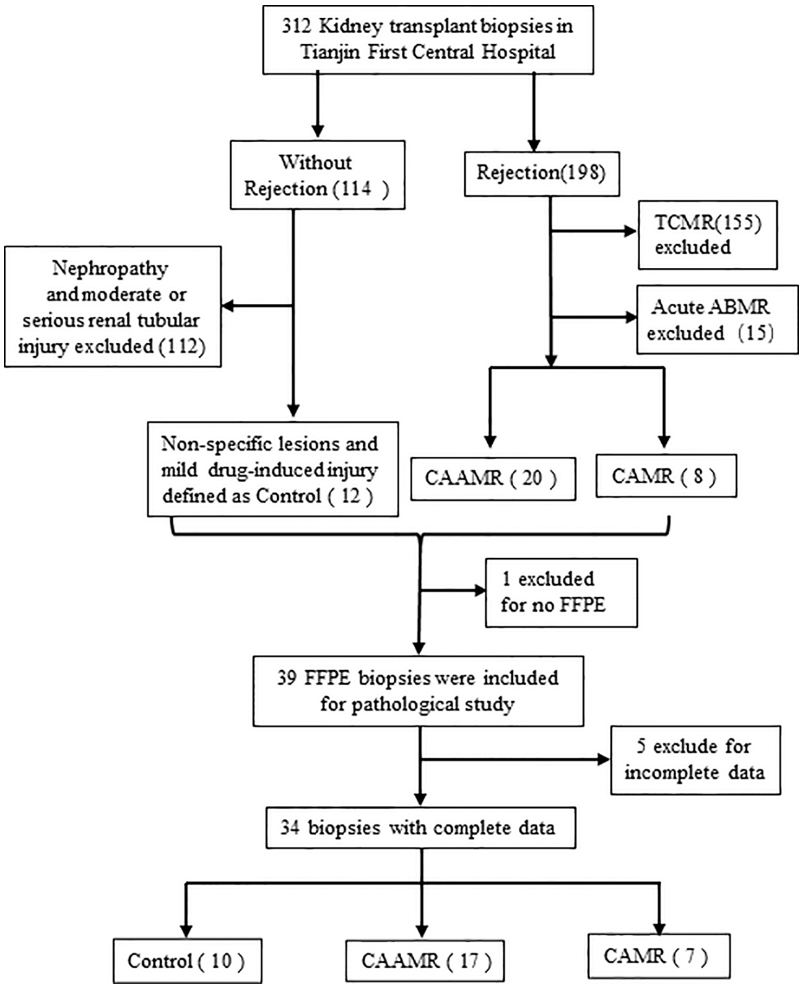

FIGURE 1 | Flow chart of biopsies inclusion and exclusions for the study. We collected 312 kidney biopsy and selected 198 biopsies with an original diagnose of rejection and 114 subjects without rejection. 20 biopsies were redefined as CAAMR and 8 biopsies were defined as CAMR by a central pathologist. In 114 subjects without rejection, 12 patients diagnosed with non-specific lesions or mild drug-induced injuries were defined as Control. We excluded 1 subject with incomplete FFPE slides and 5 subjects with incomplete central pathology data. TCMR, T cell-mediated rejection; ABMR, antibody-mediated rejection; FFPE, formalin-fixed paraffin-embedded.

the paraffin sections were dewaxed by baking for 90 min at 65°C and deparaffinized in xylene solutions and various alcohol concentrations (100%, 95%, and 75%). The sections were placed in a 3% hydrogen dioxide solution for 8 min and boiled with citrate buffer solution for 15 min. The sections were then blocked with serum for 0.5 h. The PSMP polyclonal antibody, anti-CD68 (1:100; ab125212, Abcam Inc., Cambridge, MA, USA), anti-CD163 (1:50, ZM-0428, Zhongshan Bridge, Beijing, China) were used as primary antibodies, and incubation was performed at 4°C overnight. A biotin-conjugated goat anti-mouse/rabbit IgG antibody (1:100, Zhongshan Bridge, Beijing, China) was used as the secondary antibody, and incubation was performed at 37°C for 30 min. The tissues were colored with diaminobenzidine (DAB) solution (Vector Laboratories, Inc., Burlingame, USA). A semi-quantitative assessment was conducted by Image-Pro Plus software (Image-Pro Plus 6.0, USA), the average positive cells number in at least 5 high-power field (HPF, 40×) or mean integrated optic density (IOD) was calculated.

RNA Isolation and Real-Time Polymerase Chain Reaction (RT-PCR)

RNA was isolated from biopsies using the Qiagen RNA microextraction kit (Qiagen, Valencia, CA), according to the manufacturer's instructions. RNA was reverse transcribed into cDNA using the cDNA synthesis kit (Invitrogen, Carlsbad, CA, USA) according to the manufacturer's instructions. The SYBR Premix RT-qPCR kits (Bio-Rad Laboratories, Hercules, CA) and Applied Biosystems GenAmp 7700 sequence detection system (Applied Biosystems, CA, USA) were used for the quantitative detection of mRNA levels. Glyceraldehyde 3-phosphate dehydrogenase (*GAPDH*) was employed as the normalization

control. The levels of relative gene expression were computed using the $2^{-\Delta\Delta Ct}$ approach. The following primers were used: *PSMP*, fw: 5'-CTGTGACACGGCTCAGCATC-3', rev: 5'-ATGGGCAAGCCTTTAGCTGG-3'; *GAPDH*, fw: 5'-AGGTCGGTGTGAACGGATTTG-3', rev: 5'-TGTAGACCATGTAGTTGAGGTCA-3'.

Cytokine Bead Assay

Microspheres (A37304, Life Technologies) coated with anti-rabbit polyclonal antibody were used as capture antibodies to detect the expression of PSMP in blood and urine as described (17). Gradient concentrations of PSMP monoclonal antibodies were used as detection antibodies, and phycoerythrin (PE)-labeled rabbit anti-mouse antibodies were used as secondary antibodies. The fluorescence intensity of microspheres was detected by flow cytometry, and analysis by logarithms. Finally, linear fitting was performed to obtain a standard curve, and the PSMP level was calculated in blood and urine samples.

Statistical Analysis

All data are processed by R3.6.2 statistical software. Normally distributed data are expressed as mean ± SD, comparison between groups using one-way analysis of variance (ANOVA) or 2-tailed Student's t-test. The nonnormally distributed data are expressed as median (interquartile range), comparison between groups using nonparametric Kruskal–Wallis test or nonparametric Mann–Whitney U test. Correlations between PSMP expression and other variables were analyzed by Pearson's correlation coefficient. Receiver operator characteristic (ROC) curve analysis was used to calculate the cut-off value for PSMP protein levels in renal biopsies and to assess the diagnostic ability of PSMP in CAAMR patients. Graft survival was analyzed by Kapla-Meier analysis, and survival curve was compared by Log-rank test. A value of $p \leq 0.05$ was considered significant. $*p \leq 0.05$, $**p \leq 0.01$, and $***p \leq 0.001$.

RESULTS

Patients' Baseline Characteristics

A total of 34 patients who underwent biopsy were selected and divided into three groups: Control (10/34), CAAMR (17/34), and CAMR (7/34). A comparison of the clinical characteristics among the three groups was summarized in **Table 1**. The CAAMR and CAMR groups presented positive anti-human leukocyte antigen (HLA) donor-specific antibodies (DSA) at the time of biopsy compared to Control group ($p < 0.05$), and 14 of 17 CAAMR patients were positive for anti-HLA class II antibody, as were 4 of 7 in CAMR patients. No significant

TABLE 1 | Patients Baseline Characteristics of kidney transplant patients.

Characteristics	Normal (n=10)	CAAMR (n=17)	CAMR (n=7)	p value
Age, year-mean ± SD	36.6 ± 14.49	44.78 ± 15.46	41.47 ± 14.09	0.68
Male sex- n (%)	8 (80%)	14(82.35%)	6 (85.71%)	0.99
Donor (relative)-n (%)	0 (0%)	1 (5.88%)	1 (14.29%)	0.52
Retransplantation-n (%)	0 (0%)	0 (0%)	1 (14.29%)	0.18
Time posttransplant to biopsy, days- Median (Q1-Q3)	606(545.75- 892.5)	606(614.75- 2051.5)	1932(735- 2099.5)	0.29
Biopsy times(n)	1.2 ± 0.4	1.35 ± 0.58	1.43 ± 0.49	0.66
Infections-n (%)	3 (30%)	5 (29.41%)	2 (28.57%)	0.99
Diabetic nephropathy, (%)	2 (20%)	6 (35.29%)	0 (0%)	0.3
Diabetes after transplantation-n (%)	1 (10%)	1 (5.88%)	1 (14.29%)	0.83
HLA mismatch-mean ± SD				
HLA A/B mismatch	3.33 ± 0.94	2.91 ± 0.95	2.71 ± 0.88	0.44
HLA DR mismatch	1.66 ± 0.47	1.75 ± 0.43	1.43 ± 0.73	0.49
cPRA(%)	66.2 ± 11.5	64.9 ± 13.6	64.6 ± 17.5	0.97
PRA pretransplantation	2 (20%)	2 (11.76%)	1 (14.29%)	0.88
Anti-HLA DSA at the time of biopsy-n (%)	0 (0%)	14(82.35%)	5 (71.43%)	0.03
Class I	0 (0%)	0 (0%)	1 (14.29%)	
Class II	0 (0%)	12 (70.59%)	4 (57.14%)	
Class I+II	0 (0%)	2 (11.76%)	0 (0%)	
Immunosuppressive therapy- n (%)				
CNI				0.71
FK-n (%)	8 (80%)	10 (58.82%)	6 (85.71%)	
CsA-n (%)	2 (20%)	6 (35.29%)	1(14.29%)	
Other-n (%)	0 (0%)	1(5.88%)	0 (0%)	
MMF				0.39
Mythology-n (%)	5 (50%)	9 (52.94%)	6 (85.71%)	
Myfortic-n (%)	5 (50%)	5 (29.41%)	0 (0%)	
Other-n (%)	0 (0%)	3 (17.65%)	1 (14.29%)	
Pred				
Prednisone-n (%)	10 (100%)	18 (100%)	7 (100%)	1
Allograft loss-n (%)	0	5 (29.41%)	3 (42.86%)	0.19

HLA, histocompatibility leukocyte antigen; cPRA, calculated panel reactive antibody; PRA, panel reactive antibody; DSA, donor-specific antibodies; CNI, Calcineurin inhibitor; FK, tacrolimus; CSA, cyclosporin A; MMF, mycophenolate mofetil; Pred, prednisone; CAAMR, Chronic active antibody-mediated rejection; CAMR, chronic antibody-mediated rejection.

difference was observed among the three groups for baseline characteristics including age, gender, retransplantation, infections, diabetic nephropathy, time posttransplant to biopsy, HLA mismatch, PRA pre-transplant or immunosuppressive regimen ($p > 0.05$).

Declined Graft Function and Survival Rate in CAAMR and CAMR Patients

We evaluated the changes of serum creatinine and estimated glomerular filtration rate (eGFR) in CAAMR and CAMR patients compared with Control patients without rejection from one year before the diagnosis of rejection to one year after diagnosis, which reflecting renal function during chronic rejection progression. The serum creatinine level was significantly higher and increased after diagnosis in CAAMR and CAMR patients compared to control patients (**Figures 2A, B**), while eGFR (**Figures 2C, D**) was opposite to that of creatinine, showed a declined renal graft function. Kaplan-Meier survival analysis showed that both the CAAMR and CAMR groups have lower survival rates than the non-rejection group ($p < 0.05$; **Figure 2E**).

Patients' Pathological Features

We collected the clinicopathological data for all patients, including hematoxylin and eosin (HE), Masson's trichrome and periodic acid-silver metheramine (PASM), CD20, C4d, CD3, and CD20 staining as shown in **Figure 3A**. We analyzed the differences in Banff scores among the three groups. The CAAMR group showed higher acute Banff scores include peritubular capillary (PTC), Glomerulitis (g), tubulitis (t), intimal arteritis(v) than those in CAMR and Control groups (**Figure 3B**). The CAAMR and CAMR groups showed

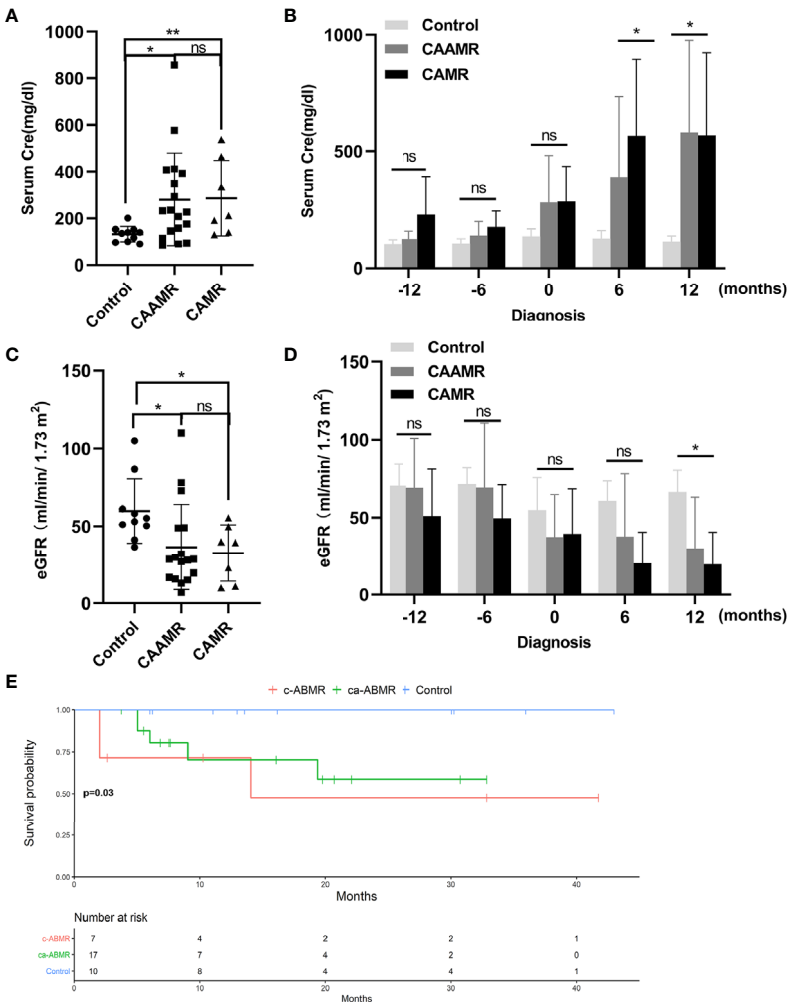

FIGURE 2 | Declined graft function and survival rate in CAAMR and CAMR patients. The serum creatinine **(A, B)** and eGFR **(C, D)** in all patients (Control, CAAMR, CAMR) were collected and analyzed at the time of diagnosis of rejection and from one year before biopsy to one year after biopsy. Kaplan-Meier survival analysis was used to compare the biopsy time to allograft failure between the three groups with the log-rank test **(E)**. Cre, creatinine; eGFR, estimated glomerular filtration rate. *p ≤ 0.05, **p ≤ 0.01. ns, no significance.

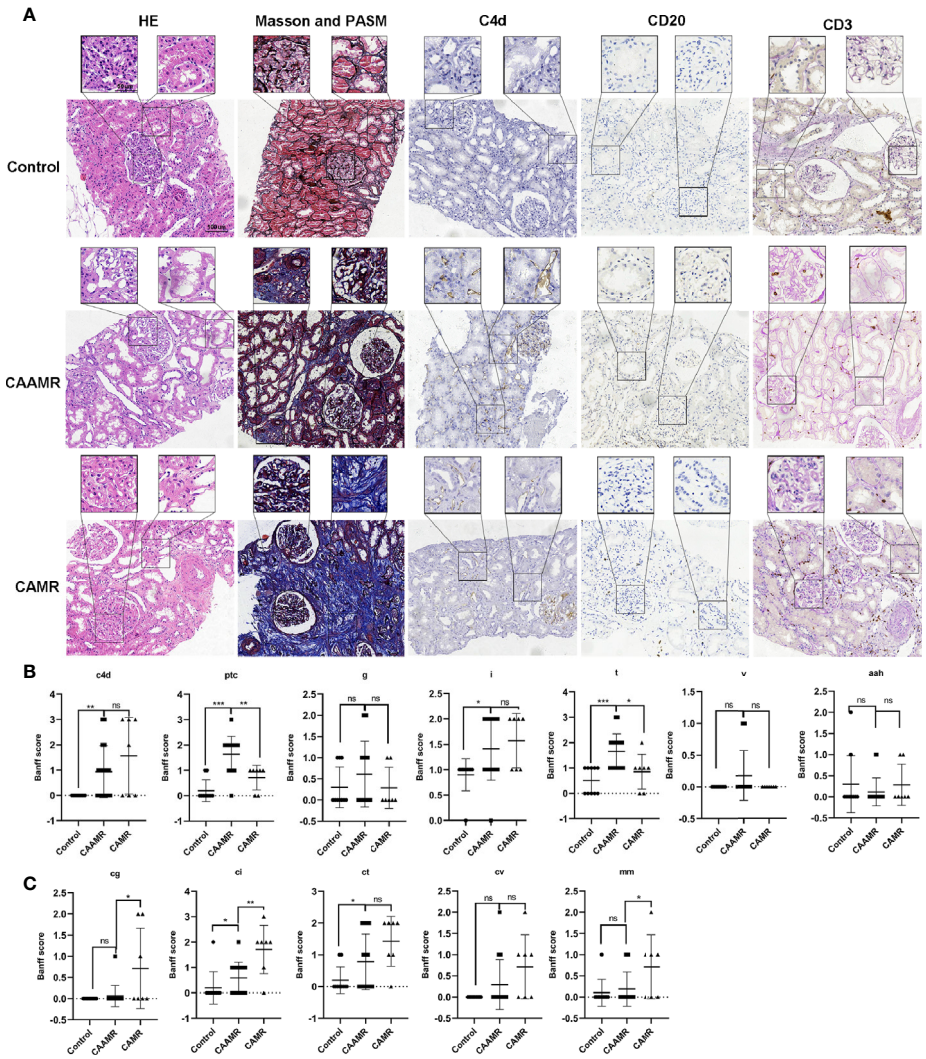

FIGURE 3 | Patients' pathological features. Patients pathological data included HE, Masson and PASM, C4d, CD20, CD3 staining **(A)** was collected and shown. Banff scores included C4d, ptc, g, i,t, v, aah **(B)** and cg, ci, ct, cv, mm **(C)** were collected and compared among three groups. HE, hematoxylin and eosin; PASM, periodic acid-silver metheramine. *p ≤ 0.05, **p ≤ 0.01, and ***p ≤ 0.001. ns, no significance.

significantly higher C4d score and chronic scores include interstitial fibrosis (ci), glomerular double contour (cg) and tubular atrophy (ct) than those in the Control group, CAMR patients revealing more distinct chronic characteristics (**Figure 3C**).

PSMP Expression in Biopsy Tissue Was a Biomarker for the Diagnosis of CAAMR

In this study, we focused on PSMP because it is a chemokine with increased expression at the site of the inflammatory injury. The immunohistochemistry analysis showed that PSMP protein was strongly expressed in the CAAMR group compared with the Control and CAMR groups ($p < 0.01$, **Figures 4A**, **B**). The PSMP mRNA expression levels in biopsy tissue were analyzed for all three groups, which showed that PSMP mRNA was detected at significantly higher levels in the biopsy tissues of CAAMR patients (five cases) compared with those from the Control group (3 cases, $p < 0.05$). No significant difference in mRNA levels was observed between the CAAMR and CAMR (3 cases) samples, which might because of the low sample size (**Figure 4C**). The ROC curve analysis showed that the PSMP protein expression level in biopsy tissues was a good discriminator for distinguishing CAAMR patients from Control and CAMR patients, with an area under the ROC curve (AUC) of 0.85 (95% confidence interval, 0.72 to 0.99), a specificity of 88.9%, and a sensitivity of 72.2% ($p < 0.001$, **Figure 4D**). We performed Kaplan-Meier survival analysis at the cut-off value of PSMP protein in biopsy, which revealed no significant differences in graft survival between high- and low-PSMP expression groups among CAAMR patients (**Figure S1A**).

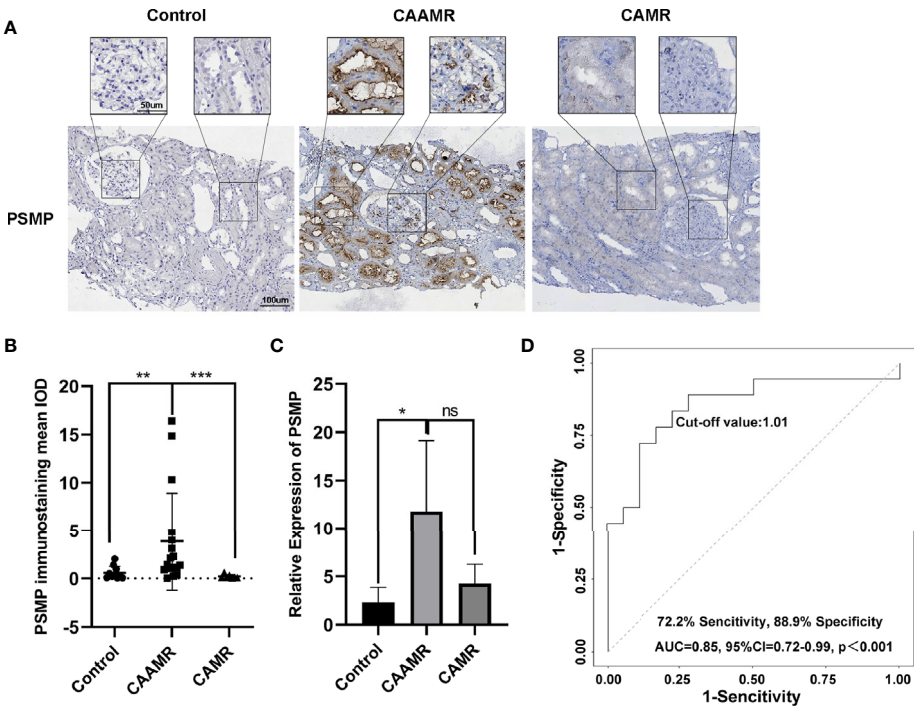

FIGURE 4 | PSMP expression in biopsy tissue may be a biomarker for the diagnosis of CAAMR. The expression of PSMP protein was detected by immunohistochemistry **(A)** and quantified by Image-pro plus software **(B)**. PSMP mRNA level was analyzed by RT-PCR in biopsy tissues **(C)**. Receiver operating characteristic (ROC) curves were used to evaluate the value of PSMP protein expression in the prediction of CAAMR from Control and CAMR patients **(D)** in graft biopsies. *p ≤ 0.05, **p ≤ 0.01, and ***p ≤ 0.001. ns, no significance.

PSMP Expression Was Related to Macrophage Infiltration in CAAMR Patients

Recently, macrophages were suggested to play a more immediate role in allograft rejection. CD68 and CD163 immunohistochemistry staining were performed in biopsies for the quantitative analysis of macrophage infiltration, which showed a higher number of $CD68^+$ cells per HPF in CAAMR and CAMR patients than in Control patients ($p < 0.01$, **Figures 5A, B**). The $CD163^+$ cells number was higher in CAAMR patients compared with control patients ($p < 0.05$) but lower than CAMR patients (**Figure 5C**). Because PSMP expression levels were higher in CAAMR patients, we used Spearman's correlation coefficient to analyze the correlation between PSMP expression and $CD68^+$ or $CD163^+$ infiltrating cells in the CAAMR and Control groups, which revealed a significant correlation between PSMP expression and the number of infiltrating $CD68^+$ cells ($p < 0.05$, **Figure 5C**), but no significant correlation between PSMP expression and the number of $CD163^+$ cells (**Figure 5E**).

PSMP Expression Was Related to V-Lesion in CAAMR Patients

We analyzed the correlation between PSMP expression quantified by immunohistochemistry staining in renal biopsies and the Banff criteria scores in CAAMR patients. The results showed that PSMP expression was significantly associated with the v-lesions in CAAMR patients ($p < 0.05$, **Figure 6A**), but no significant correlation was identified with any other Banff lesion scores (**Figure S2A).** By analyzing the pathological data of patients with intimal arteritis (v) scores > 0 in CAAMR patients, the infiltration of $CD68^+$ cells were found to be abundant in chronic intimal arteritis, suggesting that macrophage infiltration induced by the high expression of PSMP may promote the development of intimal arteritis (**Figures 6B, C**). We also found that in 3 cases with v-lesion (v > 0) in the CAAMR group, 2 cases experienced graft failure (**Table 2**). We also analyze whether PSMP levels were associated with graft function and the emergence of anti-HLA antibodies, which showed no significant correlations between PSMP expression and the eGFR or the median fluorescent intensity of anti-HLA II antibodies (**Figure S2B).**

PSMP Levels in the Serum and Urine Samples

We collected serum and urine samples of CAAMR, CAMR and Control patients, the PSMP expression levels were detected using the flow cytometry-based cytokine bead assay. However, The PSMP levels were lower in CAAMR groups compared with CAMR patients in the urine samples, ($p < 0.05$, **Figure 7A**). Based on the ROC curve analysis, urine PSMP levels could distinguish CAAMR patients from other patients, with an area under the ROC curve (AUC) of 0.77 (95% confidence interval

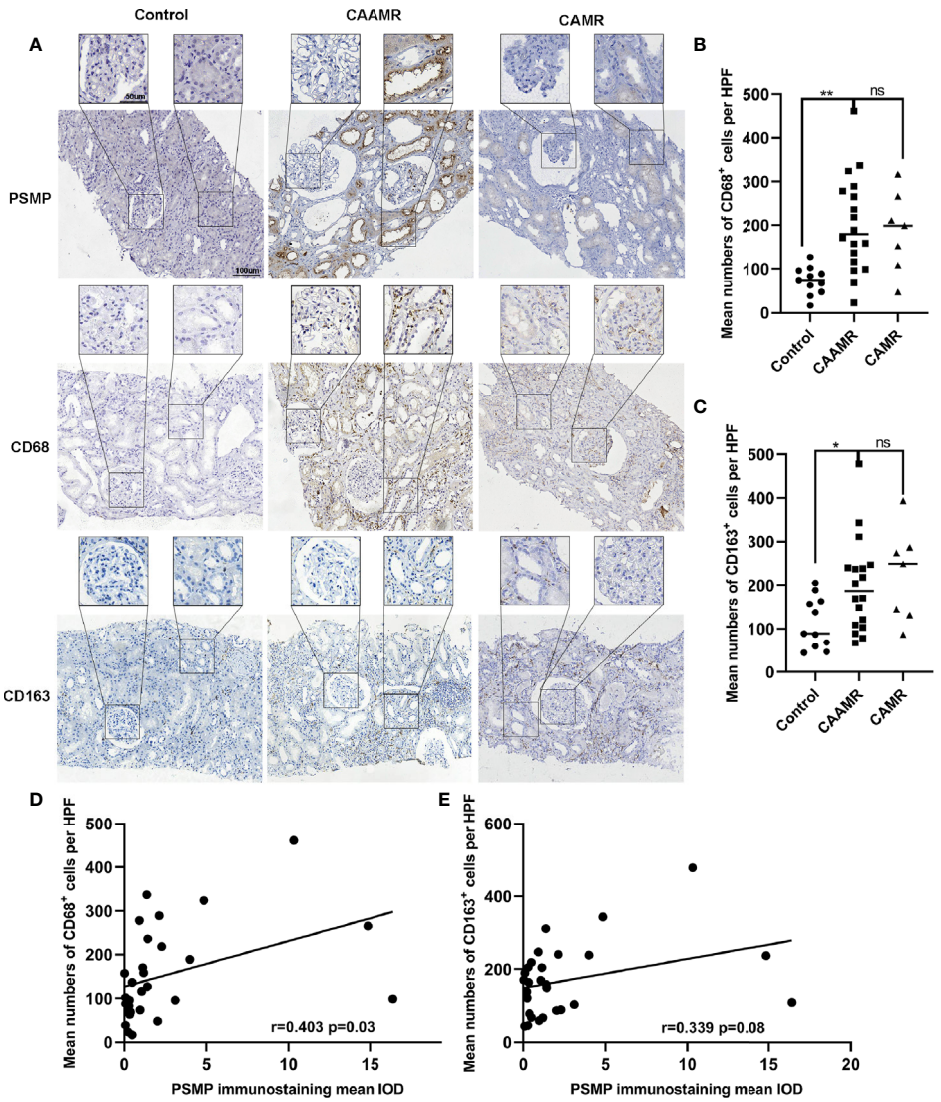

FIGURE 5 | The relationship between PSMP expression and macrophage infiltration in CAAMR patients. The $CD68^+$ and $CD163^+$ cells infiltration was detected by immunohistochemistry **(A)** and quantified as average number of positive cells per HFP (40×) by Image-pro plus software **(B, C)**. Correlations between PSMP expression and $CD68^+$ **(D)** and $CD163^+$ **(E)** cells infiltration were analyzed by Pearson's correlation coefficient. HPF, high-power field. *$p \leq 0.05$, **$p \leq 0.01$. ns, no significance.

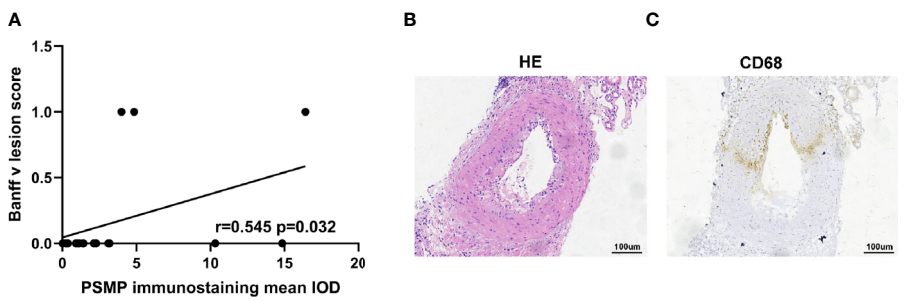

FIGURE 6 | The relationship between PSMP expression and v-lesion in CAAMR patients. Correlations between PSMP expression and Banff v-lesion scores **(A)** were analyzed by Pearson's correlation coefficient. The infiltration of $CD68^+$ cells were shown in chronic intimal arteritis by immunohistochemistry staining **(B, C)**.

TABLE 2 | v lesion in CAAMR.

Characteristics	v>0 (n=3)	v=0 (n=14)	p value
CD68 number	259.33 ± 55.26	189.53 ± 111.37	0.33
Creatinine(mg/dl)	347 ± 78.87	216.87 ± 135.31	0.07
eGFR (ml/min/1.73 m^2)	21.29 ± 26.034	36.23 ± 7.59	0.36
Graft loss-n (%)	2(66.67%)	1(7.14%)	0.07

eGFR, estimated glomerular filtration rate.

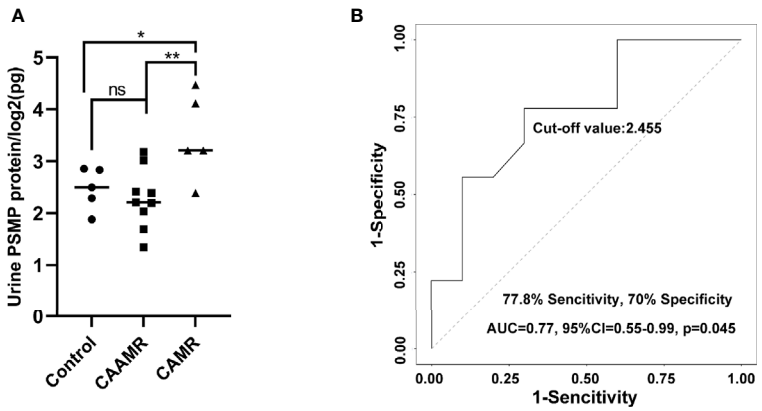

FIGURE 7 | PSMP levels in the urine samples. Urine samples were collected and measured by flow cytometry-based cytokine bead assay **(A)**. ROC curves were used to evaluate the value of urine PSMP level in discriminating CAAMR patients from other patients **(B)**. *p ≤ 0.05, **p ≤ 0.01. ns, no significance.

(0.55 to 0.99), a specificity of 70%, and a sensitivity of 77.8% ($p < 0.05$, **Figure 7B).** No significant differences in serum PSMP levels were observed among the three groups (**Figure S3A)** and could not be used as biomarkers to distinguish CAAMR patients from the other patients (**Figure S3B).**

DISCUSSION

In this study, we explored potential diagnostic and therapeutic biomarkers for chronic renal transplant rejection, include CAAMR and CAMR. Long-term graft failure caused by CAAMR has been a key challenge in renal transplantation (18). Chronic rejection needs pass through an early and active chronicity rejection phase (7) before the eventual develop to chronic graft injury. The diagnosis and treatment of early chronicity is important for blocking the progress of chronic graft injury. Although CAMR accompanied by significant microvascular inflammation was defined as CAAMR in the revised 2013 Banff classification (19), the diagnostic criteria for CAAMR have been continuously refined (20). Some specific cases that distinguish the two renal rejection types were not well known which lead to graft failure due to delayed treatment. We have shown that graft survival and function of CAAMR and CAMR patients were significantly reduced compared with those in the non-rejection group, suggesting the important effects of early active chronic development processes on graft function. Therefore, early diagnosis and treatment of CAAMR can avoid irreversible fibrosis and hold back the progress to CAMR. In our study, PSMP expression in graft biopsy tissues may be more meaningful for the diagnosis of CAAMR and distinguishing from CAMR. We have found that PSMP protein and mRNA levels both increased in CAAMR biopsy tissue, was a significant discriminatory factor that can be used to distinguish CAAMR patients from CAMR and non-rejection patients. However, there was no significant difference of PSMP protein expression in blood samples of CAAMR patients. We concluded that PSMP expression in graft biopsy tissues may be a distinguishing feature for CAAMR and should be considered an important histopathological diagnostic criterion in renal transplantation rejections. In addition, we observed that urine PSMP decreased in CAAMR patients and also can discriminated CAAMR patients from other patients. While the mechanism underlying PSMP production and metabolism is not yet clear, we will further explore this phenomenon in animal models.

According to our results, we believe that PSMP might be an important factor in the development of chronic antibody-mediated rejection. PSMP is a chemokine that recruits active monocytes-macrophages and promotes M1 polarization during the inflammatory response (17). Monocytes and macrophages infiltrate significantly in antibody-mediated rejection and can be serve as predictor of graft failure (21). In chronic rejection, macrophage infiltration plays a more important role than T cells and is positively correlated with poor graft prognosis (8, 22). We found that macrophages significantly infiltrated in CAAMR patients, PSMP expression was significantly associated with

$CD68^+$ macrophage accumulation in CAAMR graft biopsy tissues. M1 macrophages secrete pro-inflammatory cytokines that participate in the development of chronic rejection, whereas M2 macrophages secrete anti-inflammatory cytokines to promote tissue repair or graft fibrosis through the macrophage-to-myofibroblast transition (MMT) (23, 24). The M2 macrophages accumulation increased significantly 1–5 years after transplantation involved in the chronic injure progression (12), which may be associated with the fibrosis and decreased graft function (25, 26). We found $CD163^+$ M2 cells increased in CAAMR but lower than that in CAMR patients, revealed that M2 macrophages might play a more prominent role in CAMR than in CAAMR. In addition, PSMP expression was associated with $CD68^+$ macrophage infiltration but not with the accumulation of $CD163^+$ M2 macrophages in CAAMR. Therefore, we believe that PSMP expression increase and promote M1 macrophage accumulation in early CAAMR, followed by M2 polarization and decreased PSMP expression in late CAAMR. However, we require more additional data and experiments to verify this hypothesis.

Intimal arteritis caused by vascular rejection has previously considered to be a feature of acute cellular rejection (1, 27). In the revised 2013 Banff criteria, vascular arteritis (v > 0) was included in the diagnostic criteria for active antibody-mediated rejection (19). Although isolated v-lesion has been associated with reduced recipient graft survival (28, 29), this has not been evaluated in CAAMR. In CAAMR patients, 3 of 17 cases presented intimal arteritis, of which 2 of 3 grafts were lost, indicating a significant relationship between v-lesion and graft loss in CAAMR. Although there was no significant significance which might due to small size of v> 0, we can still observe that patients with v > 0 has lower graft function and higher graft failure in CAAMR patients. Anyway, more samples remain necessary to verify this relationship between v-lesion and CAAMR. Although only 3 cases (v > 0) were identified, a significant correlation was found between the expression level of PSMP and v-lesion detection in CAAMR. In acute rejection, macrophages significantly infiltrated in the interstitium and arterial intima of vascularized grafts (30, 31), but little known about the macrophages and arterial intima in CAAMR. We found that intimal arteritis showed increased macrophage infiltration in CAAMR, which may be due to the recruitment effect of PSMP on macrophages. Macrophages may be a therapeutic target for improving the long-term outcome of grafts (32). It has been proved that inhibiting the accumulation of macrophages in the graft can effectively maintain the kidney graft function and prolong the survival of the graft (33). We found that PSMP promoted macrophage accumulation in grafts of CAAMR patients, may be serve as a therapeutic target for prevention macrophages infiltration and chronic graft failure in CAAMR.

In summary, our results revealed that PSMP was significantly increased in CAAMR patients but not in CAMR patients, and PSMP expression in graft biopsy tissues was a significant discriminative biomarker that distinguishes CAAMR from CAMR patients. A significant correlation was found between the expression of PSMP and $CD68^+$ macrophage infiltration in CAAMR. Our data also revealed that v-lesions in CAAMR contributed to increased graft loss, and PSMP expression levels were significantly associated with v-lesion. These results indicated that PSMP played an important role in CAAMR development by recruiting macrophages to the renal transplant tissue and can be used as a discriminative histopathological diagnostic biomarker and therapeutic target for CAAMR.

DATA AVAILABILITY STATEMENT

The original contributions presented in the study are included in the article/**Supplementary Material**. Further inquiries can be directed to the corresponding author.

ETHICS STATEMENT

The studies involving human participants were reviewed and approved by Ethics Committee of Tianjin First Central Hospital (2020N228KY). Written informed consent for this study was not required in accordance with the national legislation and the institutional requirements.

AUTHOR CONTRIBUTIONS

PZ: research performing and manuscript writing. HL: data acquisition and statistical analysis. MH: provided guidance for planning. ZW: collection and assembly of data. JZ: pathological diagnosis of the kidney biopsies. JT: technical supporting. XS: interpreted the data. YF: conception and design of the entire study. All authors contributed to the article and approved the submitted version.

FUNDING

This study was supported by the National Natural Science Foundation of China (81970654).

SUPPLEMENTARY MATERIAL

The Supplementary Material for this article can be found online at: https://www.frontiersin.org/articles/10.3389/fimmu.2021.661911/full#supplementary-material

REFERENCES

1. Sablik KA, Clahsen-van Groningen MC, Damman J, Roelen DL, Betjes MGH. Banff lesions and renal allograft survival in chronic-active antibody mediated rejection. *Transplant Immunol* (2019) 56:101213. doi: 10.1016/j.trim.2019.101213
2. Hara S. Current pathological perspectives on chronic rejection in renal allografts. *Clin Exp Nephrol* (2017) 21(6):943–51. doi: 10.1007/s10157-016-1361-x
3. Reese SR, Wilson NA, Huang Y, Ptak L, Degner KR, Xiang D, et al. B Cell Deficiency Attenuates Transplant Glomerulopathy in a Rat Model of Chronic

Active Antibody-mediated Rejection. *Transplantation* (2020). doi: 10.1097/TP.0000000000003530
4. van der Zwan M, Hesselink DA, Baan CC, Clahsen-van Groningen MC. Chronic-active Antibody-mediated Rejection: To Belatacept or Not, That Is the HOT Question. *Transplantation* (2021) 105(3):478–9. doi: 10.1097/TP.0000000000003279
5. Roufosse C, Simmonds N, Clahsen-van Groningen M, Haas M, Henriksen KJ, Horsfield C, et al. A 2018 Reference Guide to the Banff Classification of Renal Allograft Pathology. *Transplantation* (2018) 102(11):1795–814. doi: 10.1097/TP.0000000000002366
6. Haas M, Loupy A, Lefaucheur C, Roufosse C, Glotz D, Seron D, et al. The Banff 2017 Kidney Meeting Report: Revised diagnostic criteria for chronic active T cell-mediated rejection, antibody-mediated rejection, and prospects for integrative endpoints for next-generation clinical trials. *Am J Transplant Off J Am Soc Transplant Am Soc Transplant Surgeons* (2018) 18(2):293–307. doi: 10.1111/ajt.14625
7. Haas M. The relationship between pathologic lesions of active and chronic antibody-mediated rejection in renal allografts. *Am J Transplant Off J Am Soc Transplant Am Soc Transplant Surgeons* (2018) 18(12):2849–56. doi: 10.1111/ajt.15088
8. Li J, Li C, Zhuang Q, Peng B, Zhu Y, Ye Q, et al. The Evolving Roles of Macrophages in Organ Transplantation. *J Immunol Res* (2019) 2019:5763430. doi: 10.1155/2019/5763430
9. Guillén-Gómez E, Dasilva I, Silva I, Arce Y, Facundo C, Ars E, et al. Early Macrophage Infiltration and Sustained Inflammation in Kidneys From Deceased Donors Are Associated With Long-Term Renal Function. *Am J Transplant Off J Am Soc Transplant Am Soc Transplant Surgeons* (2017) 17(3):733–43. doi: 10.1111/ajt.13998
10. Bräsen JH, Khalifa A, Schmitz J, Dai W, Einecke G, Schwarz A, et al. Macrophage density in early surveillance biopsies predicts future renal transplant function. *Kidney Int* (2017) 92(2):479–89. doi: 10.1016/j.kint.2017.01.029
11. van den Bosch TPP, Hilbrands LB, Kraaijeveld R, Litjens NHR, Rezaee F, Nieboer D, et al. Pretransplant Numbers of CD16(+) Monocytes as a Novel Biomarker to Predict Acute Rejection After Kidney Transplantation: A Pilot Study. *Am J Transplant Off J Am Soc Transplant Am Soc Transplant Surgeons* (2017) 17(10):2659–67. doi: 10.1111/ajt.14280
12. Sablik KA, Jordanova ES, Pocorni N, Clahsen-van Groningen MC, Betjes MGH. Immune Cell Infiltrate in Chronic-Active Antibody-Mediated Rejection. *Front Immunol* (2019) 10:3106. doi: 10.3389/fimmu.2019.03106
13. Pei X, Sun Q, Zhang Y, Wang P, Peng X, Guo C, et al. PC3-secreted microprotein is a novel chemoattractant protein and functions as a high-affinity ligand for CC chemokine receptor 2. *J Immunol (Baltimore Md 1950)* (2014) 192(4):1878–86. doi: 10.4049/jimmunol.1300758
14. She S, Wu X, Zheng D, Pei X, Ma J, Sun Y, et al. PSMP/MSMP promotes hepatic fibrosis through CCR2 and represents a novel therapeutic target. *J hepatology* (2020) 72(3):506–18. doi: 10.1016/j.jhep.2019.09.033
15. Loupy A, Haas M, Roufosse C, Naesens M, Adam B, Afrouzian M, et al. The Banff 2019 Kidney Meeting Report (I): Updates on and clarification of criteria for T cell- and antibody-mediated rejection. *Am J Transplant Off J Am Soc Transplant Am Soc Transplant Surgeons* (2020) 20(9):2318–31. doi: 10.1111/ajt.15898
16. Pei X, Zheng D, She S, Fang Z, Zhang S, Hu H, et al. Elevated Expression Levels of PC3-Secreted Microprotein (PSMP) in Prostate Cancer Associated With Increased Xenograft Growth and Modification of Immune-Related Microenvironment. *Front Oncol* (2019) 9:724. doi: 10.3389/fonc.2019.00724
17. Pei X, Zheng D, She S, Ma J, Guo C, Mo X, et al. The PSMP-CCR2 interactions trigger monocyte/macrophage-dependent colitis. *Sci Rep* (2017) 7(1):5107. doi: 10.1038/s41598-017-05255-7
18. Higuchi H, Kamimura D, Jiang JJ, Atsumi T, Iwami D, Hotta K, et al. Orosomucoid 1 is involved in the development of chronic allograft rejection after kidney transplantation. *Int Immunol* (2020) 32(5):335–46. doi: 10.1093/intimm/dxaa003
19. Haas M, Sis B, Racusen LC, Solez K, Glotz D, Colvin RB, et al. Banff 2013 meeting report: inclusion of c4d-negative antibody-mediated rejection and antibody-associated arterial lesions. *Am J Transplant Off J Am Soc Transplant Am Soc Transplant Surgeons* (2014) 14(2):272–83. doi: 10.1111/ajt.12590
20. Doberer K, Duerr M, Halloran PF, Eskandary F, Budde K, Regele H, et al. A Randomized Clinical Trial of Anti-IL-6 Antibody Clazakizumab in Late Antibody-Mediated Kidney Transplant Rejection. *J Am Soc Nephrol JASN* (2021) 30(3):708–22. doi: 10.1681/asn.2020071106
21. van den Bosch TP, Kannegieter NM, Hesselink DA, Baan CC, Rowshani AT. Targeting the Monocyte-Macrophage Lineage in Solid Organ Transplantation. *Front Immunol* (2017) 8:153. doi: 10.3389/fimmu.2017.00153
22. Zhao Y, Chen S, Lan P, Wu C, Dou Y, Xiao X, et al. Macrophage subpopulations and their impact on chronic allograft rejection versus graft acceptance in a mouse heart transplant model. *Am J Transplant Off J Am Soc Transplant Am Soc Transplant Surgeons* (2018) 18(3):604–16. doi: 10.1111/ajt.14543
23. Tang PM, Nikolic-Paterson DJ, Lan HY. Macrophages: versatile players in renal inflammation and fibrosis. *Nat Rev Nephrol* (2019) 15(3):144–58. doi: 10.1038/s41581-019-0110-2
24. Mosser DM, Edwards JP. Exploring the full spectrum of macrophage activation. *Nat Rev Immunol* (2008) 8(12):958–69. doi: 10.1038/nri2448
25. Toki D, Zhang W, Hor KL, Liuwantara D, Alexander SI, Yi Z, et al. The role of macrophages in the development of human renal allograft fibrosis in the first year after transplantation. *Am J Transplant Off J Am Soc Transplant Am Soc Transplant Surgeons* (2014) 14(9):2126–36. doi: 10.1111/ajt.12803
26. Aguado-Domínguez E, Cabrera-Pérez R, Suarez-Benjumea A, Abad-Molina C, Núñez-Roldán A, Aguilera I. Computer-Assisted Definition of the Inflammatory Infiltrates in Patients With Different Categories of Banff Kidney Allograft Rejection. *Front Immunol* (2019) 10:2605. doi: 10.3389/fimmu.2019.02605
27. Jeannet M, Pinn VW, Flax MH, Winn HJ, Russell PS. Humoral antibodies in renal allotransplantation in man. *New Engl J Med* (1970) 282(3):111–7. doi: 10.1056/nejm197001152820301
28. Salazar ID, Merino López M, Chang J, Halloran PF. Reassessing the Significance of Intimal Arteritis in Kidney Transplant Biopsy Specimens. *J Am Soc Nephrol JASN* (2015) 26(12):3190–8. doi: 10.1681/asn.2014111064
29. Stevenson HL, Prats MM, Isse K, Zeevi A, Avitzur Y, Ng VL, et al. Isolated vascular "v" lesions in liver allografts: How to approach this unusual finding. *Am J Transplant Off J Am Soc Transplant Am Soc Transplant Surgeons* (2018) 18(6):1534–43. doi: 10.1111/ajt.14708
30. Moreau A, Varey E, Anegon I, Cuturi MC. Effector mechanisms of rejection. *Cold Spring Harb Perspect Med* (2013) 3(11):a015461. doi: 10.1101/cshperspect.a015461
31. Matheson PJ, Dittmer ID, Beaumont BW, Merrilees MJ, Pilmore HL. The macrophage is the predominant inflammatory cell in renal allograft intimal arteritis. *Transplantation* (2005) 79(12):1658–62. doi: 10.1097/01.tp.0000167099.51275.ec
32. Azad TD, Donato M, Heylen L, Liu AB, Shen-Orr SS, Sweeney TE, et al. Inflammatory macrophage-associated 3-gene signature predicts subclinical allograft injury and graft survival. *JCI Insight* (2018) 3(2):e95659. doi: 10.1172/jci.insight.95659
33. Tillmann FP, Grotz W, Rump LC, Pisarski P. Impact of monocyte-macrophage inhibition by ibandronate on graft function and survival after kidney transplantation: a single-centre follow-up study over 15 years. *Clin Exp Nephrol* (2018) 22(2):474–80. doi: 10.1007/s10157-017-1470-1

Conflict of Interest: The authors declare that the research was conducted in the absence of any commercial or financial relationships that could be construed as a potential conflict of interest.

frontiers in Immunology

ORIGINAL RESEARCH
published: 13 April 2021
doi: 10.3389/fimmu.2021.650424

Impaired ATG16L-Dependent Autophagy Promotes Renal Interstitial Fibrosis in Chronic Renal Graft Dysfunction Through Inducing EndMT by NF-κB Signal Pathway

Zeping Gui[1,2†], Chuanjian Suo[1†], Zijie Wang[1†], Ming Zheng[1], Shuang Fei[1], Hao Chen[1], Li Sun[1], Zhijian Han[1], Jun Tao[1], Xiaobin Ju[1], Haiwei Yang[1], Min Gu[2] and Ruoyun Tan[1*]*

[1] Department of Urology, The First Affiliated Hospital of Nanjing Medical University, Nanjing, China, [2] Department of Urology, The Second Affiliated Hospital of Nanjing Medical University, Nanjing, China

OPEN ACCESS

Edited by:
Hao Wang,
Tianjin Medical University General Hospital, China

Reviewed by:
Ruiming Rong,
Fudan University, China
Stanislaw Stepkowski,
University of Toledo, United States

***Correspondence:**
Ruoyun Tan
tanruoyun112@vip.sina.com
Min Gu
lancetgu@aliyun.com

†These authors have contributed equally to this work

Specialty section:
This article was submitted to Alloimmunity and Transplantation, a section of the journal Frontiers in Immunology

Received: 07 January 2021
Accepted: 15 March 2021
Published: 13 April 2021

Citation:
Gui Z, Suo C, Wang Z, Zheng M, Fei S, Chen H, Sun L, Han Z, Tao J, Ju X, Yang H, Gu M and Tan R (2021) Impaired ATG16L-Dependent Autophagy Promotes Renal Interstitial Fibrosis in Chronic Renal Graft Dysfunction Through Inducing EndMT by NF-κB Signal Pathway. Front. Immunol. 12:650424. doi: 10.3389/fimmu.2021.650424

Chronic renal graft dysfunction (CAD) is caused by multiple factors, including glomerular sclerosis, inflammation, interstitial fibrosis and tubular atrophy (IF/TA). However, the most prominent elements of CAD are IF/TA. Our studies have confirmed that endothelial-mesenchymal transition (EndMT) is an important source to allograft IF/TA. The characteristic of EndMT is the loss of endothelial marker and the acquisition of mesenchymal or fibroblastic phenotypes. Autophagy is an intracellular degradation pathway that is regulated by autophagy-related proteins and plays a vital role in many fibrotic conditions. However, whether or not autophagy contributes to fibrosis of renal allograft and how such mechanism occurs still remains unclear. Autophagy related 16 like gene (ATG16L) is a critical autophagy-related gene (ARG) necessary for autophagosome formation. Here, we first analyzed kidney transplant patient tissues from Gene Expression Omnibus (GEO) datasets and 60 transplant patients from our center. Recipients with stable kidney function were defined as non-CAD group and all patients in CAD group were histopathologically diagnosed with CAD. Results showed that ATG16L, as one significant differential ARG, was less expressed in CAD group compared to the non-CAD group. Furthermore, we found there were less autophagosomes and autolysosomes in transplanted kidneys of CAD patients, and downregulation of autophagy is a poor prognostic factor. In vitro, we found out that the knockdown of ATG16L enhanced the process of EndMT in human renal glomerular endothelial cells (HRGECs). *In vivo*, the changes of EndMT and autophagic flux were then detected in rat renal transplant models of CAD. We demonstrated the occurrence of EndMT, and indicated that abundance of ATG16L was accompanied by the dynamic autophagic flux change along different stages of kidney transplantation. Mechanistically, knockdown of ATG16L, specifically in endothelial cells, reduced of NF-κB degradation and excreted inflammatory cytokines (IL-1β, IL-6 and TNF-α), which could facilitate EndMT. In conclusion, ATG16L-dependent autophagic flux causing by transplant showed progressive loss increase over time.

Inflammatory cytokines from this process promoted EndMT, thereby leading to progression of CAD. ATG16L served as a negative regulator of EndMT and development of renal graft fibrosis, and autophagy can be explored as a potential therapeutic target for chronic renal graft dysfunction.

Keywords: chronic renal graft dysfunction, renal interstitial fibrosis, ATG16L, autophagy, EndMT, inflammatory cytokines

INTRODUCTION

Kidney transplantation is one of the optimal treatment for patients with uremia because it significantly improves their quality of life (1). However, there is a relatively high number of renal allograft dysfunction after transplantation due to the chronic progressive deterioration of renal function, which is a key factor affecting the long-term survival of transplanted kidney (2). Chronic renal graft dysfunction (CAD), formerly known as chronic allograft nephropathy, is a multifactorial condition associated with progressive renal interstitial fibrosis. Various factors are known to contribute to the loss of renal allograft function, including, but not limited to, acute and chronic rejection, ischemia and reperfusion inflammatory and tissue rebuilding process, and drugs-related nephrotoxicity (3).

CAD is morphologically characterized by inflammation, progressive interstitial fibrosis and tubular atrophy(IF/TA), and glomerular sclerosis (4). Among them, IF/TA is key factor determining renal allograft function, but the mechanisms by which it occurs are still unknown. Several factors have been identified to contribute to the high proportion of renal allograft loss. In our previous study, we also confirmed that the main pathological process of CAD was renal allograft IF/TA, which is characterized by excessive deposition of extracellular matrix in transplanted renal tubular and interstitial tissue (5). Studies have verified that collagens are mainly secreted by myofibroblasts, and collagens secretion lead to extracellular matrix sedimentation and subsequently transplant kidney IF/TA. There are four principal cells involved in the formation of myofibroblasts: epithelial cells, endothelial cells, bone marrow-derived fibroblasts and microvascular pericytes (6, 7). They play a crucial role in repairing and protecting integrity of kidney tissue. Among them, external stimuli enable differentiation of intrinsic kidney cells such as epithelial cells to myofibroblasts, which can produce extracellular matrix. This process is called epithelial-to-mesenchymal transition (EMT). EMT usually involved three types: (I) embryogenesis, (II) tissue repair and fibrosis, (III) metastasis (8). Several studies have been done to elucidate the molecular and cellular mechanisms of type II EMT in organ fibrosis (9, 10), however, roles of EMT in different primary fibroblast-generating process during the CAD progression still remain inconclusive.

With kidney transplantation, there is always an increased likelihood of damage to the allograft macro- and microvasculature, due to the physical location of the allograft endothelium that makes it an initial target of choice for allograft injury (11). Allografts act as potential targets for immune response mediated by quite a number of serum inflammatory cytokines. Studies indicated that many inflammatory cytokines involved in CAD process (12) and endothelial cells at sites of renal allografts were not only participants in inflammation but also regulators of inflammation (11). Our previous research revealed that TNF-α more highly expressed in CAD group than non-CAD group. TNF-α also facilitated the EMT process in human proximal tubular cells (HK_2) (13). Given the intimate contact between endothelial cells and blood, circulating inflammatory cells and cytokines will first attack the allograft endothelium. Chronic stimulation from inflammatory cytokines leads to endothelial cells undergoing disorders of cell structure and internal environment, which results in endothelial injury. Emerging studies suggest that endothelial injury contributes to extracellular matrix deposition and plays a key role in the organ fibrosis diseases. Recently, Endothelial-to-mesenchymal transition (EndMT) is considered as the principal cause of the endothelial injury and promotes the progress of IF/TA during renal fibrosis disease (5, 9). EndMT is a distinctive type of EMT. It is characterized by cells that gradually lose endothelial markers, such as CD31 and CD34, and gain mesenchymal or myofibroblastic phenotype, such as a-smooth muscular actin (α-SMA), collagen I, and fibronectin (FN). The regulatory mechanism for EndMT remains a complex issue. The occurrence of EndMT could be affected by many factors such as oxidative stress, hypoxic and various injuries (14, 15). But almost all of these regulatory factors eventually come together in one direct action, which is inflammatory cytokines. In our previous studies, we showed that the EndMT was an important factor in the pathogenesis of IF/TA and CAD through the TGF-β/Smad signaling pathways (5). In addition, still other scholars suggested that TGF-β expression was up-regulated by TNF-α (16). So, inflammatory cytokines such as TNF-α may also be an important pathogenic factor in vascular endothelial injury that characterizes CAD progression. Although the initial factors of EndMT were different in various microenvironments, the final outcome was the same. Hence, it sufficed to hypothesize that there must be a central regulatory mechanism in the production of inflammatory cytokines and progression of EndMT.

Autophagy is a cellular pathway responsible for protein and organelle degradation (17). The process of autophagy is also known as autophagic flux, and the strength of this process often represents the degree of activation of autophagy. Autophagy is involved in different renal pathophysiological processes, including glomerulosclerosis, diabetic nephropathy and cystic kidney disease (18). Some studies reported that autophagy was a cytoprotective process. A classic defense for this presupposition

is as seen in mice with proximal tubule ATG5 deletion where the deletion promoted more severe renal fibrosis due to impaired autophagy (19). Other studies have also found that proximal tubule epithelial cells conditional knockdown ATG5 aggravated acute kidney injury in the early stage, but decelerated the progression of kidney fibrosis in the recovery or repair process (20). However, the specific interaction between autophagy and EMT or EndMT on fibrosis disease still remains controversial. Several studies suggested that autophagy inhibition could induce EMT and fibrosis by affecting the aberrant epithelial–fibroblast crosstalk in idiopathic pulmonary fibrosis (21). Others showed that Rapamycin promotes EndMT through the activation of autophagy during premature senescence (22). ATG16L gene mainly includes ATG16L1 and ATG16L2. ATG16L2 homo- and hetero-oligomerizes with ATG16L1. But ATG16L2 has less associated with autophagy (23). ATG16L1 has been identified as an important autophagy-related gene, promotes autophagosome formation at the plasma membrane and plays a critical role in the lipidated form of LC3 (23). Here, ATG16L1 is collectively referred to as ATG16L. As a key factor in autophagy, ATG16L was once reported that was related to the pathogenesis of several inflammatory diseases. For instance, the mutation of ATG16L conferred a strong predisposition to Crohn's disease development (24). However, the mechanism of ATG16L action and autophagy has not yet been well-studied in a targeted approach such as in the management and prognostication of kidney transplantation. So the dynamic role of autophagic flux and ATG16L-dependent autophagy must be the focus of research for potential therapeutics in CAD progression.

In this study, we explored the potential role of ATG16L-dependent autophagy in CAD progression. We revealed that the loss of ATG16L and autophagy were associated with occurrence of EndMT in clinical CAD patients and kidney transplanted rats. We then found that the levels of EndMT and renal allograft interstitial fibrosis were enhanced after altering autophagy activity by knocking down ATG16L gene. In addition, potential underlying mechanisms were also explored by RNA sequencing, we found that impairment of ATG16L contributed to the nuclear factor-κB (NF-κB) pathway activation and the inflammatory cytokines secretion, then promoted EndMT progression.

MATERIALS AND METHODS

Ethics Statement

The study's protocols complied with the Declaration of Helsinki and Istanbul. Human studies were examined and authorized by the local ethics committee of the First Affiliated Hospital of Nanjing Medical University (ID: IACUC-2010020). Informed consent was acquired from all transplant recipients as well as nephrectomy patients who were included in this research.

The studies involving rats were examined and authorized by the local ethics committee of the First Affiliated Hospital of Nanjing Medical University (ID: IACUC-2010020). Written informed consent is given by the owners for the participation of their animals in this research.

Sample Collection

Sixty adults who had received living or deceased donor kidney transplants started to be followed up from January 2010 to December 2017 at First Affiliated Hospital of Nanjing Medical University. Patients with serum creatinine level consistently < 141.46 μmol/L (1.6 mg/dl) for at least 12 months after kidney transplantation and no other complications such as episodes of significant rejection, drug toxicity injury, and infection were assigned to the non-CAD group. Patients in CAD group were defined as elevated serum creatinine greater than or equal to 141.46 μmol/L (1.6 mg/dl) for at least three months, and they were diagnosed by two independent pathology experts combined with biopsy results, laboratory indexes and imaging features. Adjacent normal kidney tissues were obtained from regions outside the tumor margin (>5cm) in patients with radical nephrectomy operations. Blood samples were obtained after patients had given informed consent. The specific step can be referred to our previous studies (5). The baseline characteristics of patients in the CAD group and non-CAD group were as shown in **Table 1**.

Rats and Animals Models

Adult male F344 and Lewis rats (Weight 250 ± 10.3 g) were obtained from Charles River Laboratories (Beijing, China) and abided by the guidelines of the Institutional Animal Care and Use Committee at Nanjing Medical University. The animals were handled in accordance with the norms of Nanjing Medical University and the guidelines published by the US National Institutes of Health.

All these animals experienced orthotopic left kidney transplantation. Lewis rats were used as recipients and syngeneic donors (Syn group), F344 rats as allogeneic donors (Allo group). The right kidney was excised simultaneously. The average time of cold ischemia was less than 20 minutes and warm ischemia was less than 35 minutes. Cyclosporine A (5 mg/kg, qd, ip; Neoral, Novartis, Switzerland) was used for 14 days to avoid the acute rejection,

Pharmaceutical Treatment and Tissue Harvest

The transplant kidneys from rats were harvested at weeks 4, 8, 12 and 16 after surgery. Paraffin-embedded formalin-fixed (10% neutral formalin) renal allograft tissue specimens were obtained for histological and IHC/IF staining. Remaining kidney stored at − 80°C refrigerator for detection of RNA and protein.

HE and Masson Trichrome Staining Assay

Protocals of HE and Masson trichrome staining assay can be referred to our previous studies (5). To identify the severity of CAD and the extent of fibrotic area, the renal allograft fibrosis area was quantified with Masson trichrome staining. For each slice, five random visual fields under × 400 microscope were selected. Area positive for Masson trichrome was measured by

TABLE 1 | Baseline characteristics of the CAD and non-CAD groups.

Clinical variables	CAD group	non-CAD group	P Value
Case number (n)	30	30	NS
Age (years, mean ± SD)	35.59 ± 3.09	38.61 ± 2.41	NS
Gender (Male/Female)	18/12	20/10	NS
BMI (kg/m2, mean ± SD)	22.64 ± 4.71	23.21 ± 4.2	NS
Transplant duration (years, range)	9.1 (6.5-13)	3.4 (2.3-4.8)	<0.001
Primary/secondary transplant	30/0	30/0	NS
PRA before renal transplant (%)	0	0	NS
Donor source			NS
Living-related	25	21	
Cadaveric	5	9	
Immunosuppressive regimen			NS
Prednisone + MMF + Tac	20	22	
Prednisone + MMF + CsA	10	8	
Biochemical parameters			
Serum creatinine (μmol/L, mean ± SD)	418.1 ± 20.8	93.37 ± 10.68	<0.001
eGFR* (min/1.73 m^2, mean ± SD)	24.71± 2.88	76.79 ± 6.23	<0.001

*SD, standard deviations; NS, no significance; CAD, Chronic allograft dysfunction; BMI, body mass index; PRA, panel reaction antibody; MMF, mycophenolate mofetil; CsA, cyclosporine A; Tac, tacrolimus; eGFR, estimated glomerular filtration rate; SD, standard deviation. *eGFR was estimated by the Cockcroft-Gault formula: eGFR = (140-age) x weight/72 x serum creatinine x (0.85 if female).*

two pathologists blinded to the experimental design using the Image-Pro Plus (Media Cybernetics, Rockville, MD).

Immunohistochemistry Staining Assay

Kidney tissues fixed with formalin were cut into 3 μm thick paraffin sections. The process of deparaffinized, hydrated, and antigen-retrieved were consistent with our previous studies (5). The antibodies [anti-ATG16L (1:100; Abcam, USA), anti-α-SMA (1:200; Abcam, USA), anti-Fibronectin (1:100; Abcam, USA) and anti-CD31 (1:100; CST, USA)] were incubated overnight at 4°C after sections blocked with 10% normal donkey serum. Next steps were also performed as described earlier with biotinylated goat anti-mouse/rabbit IgG (0.5 μg/mL; Abcam) and substrate 3-amino-9-ethylcarbazole or 3,3′ diaminobenzidine (Vector Laboratories, Burlingame, CA). The stained slides were photographed using a Nikon Eclipse 80i microscope equipped with a digital camera (DS-Ri1, Nikon, Shanghai, China).

Indirect Immunofluorescence Staining Assay

After fixing with 4% formaldehyde solution, renal allograft sections and cell climbing slices were penetrated with 0.1% Triton X-100 for 1 h, then blocked with 5% goat serum for 1 h. Afterward, sections and cell climbing slices were incubated with the anti- NF-κB p65 (1:200; Abcam, USA) at 4°C overnight. Incubation conditions of secondary antibody Dapi can refer to our previous studies (5). Slides were viewed with a Nikon Eclipse 80i fluorescence microscope (DS-Ri1, Nikon, Shanghai, China).

Autophagic Flux Detection

AAV-mRFP-GFP-LC3 (Hanbio, Shanghai, China) was stereotactically injected into left kidney of Lewis rats (3 μL) before 14 days before transplantation. The kidney was removed at 4, 8, 12, 16 weeks after transplantation and fixed with 4% paraformaldehyde for 24 h. Slides (30 μm) were viewed with a Nikon Eclipse 80i fluorescence microscope (DS-Ri1, Nikon, Shanghai, China). Yellow spots indicate autophagosomes and red spots indicate autolysosomes. When red signal stronger than the yellow signal represent autophagic flux is activated. When more yellow signal than red signal represent autophagic flux is impaired.

Electron Microscopy

The samples were fixed with ice-cold glutaraldehyde (3% in 0.1 M cacodylate buffer, pH 7.4) and further processed by the Core Facility (Servicebio, Wuhan, China). Observation was performed on a JEOL JEM-2100 transmission electron microscope.

Renal Function Detection

We used a rat QuantiChrom Creatinine Assay Kit and QuantiChrom Urea Assay Kit (Jiancheng, Beijing, China) to detected the concentrations of rat blood creatinine and urea nitrogen according to the manufacturer's instructions.

Uria Protein Detection

The 24 h urine samples were collected using metabolic cages, and urinary protein excretion was tested with the commercial kit (Mlbio, Shanghai, China) according to the instructions of the manufacturer.

Real-Time PCR Assessment

Briefly, total RNA was purified from HRGECs using the RNA extraction kits (TIANGEN, Beijing, China). cDNA (cDNA) was synthesized as described previously (5). Gene expression was measured by real-time PCR assay (Vazyme) and a DNA Engine Opticon 2 System (BioRad laboratories, Hercules, CA). The primer sequences were described as follows:

IL-1 β: 5′- TTCCTGTTGTCTACACCAATGC-3′ (F)
5′-CGGGCTTTAAGTGAGTAGGAGA-3′ (R);
IL-6: 5′-TCTCTCCGCAAGAGACTTCCA-3′ (F)

5′- ATACTGGTCTGTTGTGGGTGG-3′ (R);
TNF-α: 5′- CCTCTCTCTAATCAGCCCTCTG-3′ (F)
5′- GAGGACCTGGGAGTAGATGAG -3′ (R);
Actin: 5′- TGACGTGGACATCCGCAAAG-3′ (F)
5′- CTGGAAGGTGGACAGCGAGG-3′ (R);

Western Blot and Elisa Assay

Briefly, proteins from cells and tissues were extracted in RIPA buffer (Thermo ScientificTM, Chelmsford, MA, USA) containing phosphatases and proteases inhibitor cocktails (Sigma, St Louis, MO, USA). Proteins (20 μg) were transferred to a PVDF membrane (Millipore, IPVH00010, Massachusetts, USA) following SDS-PAGE. The slides were incubated in blocking solution (5% non-fat milk) for 60 min, and then PVDF membrane was incubated with primary antibody without washing in cold room overnight. After that, the process of PVDF membrane wash by tris buffered saline-tween (TBST) buffer, incubated by secondary antibody, ECL tableting and exposed were consistent with our previous studies (5). The primary antibodies were listed as follows: anti-GAPDH (1:1000; CST, USA), anti-CD31 (1:1000; CST, USA), anti-α-SMA (1:1000; Abcam, USA), anti-fibronectin (1:1000; BD Biosciences, USA), anti-LC3 (1:1000; CST, USA), anti-ATG16L (1:1000; CST, USA), anti-NF-κB p65 (1:1000; CST, USA), anti- Phospho-NF-κB p65 (1:1000; CST, USA). Quantification was performed by measuring the intensity of the signals with the aid of NIH image analysis software. MAP1LC3 was detected using an ELISA kit (ml000829, Mlbio, China) according to the manufacturer's instruction.

Cell Culture, Treatment, and shRNA Transfection

Human renal glomerular endothelial cells (HRGECs) were cultured in Endothelial cell medium (ECM, ScienCell Research Laboratories Carlsbad, CA, USA) containing 5% fetal bovine serum. Equipment Setup CO2 Incubator Culture HRGECs in a humidified atmosphere containing 5% CO2 at 37°C. Endothelial cells were prestarved in serum-free medium overnight and then treated with IL-1β, IL-6 and TNF-α for different hours or different concentrations.

HRGECs stable ATG16L-knockdown and ATG16L-overexpression were constructed using the lentivirus (Jikai, Shanghai, China). HRGECs was first transfected with the lipofectamine 2000, then transfected with 1.5 μL ATG16L shRNA viruses or 2.0 μL ATG16L overexpressing viruses according to the manufacturer's protocol. The endothelial cells were then switched into ECM containing 2.0 μL polybrene and incubated for an additional 6 h. We detected the infection rate of viruses with a Nikon Eclipse 80i fluorescence microscope (DS-Ri1, Nikon, Shanghai, China). Puromycin (2 μg/mL; Gibco, Thermo Fisher Scientific) was used to select stable virus-infected cells. Thereafter, HRGECs were collected for further experiments.

Statistical Analysis

GraphPad Prism 5.0 (GraphPad Software, Inc., La Jolla, CA, USA) was used for statistical analysis. Results were expressed as mean ± SD (mean ± SD) from at least three independent experiments. Comparison between and within multiple groups was performed using one-way analysis of variance followed by Student-Newman-Keuls test. P values of <0.05 were considered significant.

RESULTS

Changes of Histomorphology and Pathology in Kidney Tissues From the Non-CAD and CAD Patients

In this study, histological examination with hematoxylin-eosin (HE) and Masson's trichrome staining showed significant renal allograft IF/TA in CAD patients tissues (n = 4) compared to the kidney transplanted patients with stable renal function from our center (non-CAD group, n=4) (**Figures 1A, B**). Sample collection of materials and methods and **Table 1** describes the detailed grouping information for the original features. Immunohistochemistry staining (IHC) of human renal biopsy samples demonstrated a higher expression of α-SMA, and fibronectin (FN), and remarkably less expression of CD31 in the CAD group (**Figures 1C–H**). CD31 is a marker protein of endothelial cell, and endothelial cell lost its feature CD31 but acquired mesenchymal features such as α-SMA, FN when EndMT occurs. These results indicated that the expressions of EndMT markers were notably higher in the CAD groups compared to non-CAD group.

ATG16L Elevated After Kidney Transplantation, but ATG16L Was Downregulated in CAD Patients Comparing to the Non-CAD Patients

RNA-seq and clinical data from 25 CAD samples and 21 non-CAD patients' renal biopsies tissue samples were downloaded from GSE9493. Patients' information in the database were enrolled at Novartis Institutes for BioMedical Research, Switzerland and processed for histopathology. Histological diagnosis and biopsy classification based on Banff '05 criteria. Demographic and clinical data are provided in GEO database (https://www.ncbi.nlm.nih.gov/geo/query/acc.cgi?acc=GSE9493). Schematic diagram of the flow of analyses was as showed in **Figure 2A**. There were 1463 significant differential genes were extracted with P value <0.05. Using the criteria for [log2 fold change (log2FC)]> 1, we selected 92 up-regulated and 115 down-regulated differential genes from CAD group compared to the non-CAD group (**Figure 2B**). Then we searched genes associated with autophagy in the GeneCards database. A total of 149 ARGs with relevance score >7 were chosen. There were 14 ARGs included in CAD and non-CAD patients ARGs. Among them, we found that the ATG16L which got highest relevance score gene was downregulated in CAD samples (**Figure 2C**).

In order to avoid the batch effect and population differences, we performed a series of experiments using human specimens from our center to confirm public database results. In the first set, we

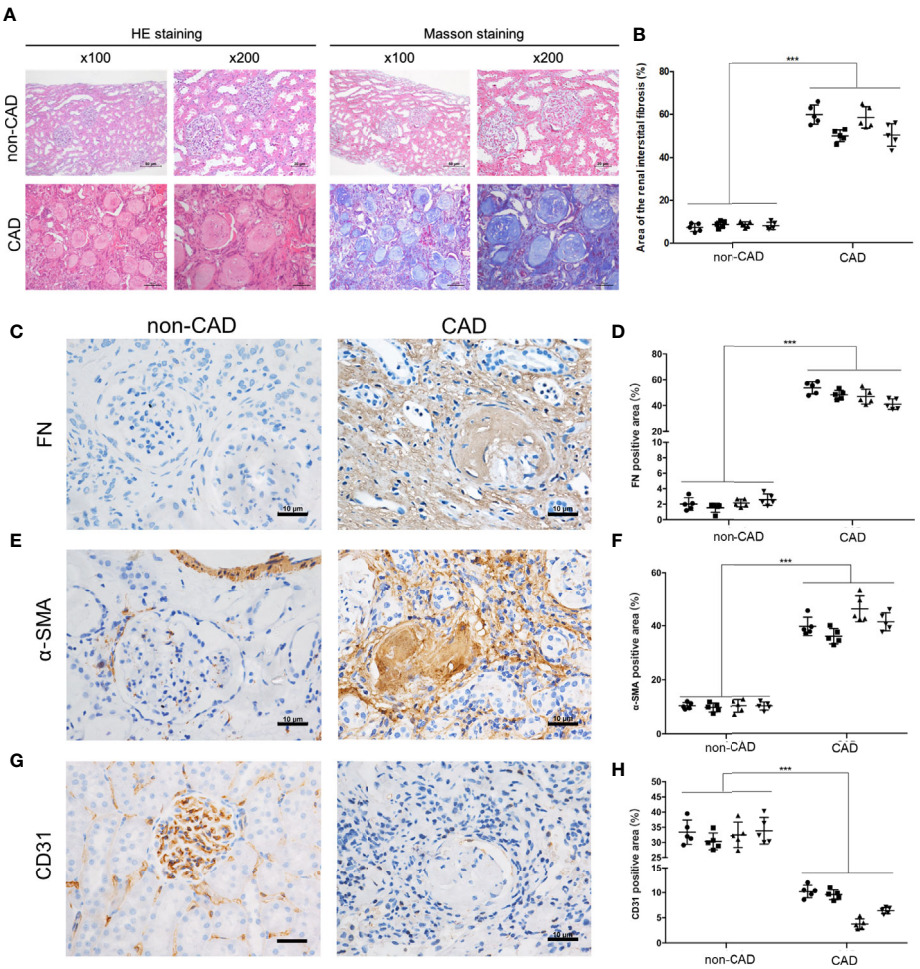

FIGURE 1 | Pathological and morphological changes in kidney tissues from the non-CAD and CAD patients. **(A)** Representative kidney sections from the non-CAD and CAD patients were stained with HE and Masson trichrome (×100, scale bar: 50 μm, ×200, scale bar: 20 μm). **(B)** Semi-quantitative analyses of the degree of fibrosis in 4 non-CAD patients' and 4 clinical CAD patients' kidney sections stained with Masson trichrome were performed. Each patient selected 5 different sites of transplanted kidney. (***P< 0.001, CAD vs. the non-CAD group, Student t test). **(C, E, G)** Distributions and expressions of FN, α-SMA and CD31 in the CAD and non-CAD group were assessed by IHC staining assays (×400, scale bar: 10 μm). **(D, F, H)** Percentage of the relative abundance of proteins were presented as the mean ± SD values of five independent experiments. Representative images of the kidney tissues of the non-CAD group (n = 4) and CAD group (n = 4) were shown. Each patient selected 5 different sites of transplanted kidney. (***P < 0.001, CAD vs. the non-CAD group, Student t test).

stained sections of normal, non-CAD and CAD renal samples with an anti-ATG16L antibody, and demonstrated that the expression of ATG16L was significantly reduced in CAD patients compared with non-CAD group (**Figure 2E**). The same conclusion was reached by western blot(WB) assay. The increase of FN represented aggravated fibrosis level of transplant kidney and one of the indicators of CAD. The WB tendency of ATG16L was congruity with the results of our IHC stain verification and consistent with the results in GEO (**Figure 2D**). These suggested that ATG16L expression was instead decreased with progression of CAD. When performing Pearson's correlation analysis, we found that ATG16L had strong negative correlation in the expression pattern of α-SMA, FN proteins and positive correlation with CD31 expression. 'r' represents the Pearson correlation value and P values denote significance of correlation (**Figures 2F–I**).

Autophagy Was Downregulated in CAD Patients, and Downregulation of MAP1LC3 Predicted Poor Prognosis in CAD Patients

In the previous experiment, a number of ARGs that regulate autophagy were identified from the GEO database. Among them, ATG16L is involved in the early step of autophagy, we speculate about the possibility that autophagy could be involved in CAD. To examine the levels of autophagy in human renal allograft tissues, we first found less autophagic vacuoles in CAD group through transmission electron microscope (TEM), compared to non-CAD group (**Figures 3A, B**). Besides the gold standard TEM for monitoring autophagy, decreased levels of SQSTM1 and increase of LC3-II expression reflect the increase of autophagy. Similar trends of protein expression levels of LC3-I (non-lipidation of LC3), LC3-II (lipidation of LC3) and SQSTM1

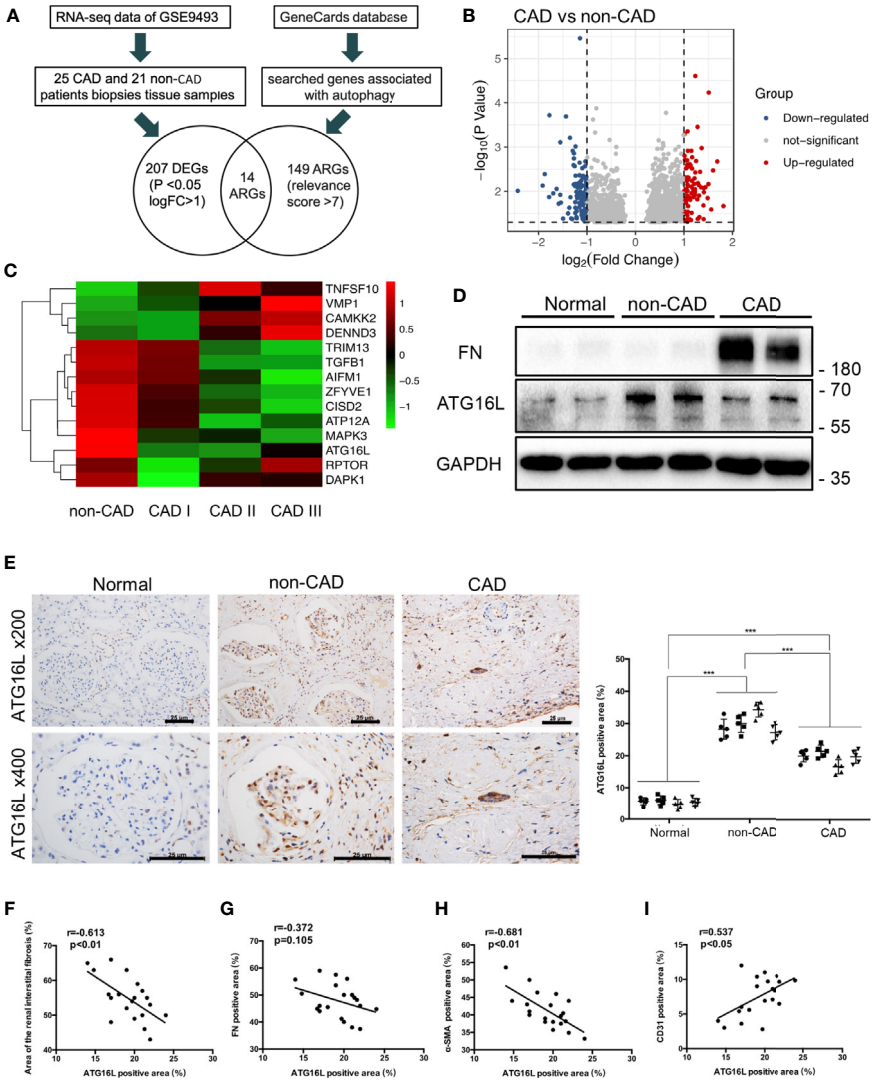

FIGURE 2 | ATG16L expressions in CAD and the non-CAD patients. **(A)** The diagram of the dataset recruitment workflow **(B)** Volcano plot of differential gene expression analysis between non-CAD (n=21) and CAD (n=25) kidney tissues from GEO profiles (GSE9493) **(C)** Heatmap indicating the differential expressions of the 20 selected ARGs. Expression values were presented in red and green to indicate expression upregulation and downregulation, respectively. **(D)** Representative western blot assay results of the protein expressions of ATG16L and FN in normal, non-CAD and CAD patient kidney tissues from our center. **(E)** Representative IHC images of ATG16L expressions in normal, non-CAD and CAD tissue (n=4) (×100, ×200, scale bar: 25 μm). Each patient selected 5 different sites of transplanted kidney. Semi-quantitative analyses of IHC staining were reported (***$P < 0.001$, vs. the non-CAD group, Student *t* test). **(F)** The correlation analysis between ATG16L and area of renal interstitial fibrosis (r=0.613, $P < 0.01$), **(G)** The correlation analysis between ATG16L and FN (r=0.372, P =0.105), **(H)** The correlation analysis between ATG16L and α-SMA (r=0.681, $P < 0.01$), **(I)** The correlation analysis between ATG16L and CD31(r=0.537, $P < 0.05$) were determined using Pearson correlation analysis. (n = 4, biological independent samples. Each patient selected 5 different sites of transplanted kidney).

in CAD group were verified by WB assay as shown in **Figures 3C, D**. P62/SQSTM1 (SQSTM1) is a selective autophagy receptor and is degraded by autophagy. Autophagosomes are associated with the lipidation of the cytosolic form of LC3 and forming of LC3-II. Thus, WB results also suggested that autophagy occurs.

Some studies have shown that there are differences of ARGs in the serum of kidney transplant patients; serum LC3 level probably was the prognostic indicator correlated with severity of the disease (25, 26). To further explore the role of autophagy in CAD procession, we examined the serum LC3 concentration of 30 non-CAD and 30 CAD patients by enzyme linked immunosorbent assay (ELISA). The demographic data presenting the basic features of the patients was in **Table 1**. Distributions of case number, patients sex, patients age, panel reactive antibodies (PRA), immunosuppressive regimen, renal function of the non-CAD and CAD groups were as shown in the **Table 1**. Sex, age, and PRA showed no major differences. There was a significant difference in serum creatinine and blood urea nitrogen (BUN) between the two groups. Then, we tried to

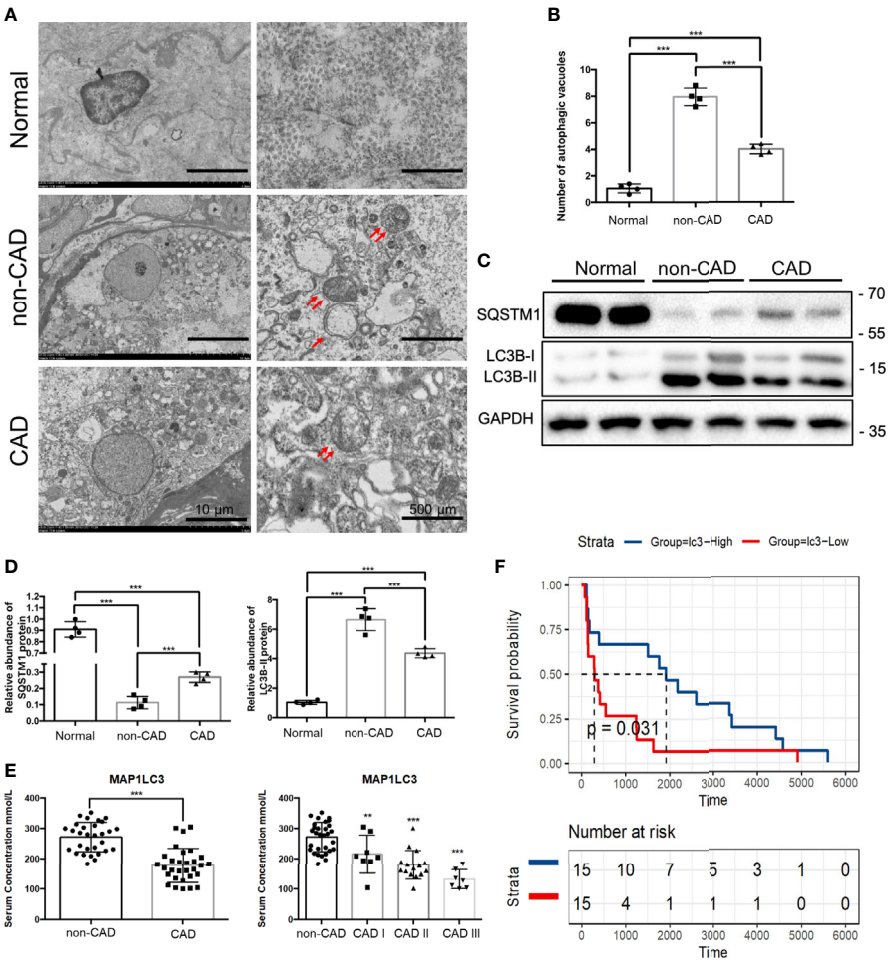

FIGURE 3 | Autophagy, MAP1LC3 expression and prognosis relationship in CAD patients. **(A)** Representative TEM images of autophagic vacuoles (red double arrow) were shown in glomerulus cells from normal, non-CAD and CAD patients (n=4) (scale bar: 10 μm and 500 μm). **(B)** Qualitative analysis of the number of autophagic vacuoles from three groups under TEM were shown. (***P < 0.001, Student t test.) **(C)** Representative western blot assay results of the protein expressions of SQSTM1 and LC3BI/II in normal, non-CAD and CAD patient kidney tissues were shown. (n=4) **(D)** Semi-quantitative analysis of Western blot assay results of SQSTM1 and LC3BI/II in normal, non-CAD and CAD patient kidney tissues. (***P < 0.001, Student t test.) **(E)** Serum concentrations of MAP1LC3 by *ELISA* assay in 30 non-CAD patients and 30 CAD patients with different degree. (***P < 0.001, **P < 0.01, vs. the non-CAD group, Student t test.) **(F)** Survival analysis of different MAPLC3 serum concentrations in 30 CAD patients based on data from *ELISA* assay. (P< 0.05, Student t test).

determine the prognostic value of autophagy in CAD patients. Through serum ELISA results, we found that the LC3 expression was lower in CAD group. There were also a progressive CAD and a simultaneous decrease in LC3 level (**Figure 3E**). In addition, we divided LC3 into high and low expression groups based on the median, survival analysis, the results revealed LC3 low expression group had shorter allograft dysfunction time (**Figure 3F**). Overall, we speculated that the deficiency of autophagy had a significant association with progression of CAD.

Downregulation of ATG16L Reduced Autophagy and Promoted Progression of EndMT

To determine whether ATG16L is involved in the change of autophagy, we first transfected HRGECs with ATG16L short hairpin RNA (shRNA). TEM was used to directly demonstrate autophagic vacuoles formation and we found that there are less autophagic vacuoles in cells transfected ATG16L shRNA compared with those transfected with scramble shNC (**Figures 4A, B**). Both of ATG16L protein expression and autophagy activity were also downregulated in knocking down ATG16L group compared with shNC group (**Figure 4C**).

The role of ATG16L-dependent autophagy in progression of EndMT was then investigated. HRGECs were transfected with ATG16L shRNA or shNC. **Figure 4D** showed that ATG16L shRNA transfection could markedly facilitate FN and α-SMA expressions and decrease CD31 expression compared with scramble shNC-transfected HRGECs. In contrast, when the ATG16L were overexpressed in HRGECs, the progression of EndMT did not significantly promote (**Figure 4E**). IHC staining results also confirmed WB trends for CD31 and α-SMA expressions in HRGECs (**Figure 4F**).

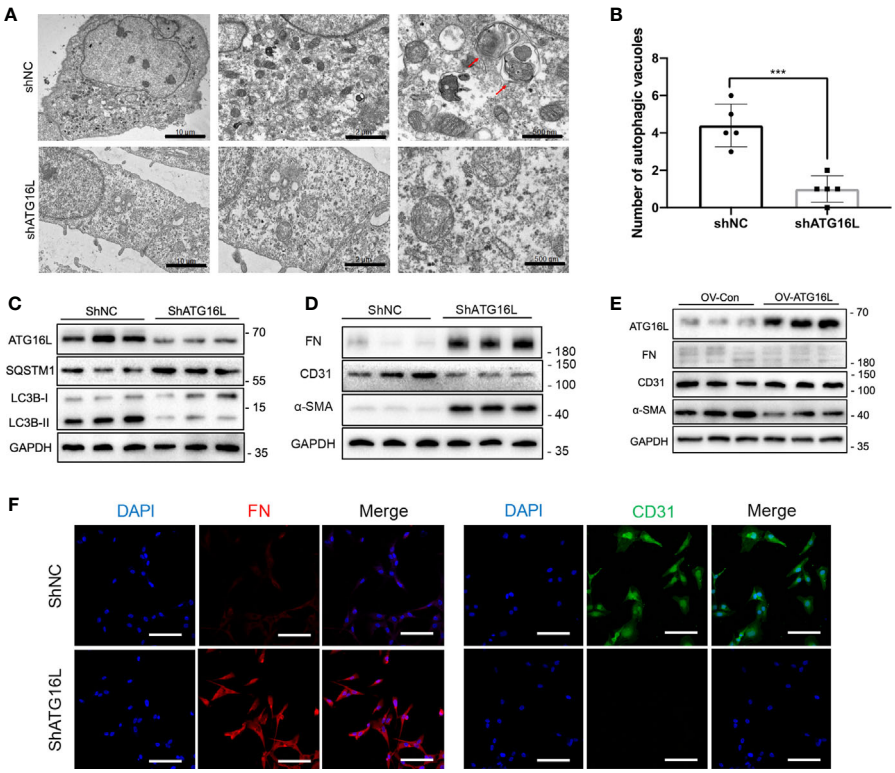

FIGURE 4 | Effects on autophagy and progression of EndMT in HRGECs after knockdown of ATG16L. **(A)** Representative TEM images of autophagic vacuoles (red arrow) were shown in shNC group and shATG16L group (n=5) (scale bar: 10 μm, 2 μm and 500 μm). **(B)** Qualitative analysis of the number of autophagic vacuoles from two groups under TEM were shown. (***$P < 0.001$, Student *t* test.) **(C)** Western blot assay results of the ATG16L, SQSTM1 and LC3BI/II proteins in HRGECs transfected with shNC or shATG16L. (n=5) **(D)** Expressions of FN, α-SMA and CD31 protein in HRGECs transfected with shNC or shATG16L. (n=5) **(E)** Expressions of ATG16L, FN, α-SMA and CD31 protein in HRGECs overexpressed of ATG16L or not. (n=5) **(F)** Representative images of IF staining of FN and CD31 in HRGECs transfected with shNC or shATG16L. Scale bar: 20 μm (n=5).

Changes of Renal Interstitial Fibrosis, Urine Protein, Renal Function and Time-Dependent Increases of EndMT in Chronic Rejection Rat Model

Next, we investigated the changes of renal interstitial fibrosis, urine protein, renal function and EndMT *in vivo*. Rat renal transplanted models of chronic rejection were established by kidney transplantation from F344 rats to Lewis rats. Renal allografts were taken at weeks 8, 12, and 16 after kidney transplantation. HE staining and Masson staining assays indicated that varying degrees of inflammatory cell infiltration, glomerulosclerosis, tubular atrophy, and interstitial fibrosis after kidney transplantation. The results of Masson staining also showed a large amount of blue-stained collagen fibers in the glomerular and renal interstitium at weeks 8, 12, 16 after kidney transplantation, compared with the syn group (**Figures 5A–C**).

In order to test the renal function of rats with allogeneic transplant, the native right kidneys were extirpated during the kidney transplantation. Four weeks after the resection of right kidney, 24 h urine protein and renal functions including the serum creatinine and BUN deteriorated gradually in allo groups until their death (**Figure 5D**). The outcomes of IHC assay revealed high expressions of FN and α-SMA while CD31 expression reduced in allo groups at 16 weeks (**Figure 5E**). Western blot assay confirmed the outcomes of immunohistochemistry assay and showed that progression of EndMT was intensified with the extension of the time after kidney transplantation (**Figure 5F**).

Kidney Transplantation Activated Autophagy but Impaired Autophagic Flux in Late Stage of Chronic Rejection Rat Model

LC3, which is considered as a defined marker for autophagy, is critical for autophagosome formation and the activation of autophagic flux. Adeno-associated virus (AAV)-mRFP-GFP-LC3 was injected into the rat renal allograft *in vivo* stereotactically. We create a mRFP-GFP-LC3 model in order to monitor autophagic activity in kidney transplantation. AAV-mRFP-GFP-LC3 is usually used to monitor autophagic flux *in vivo*. GFP signal has higher sensitivity to the acidic conditions of lysosomal lumen than mRFP. Thus, autophagosomes exhibited yellow fluorescence because of the co-location of GFP and mRFP fluorescence indicate and autolysosomes showed red

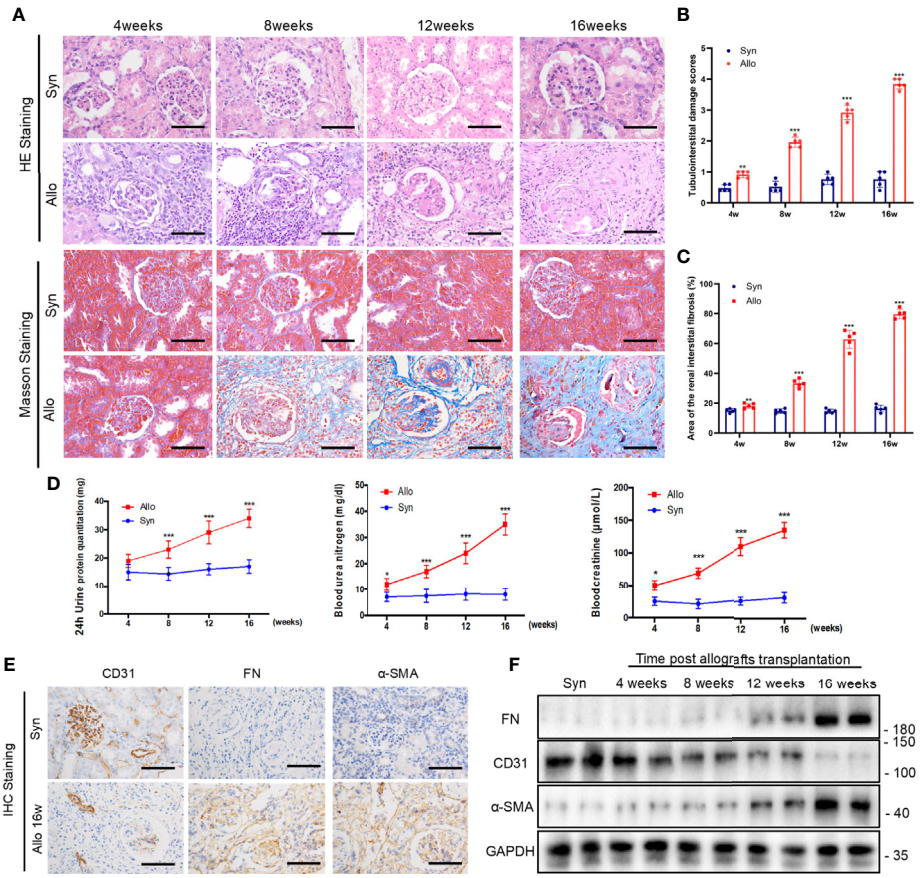

FIGURE 5 | Changes of renal interstitial fibrosis, urine protein, renal function and EndMT in chronic rejection rat model. **(A)** Representative images of HE and Masson's trichrome staining from kidney tissues of syn and allo groups (scale bar: 25 μm). **(B)** The statistical analyses of tubulointerstitial damage scores in syn and allo group. Data were expressed as the mean ± SD of each group. (n = 5, ***$P < 0.001$, **$P < 0.01$, vs. the same weeks syn group, Student *t* test.) **(C)** Semi-quantitative analyses of positive areas of renal interstitial fibrosis were performed from Masson staining assay results. Data were expressed as the mean ± SD of each group (n = 5, ***$P < 0.001$, **$P < 0.01$, vs. the same weeks syn group, Student *t* test.). **(D)** Renal function parameters (serum Cr and BUN) and 24h urine protein quantitation in syn and allo group. Values represent the mean ± SD, (n = 5, ***$P < 0.001$, *$P < 0.05$, vs. the same weeks syn group, Student *t* test.) **(E)** Representative IHC staining images of EndMT markers (FN, α-SMA and CD31) in kidney sections from syn group and 16 weeks allo group rats (scale bar: 25 μm). **(F)** Representative western blot analysis results of EndMT markers in rat kidney tissues from syn group and different allo group. (n=5).

fluorescence. Increase of red fluorescence indicated an accumulation of autolysosomes and activation of autophagy in the kidney. The positive areas of red fluorescence significantly increased at weeks 4, 8,12 and 16 in the allo group compared with the syn group. However, the red puncta weakened rapidly after reaching the peak at 8 and 12 weeks. Changes in the level of autophagy were mainly observed in the glomerular and peripheral small vessel, rather than in the distal tubules or collecting duct (**Figures 6A, B**). These results revealed that autophagy was activated in the early stages of kidney transplantation but not the late stages, and autophagosome clearance was impaired after about 8 weeks. Immunohistochemistry assay demonstrated that the expression of ATG16L was higher in 8 weeks than 16 weeks (**Figure 6C**). Western blot results also showed LC3-II and ATG16L levels peaked at 8 weeks, and then gradually decreased until 16 weeks in rat allograft kidneys after transplantation (**Figure 6D**).

NF-κB Pathway Was Activated and Promoted EndMT After Knockdown of ATG16L Expression

In light of the association between ATG16L downregulation and EndMT in chronic rejection rat model and CAD disease, we hypothesized that loss of ATG16L could directly lead to the progression of EndMT. To further explore the potential mechanism by which this progression occurs, we first performed total transcriptome sequencing (RNA-seq) in HRGECs with ShNC or ShATG16L. A total of 453 differential genes (DEGs)were obtained between two groups. Among them, 358 DEGs were up-regulated and 95 were down-regulated (**Figure 7A**). Then 20 pathways were significantly selected by KEGG enrichment. We found that NF-κB pathway was one of the pathways that were significantly activated (**Figure 7B**). Upregulation of the NF-κB pathway genes was also confirmed by Gene set enrichment analysis (GSEA) (**Figure 7C**).

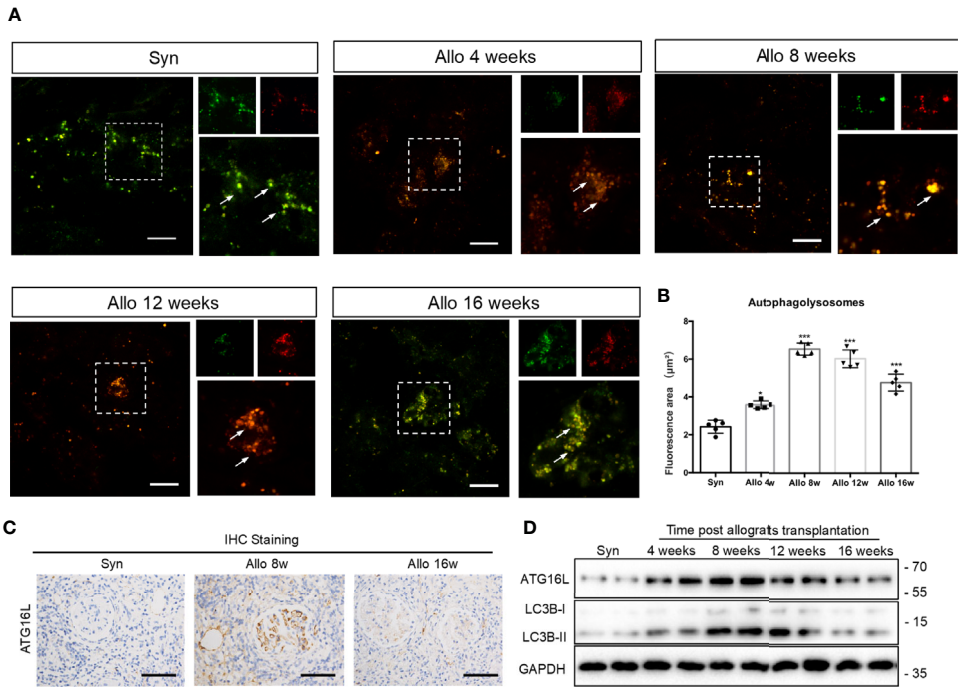

FIGURE 6 | Changes of autophagy activity in chronic rejection rat models. **(A)** Representative images of cortical kidney sections obtained from syn and different periods after kidney transplanted rats injected with AAV-mRFP-GFP-LC3. Arrows indicated the glomerular site. Scale bar: 20 μm **(B)** Semi-quantification analyses of the percentage of autolysosomes (red puncta/total puncta) in the images. The data were presented as mean ± SD (n = 5, ***$P < 0.001$, *$P < 0.05$, vs. the syn group). More than 100 cells were quantified for each image in each experiment. **(C)** Representative IHC staining images of ATG16L expressions in syn group, 8 weeks and 16 weeks allo group rats. (n=5) **(D)** Representative western blot assay results of ATG16L and LC3BI/II levels in kidney tissue from syn and allo group rats. (n=5).

NF-κB is one of the crucial transcription factor for inflammatory signaling pathways, and NF-κB will translocate from cytoplasm to nucleus when it is activated. In order to confirm the NF-κB activation and nuclear translocation, we performed the immunofluorescence staining assay using anti-p65 antibody, and found p65 and the nuclear dye were colocalized which indicated nuclear translocation (**Figure 7D**). In addition, we found that QNZ, a NF-κB signaling pathway inhibitor, significantly inhibited the expression of NF-κB in nucleus, and reversed the expressions of EndMT related proteins induced by knockdown of ATG16L (**Figure 7E**).

WB assay was also carried out to verify the specific mechanism of NF-κB pathway activation. We detected quantification of p65 (total NF-κB) and p-p65 (phosphorylated NF-κB) in HRGECs. WB results showed that p65 level was increased in ShATG16Lgroup compared to ShNC group, while p-p65 followed a similar increasing trend (**Figure 7F**). The increase in p-p65 level in HRGECs after knockdown ATG16L was accompanied by an increase in total p65 protein expression, which likely reflected an additional effect on p65 expression in HRGECs. To detected whether stabilization of NF-κB is due to decreased degradation or increased synthesis, protein synthesis inhibitor cycloheximide (CHX) was added to the cells to inhibit protein synthesis and the NF-κB protein level was analyzed. Western blot results showed that there is continued expression of p65 protein in the presence of CHX (**Figure 7G**). Meanwhile, NF-κB mRNA levels were not yet significantly altered by ShATG16L. The quantitative data for the levels of NF-κB mRNA were as indicated graphically in **Figure 7H**. This suggested that NF-κB nuclear translocation was due to decreased degradation, not increased synthesis after knockdown of ATG16L in HRGECs. To further confirm the expression of NF-κB in human tissue, we performed immunofluorescence staining assay on achieved human renal allograft tissues and found expression level of p65 significant increase in renal allografts of CAD patient (**Figures 7I, J**).

NF-κB Pathway Activation Induced Cytokines Secretion, Among Them IL-1β, IL-6, and TNF-α Could Stimulate Progression of EndMT in HRGECs

NF-κB signaling is a master regulator of the inflammatory response. We then explored the soluble factors responsible for shATG16L-induced EndMT by RT-PCR. Among the several cytokines that are relevant to the autophagy defects and inflammatory response, IL-1β, IL-6 and TNF-α, the typical downstream inflammatory factors induced by NF-κB pathway, were significantly elevated when compared with shNC-transfected HRGECs during impairment of autophagy activity (**Figure 8A**). This is in line with our previous findings of

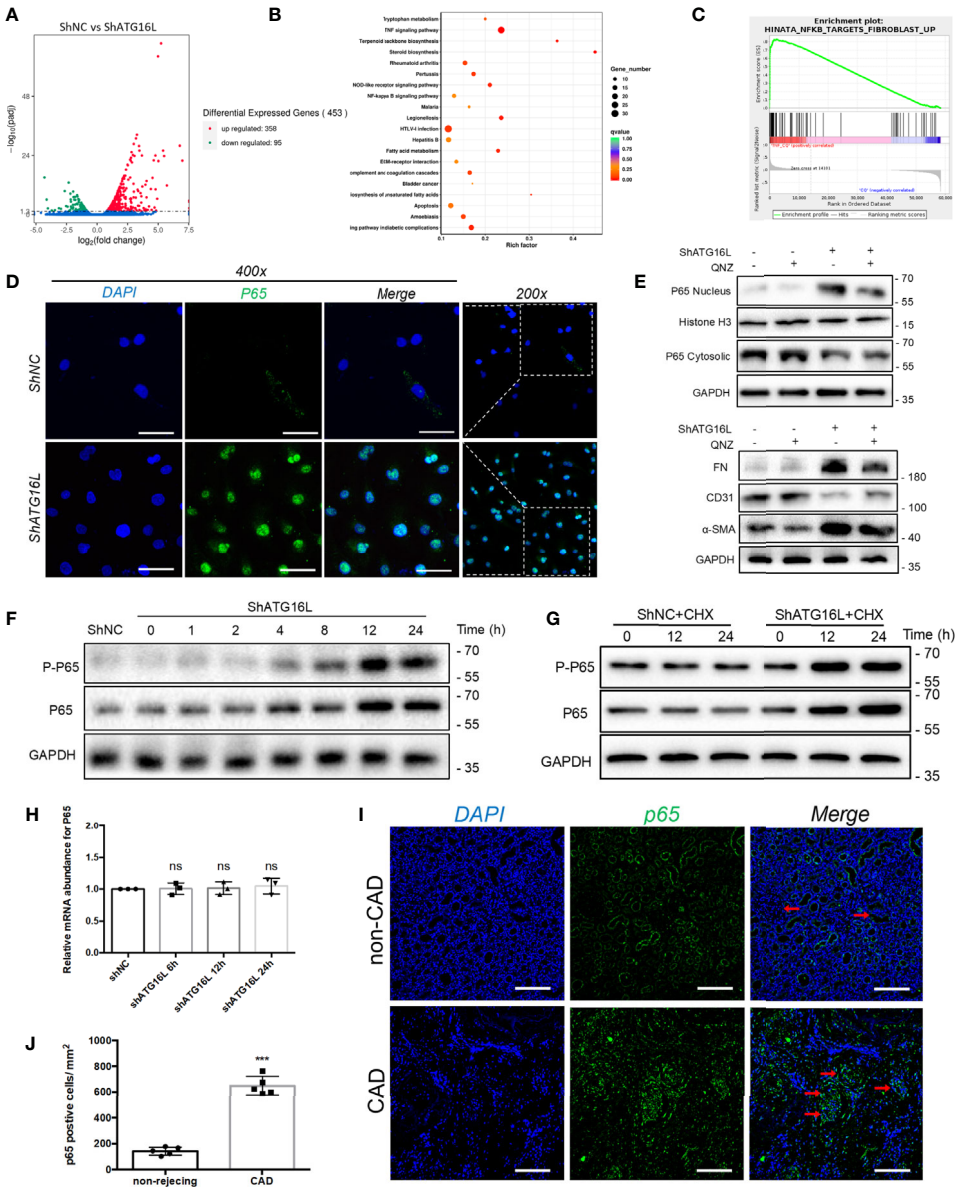

FIGURE 7 | NF-κB pathway activation and effect on EndMT in HRGECs after knockdown of ATG16L **(A)** The RNA sequencing results of differential genes in HRGECs transfected with shNC or shATG16L were plotted by volcano plot. (n=5) **(B)** KEGG pathway analyses of the top 20 KEGG enriched gene pathways. **(C)** GSEA plot of the correlation between knockdown of ATG16L and NF-κB enrichment gene signatures in the RNA sequencing results. **(D)** Representative images of p65 expression and distribution by indirect immunofluorescence staining assay in HRGECs transfected with shNC or shATG16L under confocal microscopy. Scale bar: 50 μm. (n=5) **(E)** Representative western blot results of the effects of NF-κB inhibitor (QNZ) on NF-κB nuclear translocation and EndMT markers (FN, α-SMA and CD31) expressions in HRGECs transfected with shATG16L or not. (n=5) **(F)** Representative western blot results of p65 and p-p65 (Ser536) expressions after knocking down ATG16L for different time. (n=5) **(G)** Representative western blot results of p65 and p-p65 (Ser536) expressions with CHX treatment for different time in shNC and shATG16L group. (n=5) **(H)** The mRNA levels of p65 in HRGECs transfected with shNC or shATG16L. (n=5, NS, not significant, vs. the shNC group, Student *t* test.) **(I)** Representative images of p65 expression and distribution in the non-CAD and CAD allograft renal tissues *via* indirect immunofluorescence staining assay (scale bar: 25 μm). **(J)** Semi-quantitative analysis results for indirect immunofluorescence staining assay of p65 in the non-CAD and CAD allograft renal tissue (n = 4, ***$P < 0.001$, vs. the non-CAD group, Student *t* test).

inflammatory factors such as TNF-α increase in the rat serum with chronic rejection (27).

To investigate the pathogenesis of EndMT stimulated by IL-1β, IL-6 and TNF-α, we treated the HRGECs with different concentrations of IL-1β (0~20 ng/mL), IL-6 (0~200 ng/mL) and TNF-α (0~20 ng/mL) for 24 hours. All of IL-1β, IL-6 and TNF-α could upregulate the protein level of FN and α-SMA with a dose-dependent decline of the endothelial cell markers CD31 simultaneously. These effects were peaked when HRGECs were treated with 10 ng/mL IL-1β, 200 ng/mL IL-6 or 10 ng/mL

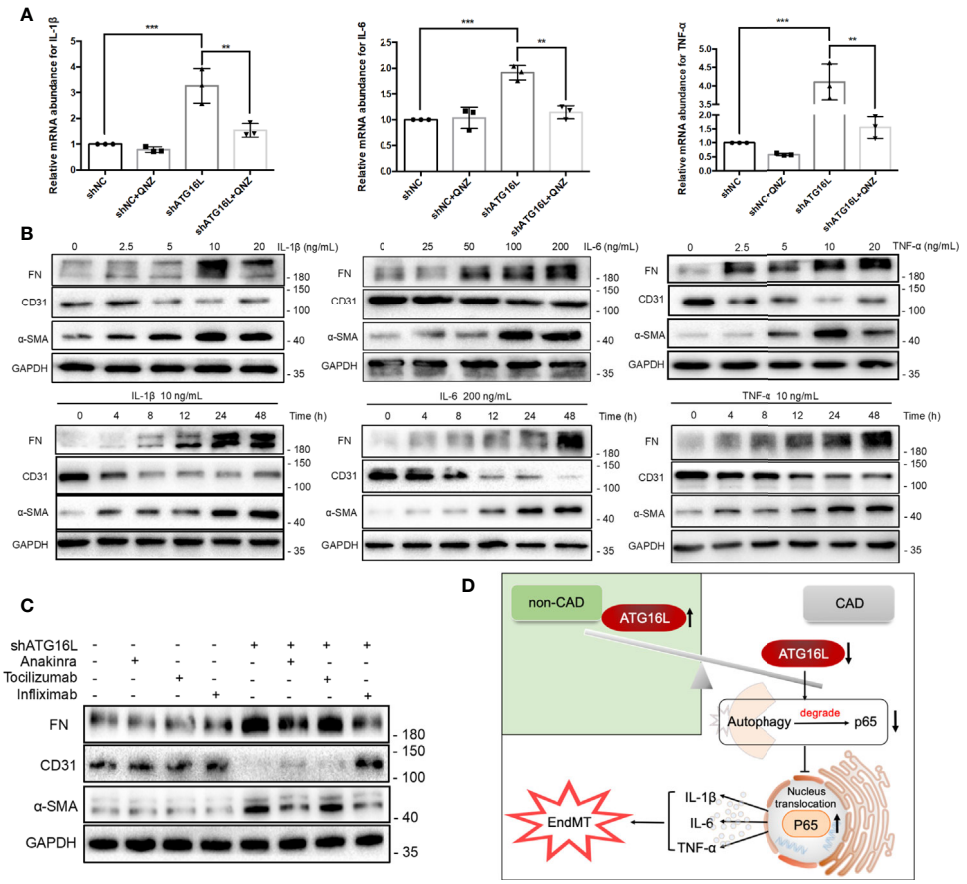

FIGURE 8 | Cytokines induced by NF-κB pathway activation and effects on progression of EndMT in HRGECs. **(A)** The graphs of the results of mRNA abundance of IL-1β, IL-6 or TNF-α after knocking down ATG16L with or without QNZ. (n = 5, ***$P < 0.001$, **$P < 0.01$, vs. the shNC group, Student *t* test.) **(B)** Representative western blotting results of the expressions of FN, CD31, α-SMA and GAPDH in HRGECs after IL-1β, IL-6 or TNF-α treatment for different times or dosage. (n=5) **(C)** Representative western blot results of FN, CD31, α-SMA and GAPDH expressions treated with or without Anakinra, Tocilizumab and Infliximab in HRGECs transfected with shATG16L or not. (n=5) **(D)** A model is proposed to illustrate the mechanisms involved in EndMT induced by loss of ATG16L in the pathogenesis of CAD and transplanted renal interstitial fibrosis.

TNF-α, respectively (**Figure 8B**). Time dependencies experiment were also performed to validate the related expressions of EndMT. As shown in **Figure 8B**, IL-1β, IL-6 or TNF-α treatment for 0~48 h could remarkably induced FN and α-SMA expressions and led to the loss of CD31 in HRGECs as the stimulus time increases. To test the effects of IL-1β, IL-6 and TNF-α on EndMT, Anakinra, Tocilizumab and Infliximab treatment were initiated when knocking down ATG16L. Anakinra is an antagonist of interleukin-1 receptor (IL-1R). Tocilizumab is an IL-6R neutralizing antibody that blocks IL-6 from binding to IL-6R. Infliximab is a monoclonal IgG1 antibody that binds specifically to TNF-α and is a TNF-α inhibitor that has been successfully used in the management of inflammatory bowel disease. WB results showed that Anakinra and Infliximab could reduce the EndMT more pronouncedly (**Figure 8C**). These results suggested that the loss of ATG16L was not only reduced autophagy activity but also promoted the secretion of inflammatory cytokines IL-1β, IL-6 and TNF-α by suppressing p65 degradation to activated the NF-κB pathway (**Figure 8D**).

DISCUSSION

In this present study, we showed that kidney transplantation impaired the autophagic flux, which was associated with an increase in the inflammatory response, EndMT and the severity of renal allografts interstitial fibrosis. Although autophagic activity was temporarily increased at the early stages of allograft transplantation, it gradually decreased due to loss of ATG16L. ATG16L-dependent autophagy, as a cytoprotective process, could attenuate the transplanted kidney interstitial fibrosis *via* the regulation of the EndMT induced by IL-1β, IL-6 and TNF-α. To the best of our knowledge, this is the first study that elucidates the role and dynamic change of autophagic flux in kidney transplantation. In this study, we also investigated the molecular pathophysiologic details underlying the way in which impairment of autophagic flux results in EndMT and renal allograft interstitial fibrosis.

Although many researches have reported that autophagy is involved in the formation and progression of renal interstitial fibrosis, ARGs has not been comprehensively analyzed to explore

their clinical value in the progression of chronic renal graft rejection. Hundreds of proteins are associated with the process of autophagy. Given the importance of autophagy in kidney transplantation, it is reasonable to speculate that ARGs hold great promises in prognostic prediction and therapeutic targets. In order to explore the original pathogenetic factors of CAD, we profiled the mRNA expressions of 149 ARGs in the GSE9493 cohort and emphatically analyzed 14 ARGs, which were most associated with autophagy between CAD and non-CAD patients. Among the downregulated ARGs in CAD group, autophagy negative regulatory genes, such as Raptor and MAPK3 (28, 29), were downregulated in CAD group. On the other hand, ATG16L as an up-regulated ARG was scaffold for LC3 lipidation by dynamically localizing to the putative source membranes and promoted autophagic vacuole formation (30). However, some studies have shown that ATG16L was not required for the elongation of the isolation membrane (23). Hence, the association between autophagy-independent or autophagy-dependent role of ATG16L and EndMT was studied.

To investigate the association among ATG16L, autophagy and EndMT in the transplanted kidneys, we knocked down ATG16L by shRNA in HRGECs. Our findings revealed that shATG16L could reduce autophagy level and induce EndMT. Similarly, *in vivo* research and clinical samples also revealed that activation of ATG16L and autophagic flux in the early stage of kidney transplantation, autophagic flux declined in a dynamic range as the fibrotic changes increased. It may be concluded that the reason for EndMT progression is probably due to autophagic flux reduction, and ATG16L-dependent autophagy play a protective role in the progression of EndMT and renal allograft interstitial fibrosis. However, some findings showed that rapamycin-induced autophagy led to activation of EndMT in HCAECs under the anoxic condition (22). These seem to be distinct from our results. We consider that role of autophagy might be different in diverse cell types. It could be cellular context- and upstream regulatory factors- dependent. Giving that ATG16L-dependent autophagy is a means of self-protection when EndMT occur in CAD, it is meaningful to determine the specific mechanism of shATG16L-induced EndMT.

We performed next-generation sequencing from the group of ATG16L knockdown and control group in HRGECs. KEGG pathways and GSEA analysis revealed that NF-κB pathway was one of the most significantly enriched pathways. NF-κB normally binds to IκB, which stabilizes NF-κB in the cytoplasm. When the NF-κB pathway is activated, NF-κB heterodimer p65 translocates to the nucleus and binds to its specific promoter (31). One of the canonical (classical) pathways for NF-κB nuclear translocation is p65 phosphorylation. However, increase in the number of non-canonical pathways have been reported in different diseases. It has also been reported that the suppressed p62/SQSTM1-mediated selective autophagy could reduce NF-κB pathway lysosomal degradation (32), autophagy defect also leads to NF-κB activation because of sustained SQSTM1 expression, which in turn promotes tumorigenesis in mouse models (33). In our study, we observed an increase in p65 and p-p65 protein levels while the mRNA levels were unchanged. In the presence of a protein synthesis inhibitor CHX, accumulation of the p65 protein still continue compared with the absence of inhibitor. We therefore speculated that NF-κB activation induced by knockdown of ATG16L was resulted from reduced protein degradation and this process might be autophagic dependent degradation suppression.

Inflammations are strictly interconnected with important consequences of kidney transplant at clinical and therapeutic level (34). The NF-κB p65 is the most important transcription factor in the regulation of cellular inflammatory factors. In this study, we also found knocking down ATG16L increased cytokine IL-1β, IL-6 and TNF-α through NF-κB pathway. This and other findings agree with the many other studies such as the ones that concluded that loss of ATG16L enhanced endotoxin-induced IL-1β production (35) and TNFAIP3/A20 binds ATG16L1 to control the autophagic response, NF-κB activation (36). Furthermore, the role of inflammatory cytokines on EndMT has been reported in some earlier studies. Nevertheless, it is probable these inflammatory cytokines play a diverse role depending on the underlying pathology and its ambient levels. In diet-induced obesity mouse model endothelial autophagy deficiency induced IL6-dependent EndMT (37). In vascular calcification disease, IL-1β and TNF-α induced EndMT in human primary aortic endothelial cells (38). Our results screened and identified IL-1β, IL-6 and TNF-α as the promoting EndMT inflammatory cytokines in pathological environments of CAD. Herewith, the reciprocal relationships between loss of ATG16L and inflammatory cytokines were researched to underline the possible therapeutic targets to control loss of ATG16L in CAD progression.

Our research has several limitations. The current validation of the effects of ATG16L on EndMT and fibrosis progression were only conducted in knockdown cell line model, the complexity of autophagy alterations *in vivo* and in the development of CAD can hardly be mimicked and underlines the need for endothelial ATG16L conditional knockout mice. We will establish ATG16L knockout mouse renal transplant model for further mechanism study. Our results showed that the loss of ATG16L and autophagy promoted EndMT, QNZ inhibited NF-κB activation and IL-1β, TNF-α monoclonal antibody antagonized specific receptors thereby slowed down the allograft fibrotic process, but it could not completely reverse this outcome. Whether other mechanisms were playing a similar role remains unknown. Additionally, besides endothelial cells, the source of myofibroblasts consists of a variety of cells, including epithelial, fibroblasts and pericytes (39). Whether the loss of ATG16L and autophagy deficiency affect these cells is still inconclusive.

In conclusion, the current studies proved that knockdown of ATG16L was vital for impairment of autophagic flux and EndMT formation induced by IL-1β, IL-6 and TNF-α in progression of transplanted renal interstitial fibrosis. This function was mediated by NF-κB reducing degradation and pathway activation. In summary, the results of our study provide novel insight into the dynamic relationship of autophagic flux and EndMT. Preventing ATG16L loss and autophagy flux inhibition could be a new option for the treatment and prevention of progression of renal interstitial fibrosis and CAD in kidney transplanted recipients.

DATA AVAILABILITY STATEMENT

The raw data supporting the conclusions of this article will be made available by the authors, without undue reservation.

ETHICS STATEMENT

The studies involving human participants were reviewed and approved by the local ethics committee of the First Affiliated Hospital of Nanjing Medical University. The patients/participants provided their written informed consent to participate in this study. The animal study was reviewed and approved by the local ethics committee of the First Affiliated Hospital of Nanjing Medical University. Written informed consent was obtained from the owners for the participation of their animals in this study.

AUTHOR CONTRIBUTIONS

RT and MG supervised and conceived the project. ZG, CS, and ZW designed and carried out most of the experiments. MZ and SF collected the samples of rats. LS, HC, ZH, JT, XJ, and HY analyzed the data. ZG and ZW made the figures. ZG and RT drafted and revised the paper. All authors contributed to the article and approved the submitted version.

FUNDING

This work has been supported by the National Natural Science Foundation of China [grant numbers 82070769, 81870512, 81770751, 81570676, 81470981, 81100532].

REFERENCES

1. Carney EF. Transplantation: Survival benefit of accepting a diabetic deceased donor kidney. *Nat Rev Nephrol* (2017) 13(8):444. doi: 10.1038/nrneph.2017.88
2. El-Husseini A, Aghil A, Ramirez J, Sawaya B, Rajagopalan N, Baz M, et al. Outcome of kidney transplant in primary, repeat, and kidney-after-nonrenal solid-organ transplantation: 15-year analysis of recent UNOS database. *Clin Transplant* (2017) 31(11). doi: 10.1111/ctr.13108
3. Schinstock CA, Stegall M, Cosio F. New insights regarding chronic antibody-mediated rejection and its progression to transplant glomerulopathy. *Curr Opin Nephrol Hypertens* (2014) 23(6):611–8. doi: 10.1097/MNH.0000000000000070
4. Goldberg RJ, Weng FL, Kandula P. Acute and Chronic Allograft Dysfunction in Kidney Transplant Recipients. *Med Clin North Am* (2016) 100(3):487–503. doi: 10.1016/j.mcna.2016.01.002
5. Wang Z, Han Z, Tao J, Wang J, Liu X, Zhou W, et al. Role of endothelial-to-mesenchymal transition induced by TGF-beta1 in transplant kidney interstitial fibrosis. *J Cell Mol Med* (2017) 21(10):2359–69. doi: 10.1111/jcmm.13157
6. An C, Jia L, Wen J, Wang Y. Targeting Bone Marrow-Derived Fibroblasts for Renal Fibrosis. *Adv Exp Med Biol* (2019) 1165:305–22. doi: 10.1007/978-981-13-8871-2_14
7. Cruz-Solbes AS, Youker K. Epithelial to Mesenchymal Transition (EMT) and Endothelial to Mesenchymal Transition (EndMT): Role and Implications in Kidney Fibrosis. *Results Probl Cell Differ* (2017) 60:345–72. doi: 10.1007/978-3-319-51436-9_13
8. Yang J, Antin P, Berx G, Blanpain C, Brabletz T, Bronner M, et al. Guidelines and definitions for research on epithelial-mesenchymal transition. *Nat Rev Mol Cell Biol* (2020) 21(6):341–52. doi: 10.1038/s41580-020-0237-9
9. Zeisberg EM, Potenta SE, Sugimoto H, Zeisberg M, Kalluri R. Fibroblasts in kidney fibrosis emerge via endothelial-to-mesenchymal transition. *J Am Soc Nephrol* (2008) 19(12):2282–7. doi: 10.1681/ASN.2008050513
10. Di Gregorio J, Robuffo I, Spalletta S, Giambuzzi G, De Iuliis V, Toniato E, et al. The Epithelial-to-Mesenchymal Transition as a Possible Therapeutic Target in Fibrotic Disorders. *Front Cell Dev Biol* (2020) 8:607483. doi: 10.3389/fcell.2020.607483
11. Cardinal H, Dieude M, Hebert MJ. Endothelial Dysfunction in Kidney Transplantation. *Front Immunol* (2018) 9:1130. doi: 10.3389/fimmu.2018.01130
12. Zhao Y, Cooper DKC, Wang H, Chen P, He C, Cai Z, et al. Potential pathological role of pro-inflammatory cytokines (IL-6, TNF-alpha, and IL-17) in xenotransplantation. *Xenotransplantation* (2019) 26(3):e12502. doi: 10.1111/xen.12502
13. Zhao C, Xu Z, Wang Z, Suo C, Tao J, Han Z, et al. Role of tumor necrosis factor-alpha in epithelial-to-mesenchymal transition in transplanted kidney cells in recipients with chronic allograft dysfunction. *Gene* (2018) 642:483–90. doi: 10.1016/j.gene.2017.11.059
14. Zhang B, Niu W, Dong HY, Liu ML, Luo Y, Li ZC. Hypoxia induces endothelialmesenchymal transition in pulmonary vascular remodeling. *Int J Mol Med* (2018) 42(1):270–8. doi: 10.3892/ijmm.2018.3584
15. Li J, Zhang Q, Ren C, Wu X, Zhang Y, Bai X, et al. Low-Intensity Pulsed Ultrasound Prevents the Oxidative Stress Induced Endothelial-Mesenchymal Transition in Human Aortic Endothelial Cells. *Cell Physiol Biochem* (2018) 45(4):1350–65. doi: 10.1159/000487561
16. Guan Q, Nguan CY, Du C. Expression of transforming growth factor-beta1 limits renal ischemia-reperfusion injury. *Transplantation* (2010) 89(11):1320–7. doi: 10.1097/TP.0b013e3181d8e9dc
17. Levine B, Kroemer G. Biological Functions of Autophagy Genes: A Disease Perspective. *Cell* (2019) 176(1-2):11–42. doi: 10.1016/j.cell.2018.09.048
18. De Rechter S, Decuypere JP, Ivanova E, van den Heuvel LP, De Smedt H, Levtchenko E, et al. Autophagy in renal diseases. *Pediatr Nephrol* (2016) 31(5):737–52. doi: 10.1007/s00467-015-3134-2
19. Li H, Peng X, Wang Y, Cao S, Xiong L, Fan J, et al. Atg5-mediated autophagy deficiency in proximal tubules promotes cell cycle G2/M arrest and renal fibrosis. *Autophagy* (2016) 12(9):1472–86. doi: 10.1080/15548627.2016.1190071
20. Baisantry A, Bhayana S, Rong S, Ermeling E, Wrede C, Hegermann J, et al. Autophagy Induces Prosenescent Changes in Proximal Tubular S3 Segments. *J Am Soc Nephrol* (2016) 27(6):1609–16. doi: 10.1681/ASN.2014111059
21. Hill C, Li J, Liu D, Conforti F, Brereton CJ, Yao L, et al. Autophagy inhibition-mediated epithelial-mesenchymal transition augments local myofibroblast differentiation in pulmonary fibrosis. *Cell Death Dis* (2019) 10(8):591. doi: 10.1038/s41419-019-1820-x
22. Sasaki N, Itakura Y, Toyoda M. Rapamycin promotes endothelial-mesenchymal transition during stress-induced premature senescence through the activation of autophagy. *Cell Commun Signal* (2020) 18(1):43. doi: 10.1186/s12964-020-00533-w
23. Ishibashi K, Fujita N, Kanno E, Omori H, Yoshimori T, Itoh T, et al. Atg16L2, a novel isoform of mammalian Atg16L that is not essential for canonical autophagy despite forming an Atg12-5-16L2 complex. *Autophagy* (2011) 7(12):1500–13. doi: 10.4161/auto.7.12.18025
24. Slowicka K, Serramito-Gomez I, Boada-Romero E, Martens A, Sze M, Petta I, et al. Physical and functional interaction between A20 and ATG16L1-WD40 domain in the control of intestinal homeostasis. *Nat Commun* (2019) 10(1):1834. doi: 10.1038/s41467-019-09667-z
25. Li L, Khatri P, Sigdel TK, Tran T, Ying L, Vitalone MJ, et al. A peripheral blood diagnostic test for acute rejection in renal transplantation. *Am J Transplant* (2012) 12(10):2710–8. doi: 10.1111/j.1600-6143.2012.04253.x
26. Kurian SM, Williams AN, Gelbart T, Campbell D, Mondala TS, Head SR, et al. Molecular classifiers for acute kidney transplant rejection in peripheral blood

by whole genome gene expression profiling. *Am J Transplant* (2014) 14 (5):1164–72. doi: 10.1111/ajt.12671
27. Zhou J, Cheng H, Wang Z, Chen H, Suo C, Zhang H, et al. Bortezomib attenuates renal interstitial fibrosis in kidney transplantation via regulating the EMT induced by TNF-alpha-Smurf1-Akt-mTOR-P70S6K pathway. *J Cell Mol Med* (2019) 23(8):5390–402. doi: 10.1111/jcmm.14420
28. Cina DP, Onay T, Paltoo A, Li C, Maezawa Y, De Arteaga J, et al. Inhibition of MTOR disrupts autophagic flux in podocytes. *J Am Soc Nephrol* (2012) 23 (3):412–20. doi: 10.1681/ASN.2011070690
29. Xiao Y, Liu H, Yu J, Zhao Z, Xiao F, Xia T, et al. MAPK1/3 regulate hepatic lipid metabolism via ATG7-dependent autophagy. *Autophagy* (2016) 12 (3):592–3. doi: 10.1080/15548627.2015.1135282
30. Fujita N, Itoh T, Omori H, Fukuda M, Noda T, Yoshimori T. The Atg16L complex specifies the site of LC3 lipidation for membrane biogenesis in autophagy. *Mol Biol Cell* (2008) 19(5):2092–100. doi: 10.1091/mbc.E07-12-1257
31. Sun SC. The non-canonical NF-kappaB pathway in immunity and inflammation. *Nat Rev Immunol* (2017) 17(9):545–58. doi: 10.1038/nri.2017.52
32. Chang CP, Su YC, Hu CW, Lei HY. TLR2-dependent selective autophagy regulates NF-kappaB lysosomal degradation in hepatoma-derived M2 macrophage differentiation. *Cell Death Differ* (2013) 20(3):515–23. doi: 10.1038/cdd.2012.146
33. Mathew R, Karp CM, Beaudoin B, Vuong N, Chen G, Chen HY, et al. Autophagy suppresses tumorigenesis through elimination of p62. *Cell* (2009) 137(6):1062–75. doi: 10.1016/j.cell.2009.03.048
34. Snoeijs MG, van Bijnen A, Swennen E, Haenen GR, Roberts LJ,2, Christiaans MH, et al. Tubular epithelial injury and inflammation after ischemia and reperfusion in human kidney transplantation. *Ann Surg* (2011) 253(3):598–604. doi: 10.1097/SLA.0b013e31820d9ae9
35. Saitoh T, Fujita N, Jang MH, Uematsu S, Yang BG, Satoh T, et al. Loss of the autophagy protein Atg16L1 enhances endotoxin-induced IL-1beta production. *Nature* (2008) 456(7219):264–8. doi: 10.1038/nature07383
36. Serramito-Gomez I, Boada-Romero E, Slowicka K, Vereecke L, Van Loo G, Pimentel-Muinos FX. The anti-inflammatory protein TNFAIP3/A20 binds the WD40 domain of ATG16L1 to control the autophagic response, NFKB/NF-kappaB activation and intestinal homeostasis. *Autophagy* (2019) 15 (9):1657–9. doi: 10.1080/15548627.2019.1628549
37. Takagaki Y, Lee SM, Dongqing Z, Kitada M, Kanasaki K, Koya D. Endothelial autophagy deficiency induces IL6 - dependent endothelial mesenchymal transition and organ fibrosis. *Autophagy* (2020) 16(10):1905–14. doi: 10.1080/15548627.2020.1713641
38. Sanchez-Duffhues G, Garcia de Vinuesa A, van de Pol V, Geerts ME, de Vries MR, Janson SG, et al. Inflammation induces endothelial-to-mesenchymal transition and promotes vascular calcification through downregulation of BMPR2. *J Pathol* (2019) 247(3):333–46. doi: 10.1002/path.5193
39. Mack M, Yanagita M. Origin of myofibroblasts and cellular events triggering fibrosis. *Kidney Int* (2015) 87(2):297–307. doi: 10.1038/ki.2014.287

Conflict of Interest: The authors declare that the research was conducted in the absence of any commercial or financial relationships that could be construed as a potential conflict of interest.

frontiers in Immunology

CASE REPORT
published: 15 April 2021
doi: 10.3389/fimmu.2021.661614

Case Report: Splenic Irradiation for the Treatment of Chronic Active Antibody-Mediated Rejection in Kidney Allograft Recipients With *De Novo* Donor-Specific Antibodies

Lan Zhu[1,2], *Zhiliang Guo*[1], *Rula Sa*[1], *Hui Guo*[1,2], *Junhua Li*[3] *and Gang Chen*[1,2*]

[1] *Tongji Hospital, Tongji Medical College, Institute of Organ Transplantation, Huazhong University of Science and Technology, Wuhan, China,* [2] *Key Laboratory of Organ Transplantation, Ministry of Education and Ministry of Public Health, Chinese Academy of Medical Sciences, Wuhan, China,* [3] *Department of Nephrology, Tongji Hospital, Tongji Medical College, Huazhong University of Science and Technology, Wuhan, China*

OPEN ACCESS

Edited by:
Hao Wang,
Tianjin Medical University General Hospital, China

Reviewed by:
Shiro Takahara,
Osaka University, Japan
Tao Lin,
Sichuan University, China

***Correspondence:**
Gang Chen
gchen@tjh.tjmu.edu.cn

Specialty section:
This article was submitted to Alloimmunity and Transplantation, a section of the journal Frontiers in Immunology

Received: *31 January 2021*
Accepted: *18 March 2021*
Published: *15 April 2021*

Citation:
Zhu L, Guo Z, Sa R, Guo H, Li J and Chen G (2021) Case Report: Splenic Irradiation for the Treatment of Chronic Active Antibody-Mediated Rejection in Kidney Allograft Recipients With De Novo Donor-Specific Antibodies. Front. Immunol. 12:661614. doi: 10.3389/fimmu.2021.661614

Chronic active antibody-mediated rejection (AMR) in renal transplantation is usually refractory to current conventional treatment with rituximab, plasmapheresis (PP), and intravenous immunoglobulins (IVIG). Splenic irradiation has been reported to be effective in the rescue of early severe acute AMR after kidney transplantation; however, its effect in chronic active AMR has not been reported to date. In order to reduce donor-specific antibody (DSA) and prevent the progression of chronic AMR, we used repetitive low-dose splenic irradiation, together with rituximab and PP/IVIG, in two living-related kidney transplant recipients with pathologically diagnosed chronic active AMR and the presence of long-term class II-*de novo* DSA. DSA monitoring and repeated renal biopsy revealed significantly reduced DSA levels as well as alleviated glomerulitis and peritubular capillaritis in both patients after treatment, and these therapies may have played a role in delaying the progression of chronic AMR. Although DSA levels in both patients eventually rebounded to some extent after treatment, serum creatinine increased slowly in one patient during the 16-month follow-up period and remained stable in the other during the 12-month follow-up period. Given the poor efficacy of conventional treatment at present, splenic irradiation may still be one of the treatment options for chronic active AMR.

Keywords: chronic active antibody-mediated rejection (cABMR), *de novo* donor-specific antibody, splenic irradiation, renal transplantation, case report

INTRODUCTION

Chronic active antibody-mediated rejection (AMR) has long been recognized as the leading cause of late allograft loss in kidney transplantation (1, 2). With the widespread adoption of single-antigen beads testing and the use of electron microscopic analysis, more and more cases of chronic active AMR have been clearly and precisely diagnosed. However, the treatment of chronic active AMR is still an unmet medical need. Current standard therapy, including rituximab plus plasmapheresis (PP)/intravenous immunoglobulins (IVIG), has generally given unsatisfactory results (3, 4). Even the most promising anti-IL-6 receptor antibodies have had controversial effects, according to the latest publication (5).

Historically, splenectomy was routinely performed in ABO-incompatible kidney transplantation (6), and it has been further used with success in the rescue of early severe acute AMR (7–9). In a recently published case report, splenic irradiation was added to the conventional treatment (PP/IVIG, rituximab, and eculizumab) to rescue early severe acute AMR in two kidney transplant recipients, achieving excellent therapeutic effects in both patients (10). Owing to the difference in immunological mechanisms between late chronic AMR and early acute AMR, whether splenic irradiation can also play an important complementary role in the treatment of chronic active AMR remains to be determined. In the present study, we describe for the first time the clinical course and efficacy of spleen irradiation as an adjunctive therapy in two kidney transplant recipients with chronic active AMR.

DONOR-SPECIFIC ANTIBODY (DSA) MONITORING

Sera were screened for HLA antibody using HLA class I and II single-antigen beads (LABScreen™ Single Antigen Beads, One Lambda Inc., Canoga Park, CA). In brief, 20 µl of 1:3 diluted sera were added to 2.5 µl of antigen beads, incubated in the dark for 30 min at room temperature, and then washed with a wash buffer. One hundred microliters of PE-conjugated goat anti-human IgG second antibody was added to the beads and the mixture was incubated for 30 min in the dark at room temperature, washed, and read on a LABScreen™100 Luminex. Antibodies were detected by measuring the mean fluorescence intensity (MFI) of each single-antigen bead. Adjusted raw MFI values >1000 were defined as positive reactions.

In addition, in order to avoid antigen saturation, we tested the serum samples at 1:6 dilution when the MFI value from the 1:3 diluted serum was >15,000. The samples were diluted with phosphate-buffered saline.

Abbreviations: AMR, antibody-mediated rejection; CDC, complement-dependent cytotoxicity; DSA, donor-specific antibody; DFPP, double filtration plasmapheresis; IVIG, intravenous immunoglobulins; MFI, mean fluorescence intensity; PP, plasmapheresis; PRA, panel reactive antibodies; TG, transplant glomerulopathy

COMPLEMENT-DEPENDENT CYTOTOXICITY (CDC) ASSAYS USING FLOW CYTOMETRY

CDC assays were assessed by flow cytometry using donor lymphocytes isolated from peripheral blood as the target cells, as described previously (11, 12). The cells were analyzed using a FACSCalibur with Cellquest Pro 6.0 software (BD Biosciences, USA). The percentage of propidium iodide-positive cells was used to determine the extent of the CDC. Cells incubated with neither human serum nor rabbit complement (cells only) and cells incubated with rabbit complement alone (cells + complement) served as negative controls.

CASE 1

The patient is a 38-year-old man who underwent living-related kidney transplantation for his IgA nephropathy 8 years ago (January 2013) following 4 years of hemodialysis. The donor was his father (59 years old at that time). The donor-recipient HLA-A, -B, -DR, -DQ mismatch grade was 4 (**Figure 1A**). The pre-transplant panel reactive antibodies (PRA) and complement-dependent cytotoxicity (CDC) test results were both negative. Given the low immunological risk, the patient did not receive any induction therapy. He recovered smoothly after the operation, and the renal allograft function soon returned to normal. Since the transplant, this patient has received triple maintenance immunosuppressive therapy with oral tacrolimus, mycophenolate mofetil, and prednisone.

Beginning 2 years after the transplantation, the patient's serum creatinine level started to increase slowly, and proteinuria began to appear. Five years after transplantation, the patient underwent renal biopsy because of significantly elevated serum creatinine (181 µmol/L) and severe proteinuria (2,260 mg/24h). The pathology results showed moderate glomerulitis (g2), severe peritubular capillaritis (ptc3), mild peritubular capillary C4d deposition (C4d1), focal glomerular basement membrane double contours (cg2), peritubular capillary basement membrane multilayering (electron microscopy), and positive IgA deposition (++), which were diagnosed as mild chronic active AMR (Banff 2017 Schema), transplant glomerulopathy (TG), and recurrent IgA nephropathy (**Figure 2A**). Meanwhile, the single-antigen bead assay detected anti-DQ7 DSA at an MFI value of 14,506. Upon admission, the patient received his first round of treatment for chronic AMR: rituximab (200 mg), three sessions of double-filtration plasmapheresis (DFPP)/IVIG (25g each time), followed by three sessions of PP/IVIG (25g each time). After the treatment, DSA detection showed no obvious decease in anti-DQ7 antibody MFI (13,576) (**Figure 1C-a**). Eight months later, the anti-IL-6 receptor monoclonal antibody (tocilizumab, 400 mg) was begun and scheduled to be given monthly. However, the treatment was terminated one month later because of the development of severe leukopenia (white cell count: 2.8 x 10^9/L). After that, we did not give the patient specific treatment of AMR.

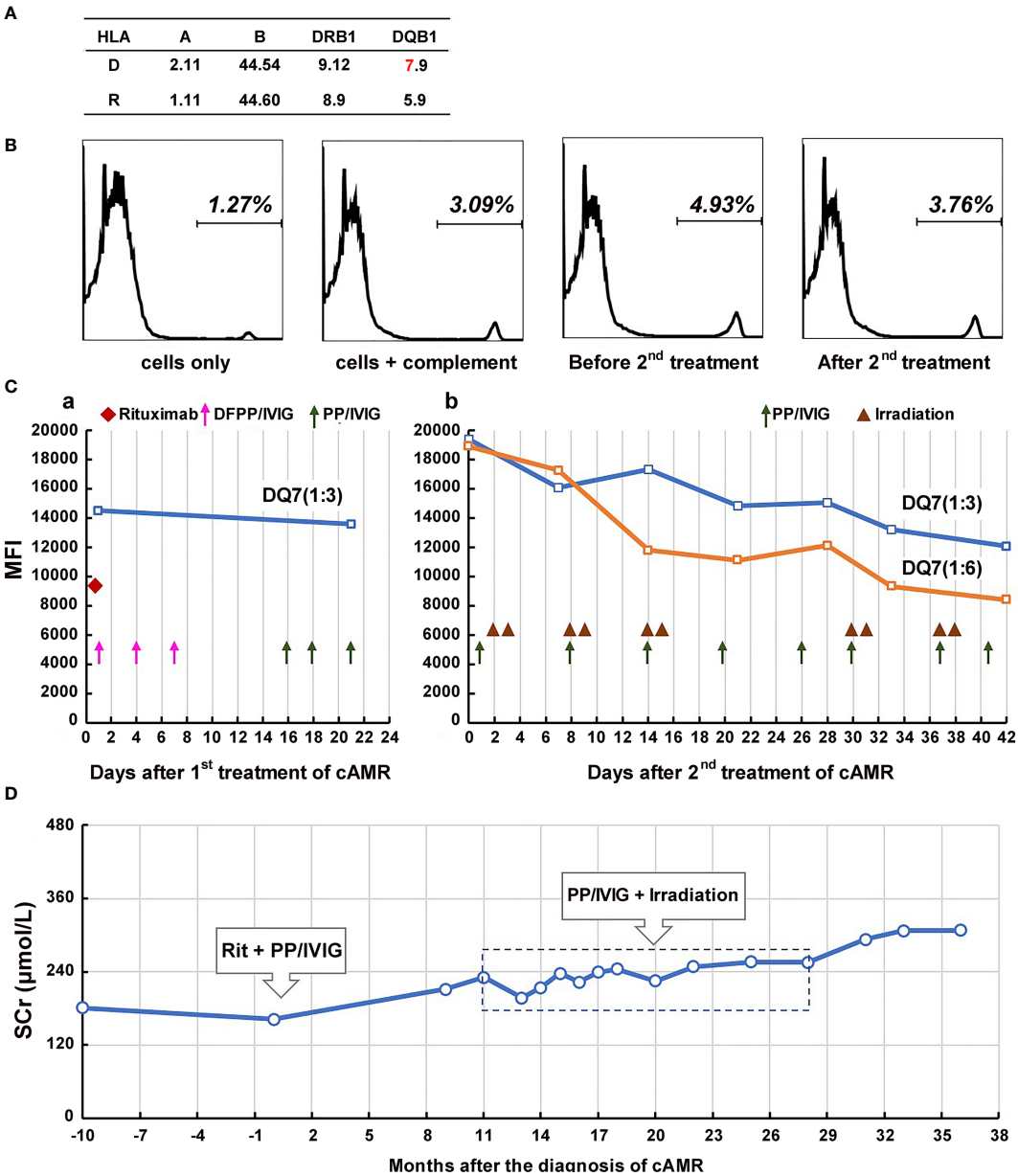

FIGURE 1 | Course of Patient 1's DSA and serum creatinine after the diagnosis of chronic active AMR. (A) HLA phenotype results of the patient 1 and his donor. **(B)** Flow-CDC results before and after the second treatment of chronic AMR. Donor lymphocytes incubated with neither the patient's serum nor rabbit complement (cells only) and cells incubated with rabbit complement alone (cells+complement) served as negative controls. **(C)** changes in MFI values of donor-specific anti-DQ7 antibody (1:3 or 1:6 diluted serum) during the first round of treatment **(a)** and the second round of treatment **(b)**. **(D)** Changes of serum creatinine levels before and after the diagnosis/treatment of chronic active AMR.

At 19 months after the first round of treatment (6 years and 7 months after transplantation), the patient's serum creatinine continued to rise (225 μmol/L), there was aggravation of the proteinuria (3,225 mg/24h), and the MFI of the anti-DQ7 DSA further increased to 19,399. Flow-CDC testing using isolated fresh donor lymphocytes as target cells showed a weakly positive result (4.93%) as compared to the negative controls (cells only: 1.27%; cells + complement: 3.09%) (**Figure 1B**). Therefore, the patient was hospitalized again and received his second round of treatment: eight PP/IVIG sessions in combination with splenic irradiation (10 times, 50 cGy each time, 500 cGy in total) within a 42-day course (**Figure 1C-b**). He tolerated the treatment well, without significant gastrointestinal problems or any signs of myelosuppression, and showed only mild fatigue. After the treatment, the MFI of the anti-DQ7 DSA decreased from 19,399 to 12,061 (1:3 diluted serum). When we further diluted the sera samples to 1:6, the MFI value of the DSA demonstrated a more obvious reduction (from 18,914 to 8,405) (**Figure 1C-b**).

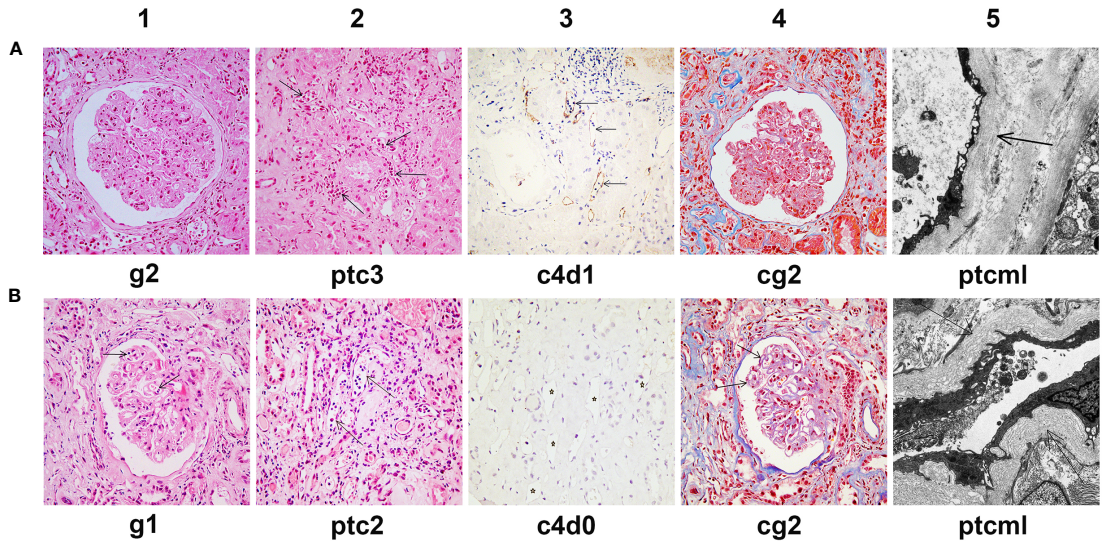

FIGURE 2 | Histological features of chronic active AMR in Patient 1 before and after treatment. **(A)** Typical histological findings of chronic AMR in Patient 1 before the first round of treatment and their Banff 2017 Scores. **(B)** Histological findings of renal allograft in Patient 1 at the 14th month after the second round of treatment and their Banff 2017 Scores. Panel A1 and B1 (hematoxylin and eosin, 400x magnification) show glomerulitis. Panel A2 and B2 (hematoxylin and eosin, 400x magnification) show peritubular capillaritis (arrow). Panel A3 and B3 (immunohistochemical staining, 400x magnification) show peritubular capillary C4d deposition (arrow). Panel A4 and B4 (Masson's trichrome, 400x magnification) show transplant glomerulopathy, characterized by focal glomerular basement membrane double contours. Panel A5 (electron microscopy, 2000x magnification) shows 5-7 circumferential layers of peritubular capillary basement membrane multilayering (ptcml, arrow). Panel B5 (electron microscopy, 3000x magnification) shows 8-10 circumferential layers of peritubular capillary basement membrane multilayering (ptcml, arrow).

Meanwhile, the Flow-CDC result decreased to 3.76%, which was very close to the negative control value.

The patient has further been followed up for 16 months since the second round of treatment. His serum creatinine remained relatively stable for the first 10 months (248-255 μmol/L) (**Figure 1D**). However, from the 11th month of follow-up, the serum creatinine gradually increased to >300 μmol/L (**Figure 1D**), the proteinuria increased (5,346 mg/24h), and the MFI of the DQ7-DSA rebounded to 14,923. At the 14th month of follow-up, the patient underwent another renal biopsy. Results showed that the acute tissue injury was alleviated (g1 and ptc2) as compared with earlier examinations, and the C4d deposition in peritubular capillaries had become negative, but the chronic tissue lesions were slightly worse (**Figure 2B**). In the latest follow-up, the patient showed mild edema, but his general condition was good. Biochemical examination of his blood revealed decreased levels of total protein (54 g/L) and albumin (29 g/L) and elevated levels of serum creatinine (316 μmol/L) and BUN (24.4 mmol/L).

CASE 2

The patient is a 44-year-old man who received a living kidney transplant from his 34-year-old wife in June, 2012 after 1.5 years of hemodialysis. The donor-recipient HLA-A, -B, -C, -DR, -DQA, -DQB, -DP mismatch grade of allele-level genotypes was 9 of 14 (**Figure 3A**). The pre-transplant PRA and CDC were both negative. His serum creatinine normalized after transplantation without any special events. Since the transplant, the patient has received a tacrolimus-based triple maintenance immunosuppressive therapy to prevent rejection.

In September 2019, the patient underwent a biopsy of his renal allograft because of proteinuria (676 mg/24h). The results showed moderate glomerulitis (g2) and peritubular capillaritis (ptc2), focal glomerular basement membrane double contours (cg1), peritubular capillary basement membrane multilayering (electron microscopy), IgA deposition (++), and focal glomerular C4d deposition, but no peritubular capillary C4d deposition (C4d0), all of which indicated mild chronic active AMR and recurrent IgA nephropathy (**Figure 4A**). Meanwhile, the single-antigen bead assay detected *de novo* DSA against DR12 (MFI: 8,023) and DQA6 (MFI: 9,780). The Flow-CDC test using isolated fresh donor lymphocytes as target cells showed a mildly positive result (8.87%) that was higher than that of the negative controls (cells only: 3.92%; cells + complement: 3.04%) (**Figure 3B**). To treat the chronic AMR, the patient was given rituximab (200 mg), eight PP/IVIG (20g each time) sessions (every 2-4 days), and splenic irradiation (10 times, 50 cGy each time, 500 cGy in total) (**Figure 3C**). After 4 weeks of treatment, the MFI levels of DSA significantly decreased (1:3 diluted serum; DR12-MFI: 1,742; DQA6-MFI: 1,222) and the Flow-CDC result became negative (3.74%) (**Figure 3B**). At the same time, the second renal biopsy showed that both the glomerulitis and peritubular capillaritis were significantly improved (g0-1, ptc0-1)

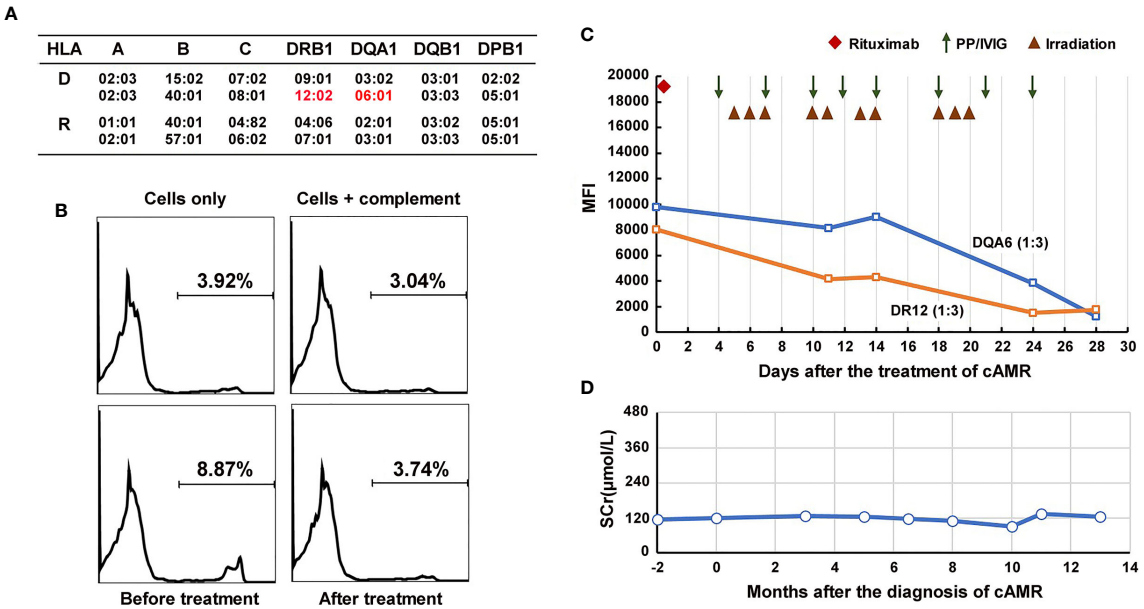

FIGURE 3 | Course of Patient 2's DSA and serum creatinine after the diagnosis of chronic active AMR. **(A)** HLA genotype results of the patient 2 and his donor. **(B)** Flow-CDC results before and after the treatment of chronic AMR. Donor lymphocytes incubated with neither the patient's serum nor rabbit complement (cells only) and cells incubated with rabbit complement alone (cells +complement) served as negative controls. **(C)** changes in MFI values of donor-specific anti-DR12 and anti-DQA6 antibodies (1:3 diluted serum) during the treatment. **(D)** Changes of serum creatinine levels after the diagnosis and treatment of chronic active AMR.

(**Figure 4B**). During the course of the treatment, the patient had no anorexia, fatigue, or other abnormal symptoms, as well as no abnormal changes in liver function or routine blood test results.

Since the treatment, the patient has been followed up for 1 year. At the tenth month of follow-up, the MFI values for DSA showed a rebound, especially in the anti-DQA6 antibody (DR12: 6,443, DQA6: 22,420). At the same time, the patient underwent a third renal biopsy. The pathology results showed that both glomerulitis and peritubular capillaritis remained mild (g1 and ptc1), and the C4d deposition was still negative (C4d0), but there was some progression in the chronic renal lesions (focal glomerular basement membrane double contours, mild interstitial fibrosis, and tubule atrophy; Banff 2017 scores: cg2, mm2, ci1, ct1; **Figure 4C**). The renal function remained quite stable during the whole follow-up period (**Figure 3D**). In the latest follow-up, his serum creatinine level was 133 μmol/L, and his total 24-hour urinary protein was 726 mg.

DISCUSSION

The development of *de novo* DSA after renal transplantation has been reported in 13%-30% of previously non-sensitized recipients (13). *De novo* DSAs are mainly directed to donor HLA class II mismatches and can appear at any time after kidney transplantation (14–16).The long-term existence of *de novo* DSA after renal transplantation has been reported to be associated with the occurrence of chronic AMR, transplant glomerulopathy, and late graft loss (17). The treatments targeting AMR vary widely, with most centers using a combination of PP and IVIG and a number of them also incorporating rituximab (18). However, there is no treatment currently proven to be effective in chronic AMR (4). In this study, we used splenic irradiation in addition to PP/IVIG and rituximab to treat chronic active AMR in two living-related kidney transplant recipients with class II *de novo* DSA production. After the treatment, the *de novo* DSA levels of both patients were significantly reduced, the acute pathological lesions of both allografts were partially reversed, and the progress of chronic lesions may have been delayed to a certain extent. Because patient 1 had an almost negative clinical response to the early treatment with rituximab in combination with 3 sessions of DFPP/IVIG and 3 sessions of PP/IVIG but showed a certain response on later treatment with repetitive low doses of splenic irradiation in addition to PP/IVIG, we think that the splenic irradiation may have played an important role in his improvement.

In the past, splenic irradiation was mainly used for treatment of chronic leukemias, myeloproliferative disorders, and some autoimmune diseases (19, 20). In the field of kidney transplantation, only one case report describes the application of splenic irradiation in the treatment of early severe acute AMR of two transplant recipients, which produced good clinical effects when used with a combination of PP/IVIG, rituximab, and eculizumab therapy (10).The immunological mechanisms by which splenic irradiation plays a role in the treatment of AMR are unclear. An animal study using a murine heart transplant model has demonstrated that the spleen is the major source of

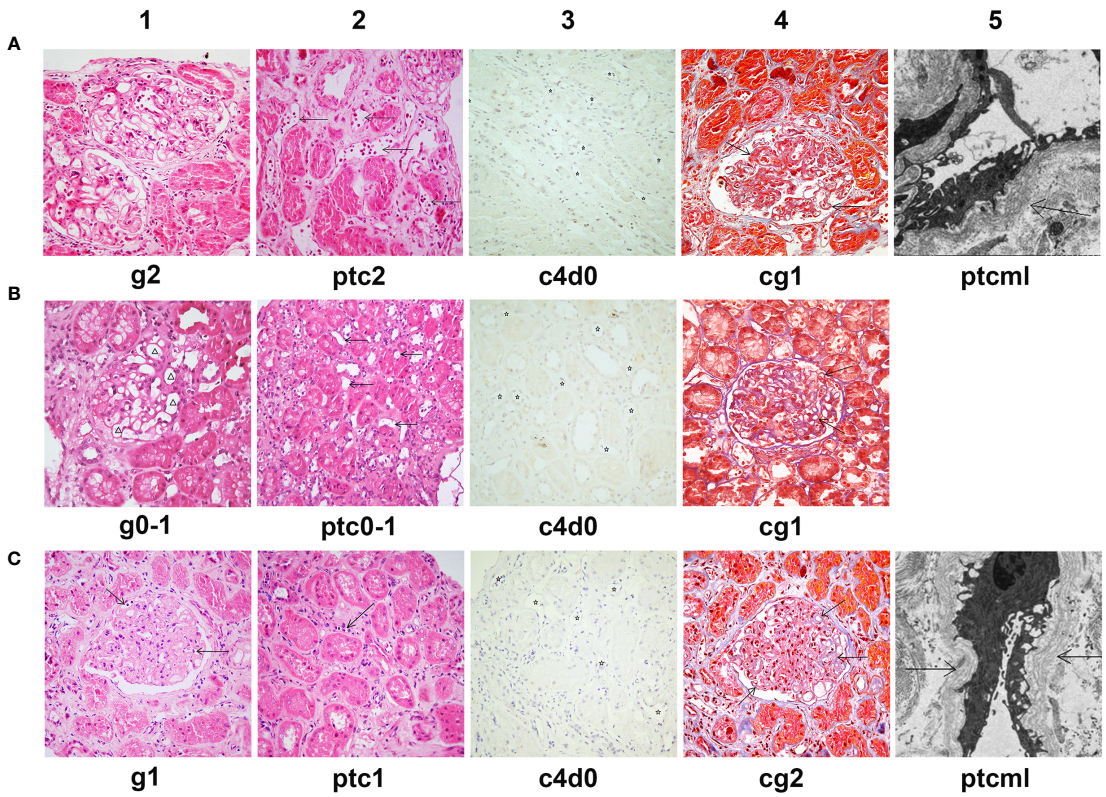

FIGURE 4 | Histological features of chronic active AMR in Patient 2 before and after treatment. **(A)** Typical histological findings of chronic AMR in Patient 2 before the treatment and their Banff 2017 Scores. **(B)** The pathology results of a second renal biopsy performed after 4 weeks of treatment and their Banff 2017 Scores. **(C)** The pathology results of a third renal biopsy performed at the tenth month after the treatment and their Banff 2017 Scores. Panel A1, B1 and C1 (hematoxylin and eosin, 400x magnification) show different degrees of glomerulitis. Panel A2, B2 and C2 (hematoxylin and eosin, 400x magnification) show different degrees of peritubular capillaritis (arrow). Panel A3, B3 and C3 (immunohistochemical staining, 400x magnification) show no C4d deposition in peritubular capillaries (asterisk). Panel A4, B4 and C4 (Masson's trichrome, 400x magnification) show different degrees of transplant glomerulopathy, characterized by focal glomerular basement membrane double contours (arrow). Panel A5 (electron microscopy, 2500x magnification) and Panel C5 (electron microscopy, 4000x magnification) show 5-7 circumferential layers of peritubular capillary basement membrane multilayering (ptcml, arrow).

anti-donor antibody-secreting cells early after transplantation in both sensitized and non-sensitized recipients (21). Another interesting case report has described a high proportion of plasma cells in the resected spleen during the development of severe acute AMR (8). Thus, splenectomy or splenic irradiation can remove or deplete a large number of antibody-secreting cells in the spleen, which may partially explain why splenic irradiation is effective in the treatment of early acute AMR. However, for late *de novo* DSA-mediated chronic active AMR, the role of splenic irradiation apparently cannot be explained by the above-described mechanism. Unlike the sharp rise in DSA caused by an anamnestic response during acute AMR, *de novo* DSA leading to chronic AMR is usually maintained at a relatively stable level for a long time and is therefore considered to be mainly produced by the long-lived plasma cells in the bone marrow. Given that splenic irradiation itself has no direct effect on the niche plasma cells in the bone marrow, why it can reduce the level of DSA during the process of treating chronic active AMR is a novel immunological issue worthy of further investigation. We have hypothesized that the chronic activated B cells in the spleen and the long-lived plasma cells in the bone marrow jointly constitute a dynamic DSA production system to maintain a relatively constant DSA level for a long period of time. Therefore, repeated low-dose splenic irradiation over a relatively long period of time interfered with this DSA production system and thus played a certain role in reducing the DSA.

Although in the two cases we describe here, adjunct therapy with splenic irradiation resulted in a moderate decline in persistent class II DSA and a marked alleviation of acute pathologic lesions (e.g., glomerulitis and peritubular capillaritis), it is not possible to accurately evaluate whether the progression of chronic renal lesions (such as TG) was significantly prevented. In addition, we cannot isolate the effect of splenic irradiation in the setting of multiple therapies. Furthermore, a rebound in DSA levels occurred in both cases after 1 to 2 years of follow-up, suggesting that our treatment regimen did not achieve long-lasting effects, and further improvement of the regimen is needed.

To the best of our knowledge, this is the first case report detailing the use of splenic irradiation for the treatment of chronic active AMR in renal transplant recipients. This integrated treatment can potentially reduce DSA levels and alleviate both glomerulitis and peritubular capillaritis, which may help delay the progression of chronic AMR. Although two cases of effective treatment alone cannot define the effectiveness of a particular therapy, given the current inadequacy of conventional treatment, splenic irradiation may still be a promising option for the treatment of chronic active AMR.

DATA AVAILABILITY STATEMENT

The raw data supporting the conclusions of this article will be made available by the authors, without undue reservation.

ETHICS STATEMENT

The studies involving human participants were reviewed and approved by the institutional review board at Tongji Hospital, Tongji Medical College, Huazhong University of Science and Technology. The patients/participants provided their written informed consent to participate in this study.

AUTHOR CONTRIBUTIONS

LZ took responsibility for the treatments of the patients, summarize clinical data, and drafting the manuscript. ZG participated in the treatment of the patients and collection of data. RS participated in data collection and drafting the manuscript. HG took responsibility for pathological diagnosis, histological images acquisition, and interpretation. JL made contributions in the treatment of plasmapheresis and double-filtration plasmapheresis. GC made substantial contributions to the study concept and design as well as revisions to the manuscript. All authors contributed to the article and approved the submitted version.

FUNDING

This work was supported by the Non-Profit Central Research Institute Fund of Chinese Academy of Medical Science (grant number 2019PT320014).

ACKNOWLEDGMENTS

We thank Dr. Deborah McClellan for editorial assistance.

REFERENCES

1. Moroni G, Binda V, Quaglini S, Sacchi L, Raffiotta F, Cosa F, et al. Causes of late transplant failure in cyclosporine-treated kidney allograft recipients. *Clin Exp Nephrol* (2019) 23(8):1076–86. doi: 10.1007/s10157-019-01740-7
2. Sellares J, de Freitas DG, Mengel M, Reeve J, Einecke G, Sis B, et al. Understanding the causes of kidney transplant failure: the dominant role of antibody-mediated rejection and nonadherence. *Am J Transplant* (2012) 12 (2):388–99. doi: 10.1111/j.1600-6143.2011.03840.x
3. Moreso F, Crespo M, Ruiz JC, Torres A, Gutierrez-Dalmau A, Osuna A, et al. Treatment of chronic antibody mediated rejection with intravenous immunoglobulins and rituximab: A multicenter, prospective, randomized, double-blind clinical trial. *Am J Transplant* (2018) 18(4):927–35. doi: 10.1111/ajt.14520
4. Bohmig GA, Eskandary F, Doberer K, Halloran PF. The therapeutic challenge of late antibody-mediated kidney allograft rejection. *Transpl Int* (2019) 32 (8):775–88. doi: 10.1111/tri.13436
5. Massat M, Congy-Jolivet N, Hebral AL, Esposito L, Marion O, Delas A, et al. Do anti-IL-6R blockers have a beneficial effect in the treatment of antibody-mediated rejection resistant to standard therapy after kidney transplantation? *Am J Transplant* (2020) 1–9. doi: 10.1111/ajt.16391.Onlineaheadofprint
6. Shimmura H, Tanabe K, Ishida H, Tokumoto T, Ishikawa N , Miyamoto N, et al. Lack of correlation between results of ABO-incompatible living kidney transplantation and anti-ABO blood type antibody titers under our current immunosuppression. *Transplantation* (2005) 80(7):985–8. doi: 10.1097/01.tp.0000173647.43616.78
7. Orandi BJ, Zachary AA, Dagher NN, Bagnasco SM, Garonzik-Wang JM , Van Arendonk KJ, et al. Eculizumab and splenectomy as salvage therapy for severe antibody-mediated rejection after HLA-incompatible kidney transplantation. *Transplantation* (2014) 98(8):857–63. doi: 10.1097/TP.0000000000000298
8. Kaplan B, Jie T, Diana R, Renz J, Whinery A , Stubbs N, et al. Histopathology and immunophenotype of the spleen during acute antibody-mediated rejection. *Am J Transplant* (2010) 10(5):1316–20. doi: 10.1111/j.1600-6143.2010.03067.x
9. Locke JE, Zachary AA, Haas M, Melancon JK, Warren DS , Simpkins CE, et al. The utility of splenectomy as rescue treatment for severe acute antibody mediated rejection. *Am J Transplant* (2007) 7(4):842–6. doi: 10.1111/j.1600-6143.2006.01709.x
10. Orandi BJ, Lonze BE, Jackson A, Terezakis S, Kraus ES, Alachkar N, et al. Splenic Irradiation for the Treatment of Severe Antibody-Mediated Rejection. *Am J Transplant* (2016) 16(10):3041–5. doi: 10.1111/ajt.13882
11. Chen G, Qian H, Starzl T, Sun H, Garcia B , Wang X, et al. Acute rejection is associated with antibodies to non-Gal antigens in baboons using Gal-knockout pig kidneys. *Nat Med* (2005) 11(12):1295–8. doi: 10.1038/nm1330
12. Chen Song S, Zhong S, Xiang Y, Li JH, Guo H, Wang WY, et al. Complement inhibition enables renal allograft accommodation and long-term engraftment in presensitized nonhuman primates. *Am J Transplant* (2011) 11(10):2057–66. doi: 10.1111/j.1600-6143.2011.03646.x
13. Zhang R. Donor-Specific Antibodies in Kidney Transplant Recipients. *Clin J Am Soc Nephrol* (2018) 13(1):182–92. doi: 10.2215/CJN.00700117
14. Guidicelli G, Guerville F, Lepreux S, Wiebe C, Thaunat O, Dubois V, et al. Non-Complement-Binding De Novo Donor-Specific Anti-HLA Antibodies and Kidney Allograft Survival. *J Am Soc Nephrol* (2016) 27(2):615–25. doi: 10.1681/ASN.2014040326
15. Ntokou IS, Iniotaki AG, Kontou EN, Darema MN, Apostolaki MD, Kostakis AG, et al. Long-term follow up for anti-HLA donor specific antibodies postrenal transplantation: high immunogenicity of HLA class II graft molecules. *Transpl Int* (2011) 24(11):1084–93. doi: 10.1111/j.1432-2277.2011.01312.x
16. Wiebe C, Gibson IW, Blydt-Hansen TD, Karpinski M, Ho J, Storsley LJ, et al. Evolution and clinical pathologic correlations of de novo donor-specific HLA antibody post kidney transplant. *Am J Transplant* (2012) 12(5):1157–67. doi: 10.1111/j.1600-6143.2012.04013.x
17. Lakkis FG, Chalasani G, Hariharan S. Antibody-Mediated Rejection of Solid-Organ Allografts. *N Engl J Med* (2018) 379(26):2580. doi: 10.1056/NEJMc1813976
18. Burton SA, Amir N, Asbury A, Lange A, Hardinger KL. Treatment of antibody-mediated rejection in renal transplant patients: a clinical practice survey. *Clin Transplant* (2015) 29(2):118–23. doi: 10.1111/ctr.12491

19. Weinmann M, Becker G, Einsele H, Bamberg M. Clinical indications and biological mechanisms of splenic irradiation in chronic leukaemias and myeloproliferative disorders. *Radiother Oncol* (2001) 58(3):235–46. doi: 10.1016/S0167-8140(00)00316-9
20. Weinmann M, Becker G, Einsele H, Bamberg M. Clinical indications and biological mechanisms of splenic irradiation in autoimmune diseases. *Strahlenther Onkol* (2001) 177(2):105–11. doi: 10.1007/PL00002384
21. Sicard A, Phares TW, Yu H, Fan R, Baldwin WM,3, Fairchild RL, et al. The spleen is the major source of antidonor antibody-secreting cells in murine heart allograft recipients. *Am J Transplant* (2012) 12(7):1708–19. doi: 10.1111/j.1600-6143.2012.04009.x

Conflict of Interest: The authors declare that the research was conducted in the absence of any commercial or financial relationships that could be construed as a potential conflict of interest.

frontiers in Immunology

ORIGINAL RESEARCH
published: 29 April 2021
doi: 10.3389/fimmu.2021.672849

Melatonin Synergizes With Mesenchymal Stromal Cells Attenuates Chronic Allograft Vasculopathy

Ya-fei Qin[1,2†], De-jun Kong[1,2†], Hong Qin[1,2†], Yang-lin Zhu[1,2], Guang-ming Li[1,2], Cheng-lu Sun[1,2], Yi-ming Zhao[1,2], Hong-da Wang[1,2], Jing-peng Hao[3] and Hao Wang[1,2]*

[1] Department of General Surgery, Tianjin Medical University General Hospital, Tianjin, China, [2] Tianjin General Surgery Institute, Tianjin Medical University General Hospital, Tianjin, China, [3] Department of Anorectal Surgery, The Second Hospital of Tianjin Medical University, Tianjin, China

OPEN ACCESS

Edited by:
Niels Olsen Saraiva Camara, University of São Paulo, Brazil

Reviewed by:
Hassan Askari, Shiraz University of Medical Sciences, Iran
Liao Tao, Third Affiliated Hospital of Sun Yat-sen University, China

***Correspondence:**
Hao Wang
hwangca272@hotmail.com; hwang1@tmu.edu.cn

Specialty section:
This article was submitted to Alloimmunity and Transplantation, a section of the journal Frontiers in Immunology

Received: *26 February 2021*
Accepted: *12 April 2021*
Published: *29 April 2021*

Citation:
Qin Y-f, Kong D-j, Qin H, Zhu Y-l, Li G-m, Sun C-l, Zhao Y-m, Wang H-d, Hao J-p and Wang H (2021) Melatonin Synergizes With Mesenchymal Stromal Cells Attenuates Chronic Allograft Vasculopathy. Front. Immunol. 12:672849. doi: 10.3389/fimmu.2021.672849

Background: Chronic rejection characterized by chronic allograft vasculopathy (CAV) remains a major obstacle to long-term graft survival. Due to multiple complicated mechanisms involved, a novel therapy for CAV remains exploration. Although mesenchymal stromal cells (MSCs) have been ubiquitously applied to various refractory immune-related diseases, rare research makes a thorough inquiry in CAV. Meanwhile, melatonin (MT), a wide spectrum of immunomodulator, plays a non-negligible role in transplantation immunity. Here, we have investigated the synergistic effects of MT in combination with MSCs in attenuation of CAV.

Methods: C57BL/6 (B6) mouse recipients receiving BALB/c mouse donor aorta transplantation have been treated with MT and/or adipose-derived MSCs. Graft pathological changes, intragraft immunocyte infiltration, splenic immune cell populations, circulating donor-specific antibodies levels, cytokine profiles were detected on post-operative day 40. The proliferation capacity of $CD4^+$ and $CD8^+$ T cells, populations of Th1, Th17, and Tregs were also assessed *in vitro*.

Results: Grafts in untreated recipients developed a typical pathological feature of CAV characterized by intimal thickening 40 days after transplantation. Compared to untreated and monotherapy groups, MT in combination with MSCs effectively ameliorated pathological changes of aorta grafts indicated by markedly decreased levels of intimal hyperplasia and the infiltration of $CD4^+$ cells, $CD8^+$ cells, and macrophages, but elevated infiltration of $Foxp3^+$ cells. MT either alone or in combination with MSCs effectively inhibited the proliferation of T cells, decreased populations of Th1 and Th17 cells, but increased the proportion of Tregs *in vitro*. MT synergized with MSCs displayed much fewer splenic populations of $CD4^+$ and $CD8^+$ T cells, Th1 cells, Th17 cells, $CD4^+$ central memory T cells (Tcm), as well as effector memory T cells (Tem) in aorta transplant recipients. In addition, the percentage of splenic Tregs was substantially increased in the combination therapy group. Furthermore, MT combined with MSCs markedly reduced serum levels of circulating allospecific IgG and IgM, as well as decreased the levels of pro-inflammatory

IFN-γ, TNF-α, IL-1β, IL-6, IL-17A, and MCP-1, but increased the level of IL-10 in the recipients.

Conclusions: These data suggest that MT has synergy with MSCs to markedly attenuate CAV and provide a novel therapeutic strategy to improve the long-term allograft acceptance in transplant recipients.

Keywords: chronic allograft vasculopathy, melatonin, mesenchymal stromal cells, aorta transplantation, mice

INTRODUCTION

Chronic rejection is supposed to be the principal obstacle to affect long-term graft or patients survival in most transplantation cases (1). The main pathological manifestation of chronic rejection is chronic allograft vasculopathy (CAV), characterized by neointimal proliferation, interstitial inflammation, parenchymal cell damage, interstitial fibrosis, and progressive narrowing of the arterial lumen, resulting in allograft dysfunction or even graft loss (2). Approximately 47.4% of allografts develop CAV during 10-year follow-up according to the International Society for Heart and Lung Transplantation (3). Although re-transplantation is an available option, currently there is no alternative novel therapy for the prevention of CAV. Therefore, CAV is considered an urgent and serious problem that needs to be solved in transplantation (4).

The immunological and non-immunological factors contributing to CAV have varied somewhat across this research area (5–7). Notably, a majority of intragraft T cells are memory T cell (Tm) phenotypes during the process of CAV (8). $CD4^+$ Tm cells have been previously documented to lead to allograft rejection by providing assistance to activate donor-reactive $CD8^+$ T cells for rapid development of direct cytotoxicity, and to B cells for alloantibody production (9–11). Furthermore, our previous research has shown that inhibiting $CD4^+$ Tm infiltration by blocking OX40/OX40L pathway can obviously alleviate the severity of CAV and greatly prolonged allograft survival in a mouse cardiac transplantation model (8). Besides, the bulk of infiltrating cells in neointima and adventitia during the development of CAV were $CD3^+$ cells, and the ratio of $CD4^+/CD8^+$ T cells was almost two (12). Activated $CD4^+$ T cells can secrete IL-2 and IFN-γ cytokines to disrupt the structure of the extracellular matrix, deposit extracellular collagen, and promote the proliferation of fibroblasts, thereby ultimately leading to the development of CAV (13). Impressively, more $CD4^+$ T helper (Th) cells and mononuclear cells are recruited into the neointima and secrete IL-1, IL-6, and TNF-α, and induce smooth muscle cell migration and proliferation in the internal elastic lamina, eventually developing CAV (14). It has been proposed that the Th1 phenotype/IFN-γ axis is one of the most important mediators of CAV through inducing macrophage activation and upregulating MHC II antigen expression that favors T cell allosensitization (15, 16). At present, although the current immunosuppressive treatment such as rapamycin and cyclosporin can dramatically prolong transplant survival, persistent immune and inflammatory responses to the MHC-mismatched transplants play a pivotal role in the development of CAV. Given the pathogenesis of CAV is multifactorial, the novel and effective therapeutic strategy should be explored.

Mesenchymal stromal cells (MSCs) are considered as "immune privileged cells" due to low expression of MHC-II as well as the absence of costimulatory molecules such as B7-1, B7-2, CD40, and CD40L on the cell surface (17, 18). They have been proposed as the promising "live" drugs being able to target the anti-donor immune response and prolong allograft survival in human and rodent studies, which may offer new insights for the prevention of CAV (19–21). Beneficial immunomodulatory effects of MSCs in downregulating the effector function of T cells, B cells, and their paracrine have been shown in experimental transplant models (22–24). Federica et al. have demonstrated that pretransplant portal vein infusion of MSCs induced tolerance which is associated with Treg expansion and compromised anti-donor Th1 activity in a mouse semiallogeneic heart transplant model (25). Similarly, we have recently reported that endometrial regenerative cells, a type of MSCs obtained from menstrual blood, are capable of alleviating CAV (26). Although the role of MSCs in immunomodulation is encouraging, concomitant immunosuppressants remain a challenge. Some immunosuppressive agents can restrict MSCs viability or function (27). For example, the beneficial role of MSCs will be antagonized by rapamycin and FK-506 *via* decreasing cell viability, differentiation, and proliferation (28–30). Consequently, additional consideration should be given when the regimens are chosen for the combination therapy with MSCs. More impressively, the life span of MSCs is severely restricted by harsh microenvironment *in vivo* leading to more than 80–90% of implanted cells being dead within 72 h after injection (31). The excessive reactive oxygen species (ROS) induced by ischemia-reperfusion injury and operation make further efforts to the apoptosis of MSCs (31). Given that all, a novel immunomodulator, which meanwhile act as an MSCs protector is urgently needed.

Melatonin (MT), also named N-acety-1-5-methoxytryptamine, is a neurohormone that is primarily known as the mediator for circadian rhythms, it also presents immunomodulatory, antioxidant, and anti-aging properties (32). It has been reported that treatment with high-dose MT (200 mg/kg/day) significantly prolonged rat cardiac allograft survival (33). Recipients receiving high-dose MT showed a marked decline in circulating allospecific IgG and IgM and lymphocyte proliferative capacity. Furthermore, high-dose MT is believed to prolong the survival of syngeneic islet

grafts by inhibiting the proliferation of Th1 cells and enhancing the level of IL-10 (34). Enhancement of the graft function and immunological compliance were also observed in experimental transplantation of liver, lungs, and kidneys (35–37). In addition to its immunomodulatory effects, MT also serves as a cell protector, which protects MSCs from oxidation, inflammation, apoptosis when they are applied as a combination therapy (38). Besides, MT is consumed by human as a dietary complement without side-effects (39).

Given the extensive immunological and non-immunological properties of MT and MSCs, we hypothesized that MT synergizes with MSCs to attenuate CAV in the mouse aorta transplantation model.

MATERIALS AND METHODS

Animals

Male adult BALB/C (H-2^d) and C57BL/6 (B6, H-2^b) mice (China Food and Drug Inspection Institute, Beijing, China) weighing 25–30 g were used as donors and recipients, respectively. All the mice were housed in a specific pathogen-free environment with the appropriate temperature, a 12 h dark/12 h light cycle, total nutrition feed, and clean water. All animal experimental procedures were approved by the Animal Care and Use Committee of Tianjin Medical University (Tianjin, China), and all the experiments were performed in accordance with the guideline of the Chinese Council on Animal Care.

Adipose-Derived MSCs Harvest and Phenotype Identification

Adipose-derived MSCs (ADMSCs) were prepared according to the protocols described previously (40). Adipose tissue obtained from B6 mice was cut into < 1 mm^3 pieces and then digested with 0.1% type I collagenase (1 mg/ml, Solarbio, Beijing, China) on the shaker (200 rpm) at 37°C for 60 min. The centrifuge was at 1,500 rpm for 5 min and the supernatant was discarded while retaining the sediment at the bottom of the centrifuge tube. After washing twice with PBS, the sediment was then resuspended in α-MEM complete medium (Hyclone, USA) with 15% fetal bovine serum (FBS, Hyclone, USA) and 1% penicillin/streptomycin (Solarbio, Beijing, China) and seeded in 6 cm plates. Then, the ADMSCs were cultured in a 37°C, 5% CO_2 incubator. After 6 days of incubation, the cells displayed a fibroblast-like morphology. Subsequently, the third generation ADMSCs were collected for the identification of surface markers (CD29, CD34, CD45, SCA-1, CD44) (41) through flow cytometry.

Orthotopic Aorta Transplantation and Experimental Groups

The recipient B6 and paired donor BALB/c mice were randomly divided into five experimental groups (n = 10 for each group): Group A, sham control group; Group B, untreated group; Group C, MT treated group; Group D, MSC treated group; Group E, MSC and MT combination treated group. Aorta transplantation, transplanting BALB/c mice aorta to B6 mice, was performed as described previously (26, 42). The recipients receiving a single dose of 1×10^6 MSCs 1 day before transplantation and on postoperative days (PODs) 1, 7, 14, 21, 28, and 35 through tail vein injection. Considering impressive immunomodulatory properties of high dose MT (200 mg/kg/day) on acute allograft rejection, the same intervention was adopted (33). MT (HY-B0075, Med Chem Express, USA) accurately weighed according to body weight of mice was dissolved in 50 ul DMSO and then suspended in 450 ul saline solution and administered through a subcutaneous injection. MT was daily administered *via* subcutaneous injection in recipients from 1 day before transplantation to the end-stage of the study. Briefly, ketamine/xylazine cocktail (80 mg/kg ketamine, 4 mg/kg xylazine, i.p.) was used for anesthesia in combination with buprenorphine (0.05 mg/kg, s.c.) for analgesia. The mice were sacrificed with an overdose of the same anesthetic at the end point of the study. Grafts and spleens were harvested for evaluation at POD 40 (26). Meanwhile, the blood samples collected on POD 40 from the tail vein were centrifuged, and the sera were stored at −80°C freezer.

Histological Assessment and Morphometric Analysis

The grafts (n = 10 for each group) were removed on POD 40 and fixed with 10% paraformaldehyde, then dehydrated for paraffin embedding, and cut into 4 μm slides. Hematoxylin and Eosin staining (H&E, G1120, Solarbio) were performed. The severity of CAV was determined by the degree of intimal hyperplasia and lumen occlusion. The scoring system, as previously described, was indicated as lumen occlusion (%) = intima/(intima+lumen). In brief, the score of 0, 1, 2, 3, 4, 5 point represents less than 10, 10–20, 20–40, 40–60, 60–80, 80–100% of lumen occlusion, respectively (43).

Immunohistochemistry

To identify the intragraft infiltration of $CD4^+$ and $CD8^+$ cells, specific markers were stained for grafts (n = 10 for each group). Briefly, 0.01 mol/L sodium citrate buffer was used on tissue sections for antigen repair. The endogenous peroxidase was eliminated through incubation with 3% hydrogen peroxide for 25 min. Then the sections were incubated with rabbit anti-mouse CD4 antibody (diluted at 1:1,000, ab183685, Abcam, Cambridge, UK), rabbit anti-mouse F4/80 antibody (diluted at 1:1,000, ab100790, Abcam, Cambridge, UK), rabbit anti-mouse CD8 antibody (diluted at 1:2,000, ab217344, Abcam, Cambridge, UK), or rabbit anti-mouse Foxp3 antibody (diluted at 1:1,000, ab215206, Abcam, Cambridge, UK), overnight at 4°C and then incubated with 100 μl enhanced enzyme-labeled goat anti-rabbit IgG polymer (DAB kit, PV9000, ZSGB-BIO, Beijing, China) for 20 min next day at room temperature. Finally, a freshly prepared DAB solution was used to visualize the labeling. Non-specific staining was determined according to the negative control. The ImageJ (version 1.53, National Institutes of Health, USA) software was applied to quantify different cell types infiltration.

Enzyme-Linked Immunosorbent Assay

The sera were obtained from the blood of all recipients after centrifuge (2,500 rpm for 8 min). Commercial ELISA kits were

used to measure the levels of IL-10 (1211002, DAKEWE, Beijing, China), IL-17A (1211702, DAKEWE, Beijing, China), IL-6 (1210602, DAKEWE, Beijing, China), TNF-α (1217202, DAKEWE, Beijing, China), IL-1β (1210122, DAKEWE, Beijing, China), MCP-1 (1217392, DAKEWE, Beijing, China), and IFN-γ (1210002, DAKEWE, Beijing, China). All experimental operations were conducted according to the manufacturer's protocols.

Real-Time Polymerase Chain Reaction (RT-PCR)

The aorta allografts were harvested at POD 40 for detection of the key cytokines in the process of CAV. Total RNA was extracted using an RNAprep Pure Tissue Kit (DP 431, TIANGEN BIOTECH, Beijing, China, http://www.tiangen.com). The concentration and purity of the extracted RNAs were measured using a UV spectrophotometer. Total RNA was reverse transcribed into cDNA for expression analysis by using the FastKing gDNA Dispelling RT supermix kit (KR118, TIANGEN BIOTECH, Beijing, China). RT-PCR was performed using the 2×SYBR Green qPCR Master Mix (B21203, TIANGEN BIOTECH, Beijing, China) according to the manufacturer's protocol. Primer sequences used in this experiment are listed in **Table 1**. The housekeeping GADPH was used as the normalization control. Relative differences of gene expression among the groups were calculated using the formula $2^{-\Delta\Delta CT}$.

Splenocytes Co-culture With MT and/or MSCs *In Vitro*

In order to identify the role of MT and/or MSCs on $CD4^+$ T cells, $CD8^+$ T cells, Th1 cells, Th17 cells, and Tregs, a co-culture system was set *in vitro*, in which the experiments were performed using B6 splenocytes in the presence or absence of MT and/or MSCs in a 24-well plate. To activate and culture T cells, CD3 and CD28 functional antibodies (CD3, 1 ug/ml, CD28 2 ug/ml, eBioscience, San Diego, CA, USA) and IL-2 (2 ng/ml, PeproTech, NJ, USA) were used in the co-culture system. In the negative control group, neither MT nor MSCs was added into activated splenocytes. Meanwhile, activated splenocytes were co-cultured with MT and/or MSCs respectively. Briefly, splenocytes (1×10^6 cells per well) were pretreated with MT (100 ug/ml) and/or MSCs (1×10^5 cells per well) 2 h before adding the stimulators according to the previous study (44, 45). The splenocytes were stimulated with corresponding stimulators for 96 h with RPMI 1640 (HyClone, GE, USA) medium containing 10% FBS (HyClone, Thermo, USA) in a 37°C and 5% CO_2 culture environment. After 96 h, the MSCs adhered to the surface of the culture dishes. Then the dishes were washed with RPMI medium and the suspended splenocytes were removed by aspiration with a pipette (46). The proliferation capacity of $CD4^+$ and $CD8^+$ T cells was evaluated by Ki67 staining through flow cytometry. In addition, Th1, Th17, and Tregs were also analyzed by flow cytometry.

TABLE 1 | The primer sequences used for real-time PCR.

Gene	Primers (5′-3′)
GADPH	Forward: AGGTCGGTGTGAACGGATTTG
	Reverse: TGTAGACCATGTAGTTGAGGTCA
IFN-γ	Forward: ATGAACGCTACACACTGCATC
	Reverse: CCATCCTTTTGCCAGTTCCTC
TNF-α	Forward: GATGGGGGGCTTCCAGAACT
	Reverse: GATGGGGGGCTTCCAGAACT
IL-1β	Forward: GAAGAGCCCATCCTCTGTGA
	Reverse: GGGTGTGCCGTCTTTCATTA
IL-6	Forward: TGACAACCACGGCCTTCCCTA
	Reverse: TCAGAATTGCCATTGCACAACTCTT
IL-17A	Forward: TTTAACTCCCTTGGCGCAAAA
	Reverse: CTTTCCCTCCGCATTGACAC
MCP-1	Forward: TTAAAAACCTGGATCGGAACCAA
	Reverse: GCATTAGCTTCAGATTTACGGGT
IL-10	Forward: ACTTCCCAGTCGGCCAGAGCCACAT
	Reverse: GATGACAGCGCCTCAGCCGCATCCT

Determination of Circulating Donor-Specific Antibodies (DSA)

To determine the levels of DSA, 5 μl serum was collected from all the recipients on POD 40. Serum was diluted 20 times with PBS and co-cultivated with the splenocytes (5×10^5 cells per well) obtained from the BALB/c at 37°C for 30 min, followed by staining with both anti-IgG-PE and anti-IgM-PE antibodies. The levels of DSA were measured by flow cytometry and presented as mean fluorescence intensity (MFI) (4).

Flow Cytometry Analysis

The spleens were obtained from different groups after sacrifice. And the splenocytes were stained with different specific markers according to the previous study (8, 47). Th1 ($CD4^+IFN\text{-}\gamma^+$), Treg ($CD4^+CD25^+Foxp3^+$), Th17 ($CD4^+IL\text{-}17A^+$), $CD4^+$ central memory T cell (Tcm, $CD4^+CD44^{high}CD62L^{high}$), and effector memory T cell (Tem, $CD4^+CD44^{high}CD62L^{low}$) were stained with corresponding antibodies, including anti-CD4-FITC, anti-Foxp3-APC, anti-IFN-γ-PE, anti-IL-4-APC, anti-IL-17A-perCP, anti-CD62L-perCP, anti-CD44-APC. The detailed procedure of staining was the same as that previously described (48). All fluorescent-labeled antibodies, FcR blockers, and intracellular staining reagents for flow cytometry were purchased from either eBioscience (eBioscience, San Diego, CA, USA) or BioLegend (BioLegend, San Diego, CA, USA). The FlowJo (version 10.7.1, https://www.flowjo.com) software was applied to analyze the data.

Statistical Analysis

All data were expressed as mean ± standard error of mean (SEM). Sample comparison between multiple groups was analyzed by one-way analysis of variance (ANOVA) after the normality test and followed by *post hoc* analysis with the least significant difference (LSD) test; $P < 0.05$ was considered statistically significant. SPSS (IBM SPSS Statistics version 22.0) software was used for statistical analysis.

RESULTS

Characterization of MSCs

To identify the phenotype of MSCs, the iconic markers of MSCs were determined by flow cytometry. As shown in **Figure 1**, MSCs

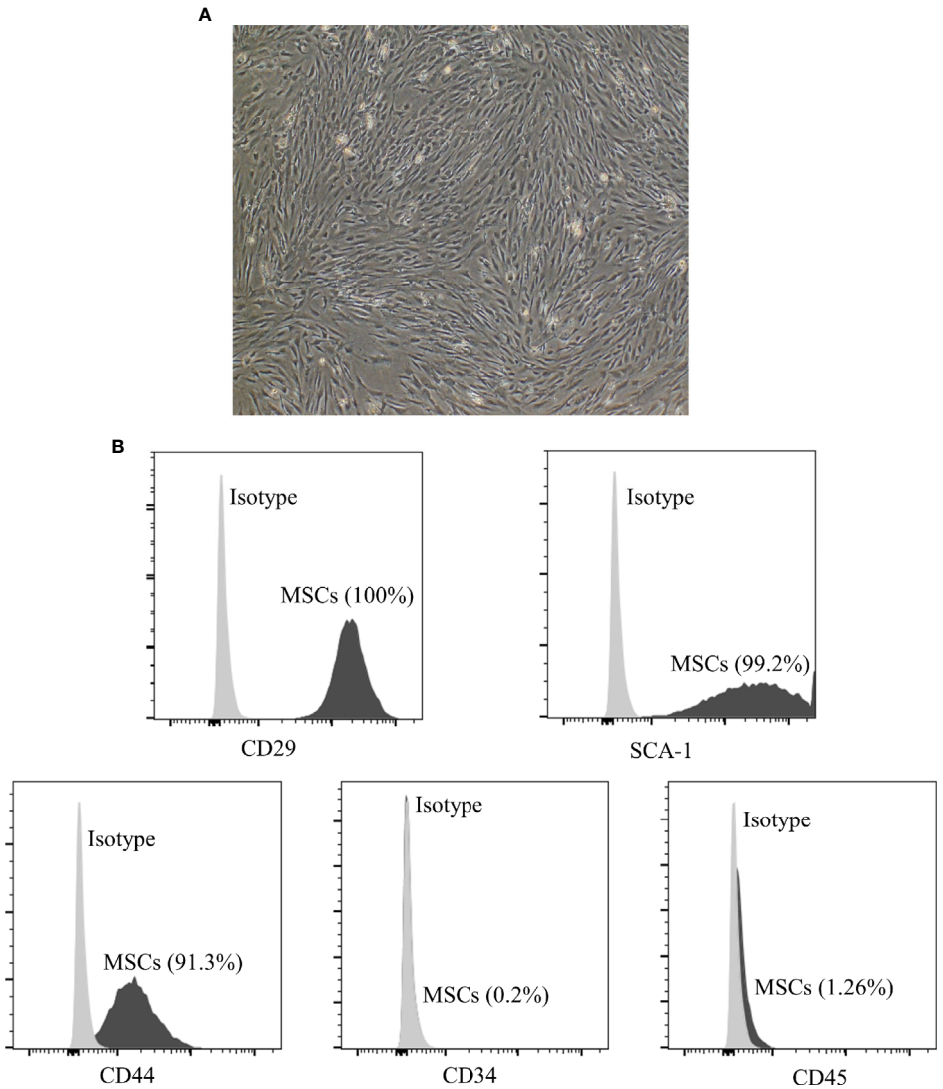

FIGURE 1 | Characterization of adipose derived MSCs. **(A)** Morphology of p3 passage MSCs. The section is displayed at 100× magnification. The MSCs display a fibroblast-like or spindle-shaped morphology. **(B)** The expression of cell markers on the surface of MSCs measured by flow cytometry analysis. MSCs are positive for CD29 (100%), SCA-1 (99.2%), CD44 (91.3%), while negative for CD34 (0.2%) and CD45 (1.26%). MSCs, mesenchymal stromal cells.

displayed a fibroblast-like morphology and were positive for CD29 (100%), SCA-1 (99.2%), CD44 (91.3%), while negative for CD34 (0.2%) and CD45 (1.26%).

MT Either Alone or Combined With MSCs Suppressed T Cell Proliferation *In Vitro*

It has been previously demonstrated that MSCs could inhibit the proliferation of T cells. However, whether this effect can be augmented by MT remains unknown (49). The splenocytes obtained from B6 mice were stimulated with anti-CD3 Abs, anti-CD28 Abs, and IL-2, and co-cultured with MT, MSCs, and MT+MSCs, respectively *in vitro*. As shown in **Figures 2A, C, D**, the population of $CD4^+$ and $CD8^+$ T cells declined obviously in MT treated group (*vs.* Sp+St group: CD4, p <.001; CD8, p <.01). Moreover, the proportions further decreased strikingly after co-culture with MT+MSCs (*vs.* Sp+St group: CD4, p <.001; CD8, p <.001; *vs.* Sp+St+MT group: CD4, p <.01; CD8, p <.01; *vs.* Sp+St+MSCs group: CD4, p <.01; CD8, p <.01).

Ki67, a nuclear cell proliferation-associated antigen, was also stained to reflect T cell proliferation rate. When compared with untreated group, the proliferation of $CD4^+$ and $CD8^+$ T cells was significantly inhibited by MT treatment (**Figures 2B, E, F**, *vs.* Sp +St group: CD4, p <.001; CD8, p <.001). Additionally, MT +MSCs further inhibited $CD4^+$ and $CD8^+$ T cell proliferation (*vs.* Sp+St group: CD4, p <.001; CD8, p <.001; *vs.* Sp+St+MT group: CD4, p <.01; CD8, p <.01; *vs.* Sp+St+MSCs group; CD4, p <.01; CD8, p <.01). Given together, these results showed that MT either alone or in combination with MSCs could obviously decrease the proportion of $CD4^+$ and $CD8^+$ T cells and significantly inhibit T cell proliferation *in vitro*.

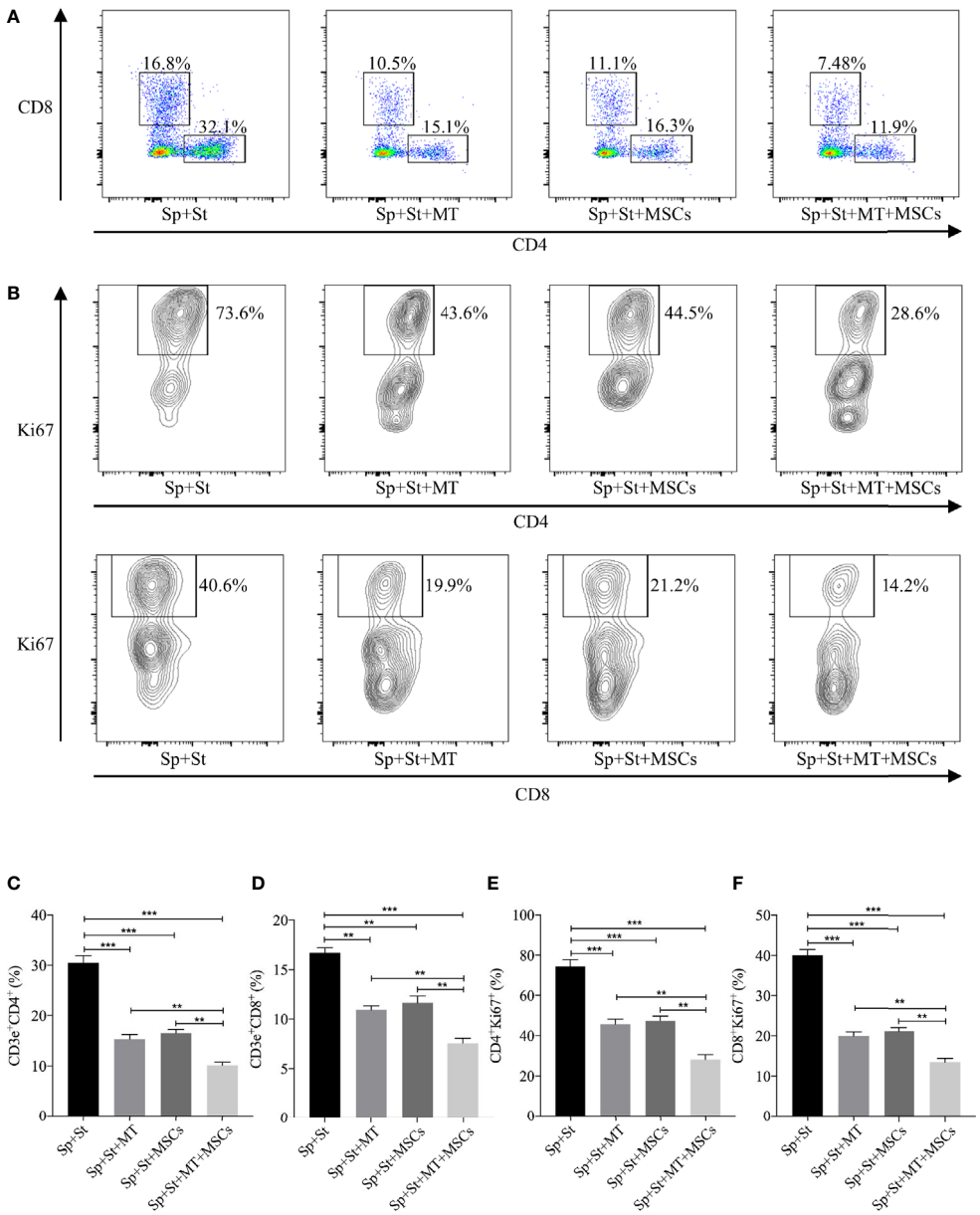

FIGURE 2 | MT either alone or combined with MSCs suppresses T cell proliferation *in vitro*. The splenocytes derived from B6 mice are co-cultured with MT, MSCs, and MT+MSCs respectively in the presence of the stimulators of anti-CD3 Abs, anti-CD28 Abs and IL-2 *in vitro*. **(A)** The pseudocolor of $CD4^+$ and $CD8^+$ T cells *in vitro*; **(B)** Contour plot of $CD4^+Ki67^+$ and $CD8^+Ki67^+$ T cells *in vitro*; **(C)** The percentage of $CD4^+$ T cells; **(D)** The percentage of $CD8^+$ T cells; **(E)** The percentage of $CD4^+Ki67^+$ T cells; **(F)** The percentage of $CD8^+Ki67^+$ T cells. Statistical analysis is performed by one-way analysis of variance (ANOVA), $^{**}p < .01$ and $^{***}p < .001$. Bar graphs represent mean ± SEM. MT, melatonin; MSCs, mesenchymal stromal cells; Sp, splenocytes; St, stimulators. The assay was conducted three times with three replicates each time.

MT Either Alone or Combined With MSCs Reduced Th1 and Th17 Population While Promoting Tregs *In Vitro*

$CD4^+$ Th cells are considered to be the vital driving factors in the process of CAV (50, 51). In this experiment, the percentage of Th1 and Th17 cells were detected *in vitro*. Compared to negative control group, both $CD4^+IFN\gamma^+$ and $CD4^+IL\text{-}17A^+$ cells were decreased after co-culture with MT (**Figures 3A, C, D**, *vs.* Sp+St group: Th1, $p < .01$; Th17, $p < .001$), and further reduced in the combination group (*vs.* Sp+St group: Th1, $p < .001$; Th17, $p < .001$; *vs.* Sp+St+MT group: Th1, $p < .05$; Th17, $p < .001$; *vs.* Sp+St+MSCs group: Th1, $p < .01$; Th17, $p < .001$). On the contrary, Tregs could hamper the immune reaction of Th1 and Th17 cells. Therefore, the effect of MT and MSCs on regulating

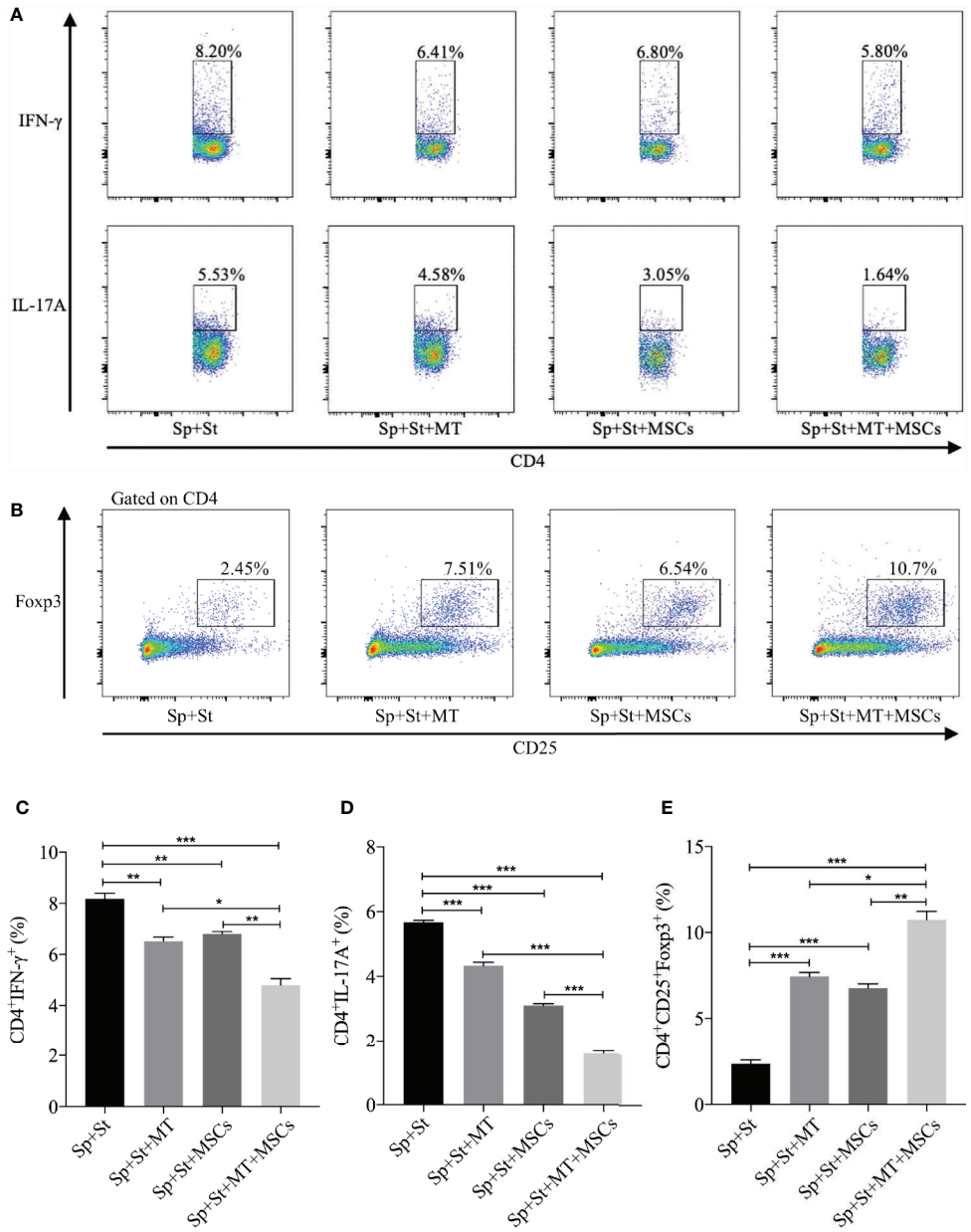

FIGURE 3 | MT either alone or combined with MSCs reduces Th1 and Th17 populations while promoting Treg population *in vitro*. The splenocytes derived from B6 mice were co-cultured with MT, MSCs, and MT+MSCs respectively in the presence of the stimulators of anti-CD3 Abs, anti-CD28 Abs, and IL-2 *in vitro*. **(A)** The pseudocolor of Th1 ($CD4^+IFN\text{-}\gamma^+$) cells and Th17 ($CD4^+IL\text{-}17A^+$) cells *in vitro*; **(B)** The pseudocolor of Tregs ($CD4^+CD25^+Foxp3^+$) *in vitro*; **(C)** The percentage of Th1 cells; **(D)** The percentage of Th17 cells; **(E)** The percentage of Tregs. Statistical analysis is performed by one-way analysis of variance (ANOVA), $^*p < .05$, $^{**}p < .01$, and $^{***}p < .001$. Bar graphs represent mean ± SEM. MT, melatonin; MSCs, mesenchymal stromal cells; Sp, splenocytes; St, stimulators. The assay was conducted three times with three replicates each time.

$CD4^+CD25^+Foxp3^+$ T cells were also evaluated. As shown in **Figures 3B, E**, the percentage of $CD4^+CD25^+Foxp3^+$ T cells was increased in MT (*vs.* Sp+St group, $p < .001$) or MSC monotherapy group. And the proportion tended to be the highest in combination treatment group (*vs.* Sp+St group, $p < .001$; *vs.* Sp+St+MT group, $p < .05$; *vs.* Sp+St+MSCs group, $p < .01$). This result suggests that MT synergizes with MSCs can significantly reduce Th1 and Th17 population, but augment Treg population *in vitro*.

MT Synergized With MSCs Significantly Ameliorate CAV

Based on the striking inhibition effect of MT and/or MSCs on $CD4^+$ T and $CD8^+$ T cells activation *in vivo*, we then assessed the

role of MT and MSCs in the allogeneic aorta transplantation model. We have previously reported that aorta allografts collected at POD 40 developed typical features of vasculopathy in mice (52). In this study, **Figure 4A** showed that there was obvious lumen occlusion accompanied by the thickest neointima in aorta allografts of untreated mice. Either MT or MSC monotherapy could ameliorate intimal thickening of aorta grafts. Furthermore, when MT was added to MSC treatment,

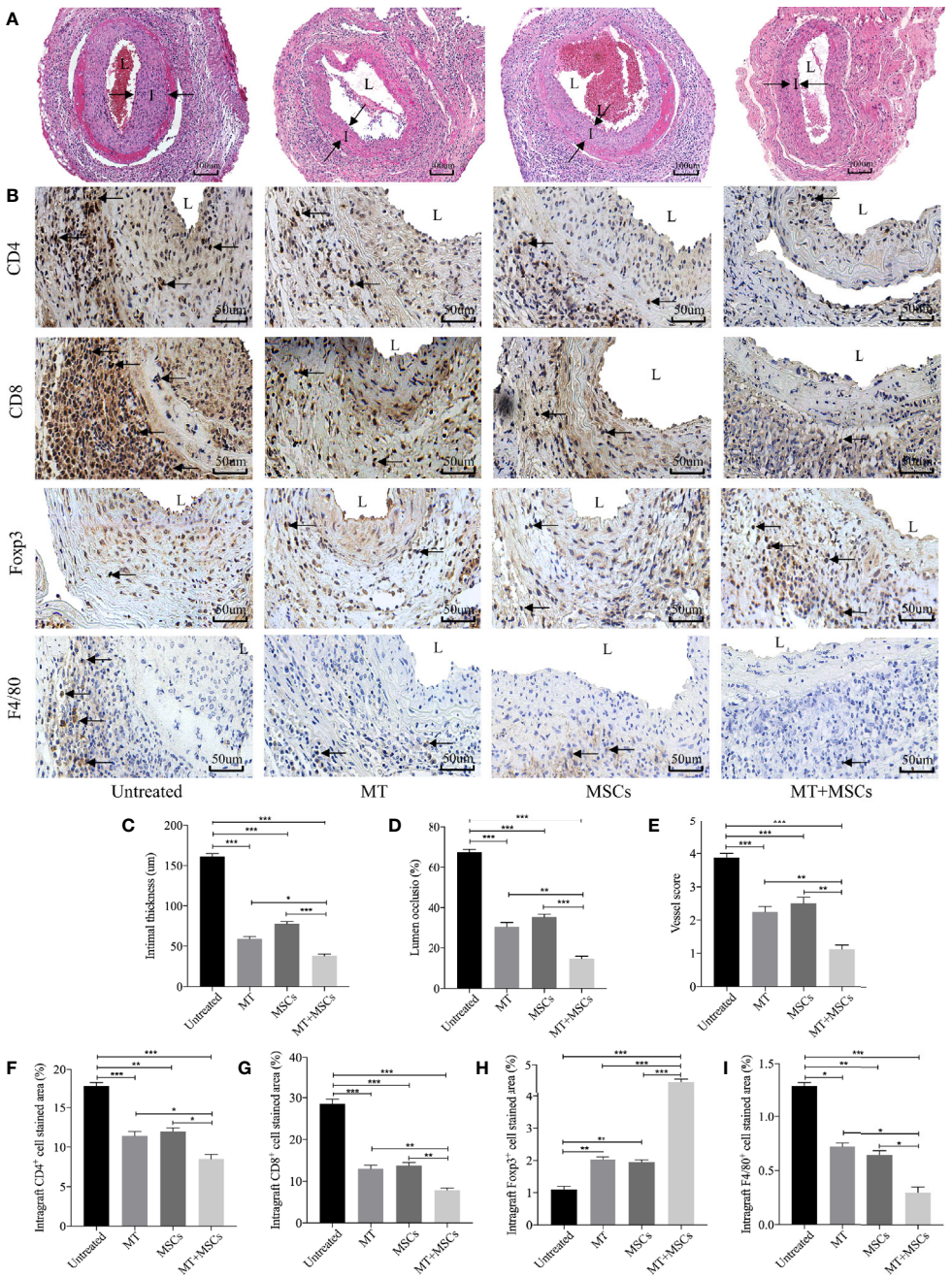

FIGURE 4 | MT synergized with MSCs significantly ameliorates CAV. Each section is displayed at 400× magnification. "I" indicates neointima. "L" indicates lumen. **(A)** Histology of aorta allografts in transplant recipients; **(B)** Graft sections for immunohistochemical staining of $CD4^+$ cells, $CD8^+$ cells, Tregs and macrophages; **(C)** Intimal thickness of the aorta allografts in different groups; **(D)** Lumen occlusion of the aorta allografts in different groups; **(E)** Vessel score of the aorta allografts in different groups; **(F)** The percentage of intragraft $CD4^+$ cells; **(G)** The percentage of intragraft $CD8^+$ cells; **(H)** The percentage of intragraft Tregs; **(I)** The percentage of intragraft macrophages. Statistical analysis is performed by one-way analysis of variance (ANOVA), n = 10 per group, $^*p$ <.05, $^{**}p$ <.01, and $^{***}p$ <.001. Bar graphs represent mean ± SEM. MT, melatonin; MSCs, mesenchymal stromal cells. The experiments were repeated three times independently.

the vasculopathy was effectively inhibited in aorta allografts. As shown in **Figure 4C**, the intimal hyperplasia of aorta allografts was decreased by the treatment of either MT (*vs.* untreated group, p <.001) or MSCs, and further attenuated by the combination therapy (*vs.* untreated group, p <.001; *vs.* MT alone group, p <.05; *vs.* MSC alone group, p <.001). Additionally, we measured the intima/(intima+lumen) ratio in the grafts among different groups. As shown in **Figure 4D**, minimal intima/(intima+lumen) ratio was found in the MT+MSC group (*vs.* untreated group, p <.001; *vs.* MT alone group, p <.01; *vs.* MSC alone group, p <.001). Moreover, the vessel score, indicating the severity of CAV, was also the lowest in the combination therapy group (**Figure 4E**, *vs.* untreated group, p <.001; *vs.* MT alone group, p <.01; *vs.* MSC alone group, p <.01). Taken together, these data indicate that MT has a synergistic effect with MSCs to prevent the progression of CAV.

MT Either Alone or Combined With MSCs Decreased $CD4^+$ Cell, $CD8^+$ Cell, and Macrophage Infiltration but Augmented Treg Infiltration in Aorta Allografts

To determine the intragraft infiltration of immune cells, immunohistology staining of $CD4^+$ and $CD8^+$ cells was performed. As shown in **Figures 4B, F–I**, a large number of $CD4^+$ and $CD8^+$ cells were localized in the graft neointima of untreated mice. Both $CD4^+$ and $CD8^+$ cells were decreased in either MT (*vs.* untreated group, CD4, p <.001; CD8, p <.001) or MSC treated group, and further dramatically reduced in the combination therapy group (*vs.* untreated group, CD4, p <.001; CD8, p <.001; *vs.* MT alone group: CD4, p <.05; CD8, p <.01; *vs.* MSC alone group: CD4, p <.05; CD8, p <.01). Conversely, MT effectively increased intragraft Treg infiltration (*vs.* untreated group, p <.01). Furthermore, MT synergizes with MSCs achieved highest infiltration level of Tregs in aorta allografts (*vs.* untreated group, p <.001; *vs.* MT group, p <.001; *vs.* MSC group, p <.001). Given that macrophages play an important role in the development of CAV, we sought to observe the infiltration of macrophages in the grafts. Either MT (*vs.* untreated group, p <.05) or MSC monotherapy could reduce intragraft macrophage infiltration. Notably, the lowest level of macrophages was detected in the combination therapy group (*vs.* untreated group, p <.001; *vs.* MT group, p <.05; *vs.* MSC group, p <.05). The above results indicate that synergistic effects of MT and MSCs in attenuating CAV are associated with the reduced infiltration of $CD4^+$ cells, $CD8^+$ cells, and macrophages, but increased infiltration of Tregs in the allografts.

MT Acted Synergistically With MSCs to Reduce Splenic $CD4^+$ and $CD8^+$ T Cells, Inhibit B Cell Activation and DSA Production

We have found the obviously decreased proliferation propriety and proportion of $CD4^+$ and $CD8^+$ T cells *in vitro*. Therefore, the systemic levels of $CD4^+$ and $CD8^+$ T cells in recipients were also detected in this study. In **Figures 5A, C, D**, the percentage of $CD4^+$ and $CD8^+$ T cells were highly increased in untreated group (*vs.* sham group: CD4, p <.001; CD8, p <.001). However, the population of $CD4^+$ and $CD8^+$ T cells obviously declined in MT treated group (*vs.* untreated group: CD4, p <.001; CD8, p <.01). Moreover, the proportion further decreased strikingly in MT+ MSC treated group (*vs.* untreated group: CD4, p <.001; CD8, p <.001; *vs.* MT alone group: CD4, p <.05; CD8, p <.01; *vs.* MSC alone group: CD4, p <.001; CD8, p <.01).

Meanwhile, the features of B cells in driving immune response including antigen presentation to T lymphocytes, transition into plasma cells, and generation of DSA cannot be ignored in the process of CAV. In this study, $CD19^+CD86^+$ B cells were measured among different groups and the results were shown in **Figures 5B, E**. Compared to the sham group, the proportion of $CD19^+CD86^+$ B cells increased significantly in untreated group (*vs.* sham group, p <.001). Phenomenally, the population of $CD19^+CD86^+$ B cells was decreased greatly in MT (*vs.* untreated group, p <.001) or MSC treated group and was further decreased in the combination group (*vs.* untreated group, p <.001; *vs.* MT alone group, p <.01; *vs.* MSC alone group, p <.01). In addition, DSA produced by plasma cells was also evaluated among groups. Splenocytes obtained from the BALB/c mice were co-cultured with diluted B6 recipient serum and then stained with anti-IgG-PE and anti-IgM-PE antibodies, respectively. As shown in **Figures 5F, G**, both donor-specific IgG and IgM were decreased in MT (*vs.* untreated group, IgG, p <.001; IgM, p <.01) or MSC (*vs.* untreated group, IgG, p <.001; IgM, p <.001) treated group, indicating that either MT or MSC treatment restrained the formation of DSA. And this inhibitory effect was further strengthened in the combination therapy group (*vs.* untreated group, IgG, p <.001; IgM, p <.001; *vs.* MT alone group: IgG, p <.001; IgM, p <.01; *vs.* MSCs alone group: IgG, p <.01; IgM, p <.01). These data indicated that MT acts synergistically with MSCs to attenuate CAV through inhibiting B cell activation and alleviating DSA production in the transplant recipients.

MT Either Alone or Combined With MSCs Reduced Splenic Th1, Th17, $CD4^+$ Tm Populations but Enhanced Treg Population in the Aorta Transplant Recipients

Based on the direct inhibitory effect of MT combined with MSCs on activation of Th1 and Th17 cells *in vitro*, we further determined whether MT and/or MSCs could modulate Th populations in the splenocytes of the aorta transplant recipients. Splenocytes of different groups were harvested and stained for Th1 ($CD4^+IFN\text{-}\gamma^+$) and Th17 ($CD4^+IL\text{-}17A^+$) cells. The percentage of Th1 and Th17 cells increased obviously in untreated group (*vs.* sham group: Th1, p <.001; Th17, p <.001). As compared with those of the untreated group, the percentages of both Th1 and Th17 cells were significantly decreased in MT (**Figure 6A**, Th1, p <.001; Th17, p <.001) or MSC group, and they were further reduced in the combination therapy group (*vs.* untreated group: Th1, p <.001; Th17, p<.001; *vs.* MT alone group: Th1, p <.001; Th17, p <.001; *vs.* MSC alone group: Th1, p <.001; Th17, p <.001).

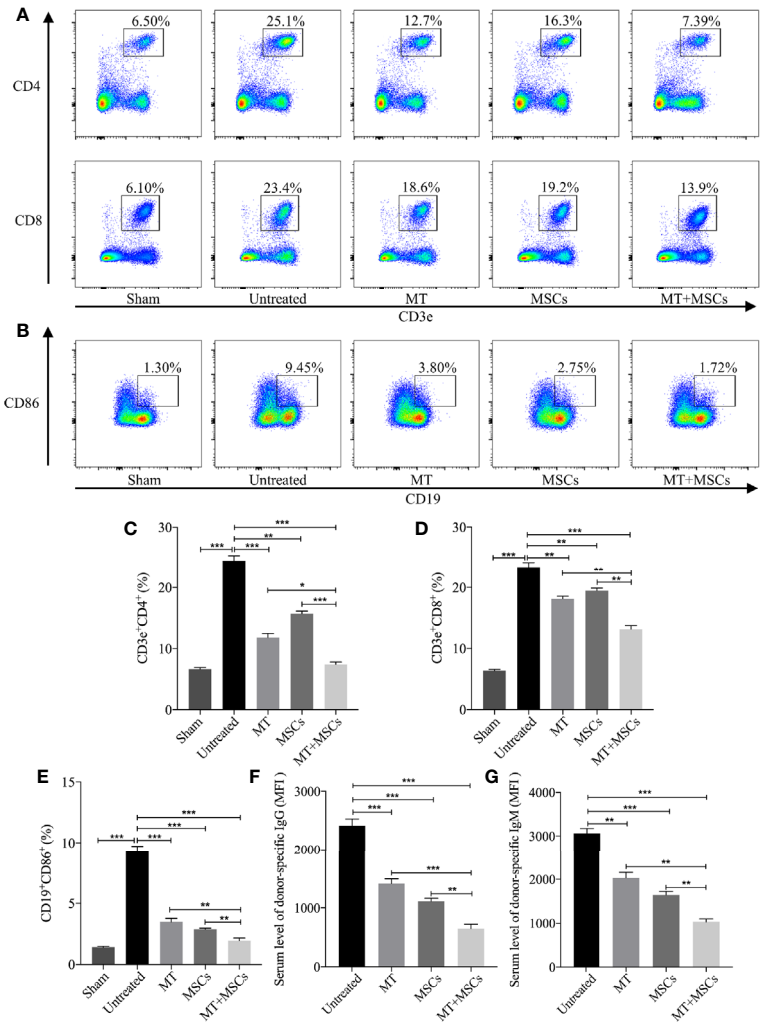

FIGURE 5 | MT acts synergistically with MSCs to reduce splenic $CD4^+$ and $CD8^+$ T cells, inhibit B cell activation and DSA production. Splenocytes are collected from the B6 recipient mice of each group at postoperative day 40. **(A)** The pseudocolor of $CD4^+$ and $CD8^+$ T cells in recipient splenocytes; **(B)** The pseudocolor of B ($CD19^+CD86^+$) cells *in vivo*; **(C)** The percentage of $CD4^+$ T cells; **(D)** The percentage of $CD8^+$ T cells; **(E)** The percentage of B cells; **(F)** The serum level of donor-specific IgG; **(G)** The serum level of donor-specific IgM. Statistical analysis is performed by one-way analysis of variance (ANOVA), n = 10 per group, $^*p$ <.05, $^{**}p$ <.01, and $^{***}p$ <.001. Bar graphs represent mean ± SEM. MT, melatonin; MSCs, mesenchymal stem cells; MFI, mean fluorescence intensity. Data shown are representative of three separate experiments.

In correlation with *in vitro* experiments and immunohistology staining, we have further measured the splenic Treg population in the recipients. As shown in **Figures 6A, C–E**, when compared with the untreated group, the percentage of splenic Tregs was obviously increased in MT (*vs.* untreated group, p <.01) or MSC treated recipients. And consistently, the Treg population was further increased significantly in the combined therapy group (*vs.* untreated group, p <.001; *vs.* MT alone group, p <.001; *vs.* MSC alone group, p <.001). This result suggested that MT combined with MSCs can modulate Th1, Th17, and Treg populations which are associated with attenuation of CAV in transplant recipients.

It has been proven that the blocking of $CD4^+$ Tm cells (Tcm and Tem) could alleviate the severity of CAV (53). To identify whether MT and MSCs have synergistic effect in modulating $CD4^+$ Tm, splenic Tcm ($CD4^+CD44^{high}CD62L^{high}$) and Tem ($CD4^+CD44^{high}CD62L^{low}$) were detected among different groups. The results were analyzed by flow cytometry, and the contour plot among the groups is shown in **Figures 6B, F, G**. As compared to sham group, the proportion of Tcm and Tem markedly increased in untreated group (*vs.* sham group, Tcm, p <.001; Tem, p <.001). However, the percentages of both Tcm and Tem were decreased in MT (*vs.* untreated group, Tcm, p <.01; Tem, p <.01) or MSC monotherapy group, and these two populations were further significantly reduced in combination therapy group (*vs.* untreated group, Tcm, p <.001; Tem, p <.001; *vs.* MT alone group: Tcm, p <.01; Tem, p <.001; *vs.* MSCs alone

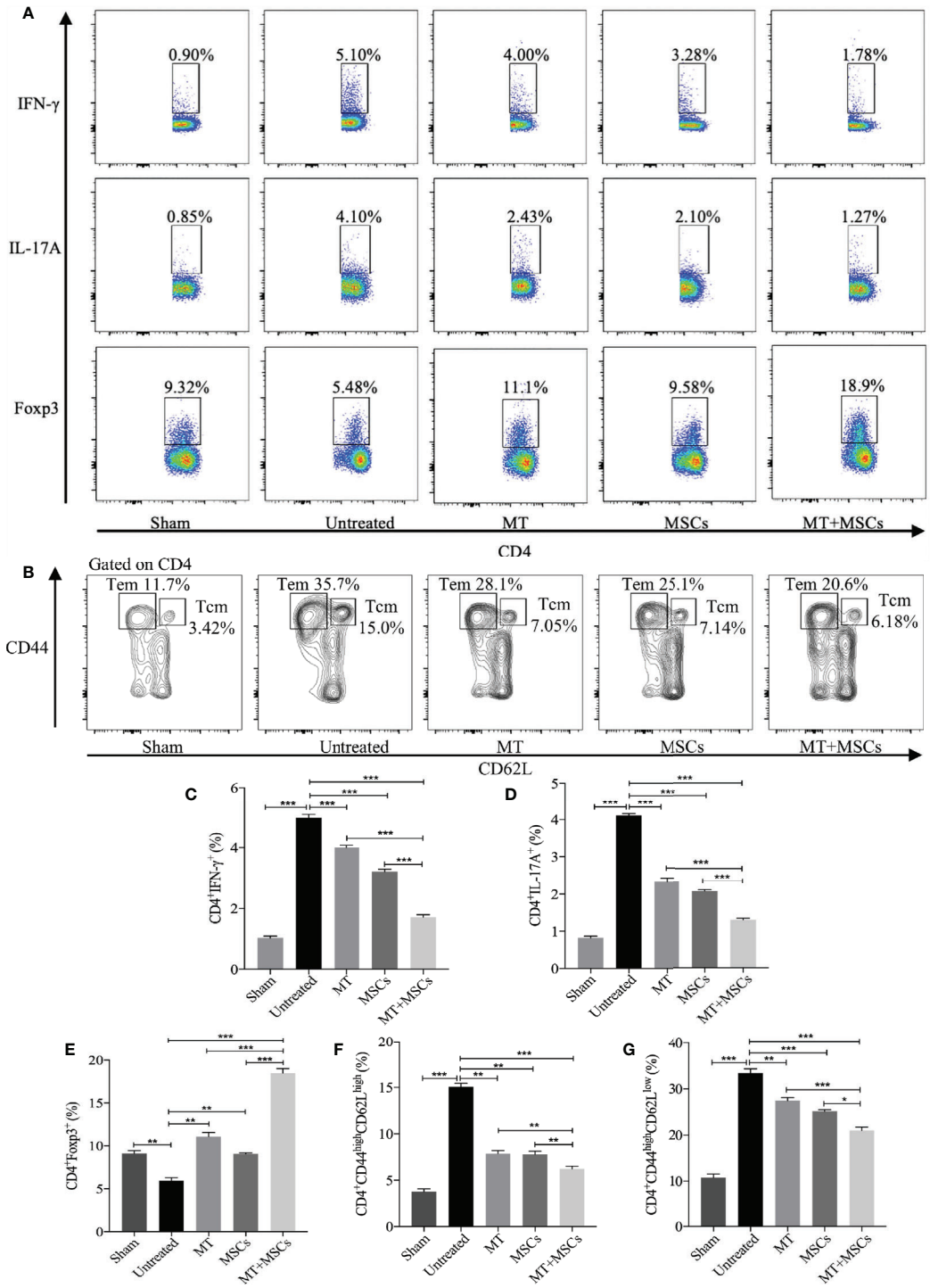

FIGURE 6 | MT either alone or combined with MSCs reduces splenic Th1, Th17, $CD4^+$ Tcm, and $CD4^+$ Tem, but enhances Treg population in the aorta transplant recipients. Splenocytes are collected from the B6 recipient mice of each group at postoperative day 40. **(A)** The pseudocolor of Th1 ($CD4^+IFN\text{-}\gamma^+$) cells, Th17 ($CD4^+IL\text{-}17A^+$) cells, and $CD4^+Foxp3^+$ Tregs *in vivo*; **(B)** The contour plot of Tem ($CD4^+CD44^{high}CD62L^{low}$) and Tcm ($CD4^+CD44^{high}CD62L^{high}$) *in vivo*; **(C)** The percentage of Th1 cells; **(D)** The percentage of Th17 cells; **(E)** The percentage of Tregs; **(F)** The percentage of Tcm *in vivo*; **(G)** The percentage of Tem *in vivo*. Statistical analysis is performed by one-way analysis of variance (ANOVA), n = 10 per group, $^*p < .05$, $^{**}p < .01$, and $^{***}p < .001$. Bar graphs represent mean ± SEM. MT, melatonin; MSCs, mesenchymal stromal cells. The experiments were independently repeated three times.

group: Tcm, p <.01; Tem, p <.05). These results suggested that Tm, which is critical to the pathogenesis of CAV, can be attenuated by the combination therapy of MT and MSC in allograft recipients.

MT in Combination With MSCs Further Achieved the Reduced Levels of Pro-inflammatory Cytokines but Increased Level of IL-10 in Transplant Recipients

To further determine the cytokine profiles locally and systemically in the development of CAV, the levels of anti-inflammatory and pro-inflammatory cytokines were detected in both the grafts and the sera. As shown in **Figures 7A–G**, the serum levels of inflammatory cytokines were significantly increased in the untreated group (*vs.* sham group, IFN-γ, p <.001; TNF-α, p <.001; IL-1β, p <.001; IL-6, p <.001; IL-17A, p <.001; MCP-1, p <.001). As compared with those of untreated recipients, the serum levels of inflammatory cytokines (IFN-γ, TNF-α, IL-1β, IL-6, IL-17A, and MCP-1) were significantly decreased in the recipients receiving MT (*vs.* untreated group, IFN-γ, p <.001; TNF-α, p <.01; IL-1β, p <.01; IL-6, p <.01; IL-17A, p <.001; MCP-1, p <.001) or MSC monotherapy. Moreover, these cytokine levels were further reduced in the combination therapy group. In contrast, the serum level of IL-10 was significantly increased in MT (*vs.* untreated group, p <.001) or MSC monotherapy group, and it was further increased in the combination therapy group (*vs.* untreated group, p <.001; *vs.* MT alone group, p <.01; *vs.* MSC alone group, p <.01). Meanwhile, the levels of anti-inflammatory and pro-inflammatory cytokines were also examined in aorta allografts by RT-PCR. As shown in **Figures 7H-N**, similar to the results of serological tests, the intragraft levels of inflammatory cytokines were significantly increased in the untreated group. As compared with those of untreated recipients, the intragraft levels of inflammatory cytokines (IFN-γ, TNF-α, IL-1β, IL-6, IL-17A, and MCP-1) were significantly decreased in the recipients receiving MT (*vs.* untreated group, IFN-γ, p <.001; TNF-α, p <.001; IL-1β, p <.001; IL-6, p <.01; IL-17A, p <.001; MCP-1, p <.01) or MSC monotherapy. Moreover, these intragraft cytokine levels were further reduced in the combination therapy group. In contrast, the intragraft level of IL-10 was significantly increased in MT (*vs.* untreated group, p <.001) or MSC monotherapy group, and it was further increased in the combination therapy group (*vs.* untreated group, p <.001; *vs.* MT alone group, p <.01; *vs.* MSC alone group, p <.01). These data demonstrate that MT and MSCs act synergistically to ameliorate CAV by regulating cytokine profiles locally and systemically in the transplant recipients.

DISCUSSION

Chronic vasculopathy is the major cause of end-stage graft loss. It has been reported that infection, ischemic injury, oxidative stress, adaptive immune response, and other risk factors are linked to the development of CAV (51). As of yet, a novel therapy that directly targets chronic vasculopathy is still lacking. MSCs have been proposed as promising drugs due to their distinct immunomodulatory features. ADMSCs represent biological advantages in immunomodulatory effects, such as downregulating the effector function of dendritic cells and promoting the transfer of tolerogenic dendritic cells (54). Meanwhile, the immunomodulatory, antioxidant, and anti-apoptotic properties of MT have attracted extensive attention for its therapeutic application (32). Our study has, for the first time, provided strong evidence that MT has synergy with MSCs to effectively ameliorate graft pathological changes of CAV. The dosage of MT used in this study was based on the previous reports (33, 34). It has been previously reported that high-dose of MT (200 mg/kg/day) used for treatment of Parkinsonism had no any signs of serious adverse effects apart from transient sedation (55). In addition, no adverse effects were observed when the repeated high-dose of MT was applied intravenously to the recipients (56, 57). Furthermore, in the current study we have also demonstrated that the same dosage (200 mg/kg/day) of MT has no side-effects observed and is safe in transplant recipients.

Based on the evaluation of the infiltrating cells in the neointima and the endothelial layer of aorta allografts, it was observed that the majority of infiltrating cells were $CD4^+$ and $CD8^+$ cells (12) which were recognized as key contributors to CAV (58). *In vitro*, the population of $CD4^+$ and $CD8^+$ T cells declined obviously in the MT treated group and further decreased strikingly after co-culture with MT+MSCs. Meanwhile, $CD4^+$ and $CD8^+$ T cells proliferation rate was further detected according to Ki67 staining. We have also identified that the proliferation of $CD4^+$ and $CD8^+$ T cells were significantly inhibited by MT and/or MSCs *in vitro*. Consistently, it was found that the local (aorta allografts) and systemic (recipient spleens) levels of $CD4^+$ and $CD8^+$ T cells in the recipients were also significantly declined by the treatment of MT and/or MSCs. According to the literature reports, the expressions of T cell activating factors (CD3e, lck, ZAP 70, LAT, and slp76) were significantly decreased when the MT dosage was increased. Similarly, the expression of CD69, a classic marker of early lymphocyte and T cell activation was significantly higher than that of normal group when the level of internal MT dropped after 6 weeks (59). Meanwhile, the interplay between MSCs and T cells have been extensively investigated. The proliferation-inhibiting effect of MSCs on T cells is thought to be meditated by the release of transforming growth factor-beta (TGF-β) and hepatocyte growth factor (HGF), which leads to the decrease of cyclin D2 and increase of $p27^{kipl}$ expression in T cells, resulting in arrest of proliferation in the G1 phase (60). The data obtained from our study have demonstrated that the inhibitory effect of MT and/or MSCs on the proliferation of $CD4^+$ and $CD8^+$ T cells is crucial for the prevention of CAV.

Th1 and its hallmark secretion factor IFN-γ play an essential role in initiating inflammatory response, thereby contributing to the development of CAV (61). IFN-γ has been demonstrated to

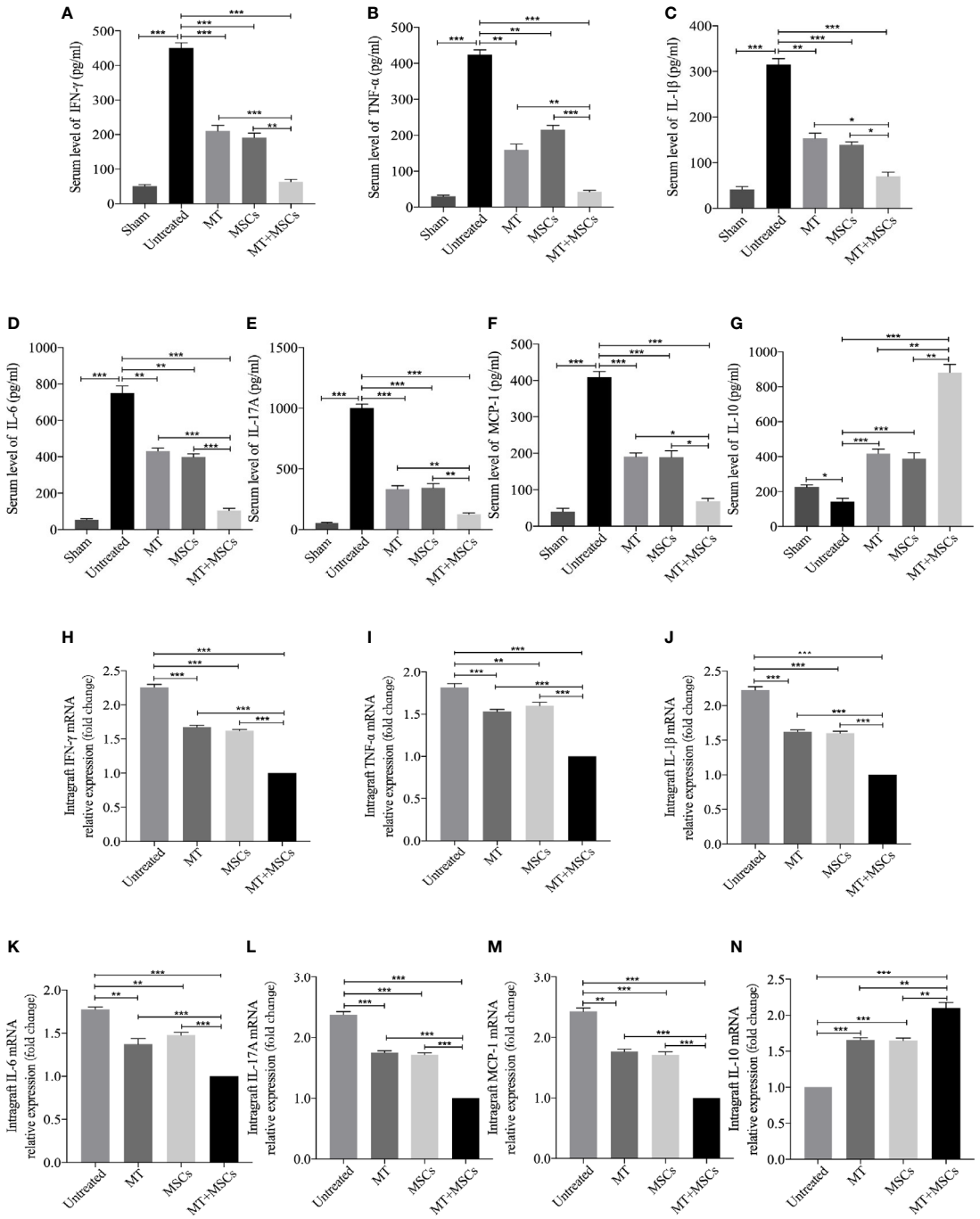

FIGURE 7 | MT in combination with MSCs further achieves reduce levels of pro-inflammatory cytokines, but increased level of IL-10 in transplant recipients. The IFN-γ, TNF-α, IL-1β, IL-6, IL-17A, MCP-1, and IL-10 are detected the in the recipient sera and grafts. **(A)** The level of serum IFN-γ among the groups; **(B)** The level of serum TNF-α among the groups; **(C)** The level of serum IL-1β among the groups; **(D)** The level of serum IL-6 among the groups; **(E)** The level of serum IL-17A among the groups; **(F)** The level of serum MCP-1 among the groups; **(G)** The level of serum IL-10 among the groups; **(H)** The mRNA expression levels of IFN-γ among the groups; **(I)** The mRNA expression level of TNF-α among the groups; **(J)** The mRNA expression level of IL-1β among the groups; **(K)** The mRNA expression level of IL-6 among the groups; **(L)** The mRNA expression level of IL-17A among the groups; **(M)** The mRNA expression level of MCP-1 among the groups; **(N)** The mRNA expression level of IL-10 among the groups. Statistical analysis is performed by one-way analysis of variance (ANOVA), n = 10 per group, $^{*}p < .05$, $^{**}p < .01$, and $^{***}p < .001$. Bar graphs represent mean ± SEM. MT, melatonin; MSCs, mesenchymal stromal cells. The experiments were independently repeated three times.

play a vital role in destroying the structure of the extracellular matrix, facilitating the proliferation of vascular smooth muscle cells and the deposition of extracellular collagen, ultimately leading to the development of CAV (13). The grafts in IFN-$\gamma^{-/-}$ mice have no signs of CAV for up to 8 weeks post-transplantation. In contrast, the grafts in wildtype recipients developed severe CAV in 50% of the recipients (62). There is increasing evidence that MSCs are capable of suppressing the expression of T-bet, a Th1-specific transcription factor and decreasing the level of IFN-γ (63). Furthermore, high-dose MT is believed to prolong the survival of syngeneic islet grafts by inhibiting the proliferation of Th1 cells (34). The above findings were further verified by our current study. We observed that infusion of both MT and MSCs to the recipients could synergistically inhibit Th1 cell response, thus preventing the progression of the CAV. Similarly, our *in vitro* co-culture experiments demonstrated that either MT or MSCs were capable of suppressing the activation of Th1 cells, and this inhibitory effect was further strengthened in the combination therapy group. In addition, MT in synergy with MSCs dramatically downregulated the level of IFN-γ in both the circulation and the allografts, and played a key role in the process of CAV.

IL-17, secreted by Th17 cells, is a potent proinflammatory cytokine that induces chemokine expression and leukocyte infiltration (64). The recent study suggested that, in addition to Th1 response, Th17 cell response exists in the process of CAV, and neutralization of IL-17 can ameliorate CAV (62). It comes to light that the infiltration of IL-17-producing $CD4^+$ T cells are predominant in an established MHC II mismatched (bm12-to-B6) model accompanied by early vascular inflammation and CAV (62). Nuria et al. (65) have discovered that the peripheral and central Th17 responses were distinctly inhibited by MT in the immunized experimental autoimmune encephalomyelitis model. In the current study, we have also observed that MT could significantly decrease the population of Th17 and the serum level of IL-17 in aorta transplant recipients. The underlying interaction between RORα, a lineage-specific transcription factor for Th17 cells, and MT could be the potential mechanism for the inhibition of Th17 cell differentiation. RORα highly promotes the generation of Th17 from naive T cells, while a deficiency of RORα inhibits the expression of IL-17 *in vitro* and *in vivo* (66). The degradation of RORα or translocation of RORα from the nucleus induced by MT may lead to this inhibitory effect (67). Also, after binding to MT1 receptor, MT promotes the phosphorylation of Erk1/2, which in turn induces the activation of CAAT/enhancer-binding protein α (C/EBPα). C/EBPα binds to the promoter of REV-ERBα and inhibits the expression of REV-ERBα. Subsequently, REV-ERBα reduces the expression of NFIL3 by binding to a consensus sequence in the Nfil3 gene locus. The recruitment of NFIL3 to the promoters of rora and rorc gene inhibits the expression of RORα (67). A similar trend was observed in the MSC monotherapy group, which is consistent with our previous research concerning that Th17 response was inhibited by MSCs in acute cardiac allograft rejection (68). Novel findings have indicated that the inhibition of Th17 cells by MSCs is also mediated by HGF (69). Furthermore, it has been reported that MSCs impair the IL-17 production by Th17 cells in a contact-dependent manner (70). The decreased expressions of allograft IL-17A and splenic Th17 cells have suggested that MT has synergy with MSCs in inhibiting Th17 response.

Compared with naive T cells, $CD4^+$ Tm cells have a lower activation threshold and are less dependent on co-stimulator molecules (71). Besides, the immune response of antigen-experienced $CD4^+$ Tm is much faster and stronger than those of naive T cells during a second-time immune response (72). It has been shown that $CD4^+$ Tm cells were a major population of infiltrating mononuclear cells in patients with CAV (12). Thus, alternative immunomodulatory protocols aiming to reduce $CD4^+$ Tm response are required. In this study, we have demonstrated that the splenic population of both $CD4^+$ Tcm and $CD4^+$ Tem were reduced in recipients treated with MT and/or MSCs. This finding was correlated with the previous reports demonstrating that MSCs and MT could independently inhibit $CD4^+$ Tcm and $CD4^+$ Tem (65, 73, 74). To our knowledge, lacking expression of CD44 on the surface of splenic $CD4^+$ T cells impairs the T cell adhesion to vascular endothelial cell (65, 75). Álvarez-Sánchez et al. have also reported that MT treatment could reduce CD44 expression in both peripheral Tem and Tcm, as well as downregulate the levels of IL-17A, IFN-γ, TNF-α in Tem (65). The results obtained from the present study demonstrated the reduced numbers of $CD4^+$ Tcm and $CD4^+$ Tem with a marked decrease in CD44 expression following the combination treatment of MT and MSCs, which are in line with the previous reports (65). On the basis of the *in vitro* data, we speculated that the sharp inhibition of $CD4^+$ T cell proliferation is one of the causes for the decrease of $CD4^+$ Tcm and $CD4^+$ Tem. We believe that the low expressions of $CD4^+$ Tcm and $CD4^+$ Tem are associated with ameliorated pathological changes of CAV.

Tregs play a major role in maintaining immune balance and preventing CAV (48, 76). Here, we further evaluated the effect of the combination therapy on the regulation of Treg population. MT monotherapy distinctly increased the proportion of splenic Tregs in transplant recipients and promoted $Foxp3^+$ Treg infiltration in allografts. Although MT caused a reduction in the number of Tregs in patients with metastatic solid tumors, it augments the number of $CD3^+CD4^+Foxp3^+$ cells in SLE (77). Based on the present study, we believe that MT increased the formation of Tregs under an inflammatory status. The previous research by Zhao et al. assumed that the upregulation of the Tregs was due to the inhibition of calcium/calmodulin-dependent kinase IV (CAMKIV) by MT (78). CAMKIV has been considered as a putative MT target. Silencing of CAMKIV increases Foxp3 production upon TGF-β stimulation from untreated lupus patients, indicating that CAMKIV acts as a negative Tregs regulator (79). However, detailed mechanisms still need to be elaborated. Instead, it is known that the generation of Treg induced by MSCs is predominantly dependent on TGF-β1 and IL-10 cytokines (80). Likewise, in the present study, the IL-10 levels in both the sera and the

allografts were increased in either MT or MSC monotherapy group. Thus, the elevated level of IL-10 could be a cause for Treg generation. Furthermore, we have also found that MT in synergy with MSCs prevented the development of CAV, suggesting that this finding is associated with the augment of Tregs.

DSA can activate complement and combine with intimal matrix and type IV collagen of endothelial cells, thus resulting in an unnational disorder of vascular endothelium and structural damage (81, 82). In the present study, we found that MT synergized with MSCs markedly inhibited allospecific IgG and IgM on POD 40. Based on the stimulating effect of $CD4^+$ Tm on the alloantibody production of B cells, we consider that the decreased proportion of $CD4^+$ Tcm and $CD4^+$ Tem in the present study may contribute to the low level of DSA. However, we did not find significant differences in total IgM and IgG among the experimental groups (data not shown), indicating that both MT and MSCs can effectively inhibit the generation of donor-specific immunoglobulins. Similar to the tendency of DSA, the population of $CD19^+CD86^+$ B cells were dramatically decreased in the recipients when treated with MT and MSCs, suggesting that MT synergized with MSCs could block DSA formation and restrain the response of $CD19^+CD86^+$ B cells. Several lines of evidences have demonstrated that MSCs are capable of suppressing the proliferation, differentiation, and activation of plasma cell generation, immunoglobulin-secreting ability of B cells through soluble factors secretion and cell-cell contact (83). Similarly, it has been previously reported that the expression of B cell activating factors CD19 were downregulated when pinealectomy mice were treated with exogenous MT (59), and this finding is in concurrence with our results.

In this study, untreated group developed a typical pathological feature of CAV accompanying with markedly increased infiltration of $CD4^+$ cells, $CD8^+$ cells, and macrophages, as well as the upregulated populations of splenic Th1, Th17, and $CD4^+$ Tm, and the enhanced levels of circulating allospecific IgG and IgM. In addition, our pilot study showed that these results had no significant differences between untreated group and DMSO vehicle control group (data not shown). Ultimately, we have demonstrated that either MT or MSC monotherapy could ameliorate the pathological changes of CAV. In addition to its immunomodulatory effects, MT could work through alleviating ischemia reperfusion and blocking oxidative stress of allografts. Therefore, it suggests that MT exerts its modulatory effect through both immunological and non-immunological properties. Moreover, we have elaborated that MT combined with MSCs dramatically abrogated allograft CAV, and the superposition of the effects of the two agents is warranted. Although the in-depth mechanisms and specific signaling pathways of MT in regulating chronic immune response still need to be elucidated, the present study highlights that MT has synergy with MSCs in suppressing CAV, and provides a novel therapeutic strategy for the prevention of chronic allograft rejection.

CONCLUSION

In the present study, we have investigated synergistic effects of MT and MSCs in attenuation of CAV in a mouse aorta transplantation model. Our results have demonstrated that MT synergizes with MSCs to significantly suppress allogeneic Th1, Th17, and $CD4^+$ Tm cell responses, decrease DSA production as well as promote the Treg population. These encouraging data were further convinced by obviously ameliorated pathological manifestations of CAV. Our study highlights the efficacy of MT and MSC combination therapy in inhibiting CAV and provides a novel therapeutic strategy to prevent CAV and thereby achieving long-term allograft survival following transplantation.

DATA AVAILABILITY STATEMENT

The original contributions presented in the study are included in the article/supplementary material. Further inquiries can be directed to the corresponding author.

ETHICS STATEMENT

The animal study was reviewed and approved by the Animal Care and Use Committee of Tianjin Medical University.

AUTHOR CONTRIBUTIONS

Y-FQ: conception and design, collection and assembly of data, data analysis and interpretation, and manuscript writing. D-JK and HQ: collection and assembly of data, data analysis and interpretation, and manuscript writing. Y-LZ, G-ML, C-LS, Y-MZ, H-DW, and J-PH: collection of data, data analysis and interpretation. HW: conception and design, financial support, administrative support, manuscript writing, and final approval of the manuscript. All authors contributed to the article and approved the submitted version.

FUNDING

This work was supported by grants to HW from the National Natural Science Foundation of China (No. 82071802), Tianjin Application Basis and Cutting-Edge Technology Research Grant (No. 14JCZDJC35700), Li Jieshou Intestinal Barrier Research Special Fund (No. LJS_201412), Natural Science Foundation of Tianjin (No. 18JCZDJC35800), and Tianjin Medical University Talent Fund; by a grant to D-JK from Tianjin Research Innovation Project for Postgraduate Students (No. 2019YJSS184); by a grant to G-ML from Tianjin Research Innovation Project for Postgraduate Students (2020YJSS176); and by a grant to H-DW from Tianjin Research Innovation Project for Postgraduate Students (2020YJSS177).

REFERENCES

1. Justiz Vaillant AA, Mohseni M. *Chronic Transplantation Rejection. Statpearls*. Treasure Island, FL: StatPearls Publishing Copyright © 2020, StatPearls Publishing LLC (2020).
2. Taylor DO, Edwards LB, Aurora P, Christie JD, Dobbels F, Kirk R, et al. Registry of the International Society for Heart and Lung Transplantation: Twenty-Fifth Official Adult Heart Transplant Report–2008. *J Heart Lung Transplant* (2008) 27(9):943–56. doi: 10.1016/j.healun.2008.06.017
3. Lund LH, Khush KK, Cherikh WS, Goldfarb S, Kucheryavaya AY, Levvey BJ, et al. The Registry of the International Society for Heart and Lung Transplantation: Thirty-fourth Adult Heart Transplantation Report-2017; Focus Theme: Allograft Ischemic Time. *J Heart Lung Transplant* (2017) 36 (10):1037–46. doi: 10.1016/j.healun.2017.07.019
4. Luo Z, Liao T, Zhang Y, Zheng H, Sun Q, Han F, et al. Triptolide Attenuates Transplant Vasculopathy Through Multiple Pathways. *Front Immunol* (2020) 11:612. doi: 10.3389/fimmu.2020.00612
5. Wang CY, Aronson I, Takuma S, Homma S, Naka Y, Alshafie T, et al. cAMP Pulse During Preservation Inhibits the Late Development of Cardiac Isograft and Allograft Vasculopathy. *Circ Res* (2000) 86(9):982–8. doi: 10.1161/01.res.86.9.982
6. Banner NR, Thomas HL, Curnow E, Hussey JC, Rogers CA, Bonser RS. The Importance of Cold and Warm Cardiac Ischemia for Survival After Heart Transplantation. *Transplantation* (2008) 86(4):542–7. doi: 10.1097/TP.0b013e31818149b9
7. Antunes A, Prieto D, Pinto C, Branco C, Correia P, Batista M, et al. Coronary Allograft Vasculopathy After Cardiac Transplantation: Prevalence, Prognostic and Risk Factors. *Rev Portuguesa Cirurgia Cardio-toracica e Vasc Orgao Oficial da Sociedade Portuguesa Cirurgia Cardio-Toracica e Vasc* (2017) 24(3-4):158.
8. Wang H, Zhang Z, Tian W, Liu T, Han H, Garcia B, et al. Memory T Cells Mediate Cardiac Allograft Vasculopathy and are Inactivated by Anti-OX40L Monoclonal Antibody. *Cardiovasc Drugs Ther* (2014) 28(2):115–22. doi: 10.1007/s10557-013-6502-9
9. Chen Y, Heeger PS, Valujskikh A. In Vivo Helper Functions of Alloreactive Memory CD4+ T Cells Remain Intact Despite Donor-Specific Transfusion and anti-CD40 Ligand Therapy. *J Immunol (Baltimore Md 1950)* (2004) 172 (9):5456–66. doi: 10.4049/jimmunol.172.9.5456
10. Zhang Q, Chen Y, Fairchild RL, Heeger PS, Valujskikh A. Lymphoid Sequestration of Alloreactive Memory CD4 T Cells Promotes Cardiac Allograft Survival. *J Immunol (Baltimore Md 1950)* (2006) 176(2):770–7. doi: 10.4049/jimmunol.176.2.770
11. Zhang QW, Rabant M, Schenk A, Valujskikh A. Icos-Dependent and -Independent Functions of Memory CD4 T Cells in Allograft Rejection. *Am J Transplant* (2008) 8(3):497–506. doi: 10.1111/j.1600-6143.2007.02096.x
12. van Loosdregt J, van Oosterhout MF, Bruggink AH, van Wichen DF, van Kuik J, de Koning E, et al. The Chemokine and Chemokine Receptor Profile of Infiltrating Cells in the Wall of Arteries With Cardiac Allograft Vasculopathy is Indicative of a Memory T-helper 1 Response. *Circulation* (2006) 114 (15):1599–607. doi: 10.1161/circulationaha.105.597526
13. Pichler M, Rainer PP, Schauer S, Hoefler G. Cardiac Fibrosis in Human Transplanted Hearts is Mainly Driven by Cells of Intracardiac Origin. *J Am Coll Cardiol* (2012) 59(11):1008–16. doi: 10.1016/j.jacc.2011.11.036
14. Chih S, Chong AY, Mielniczuk LM, Bhatt DL, Beanlands RS. Allograft Vasculopathy: The Achilles' Heel of Heart Transplantation. *J Am Coll Cardiol* (2016) 68(1):80–91. doi: 10.1016/j.jacc.2016.04.033
15. Nagano H, Mitchell RN, Taylor MK, Hasegawa S, Tilney NL, Libby P. Interferon-Gamma Deficiency Prevents Coronary Arteriosclerosis But Not Myocardial Rejection in Transplanted Mouse Hearts. *J Clin Invest* (1997) 100 (3):550–7. doi: 10.1172/jci119564
16. Murayama H, Takahashi M, Takamoto M, Shiba Y, Ise H, Koyama J, et al. Deficiency of Tumour Necrosis Factor-Alpha and Interferon-Gamma in Bone Marrow Cells Synergistically Inhibits Neointimal Formation Following Vascular Injury. *Cardiovasc Res* (2008) 80(2):175–80. doi: 10.1093/cvr/cvn250
17. Quaranta P, Focosi D, Freer G, Pistello M. Tweaking Mesenchymal Stem/Progenitor Cell Immunomodulatory Properties With Viral Vectors Delivering Cytokines. *Stem Cells Dev* (2016) 25(18):1321–41. doi: 10.1089/scd.2016.0145
18. Voisin C, Cauchois G, Reppel L, Laroye C, Louarn L, Schenowitz C, et al. Are the Immune Properties of Mesenchymal Stem Cells From Wharton's Jelly Maintained During Chondrogenic Differentiation? *J Clin Med* (2020) 9 (2):423. doi: 10.3390/jcm9020423
19. Chen C, Hou J. Mesenchymal Stem Cell-Based Therapy in Kidney Transplantation. *Stem Cell Res Ther* (2016) 7:16. doi: 10.1186/s13287-016-0283-6
20. Leventhal JR, Ildstad ST. Tolerance Induction in HLA Disparate Living Donor Kidney Transplantation by Facilitating Cell-Enriched Donor Stem Cell Infusion: The Importance of Durable Chimerism. *Hum Immunol* (2018) 79 (5):272–6. doi: 10.1016/j.humimm.2018.01.007
21. Li J, Meng X, Tao K, Dou K. Prolongation of Cardiac Allograft Survival by Syngeneic Hematopoietic Stem/Progenitor Cell Transplantation in Mice. *Adv Ther* (2008) 25(9):935–42. doi: 10.1007/s12325-008-0091-1
22. Casiraghi F, Perico N, Cortinovis M, Remuzzi G. Mesenchymal Stromal Cells in Renal Transplantation: Opportunities and Challenges. *Nat Rev Nephrol* (2016) 12(4):241–53. doi: 10.1038/nrneph.2016.7
23. Mannon RB. Macrophages: Contributors to Allograft Dysfunction, Repair, or Innocent Bystanders? *Curr Opin Organ Transplant* (2012) 17(1):20–5. doi: 10.1097/MOT.0b013e32834ee5b6
24. Di Ianni M, Del Papa B, De Ioanni M, Moretti L, Bonifacio E, Cecchini D, et al. Mesenchymal Cells Recruit and Regulate T Regulatory Cells. *Exp Hematol* (2008) 36(3):309–18. doi: 10.1016/j.exphem.2007.11.007
25. Casiraghi F, Azzollini N, Cassis P, Imberti B, Morigi M, Cugini D, et al. Pretransplant Infusion of Mesenchymal Stem Cells Prolongs the Survival of a Semiallogeneic Heart Transplant Through the Generation of Regulatory T Cells. *J Immunol (Baltimore Md 1950)* (2008) 181(6):3933–46. doi: 10.4049/jimmunol.181.6.3933
26. Ye K, Lan X, Wang G, Zhang B, Xu X, Li X, et al. B7-H1 Expression is Required for Human Endometrial Regenerative Cells in the Prevention of Transplant Vasculopathy in Mice. *Stem Cells Int* (2018) 2018:2405698. doi: 10.1155/2018/2405698
27. Huang WC, Liao SK, Wallace CG, Chang NJ, Lin JY, Wei FC. Greater Efficacy of Tolerance Induction With Cyclosporine Versus Tacrolimus in Composite Tissue Allotransplants With Less Myeloablative Conditioning. *Plast Reconstruct Surg* (2011) 127(3):1141–8. doi: 10.1097/PRS.0b013e3182043695
28. Buron F, Perrin H, Malcus C, Héquet O, Thaunat O, Kholopp-Sarda MN, et al. Human Mesenchymal Stem Cells and Immunosuppressive Drug Interactions in Allogeneic Responses: An In Vitro Study Using Human Cells. *Transplant Proc* (2009) 41(8):3347–52. doi: 10.1016/j.transproceed.2009.08.030
29. Hoogduijn MJ, Crop MJ, Korevaar SS, Peeters AM, Eijken M, Maat LP, et al. Susceptibility of Human Mesenchymal Stem Cells to Tacrolimus, Mycophenolic Acid, and Rapamycin. *Transplantation* (2008) 86(9):1283–91. doi: 10.1097/TP.0b013e31818aa536
30. Tsuji W, Schnider JT, McLaughlin MM, Schweizer R, Zhang W, Solari MG, et al. Effects of Immunosuppressive Drugs on Viability and Susceptibility of Adipose- and Bone Marrow-Derived Mesenchymal Stem Cells. *Front Immunol* (2015) 6:131. doi: 10.3389/fimmu.2015.00131
31. Hu C, Li L. Melatonin Plays Critical Role in Mesenchymal Stem Cell-Based Regenerative Medicine In Vitro and In Vivo. *Stem Cell Res Ther* (2019) 10 (1):13. doi: 10.1186/s13287-018-1114-8
32. Reiter RJ, Tan DX, Fuentes-Broto L. Melatonin: A Multitasking Molecule. *Prog Brain Res* (2010) 181:127–51. doi: 10.1016/s0079-6123(08)81008-4
33. Jung FJ, Yang L, Harter L, Inci I, Schneiter D, Lardinois D, et al. Melatonin In Vivo Prolongs Cardiac Allograft Survival in Rats. *J Pineal Res* (2004) 37(1):36–41. doi: 10.1111/j.1600-079X.2004.00133.x
34. Lin GJ, Huang SH, Chen YW, Hueng DY, Chien MW, Chia WT, et al. Melatonin Prolongs Islet Graft Survival in Diabetic NOD Mice. *J Pineal Res* (2009) 47(3):284–92. doi: 10.1111/j.1600-079X.2009.00712.x
35. Vairetti M, Ferrigno A, Bertone R, Rizzo V, Richelmi P, Bertè F, et al. Exogenous Melatonin Enhances Bile Flow and ATP Levels After Cold Storage and Reperfusion in Rat Liver: Implications for Liver Transplantation. *J Pineal Res* (2005) 38(4):223–30. doi: 10.1111/j.1600-079X.2004.00193.x
36. Inci I, Inci D, Dutly A, Boehler A, Weder W. Melatonin Attenuates Posttransplant Lung Ischemia-Reperfusion Injury. *Ann Thorac Surg* (2002) 73(1):220–5. doi: 10.1016/s0003-4975(01)03101-0

37. Li Z, Nickkholgh A, Yi X, Bruns H, Gross ML, Hoffmann K, et al. Melatonin Protects Kidney Grafts From Ischemia/Reperfusion Injury Through Inhibition of NF-kB and Apoptosis After Experimental Kidney Transplantation. *J Pineal Res* (2009) 46(4):365–72. doi: 10.1111/j.1600-079X.2009.00672.x
38. Calvo JR, González-Yanes C, Maldonado MD. The Role of Melatonin in the Cells of the Innate Immunity: A Review. *J Pineal Res* (2013) 55(2):103–20. doi: 10.1111/jpi.12075
39. Zahran R, Ghozy A, Elkholy SS, El-Taweel F, El-Magd MA. Combination Therapy With Melatonin, Stem Cells and Extracellular Vesicles is Effective in Limiting Renal Ischemia–Reperfusion Injury in a Rat Model. *Int J Urol* (2020) 27(11):1039–49. doi: 10.1111/iju.14345
40. Yu S, Cheng Y, Zhang L, Yin Y, Xue J, Li B, et al. Treatment With Adipose Tissue-Derived Mesenchymal Stem Cells Exerts Anti-Diabetic Effects, Improves Long-Term Complications, and Attenuates Inflammation in Type 2 Diabetic Rats. *Stem Cell Res Ther* (2019) 10(1):333. doi: 10.1186/s13287-019-1474-8
41. Mazini L, Rochette L, Amine M, Malka G. Regenerative Capacity of Adipose Derived Stem Cells (Adscs), Comparison With Mesenchymal Stem Cells (Mscs). *Int J Mol Sci* (2019) 20(10):2523. doi: 10.3390/ijms20102523
42. Labat A, Calise D, Thiers JC, Pieraggi MT, Cerene A, Fournial G, et al. Simultaneous Orthotopic Transplantation of Carotid and Aorta in the Rat by the Sleeve Technique. *Lab Anim* (2002) 36(4):426–31. doi: 10.1258/002367702320389099
43. Sho M, Harada H, Rothstein DM, Sayegh MH. CD45RB-Targeting Strategies for Promoting Long-Term Allograft Survival and Preventingchronic Allograft Vasculopathy. *Transplantation* (2003) 75(8):1142–6. doi: 10.1097/01.Tp.0000060567.48258.9d
44. Lee JH, Han YS, Lee SH. Potentiation of Biological Effects of Mesenchymal Stem Cells in Ischemic Conditions by Melatonin Via Upregulation of Cellular Prion Protein Expression. *J Pineal Res* (2017) 62(2):10.1111/jpi.12385. doi: 10.1111/jpi.12385
45. Shaji AV, Kulkarni SK, Agrewala JN. Regulation of Secretion of IL-4 and IgG1 Isotype by Melatonin-Stimulated Ovalbumin-Specific T Cells. *Clin Exp Immunol* (1998) 111(1):181–5. doi: 10.1046/j.1365-2249.1998.00493.x
46. Pasztorek M, Rossmanith E, Mayr C, Hauser F, Jacak J, Ebner A, et al. Influence of Platelet Lysate on 2D and 3D Amniotic Mesenchymal Stem Cell Cultures. *Front Bioeng Biotechnol* (2019) 7:338. doi: 10.3389/fbioe.2019.00338
47. Lan X, Wang G, Xu X, Lu S, Li X, Zhang B, et al. Stromal Cell-Derived Factor-1 Mediates Cardiac Allograft Tolerance Induced by Human Endometrial Regenerative Cell-Based Therapy. *Stem Cells Transl Med* (2017) 6(11):1997–2008. doi: 10.1002/sctm.17-0091
48. Wang H, Qi F, Dai X, Tian W, Liu T, Han H, et al. Requirement of B7-H1 in Mesenchymal Stem Cells for Immune Tolerance to Cardiac Allografts in Combination Therapy With Rapamycin. *Transplant Immunol* (2014) 31 (2):65–74. doi: 10.1016/j.trim.2014.06.005
49. Bartholomew A, Sturgeon C, Siatskas M, Ferrer K, McIntosh K, Patil S, et al. Mesenchymal Stem Cells Suppress Lymphocyte Proliferation In Vitro and Prolong Skin Graft Survival In Vivo. *Exp Hematol* (2002) 30(1):42–8. doi: 10.1016/s0301-472x(01)00769-x
50. Illigens BM, Yamada A, Anosova N, Dong VM, Sayegh MH, Benichou G. Dual Effects of the Alloresponse by Th1 and Th2 Cells on Acute and Chronic Rejection of Allotransplants. *Eur J Immunol* (2009) 39(11):3000–9. doi: 10.1002/eji.200838980
51. Syrjala SO, Keranen MA, Tuuminen R, Nykanen AI, Tammi M, Krebs R, et al. Increased Th17 Rather Than Th1 Alloimmune Response is Associated With Cardiac Allograft Vasculopathy After Hypothermic Preservation in the Rat. *J Heart Lung Transplant* (2010) 29(9):1047–57. doi: 10.1016/j.healun.2010.04.012
52. Ye K, Lan X, Wang G, Zhang B, Xu X, Li X, et al. B7-H1 Expression is Required for Human Endometrial Regenerative Cells in the Prevention of Transplant Vasculopathy in Mice. *Stem Cells Int* (2018) 2018:1–12. doi: 10.1155/2018/2405698
53. Abele-Ohl S, Leis M, Mahmoudian S, Weyand M, Stamminger T, Ensminger SM. Rag2-/- Gamma-Chain-/- Mice as Hosts for Human Vessel Transplantation and Allogeneic Human Leukocyte Reconstitution. *Transpl Immunol* (2010) 23(1-2):59–64. doi: 10.1016/j.trim.2010.04.003
54. Rafat A, Mohammadi Roushandeh A, Alizadeh A, Hashemi-Firouzi N, Golipoor Z. Comparison of The Melatonin Preconditioning Efficacy Between Bone Marrow and Adipose-Derived Mesenchymal Stem Cells. *Cell J* (2019) 20(4):450–8. doi: 10.22074/cellj.2019.5507
55. Shaw KM, Stern GM, Sandler M. Melatonin and Parkinsonism. *Lancet (London England)* (1973) 1(7797):271. doi: 10.1016/s0140-6736(73)90118-9
56. Gitto E, Reiter RJ, Sabatino G, Buonocore G, Romeo C, Gitto P, et al. Correlation Among Cytokines, Bronchopulmonary Dysplasia and Modality of Ventilation in Preterm Newborns: Improvement With Melatonin Treatment. *J Pineal Res* (2005) 39(3):287–93. doi: 10.1111/j.1600-079X.2005.00251.x
57. Andersen LP, Gogenur I, Rosenberg J, Reiter RJ. The Safety of Melatonin in Humans. *Clin Drug Investig* (2016) 36(3):169–75. doi: 10.1007/s40261-015-0368-5
58. Fischbein MP, Yun J, Laks H, Irie Y, Fishbein MC, Bonavida B, et al. Role of CD8+ Lymphocytes in Chronic Rejection of Transplanted Hearts. *J Thoracic Cardiovasc Surg* (2002) 123(4):803–9. doi: 10.1067/mtc.2002.120008
59. Luo J, Zhang Z, Sun H, Song J, Chen X, Huang J, et al. Effect of Melatonin on T/B Cell Activation and Immune Regulation in Pinealectomy Mice. *Life Sci* (2020) 242:117191. doi: 10.1016/j.lfs.2019.117191
60. Di Nicola M, Carlo-Stella C, Magni M, Milanesi M, Longoni PD, Matteucci P, et al. Human Bone Marrow Stromal Cells Suppress T-lymphocyte Proliferation Induced by Cellular or Nonspecific Mitogenic Stimuli. *Blood* (2002) 99(10):3838–43. doi: 10.1182/blood.v99.10.3838
61. Hamano K, Bashuda H, Ito H, Shirasawa B, Okumura K, Esato K. Graft Vasculopathy and Tolerance: Does the Balance of Th Cells Contribute to Graft Vasculopathy? *J Surg Res* (2000) 93(1):28–34. doi: 10.1006/jsre.2000.5967
62. Yuan X, Paez-Cortez J, Schmitt-Knosalla I, D'Addio F, Mfarrej B, Donnarumma M, et al. A Novel Role of CD4 Th17 Cells in Mediating Cardiac Allograft Rejection and Vasculopathy. *J Exp Med* (2008) 205 (13):3133–44. doi: 10.1084/jem.20081937
63. Özdemir AT, Özgül Özdemir RB, Kırmaz C, Sarıboyacı AE, Ünal Halbutoğlları ZS, Özel C, et al. The Paracrine Immunomodulatory Interactions Between the Human Dental Pulp Derived Mesenchymal Stem Cells and CD4 T Cell Subsets. *Cell Immunol* (2016) 310:108–15. doi: 10.1016/j.cellimm.2016.08.008
64. Park H, Li Z, Yang XO, Chang SH, Nurieva R, Wang YH, et al. A Distinct Lineage of CD4 T Cells Regulates Tissue Inflammation by Producing Interleukin 17. *Nat Immunol* (2005) 6(11):1133–41. doi: 10.1038/ni1261
65. Alvarez-Sanchez N, Cruz-Chamorro I, Lopez-Gonzalez A, Utrilla JC, Fernandez-Santos JM, Martinez-Lopez A, et al. Melatonin Controls Experimental Autoimmune Encephalomyelitis by Altering the T Effector/Regulatory Balance. *Brain Behav Immun* (2015) 50:101–14. doi: 10.1016/j.bbi.2015.06.021
66. Yang XO, Pappu BP, Nurieva R, Akimzhanov A, Kang HS, Chung Y, et al. T Helper 17 Lineage Differentiation is Programmed by Orphan Nuclear Receptors ROR Alpha and ROR Gamma. *Immunity* (2008) 28(1):29–39. doi: 10.1016/j.immuni.2007.11.016
67. Ren W, Liu G, Chen S, Yin J, Wang J, Tan B, et al. Melatonin Signaling in T Cells: Functions and Applications. *J Pineal Res* (2017) 62(3):10.1111/jpi.12394. doi: 10.1111/jpi.12394
68. Zhao Y, Li X, Yu D, Hu Y, Jin W, Qin Y, et al. Galectin-9 is Required for Endometrial Regenerative Cells to Induce Long-Term Cardiac Allograft Survival in Mice. *Stem Cell Res Ther* (2020) 11(1):471. doi: 10.1186/s13287-020-01985-0
69. Chen QH, Wu F, Liu L, Chen HB, Zheng RQ, Wang HL, et al. Mesenchymal Stem Cells Regulate the Th17/Treg Cell Balance Partly Through Hepatocyte Growth Factor In Vitro. *Stem Cell Res Ther* (2020) 11(1):91. doi: 10.1186/s13287-020-01612-y
70. Luz-Crawford P, Hernandez J, Djouad F, Luque-Campos N, Caicedo A, Carrère-Kremer S, et al. Mesenchymal Stem Cell Repression of Th17 Cells is Triggered by Mitochondrial Transfer. *Stem Cell Res Ther* (2019) 10(1):232. doi: 10.1186/s13287-019-1307-9
71. Mishima T, Toda S, Ando Y, Matsunaga T, Inobe M. Rapid Proliferation of Activated Lymph Node CD4(+) T Cells is Achieved by Greatly Curtailing the Duration of Gap Phases in Cell Cycle Progression. *Cell Mol Biol Lett* (2014) 19 (4):638–48. doi: 10.2478/s11658-014-0219-z

72. Blattman JN, Antia R, Sourdive DJ, Wang X, Kaech SM, Murali-Krishna K, et al. Estimating the Precursor Frequency of Naive Antigen-Specific CD8 T Cells. *J Exp Med* (2002) 195(5):657–64. doi: 10.1084/jem.20001021
73. Ribeiro A, Laranjeira P, Mendes S, Velada I, Leite C, Andrade P, et al. Mesenchymal Stem Cells From Umbilical Cord Matrix, Adipose Tissue and Bone Marrow Exhibit Different Capability to Suppress Peripheral Blood B, Natural Killer and T Cells. *Stem Cell Res Ther* (2013) 4(5):125. doi: 10.1186/scrt336
74. Luque-Campos N, Contreras-López RA, Jose Paredes-Martínez M, Torres MJ, Bahraoui S, Wei M, et al. Mesenchymal Stem Cells Improve Rheumatoid Arthritis Progression by Controlling Memory T Cell Response. *Front Immunol* (2019) 10:798. doi: 10.3389/fimmu.2019.00798
75. Baaten BJ, Tinoco R, Chen AT, Bradley LM. Regulation of Antigen-Experienced T Cells: Lessons From the Quintessential Memory Marker Cd44. *Front Immunol* (2012) 3:23. doi: 10.3389/fimmu.2012.00023
76. Roldan C, Mirabet S, Brossa V, Molto E, Lopez L, Alvaro Y, et al. Correlation of Immunological Markers With Graft Vasculopathy Development in Heart Transplantation. *Transplant Proc* (2012) 44(9):2653–6. doi: 10.1016/j.transproceed.2012.09.048
77. Medrano-Campillo P, Sarmiento-Soto H, Alvarez-Sanchez N, Alvarez-Rios AI, Guerrero JM, Rodriguez-Prieto I, et al. Evaluation of the Immunomodulatory Effect of Melatonin on the T-cell Response in Peripheral Blood From Systemic Lupus Erythematosus Patients. *J Pineal Res* (2015) 58(2):219–26. doi: 10.1111/jpi.12208
78. Zhao CN, Wang P, Mao YM, Dan YL, Wu Q, Li XM, et al. Potential Role of Melatonin in Autoimmune Diseases. *Cytokine Growth Factor Rev* (2019) 48:1–10. doi: 10.1016/j.cytogfr.2019.07.002
79. Koga T, Ichinose K, Mizui M, Crispín JC, Tsokos GC. Calcium/Calmodulin-Dependent Protein Kinase IV Suppresses IL-2 Production and Regulatory T Cell Activity in Lupus. *J Immunol (Baltimore Md 1950)* (2012) 189(7):3490–6. doi: 10.4049/jimmunol.1201785
80. Sakaguchi S, Ono M, Setoguchi R, Yagi H, Hori S, Fehervari Z, et al. Foxp3+ CD25+ CD4+ Natural Regulatory T Cells in Dominant Self-Tolerance and Autoimmune Disease. *Immunol Rev* (2006) 212:8–27. doi: 10.1111/j.0105-2896.2006.00427.x
81. Zorn E. Effector B Cells in Cardiac Allograft Vasculopathy. *Curr Opin Organ Transplant* (2019) 24(1):31–6. doi: 10.1097/mot.0000000000000591
82. Jansen MA, Otten HG, de Weger RA, Huibers MM. Immunological and Fibrotic Mechanisms in Cardiac Allograft Vasculopathy. *Transplantation* (2015) 99(12):2467–75. doi: 10.1097/tp.0000000000000848
83. Corcione A, Benvenuto F, Ferretti E, Giunti D, Cappiello V, Cazzanti F, et al. Human Mesenchymal Stem Cells Modulate B-cell Functions. *Blood* (2006) 107(1):367–72. doi: 10.1182/blood-2005-07-2657

Conflict of Interest: The authors declare that the research was conducted in the absence of any commercial or financial relationships that could be construed as a potential conflict of interest.

frontiers in Immunology

MINI REVIEW
published: 20 May 2021
doi: 10.3389/fimmu.2021.661643

Tackling Chronic Kidney Transplant Rejection: Challenges and Promises

Xingqiang Lai[1,2,3], *Xin Zheng*[4], *James M. Mathew*[1,2], *Lorenzo Gallon*[1,5], *Joseph R. Leventhal*[1,2] *and Zheng Jenny Zhang*[1,2*]

[1] Comprehensive Transplant Center, Northwestern University Feinberg School of Medicine, Chicago, IL, United States, [2] Department of Surgery, Northwestern University Feinberg School of Medicine, Chicago, IL, United States, [3] Organ Transplant Center, the Second Affiliated Hospital of Guangzhou Medical University, Guangzhou, China, [4] Department of Urology, Beijing Youan Hospital, Capital Medical University, Beijing, China, [5] Department of Medicine, Nephrology, Northwestern University Feinberg School of Medicine, Chicago, IL, United States

Despite advances in post-transplant management, the long-term survival rate of kidney grafts and patients has not improved as approximately forty percent of transplants fails within ten years after transplantation. Both immunologic and non-immunologic factors contribute to late allograft loss. Chronic kidney transplant rejection (CKTR) is often clinically silent yet progressive allogeneic immune process that leads to cumulative graft injury, deterioration of graft function. Chronic active T cell mediated rejection (TCMR) and chronic active antibody-mediated rejection (ABMR) are classified as two principal subtypes of CKTR. While significant improvements have been made towards a better understanding of cellular and molecular mechanisms and diagnostic classifications of CKTR, lack of early detection, differential diagnosis and effective therapies continue to pose major challenges for long-term management. Recent development of high throughput cellular and molecular biotechnologies has allowed rapid development of new biomarkers associated with chronic renal injury, which not only provide insight into pathogenesis of chronic rejection but also allow for early detection. In parallel, several novel therapeutic strategies have emerged which may hold great promise for improvement of long-term graft and patient survival. With a brief overview of current understanding of pathogenesis, standard diagnosis and challenges in the context of CKTR, this mini-review aims to provide updates and insights into the latest development of promising novel biomarkers for diagnosis and novel therapeutic interventions to prevent and treat CKTR.

Keywords: chronic allograft rejection, kidney transplant, biomarkers, IFTA, T cells mediated rejection

OPEN ACCESS

Edited by:
Hao Wang,
Tianjin Medical University General Hospital, China

Reviewed by:
Maarten Naesens,
KU Leuven, Belgium
Longshan Liu,
Sun Yat-Sen University, China
Dengping Yin,
University of Chicago, United States

****Correspondence:***
Zheng Jenny Zhang
zjzhang@northwestern.edu

Specialty section:
This article was submitted to Alloimmunity and Transplantation, a section of the journal Frontiers in Immunology

Received: *31 January 2021*
Accepted: *27 April 2021*
Published: *20 May 2021*

Citation:
Lai X, Zheng X, Mathew JM, Gallon L, Leventhal JR and Zhang ZJ (2021) Tackling Chronic Kidney Transplant Rejection: Challenges and Promises. Front. Immunol. 12:661643. doi: 10.3389/fimmu.2021.661643

INTRODUCTION

Chronic kidney transplant rejection (CKTR) is characterized by progressive decrease of renal graft function that starts to manifest at one-year after the transplantation and usually accompanied by hypertension and proteinuria (1). CKTR usually occurs in patients with insufficient immunosuppression or medication nonadherence (2). While Persistent allogeneic immune response remains a major cause (3, 4), multiple risk factors, e.g. early ischemia reperfusion injury, acute rejection episodes and transplant infectious diseases, can contribute to the development and

progression of CKTR. Histologically, there are two principal distinct subtypes of CKTR, namely chronic active antibody-mediated rejection (ABMR) and chronic active T cell-mediated rejection (TCMR) according to the revised Banff criteria (5, 6). It is not uncommon that both chronic active TCMR/ABMR co-exist and lead to rapid loss of graft function (7–9).

Effective treatment and prognosis of CKTR are largely dependent upon the severity and reversibility of rejection at the time of diagnosis. However, it remains a major challenge to identify early changes before irreversible damage to the graft occurs. Currently, no immunotherapies are clinically proven to be effective in prevention and treatment of CKTR, particularly ABMR. Recent advances in high-throughput cellular and molecular biotechnologies have allowed for in-depth analyses of cellular and molecular processes and deconvolutions of mechanisms underlying CKTR and have led to identification and validation of new molecular and cellular biomarkers through non-invasive or minimal-invasive approaches. The discovery of these biomarkers holds tremendous promise for early detection and development of promising novel therapies for improvement of kidney transplant outcomes. This review will first provide a brief summary on current understanding of pathogenesis and standard mothed challenges for the diagnosis of CKTR, and then, focus on more in-depth discussions to the area of biomarker discovery and novel therapeutic interventions to improve long term transplant outcome.

PATHOGENESIS OF CHRONIC ACTIVE ABMR AND CHRONIC TCMR

Chronic active ABMR represents most cases of CKTR (2), featuring transplant glomerulopathy along with severe peritubular capillary basement membrane multilayering and new onset arterial intimal fibrosis. In contract, chronic active TCMR is determined based on inflammation in areas of the cortex with interstitial fibrosis and tubular atrophy (i-IFTA), a hallmark feature of CKTR in addition to tubulitis. The newly revised Banff criteria of chronic active TCMR recognize the pathogenic importance of TCMR in the development of chronic interstitial inflammation leading to i-IFTA, nonetheless, it does not discriminate alloimmune-mediated tissue injury from 'non-specific injuries, particularly calcineuirn inhibitor (CNI) mediated nephrotoxicities (10, 11).

While precise mechanisms underlying ABMR remain elusive, it is believed that the interaction of donor-specific alloantibodies (DSAs) against donor HLA antigens, especially HLA class II antigens expressed by endothelial cells of the microvascular circulation, initiates ABMR (12). DSAs binding to endothelial cells leads to a cascade of molecular events, including complement activation that may contribute to endothelial dysfunction, microvascular inflammation and remodeling, and ultimately results in irreversible tissue injury (13). B cell deficiency resulted in reduced transplant glomerulopathy, decreased microvascular inflammation, reduced macrophage infiltration and IFNγ transcripts in the allograft (14), which underscores the importance of B cells in the pathogenesis of ABMR. In addition to uncontrolled allogeneic immune response due to insufficient immunosuppression or nonadherence, early inflammatory events such as acute TCMR and viral infection are suggested to be risk factors for DSA (dnDSA) production (15–17). Preceding TCMR is found to be strongly correlated with development of chronic active ABMR dnDSA (7). Moreover, it has been shown in biopsy-proven chronic active ABMR cases that T cells (especially CD8+ T cells) and macrophages are the dominant infiltrating cell types in glomerulus, whereas B cells are frequently observed in the tubulointerstitial compartment, indicating that both T cells and macrophages play a pivotal role in renal chronic ABMR (18). The involvement of NK cells in ABMR has recently gained attention. Recent studies have revealed that NK cells are involved in ABMR *via* CD16a Fc receptors (19, 20). Depletion of NK cells significantly mitigates DSA-induced chronic allograft vasculopathy (CAV) (21). NK cells increase IFNγ production after exposure to alloantigens through an antibody-dependent cellular cytotoxicity-like mechanisms, which is associated with an increased risk for ABMR (22) and NK cell infiltration predicts poor outcome after kidney transplantation (23).

Persistent T cell–mediated injuries can lead to chronic active TCMR (24). Alloreactive effector memory T Cells (Tem), particularly CD8+ Tem subsets (express increased CD44hi, CD45RO+, OX40, KLRG-1 and BLIMP-1), are implicated in the development of TCMR (25). Unlike naïve T cells, Tem cells are known for their low activation threshold, robust effector functions, and resistance to conventional immunosuppression and costimulation blockade (26). Memory T cells are originated from environmental antigens or generated from previous rejection episodes and once activated, they enter into the renal interstitium and secrete several cytokines such as IFNγ and TGFβ, and subsequently trigger a cascade of inflammation leading to tubulitis (27). Chronic TCMR also results in renal vasculature injuries, such as arterial inflammation and intimal fibrosis (6). In a recent study, Claudia and colleagues (25) demonstrated that CD8+ effector memory T cells mediated by the OX40 gene pathway play an important role in the pathogenesis of chronic TCMR.

CURRENT DIAGNOSIS AND CHALLENGES

Early diagnosis of CKTR determines successful therapeutic interventions and prognosis. CKTR is a slowly progressive process in which pathologic changes as such vascular inflammation and i-IFTA do not have clinical manifestations until late stages. In addition, differential diagnosis is extremely important to distinguish CKTR from late graft dysfunction caused by other complications including CNI toxicity, BK-virus associated nephropathy and recurrent renal diseases, each of which requires different treatment. Transplant patients are subjected to routine laboratory tests for continuous graft monitoring. Serum creatinine (sCr), blood urea nitrogen (BUN) and cystatin C are commonly used to evaluate graft function. The estimated glomerular filtration rate (eGFR),

calculated based on sCr level, age, weight and gender, is considered as an accurate indicator and predictor for graft function and long-term graft survival (28). Proteinuria>500 mg/day is also considered as a marker of chronic kidney allograft dysfunction (29). However, because chronic rejection is an indolent process with slow progression in pathologic changes (30), these aforementioned tests are non-specific, often failing to detect renal damage at early stages and easily influenced by other non-immune injuries can also influence the results. Emergence of circulating *de novo* DSAs is associated with increased risk for graft failure as a result of chronic active ABMR (31, 32). Prospective monitoring for DSAs may be indicative for early treatment before irreversible graft injury (33, 34), however, not all DSAs are doomed to be pathogenic (35) and DSA levels may not correlate with tissue injury (15). Imaging technologies such as Doppler ultrasonography (US), Contrast-enhanced ultrasound (CEUS) and Magnetic Resonance Imaging (MRI) are non-invasive complementary methodologies used to assist in the early diagnosis of both acute and chronic graft rejection by evaluating renal vasculature resistance (US) (36, 37), graft blood perfusion (CEUS) (38), and anatomical changes (MRI) such as fibrosis (39). However, findings from these tests are mostly non-specific with limited value in guiding the clinical treatment.

Currently, graft biopsies still remain the gold standard for diagnosing graft rejection. Graft histology provides visual evidence of the underlying pathology and pathogenesis of graft dysfunction. More recently, genetic analysis of biopsy tissue has been used to assist in the differential diagnosis of allograft rejection in conjunction with histology and immunohistochemistry. The Banff classification, founded in 1991, has established specific criteria for the diagnosis of kidney allograft rejection. It has been updated multiple times in the past two decades (5). C4d complement fragment deposition in the peritubular capillaries was regarded as a marker for ABMR (40), but removed as a diagnostic criterion in the latest Banff (2019) Classification Criteria for chronic active ABMR due to the emergence of C4d negative ABMR (41). Although histological examination through renal biopsy remains the diagnostic gold standard criterion, it cannot be carried out too often due to its invasiveness. Graft needle biopsy can cause various surgery-related complications, such as perinephric hematoma, arteriovenous fistula, bleeding, infection. In addition, there are other limitations associated with histologic examination, e.g. lack of standardization and quantitation, sampling errors and accurate diagnosis largely relies on the pathologists' skills (42). Therefore, non-/minimally-invasive and predictive biomarkers are highly desirable for early diagnosis and tailored inventions to delay or prevent CKTR and improve graft longevity.

POTENTIAL BIOMARKERS FOR EARLY DIAGNOSIS AND PROGNOSIS

Recent development of high-throughput cellular and molecular biotechnologies has led to tremendous advances in biomarker discoveries in the field of transplantation, with great promise for better understanding and management of CKTR. Contributions of biomarker studies are multifold, including 1) generating new insight into molecular mechanisms of CKTR, 2) allowing for early and differential diagnosis, 3) providing evaluation of therapeutic intervention, and 4) predicting prognosis. Principal characteristics of the biomarkers have been thoroughly reviewed elsewhere (42–44). Although most studies have centered in exploring non-invasive biomarkers for ischemia/reperfusion injury and acute allograft rejection in blood and urine (42), a variety of biomarkers generated from studies in renal protocol biopsies and blood and urine samples are suggestive for diagnosis and prognosticator for CKTR. Based on the characteristics of the biomarkers and technologies used, biomarkers pertaining to CKTR can be divided into five main categories: transcriptomic biomarkers, Epigenetic biomarkers, Proteomic biomarkers, and Metabolomic biomarkers, and cellular biomarkers, which are summarized **Table 1**, and also briefly discussed in the following sections.

Transcriptomic Biomarkers

These biomarkers are generated by high-throughput gene or transcriptome profiling, also termed transcriptomics, using microarray and next generation gene sequencing technologies. These studies have been more commonly performed on renal biopsy samples as they provide sufficient material for RNA extraction. As listed in **Table 1**, gene signatures associated with fibrosis, i-IFTA, chronic rejection (ABMR and TCMR) and graft failure can be identified by determining gene expression profiling (45–53). Importantly, the gene set has higher predictive capacity than that of baseline clinical variables, and clinical and pathological variables. One notion from these studies is that similar gene signatures for acute rejection are also indicative of CKTR. For example, a study by Khatri et al. (85) revealed 11 genes associated with acute rejection across different engrafted tissues, among which 7 genes (*CD6, INPP5D, ISG20, NKG7, PSMB9, RUNX3*, and *TAP1*) were identified as predictors for the development of progressive i-IFTA at 24 months posttransplant (45). More interestingly, a set of four gene markers (*vimentin, NKCC2, E-cadherin, and 18S rRNA*) in urine samples has been identified as reliable non-invasive biomarkers for i-IFTA (46).

Epigenetic Biomarkers

Epigenetic modifications and regulators control relevant gene expression and function in response to altered biological process, and thereby can be employed as disease biomarkers (86). Epigenetic modifications include cytosine methylation of DNA at cytosine-phosphate diester-guanine dinucleotides, microRNA interactions, histone modifications, and chromatin remodeling complexes (87), which occur to genome without alteration of the DNA sequence. Epigenetics is an emerging field of research in kidney transplantation. Most studies have been performed in the context of ischemia and reperfusion injury and acute rejection, demonstrating the implication of aberrant DNA methylation (88). Recent studies in both humans and animals (54, 89) have shown that altered epigenetic modifications, particularly DNA methylation, influences the activation, proliferation,

TABLE 1 | Potential biomarkers for chronic rejection.

Biomarker classification	Biomarker candidate	Sample type	AUC	Sensitivity/ Specificity	Application	Ref
Transcriptomic biomarker	CD6, INPP5D, ISG20, NKG7, PSMB9, RUNX3, TAP1 (↑)	Kidney graft	n/a	n/a	Predict the development of progressive i-IFTA at 24 months	Sigdel TK, et al. (45)
	vimentin, NKCC2, E-cadherin, 18S rRNA (↑)	Urine	0.95	0.938/0.841	As a 4-gene model diagnostic of i-IFTA	Lee JR, et al. (46)
	CHCHD10, KLHL13, FJX1, MET, SERINC5, RNF149, SPRY4, TGIF1, KAAG1, ST5, WNT9A, ASB15, RXRA	Kidney graft	0.889 (average)	0.81/0.79 (average)	Predict fibrosis and graft failure	O'Connell PJ, et al. (47)
	RSAD2, ETV7 (↑)	PBMC	0.761 (RSAD2) 0.84 (ETV7)	n/a	Diagnose of ABMR	Matz M, et al. (48)
	TIM-3 (↑)	PBMC	0.71	0.83/0.75	Predict CAD	Shahbaz SK, et al. (49)
		Urine	0.75	0.83/0.75		
	TIM-3, KIM-1 (↑)	PBMC	0.99 (TIM-3)	1/0.98 (TIM-3)	Predict CAD	Shahbaz SK, et al. (50)
			0.97 (KIM-1)	1/0.7 (KIM-1)		
		Urine	0.95 (TIM-3)	1/0.81 (TIM-3)		
			0.99 (KIM-1)	1/0.93 (KIM-1)		
			0.95 (KIM-1 concentration)	1/74 (KIM-1 concentration)		
	CIITA (↓), CTLA-4 (↑)	PBMC	0.902 (CIITA) 0.785 (CTLA4)	n/a	Predict dnDSA and chronic ABMR	Yamamoto T, et al. (51)
	TLR-2, TLR-4, MyD88 (↑)	PBMC	0.94 (TLR2)	0.93/0.93 (TLR2)	Predict early and late CAD	Hosseinzadeh M, et al. (52)
			0.95 (TLR4)	0.93/0.93 (TLR4)		
			0.94 (MyD88)	1/0.93 (MyD88)		
		Kidney graft	0.94 (TLR2)	0.93/0.93 (TLR2)		
			0.95 (TLR4)	0.93/1 (TLR4)		
			0.98 (MyD88)	1/0.93 (MyD88)		
	CASP3, FAS, IL-18 (↓)	PBMC	0.79 (CASP3)	0.71/0.88 (CASP3)	Predict graft function	Kaminska D, et al. (53)
			0.75 (FAS)	0.64/0.8 (FAS)		
			0.77 (IL-18)	0.71/0.8 (IL-18)		
Epigenetic biomarkers	Foxp3 DNA demethylation	Kidney graft	n/a	n/a	Protector for long-term allograft outcome	Bestard O, et al. (54)
	PD1 DNA methylation in memory CD8+ T cells (↑)	PBMC	n/a	n/a	PD1 DNA methylation increases in recipients with rejection	Karin Boer, et al. (55)
	miR-21, miR-200b (↑)	Urine	0.89 (miR-21)	0.85/0.8 (miR-21)	Corelate with renal allograft	Zununi VS, et al. (56)
			0.81 (miR-200b)	0.84/0.95 (miR-200b)	dysfunction and i-IFTA; diagnostic biomarkers for renal allograft monitoring	
	miR-150 (↑), miR-423-3p (↑), miR192 (↓), miR-200b (↓)	Plasma	0.87 (all)	0.78/0.91	Predict graft outcome in recipients with CAD	Zununi VS, et al. (57)

(Continued)

TABLE 1 | Continued

Biomarker classification	Biomarker candidate	Sample type	AUC	Sensitivity/ Specificity	Application	Ref
	miR21, miR-155, miR-142-3p (↑)	Plasma	0.82 (all)	0.81/0.92	Upregulate in recipients with i-IFTA; corelate with renal allograft dysfunction; can be used for graft monitoring	Zununi VS, et al. (58)
	miR-145-5p (↓)	Plasma	0.891	0.933/0.731	Diagnostic biomarker of i-IFTA	Matz M, e al (59)
	miR-148a (↓)	Plasma	0.89	0.97/0.72	Correlated with renal function and histological grades; biomarker of the progression to i-IFTA	Nariman-Saleh-Fam Z, et al. (60)
	miR-142-3p(↓), miR-204 (↑), miR-211 (↑)	Urine, kidney graft	0.974 (miR-142-3p) 0.967 (miR-204) 1 (miR-211)	0.89/1 (miR-142-3p) 0.95/1 (miR-204) 1/1 (miR-211)	As markers of CAD with i-IFTA and for monitoring graft function	Scian MJ, et al. (61)
	miR-142-5p (↓), miR-486-5p (↑)	PBMC	n/a	n/a	Predict chronic ABMR	Iwasaki K, et al. (62)
Proteomic biomarker	V305_HUMAN_NTLYLNMNSLR, RL18_HUMAN_ILTFDQLALDSPK, F151A_HUMAN_AVGPSLDLLR, TGFR2_HUMAN_LTAQCVAER, LYAM1_HUMAN_AEIEYLEK, K2C8_HUMAN_LSELEAALQR, F151A_HUMAN_TYTQAMVEK, PLGB_Human_AFQYHSK, K1C19_HUMAN_ILGATIENSR, IBP7_HUMAN_GTCEQGPSIVTPPK, LV102_HUMAN_WYQQLPGTAPK DSRAD_Human_YLNTNPVGGLLEYAR,	Urine	0.995	n/a	Predict CAD	Sigdel TK, et al. (63)
	PARP1 (↓)	Serum	0.871	n/a	Predict AR and chronic graft injury	Srivastava M, et al. (64)
	TNF-α, ANXA11, Integrin α3, Integrin β3 (↑)	Urine	0.805 (TNFα) 0.855 (Integrin α3) 0.813 (integrin β3) 0.963 (ANXA11)	n/a	Diagnose AR and CR	Srivastava M, et al. (65)
	CXCL9, CXCL10 (↑) CXCL9/Cr ratio (↑) CXCL10/Cr ratio (↑)	Urine	0.86 (CXCL9), 0.9 (CXCL9/Cr)	n/a	Predict TCMR	Rabant M, et al. (66)
			0.8 (CXCL10), 0.82 (CXCL10/Cr)	n/a	Predict mixed rejection	
			0.7 (CXCL10), 0.7 (CXCL10/Cr)	n/a	Predict ABMR	
	CXCL10/Cr ratio (↑)	Urine	0.81 (sub-clinical TCMR)	0.59/0.67 (subclinical TCMR)	Predict TCMR for pediatric recipients	Blydt-Hansen TD, et al. (67)
			0.88 (clinical TCMR)	0.77/0.6 (clinical TCMR)		
	Vitronectin (↑)	Urine	0.963	n/a	Monitor fibrotic changes in kidney allograft	Carreras-Planella L, et al. (68)
	Properdin, sC5b-9 (↑)	Urine	n/a	n/a	As risk factors of graft failure	Lammerts R, et al. (69)
	AZGP1 (↑)	Urine	0.946	0.846/0.8	Predict and diagnose chronic ABMR	Jung HY, et al. (70)

(Continued)

TABLE 1 | Continued

Biomarker classification	Biomarker candidate	Sample type	AUC	Sensitivity/ Specificity	Application	Ref
	β2 microglobulin, NGAL, clusterin, KIM-1 (↑)	Urine	n/a	n/a	Predict chronic allograft nephropathy	Cassidy H, et al. (71)
Metabolomic biomarkers	Newly Synthesized DNA and ATP	PBMC	n/a	n/a	Analyze lymphocyte subset activation responses	Sottong PR, et al. (72)
	NAD, 1-MN, cholesterol sulfate, GABA, nicotinic acid, NADPH, proline, spermidine, alpha-hydroxyhippuric acid	Urine	n/a	n/a	Predict TCMR	Kalantari S, et al. (73)
	Alanine, Citrate, Lactate, combined with urea or glucose or glucutonate	Urine	0.76	n/a	Diagnose AR	Miriam B, et al. (74)
	threitol, inositol, glucose, xylono-1, 5-lactone, xylitol, xylopyranoside, 2,3-dihydroxybutanoic acid, glucitol, ribonic acid, octadecanoic acid, phosphate (↑) fructose, glycolic acid, 3-hydroxyisovaleric acid (↓)	Urine	n/a	0.867/0.677	Diagnose AR	Long Zheng, et al. (75)
	guanidoacetic acid, methylimidazoleacetic acid, dopamine (↑) 4-guanidinobutyric acid, L-tryptophan (↓)	Urine	0.926	0.9/0.846	Diagnose AR	Kim S, et al. (76)
	Itaconate, kynurenine (↑)	Kidney graft	n/a	n/a	Distinguish acute cellular rejection from IRI	Beier UH, et al. (77)
	glycine, glutaric acid, adipic acid, inulobiose, threose, sulfuric acid, taurine, *N*-methylalanine, asparagine, 5-aminovaleric acid lactam, myo-inositol	Urine	0.985	0.929/0.963	Diagnose AR	Sigdel TK, et al. (78)
Cellular biomarker	TEMRA/EM CD8 T cell ratio (↑)	PBMC	0.75 (8 year graft failure) 0.79 (11 year graft failure)	n/a	Predict graft failure	Jacquemont L, et al. (79)
	CD154+ T-cytotoxic memory cells (↑)	PBMC	0.968	0.923/0.846	Predict rejections (liver)	Ashokkumar C, et al. (80)
		PBMC	0.938	1/0.88	Predict AR (kidney)	Ashokkumar C, et al. (81)
	alloreactive memory IFN-γ-producing T cells (↑)	PBMC	0.725	0.8/0.64	Predict subclinical TCMR and DSA	Crespo E, et al. (82)
	Ratio of T follicular helper cells and T follicular regulatory cells (Tfc/Tfr) (↑)	PBMC	n/a	n/a	Risk factor of CAD	Yan L, et al. (83)
	Myofibroblast	Kidney graft	n/a	n/a	Identify CR	Liu YG, et al. (84)

NKCC2, Na-K-Cl cotransporter 2; CD6, cluster of differentiation 6; INPP5D, inositol polyphosphate-5-phosphatase D; ISG20, interferon-stimulated gene 20; NKG7, natural killer cell granule protein 7; PSMB9, proteasome subunit beta type-9; RUNX3, runt-related transcription factor 3; TAP1, transporter associated with antigen processing 1; CHCHD10, Coiled-coil-helix-coiled-coil-helix domain containing 10; KLHL13, Kelch-like family member 13; FJX1, Four jointed box 1; MET, Met proto-oncogene; SERINC5, Serine incorporator 5; RNF149, Ring finger protein 149; SPRY4, Sprouty homolog 4; TGIF1, TGFB-induced factor homeobox 1; KAAG1, Kidney associated antigen 1; ST5, Suppression of tumorigenicity 5; WNT9A, Wingless-type MMTV integration site family member 9A; ASB15, Ankyrin repeat and SOCS box-containing 15; RXRA, Retinoid X receptor alpha; TIM-3, T cell immunoglobulin and mucin domain 3; KIM-1, kidney injury molecule-1; CIITA, class II transactivator; CTLA-4, cytotoxic T-lymphocyte antigen; TLR, toll-like receptor; MyD88, myeloid differentiation factor 88; CASP3, caspase 3; FAS, first apoptotic signal; PD1, programmed death 1; miR, micro RNA; PARP1, Poly(ADP-ribose) polymerase 1; CXCL9, chemokine C-X-C motif ligand 9; CXCL10, chemokine C-X-C motif ligand 10; AZGP1, zinc-alpha-2-glycoprotein; NAD, nicotinamide adenine dinucleotide; 1-MN, 1-methylnicotinamide; GABA, gamma-aminobutyric acid; NADPH, nicotinamide adenine dinucleotide phosphate; IRI, ischemia reperfusion injury; NGAL, neutrophil gelatinase-associated lipocalin; TEMRA, terminally differentiated effector memory; EM, effector memory; PBMC, Peripheral blood mononuclear cell; AUC, area under curve; n/a, not available; I-IFTA, interstitial fibrosis and tubular atrophy; AR, acute rejection; CR, chronic rejection; ABMR, antibody-mediated rejection; TCMR, T cell-mediated rejection; CAD, chronic allograft dysfunction; dnDSA, de novo donor specific antibody.

differentiation, and migration of a variety of cell types, e.g. helper T cells (90, 91) or regulatory T cells (54) and fibroblast (92), which are implicated in allograft survival and kidney fibrosis. For example, Foxp3 demethylation at the T(reg)-specific demethylation region positively correlates with numbers of intragraft Foxp3-expressing T cells in patients with subclinical rejection with i-IFTA *via* protocol biopsies; consequently, patients with more Foxp3+ T(reg) cells within graft infiltrates showed significantly better 5-year graft function evolution than patients without Foxp3+ T(reg) cell infiltration (54). Boer et al. (55) studied DNA methylation (DNAm) of the pro-inflammatory cytokine interferon γ (IFNγ) and the inhibitory receptor programmed death 1 (PD1) in naïve and memory CD8+ T cell subsets in kidney transplant recipients. Increased DNAm of IFN-γ and PD1 was observed in memory CD8+ T cells in kidney transplant recipients 3 months after transplantation, regardless of a rejection episode or not, suggesting that it was a non-specific change associated with transplant surgery or use of immunosuppressive drugs. However, PD1 methylation in the CD27− memory CD8+ T cells was more prominently increased in recipients with rejection episode than those without. In a more recent study concerning the role of DNAm in progression of IFTA in renal biopsies, normal allograft

biopsies at 2-years post-transplantation showed similar DNAm patterns comparable to preimplantation biopsies, whereas persistent differentially methylation was associated with progression of allografts to chronic renal allograft dysfunction (93). Epigenetic mechanisms such as hypomethylation could directly boost and indirectly modulate their expression by controlling miRNAs (93). Recent studies have revealed that miR21 and miR200b expression in urine are associated with IFTA and CAD (56), while circulating miR-150, miR192, miR-200b, and miR-423-3p in plasma are related to IFTA (57). Meanwhile, expression of miR21, miR-155, and miR-142-3p was up-regulated in the plasma of patients with IFTA (58), while miR-145-5p and miR-148a were down-regulated (59, 60). Another study showed that expression of miR-142-3p was up-regulated, whereas miR-204 and miR-211 were down-regulated both in urine and kidney graft of recipients with CAD-IFTA (61). In addition, up-regulation of miR142-5p, and down-regulation of miR-486-5p may serve as biomarkers for early detection of chronic ABMR (62). These markers could, therefore, be considered as potential markers for CAD.

Proteomic Biomarkers

Scores of non-invasive proteomic biomarkers of CKTR are generated using high-throughput proteomic techniques, such as liquid chromatography-mass spectrometry (LC-MS), isobaric tag for relative and absolute quantitation (iTRAQ), protein microarray, and bead-based immunoassay. Studies investigating non-invasive proteomic biomarkers in urine and blood (94), have discovered unique protein sets valuable for differential diagnosis. For example, one study on a set of 245 urine samples from a pediatric and young adult kidney allograft recipient cohort, identified 35 proteins that could discriminate three types of graft injury, 11 peptides for acute rejection, 12 urinary peptides for chronic allograft nephropathy and 12 peptides for BK virus nephritis (63). Metzger et al. (95) validated a multi-marker urinary peptide classifier constructed from capillary electrophoresis mass spectrometry (CE-MS) peptide spectra of urine from a training set of 39 allograft patients to discriminate TCMR from healthy allografts. Srivastava et al. (64, 65) identified that the up-expression of urine ANXA11, Integrin α3, Integrin β3 and TNF-α, and the downregulation of serum PARP1 could be used as candidate proteomic biomarkers for kidney allograft rejection. Furthermore, several proteins, some chemokines and cytokines in blood and urine are also identified as biomarkers for diagnosing CKTR and predicting graft outcomes (66–71). Several recent efforts have established urinary C-X-C motif chemokine 9 (CXCL9) and CXCL10 as reliable biomarkers for subclinical allograft rejection and for guiding the post-transplant management (66, 67). A recent study shows that platelets contain a wide array of mediators that could potentially promote acute and chronic ABMR (96, 97). In fact, platelet factor 4 (PF4, also known as CXCL4), the most abundant platelet-related mediator detected in the allograft with large quantities, has multiple consequences on allografts, one of which is to promote monocytes survival and macrophage differentiation (98), predicting poorer graft outcomes (99).

Metabolomic Biomarkers

Metabolomics is a rapidly emerging research field that involves comprehensive analysis of all metabolites in a single biological sample (100) and has recently gained tremendous interest in the biomarker study in organ transplantation. Compared to proteomic or transcriptomic markers, metabolomic biomarkers may be more precise in reflecting cellular functions (101). Metabolomics can be used in two ways: intensively analyzing and identifying individual metabolites; or using pattern recognition to record spectral patterns and intensities instead of recording individual molecules (100, 102). Researchers recommend that metabolomic markers improve observing rejection and other organ injuries (103). In children, urinary metabolomics improved detection of borderline TCMR and demonstrated promise in ABMR (104). Measuring adenosine triphosphate (ATP) generation by mitogen-stimulated CD4 lymphocytes (ImmuKnow assay) is an FDA-approved biomarker potentially effective in transplant recipients (72). In a randomized prospective study, based on immune function values determined by ImmuKnow assay, one-year patient survival was markedly improved and infection rates were reduced in the group receiving ATP release biomarker-guided immunosuppressant regulation (105). In a recent study, a panel of nine differential metabolites in urine were identified as novel potential metabolite biomarkers of TCMR (73). The metabolomic biomarkers that considered as potential markers for rejection episodes are listed in **Table 1** (72–78).

Cellular Biomarkers

There has been significant attentions drawn to quantify alloreactive CD8+ T cells as potential cellular biomarkers of rejection (25, 79, 106), or tolerance (107). Ashokkumar et al. (80) found that allospecific CD154+ T-cytotoxic memory cells were associated with rejection risk in liver transplant recipients. Limited data showed that an increase in CD154+ subset is implicated in acute kidney transplant rejection (81). Resent studies showed that monitoring alloreactive memory IFN-γ-producing T cells could assess subclinical TCMR and predict *de novo* DSA (82), while ratio of T follicular helper cells and T follicular regulatory cells (Tfc/Tfr) was an independent risk factor for CAD (83). However, multicenter validation of its diagnostic/prognostic biomarker utility in CKTR remains to be determined (108). Both macrophages and NK cells are implicated in chronic rejection (21, 109–111). However, it remains to be determined whether a specific subset of macrophages or NK cells could be served as cellular markers for CKTR. Recently, single-cell sequencing technologies have been rapidly developed and have evolved as a power tool for unbiased assessments of genomic, epigenomic, and transcriptomic profiling at the single-cell level. Compared with traditional sequencing technology, single-cell technologies have the advantages of detecting heterogeneity among individual cells, distinguishing a small number of cells, and delineating cell maps (112, 113). Using scRNA-seq technique, Liu et al. revealed multiple novel subsets of immune cells, including five subclasses of NKT cells, two subtypes in memory B cells, a classic CD14+ group and a nonclassical CD16+ group in

monocytes, in patients with CKTR. They also identified a novel subpopulation [myofibroblasts (MyoF)] in fibroblasts, which express collagen and extracellular matrix components in CKTR group (84). While still in its early infancy, scRNA-seq is considered as diagnostic tool for identifying cellular and molecular biomarkers specific for CKTR. With improved understanding of cellular mechanisms underlying CKTR and advances in the multi-color flow cytometry analyses combining with more recent development of single-cell genomics studies, it is conceivable that more precise cellular biomarkers will be identified for CKTR.

Several considerations ought to be adequately addressed before these biomarkers can be regularly used in the clinical practice for kidney transplants (114–116). First, sensitivity, specificity, positive and negative predictive values must be considered, and receiver operating characteristic (ROC) curves need to be thoroughly assessed for their clinical utility. Secondly, integration of different biomarkers is necessary for accurate diagnosis. Thirdly, robust validation studies and standardization of measurements are required to identify new biomarkers. Finally, timing required for generating results and cost of assessment should be reasonable.

NEW THERAPIES FOR THE TREATMENT OF CKTR

Chronic active ABMR is the most widely recognized cause of allograft failure (117), whereas TCMR usually exists in a mixed rejection phenotype (118). Given current understanding that that chronic active TCMR is often associated with insufficient immunosuppression, TCMR treatment has been directed to increasing doses and types of anti-T cell immunosuppressive agents such as combinations of therapies with basiliximab, everolimus in addition to tacrolimus (119). Numerous therapies have been used in the clinical setting, mostly focusing on chronic active ABMR. The strategies include plasmapheresis, intravenous immunoglobulin (IVIG), CD20 antibody (rituximab), proteasome inhibitor (bortezomib) (120–122) and anti-complement monoclonal antibody (eculizumab), single or combined therapies (123, 124). Their therapeutic effectiveness in treatment of chronic active ABMR have been evaluated in recent randomized controlled trials and results have been extensively reviewed (125), suggesting limited success being achieved by using these agents alone or in combination despite their effectiveness in treating acute ABMR. Through biomarker discovery, understanding of CKTR has been tremendously improved over the last five years. Recognition of biological similarities shared by CKTR, cancer immunology and autoimmune diseases has led to frontier investigations in repurposing of several treatment strategies from cancer therapy or autoimmune diseases to ABMR. IL-6/IL-6R blockade (Tocilizumab), C1 esterase inhibitor (C1 INH), and B-lymphocyte stimulator (BLyS) inhibitor (Belimumab) are among those that have been tested for their therapeutic potentials in mitigating ABMR and have shown promising results as described below and summarized in **Table 2**.

IL-6/IL-6R Blockade

IL-6 is a pleotropic cytokine associated to many facets of innate and adaptive immunity, which plays an important role in DSA generation and chronic ABMR, including its effects on B cell immunity and antibody-producing plasma cells, as well as the balance between effector and regulatory T cells (130). Blockade of the IL-6/IL-6R axis with Tocilizumab, anti–interleukin-6 receptor monoclonal antibody has been well-established for the treatment of rheumatoid arthritis (131), and is recently

TABLE 2 | Clinical trials - new therapies for chronic ABMR after kidney transplantation.

Trial design	Inclusion criteria	Test therapeutics	Other Immuno suppression	Patients	Follow up	Major results	Ref
single center, open-label case study, historical control	chronic ABMR, DSA+, TG	**Tocilizumab** (8 mg/kg monthly, maximal dose 800 mg for 6–25 months)	Tac/MMF/Pred	36	6 years	reduction in DSAs and stabilization of renal function at 2 years; graft survival rate of 80%, patient survival rate of 91% at 6 years	Choi J, et al. (126)
randomized controlled trials	ABMR, DSA+	**C1 INH** (5000 U on day 1 of ABMR, 2500 U on days 3, 5, 7, 9, 11, and 13) add-on standard of care (PP+IVIG+/- anti-CD20)	n/a	18 (treatment: n=9; placebo: n=9)	6 months	reduction of transplant glomerulopathy	Montgomery RA, et al. (127)
single center, observational study, historical control	refractory active ABMR with acute allograft dysfunction, DSA>3000 MFI, g +ptc≥2	**C1 INH** (20 units/kg on days 1, 2, and 3 and then twice weekly; IVIG at 2 g/kg every month for 6 months	Tac/MMF/Pred	6	6 months	improvement in eGFR, reduced DSA; no change in histological features	Viglietti D, et al. (128)
randomized controlled trials	adult patient receiving a kidney transplant	**Belimumab** (10 mg/kg on day 0, 14, and 28, and then every 4 weeks for a total of 7 infusions)	Tac/MMF/Pred	28 (treatment: n=14; placebo: n=14)	6 months	similar proportions of adverse events; no change in the number of naive B cells	Banham GD, et al. (129)

TG, transplant glomerulopathy; Tac, tacrolimus; MMF, mycophenolate mofetil; Pred, prednisone; n/a, not available.

considered as a new therapy to prevent ABMR progression (126). It has been shown that tocilizumab markedly reduced DSAs and stabilized renal function at 2 years post-transplant, suggesting a therapeutic effect of tocilizumab in ABMR. Tocilizumab has also been evaluated in combination with IVIG and rituximab for patients who failed standard desensitization, and it appeared well tolerated and safe (132). However, there is still a lack of randomized controlled trials to systematically evaluate the efficacy and safety of tocilizumab to date. Another new inhibitor for IL-6/IL-6R axis is clazakizumab, a genetically engineered humanized monoclonal antibody directed against IL-6. Two pilot trials (NCT03444103, NCT03380377) (132–134) and a large multicenter trial evaluating clazakizumab in late/chronic ABMR (NCT03744910) (135) are underway.

C1 Esterase Inhibitor (C1 INH)

Since the efficacy of C5 blockade in late ABMR is limited (123, 124), blockade of early complement pathway at the level of key component C1 has attracted a great deal of attention. One potential strategy being studied is the use of C1 INH, which has been used to prevent and/or treat attacks of hereditary angioedema for years and has an established safety record (136). C1-INH is a serum protease inhibitor that binds covalently and inactivates C1r, C1s, and mannan-binding protein-associated proteases (136, 137). In a double-blind RCT, C1-INH was tested as a treatment for biopsy-proven ABMR. Both C1-INH and placebo groups showed improvements in early follow-up biopsies. However, in a subset of patients with late follow-up biopsies (6 months), a decreased rate of transplant glomerulopathy was seen in C1-INH treated group, accompanied by improved graft function, suggesting C1-NIH may be effective in preventing the development of chronic injury (127). In a prospective, single-arm pilot clinical trail, C1-INH was added to IVIG to treat refractory acute ABMR. In comparison with historical controls, patients treated with C1-INH showed decreased C4d deposition and improved renal function, whereas microcirculatory damage still persisted (glomerulitis, peritubular capillaritis, and allograft glomerulopathy) (128). Currently, a large multicenter clinical trials evaluating C1-INH added to standard treatment of ABMR (NCT02547220) (138) is underway, while another clinical trial evaluating C1-NIH for the treatment of refractory AMR (NCT03221842) in renal transplant recipients (139) is also ongoing.

Inhibition of B-lymphocyte Stimulator

B-lymphocyte stimulator (BLyS) is a critical cytokine that enhances B cell and plasma cell survival (140). Targeting BLyS has recently driven increasing interest in transplant by modulating B cell alloimmunity. Belimumab, a humanized anti-BLyS antibody, which has shown therapeutic efficacy in systemic lupus erythematosus (141), has now been applied in organ transplantation. In a double-blind, randomized, placebo-controlled phase 2 trial, belimumab was evaluated in 28 kidney transplant recipients (129). The findings revealed that treatment of belimumab showed no effect on reducing the number of naïve B cells from baseline to 24 weeks after transplant. However, the activated memory B cells and plasmablasts were significantly reduced, and tissue-specific antibodies in serum were lowered. In addition, treatment with belimumab modulated the B cell profile towards a regulatory profile by changing the IL-10/IL-6 ratio. In parallel, genes coding for IgG and markers of T cell proliferation were reduced (129). To date, there is still lack of clinical trial using belimumab to treat chronic rejection. In a murine chronic ABMR kidney transplant model, blockade of APRIL/BLyS by TAC-Ig resulted in decreased antinuclear antibody (ANA) and disruption of splenic germinal center architecture, but have no significant difference in lymphocyte infiltration and kidney graft pathology compared with control grafts, which may be due to the absence of T cell immunosuppression (142).

CONCLUSION

Discovery of novel earlier diagnostic biomarkers will not only allows designing individualized therapy for timely therapeutic intervention, but also further advance understanding of pathogenesis of CKTR. Although many biomarkers listed in **Table 1** still require validation and standardization in several independent cohorts, considerable progress has been made in recent years (115, 116, 143). The management of CKTR remains a daunting task due to the complex pathogenesis of CKTR and irreversibility at the time of diagnosis. Nevertheless, several promising therapies have been in robust intervention trials with promising results. With the emergence of new technologies, such as single cell genomics, computational biology along with artificial intelligence-based assistance, it is conceivable that more specific biomarkers and therapeutic targets for CKTR will be identified and translated into the clinical practice in the very near future.

AUTHOR CONTRIBUTIONS

XL and XZ: participated in manuscript preparation and writing. JM, LG, and JL: provided suggestion and edits. ZZ conceptualized, wrote, and revised manuscript All authors contributed to the article and approved the submitted version.

REFERENCES

1. Kasiske BL, Andany MA, Danielson B. A Thirty Percent Chronic Decline in Inverse Serum Creatinine Is an Excellent Predictor of Late Renal Allograft Failure. *Am J Kidney Dis* (2002) 39:762–8. doi: 10.1053/ajkd.2002.31996
2. Hara S. Current Pathological Perspectives on Chronic Rejection in Renal Allografts. *Clin Exp Nephrol* (2017) 21:943–51. doi: 10.1007/s10157-016-1361-x
3. Stegall MD, Park WD, Larson TS, Gloor JM, Cornell LD, Sethi S, et al. The Histology of Solitary Renal Allografts At 1 and 5 Years After Transplantation. *Am J Transplant* (2011) 11:698–707. doi: 10.1111/j.1600-6143.2010.03312.x

4. Shiu KY, Stringer D, McLaughlin L, Shaw O, Brookes P, Burton H, et al. Effect of Optimized Immunosuppression (Including Rituximab) on Anti-Donor Alloresponses in Patients With Chronically Rejecting Renal Allografts. *Front Immunol* (2020) 11:79. doi: 10.3389/fimmu.2020.00079
5. Loupy A, Haas M, Roufosse C, Naesens M, Adam B, Afrouzian M, et al. The Banff 2019 Kidney Meeting Report (I): Updates on and Clarification of Criteria for T Cell- and Antibody-Mediated Rejection. *Am J Transplant* (2020) 20:2318–31. doi: 10.1111/ajt.15898
6. Haas M, Loupy A, Lefaucheur C, Roufosse C, Glotz D, Seron D, et al. The Banff 2017 Kidney Meeting Report: Revised Diagnostic Criteria for Chronic Active T Cell-Mediated Rejection, Antibody-Mediated Rejection, and Prospects for Integrative Endpoints for Next-Generation Clinical Trials. *Am J Transplant* (2018) 18:293–307. doi: 10.1111/ajt.14625
7. Tsuji T, Iwasaki S, Makita K, Imamoto T, Ishidate N, Mitsuke A, et al. Preceding T-Cell-Mediated Rejection Is Associated With the Development of Chronic Active Antibody-Mediated Rejection by De Novo Donor-Specific Antibody. *Nephron* (2020) 144:13–7. doi: 10.1159/000512659
8. Everly MJ, Everly JJ, Arend LJ, Brailey P, Susskind B, Govil A, et al. Reducing De Novo Donor-Specific Antibody Levels During Acute Rejection Diminishes Renal Allograft Loss. *Am J Transplant* (2009) 9:1063–71. doi: 10.1111/j.1600-6143.2009.02577.x
9. Halloran PF, Chang J, Famulski K, Hidalgo LG, Salazar ID, Merino LM, et al. Disappearance of T Cell-Mediated Rejection Despite Continued Antibody-Mediated Rejection in Late Kidney Transplant Recipients. *J Am Soc Nephrol* (2015) 26:1711–20. doi: 10.1681/ASN.2014060588
10. Nankivell BJ, Shingde M, Keung KL, Fung CL, Borrows RJ, O'Connell PJ, et al. The Causes, Significance and Consequences of Inflammatory Fibrosis in Kidney Transplantation: The Banff i-IFTA Lesion. *Am J Transplant* (2018) 18:364–76. doi: 10.1111/ajt.14609
11. Roos-van GM, Scholten EM, Lelieveld PM, Rowshani AT, Baelde HJ, Bajema IM, et al. Molecular Comparison of Calcineurin Inhibitor-Induced Fibrogenic Responses in Protocol Renal Transplant Biopsies. *J Am Soc Nephrol* (2006) 17:881–8. doi: 10.1681/ASN.2005080891
12. Lefaucheur C, Loupy A. Antibody-Mediated Rejection of Solid-Organ Allografts. *N Engl J Med* (2018) 379:2580–2. doi: 10.1056/NEJMc1813976
13. Thomas KA, Valenzuela NM, Reed EF. The Perfect Storm: HLA Antibodies, Complement, FcgammaRs, and Endothelium in Transplant Rejection. *Trends Mol Med* (2015) 21:319–29. doi: 10.1016/j.molmed.2015.02.004
14. Reese SR, Wilson NA, Huang Y, Ptak L, Degner KR, Xiang D, et al. B Cell Deficiency Attenuates Transplant Glomerulopathy in a Rat Model of Chronic Active Antibody-mediated Rejection. *Transplantation* (2020). doi: 10.1097/TP.0000000000003530
15. Zhang R. Donor-Specific Antibodies in Kidney Transplant Recipients. *Clin J Am Soc Nephrol* (2018) 13:182–92. doi: 10.2215/CJN.00700117
16. Dieplinger G, Everly MJ, Briley KP, Haisch CE, Bolin P, Maldonado AQ, et al. Onset and Progression of De Novo Donor-Specific Anti-Human Leukocyte Antigen Antibodies After BK Polyomavirus and Preemptive Immunosuppression Reduction. *Transpl Infect Dis* (2015) 17:848–58. doi: 10.1111/tid.12467
17. De Keyzer K, Van Laecke S, Peeters P, Vanholder R. Human Cytomegalovirus and Kidney Transplantation: A Clinician's Update. *Am J Kidney Dis* (2011) 58:118–26. doi: 10.1053/j.ajkd.2011.04.010
18. Sablik KA, Jordanova ES, Pocorni N, Clahsen-van GM, Betjes M. Immune Cell Infiltrate in Chronic-Active Antibody-Mediated Rejection. *Front Immunol* (2019) 10:3106. doi: 10.3389/fimmu.2019.03106
19. Venner JM, Hidalgo LG, Famulski KS, Chang J, Halloran PF. The Molecular Landscape of Antibody-Mediated Kidney Transplant Rejection: Evidence for NK Involvement Through CD16a Fc Receptors. *Am J Transplant* (2015) 15:1336–48. doi: 10.1111/ajt.13115
20. Parkes MD, Halloran PF, Hidalgo LG. Evidence for CD16a-Mediated Nk Cell Stimulation in Antibody-Mediated Kidney Transplant Rejection. *Transplantation* (2017) 101:e102–11. doi: 10.1097/TP.0000000000001586
21. Hirohashi T, Chase CM, Della PP, Sebastian D, Alessandrini A, Madsen JC, et al. A Novel Pathway of Chronic Allograft Rejection Mediated by NK Cells and Alloantibody. *Am J Transplant* (2012) 12:313–21. doi: 10.1111/j.1600-6143.2011.03836.x
22. Ge S, Chu M, Choi J, Louie S, Vo A, Jordan SC, et al. Imlifidase Inhibits Hla Antibody-mediated Nk Cell Activation and Antibody-Dependent Cell-Mediated Cytotoxicity (Adcc) In Vitro. *Transplantation* (2020) 104:1574–9. doi: 10.1097/TP.0000000000003023
23. Yazdani S, Callemeyn J, Gazut S, Lerut E, de Loor H, Wevers M, et al. Natural Killer Cell Infiltration Is Discriminative for Antibody-Mediated Rejection and Predicts Outcome After Kidney Transplantation. *Kidney Int* (2019) 95:188–98. doi: 10.1016/j.kint.2018.08.027
24. Lefaucheur C, Gosset C, Rabant M, Viglietti D, Verine J, Aubert O, et al. T Cell-Mediated Rejection Is a Major Determinant of Inflammation in Scarred Areas in Kidney Allografts. *Am J Transplant* (2018) 18:377–90. doi: 10.1111/ajt.14565
25. Curci C, Sallustio F, Serino G, De Palma G, Trpevski M, Fiorentino M, et al. Potential Role of Effector Memory T Cells in Chronic T Cell-Mediated Kidney Graft Rejection. *Nephrol Dial Transplant* (2016) 31:2131–42. doi: 10.1093/ndt/gfw245
26. Benichou G, Gonzalez B, Marino J, Ayasoufi K, Valujskikh A. Role of Memory T Cells in Allograft Rejection and Tolerance. *Front Immunol* (2017) 8:170. doi: 10.3389/fimmu.2017.00170
27. Halloran PF. T Cell-Mediated Rejection of Kidney Transplants: A Personal Viewpoint. *Am J Transplant* (2010) 10:1126–34. doi: 10.1111/j.1600-6143.2010.03053.x
28. Stegall MD, Gaston RS, Cosio FG, Matas A. Through a Glass Darkly: Seeking Clarity in Preventing Late Kidney Transplant Failure. *J Am Soc Nephrol* (2015) 26:20–9. doi: 10.1681/ASN.2014040378
29. Kasiske BL, Zeier MG, Chapman JR, Craig JC, Ekberg H, Garvey CA, et al. KDIGO Clinical Practice Guideline for the Care of Kidney Transplant Recipients: A Summary. *Kidney Int* (2010) 77:299–311. doi: 10.1038/ki.2009.377
30. Ivanyi B. Transplant Capillaropathy and Transplant Glomerulopathy: Ultrastructural Markers of Chronic Renal Allograft Rejection. *Nephrol Dial Transplant* (2003) 18:655–60. doi: 10.1093/ndt/gfg139
31. Zhang Q, Liang LW, Gjertson DW, Lassman C, Wilkinson AH, Kendrick E, et al. Development of Posttransplant Antidonor HLA Antibodies is Associated With Acute Humoral Rejection and Early Graft Dysfunction. *Transplantation* (2005) 79:591–8. doi: 10.1097/01.TP.0000155246.52249.AC
32. Scornik JC, Guerra G, Schold JD, Srinivas TR, Dragun D, Meier-Kriesche HU. Value of Posttransplant Antibody Tests in the Evaluation of Patients With Renal Graft Dysfunction. *Am J Transplant* (2007) 7:1808–14. doi: 10.1111/j.1600-6143.2007.01855.x
33. Wiebe C, Nickerson P. Posttransplant Monitoring of De Novo Human Leukocyte Antigen Donor-Specific Antibodies in Kidney Transplantation. *Curr Opin Organ Transplant* (2013) 18:470–7. doi: 10.1097/MOT.0b013e3283626149
34. Everly MJ, Rebellato LM, Haisch CE, Ozawa M, Parker K, Briley KP, et al. Incidence and Impact of De Novo Donor-Specific Alloantibody in Primary Renal Allografts. *Transplantation* (2013) 95:410–7. doi: 10.1097/TP.0b013e31827d62e3
35. Loupy A, Lefaucheur C, Vernerey D, Prugger C, Duong VHJ, Mooney N, et al. Complement-Binding Anti-HLA Antibodies and Kidney-Allograft Survival. *N Engl J Med* (2013) 369:1215–26. doi: 10.1056/NEJMoa1302506
36. Radermacher J, Mengel M, Ellis S, Stuht S, Hiss M, Schwarz A, et al. The Renal Arterial Resistance Index and Renal Allograft Survival. *N Engl J Med* (2003) 349:115–24. doi: 10.1056/NEJMoa022602
37. Kramann R, Frank D, Brandenburg VM, Heussen N, Takahama J, Kruger T, et al. Prognostic Impact of Renal Arterial Resistance Index Upon Renal Allograft Survival: The Time Point Matters. *Nephrol Dial Transplant* (2012) 27:3958–63. doi: 10.1093/ndt/gfr772
38. Schwenger V, Korosoglou G, Hinkel UP, Morath C, Hansen A, Sommerer C, et al. Real-Time Contrast-Enhanced Sonography of Renal Transplant Recipients Predicts Chronic Allograft Nephropathy. *Am J Transplant* (2006) 6:609–15. doi: 10.1111/j.1600-6143.2005.01224.x
39. Beck-Tolly A, Eder M, Beitzke D, Eskandary F, Agibetov A, Lampichler K, et al. Magnetic Resonance Imaging for Evaluation of Interstitial Fibrosis in Kidney Allografts. *Transplant Direct* (2020) 6:e577. doi: 10.1097/TXD.0000000000001009
40. Solez K, Colvin RB, Racusen LC, Sis B, Halloran PF, Birk PE, et al. Banff '05 Meeting Report: Differential Diagnosis of Chronic Allograft Injury and Elimination of Chronic Allograft Nephropathy ('Can'). *Am J Transplant* (2007) 7:518–26. doi: 10.1111/j.1600-6143.2006.01688.x

41. Haas M, Sis B, Racusen LC, Solez K, Glotz D, Colvin RB, et al. Banff 2013 Meeting Report: Inclusion of c4d-Negative Antibody-Mediated Rejection and Antibody-Associated Arterial Lesions. *Am J Transplant* (2014) 14:272–83. doi: 10.1111/ajt.12590
42. Quaglia M, Merlotti G, Guglielmetti G, Castellano G, Cantaluppi V. Recent Advances on Biomarkers of Early and Late Kidney Graft Dysfunction. *Int J Mol Sci* (2020) 21:5404. doi: 10.3390/ijms21155404
43. Califf RM. Biomarker Definitions and Their Applications. *Exp Biol Med (Maywood)* (2018) 243:213–21. doi: 10.1177/1535370217750088
44. Salvadori M, Tsalouchos A. Biomarkers in Renal Transplantation: An Updated Review. *World J Transplant* (2017) 7:161–78. doi: 10.5500/wjt.v7.i3.161
45. Sigdel TK, Bestard O, Tran TQ, Hsieh SC, Roedder S, Damm I, et al. A Computational Gene Expression Score for Predicting Immune Injury in Renal Allografts. *PLoS One* (2015) 10:e138133. doi: 10.1371/journal.pone.0138133
46. Lee JR, Muthukumar T, Dadhania D, Ding R, Sharma VK, Schwartz JE, et al. Urinary Cell mRNA Profiles Predictive of Human Kidney Allograft Status. *Immunol Rev* (2014) 258:218–40. doi: 10.1111/imr.12159
47. O'Connell PJ, Zhang W, Menon MC, Yi Z, Schroppel B, Gallon L, et al. Biopsy Transcriptome Expression Profiling to Identify Kidney Transplants At Risk of Chronic Injury: A Multicentre, Prospective Study. *Lancet* (2016) 388:983–93. doi: 10.1016/S0140-6736(16)30826-1
48. Matz M, Heinrich F, Zhang Q, Lorkowski C, Seelow E, Wu K, et al. The Regulation of Interferon Type I Pathway-Related Genes RSAD2 and ETV7 Specifically Indicates Antibody-Mediated Rejection After Kidney Transplantation. *Clin Transplant* (2018) 32:e13429. doi: 10.1111/ctr.13429
49. Shahbaz SK, Barabadi M, Ahmadpour P, Pourrezagholi F, Nafar M, Foroughi F, et al. Sequential Monitoring of TIM-3 mRNA Expression in Blood and Urine Samples of Renal Transplant Recipients. *Transpl Immunol* (2019) 54:9–16. doi: 10.1016/j.trim.2018.10.007
50. Shahbaz SK, Pourrezagholi F, Barabadi M, Foroughi F, Hosseinzadeh M, Ahmadpoor P, et al. High Expression of TIM-3 and KIM-1 in Blood and Urine of Renal Allograft Rejection Patients. *Transpl Immunol* (2017) 43-44:11–20. doi: 10.1016/j.trim.2017.07.002
51. Yamamoto T, Iwasaki K, Murotani K, Takeda A, Futamura K, Okada M, et al. Peripheral Blood Immune Response-Related Gene Analysis for Evaluating the Potential Risk of Chronic Antibody-Mediated Rejection. *Hum Immunol* (2018) 79:432–8. doi: 10.1016/j.humimm.2018.03.012
52. Hosseinzadeh M, Ahmadpoor P, Yekaninejad MS, Pourrezagholi F, Foroughi F, Ghorbanpour M, et al. Expression Patterns of Toll Like Receptor (TLR)-2, TLR-4 and Myeloid Differentiation Primary Response Gene 88 (MYD88) in Renal Transplant Patients Developing Allograft Dysfunction; a Cohort Study. *Transpl Immunol* (2018) 48:26–31. doi: 10.1016/j.trim.2018.02.005
53. Kaminska D, Koscielska-Kasprzak K, Chudoba P, Mazanowska O, Banasik M, Zabinska M, et al. Pretransplant Immune- and Apoptosis-Related Gene Expression is Associated With Kidney Allograft Function. *Mediators Inflamm* (2016) 2016:8970291. doi: 10.1155/2016/8970291
54. Bestard O, Cunetti L, Cruzado JM, Lucia M, Valdez R, Olek S, et al. Intragraft Regulatory T Cells in Protocol Biopsies Retain Foxp3 Demethylation and are Protective Biomarkers for Kidney Graft Outcome. *Am J Transplant* (2011) 11:2162–72. doi: 10.1111/j.1600-6143.2011.03633.x
55. Boer K, de Wit LE, Peters FS, Hesselink DA, Hofland LJ, Betjes MG, et al. Variations in DNA Methylation of Interferon Gamma and Programmed Death 1 in Allograft Rejection After Kidney Transplantation. *Clin Epigenet* (2016) 8:116. doi: 10.1186/s13148-016-0288-0
56. Zununi VS, Omidi Y, Ardalan M, Samadi N. Dysregulation of Urinary miR-21 and miR-200b Associated With Interstitial Fibrosis and Tubular Atrophy (IFTA) in Renal Transplant Recipients. *Clin Biochem* (2017) 50:32–9. doi: 10.1016/j.clinbiochem.2016.08.007
57. Zununi VS, Poursadegh ZA, Mahmoodpoor F, Samadi N, Ardalan M, Omidi Y. Circulating miR-150, miR-192, miR-200b, and miR-423-3p as Non-Invasive Biomarkers of Chronic Allograft Dysfunction. *Arch Med Res* (2017) 48:96–104. doi: 10.1016/j.arcmed.2017.03.004
58. Zununi VS, Poursadegh ZA, Ghanbarian H, Ghojazadeh M, Samadi N, Omidi Y, et al. Differential Expression of Circulating miR-21, miR-142-3p and miR-155 in Renal Transplant Recipients With Impaired Graft Function. *Int Urol Nephrol* (2017) 49:1681–9. doi: 10.1007/s11255-017-1602-2
59. Matz M, Heinrich F, Lorkowski C, Wu K, Klotsche J, Zhang Q, et al. MicroRNA Regulation in Blood Cells of Renal Transplanted Patients With Interstitial Fibrosis/Tubular Atrophy and Antibody-Mediated Rejection. *PLoS One* (2018) 13:e201925. doi: 10.1371/journal.pone.0201925
60. Nariman-Saleh-Fam Z, Bastami M, Ardalan M, Sharifi S, Hosseinian KS, Zununi VS. Cell-Free microRNA-148a Is Associated With Renal Allograft Dysfunction: Implication for Biomarker Discovery. *J Cell Biochem* (2019) 120:5737–46. doi: 10.1002/jcb.27860
61. Scian MJ, Maluf DG, David KG, Archer KJ, Suh JL, Wolen AR, et al. MicroRNA Profiles in Allograft Tissues and Paired Urines Associate With Chronic Allograft Dysfunction With IF/TA. *Am J Transplant* (2011) 11:2110–22. doi: 10.1111/j.1600-6143.2011.03666.x
62. Iwasaki K, Yamamoto T, Inanaga Y, Hiramitsu T, Miwa Y, Murotani K, et al. MiR-142-5p and miR-486-5p as Biomarkers for Early Detection of Chronic Antibody-Mediated Rejection in Kidney Transplantation. *Biomarkers* (2017) 22:45–54. doi: 10.1080/1354750X.2016.1204000
63. Sigdel TK, Gao Y, He J, Wang A, Nicora CD, Fillmore TL, et al. Mining the Human Urine Proteome for Monitoring Renal Transplant Injury. *Kidney Int* (2016) 89:1244–52. doi: 10.1016/j.kint.2015.12.049
64. Srivastava M, Torosyan Y, Eidelman O, Jozwik C, Pollard HB, Mannon R. Reduced PARP1 as a Serum Biomarker for Graft Rejection in Kidney Transplantation. *J Proteomics Bioinform* (2015) 8:31–8. doi: 10.4172/jpb.1000350
65. Srivastava M, Eidelman O, Torosyan Y, Jozwik C, Mannon RB, Pollard HB. Elevated Expression Levels of ANXA11, Integrins Beta3 and Alpha3, and TNF-alpha Contribute to a Candidate Proteomic Signature in Urine for Kidney Allograft Rejection. *Proteomics Clin Appl* (2011) 5:311–21. doi: 10.1002/prca.201000109
66. Rabant M, Amrouche L, Lebreton X, Aulagnon F, Benon A, Sauvaget V, et al. Urinary C-X-C Motif Chemokine 10 Independently Improves the Noninvasive Diagnosis of Antibody-Mediated Kidney Allograft Rejection. *J Am Soc Nephrol* (2015) 26:2840–51. doi: 10.1681/ASN.2014080797
67. Blydt-Hansen TD, Gibson IW, Gao A, Dufault B, Ho J. Elevated Urinary CXCL10-to-creatinine Ratio is Associated With Subclinical and Clinical Rejection in Pediatric Renal Transplantation. *Transplantation* (2015) 99:797–804. doi: 10.1097/TP.0000000000000419
68. Carreras-Planella L, Cucchiari D, Canas L, Juega J, Franquesa M, Bonet J, et al. Urinary Vitronectin Identifies Patients With High Levels of Fibrosis in Kidney Grafts. *J Nephrol* (2020). doi: 10.1007/s40620-020-00886-y
69. Lammerts R, Eisenga MF, Alyami M, Daha MR, Seelen MA, Pol RA, et al. Urinary Properdin and Sc5b-9 Are Independently Associated With Increased Risk for Graft Failure in Renal Transplant Recipients. *Front Immunol* (2019) 10:2511. doi: 10.3389/fimmu.2019.02511
70. Jung HY, Lee CH, Choi JY, Cho JH, Park SH, Kim YL, et al. Potential Urinary Extracellular Vesicle Protein Biomarkers of Chronic Active Antibody-Mediated Rejection in Kidney Transplant Recipients. *J Chromatogr B Analyt Technol BioMed Life Sci* (2020) 1138:121958. doi: 10.1016/j.jchromb.2019.121958
71. Cassidy H, Slyne J, O'Kelly P, Traynor C, Conlon PJ, Johnston O, et al. Urinary Biomarkers of Chronic Allograft Nephropathy. *Proteomics Clin Appl* (2015) 9:574–85. doi: 10.1002/prca.201400200
72. Sottong PR, Rosebrock JA, Britz JA, Kramer TR. Measurement of T-Lymphocyte Responses in Whole-Blood Cultures Using Newly Synthesized DNA and ATP. *Clin Diagn Lab Immunol* (2000) 7:307–11. doi: 10.1128/CDLI.7.2.307-311.2000
73. Kalantari S, Chashmniam S, Nafar M, Samavat S, Rezaie D, Dalili N. A Noninvasive Urine Metabolome Panel as Potential Biomarkers for Diagnosis of T Cell-Mediated Renal Transplant Rejection. *Omics* (2020) 24:140–7. doi: 10.1089/omi.2019.0158
74. Banas M, Neumann S, Eiglsperger J, Schiffer E, Putz FJ, Reichelt-Wurm S, et al. Identification of a Urine Metabolite Constellation Characteristic for Kidney Allograft Rejection. *Metabolomics* (2018) 14:116. doi: 10.1007/s11306-018-1419-8
75. Zheng L, Wang J, Gao W, Hu C, Wang S, Rong R, et al. GC/MS-Based Urine Metabolomics Analysis of Renal Allograft Recipients With Acute Rejection. *J Transl Med* (2018) 16:202. doi: 10.1186/s12967-018-1584-6
76. Kim SY, Kim BK, Gwon MR, Seong SJ, Ohk B, Kang WY, et al. Urinary Metabolomic Profiling for Noninvasive Diagnosis of Acute T Cell-Mediated

Rejection After Kidney Transplantation. *J Chromatogr B Analyt Technol BioMed Life Sci* (2019) 1118-1119:157–63. doi: 10.1016/j.jchromb.2019.04.047
77. Beier UH, Hartung EA, Concors S, Hernandez PT, Wang Z, Perry C, et al. Tissue Metabolic Profiling Shows That Saccharopine Accumulates During Renal Ischemic-Reperfusion Injury, While Kynurenine and Itaconate Accumulate in Renal Allograft Rejection. *Metabolomics* (2020) 16:65. doi: 10.1007/s11306-020-01682-2
78. Sigdel TK, Schroeder AW, Yang J, Sarwal RD, Liberto JM, Sarwal MM. Targeted Urine Metabolomics for Monitoring Renal Allograft Injury and Immunosuppression in Pediatric Patients. *J Clin Med* (2020) 9:2341. doi: 10.3390/jcm9082341
79. Jacquemont L, Tilly G, Yap M, Doan-Ngoc TM, Danger R, Guerif P, et al. Terminally Differentiated Effector Memory Cd8(+) T Cells Identify Kidney Transplant Recipients At High Risk of Graft Failure. *J Am Soc Nephrol* (2020) 31:876–91. doi: 10.1681/ASN.2019080847
80. Ashokkumar C, Talukdar A, Sun Q, Higgs BW, Janosky J, Wilson P, et al. Allospecific CD154+ T Cells Associate With Rejection Risk After Pediatric Liver Transplantation. *Am J Transplant* (2009) 9:179–91. doi: 10.1111/j.1600-6143.2008.02459.x
81. Ashokkumar C, Shapiro R, Tan H, Ningappa M, Elinoff B, Fedorek S, et al. Allospecific CD154+ T-Cytotoxic Memory Cells Identify Recipients Experiencing Acute Cellular Rejection After Renal Transplantation. *Transplantation* (2011) 92:433–8. doi: 10.1097/TP.0b013e318225276d
82. Crespo E, Cravedi P, Martorell J, Luque S, Melilli E, Cruzado JM, et al. Posttransplant Peripheral Blood Donor-Specific Interferon-Gamma Enzyme-Linked Immune Spot Assay Differentiates Risk of Subclinical Rejection and De Novo Donor-Specific Alloantibodies in Kidney Transplant Recipients. *Kidney Int* (2017) 92:201–13. doi: 10.1016/j.kint.2016.12.024
83. Yan L, Li Y, Li Y, Wu X, Wang X, Wang L, et al. Increased Circulating Tfh to Tfr Ratio in Chronic Renal Allograft Dysfunction: A Pilot Study. *BMC Immunol* (2019) 20:26. doi: 10.1186/s12865-019-0308-x
84. Liu Y, Hu J, Liu D, Zhou S, Liao J, Liao G, et al. Single-Cell Analysis Reveals Immune Landscape in Kidneys of Patients With Chronic Transplant Rejection. *Theranostics* (2020) 10:8851–62. doi: 10.7150/thno.48201
85. Khatri P, Roedder S, Kimura N, De Vusser K, Morgan AA, Gong Y, et al. A Common Rejection Module (CRM) for Acute Rejection Across Multiple Organs Identifies Novel Therapeutics for Organ Transplantation. *J Exp Med* (2013) 210:2205–21. doi: 10.1084/jem.20122709
86. Garcia-Gimenez JL, Seco-Cervera M, Tollefsbol TO, Roma-Mateo C, Peiro-Chova L, Lapunzina P, et al. Epigenetic Biomarkers: Current Strategies and Future Challenges for Their Use in the Clinical Laboratory. *Crit Rev Clin Lab Sci* (2017) 54:529–50. doi: 10.1080/10408363.2017.1410520
87. Liu H, Li P, Wei Z, Zhang C, Xia M, Du Q, et al. Regulation of T Cell Differentiation and Function by Epigenetic Modification Enzymes. *Semin Immunopathol* (2019) 41:315–26. doi: 10.1007/s00281-019-00731-w
88. Mas VR, Le TH, Maluf DG. Epigenetics in Kidney Transplantation: Current Evidence, Predictions, and Future Research Directions. *Transplantation* (2016) 100:23–38. doi: 10.1097/TP.0000000000000878
89. Wing MR, Devaney JM, Joffe MM, Xie D, Feldman HI, Dominic EA, et al. DNA Methylation Profile Associated With Rapid Decline in Kidney Function: Findings From the CRIC Study. *Nephrol Dial Transplant* (2014) 29:864–72. doi: 10.1093/ndt/gft537
90. Rodriguez RM, Lopez-Larrea C, Suarez-Alvarez B. Epigenetic Dynamics During CD4(+) T Cells Lineage Commitment. *Int J Biochem Cell Biol* (2015) 67:75–85. doi: 10.1016/j.biocel.2015.04.020
91. Jones B, Chen J. Inhibition of IFN-gamma Transcription by Site-Specific Methylation During T Helper Cell Development. *EMBO J* (2006) 25:2443–52. doi: 10.1038/sj.emboj.7601148
92. Bechtel W, McGoohan S, Zeisberg EM, Muller GA, Kalbacher H, Salant DJ, et al. Methylation Determines Fibroblast Activation and Fibrogenesis in the Kidney. *Nat Med* (2010) 16:544–50. doi: 10.1038/nm.2135
93. Bontha SV, Maluf DG, Archer KJ, Dumur CI, Dozmorov MG, King AL, et al. Effects of DNA Methylation on Progression to Interstitial Fibrosis and Tubular Atrophy in Renal Allograft Biopsies: A Multi-Omics Approach. *Am J Transplant* (2017) 17:3060–75. doi: 10.1111/ajt.14372
94. Sigdel TK, Kaushal A, Gritsenko M, Norbeck AD, Qian WJ, Xiao W, et al. Shotgun Proteomics Identifies Proteins Specific for Acute Renal Transplant Rejection. *Proteomics Clin Appl* (2010) 4:32–47. doi: 10.1002/prca.200900124
95. Metzger J, Chatzikyrkou C, Broecker V, Schiffer E, Jaensch L, Iphoefer A, et al. Diagnosis of Subclinical and Clinical Acute T-cell-mediated Rejection in Renal Transplant Patients by Urinary Proteome Analysis. *Proteomics Clin Appl* (2011) 5:322–33. doi: 10.1002/prca.201000153
96. Kuo HH, Fan R, Dvorina N, Chiesa-Vottero A, Baldwin WR. Platelets in Early Antibody-Mediated Rejection of Renal Transplants. *J Am Soc Nephrol* (2015) 26:855–63. doi: 10.1681/ASN.2013121289
97. Morrell CN, Sun H, Swaim AM, Baldwin WR. Platelets an Inflammatory Force in Transplantation. *Am J Transplant* (2007) 7:2447–54. doi: 10.1111/j.1600-6143.2007.01958.x
98. Scheuerer B, Ernst M, Durrbaum-Landmann I, Fleischer J, Grage-Griebenow E, Brandt E, et al. The CXC-chemokine Platelet Factor 4 Promotes Monocyte Survival and Induces Monocyte Differentiation Into Macrophages. *Blood* (2000) 95:1158–66. doi: 10.1182/blood.V95.4.1158.004k31_1158_1166
99. Tinckam KJ, Djurdjev O, Magil AB. Glomerular Monocytes Predict Worse Outcomes After Acute Renal Allograft Rejection Independent of C4d Status. *Kidney Int* (2005) 68:1866–74. doi: 10.1111/j.1523-1755.2005.00606.x
100. Wishart DS. Metabolomics: A Complementary Tool in Renal Transplantation. *Contrib Nephrol* (2008) 160:76–87. doi: 10.1159/000125935
101. Naesens M, Sarwal MM. Molecular Diagnostics in Transplantation. *Nat Rev Nephrol* (2010) 6:614–28. doi: 10.1038/nrneph.2010.113
102. Nasr M, Sigdel T, Sarwal M. Advances in Diagnostics for Transplant Rejection. *Expert Rev Mol Diagn* (2016) 16:1121–32. doi: 10.1080/14737159.2016.1239530
103. Blydt-Hansen TD, Sharma A, Gibson IW, Wishart DS, Mandal R, Ho J, et al. Urinary Metabolomics for Noninvasive Detection of Antibody-Mediated Rejection in Children After Kidney Transplantation. *Transplantation* (2017) 101:2553–61. doi: 10.1097/TP.0000000000001662
104. Mincham CM, Gibson IW, Sharma A, Wiebe C, Mandal R, Rush D, et al. Evolution of Renal Function and Urinary Biomarker Indicators of Inflammation on Serial Kidney Biopsies in Pediatric Kidney Transplant Recipients With and Without Rejection. *Pediatr Transplant* (2018) 22:e13202. doi: 10.1111/petr.13202
105. Ravaioli M, Neri F, Lazzarotto T, Bertuzzo VR, Di Gioia P, Stacchini G, et al. Immunosuppression Modifications Based on an Immune Response Assay: Results of a Randomized, Controlled Trial. *Transplantation* (2015) 99:1625–32. doi: 10.1097/TP.0000000000000650
106. Bestard O, Nickel P, Cruzado JM, Schoenemann C, Boenisch O, Sefrin A, et al. Circulating Alloreactive T Cells Correlate With Graft Function in Longstanding Renal Transplant Recipients. *J Am Soc Nephrol* (2008) 19:1419–29. doi: 10.1681/ASN.2007050539
107. Koyama I, Nadazdin O, Boskovic S, Ochiai T, Smith RN, Sykes M, et al. Depletion of CD8 Memory T Cells for Induction of Tolerance of a Previously Transplanted Kidney Allograft. *Am J Transplant* (2007) 7:1055–61. doi: 10.1111/j.1600-6143.2006.01703.x
108. Rohan VS, Soliman KM, Alqassieh A, Alkhader D, Patel N, Nadig SN. Renal Allograft Surveillance With Allospecific T-cytotoxic Memory Cells. *Ren Fail* (2020) 42:1152–6. doi: 10.1080/0886022X.2020.1846054
109. Chazaud B. Macrophages: Supportive Cells for Tissue Repair and Regeneration. *Immunobiology* (2014) 219:172–8. doi: 10.1016/j.imbio.2013.09.001
110. Pilmore HL, Painter DM, Bishop GA, McCaughan GW, Eris JM. Early Up-Regulation of Macrophages and Myofibroblasts: A New Marker for Development of Chronic Renal Allograft Rejection. *Transplantation* (2000) 69:2658–62. doi: 10.1097/00007890-200006270-00028
111. Ziai F, Nagano H, Kusaka M, Coito AJ, Troy JL, Nadeau KC, et al. Renal Allograft Protection With Losartan in Fisher–>Lewis Rats: Hemodynamics, Macrophages, and Cytokines. *Kidney Int* (2000) 57:2618–25. doi: 10.1046/j.1523-1755.2000.00122.x
112. Hwang B, Lee JH, Bang D. Single-Cell RNA Sequencing Technologies and Bioinformatics Pipelines. *Exp Mol Med* (2018) 50:1–14. doi: 10.1038/s12276-018-0071-8
113. Haque A, Engel J, Teichmann SA, Lonnberg T. A Practical Guide to Single-Cell RNA-sequencing for Biomedical Research and Clinical Applications. *Genome Med* (2017) 9:75. doi: 10.1186/s13073-017-0467-4

114. Mao S, Wang C, Dong G. Evaluation of Inter-Laboratory and Cross-Platform Concordance of DNA Microarrays Through Discriminating Genes and Classifier Transferability. *J Bioinform Comput Biol* (2009) 7:157–73. doi: 10.1142/S0219720009004011
115. Salcido-Ochoa F, Allen JJ. Biomarkers and a Tailored Approach for Immune Monitoring in Kidney Transplantation. *World J Transplant* (2017) 7:276–84. doi: 10.5500/wjt.v7.i6.276
116. Madill-Thomsen K, Perkowska-Ptasinska A, Bohmig GA, Eskandary F, Einecke G, Gupta G, et al. Discrepancy Analysis Comparing Molecular and Histology Diagnoses in Kidney Transplant Biopsies. *Am J Transplant* (2020) 20:1341–50. doi: 10.1111/ajt.15752
117. Loupy A, Lefaucheur C. Antibody-Mediated Rejection of Solid-Organ Allografts. *N Engl J Med* (2018) 379:1150–60. doi: 10.1056/NEJMra1802677
118. Haas M, Mirocha J, Reinsmoen NL, Vo AA, Choi J, Kahwaji JM, et al. Differences in Pathologic Features and Graft Outcomes in Antibody-Mediated Rejection of Renal Allografts Due to Persistent/Recurrent Versus De Novo Donor-Specific Antibodies. *Kidney Int* (2017) 91:729–37. doi: 10.1016/j.kint.2016.10.040
119. Noguchi H, Nakagawa K, Ueki K, Tsuchimoto A, Kaku K, Okabe Y, et al. Response to Treatment for Chronic-Active T Cell-Mediated Rejection in Kidney Transplantation: A Report of 3 Cases. *Transplant Direct* (2020) 6: e628. doi: 10.1097/TXD.0000000000001079
120. Trivedi HL, Terasaki PI, Feroz A, Everly MJ, Vanikar AV, Shankar V, et al. Abrogation of Anti-HLA Antibodies Via Proteasome Inhibition. *Transplantation* (2009) 87:1555–61. doi: 10.1097/TP.0b013e3181a4b91b
121. Waiser J, Budde K, Schutz M, Liefeldt L, Rudolph B, Schonemann C, et al. Comparison Between Bortezomib and Rituximab in the Treatment of Antibody-Mediated Renal Allograft Rejection. *Nephrol Dial Transplant* (2012) 27:1246–51. doi: 10.1093/ndt/gfr465
122. Eskandary F, Regele H, Baumann L, Bond G, Kozakowski N, Wahrmann M, et al. A Randomized Trial of Bortezomib in Late Antibody-Mediated Kidney Transplant Rejection. *J Am Soc Nephrol* (2018) 29:591–605. doi: 10.1681/ASN.2017070818
123. Cornell LD, Schinstock CA, Gandhi MJ, Kremers WK, Stegall MD. Positive Crossmatch Kidney Transplant Recipients Treated With Eculizumab: Outcomes Beyond 1 Year. *Am J Transplant* (2015) 15:1293–302. doi: 10.1111/ajt.13168
124. Kulkarni S, Kirkiles-Smith NC, Deng YH, Formica RN, Moeckel G, Broecker V, et al. Eculizumab Therapy for Chronic Antibody-Mediated Injury in Kidney Transplant Recipients: A Pilot Randomized Controlled Trial. *Am J Transplant* (2017) 17:682–91. doi: 10.1111/ajt.14001
125. Montgomery RA, Loupy A, Segev DL. Antibody-Mediated Rejection: New Approaches in Prevention and Management. *Am J Transplant* (2018) 18:3–17. doi: 10.1111/ajt.14584
126. Choi J, Aubert O, Vo A, Loupy A, Haas M, Puliyanda D, et al. Assessment of Tocilizumab (Anti-Interleukin-6 Receptor Monoclonal) as a Potential Treatment for Chronic Antibody-Mediated Rejection and Transplant Glomerulopathy in HLA-Sensitized Renal Allograft Recipients. *Am J Transplant* (2017) 17:2381–9. doi: 10.1111/ajt.14228
127. Montgomery RA, Orandi BJ, Racusen L, Jackson AM, Garonzik-Wang JM, Shah T, et al. Plasma-Derived C1 Esterase Inhibitor for Acute Antibody-Mediated Rejection Following Kidney Transplantation: Results of a Randomized Double-Blind Placebo-Controlled Pilot Study. *Am J Transplant* (2016) 16:3468–78. doi: 10.1111/ajt.13871
128. Viglietti D, Gosset C, Loupy A, Deville L, Verine J, Zeevi A, et al. C1 Inhibitor in Acute Antibody-Mediated Rejection Nonresponsive to Conventional Therapy in Kidney Transplant Recipients: A Pilot Study. *Am J Transplant* (2016) 16:1596–603. doi: 10.1111/ajt.13663
129. Banham GD, Flint SM, Torpey N, Lyons PA, Shanahan DN, Gibson A, et al. Belimumab in Kidney Transplantation: An Experimental Medicine, Randomised, Placebo-Controlled Phase 2 Trial. *Lancet* (2018) 391:2619–30. doi: 10.1016/S0140-6736(18)30984-X
130. Jordan SC, Choi J, Kim I, Wu G, Toyoda M, Shin B, et al. Interleukin-6, A Cytokine Critical to Mediation of Inflammation, Autoimmunity and Allograft Rejection: Therapeutic Implications of IL-6 Receptor Blockade. *Transplantation* (2017) 101:32–44. doi: 10.1097/TP.0000000000001452
131. Aletaha D, Smolen JS. Diagnosis and Management of Rheumatoid Arthritis: A Review. *JAMA* (2018) 320:1360–72. doi: 10.1001/jama.2018.13103
132. Vo AA, Choi J, Kim I, Louie S, Cisneros K, Kahwaji J, et al. A Phase I/Ii Trial of the Interleukin-6 Receptor-Specific Humanized Monoclonal (Tocilizumab) + Intravenous Immunoglobulin in Difficult to Desensitize Patients. *Transplantation* (2015) 99:2356–63. doi: 10.1097/TP.0000000000000741
133. Eskandary F, Durr M, Budde K, Doberer K, Reindl-Schwaighofer R, Waiser J, et al. Clazakizumab in Late Antibody-Mediated Rejection: Study Protocol of a Randomized Controlled Pilot Trial. *Trials* (2019) 20:37. doi: 10.1186/s13063-018-3158-6
134. NIH U.S. National Library of Medicine. *A Pilot Trial of Clazakizumab in Late Abmr*. Available at: https://clinicaltrials.gov/ct2/show/NCT03444103.
135. NIH U.S. National Library of Medicine. *Interleukin 6 Blockade Modifying Antibody-Mediated Graft Injury and Estimated Glomerular Filtration Rate (Egfr) Decline (Imagine)*. Available at: https://ClinicalTrials.gov/show/NCT03744910.
136. Berger M, Baldwin WR, Jordan SC. Potential Roles for C1 Inhibitor in Transplantation. *Transplantation* (2016) 100:1415–24. doi: 10.1097/TP.0000000000000995
137. Davis AR, Lu F, Mejia P. C1 Inhibitor, a Multi-Functional Serine Protease Inhibitor. *Thromb Haemost* (2010) 104:886–93. doi: 10.1160/TH10-01-0073
138. NIH U.S. National Library of Medicine. *A Multicenter Study to Evaluate the Efficacy and Safety of Cinryze® for the Treatment of Acute Antibody-Mediated Rejection in Participants With Kidney Transplant*. Available at: https://clinicaltrials.gov/ct2/show/NCT02547220.
139. NIH U.S. National Library of Medicine. *Efficacy and Safety of Human Plasma-Derived C1-esterase Inhibitor as Add-on to Standard of Care for the Treatment of Refractory Antibody Mediated Rejection (AMR) in Adult Renal Transplant Recipients*. Available at: https://ClinicalTrials.gov/show/NCT03221842.
140. Clatworthy MR. B-Cell Regulation and its Application to Transplantation. *Transpl Int* (2014) 27:117–28. doi: 10.1111/tri.12160
141. Navarra SV, Guzman RM, Gallacher AE, Hall S, Levy RA, Jimenez RE, et al. Efficacy and Safety of Belimumab in Patients With Active Systemic Lupus Erythematosus: A Randomised, Placebo-Controlled, Phase 3 Trial. *Lancet* (2011) 377:721–31. doi: 10.1016/S0140-6736(10)61354-2
142. Bath NM, Ding X, Verhoven BM, Wilson NA, Coons L, Sukhwal A, et al. Autoantibody Production Significantly Decreased With APRIL/BLyS Blockade in Murine Chronic Rejection Kidney Transplant Model. *PLoS One* (2019) 14:e223889. doi: 10.1371/journal.pone.0223889
143. Bloom RD, Bromberg JS, Poggio ED, Bunnapradist S, Langone AJ, Sood P, et al. Cell-Free DNA and Active Rejection in Kidney Allografts. *J Am Soc Nephrol* (2017) 28:2221–32. doi: 10.1681/ASN.2016091034
144. NIH U.S. National Library of Medicine. *Clazakizumab for Chronic and Active Antibody Mediated Rejection Post-Kidney Transplant* . Available at: https://clinicaltrials.gov/ct2/show/NCT03380377.

Conflict of Interest: The authors declare that the research was conducted in the absence of any commercial or financial relationships that could be construed as a potential conflict of interest.

frontiers in Immunology

ORIGINAL RESEARCH
published: 25 May 2021
doi: 10.3389/fimmu.2021.661761

Connective Tissue Growth Factor Is Overexpressed in Explant Lung Tissue and Broncho-Alveolar Lavage in Transplant-Related Pulmonary Fibrosis

*Arno Vanstapel[1,2], Roel Goldschmeding[3], Roel Broekhuizen[3], Tri Nguyen[3], Annelore Sacreas[1], Janne Kaes[1], Tobias Heigl[1], Stijn E. Verleden[1], Alexandra De Zutter[4], Geert Verleden[1,5], Birgit Weynand[1,2], Erik Verbeken[1,2], Laurens J. Ceulemans[1,6], Dirk E. Van Raemdonck[1,6], Arne P. Neyrinck[7,8], Helene M. Schoemans[9], Bart M. Vanaudenaerde[1] and Robin Vos[1,5]**

[1] Department of Chronic Diseases and Metabolism, Katholieke Universiteit, Leuven, Belgium, [2] Department of Pathology, University Hospital Leuven, Leuven, Belgium, [3] Department of Pathology, University Medical Center Utrecht, Utrecht, Netherlands, [4] Department of Microbiology, Immunology and Transplantation, Katholieke Universiteit, Leuven, Belgium, [5] Department of Respiratory Diseases, Lung Transplant Unit, University Hospital Leuven, Leuven, Belgium, [6] Department of Thoracic Surgery, University Hospital Leuven, Leuven, Belgium, [7] Department of Cardiovascular Sciences, Katholieke Universiteit, Leuven, Belgium, [8] Department of Anesthesiology, University Hospital Leuven, Leuven, Belgium, [9] Department of Hematology, University Hospital Leuven, Leuven, Belgium

Background: Connective tissue growth factor (CTGF) is an important mediator in several fibrotic diseases, including lung fibrosis. We investigated CTGF-expression in chronic lung allograft dysfunction (CLAD) and pulmonary graft-versus-host disease (GVHD).

Materials and Methods: CTGF expression was assessed by quantitative real-time polymerase chain reaction (qPCR) and immunohistochemistry in end-stage CLAD explant lung tissue (bronchiolitis obliterans syndrome (BOS), n=20; restrictive allograft syndrome (RAS), n=20), pulmonary GHVD (n=9). Unused donor lungs served as control group (n=20). Next, 60 matched lung transplant recipients (BOS, n=20; RAS, n=20; stable lung transplant recipients, n=20) were included for analysis of CTGF protein levels in plasma and broncho-alveolar lavage (BAL) fluid at 3 months post-transplant, 1 year post-transplant, at CLAD diagnosis or 2 years post-transplant in stable patients.

Results: qPCR revealed an overall significant difference in the relative content of CTGF mRNA in BOS, RAS and pulmonary GVHD vs. controls (p=0.014). Immunohistochemistry showed a significant higher percentage and intensity of CTGF-positive respiratory epithelial cells in BOS, RAS and pulmonary GVHD patients vs. controls (p<0.0001). BAL CTGF protein levels were significantly higher at 3 months post-transplant in future RAS vs. stable or BOS (p=0.028). At CLAD diagnosis, BAL protein content was

OPEN ACCESS

Edited by:
Hao Wang,
Tianjin Medical University General Hospital, China

Reviewed by:
Antoine Magnan,
Université de Nantes, France
Caigan Du,
University of British Columbia, Canada

***Correspondence:**
Robin Vos
robin.vos@uzleuven.be

Specialty section:
This article was submitted to Alloimmunity and Transplantation, a section of the journal Frontiers in Immunology

Received: 31 January 2021
Accepted: 07 May 2021
Published: 25 May 2021

Citation:
Vanstapel A, Goldschmeding R, Broekhuizen R, Nguyen T, Sacreas A, Kaes J, Heigl T, Verleden SE, De Zutter A, Verleden G, Weynand B, Verbeken E, Ceulemans LJ, Van Raemdonck DE, Neyrinck AP, Schoemans HM, Vanaudenaerde BM and Vos R (2021) Connective Tissue Growth Factor Is Overexpressed in Explant Lung Tissue and Broncho-Alveolar Lavage in Transplant-Related Pulmonary Fibrosis. Front. Immunol. 12:661761. doi: 10.3389/fimmu.2021.661761

significantly increased in RAS patients vs. stable (p=0.0007) and BOS patients (p=0.042). CTGF plasma values were similar in BOS, RAS, and stable patients (p=0.74).

Conclusions: Lung CTGF-expression is increased in end-stage CLAD and pulmonary GVHD; and higher CTGF-levels are present in BAL of RAS patients at CLAD diagnosis. Our results suggest a potential role for CTGF in CLAD, especially RAS, and pulmonary GVHD.

Keywords: GVHD, RAS, BOS, lung transplantation, fibrosis, CTGF, CLAD

INTRODUCTION

Connective tissue growth factor (CTGF, CCN2), a cysteine-rich matricellular protein, is an important profibrotic mediator in several fibrotic disorders, including idiopathic pulmonary fibrosis (IPF) (1, 2). In IPF, promising results of the PRAISE trial were recently published, which was a phase II randomized trial of Pamrevlumab (FG-3019), a fully recombinant human monoclonal antibody against CTGF, demonstrating attenuation of disease progression (2).

Currently, no data are available regarding the potential role of CTGF in the development of chronic lung allograft dysfunction (CLAD) after lung transplantation (LTx); nor in lung graft-versus-host disease (GVHD) after allogeneic hematopoietic stem cell transplantation (HCT). However, as in IPF, fibrotic lung remodeling forms the pathologic hallmark of both CLAD and pulmonary GVHD.

CLAD affects more than 50% of patients within 5 years after lung transplantation (LTx) (3, 4) and remains the major limitation to long term graft survival. CLAD is a clinical diagnosis, defined by a persistent decline in forced expiratory volume in one second (FEV1) of at least >20% compared to baseline. There are currently two main phenotypes described, which are both characterized by distinct fibrotic remodeling (5). Bronchiolitis obliterans syndrome (BOS) is characterized by an obstructive pulmonary function deficit and air trapping on computed tomography (CT) (5). The pathologic hallmark of BOS are bronchiolitis obliterans (BO) lesions, which are characterized by sub-epithelial fibrosis of the small airways. Although several risk factors have been identified for CLAD development (e.g. infection, cellular rejection), the underlying pathogenesis remains largely unknown, but likely results from a complex interplay and dysregulation of pro- and anti-fibrotic mediators. Molecular analysis revealed distinct gene expression patterns, with upregulated transforming growth factor beta (TGF-β), fibroblast growth factor-2, tumor necrosis factor-α and endothelin-1, which interfere with the mediators of myofibroblast homeostasis and extracellular matrix turnover [e.g. matrix metalloproteinases (MMPs) and tissue inhibitors of metalloproteinases (TIMPs)] (6–8).

The second main phenotype of CLAD, restrictive allograft syndrome (RAS), is defined by a restrictive pulmonary function deficit [i.e. >10% decline in total lung capacity (TLC))]and the presence of persistent radiological opacities (9, 10). Pleuroparenchymal fibro-elastosis forms the dominant fibrosis pattern in RAS and non-specific interstitial pneumonia, another fibrotic pattern, is observed in approximately a quarter of RAS patients (11). Interestingly, BO lesions are also present in the majority of end-stage RAS explant lungs, indicating potential overlap of BOS and RAS regarding the underlying fibrogenesis.

CLAD further shows considerable clinical, histopathologic and molecular overlap with pulmonary graft-versus-host-disease (GVHD) after HCT, including development of BO, pleuroparenchymal fibro-elastosis, and an adverse outcome (12, 13). Molecular analysis previously revealed large overlap in the fibrosis-associated gene expression signatures (e.g. MMP, TGF-β) of CLAD vs. pulmonary GVHD (14), indicating potential overlap in pathophysiology.

Since the development of fibrotic lung lesions is central in the pathogenesis of both CLAD and pulmonary GVHD, and given the afore mentioned advancements in CTGF as a promising therapeutic target in IPF, we tested the hypothesis that CTGF may play a role in CLAD and pulmonary GVHD. We therefore analyzed CTGF expression in end-stage lung tissue of well-defined BOS, RAS, pulmonary GVHD and control lungs. In addition, we explored the potential of CTGF as a biomarker, by analyzing CTGF protein expression in broncho-alveolar lavage (BAL) and plasma of CLAD and stable LTx patients.

MATERIALS AND METHODS

CLAD and Pulmonary GVHD Diagnosis

CLAD was defined as per recent ISHLT consensus guidelines (5, 10). CLAD was defined by a persistent (> 3 months) decline in FEV_1 of at least 20% compared to the best post-operative baseline (mean of the two highest FEV_1 values post-LTx taken at least 3 weeks apart), in absence of another cause of pulmonary function decline (e.g. infection) (5). BOS was diagnosed when patients presented with a purely obstructive lung function deficit

Abbreviations: BAL, broncho-alveolar lavage; BOS, bronchiolitis obliterans syndrome; CKD-EPI, Chronic Kidney Disease Epidemiology Collaboration formula; CLAD, chronic lung allograft dysfunction; CT, computed tomography; CTGF, connective tissue growth factor; eGFR, estimated glomerular filtration rate; FEV1, forced expiratory volume in one second; FFPE, formalin-fixed and paraffin-embedded; FVC, forced vital capacity; GVHD, graft-versus-host-disease; HCT, hematopoietic stem cell transplantation; IPF, idiopathic pulmonary fibrosis; LTx, lung transplantation; MMP, matrix metalloproteinases; qPCR, quantitative real-time polymerase chain reaction; RAS, restrictive allograft syndrome; TGF-β, transforming growth factor beta; TIMP, tissue inhibitors of metalloproteinases; TLC, total lung capacity.

(i.e. ≥20% FEV_1 decline with FEV_1/FVC ratio of <0.7, and <10% TLC decline), and without persistent radiological opacities. RAS was diagnosed based on the presence of a restrictive pulmonary function decline (i.e. an additional decline in TLC of ≥10% compared to the best baseline post-LTx, or if unavailable, a decline in FVC of ≥20%) in combination with the presence of persistent opacities on chest CT (10). Stable LTx recipients were defined by a stable lung function (i.e. <10% FEV_1 decline, <10% forced vital capacity (FVC) decline, and <10% TLC decline) for the entire available follow up period, with a minimum of at least three years post-LTx follow up available. Graft loss was defined as death or redo-transplantation (follow-up until July 2020). Pulmonary GVHD was diagnosed by an experienced hematologist, according to the 2014 NIH definition (15). Briefly, this included lung function testing, CT evaluation and clinical symptom assessment.

Explant Lung Tissue Selection

Fresh-frozen explant lung tissue (obtained at redo-LTx or autopsy), collected as previously described and stored in our lung research biobank (16), was used for quantitative real-time polymerase chain reaction (qPCR) analysis of CTGF mRNA levels. We included CLAD patients with BOS (n=20) and RAS (n=20). As no explant tissue was available from stable LTx patients, unused donor lungs (n=20) were matched for age and gender and served as control group. In addition, fresh-frozen explant lung tissue was included from patients suffering from pulmonary GVHD after allogeneic HCT (n=9), which was obtained at LTx or autopsy. A flowchart of patient and tissue selection is provided in **Supplementary Figure S1**. For the immunohistochemical analysis, formalin-fixed and paraffin-embedded (FFPE) explant tissue samples, previously obtained for diagnostic purposes, were retrieved from the pathology archives. For 6/20 (30%) BOS lungs and 7/20 (35%) RAS lungs included in the qPCR analysis, no FFPE material was available in the pathology archives. Therefore, additional CLAD patients were included following the same criteria. In addition, FFPE explant material from all non-transplanted donor lungs (n=20) and pulmonary GVHD patients (n=9) included in the qPCR analysis was available and included in the immunohistochemical analysis.

qPCR Analysis

RNA extraction of fresh-frozen lung tissue was performed by placing the tissue in Trizol reagent (Thermo Fisher), with subsequent disruption using inert zirconium beads and a tissue homogenizer (Precellys). RNA was isolated from the Trizol fractions and further purified using the RNeasy Mini Kit (Qiagen). cDNA synthesis from 3 µg RNA was done using Superscript III reverse transciptase (Thermo Fisher). qPCR was performed with a ViiA7 real-time PCR system (Thermo Fisher), using TaqMan Gene Expression Assays for CTGF (ThermoFisher Hs00170014_m1), TBP (ThermoFisher Hs99999905_m1, and GAPDH (ThermoFisher Hs00427620_m1). Amplification reactions were run in duplicate and analyzed using ViiA7 Software (version 1.2.4). CTGF expression was analyzed using the comparative cycle threshold method, and normalized to the geometric mean of the two housekeeping genes (TBP and GAPDH).

CTGF Immunohistochemistry and Histological Analysis

A representative 3µm tissue section of FFPE material was used for CTGF immunohistochemistry (sc-14939; Santa Cruz Biotechnology Inc., Heidelberg, Germany), as previously described (17). Tissue slides were subsequently digitalized using a Nanozoom XR scanner (Hamamatsu Photonics, München, Germany) and assessed through digital pathology slide viewing software (Aperio ImageScope version 12.4.3., Leica Biosystems, Wetzlar, Germany). CTGF expression of the respiratory epithelium was assessed by a semi-automated approach using open-source image analysis QuPath software (18). The respiratory epithelium was manually delineated and subsequently automatically analyzed using the '*positive cell detection*' tool, that uses an automated cell segmentation algorithm to identify (positive) cells. After visual confirmation and optimization of the different thresholds for cell detection and staining intensities (i.e. negative, 1+, 2+ and 3+), thresholds were consistently applied for all slides. In addition, CTGF expression patterns of other cell types (e.g. endothelial cells, fibroblasts) and further histological findings were reviewed qualitatively by an experienced pulmonary pathologist.

LTx Patient Selection for BAL and Blood Analysis

Sixty patients who underwent LTx at the University Hospitals Leuven between 2007 and 2018 were included for BAL and plasma analysis in this study (**Supplementary Figure S1B**). Patient inclusion was based on retrospective diagnosis of CLAD following the above stated criteria. We selected BOS (n=20), RAS (n= 20), and stable LTx recipients (n=20). BOS and RAS patients were matched with stable LTx recipients for age, gender, and underlying native lung disease; and further selected based on the availability of BAL and plasma samples at the different matched time points. For 2/20 (10%) BOS patients and 8/20 (40%) RAS patients, fresh-frozen and FFPE explant lung tissue was also included.

BAL Collection

All LTx recipients received routine follow-up visits at fixed time points, as described earlier (19). BAL samples, obtained at three different time points and stored at -80°C, were included in this study: at 3 months post-LTx, 1 year post-LTx, and at CLAD diagnosis for BOS and RAS patients, or at 2 years post-LTx for stable LTx recipients (i.e. the last routine bronchoscopic evaluation and the closest matched time point as comparison for BAL samples at CLAD diagnosis). The applied BAL protocol was in accordance with the recently published consensus statement for the standardization of BAL in LTx (20) (**Supplementary methods**).

Peripheral Blood Collection

Peripheral blood samples were collected at the time of bronchoscopy at initial CLAD diagnosis, or if unavailable, the first available sample following CLAD diagnosis. (BD Vacutainer® EDTA-lined plastic tubes, Franklin Lakes, NJ, USA). For stable LTx recipients, samples from the routine 2 years post-LTx visit were included. Blood plasma was isolated and stored at -80°C. As CTGF has a predominant renal clearance (21), plasma creatinine levels and the estimated glomerular filtration rate (eGFR - Chronic Kidney Disease Epidemiology Collaboration formula) were compared between groups as surrogate for potential differences in renal CTGF clearance.

CTGF Enzyme-Linked Immunosorbent Assay

CTGF was determined by sandwich enzyme-linked immunosorbent assay (ELISA) as described previously (22, 23), using monoclonal antibodies against two distinct epitopes on the NH2-terminal part of human CTGF (FibroGen, South San Francisco, CA, USA). Twenty µl of undiluted BAL supernatants or 50 µl 1:5 diluted plasma were added to each well together with an equal volume of CTGF detection antibody conjugated to alkaline phosphatase. Purified recombinant human N-CTGF (FibroGen, South San Francisco, CA, USA) was used for calibration and absorbance was read at 405 nm. Measurements were performed in duplicate and the mean of these values was used for further analysis.

Statistics and Ethics Statement

Results are presented as median and interquartile range (IQR), unless stated otherwise. All datasets were formally tested for normality using D'Agostino Pearson test. Discrete data were compared *via* contingency tables and Chi-square test. For continuous data, Mann-Whitney U and Kruskall-Wallis test was used with post-hoc testing using Dunn's multiple comparison test, where appropriate. GraphPad prism version 8.0 software (San Diego, CA, USA) was used for all analyses. A two-tailed p-value of <0.05 was considered significant. This retrospective study was approved by the Leuven University Hospital institutional review board (S52174, S57742, S51577, S61653, S59648, ML6385) and performed according to the principles of the Declaration of Helsinki. Written informed consent to participate in biobanking and scientific research was provided by all CLAD and pulmonary GVHD patients included in the study. In addition, Belgian law states that donor organs not suitable for transplantation can be used in approved research programs.

RESULTS

CTGF Explant Tissue Analysis

An overview of the patient characteristics of BOS, RAS, and control lungs included in the qPCR and immunohistochemical CTGF analysis is provided in **Tables S1** and **S2**, *respectively*. Control lungs (n=20) consisted of lungs not used for LTx for the following reasons: logistical issue (n=8), used for single/lobar transplant (n=7), extra-pulmonary tumor (n=3), and other (n=2). The cause of death of these donors was cerebrovascular accident (n=6), trauma (n=4), suicide (n=3), cardiac arrest (n=3), euthanasia (n=1), death during surgery (n=1), subarachnoid hemorrhage (n=1), and bacterial meningitis (n=1). Explant lung tissue from 9 patients with pulmonary GVHD was available (patient characteristics are provided in **Table S3**). Five (56%) of 9 patients suffered from an obstructive lung function deficit without prominent opacities on CT (i.e. obstructive pulmonary GVHD or BOS), while 4 (44%) patients suffered from a restrictive lung function deficit with ground glass opacities and consolidation on chest CT (i.e. restrictive pulmonary GVHD or late-onset non-infectious pulmonary complication other than BOS). An overview of the results of qPCR analysis, immunohistochemistry, BAL and blood plasma ELISA is provided in **Table S4**.

qPCR Analysis

qPCR analysis of BOS, RAS, pulmonary GVHD and control lungs revealed an overall significant difference in the relative fold change expression of CTGF mRNA compared to controls, normalized to the geometric mean of the two housekeeping genes (TBP, GAPDH) (p=0.014) (**Figure 1**). Post-hoc analysis revealed significant increased relative CTGF mRNA levels in BOS vs. controls (p=0.0020), GVHD vs. controls (p=0.0097), and trend towards higher CTGF mRNA content in RAS vs. controls (p=0.052).

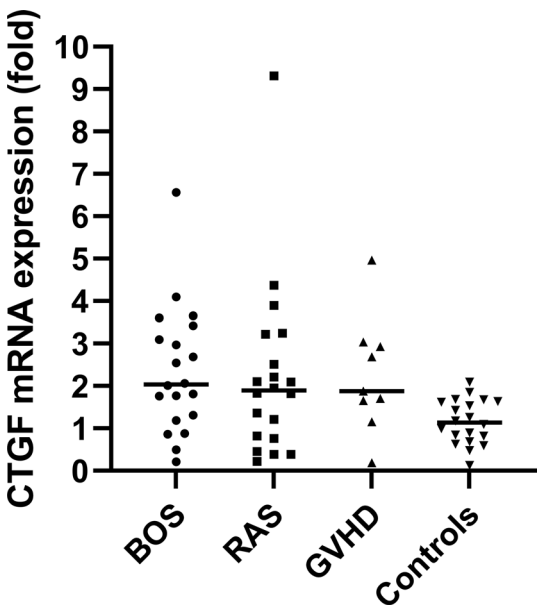

FIGURE 1 | qPCR analysis with visualization of the difference in relative fold change levels of CTGF mRNA, relative to the geometric mean of the two housekeeping genes (TBP, GAPDH). Overall, CTGF levels were significantly increased compared to controls (Kruskal Wallis: p=0.014). *Post-hoc* analysis revealed significant increased relative CTGF mRNA levels in BOS *vs.* controls (p=0.0020) and GVHD vs. controls (p=0.0097).

CTGF Staining in CLAD Explant Tissue

To validate and further explore the overall higher CTGF mRNA levels compared to control lungs, CTGF immunohistochemistry was performed to assess and compare protein expression patterns. Immunohistochemistry revealed a significant higher percentage of CTGF-positive respiratory epithelial cells (staining intensity ≥ 1+) in both end-stage BOS and RAS lungs (median: 77.81% [60.73-90.52], and median: 95.53%, [75.05-98.84]; respectively), compared to control lungs (median: 30.34%, [12.55-37.75], p<0.0001); while there was no significant difference between BOS and RAS (p=0.47) (**Figure 2** and comparison of different staining intensities is provided in **Table S4**).

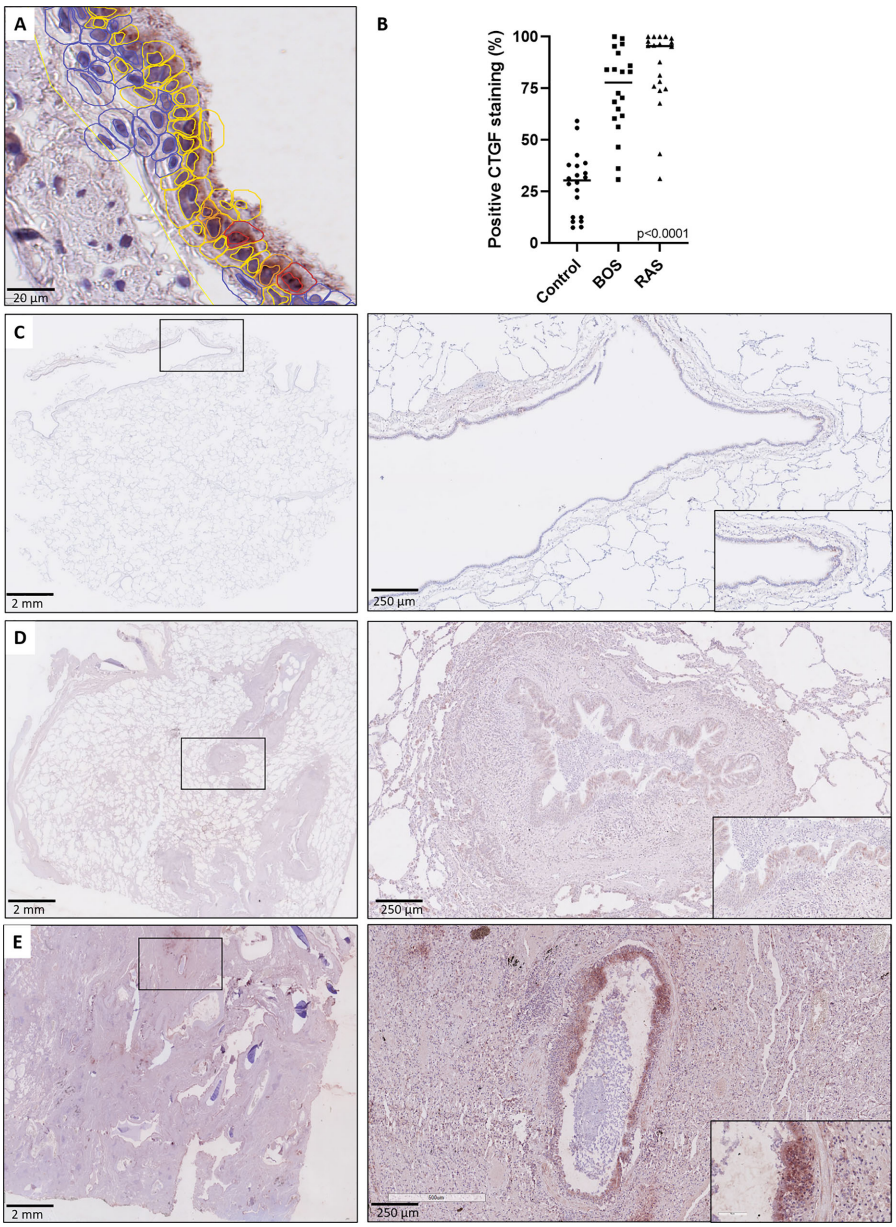

FIGURE 2 | CTGF staining in respiratory epithelium. **(A)** High-detailed illustration of semi-automated cell segmentation and analysis method using QuPath software to assess the respiratory epithelium. Blue lining indicates no CTGF positive staining, yellow indicates mild (1+) staining, orange indicates moderate (2+) staining and red indicates strongly positive (3+) staining. **(B)** Comparison of CTGF immunohistochemistry revealed a significant higher percentage of CTGF-positive respiratory cells (staining intensity ≥1+) in both BOS and RAS, compared to control lungs (p<0.0001). **(C)** Control lung, normal lung parenchyma with presence of a larger normal airway. Inset: higher magnification of the normal lining respiratory epithelium, with presence of only few cells with a positive CTGF staining. **(D)** Bronchiolitis obliterans syndrome with normally preserved alveoli and the presence of several larger airways displaying mild to moderate sub-epithelial fibrosis. Inset: higher magnification of airway with diffuse cytoplasmic CTGF staining of the respiratory epithelium. **(E)** Restrictive allograft syndrome with severe fibrotic remodeling. Inset: airway with prominent and diffuse CTGF positive respiratory epithelium.

Histopathological examination further revealed that the respiratory epithelium in active BO lesions, which are characterized by sub-epithelial fibrosis and potential inflammation of the small bronchioles, displayed a uniform prominent cytoplasmic CTGF staining (**Figures 3A, B**). Similarly, there was prominent staining in bronchioles with lymphocytic bronchiolitis (**Figure 3C**). In end-stage BO lesions, the respiratory epithelium was no longer discernable and only fibrotic lesions, with CTGF positive stromal cells, remained (**Figure 3D**). In contrast, normal bronchioles from the same size revealed only mild and limited focal CTGF staining of the respiratory epithelium in control lungs (**Figures 3E, F**).

A consistent finding was the presence of strongly positive CTGF stained stromal fibroblasts in fibrotic regions of RAS lungs. This included fibrosis in regions of (sub)pleural fibrosis and alveolar fibrosis (e.g. diffuse fibrotic thickening of alveolar septa) (**Figures 4A, B**, respectively). In addition, microscopic interstitial foci of fibrosis in BOS lungs, beyond the fibrosis in the setting of (end-stage) BO lesions, displayed a comparable and consistent strongly positive staining of CTGF positive fibroblasts (**Figure 4C**). CTGF immunohistochemical staining of endothelial cells was variable, but consistently prominently expressed in fibrotic regions of RAS patients (**Figures 5A, B**). CTGF staining of macrophages also displayed considerable variation in staining intensities. The most prominent finding was CTGF positive staining of collections of intra-alveolar macrophages, which were most abundant in RAS and typically distributed around zones of interstitial fibrosis (**Supplementary Figure S2**). However, even within and between these collections of intra-alveolar macrophages, staining intensity varied.

CTGF Expression in GVHD

Immunohistochemical CTGF analysis of GVHD lung tissue revealed similar histological findings compared to BOS and RAS. GVHD lungs displayed prominent staining intensity (≥ 1+) of the respiratory epithelium (median percentage of positive cells: 88.87% [83.13-91.64]), significantly increased compared to unused donor lungs ($p<0.0001$). Similar to CLAD, a diffuse cytoplasmic CTGF positivity of the respiratory epithelium in small bronchioles with

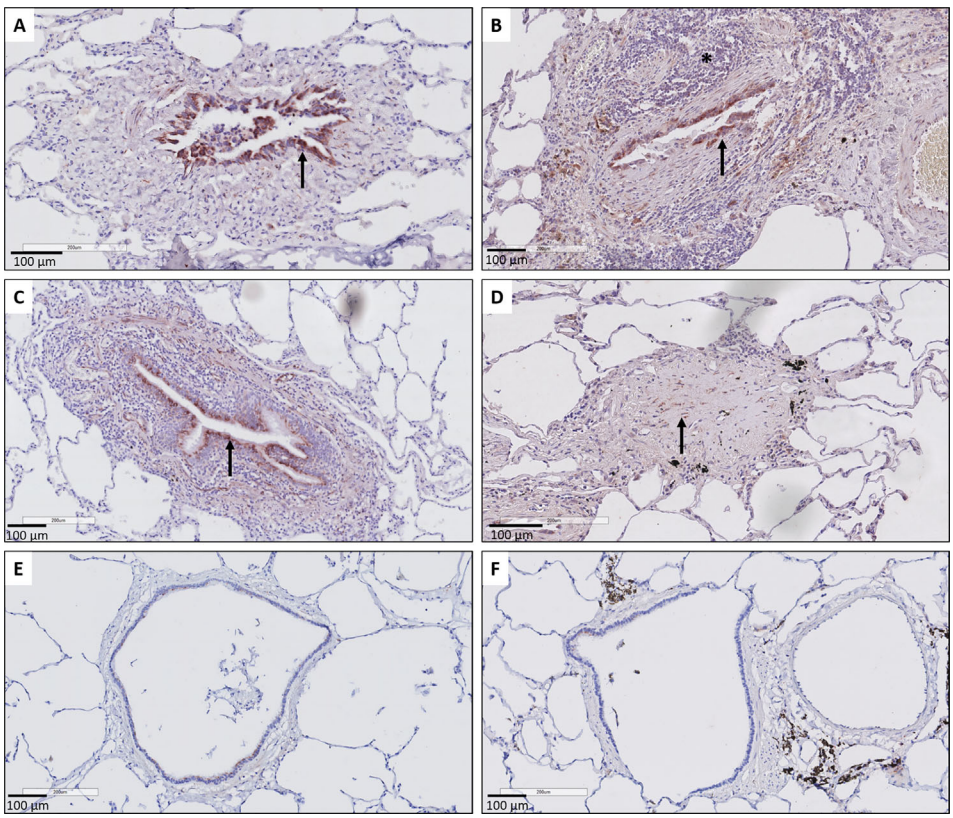

FIGURE 3 | Representative immunohistochemical illustrations of CTGF staining in airway lesions in CLAD versus in normal bronchioles from control lungs. **(A, B)** BO lesions, characterized by sup-epithelial fibrosis are lined by respiratory epithelium with a diffuse and prominent CTGF positivity (arrows). In figure **(B)** there is also an accompanying prominent lymphocytic inflammation (asterisk). **(C)** Lymphocytic bronchiolitis characterized by diffuse submucosal invasion of lymphocytes with diffuse and strong CTGF positive stained respiratory epithelium (arrow). **(D)** end-stage BO lesion without recognizable airway lumen, with partly CTGF positive stromal cells (arrow). **(E, F)** bronchioles from control lungs, approximately the same size as the airways with obliterative airway remodeling in CLAD, displaying only limited and focal CTGF positive staining of the respiratory epithelium. In figure **(F)** there is also prominent presence of black pigment-laden macrophages.

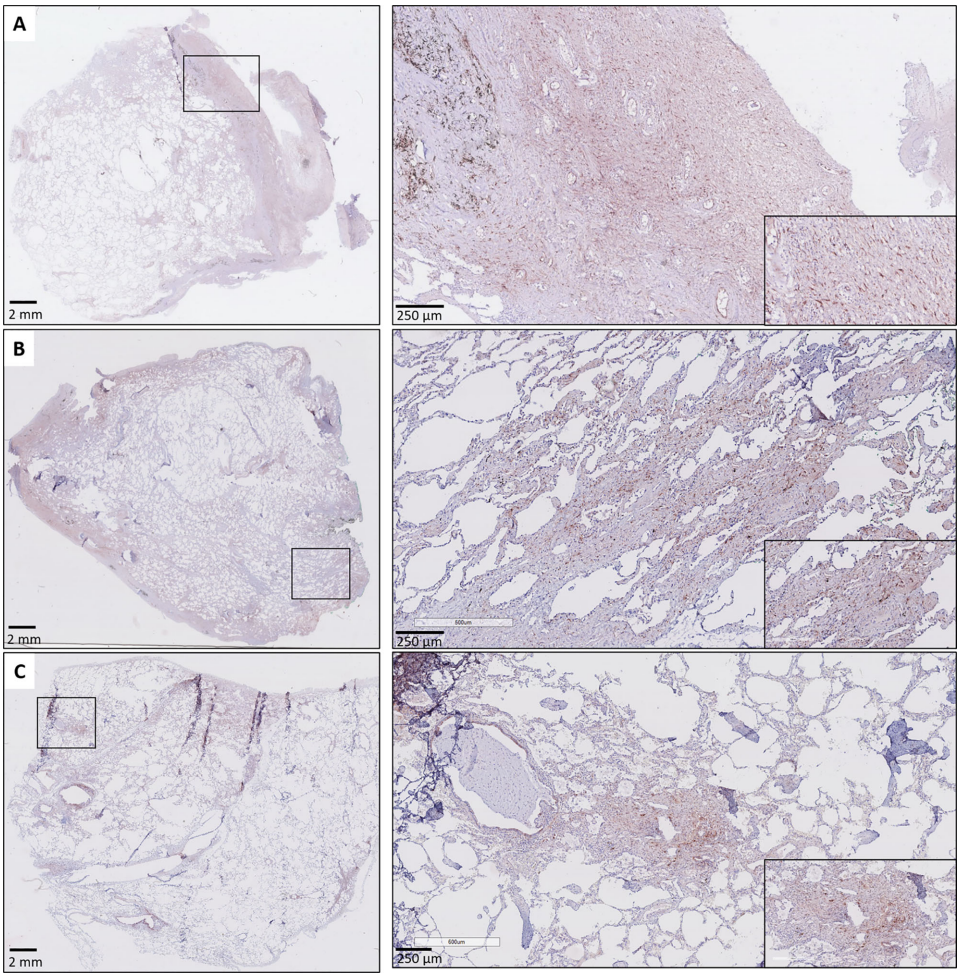

FIGURE 4 | Fibrosis in CLAD. **(A)** Subpleural fibrosis in a patient with RAS. The inset illustrates prominent and diffuse (myo)fibroblast staining in the (sub)pleural region. **(B)** RAS, with both subpleural fibrosis and alveolar fibrosis. The inset illustrates prominent CTGF staining in a zone with thickened fibrotic alveolar septa. **(C)** BOS. The lung parenchyma has signs of mild emphysema, but no obvious fibrotic remodeling is present. The inset highlights a microscopic focus of fibrosis, in which there is also prominent CTGF staining of fibroblasts.

fibrotic remodeling was found (**Figure 6A**). In fibrotic zones, similar to RAS, there was strong and diffuse CTGF staining of the fibroblasts (**Figures 6B, C**). Endothelial cells also displayed variable CTGF staining, but, similar as in RAS, were consistently highly expressed in fibrotic regions.

CTGF Biomarker Exploration

Since end-stage explant lung tissue analysis revealed higher CTGF expression in CLAD compared to control lungs, with prominent CTGF expression in the respiratory epithelium and endothelium, we aimed to explore the role of CTGF as a potential biomarker for CLAD, based on CTGF levels in BAL and plasma. Patient characteristics of BOS (n=20), RAS (n=20) and stable LTx (n=20) recipients included for BAL and plasma CTGF analysis are provided in **Table S5**. For pulmonary GVHD patients, no BAL and plasma samples were available. Patients had a median time to BOS of 3.10 years [1.46-4.58] and to RAS of 3.38 years [1.81-4.60]. Graft loss occurred in 6/20 (30%) BOS patients and 11/20 (55%) RAS patients. In addition, graft loss occurred in 2/20 (10%) patients from the stable group (i.e. 9 and 10 years after LTx due to hospital acquired pneumonia following orthopedic surgery, and sudden cardiac arrest, respectively), without available explant tissue.

BAL CTGF ELISA

BAL CTGF content was assessed at three distinct time points: at 3 months post-LTx, 1 year post-LTx, and at CLAD diagnosis or at 2 years post-LTx in stable LTx recipients. CTGF levels were significantly higher at 3 months post-LTx in patients who later developed RAS compared to stable LTx recipients (p=0.025), while there was no significant difference with patients who later developed BOS (p=0.28) (**Figure 7A**). At 1 year post-LTx, there was no significant difference between groups (p=0.20) (**Figure 7B**). At CLAD diagnosis, CTGF levels were

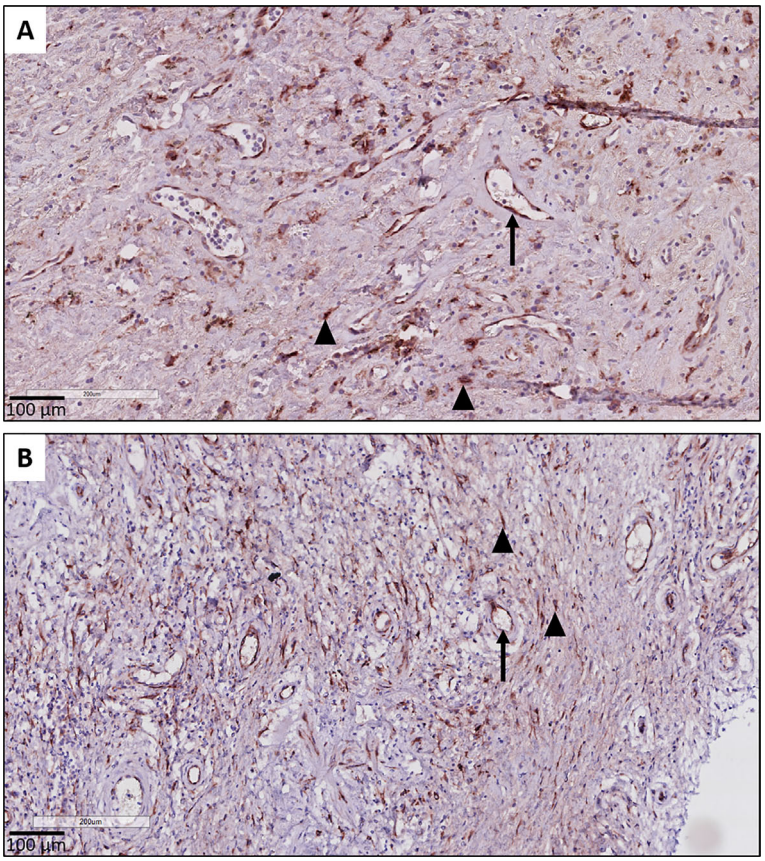

FIGURE 5 | CTGF staining in endothelial cells. **(A, B)** Illustration of prominent endothelial staining (arrows) in fibrotic zones of two patients with RAS. The (myo) fibroblasts are also strongly CTGF positive (arrow heads).

significantly higher in RAS patients compared to stable LTx recipients (p=0.0007) and BOS patients (p=0.042) (**Figure 7C**). Paired analysis revealed no significant difference in CTGF values at the different time points for stable and BOS patients (p=0.84 and p=0.92, respectively) (**Figures 8A, B**), whereas values had significantly increased in RAS patients at the moment of CLAD diagnosis compared to 1 year post-LTx (p=0.029) (**Figure 8C** and **Supplementary Figure S3**).

Plasma CTGF ELISA

Plasma CTGF analysis from BOS, RAS, and stable LTx patients (obtained at routine 2 years post-LTx visit) revealed no significant differences (p=0.74) (**Figure 9**). Blood samples were collected at initial BOS diagnosis for 3/20 (15%) BOS patients, and at initial RAS diagnosis for 12/20 (60%) RAS patients, while the remaining samples were obtained after initial CLAD diagnosis (median time after CLAD diagnosis was 2.30 years [0.89-4.92]). Median plasma creatinine levels and the estimated glomerular filtration rate did not significantly differ between groups, indicating no difference in renal function and therefore presumably no difference in renal CTGF clearance (p=0.95 and p=0.80, respectively) (**Table S4**).

DISCUSSION

This explorative study investigated the expression of CTGF in CLAD and pulmonary GVHD. The main findings of this study are (i) higher levels of tissue CTGF expression in end-stage explant lungs of BOS, RAS and pulmonary GVHD patients compared to control lungs and (ii) increased CTGF levels in BAL at RAS diagnosis compared to stable LTx patients and compared to BOS patients.

CTGF has an important role in many biological processes, such as cell adhesion, proliferation, differentiation, and tissue repair. It stands as a central profibrotic mediator, and its transcription is regulated by several factors, both directly from external stimuli (e.g. hypoxia, mechanical stimulation) and through cross-talks (e.g. TGF-β) (24). CTGF has been studied in several organs, including kidney, liver, cardiac and lung fibrosis (1). In IPF, CTGF was found to be upregulated in cultured fibroblasts, broncho-alveolar lavage, plasma, and lung tissue (25–28). In animal models, CTGF levels were increased in fibroblasts of a bleomycin-induced mouse model of IPF (29), and CTGF was an essential factor to induce a profibrotic environment in "fibrosis-resistant" mice lungs (30). These

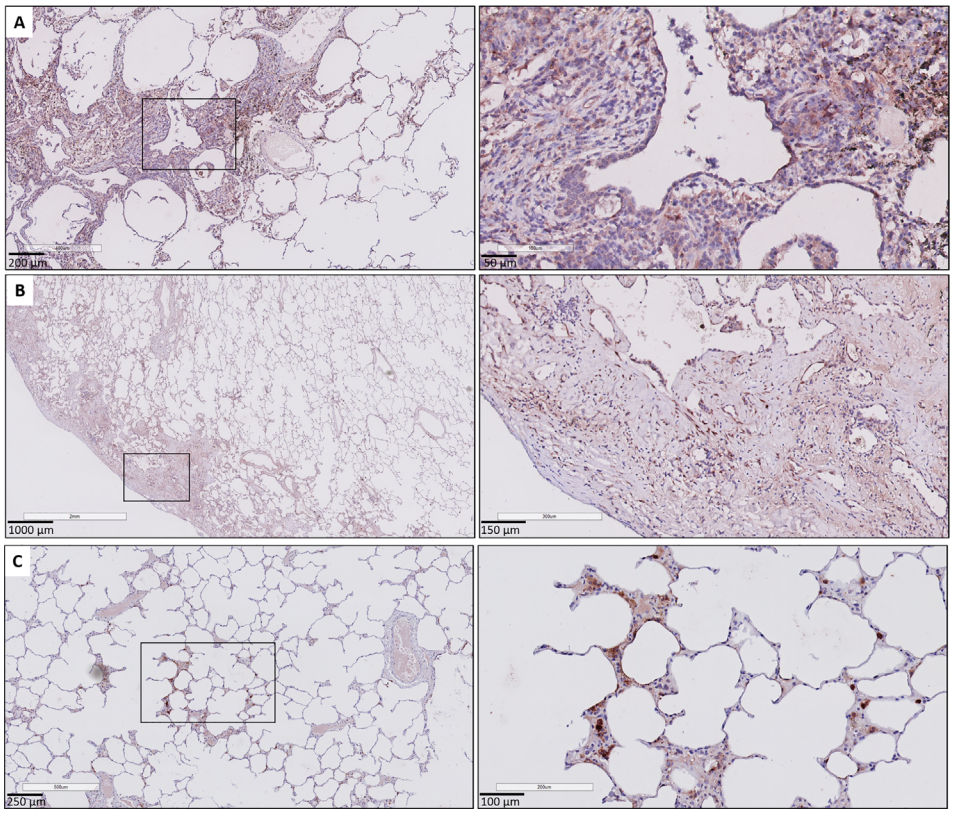

FIGURE 6 | CTGF immunohistochemistry in patients with pulmonary GVHD after HCT. **(A)** Illustration of small bronchiole surrounded by fibrous remodeling with limited inflammation, with CTFG positive respiratory epithelium and stromal cells. **(B)** Presence of subpleural fibrosis characterized by prominent staining of the (myo) fibroblasts in these fibrotic regions. **(C)** Presence of focal, minimal fibrous thickening of the alveolar septa, with presence of prominent staining of interstitial macrophages and the alveolar epithelial cells. The surrounding alveolar parenchyma is normally preserved.

findings in the field of IPF, combined with overt fibrotic lung remodeling in CLAD and pulmonary GVHD, therefore also provide a theoretical basis for studying the role of CTGF in CLAD. However, in the context of CLAD after LTx or pulmonary GVHD after HCT, no data are currently available regarding CTGF expression. To the best of our knowledge, this study therefore forms the first to explore the role of CTGF in CLAD and pulmonary GVHD.

Exploration of CTGF expression in explant lungs revealed prominent differences between CLAD (BOS/RAS) and pulmonary GVHD on the one hand, and control lungs on the other hand. CTGF staining was significantly increased in the

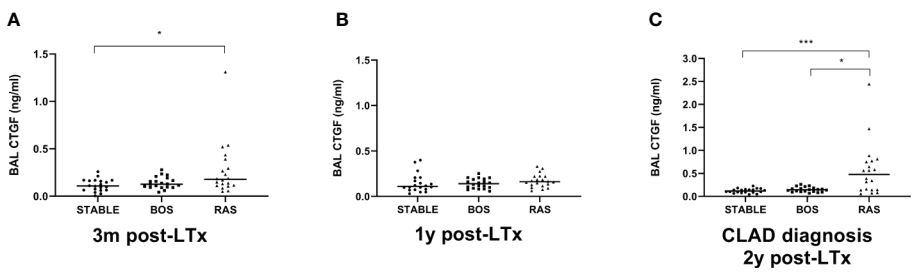

FIGURE 7 | Comparison of BAL CTGF protein levels between groups at different time points. **(A)** CTGF values at 3 months after LTx (p=0.028). CTGF values are significantly higher in patients that later developed RAS, compared to stable LTx recipients (p=0.025). **(B)** CTGF values at 1 year after LTx, there are no significant differences between groups (p=0.20). **(C)** CTGF values at CLAD diagnosis and at 2 years post-LTx for stable LTx recipients (p=0.0009). CTGF values are significantly higher at RAS diagnosis compared to stable LTx recipients at 2 years post LTx (p=0.0007) and compared to CTGF values at BOS diagnosis (p=0.042). BAL, broncho-alveolar lavage; BOS, bronchiolitis obliterans syndrome; RAS, restrictive allograft syndrome; CLAD, chronic lung allograft dysfunction.

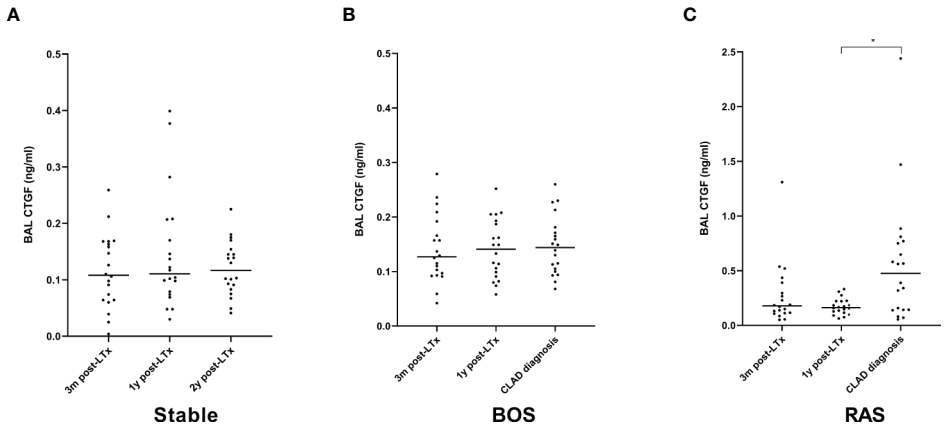

FIGURE 8 | Paired analysis of BAL CTGF protein levels at the different time points after LTx. **(A)** CTGF values for stable LTx recipients; there was no significant difference between different time points (p=0.84). **(B)** CTGF values for BOS patients; no significant difference was observed between different time points (p=0.92). **(C)** CTGF values for RAS patients; CTGF values were significantly higher at CLAD diagnosis (p=0.026); *post-hoc* analysis confirmed higher CTGF values at CLAD diagnosis compared to 1y post-LTx (p=0.029), but not compared to 3 months post-LTx (p=0.15). BOS, bronchiolitis obliterans syndrome; RAS, restrictive allograft syndrome.

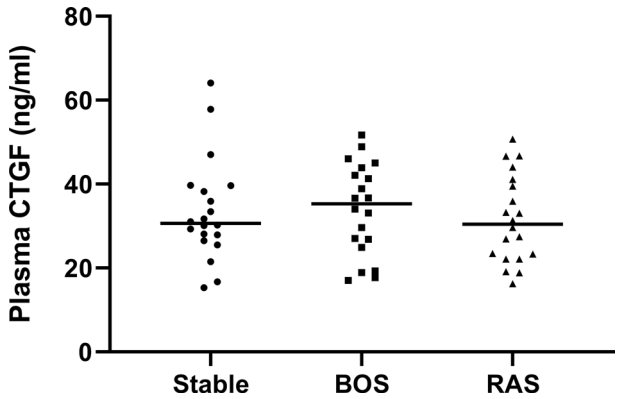

FIGURE 9 | Plasma CTGF protein levels. There was no significant difference in plasma CTGF levels between groups (p=0.74).

respiratory epithelium in CLAD and pulmonary GVHD compared to control lungs, with especially prominent staining of the respiratory epithelium in BO lesions. Interestingly, higher respiratory CTGF expression has previously been demonstrated in chronic obstructive pulmonary disease, and correlated with disease severity (31). Further, CLAD explant lungs displayed consistent and strong CTGF positivity in fibroblasts, comparable to previously described findings in IPF (28). In addition, CTGF expression in endothelial cells was specifically prominent in fibrotic zones of RAS patients. CTGF is known to exacerbate vascular remodeling in the lung, and CTGF transcription can be induced by hypoxia (1). In transgenic mouse models, down-regulation of CTGF was protective against development of pulmonary hypertension associated with hypoxia and against bleomycin-induced pulmonary hypertension (32). Modulation of endothelial CTGF expression may therefore be a potential interesting mechanism of action for CTGF-inhibitors, especially since pulmonary hypertension and vascular remodeling is highly prevalent in CLAD patients (33).

As immunohistochemical analysis revealed prominent CTGF expression in the respiratory epithelium and endothelium, monitoring of CTGF levels in BAL and plasma might hold potential as a biomarker. CTGF ELISA, mostly measured in plasma and urine, has previously been proposed as a biomarker monitoring tool to measure the extent of ongoing fibrosis in several fibrotic diseases (liver fibrosis, diabetic nephropathy, systemic sclerosis), and correlated with disease severity (1). Our current findings confirm that CTGF expression in BAL may be associated with fibrosis in CLAD, although the results were variable between patients, potentially due to the inherent sampling-variability observed in fibrotic remodeling in CLAD patients. In addition, we found no increased plasma CTGF expression in our cohort. While BAL CTGF was higher in RAS at 3 months post-LTx compared to stable LTx patients, this difference did not persist in consecutive samples at 1 year post-LTx. This lowers the current evidence of CTGF as potential biomarker to predict CLAD onset and advocates further investigation of CTGF biomarker potential in successive BAL samples of a larger cohort. However, it is important to note that a BAL procedure gives no information about the whole lung, but rather for a limited bronchopulmonary segment. As fibrotic remodeling in CLAD is a heterogeneous phenomenon, especially given the preferential apical fibrosis in RAS, BAL fluid analysis might underestimate the true observed difference. Moreover, BAL samples were obtained at CLAD diagnosis, when fibrotic remodeling may still be limited.

Exploration of potential biomarkers to predict CLAD development has been performed by several groups (34). Despite the fact that no single clinically useful biomarker has

been identified yet, several interesting markers have been linked to CLAD development in BAL, blood and lung tissue. Todd et al. recently identified upregulation of amphiregulin, an epidermal growth factor receptor (EGFR) ligand with putative role in airway injury and repair regulation, in BAL fluid of CLAD patients (20). *In situ* hybridization of CLAD tissue identified abundant EGFR and amphiregulin transcript expression in the airway epithelial cells of fibrotic regions. Moreover, *ex vivo* stimulation of cultured bronchial epithelial cells with amphiregulin led to increased hyaluronan expression through an EGRF-dependent pathway. Hyaluronan is an important glycosaminoglycan previously found to be increased in both BAL and blood of CLAD patients (35). In addition, a murine orthotopic lung transplant model demonstrated that hyaluronan might contribute to CLAD by activation of innate immune signaling pathways in a toll-like receptor (TLR) 2/4 and myeloid differentiation primary response (MyD)-88 dependent manner (35). Shino et al. analyzed BAL expression of Chemokine (C-X-C motif) ligand (CXCL) 9, CXCL10 and CXCL11, which form CXC chemokine receptor (CXCR) 3 chemokine ligands and which act as chemoattractants of mononuclear cells. They found, in a multivariate adjusted model that higher expression of these CXCR3 chemokine ligands in BAL, in co-presence with organizing pneumonia, led to significantly increased CLAD risk (36). Very recently, the same group reported increased BAL levels of CXCL9 and CXCL10 in a prospective multicenter study during episodes of acute rejection and acute lung injury in the first year post-LTx, which form known risk factors for future CLAD development (37).

Micro-array based gene expression analysis of BAL cell pellets by Weigt et al., obtained at one year post transplant surveillance in a small nested-case control study, revealed differential gene expression related to mainly CD8 cytotoxic lymphocytes and NK cell activation and proliferation in patients who developed CLAD within two years after bronchoscopy (38). Micro-array analysis of blood samples however mostly pointed towards a qualitative B cell defect, with identification of a three gene based predictive model of CLAD (downregulation of POU class 2 associating factor 1 (POU2AF1), T cell leukemia/lymphoma protein 1A (TCL1A) and B cell lymphocyte kinase (BLK)) (39). In blood, especially MMP-9 has further gained interest as a potential biomarker. Pain et al. reported that increased expression of MMP-9 was independently associated with CLAD and detection preceded functional CLAD diagnosis by 12 months (40). Interestingly, in an associated *ex vivo* study, they identified that activated T cells promote specific MMP-9 production by bronchial epithelial cells trough the CCL2/CCR2 axis in synergy with TGF-β and initiate epithelial-to-mesenchymal transition (40). Recently, increased expression of lipocalin-2, which stabilizes MMP-9 activity, was also proposed as potential biomarker to distinguish RAS from BOS patients and stable-LTx patients (41). TGF-β forms the most potent inducer of CTGF, and CTGF overproduction plays a crucial role in fibrosis development (42, 43), but appears to induce fibrosis mostly in the co-presence of TGF-β (44). We previously reported that TGF-β was mainly upregulated in RAS patients, both in BAL fluid and explant lung tissue, and TGF-β stimulation of pleural mesothelial cells led to a phenotypical switch to mesenchymal cells, indicating a potential role in the epithelial-to-mesenchymal transition (45).

In a molecular profiling study based on lung biopsies obtained in the first year post-LTx, Jonigk et al. assessed 45 tissue remodeling-associated genes in a cohort that rapidly developed CLAD within 3y post-LTx versus a matched stable cohort without CLAD development (8). By combining mRNA expression levels of the five most significantly differentially expressed genes from the TGF-β axis (BMP-4, IL-6, MMP-1, SMAD1, and THBS1), they could predict patient outcomes. In addition, the same group performed laser-assisted microdissection of airway lesions in both CLAD and IPF explant lungs, and reported a large and important molecular overlap of pivotal fibrotic pathways, with shared upregulation of TGF-β, MMP-9, RANTES, TIMP-1, TIMP-2, BMP-2, PLA-1 and COL1/2/3 (6).

There is currently no effective treatment for CLAD, and especially RAS patients typically experience a rapid inevitable decline of pulmonary function after diagnosis, with a median survival of only 1-1.5 years (9). Given the clinical, radiological and pathological similarities with IPF, attempted treatment strategies are mainly based on approved IPF treatments. Pirfenidone appears safe and may attenuate the rate of decline in lung function in patients with RAS, although prospective trials are lacking (46, 47). In BOS patients, both Pirfenidone and Nintedanib, another approved IPF treatment, are currently investigated in prospective clinical trials (NCT02262299 and NCT03283007, respectively). CTGF has also gained interest as a potential therapeutic target for IPF. A clinical phase II placebo-controlled trial of a fully recombinant human monoclonal antibody against CTGF (FG-3019) was recently found to attenuate progression of IPF (2). Despite that the phase III trial is currently still ongoing, this might perhaps become a third therapeutic option for IPF in the near future (NCT03955146). Given the striking similarities between IPF and CLAD, and given our current findings, this might also indirectly advocate to study CTGF as potential therapeutic target in CLAD, and by extrapolation, in pulmonary GVHD.

There are some limitations to our study. First, this is an explorative and descriptive retrospective single center study with limited sample size and although patients were well-characterized, extrapolation of these results might therefore be limited. Second, serum samples at CLAD diagnosis were not available for most CLAD patients due to the fact that serum samples were only routinely obtained from 2015 onwards. Further exploration of the biomarker potential of CTGF ELISA remains to be investigated in a larger cohort. Third, no lung tissue was available from stable LTx recipients due to inherent limitations in collecting explant material and no immunohistochemical comparison could therefore be made between CLAD and stable LTx patients. However, matched unused donor lungs served as a valuable and unique control group. Finally, no BAL or blood samples were available from pulmonary GVHD patients, as well as only a limited number of

lungs, which is directly related to the low number of GVHD patients qualifying for LTx and the limited number of LTx for this indication in most centers.

In conclusion, lung tissue CTGF expression levels are mainly increased in end-stage RAS, but also in established BOS and pulmonary GVHD. CTGF protein expression is increased in BAL fluid from RAS patients at CLAD diagnosis compared to BOS and stable LTx patients. Our results therefore suggest a potential role for CTGF in CLAD, especially RAS, and pulmonary GvHD, which advocates further investigation of the role of CTGF in the pathophysiology of CLAD and the potential therapeutic modulation of CTGF in onset and progression of both disorders.

DATA AVAILABILITY STATEMENT

The raw data supporting the conclusions of this article will be made available by the authors, without undue reservation.

ETHICS STATEMENT

The studies involving human participants were reviewed and approved by UZ Leuven Ethical Committee. The patients/participants provided their written informed consent to participate in this study.

AUTHOR CONTRIBUTIONS

Concept and design: AV, RG, RB, TN, AS, SV, BW, and RV. Data analysis and interpretation: AV, RG, RB, TN, AS, JK, TH, SV, AZ, GV, BW, EV, LC, DR, AN, HS, BV, and RV. Drafting the manuscript for important intellectual content: AV, RG, RB, TN, AS, JK, TH, SV, AZ, GV, BW, EV, LC, DR, AN, HS, BV, and RV. All authors contributed to the article and approved the submitted version.

FUNDING

AV is sponsored by a fundamental research grant from the FWO (1102020N). JK is sponsored by a fundamental research grant from the FWO (1198920N). SV is sponsored by a grant from the FWO (FWO12G8715N) and the KU Leuven (C24/18/073). BV is funded by the KU Leuven (C24/050). RV is supported by the FWO (senior clinical researcher) and by a Roche Research Grant from the Belgian Transplant Society. LC is supported by a KU Leuven University chair sponsored by the company Medtronic. DR and GV are supported by the Broere Charitable foundation.

ACKNOWLEDGMENTS

We would like to thank "The Leuven Lung Transplant Group": this includes the following important collaborators of our lung transplant program who were directly involved in the care of our lung transplant recipients during the past years: Lieven J. Dupont, MD, PhD, Jonas Yserbyt, MD, PhD, Laurent Godinas, MD, PhD, Anke Van Herck, MD, PhD, Veronique Schaevers, MSc, Paul De Leyn, MD, PhD, Herbert Decaluwé, MD, PhD, Hans Van Veer, MD, Lieven Depypere, MD, PhD, Marie-Paule Emonds, MD, PhD, Liesbeth Daniëls, MD, Jan Van Slambrouck, MD, and Michaela Orlitová, MD.

SUPPLEMENTARY MATERIAL

The Supplementary Material for this article can be found online at: https://www.frontiersin.org/articles/10.3389/fimmu.2021.661761/full#supplementary-material

REFERENCES

1. Ramazani Y, Knops N, Elmonem MA, Nguyen TQ, Arcolino FO, van den Heuvel L, et al. Connective Tissue Growth Factor (CTGF) From Basics to Clinics. *Matrix Biol* (2018) 68–69:44–66. doi: 10.1016/j.matbio.2018.03.007
2. Richeldi L, Fernández Pérez ER, Costabel U, Albera C, Lederer DJ, Flaherty KR, et al. Pamrevlumab, an Anti-Connective Tissue Growth Factor Therapy, for Idiopathic Pulmonary Fibrosis (PRAISE): A Phase 2, Randomised, Double-Blind, Placebo-Controlled Trial. *Lancet Respir Med* (2020) 8(1):25–33. doi: 10.1016/S2213-2600(19)30262-0
3. Chambers DC, Yusen RD, Cherikh WS, Goldfarb SB, Kucheryavaya AY, Khusch K, et al. The Registry of the International Society for Heart and Lung Transplantation: Thirty-Fourth Adult Lung and Heart-Lung Transplantation Report—2017; Focus Theme: Allograft Ischemic Time. *J Heart Lung Transplant* (2017) 36(10):1047–59. doi: 10.1016/j.healun.2017.07.016
4. Kulkarni HS, Cherikh WS, Chambers DC, Garcia VC, Hachem RR, Kreisel D, et al. Bronchiolitis Obliterans Syndrome–Free Survival After Lung Transplantation: An International Society for Heart and Lung Transplantation Thoracic Transplant Registry Analysis. *J Heart Lung Transplant* (2019) 38(1):5–16. doi: 10.1016/j.healun.2018.09.016
5. Verleden GM, Glanville AR, Lease ED, Fisher AJ, Calabrese F, Corris PA, et al. Chronic Lung Allograft Dysfunction: Definition, Diagnostic Criteria, and Approaches to Treatment——a Consensus Report From the Pulmonary Council of the ISHLT. *J Heart Lung Transplant* (2019) 38(5):493–503. doi: 10.1016/j.healun.2019.03.009
6. Jonigk D, Merk M, Hussein K, Maegel L, Theophile K, Muth M, et al. Obliterative Airway Remodeling Molecular Evidence for Shared Pathways in Transplanted and Native Lungs. *Am J Pathol* (2011) 178(2):599–608. doi: 10.1016/j.ajpath.2010.10.032
7. Kuehnel M, Maegel L, Vogel-Claussen J, Robertus JL, Jonigk D. Airway Remodelling in the Transplanted Lung. *Cell Tissue Res* (2017) 367(3):663–75. doi: 10.1007/s00441-016-2529-0
8. Jonigk D, Izykowski N, Rische J, Braubach P, Kühnel M, Warnecke G, et al. Molecular Profiling in Lung Biopsies of Human Pulmonary Allografts to Predict Chronic Lung Allograft Dysfunction. *Am J Pathol* (2015) 185(12):3178–88. doi: 10.1016/j.ajpath.2015.08.016
9. Sato M, Waddell TK, Wagnetz U, Roberts HC, Hwang DM, Haroon A, et al. Restrictive Allograft Syndrome (RAS): A Novel Form of Chronic Lung Allograft Dysfunction. *J Heart Lung Transplant* (2011) 30(7):735–42. doi: 10.1016/j.healun.2011.01.712
10. Glanville AR, Verleden GM, Todd JL, Benden C, Calabrese F, Gottlieb J, et al. Chronic Lung Allograft Dysfunction: Definition and Update of Restrictive

Allograft Syndrome——a Consensus Report From the Pulmonary Council of the ISHLT. *J Heart Lung Transplant* (2019) 38(5):483–92. doi: 10.1016/j.healun.2019.03.008
11. Ofek E, Sato M, Saito T, Wagnetz U, Roberts HC, Chaparro C, et al. Restrictive Allograft Syndrome Post Lung Transplantation is Characterized by Pleuroparenchymal Fibroelastosis. *Modern Pathol* (2013) 26:350–6. doi: 10.1038/modpathol.2012.171
12. Palmer J, Williams K, Inamoto Y, Chai X, Martin PJ, Tomas LS, et al. Pulmonary Symptoms Measured by the National Institutes of Health Lung Score Predict Overall Survival, Nonrelapse Mortality, and Patient-Reported Outcomes in Chronic Graft-Versus-Host Disease. *Biol Blood Marrow Transplant* (2014) 20(3):337–44. doi: 10.1016/j.bbmt.2013.11.025
13. Takeuchi Y, Miyagawa-Hayashino A, Chen F, Kubo T, Handa T, Date H, et al. Pleuroparenchymal Fibroelastosis and Non-Specific Interstitial Pneumonia: Frequent Pulmonary Sequelae of Haematopoietic Stem Cell Transplantation. *Histopathology* (2015) 66(4):536–44. doi: 10.1111/his.12553
14. Jonigk D, Rath B, Borchert P, Braubach P, Maegel L, Izykowski N, et al. Comparative Analysis of Morphological and Molecular Motifs in Bronchiolitis Obliterans and Alveolar Fibroelastosis After Lung and Stem Cell Transplantation. *J Pathol Clin Res* (2017) 3(1):17–28. doi: 10.1002/cjp2.60
15. Jagasia MH, Greinix HT, Arora M, Williams KM, Wolff D, Cowen EW, et al. National Institutes of Health Consensus Development Project on Criteria for Clinical Trials in Chronic Graft-Versus-Host Disease: I. the 2014 Diagnosis and Staging Working Group Report. *Biol Blood Marrow Transplant* (2015) 21(3):389–401. doi: 10.1016/j.bbmt.2015.02.025
16. Verleden SE, Kirby M, Everaerts S, Vanstapel A, McDonough JE, Verbeken EK, et al. Small Airway Loss in the Physiologically Ageing Lung: A Cross-Sectional Study in Unused Donor Lungs. *Lancet Respir Med* (2021) 9(2):167–174. doi: 10.1016/S2213-2600(20)30324-6
17. Falke LL, Kinashi H, Dendooven A, Broekhuizen R, Stoop R, Joles JA, et al. Age-Dependent Shifts in Renal Response to Injury Relate to Altered BMP6/CTGF Expression and Signaling. *Am J Physiol Physiol* (2016) 311(5):926–34. doi: 10.1152/ajprenal.00324.2016
18. Bankhead P, Loughrey MB, Fernández JA, Dombrowski Y, Mcart DG, Dunne PD, et al. Qupath: Open Source Software for Digital Pathology Image Analysis. *Sci Rep* (2017) 7(1):16878. doi: 10.1038/s41598-017-17204-5
19. Vanstapel A, Verleden SE, Weynand B, Verbeken E, De Sadeleer L, Vanaudenaerde BM, et al. Late-Onset "Acute Fibrinous and Organising Pneumonia" Impairs Long-Term Lung Allograft Function and Survival. *Eur Respir J* (2020) 56(3):1902292. doi: 10.1183/13993003.02292-2019
20. Martinu T, Koutsokera A, Benden C, Cantu E, Chambers D, Cypel M, et al. Ishlt Consensus Statement for the Standardization of Bronchoalveolar Lavage in Lung Transplantation. *J Heart Lung Transplant* (2020) 39(11):1171–90. doi: 10.1016/j.healun.2020.07.006
21. Gerritsen KG, Abrahams AC, Peters HP, Nguyen TQ, Koeners MP, Den Hoedt CH, et al. Effect of GFR on Plasma N-Terminal Connective Tissue Growth Factor (CTGF) Concentrations. *Am J Kidney Dis* (2012) 59(5):619–27. doi: 10.1053/j.ajkd.2011.12.019
22. Nguyen TQ, Tarnow L, Andersen S, Hovind P, Parving HH, Goldschmeding R, et al. Urinary Connective Tissue Growth Factor Excretion Correlates With Clinical Markers of Renal Disease in a Large Population of Type 1 Diabetic Patients With Diabetic Nephropathy. *Diabetes Care* (2006) 29(1):83–8. doi: 10.2337/diacare.29.01.06.dc05-1670
23. Murphy M, Godson C, Cannon S, Kato S, Mackenzie HS, Martin F, et al. Suppression Subtractive Hybridization Identifies High Glucose Levels as a Stimulus for Expression of Connective Tissue Growth Factor and Other Genes in Human Mesangial Cells. *J Biol Chem* (1999) 274(9):5830–4. doi: 10.1074/jbc.274.9.5830
24. Kubota S, Takigawa M. Cellular and Molecular Actions of CCN2/CTGF and Its Role Under Physiological and Pathological Conditions. *Clin Sci* (2014) 128(3):181–96. doi: 10.1042/CS20140264
25. Plantier L, Renaud H, Respaud R, Marchand-Adam S, Crestani B. Transcriptome of Cultured Lung Fibroblasts in Idiopathic Pulmonary Fibrosis: Meta-Analysis of Publically Available Microarray Datasets Reveals Repression of Inflammation and Immunity Pathways. *Int J Mol Sci* (2016) 17(12):2091. doi: 10.3390/ijms17122091
26. Allen JT, Knight RA, Bloor CA, Spiteri MA. Enhanced Insulin-Like Growth Factor Binding Protein-Related Protein 2 (Connective Tissue Growth Factor) Expression in Patients With Idiopathic Pulmonary Fibrosis and Pulmonary Sarcoidosis. *Am J Respir Cell Mol Biol* (1999) 21(6):693–700. doi: 10.1165/ajrcmb.21.6.3719
27. Kono M, Nakamura Y, Suda T, Kato M, Kaida Y, Hashimoto D, et al. Plasma CCN2 (Connective Tissue Growth Factor; CTGF) is a Potential Biomarker in Idiopathic Pulmonary Fibrosis (IPF). *Clin Chim Acta* (2011) 412(23–24):2211–5. doi: 10.1016/j.cca.2011.08.008
28. Pan L-H, Yamauchi K, Uzuki M, Nakanishi T, Takigawa M, Inoue H, et al. Type II Alveolar Epithelial Cells and Interstitial Fibroblasts Express Connective Tissue Growth Factor in IPF. *Eur Respir J* (2001) 17(6):1220–7. doi: 10.1183/09031936.01.00074101
29. Lasky JA, Ortiz LA, Tonthat B, Hoyle GW, Corti M, Athas G, et al. Connective Tissue Growth Factor Mrna Expression is Upregulated in Bleomycin-Induced Lung Fibrosis. 1998. *Am J Physiol* (1998) 275(2):365–71. doi: 10.1152/ajplung.1998.275.2.L365
30. Bonniaud P, Martin G, Margetts PJ, Ask K, Robertson J, Gauldie J, et al. Connective Tissue Growth Factor is Crucial to Inducing a Profibrotic Environment in "Fibrosis-Resistant" Balb/C Mouse Lungs. *Am J Respir Cell Mol Biol* (2004) 31(5):510–6. doi: 10.1165/rcmb.2004-0158OC
31. Ning W, Li CJ, Kaminski N, Feghali-Bostwick CA, Alber SM, Di YP, et al. Comprehensive Gene Expression Profiles Reveal Pathways Related to the Pathogenesis of Chronic Obstructive Pulmonary Disease. *Proc Natl Acad Sci U S A* (2004) 101(41):14895–900. doi: 10.1073/pnas.0401168101
32. Pi L, Fu C, Lu Y, Zhou J, Jorgensen M, Shenoy V, et al. Vascular Endothelial Cell-Specific Connective Tissue Growth Factor (CTGF) is Necessary for Development of Chronic Hypoxia-Induced Pulmonary Hypertension. *Front Physiol* (2018) 9:138. doi: 10.3389/fphys.2018.00138
33. Saggar R, Ross DJ, Saggar R, Zisman DA, Gregson A, Lynch JP, et al. Pulmonary Hypertension Associated With Lung Transplantation Obliterative Bronchiolitis and Vascular Remodeling of the Allograft. *Am J Transplant* (2008) 8(9):1921–30. doi: 10.1111/j.1600-6143.2008.02338.x
34. Tissot A, Danger R, Claustre J, Magnan A, Brouard S. Early Identification of Chronic Lung Allograft Dysfunction: The Need of Biomarkers. *Front Immunol* (2019) 10:1681. doi: 10.3389/fimmu.2019.01681
35. Todd JL, Wang X, Sugimoto S, Kennedy VE, Zhang HL, Pavlisko EN, et al. Hyaluronan Contributes to Bronchiolitis Obliterans Syndrome and Stimulates Lung Allograft Rejection Through Activation of Innate Immunity. *Am J Respir Crit Care Med* (2014) 189(5):556–66. doi: 10.1164/rccm.201308-1481OC
36. Shino MY, Weigt SS, Li N, Palchevskiy V, Derhovanessian A, Saggar R, et al. The Prognostic Importance of CXCR3 Chemokine During Organizing Pneumonia on the Risk of Chronic Lung Allograft Dysfunction After Lung Transplantation. *PLoS One* (2017) 12(7):e0180281. doi: 10.1371/journal.pone.0180281
37. Shino MY, Li N, Todd JL, Neely ML, Kopetskie H, Sever ML, et al. Correlation Between BAL CXCR3 Chemokines and Lung Allograft Histopathologies: A Multi-Center Study. *Am J Transplant* (2021). doi: 10.1111/ajt.16601 Online ahead of print
38. Weigt SS, Wang X, Palchevskiy V, Gregson AL, Patel N, Der Hovanessian A, et al. Gene Expression Profiling of Bronchoalveolar Lavage Cells Preceding a Clinical Diagnosis of Chronic Lung Allograft Dysfunction. *PLoS One* (2017) 12(1):e0169894. doi: 10.1371/journal.pone.0169894
39. Danger R, Royer PJ, Reboulleau D, Durand E, Loy J, Tissot A, et al. Blood Gene Expression Predicts Bronchiolitis Obliterans Syndrome. *Front Immunol* (2018) 8:1841. doi: 10.3389/fimmu.2017.01841
40. Pain M, Royer PJ, Loy J, Girardeau A, Tissot A, Lacoste P, et al. T Cells Promote Bronchial Epithelial Cell Secretion of Matrix Metalloproteinase-9 Via a C-C Chemokine Receptor Type 2 Pathway: Implications for Chronic Lung Allograft Dysfunction. *Am J Transplant* (2017) 17(6):1502–14. doi: 10.1111/ajt.14166
41. Veraar C, Kliman J, Benazzo A, Oberndorfer F, Laggner M, Hacker P, et al. Potential Novel Biomarkers for Chronic Lung Allograft Dysfunction and Azithromycin Responsive Allograft Dysfunction. *Sci Rep* (2021) 11(1):6799. doi: 10.1038/s41598-021-85949-1
42. Igarashi A, Okochi H, Bradham DM, Grotendorst GR. Regulation of Connective Tissue Growth Factor Gene Expression in Human Skin Fibroblasts and During Wound Repair. *Mol Biol Cell* (1993) 4(6):637–45. doi: 10.1091/mbc.4.6.637
43. Frazier K, Williams S, Kothapallj D, Klapper H, Gwtendorst GR. Stimulation of Fibroblast Cell Growth, Matrix Production, and Granulation Tissue

Fortnation by Connective Tissue Growth Factor. *J Invest Dermatol* (1996) 107 (3):404–11. doi: 10.1111/1523-1747.ep12363389
44. Mori T, Kawara S, Shinozaki M, Hayashi N, Kakinuma T, Igarashi A, et al. Role and Interaction of Connective Tissue Growth Factor With Transforming Growth Factor-in Persistent Fibrosis. In: A mouse fibrosis model. *J Cell Physiol* (1999) 181 (1):153–9. doi: 10.1002/(SICI)1097-4652(199910)181:1<153::AID-JCP16>3.0.CO;2-K
45. Sacreas A, von der Thüsen JH, van den Bosch TPP, Weynand B, Verbeken EK, Debbaut C, et al. The Pleural Mesothelium and Transforming Growth Factor-B 1 Pathways in Restrictive Allograft Syndrome: A Pre-Clinical Investigation. *J Heart Lung Transplant* (2019) 38(5):570–9. doi: 10.1016/j.healun.2019.02.001
46. Vos R, Wuyts WA, Gheysens O, Goffin KE, Schaevers V, Verleden SE, et al. Pirfenidone in Restrictive Allograft Syndrome After Lung Transplantation: A Case Series. *Am J Transplant* (2018) 18(12):3045–59. doi: 10.1111/ajt.15019
47. Bennett D, Lanzarone N, Fossi A, Perillo F, De Vita E, Luzzi L, et al. Pirfenidone in Chronic Lung Allograft Dysfunction: A Single Cohort Study. *Panminerva Med* (2020) 62(3):143–9. doi: 10.23736/S0031-0808.19.03840-0

Conflict of Interest: RG has received research support from Fibrogen Inc.

The remaining authors declare that the research was conducted in the absence of any commercial or financial relationships that could be construed as a potential conflict of interest.

frontiers in Immunology

ORIGINAL RESEARCH
published: 25 June 2021
doi: 10.3389/fimmu.2021.662441

Efficacy and Safety of Bone Marrow-Derived Mesenchymal Stem Cells for Chronic Antibody-Mediated Rejection After Kidney Transplantation- A Single-Arm, Two-Dosing-Regimen, Phase I/II Study

Yongcheng Wei[1†], Xiaoyong Chen[2†], Huanxi Zhang[1†], Qun Su[1], Yanwen Peng[3], Qian Fu[1], Jun Li[1], Yifang Gao[1], Xirui Li[1], Shicong Yang[4], Qianyu Ye[1], Huiting Huang[1], Ronghai Deng[1], Gang Li[2], Bowen Xu[1], Chenglin Wu[1], Jiali Wang[5], Xiaoran Zhang[2], Xiaojun Su[1], Longshan Liu[1], Andy Peng Xiang[2*] and Changxi Wang[1*]*

[1] Organ Transplant Center, the First Affiliated Hospital, Sun Yat-sen University, Guangzhou, China, [2] Center for Stem Cell Biology and Tissue Engineering, Key Laboratory for Stem Cells and Tissue Engineering, Ministry of Education, Sun Yat-Sen University, Guangzhou, China, [3] The Biotherapy Center, The Third Affiliated Hospital, Sun Yat-sen University, Guangzhou, China, [4] Department of Pathology, The First Affiliated Hospital, Sun Yat-sen University, Guangzhou, China, [5] Department of Nephrology, The First Affiliated Hospital, Sun Yat-sen University, Guangzhou, China

Objective: To investigate the efficacy and safety of bone marrow-derived mesenchymal stem cells (BM-MSCs) on chronic active antibody-mediated rejection (cABMR) in the kidney allograft.

Methods: Kidney recipients with biopsy-proven cABMR were treated with allogeneic third-party BM-MSCs in this open-label, single-arm, single-center, two-dosing-regimen phase I/II clinical trial. In Regimen 1 (n=8), BM-MSCs were administered intravenously at a dose of 1.0×10^6 cells/kg monthly for four consecutive months, while in Regimen 2 (n=15), the BM-MSCs dose was 1.0×10^6 cells/kg weekly during four consecutive weeks. The primary endpoints were the absolute change of estimated glomerular filtration rate (eGFR) from baseline (delta eGFR) and the incidence of adverse events associated with BM-MSCs administration 24 months after the treatment. Contemporaneous cABMR patients who did not receive BM-MSCs were retrospectively analyzed as the control group (n =30).

Results: Twenty-three recipients with cABMR received BM-MSCs. The median delta eGFR of the total BM-MSCs treated patients was -4.3 ml/min per $1.73m^2$ (interquartile range, IQR -11.2 to 1.2) 2 years after BM-MSCs treatment (P=0.0233). The median delta maximum donor-specific antibody (maxDSA) was -4310 (IQR -9187 to 1129) at 2 years (P=0.0040). The median delta eGFR of the control group was -12.7 ml/min per 1.73 m^2 (IQR -22.2 to -3.5) 2 years after the diagnosis, which was greater than that of the BM-MSCs treated group (P=0.0342). The incidence of hepatic enzyme elevation, BK polyomaviruses (BKV) infection, cytomegalovirus (CMV) infection was 17.4%, 17.4%,

OPEN ACCESS

Edited by:
Hao Wang,
Tianjin Medical University General Hospital, China

Reviewed by:
Cheng Yang,
Fudan University, China
Yuanyuan Zhang,
Wake Forest Baptist Medical Center, United States

***Correspondence:**
Changxi Wang
wangchx@mail.sysu.edu.cn
Andy Peng Xiang
xiangp@mail.sysu.edu.cn
Longshan Liu
Liulshan@mail.sysu.edu.cn

†These authors have contributed equally to this work

Specialty section:
This article was submitted to Alloimmunity and Transplantation, a section of the journal Frontiers in Immunology

Received: *01 February 2021*
Accepted: *02 June 2021*
Published: *25 June 2021*

Citation:
Wei Y, Chen X, Zhang H, Su Q, Peng Y, Fu Q, Li J, Gao Y, Li X, Yang S, Ye Q, Huang H, Deng R, Li G, Xu B, Wu C, Wang J, Zhang X, Su X, Liu L, Xiang AP and Wang C (2021) Efficacy and Safety of Bone Marrow-Derived Mesenchymal Stem Cells for Chronic Antibody-Mediated Rejection After Kidney Transplantation- A Single-Arm, Two-Dosing-Regimen, Phase I/II Study. Front. Immunol. 12:662441. doi: 10.3389/fimmu.2021.662441

8.7%, respectively. There was no fever, anaphylaxis, phlebitis or venous thrombosis, cardiovascular complications, or malignancy after BM-MSCs administration. Flow cytometry analysis showed a significant decreasing trend of $CD27^{-}IgD^{-}$ double negative B cells subsets and trend towards the increase of $CD3^{+}CD4^{+}PD\text{-}1^{+}$/lymphocyte population after MSCs therapy. Multiplex analysis found TNF-α, CXCL10, CCL4, CCL11 and RANTES decreased after MSCs treatment.

Conclusion: Kidney allograft recipients with cABMR are tolerable to BM-MSCs. Immunosuppressive drugs combined with intravenous BM-MSCs can delay the deterioration of allograft function, probably by decreasing DSA level and reducing DSA-induced injury. The underlying mechanism may involve immunomodulatory effect of MSCs on peripheral B and T cells subsets.

Keywords: mesenchymal stem cells, kidney transplantation, antibody-mediated allograft rejection, stem cell therapy, alloimmunity

INTRODUCTION

Kidney transplantation is the most effective treatment for end-stage renal disease (ESRD) as it can significantly prolong life expectancy and improve life quality of patients with ESRD. Over the last decades, the 1-year graft survival rate has increased to nearly 95%. However, long-term survival is still unsatisfactory, and the 10-year graft survival rate is nearly 60% (1). Antibody-mediated rejection (ABMR) is the main cause of long-term graft loss after kidney transplantation (2). B cells can be activated under many circumstances prior to or after transplantation to produce donor-specific antibodies (DSA) which are mainly anti-HLA (human leukocyte antigen) antibodies. The DSA attack vascular endothelium of renal allografts through complement-dependent cytotoxicity (CDC) and antibody-dependent cellular cytotoxicity (ADCC) pathways, causing microvascular inflammation and leading, to chronic damage, in the long-term including transplant glomerulopathy, arterial intimal thickening, renal tubular atrophy and interstitial fibrosis, etc (3).

ABMR, which presents largely heterogenic clinical manifestation, can be pathologically classified into active ABMR and chronic active ABMR (cABMR), according to 2019 Banff classification criteria (4). Patients with cABMR often present a gradual increment in serum creatinine with or without deteriorative proteinuria months or even years after the development of *de novo* DSA. Contrary to the improvement achieved on diagnostic techniques and mechanism understanding, there is still a lack of efficient treatment for cABMR. In this sense, a comprehensive treatment strategy involving the administration of plasmapheresis (PP) and/or intravenous immunoglobulin (IVIG), combing with rituximab, bortezomib or daclizumab, etc. is currently being used. Unfortunately, most studies on these treatments are small, lack solid evidence, and the reported findings are often inconsistent or even opposite (5). Many patients with cABMR ultimately progress to renal allograft failure despite receiving a strong comprehensive treatment, which increases medical cost and risk of infection. Therefore, there is an urgent need to develop novel therapeutic strategies for cABMR treatment.

Mesenchymal stem cells (MSCs) are widely distributed in various tissues and organs of the human body and exert immunomodulatory potential with low immunogenicity (6). Since 2004, when MSCs were introduced to treat graft versus host disease (GvHD) after bone marrow transplantation (7), its therapeutic effect on inflammatory and autoimmune diseases have been widely reported (8). Multiple studies have demonstrated the potential effect of MSCs in kidney transplantation as induction therapy, minimizing calcineurin inhibitors (CNIs), rejection treatment and tolerance induction (9–15). In addition, preclinical studies have showed that MSCs therapy prevents interstitial fibrosis and tubular atrophy in a chronic rejection model of rat kidney transplantation (16, 17). Moreover, a phase I study indicates that MSCs are clinically feasible and safe treatment for subclinical rejection and interstitial fibrosis in kidney transplantation (18). These findings suggest that MSCs may have protective effects on renal allograft function in the setting of chronic rejection. Despite its overall safety, reported in many studies, MSCs infusion has also been reported to increase serum creatinine, drawing the attention to its adverse effects in kidney transplantation (19). Nevertheless, the efficacy and safety of MSCs to treat cABMR in kidney transplantation has not been well investigated. In this prospective two-dosing-regimen phase I/II clinical trial, MSCs were intravenously administered to 23 biopsy-proven cABMR patients.The renal allograft function, DSA level and adverse events were subsequently assessed during 24 months after treatment. The mechanism involved in the effect of MSCs in patients with cABMR was also explored.

PATIENTS AND METHODS

Study Design and Participants

We designed an open-label, single-arm, single-center, two-dosing-regimen, phase I/II clinical trial with a 24-month follow-up period. The study was conducted in the

First Affiliated Hospital of Sun Yat-sen University between 2013 and 2020. Kidney recipients with histological-proven cABMR, with presence or absence of circulating donor-specific anti-human leukocyte antigen (HLA) antibodies (DSA), between 18 and 65 years old were eligible for the study. Histological evaluation of renal biopsies was performed in accordance with Banff criteria (4). The patients were administered with a maintenance immunosuppressive regimen consisting of calcineurin inhibitors, mycophenolate with or without glucocorticoids, and were treated with BM-MSCs as the initial regimen or second-line regimen after previous failed ABMR treatment, including plasmapheresis, intravenous immunoglobulin, rituximab, bortezomib and methylprednisolone (**Supplemental Table 1**). The exclusion criteria included pregnancy, combined organ transplantation, active infection, white blood cell count < 3×10^9/L, hemoglobin < 50 g/L, and severe cardiovascular or gastrointestinal complications. This study was approved by the Ethics Committee of the First Affiliated Hospital of Sun Yat-sen University and was conducted in accordance with the principles of the World Medical Association Declaration of Helsinki. Written informed consent was obtained from all the participants.

For comparison with the BM-MSCs treated group, adult kidney recipients (≥18 years old) who were histologically diagnosed as cABMR in the same transplant center between 2013 and 2020 were retrospectively enrolled as the contemporaneous control group. Patients with a baseline eGFR lower than 15 ml/min per $1.73m^2$ at the time of diagnosis were excluded.

Procedures

Between 2013 and 2015, BM-MSCs were administered intravenously at a dose of 1.0×10^6 cells/kg per month for four consecutive months (Regimen 1). Since 2016, a strengthened therapy was used. BM-MSCs were intravenously infused at a dose of 1.0×10^6 cells/kg per week for four consecutive weeks (Regimen 2). The BM-MSCs were added to 30 ml sterilized normal saline and infused within 30 minutes. The primary endpoints were the absolute change of estimated glomerular filtration rate (eGFR) from baseline, and the incidence of adverse events (AEs) associated with BM-MSCs administration 24 months after BM-MSCs treatment. eGFR was calculated by the modification of diet in renal disease (MDRD) equation. The secondary endpoints included absolute change of maximum DSA (maxDSA) mean fluorescence intensity (MFI) level from baseline, and patient and graft survival. maxDSA is defined as the DSA loci with the highest MFI value. In Regimen 1, the patients were evaluated at screening, monthly during the first 4 months, and then at 6, 12 and 24 months after BM-MSCs treatment. In Regimen 2, the patients were examined at screening, weekly during the first month, and then at 1, 3, 6, 12 and 24 months after BM-MSCs treatment. Routine laboratory tests and adverse events monitoring were performed at every visit. DSA MFI level was measured at 1, 6, 12 and 24 months. Blood samples were collected at every visit and stored for further examinations. In the control group, the demographic, clinical, laboratory, treatment and outcome data in the following two years after diagnosis were collected from medical records.

Isolation and Characterization of BM-MSCs

Human bone marrow samples donated from four male and two female third-party healthy donors were used to isolate and expand BM-MSCs, after informed consent. All the donors were negative for human immunodeficiency virus (HIV), hepatitis B virus (HBV), hepatitis C virus (HCV), human T cell virus, human herpes virus (HTLV), Epstein-Barr virus (EBV), human cytomegalovirus (HCMV), and treponema pallidum (TP). The age of the healthy donors was 27.8 ± 5.8 years old. The donors were healthy and did not presented hematopoietic, genetic, autoimmune diseases, nor mental disorders.

The bone marrow was diluted 1:1 with human MSCs culture medium (Xeno-free media, GIBCO, Grand Island, NY, USA). Bone marrow mononuclear cells were separated by Ficoll-Paque (1.077 g/mL; GE Healthcare Life Sciences, Little Chalfont, Buckinghamshire, UK) using density gradient centrifugation and were seeded at a density of $1x10^5$ cells/cm^2 in T75 cell culture flasks. When 80% confluence was reached, the cells were detached using Trypsin-EDTA (0.25%, GIBCO, Grand Island, NY, USA) and were designated as passage 1. These cells were further passaged at a ratio of 1:3. The culture-expanded BM-MSCs exhibit fibroblast-like (spindle and fusiform) and uniform morphology in adherent cultures, expressed CD29, CD44, CD73, CD90, CD105 and CD166, but not CD34 or CD45 (**Supplemental Figure 1**). They were able to differentiate into osteoblasts, adipocytes and chondroblasts under standard *in vitro* differentiating conditions.

BM-MSCs at passage 7 to 8 were used for the treatments described in the study. The selection criteria of the BM-MSCs used in the trial includes: presence of normal karyotypes; cell viability greater than 95%; absence of visible clumps; sterility: negative for fungi, bacteria, mycoplasma, HIV, HBV, HCV, HTLV, EBV, HCMV, TP and endotoxin; and cell purity: their expression of CD29, CD44, CD73, CD90, CD105 and CD166 must be above 95% and must lack expression of CD34 and CD45 (<2%).

Peripheral Blood Lymphocyte Immunophenotyping

Principal lymphocyte subsets of monocytes, B lymphocytes, T lymphocytes, dendritic cells, regulatory T cells and TCR αβ and TCR γδ protein chain expression, and detection of Vδ1+ and Vδ2+ subsets among TCRγδ+ T cells, were assessed by flow-cytometry using the following DuraClone panels (Beckman Coulter, Miami, FL, USA): IM Phenotyping Basic panel, IM B cell panel, IM T Cell Subsets panel, IM Dendritic Cell panel, IM Treg panel and IM TCRs panel (**Supplemental Table 2**).

Sample preparation was performed according to the manufacturer's instructions. Sample acquisition was conducted on an eight-color Navios flow cytometer and the data generated were analyzed using Kaluza Analysis 2.1 software (Beckman Coulter, Miami, FL, USA). Representative figures depicting the gating strategy are shown in **Supplemental Figure 2**.

Detection of Anti-HLA Antibody

Anti-HLA antibody profiling of serum from kidney recipients was performed according to the instruction of LIFECODES®

LSA™ Class I/II kit (Immucor GTI Diagnostics, Inc. Waukesha, WI, USA). Briefly, Millipore multiscreen filter plate wells were pre-wet with distilled water for five minutes, then the water was removed. The LSA™ Beads were briefly centrifugated and then thoroughly vortexed for one minute. Then, 40 µl of LSA™ Beads were added to each of the assigned wells. Re-vortex intermittently and add 5 µl of patient serum and control sera and mix well. Then were incubate for 30 minutes on a rotating platform in the dark and at room temperature. After incubation, the beads were resuspended and washed three times with Wash Buffer. Then, 50 µl of 1 X conjugate was added to each well, placed on a rotating platform for 10 minutes, and incubate for 30 minutes in dark. Finally, 150 µl of Wash Buffer were added to resuspend the beads, and the solution was read on the Luminex® 200 platform. The result were analyzed with the LIFECODES® MatchIT! Antibody software (Immucor GTI Diagnostics, Inc. Waukesha, WI, USA). Mean fluorescence intensity (MFI)>1000 was considered positive.

Detection of Serum Cytokines and Chemokines

Serum cytokines and chemokines were assessed according to the instruction of Luminex® Assay Human Premixed Multi-Analyte Kit (R&D Systems, Inc. Minneapolis, MN, USA). The kit detects BAFF, CCL3, CCL11, CXCL10, IFN-γ, IL-2, IL-5, IL-8, IL-12 p70, CCL2, CCL4, CXCL1, GM-CSF, IL-1β, IL-4, IL-6, IL-10, IL-13, TNF-α, CXCL12 and RANTES. Briefly, 50 µl of standard or sample was added to each well of a microplate followed by the addition of 50 µl of diluted Microparticle Cocktail. The microplate was then covered with a foil plate sealer and incubated on a horizontal orbital microplate shaker at 800 rpm at room temperature for two hours. The plate was washed three times with Wash Buffer. Then, 50 µl of diluted Biotin-Antibody Cocktail was added to each well and incubated again on a horizontal orbital microplate shaker at 800 rpm at room temperature for one hour with a foil plate sealer. After that, the plate was washed 3 times, 50 µl of diluted Streptavidin-PE were added to each well, and the plate was incubated on a horizontal orbital microplate shaker at 800 rpm at room temperature for 30 minutes with a foil plate sealer. Finally, the plate was washed three times, 100 µl of Wash Buffer were added to each well, and the plate was incubated for 2 minutes at room temperature. The samples were then read in a Luminex® MAGPIX® analyzer (R&D Systems, Inc. Minneapolis, MN, USA).

Statistical Analysis

Continuous data with normal distribution was presented as mean ± standard deviation (SD) and compared using Student's t-test, while continuous data without normal distribution was expressed as median (lower quartile-higher quartile) and compared using Mann-Whitney U test. Categorical data was reported as counts and percentages and compared using Chi-square test or Fisher's exact test. Kaplan-Meier method was used for survival analysis and the log-rank test was used to compare two survival curves. Paired t-test or Wilcoxon signed-rank test was used to analyze paired differences. The linear trend test was used to determine the significance of trends over time. Multivariate linear regression was performed to adjust for confounding factors affecting the decline rate of eGFR. Last observation carried forward (LOCF) was used for data imputation (20). Significance was set at $p < 0.05$. Statistical analyses were performed using GraphPad Prism 8.0.1 software (GraphPad Corporation, La Jolla, CA, USA) and 'R', a free software environment for statistical computing and graphics (www.r-project.org).

RESULTS

Baseline Characteristics of Kidney Transplant Recipients With Chronic Antibody-Mediated Rejection

The baseline characteristics of the 23 kidney recipients with BM-MSCs treatment were shown in **Table 1**. Eight patients were enrolled in Regimen 1 and fifteen in Regimen 2. The baseline characteristics between patients enrolled in Regimen 1 and Regimen 2 were not significantly different. Regarding combined histological lesions, there were two cases of IgA nephropathy (IgAN) (8.7%), one of CNI nephrotoxicity (4.3%), and one of borderline rejection (4.3%); all the cases were in Regimen 2 group. In addition, no acute/chronic T cell-mediated rejection or acute ABMR were identified. Other medications used for cABMR before or after MSCs treatment are listed in **Supplemental Table 1**. The histological scores at the time of cABMR diagnosis, summarized in **Table 2**, were similar between Regimen 1 and Regimen 2.

Renal Allograft Function

Figures 1A–C shows the changes in estimated glomerular filtration rate (eGFR) for the total study population, Regimen 1 and Regimen 2 patients, respectively. Delta eGFR did not significantly change in one year. At one and two years after BM-MSCs treatment, the median delta eGFR of the total participants was -2.2 ml/min per 1.73m^2 (IQR -9.3 to 1.2, P>0.05) and -4.3 ml/min per 1.73m^2 (IQR -11.2 to 1.2, P=0.0233), respectively. Moreover, one year after BM-MSCs treatment, the median delta eGFR was -4.7 ml/min per 1.73m^2 (IQR -21.6 to 7.1, P=0.3828) in Regimen 1 group and -2.2 ml/min per 1.73m^2 (IQR -7.3 to 0.9, P=0.0554) in Regimen 2 group. At two years after treatment, the median delta eGFR was -5.4 ml/min per 1.73m^2 (IQR -21.6 to 1.3, P=0.1953) in Regimen 1 group and -2.2 ml/min per 1.73m^2 (IQR -11.2 to 1.2, P=0.0833) in Regimen 2 group. eGFR remained stable in one year (**Figures 1D–F**). The median eGFR of the total participants, and those from Regimen 1 and Regimen 2 one year after MSCs treatment was 35.6 ml/min per 1.73m^2 (IQR 26.3 to 47.8), 45.4 ml/min per 1.73m^2 (IQR 26.7 to 50.7) and 35.2 ml/min per 1.73m^2 (IQR 26.3 to 47.7), respectively. This parameter was respectively 34.9 ml/min per 1.73m^2 (IQR 27.7 to 46.9), 41.8 ml/min per 1.73m^2 (IQR 32.5 to 47.1) and 31.5 ml/min per 1.73m^2 (IQR 26.1 to 40.8) two years after BM-MSCs treatment.

TABLE 1 | Baseline characteristics of chronic antibody-mediated rejection patients before BM-MSCs treatment and the contemporaneous control.

Characteristics	Total	MSCs			Control	P value*	P value†
		Total	Regimen 1	Regimen 2			
Patient number (n)	53	23	8	15	30		
Age (years), mean (SD)	45.5 (11.3)	42.9 (11.0)	40.6 (12.9)	44.07 (10.1)	47.4 (11.4)	0.4869	0.1473
Gender						0.3452	0.2352
Male, No. (%)	41 (77.4%)	16 (69.6%)	7 (87.5%)	9 (60.0%)	25 (83.3%)		
Female, No. (%)	12 (22.6%)	7 (30.4%)	1 (12.5%)	6 (40.0%)	5 (16.7%)		
BMI (kg/m^2), mean (SD)	22.6 (3.9)	22.3 (3.6)	21.2 (3.7)	22.9 (3.6)	22.9 (4.1)	0.2943	0.6113
Baseline eGFR (ml/min/1.73m^2), mean (SD)	38.3 (18.3)	42.6 (19.0)	48.0 (22.6)	39.7 (16.8)	35.1 (17.4)	0.3296	0.1412
Baseline maxDSA MFI※, mean (SD)	12103 (5750)	12554 (4164)	11357 (4215)	13153 (4189)	11750 (6813)	0.4048	0.6624
Time from transplantation to treatment (years), mean (SD)		8.5 (5.7)	4.8 (2.8)	10.5 (6.0)		0.0191	
Maintenance immunosuppressants, No. (%)						0.5576	0.1472
Tacrolimus + MPA + Steroids	40 (75.5%)	21 (91.3%)	8 (100%)	13 (86.7%)	19 (63.3%)		
Tacrolimus + MPA + Steroids + Rapamycin	2 (3.8%)	0 (0)			2 (6.7%)		
Cyclosporine A + MPA + Steroids	8 (15.1%)	1 (4.3%)	0 (0)	1 (6.7%)	7 (23.3%)		
Tacrolimus + MPA (Steroids free)	2 (3.8%)	1 (4.3%)	0 (0)	1 (6.7%)	1 (3.3%)		
Cyclosporine A + MPA (Steroids free)	1 (1.9%)	0 (0)			1 (3.3%)		
Combined histological lesions						0.4921	0.6729
IgAN, No. (%)	5 (9.4%)	2 (8.7%)	0 (0)	2 (13.3%)	3 (10%)		
CNI nephrotoxicity, No. (%)	6 (11.3%)	1 (4.3%)	0 (0)	1 (6%)	5 (16.7%)		
Borderline rejection, No. (%)	3 (5.7%)	1 (4.3%)	0 (0)	1 (6%)	2 (6.7%)		
Other, No. (%)	2 (3.8%)	1 (4.3%)	0 (0)	1 (6%)	1 (3.3%)		

*BM-MSCs, bone marrow derived mesenchymal stem cells; BMI, body mass index; Baseline maxDSA MFI※, maximum donor-specific antibody mean fluorescence intensity pre-MSCs treatment or at diagnosis; Scr, serum creatinine; eGFR, estimated glomerular filtration rate; SD, standard deviation; IgAN, IgA nephropathy; CNI, calcineurin inhibitors; MPA, mycophenolate acid. *P value between Regimen 1 and Regimen 2. †P value between total BM-MSCs treatment group and contemporaneous control.*

DSA Changes

Serum maxDSA intensity of the total BM-MSCs population tended to decline six months after BM-MSCs infusions (**Figures 2A, D**). Median serum maxDSA decreased from 13534 to 8797 one year after treatment, and to 7952 two years after MSCs treatment. The median delta maxDSA was -4310 (IQR -9187 to 1129) in the second year (P=0.0040). In patients from Regimen 1, serum maxDSA tended to decline (**Figures 2B, E**), while in Regimen 2 patients maxDSA significantly decreased after one and two years of the first dose of BM-MSCs (**Figures 2C, F**).

Patient and Graft Survival

No patient died in two years after BM-MSCs treatment. Graft loss was observed in three patients after BM-MSCs infusion within two years of follow-up. One graft loss was detected in Regimen 1 group and two in Regimen 2. The graft survival rate after two years of BM-MSCs treatment was 87.0% (**Figure 3**).

Adverse Events

We assessed the adverse events (AEs) associated with BM-MSCs administration. Two years after BM-MSCs infusion, one patient presented severe bacterial pneumonia and recovered after receiving appropriate medication, which was considered to be unrelated to the BM-MSCs treatment (**Table 3**). Elevated hepatic enzyme was observed in four patients, three of which resulted from replication of pre-existing hepatitis B virus (HBV) or hepatitis C virus (HCV). Several BK polyomaviruses infections and cytomegalovirus infections were observed and were solved with treatment. Furthermore, no fever, anaphylaxis, phlebitis or venous thrombosis, cardiovascular complications or malignancy were identified during this study.

Effect of Combined Medications

In order to exclude confounding by other combined medications for ABMR, subgroup analysis was conducted. All BM-MSCs treated patients were divided into BM-MSCs alone subgroup and BM-MSCs combined with other treatments subgroup. Baseline eGFR and maxDSA were similar in these two subgroups. Two years after BM-MSCs treatment, the median delta eGFR of BM-MSCs alone subgroup was similar with that of the BM-MSCs combined with other treatments subgroup [median, -3.8 ml/min per 1.73m^2 (IQR -10.7 to 1.4) *vs* -4.3 ml/min per 1.73m^2 (IQR -20.9 to 0.9), P=0.9279]. The median delta maxDSA of BM-MSCs alone subgroup was -4899 (IQR -8320 to 285.5) while in the BM-MSCs combined with other treatments subgroup was -3824 (IQR -10961 to 1576) (p=0.7618).

Comparison With the Contemporaneous Control Cohort

There were no significant differences in the baseline characteristics and Banff scores between the total BM-MSCs treatment population and the control cohort (**Tables 1**, **2**). The median delta eGFR of the control cohort was -7.0 ml/min per 1.73m^2 (IQR -17.1 to 3.1) one year after diagnosis, and -12.7 ml/min/1.73m^2 (IQR -22.2 to -3.5) after two years (**Figure 1G**). The median eGFR of the control cohort was 25.1 ml/min per 1.73m^2 (IQR 12.2 to 42.8) one year after diagnosis and 17.2 ml/min per 1.73m^2 (IQR 0 to 33.7) after two years (**Figure 1H**). In addition, it was observed that eGFR significantly declined more rapidly in the control cohort than that in the BM-MSCs treated group (p=0.4382, year one; p=0.0342, year two) (**Figure 1I**). The graft survival rate after two years of cABMR diagnosis of the control cohort was 66.7%, while in the BM-MSCs treated group, after two years of BM-MSCs

TABLE 2 | Baseline Banff scores at the time of BM-MSCs treatment initiation for the BM-MSCs group, or at the time of histologic diagnosis of cABMR for the contemporaneous control.

Total (N = 53), No. (%)		MSCs			Control (N = 30), No. (%)	P value*	P value†
		Total (N = 23), No. (%)	Regimen 1 (N = 8), No. (%)	Regimen 2 (N = 15), No. (%)			
Glomerulitis (g)						0.9802	0.6246
1	15 (28.3%)	6 (26.1%)	2 (25.0%)	4 (26.7%)	9 (30.0%)		
2	21 (39.6%)	8 (34.8%)	3 (37.5%)	5 (33.3%)	13 (43.3%)		
3	17 (32.1%)	9 (39.1%)	3 (37.5%)	6 (40.0%)	8 (26.7%)		
Peritubular capillaritis (ptc)						0.2136	0.3614
0	3 (5.7%)	2 (8.7%)	0 (0)	2 (13.3%)	1 (3.3%)		
1	18 (34.0%)	5 (21.7%)	2 (25.0%)	3 (20.0%)	13 (43.3%)		
2	25 (47.2%)	12 (52.2%)	6 (75.0%)	6 (40.0%)	13 (43.3%)		
3	7 (13.2%)	4 (17.4%)	0 (0)	4 (26.7%)	3 (10.0%)		
Tubulitis (t)						0.6077	0.4726
0	23 (43.4%)	9 (39.1%)	4 (50.0%)	5 (33.3%)	14 (46.7%)		
1	29 (54.7%)	13 (56.5%)	4 (50.0%)	9 (60.0%)	16 (53.3%)		
3	1 (1.9%)	1 (4.3%)	0 (0)	1 (6.7%)	0 (0)		
Intimal or transmural arteritis (v)						0.2137	0.4312
0	48 (90.6%)	20 (87.0%)	6 (75.0%)	14 (93.3%)	28 (93.3%)		
1	5 (9.4%)	3 (13.0%)	2 (25.0%)	1 (6.7%)	2 (6.7%)		
Inflammation (i)						0.5396	0.3362
0	41 (77.4%)	16 (69.6%)	5 (62.5%)	11 (73.3%)	25 (83.3%)		
1	11 (20.8%)	6 (26.1%)	3 (37.5%)	3 (20.0%)	5 (16.7%)		
3	1 (1.9%)	1 (4.3%)	0 (0)	1 (6.7%)	0 (0)		
Double contour (cg)						0.8485	0.9503
1	15 (28.3%)	7 (30.4%)	3 (37.5%)	4 (26.7%)	8 (26.7%)		
2	17 (32.1%)	7 (30.4%)	2 (25.0%)	5 (33.3%)	10 (33.3%)		
3	21 (39.6%)	9 (39.1%)	3 (37.5%)	6 (40.0%)	12 (40.0%)		
Interstitial fibrosis (ci)						0.1501	0.6907
0	3 (5.7%)	2 (8.7%)	0 (0)	2 (13.3%)	1 (3.3%)		
1	32 (60.4%)	14 (60.9%)	7 (87.5%)	7 (46.7%)	18 (60.0%)		
2	17 (32.1%)	7 (30.4%)	1 (12.5%)	6 (40.0%)	10 (33.3%)		
3	1 (1.9%)	0 (0)	0 (0)	0 (0)	1 (3.3%)		
Tubular atrophy (ct)						0.1501	0.2901
0	2 (3.8%)	2 (8.7%)	0 (0)	2 (13.3%)	0 (0)		
1	31 (58.5%)	14 (60.9%)	7 (87.5%)	7 (46.7%)	17 (56.7%)		
2	19 (35.8%)	7 (30.4%)	1 (12.5%)	6 (40.0%)	12 (40.0%)		
3	1 (1.9%)	0 (0)	0 (0)	0 (0)	1 (3.3%)		
Fibrous intimal thickening (cv)						0.1468	0.0556
0	8 (15.1%)	6 (26.1%)	0 (0)	6 (40.0%)	2 (6.7%)		
1	24 (45.3%)	12 (52.2%)	6 (75.0%)	6 (40.0%)	12 (40.0%)		
2	19 (35.8%)	4 (17.4%)	2 (25.0%)	2 (13.3%)	15 (50.0%)		
3	2 (3.8%)	1 (4.3%)	0 (0)	1 (6.7%)	1 (3.3%)		
C4d staining						0.2516	0.9979
0	21 (39.6%)	9 (39.1%)	1 (12.5%)	8 (53.3%)	12 (40.0%)		
1	9 (17.0%)	4 (17.4%)	2 (25.0%)	2 (13.3%)	5 (16.7%)		
2	11 (20.8%)	5 (21.7%)	3 (37.5%)	2 (13.3%)	6 (20.0%)		
3	12 (22.6%)	5 (21.7%)	2 (25.0%)	3 (20.0%)	7 (23.3%)		

**P value between Regimen 1 and Regimen 2. †P value between total BM-MSCs treatment group and contemporaneous control.*

treatment, was 87.0% (P=0.1012) (**Figure 3**). Multivariate linear regression was performed to adjust for the confounding effect of baseline eGFR on delta eGFR at two years and the eGFR of the BM-MSCs treated group declined slower (hazard ratio, 8.691; 95% confidence interval, 0.496-16.885; p=0.038) (**Table 4**).

Changes in Peripheral Blood Lymphocytes Subsets

The changes in peripheral lymphocytes subsets including T cells, B cells, monocytes and NK cells were analyzed in the pre-treatment stage and at days 7, 14, 21, and 30 post-treatment. The blood samples collected belonged to seven patients from Regimen 2 group. **Figures 4A, C** shows that the proportion of $CD27^{-}CD38^{-/+}/IgD^{-}IgM^{-}$ (double negative B cell) decreased after BM-MSCs treatment. In addition, $CD3^{+}CD4^{+}PD\text{-}1^{+}$/lymphocyte (**Figures 4B, D**) also trended to increase in time (although this was not significant). Significant variations were not detected in other representative subsets of T cell (**Supplemental Figure 3-1**), B cells (**Supplemental Figure 3-2**), NK cells (**Supplemental Figure 3-3**), monocytes (**Supplemental Figure 3-3**), dendritic cells (**Supplemental Figure 3-4**), and regulatory T cells (**Supplemental Figure 3-5**) were not found significantly changed.

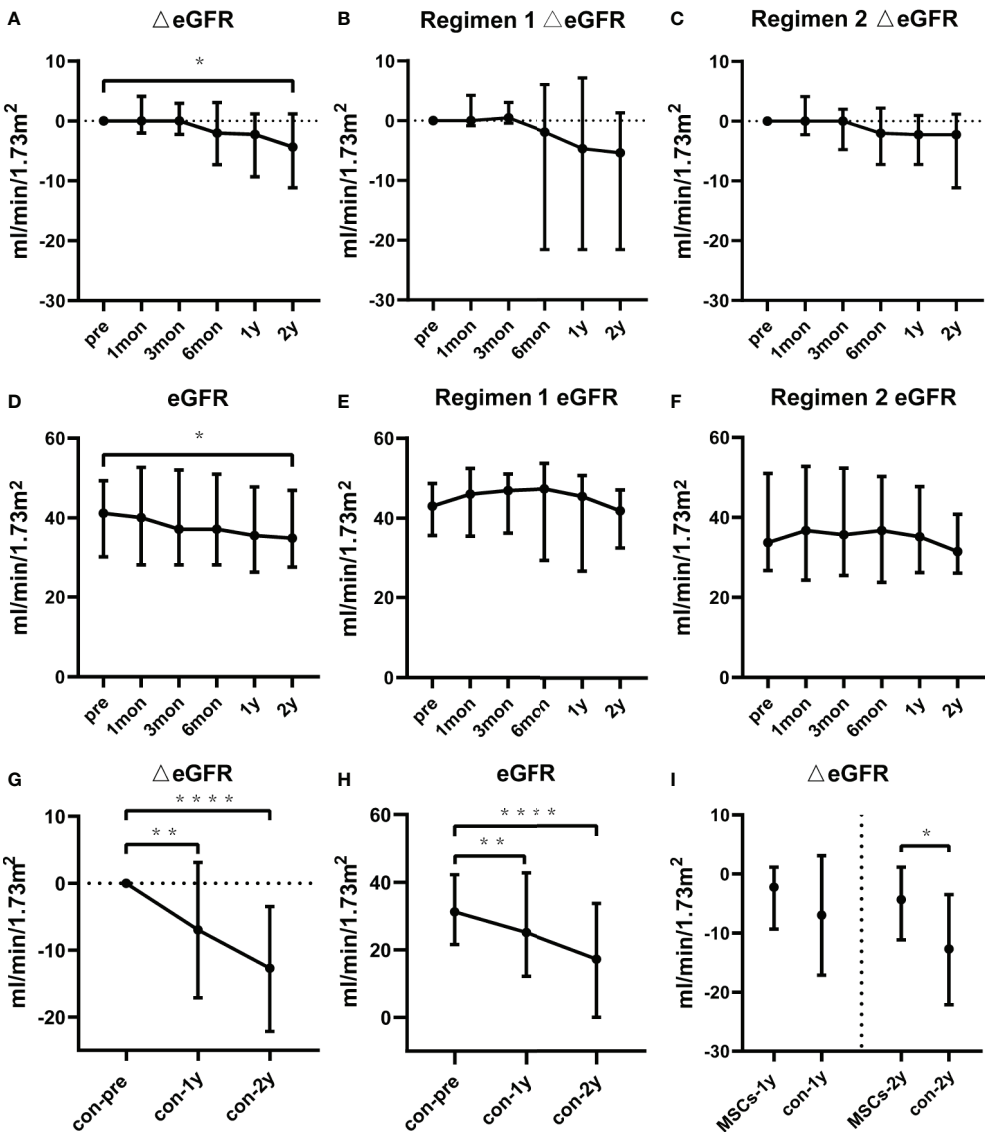

FIGURE 1 | Renal function of the BM-MSCs treated group and the contemporaneous control group in two years of follow-up. Delta estimated glomerular filtration rate (eGFR) pre and after BM-MSCs treatment in total BM-MSCs treated **(A)**, Regimen 1 **(B)**, and Regimen 2 populations **(C)**. eGFR pre and after BM-MSCs treatment in total BM-MSCs treated **(D)**, Regimen 1 **(E)**, and Regimen 2 populations **(F)** during the study period. Delta eGFR of the control group two years after histological diagnosis **(G)**. eGFR of the control group two years after histological diagnosis **(H)**. Comparison of delta eGFR between BM-MSCs treated group and the control group **(I)**. Points represent median. Bars represent the lower quartile and upper quartile. Data before and after BM-MSCs treatment or histological diagnosis were analyzed by Wilcoxon test. Data comparing BM-MSCs-treated and control groups were analyzed by Mann-Whitney test. *p < 0.05, **p < 0.01, ****p < 0.0001.

Variation in Peripheral Blood Cytokines and Chemokines

Serum concentrations of cytokines and chemokines were examined at different times after BM-MSCs treatment. we found that the concentration of the proinflammatory cytokine TNF-α significantly decreased after four doses of BM-MSCs infusion (**Figure 5A**). The mean level of TNF-α pre-treatment was 2.12 ± 1.09 pg/ml and declined to 1.12 ± 0.63 pg/ml six months after treatment. After two years, TNF-α concentration further decreased to 0.92 ± 0.56 pg/ml. Moreover, RANTES, CXCL10, CCL11 and CCL4 concentrations declined after BM-MSCs treatment (**Figures 5B–E**). The cytokines and chemokines that did not show significant variations are listed in **Supplemental Figures 4-1** and **4-2**.

DISCUSSION

To the best of our knowledge, this is the first clinical trial demonstrating the efficacy and safety of allogeneic BM-MSCs

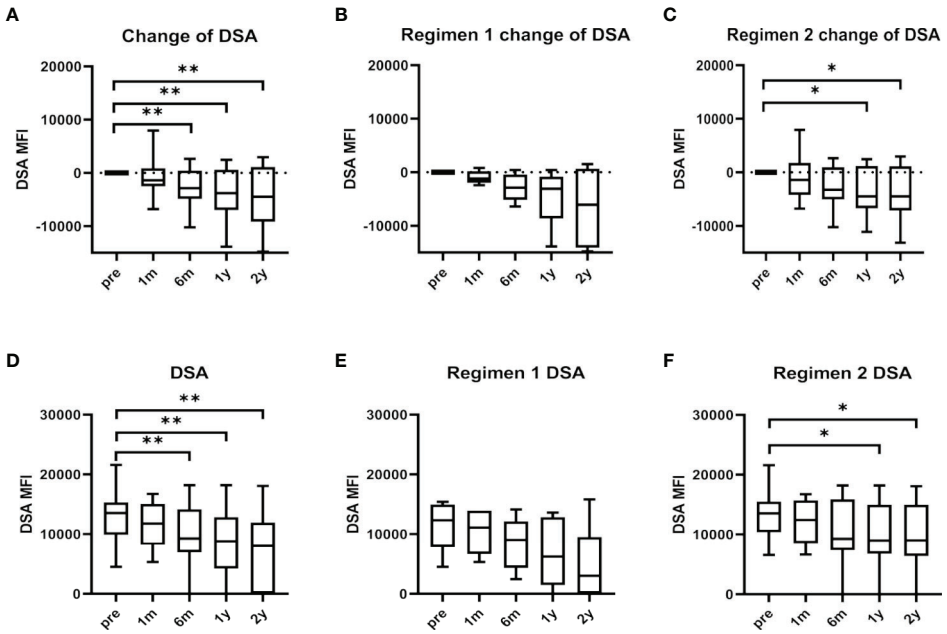

FIGURE 2 | Maximum donor-specific antibody (maxDSA) value pre and after BM-MSCs treatment. Change of maxDSA MFI pre and after BM-MSCs treatment in total BM-MSCs treated **(A)**, Regimen 1 **(B)**, and Regimen 2 populations **(C)**. MaxDSA MFI pre and after BM-MSCs treatment in total BM-MSCs treated **(D)**, Regimen 1 population **(E)**, and Regimen 2 population **(F)** during the study period. Boxplots represent the lower quartile, median and upper quartile. Bars represent minimum and maximum. Data were analyzed by Wilcoxon test. *p < 0.05, **p < 0.01.

administration for treatment of cABMR in kidney transplantation. A previous multi-centered study has demonstrated that the eGFR of patients with biopsy-proven late active ABMR significantly declines by a delta value of -9.084 ml/min per 1.73m^2 one year after cABMR diagnosis (21). Our study found the eGFR of cABMR patients treated with BM-MSCs declined by a median of 2.2 ml/min per 1.73m^2 and 4.3 ml/min per 1.73m^2 one and two years after BM-MSCs treatment, respectively. However, the eGFR of the contemporaneous control cohort declined by a median of 12.7 ml/min per 1.73m^2 two years after cABMR diagnosis. The two-year allograft survival of patients treated with BM-MSCs was higher than that of the contemporaneous control cohort (87.0% *vs.* 66.7%), although the difference did not reach statistical significance. Allogeneic MSCs was previously deemed to increase the risk of sensitization and antibody-mediated allograft rejection (22, 23). Nonetheless, in our study, we found that four doses of intravenous BM-MSCs did neither increase cABMR episodes nor deteriorate renal allograft

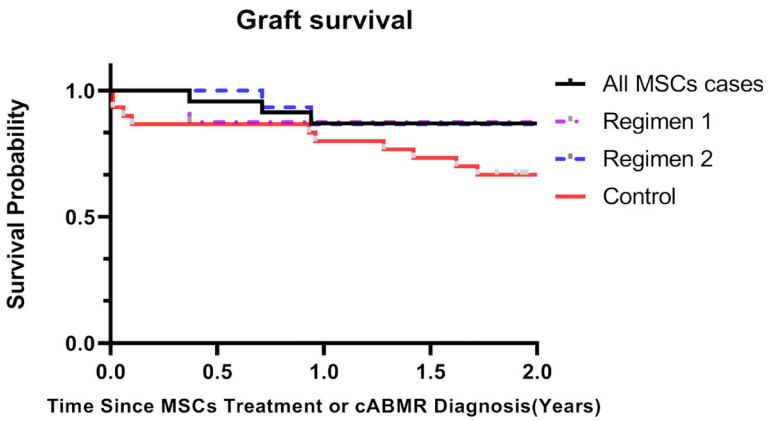

FIGURE 3 | Kaplan-Meier curves of kidney graft survival for chronic antibody-mediated rejection (cABMR) patients after BM-MSCs infusion or histological diagnosis within two years. Kaplan-Meier of graft survival of the total BM-MSCs treated (black), Regimen 1 (purple), and Regimen 2 populations (blue), and of the control group after histological diagnosis of cABMR (red).

TABLE 3 | Adverse events of cABMR patients treated with BM-MSCs.

Adverse event, No. (%)	Total, (n = 23)	Regimen 1, (n = 8)	Regimen 2, (n = 15)
Hepatic enzyme elevation	4 (17.4%)	3 (37.5%)	1 (6.7%)
Bacterial pneumonia	1 (4.3%)	0 (0)	1 (6.7%)
Polyoma BK virus infection	4 (17.4%)	2 (25.0%)	2 (13.3%)
Cytomegalovirus infection	2 (8.7%)	0 (0)	2 (13.3%)

function when compared to the control cohort and data from a published patient cohort with cABMR (21). Instead, we observed BM-MSCs treatment decelerated the loss of renal allograft function.

It has been previously proven that MSCs could reduce pathogenic antibodies in patients with SLE (24, 25). In agreement, in our study, BM-MSCs treatment significantly reduced DSA level after one and two years of its initial administration. Considering the eGFR was maintained, the results indicate that BM-MSCs presents therapeutic potential for cABMR treatment. In addition, three grafts lost function within two years of follow-up. We retrospectively analyzed the baseline data and found that their eGFR were respectively 25.6, 20.9 and 25.4 ml/min per 1.73m^2. These results indicate that MSCs may not be suitable for cABMR patients with severely deteriorated renal allograft function. It is of note that many enrolled patients in this study received other treatments for cABMR besides MSCs infusion. To further address the efficacy of MSCs on cABMR, we divided the enrolled patients into two subgroups, i.e. MSCs alone, and MSCs combined with other treatments. These two subgroups were comparable in baseline eGFR and maxDSA, and outcome result showed delta eGFR (-4.3 ml/min/1.73m2 *vs* -3.8 ml/min/1.73m2; p=0.9279) and delta maxDSA (-3824 *vs* -4899; p = 0.7618) were not significant different between these two subgroups. This result indicates the combined treatment administered before or after MSCs may not affect the evaluation of MSCs efficacy on cABMR in this study.

A clinical study has reported the safety of third-party BM-MSCs administration among kidney transplantation recipients (16). The only reported adverse event was the non-ST elevation of myocardial infarction hours after MSCs infusion in one patient with ischemic heart disease and postoperative anemia. Another publication reported the safety of multiple injection of third-party BM-MSCs for treatment of two kidney transplant patients with refractory cABMR, and only diarrhea and hypertension were observed, while the renal allografts deteriorated six months after MSCs treatment (26). Herein, we observed four cases of elevated hepatic enzymes, three of which resulted from replication of pre-existing HBV or HCV. Moreover, BKV and CMV infections were also observed in our study. In accordance, BKV and CMV infections were also reported by Erpicum et al., but there was no difference compared with the concurrent controls (16). Furthermore, no fever, anaphylaxis, phlebitis or venous thrombosis, cardiovascular complications or malignancy were identified in our study. The results indicate the safety of multiple doses of third-party BM-MSCs infusion in kidney recipients with cABMR.

Previous studies have demonstrated MSCs can modulate the humoral immunity by inhibiting the maturation and proliferation of B cells, modulating their activation and inducing regulatory B cells (Breg) (27–30). An *in vivo* study has showed that administration of MSCs combined with rapamycin generates suppression of antibody production and B cell proliferation (31). In this sense, clinical studies have confirmed that MSCs can induce Breg in human (32). Furthermore, MSCs have been used to treat systemic lupus erythematosus (SLE), rheumatoid arthritis and other autoimmune diseases. In this study, we conducted short-term immunosurveillance after BM-MSCs treatment. Immune monitoring was performed according to the methods validated in "The One Study" as described by Streitz et al., with minor modification (33). We found $CD27^-CD38^{-/+}/IgD^-IgM^-$ (Double Negative B cells, DN B cells) population trended to decrease in a dose-dependent manner after BM-MSCs treatment. DN B cells have been recently describe as a novel memory B cells population lacking CD27 expression, a generally used memory B cells marker which expression correlates to somatic mutations in the immunoglobulin genes (34, 35). These B cells do not express IgD indicating that they have undergone class switching, although they do not gain CD27 expression. DN B cells are suggested to be the precursors of antibody secreting cells in SLE patients and to develop outside the germinal center (36, 37). While DN B cells can be detected in healthy individuals, they expand in patients with SLE (38), rheumatoid arthritis (39), non-small cell lung cancer (40), and COVID-19 (41). Furthermore, it has been reported that DN B cells increased in pediatric acute renal allograft rejection recipients who received steroid pulsing, compared to patients with stable graft function (42). The expansion of this cell population has also been observed in pediatric kidney transplant recipients who developed anti-HLA antibodies (43). It has been reported to correlated with poor

TABLE 4 | Effect of BM-MSCs treatment on delta eGFR at two year.

	Univariate analysis		Multivariate analysis	
	HR (95%CI)	P value	HR (95%CI)	P value
Treatment (BM-MSCs *vs* control)	7.284 (-0.875-15.444)	0.079	8.691 (0.496-16.885)	0.038
Pre-eGFR (per 1 ml/min/1.73m^2)	-0.139 (-0.366-0.088)	0.224	-0.188 (-0.412-0.036)	0.099

BM-MSCs, bone marrow derived mesenchymal stem cells; Pre-eGFR, estimated glomerular filtration rate pre-MSCs treatment or at diagnosis; HR, hazard ratio. 95%CI, 95% confidence interval.

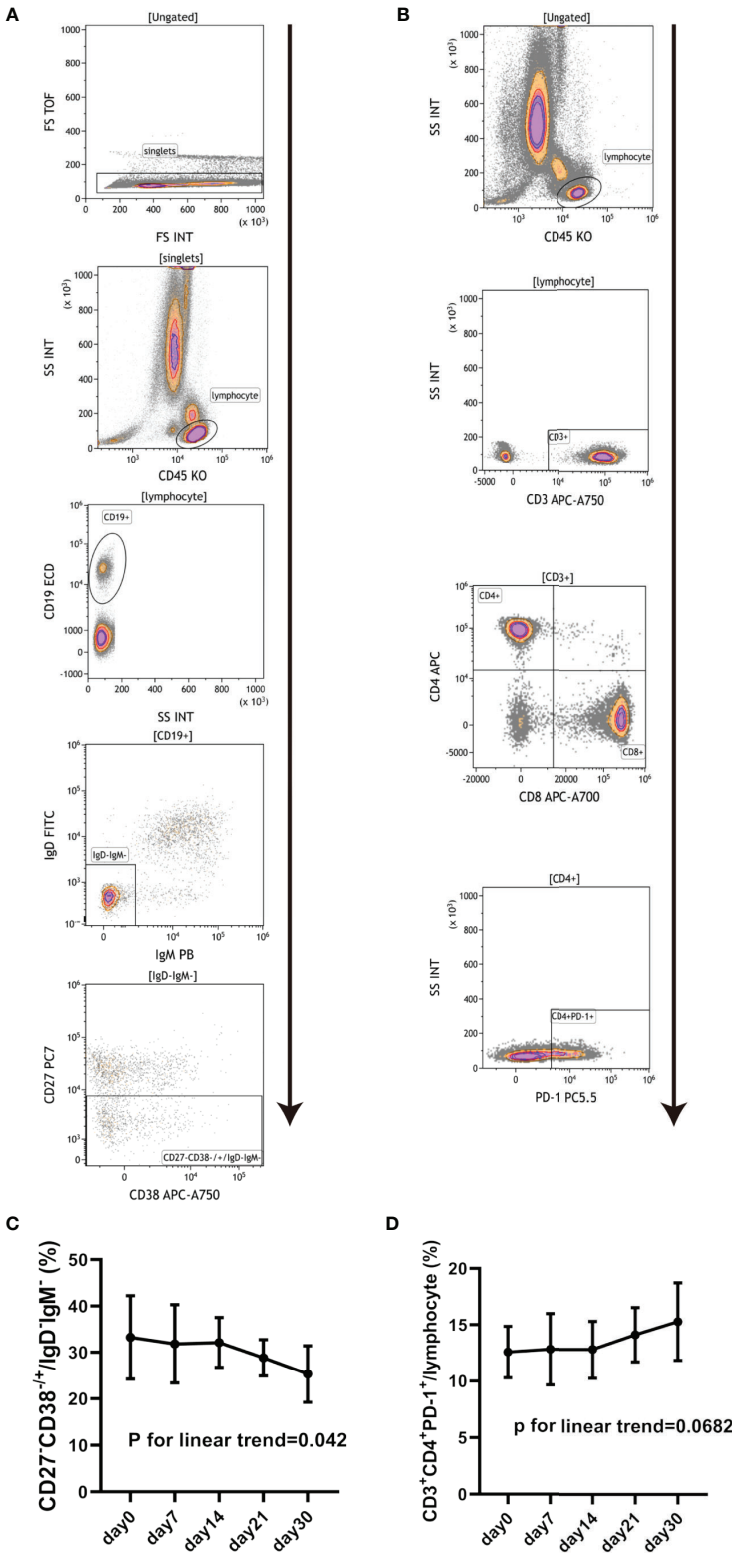

FIGURE 4 | Changes in peripheral blood lymphocyte subsets in cABMR patients after BM-MSCs treatment. Representative flow cytometry plots of $CD27^{-}CD38^{-/+}/IgD^{-}IgM^{-}$ **(A)** and $CD3^{+}CD4^{+}PD\text{-}1^{+}$/lymphocyte **(B)**. Percentage of $CD27^{-}CD38^{-/+}/IgD^{-}IgM^{-}$ pre and after BM-MSCs treatment in one month **(C)**. Percentage of $CD3^{+}CD4^{+}PD\text{-}1^{+}$/lymphocyte pre and after BM-MSCs treatment in one month **(D)**. Points represent mean. Bars represent standard deviation. Data were analyzed by linear trend test.

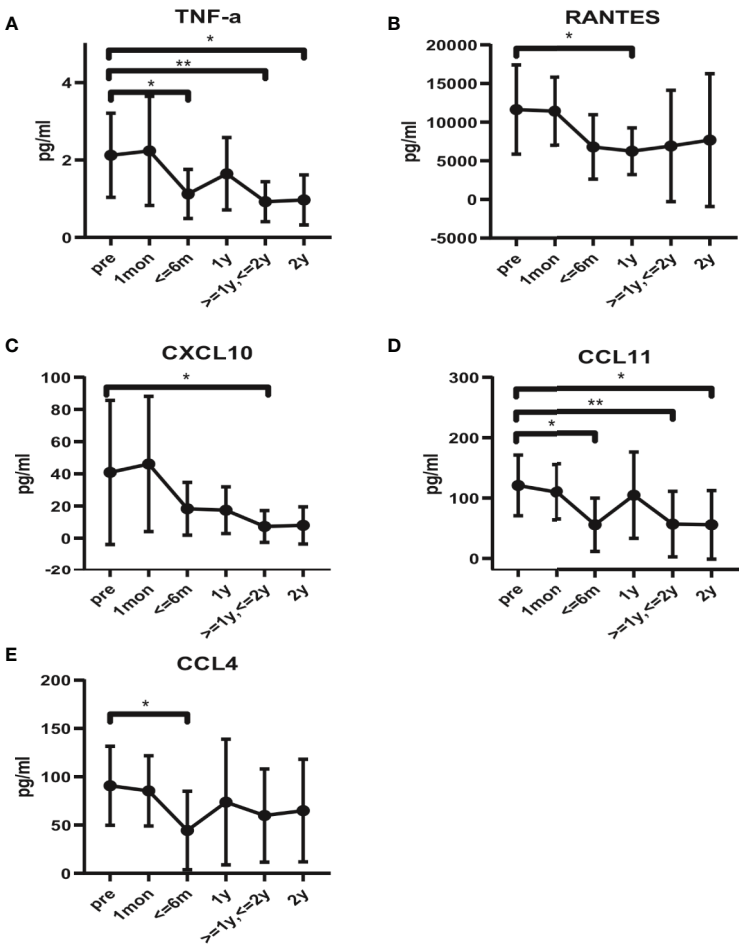

FIGURE 5 | Alteration in serum cytokines and chemokines profile in BM-MSCs treated cABMR patients. Serum levels of TNF-α **(A)**, RANTES **(B)**, CXCL10 **(C)**, CCL11 **(D)**, and CCL4 **(E)**. Points represent mean. Bars represent standard deviation. Data were analyzed by unpaired t-test. *p<0.05, **p<0.01.

response to B cell depletion therapy and active disease in SLE (34, 36, 44). In addition, DN B cells can contribute excess of 40% of all B cells in active SLE and may become the largest circulating population of isotype switched IgD^{-} cells (45). Among these expanded DN B cells, most were DN2 B cells ($CXCR5^{-}$ $CD11c^{+}$), which representing pre-plasma cells (36). Thus, we speculated that BM-MSCs plays a role in the treatment of cABMR by decreasing DN B cells, probably DN2 B cells. We also found that the proportion of $CD3^{+}CD4^{+}PD\text{-}1^{+}$/lymphocyte tended to increase after BM-MSCs infusion. Programmed cell death protein 1 (PD-1) is an important costimulatory molecule that involved in the downregulation of activated T cells (46, 47). The T cells that upregulate PD-1 expression show an exhausted state and functional unresponsiveness, preventing massive immunoactivation (48). Therefore, this might indicate that BM-MSCs could modulate the immune status in cABMR patients by inducing PD-1 positive CD4+ T cells.

MSCs can orchestrate the inflammatory state of micro environments by modulating the secretion of multiple components including cytokines, chemokines, anti-inflammatory mediators and exosomes, which exert immunoregulatory effects on various immune cells (49–51). Our study showed that the proinflammatory cytokine TNF-α and the chemokines CXCL10, CCL4, CCL11 and RANTES decreased after BM-MSCs treatment. Previous studies have found that TNF, CXCL10, CCL4, and RANTES are among the prime genes of ABMR, which are the potential diagnostic and prognostic molecular endpoints and biomarkers for clinical trials recommended by the Banff 2017 kidney meeting report (52). This indicated that BM-MSCs administration may alleviate inflammatory responses in cABMR patients.

The study is subjected to some limitations. This is a single-arm and single-center study with small sample size. The pathological change of renal allografts was not examined since protocol biopsy was unable to be performed. This prospective phase I/II study demonstrated the promising potential of MSCs for treatment of cABMR in kidney transplantation, and a large well-designed study is advocated to further determine its efficacy.

In conclusion, this study demonstrated that immunosuppressive drugs combined with intravenous administration of BM-MSCs decrease DSA and facilitates the maintenance of renal allograft function for kidney transplant recipients with chronic active ABMR without significant adverse events. The underlying mechanisms might involve immunomodulatory effect of MSCs on peripheral $CD27^{-}IgD^{-}$ B cells and $CD4^{+}PD\text{-}1^{+}$ T cells.

DATA AVAILABILITY STATEMENT

The raw data supporting the conclusions of this article will be made available by the authors, without undue reservation.

ETHICS STATEMENT

This study was reviewed and approved by the Ethics Committee and the Research Board, the First Affiliated Hospital of Sun Yat-sen University and was in accordance with the principles of the World Medical Association Declaration of Helsinki. The patients receiving BM-MSCs treatment provided their written consent to participate this study. Consent of patients from the contemporaneous control cohort was waived.

AUTHOR CONTRIBUTIONS

As for individual contribution, YW, LL, and HZ, study design, data analysis and interpretation and manuscript preparation. XC, GL, XZ, and APX, MSCs preparation and quality control. LL, QF, JL, RD, CXW, and CLW, patient enrollment and informed consent. QS, XL, and QY, laboratory examination and data analysis. SY, pathology examination. YP and YG, academic consult. JW and XS, clinical data collection. HH and BX, sample collection. APX and CXW, funding support, study supervision and critical review of manuscript. CXW, APX and LL are responsible for the decision to submit for publication. All authors contributed to the article and approved the submitted version.

FUNDING

This study was supported by Science and Technology Planning Project of Guangdong Province, China (2015B020226002, 2014B020212006, 2017A020215012), National Natural Science Foundation of China (81870511, 81670680, 81700655, 81970109, 81300623), Key Scientific and Technological Program of Guangzhou City (201803040011), Guangdong Basic and Applied Basic Research Foundation (2020A1515010884), Guangdong Natural Science Foundation (2018A030313016), Pearl River S&T Nova Program of Guangzhou (201906010095), Guangdong Provincial Key Laboratory on Organ Donation and Transplant Immunology (2013A061401007, 2017B030314018), and Guangdong Provincial International Cooperation Base of Science and Technology (Organ Transplantation, 2015B050501002).

SUPPLEMENTARY MATERIAL

The Supplementary Material for this article can be found online at: https://www.frontiersin.org/articles/10.3389/fimmu.2021.662441/full#supplementary-material

REFERENCES

1. Matas AJ, Smith JM, Skeans MA, Thompson B, Gustafson SK, Stewart DE, et al. OPTN/SRTR 2013 Annual Data Report: Kidney. *Am J Transplant* (2015) 15 Suppl 2:1–34. doi: 10.1111/ajt.13195
2. Loupy A, Lefaucheur C, Vernerey D, Prugger C, Duong VHJ, Mooney N, et al. Complement-Binding Anti-HLA Antibodies and Kidney-Allograft Survival. *N Engl J Med* (2013) 369:1215–26. doi: 10.1056/NEJMoa1302506
3. Loupy A, Lefaucheur C. Antibody-Mediated Rejection of Solid-Organ Allografts. *N Engl J Med* (2018) 379:1150–60. doi: 10.1056/NEJMra1802677
4. Loupy A, Haas M, Roufosse C, Naesens M, Adam B, Afrouzian M, et al. The Banff 2019 Kidney Meeting Report (I): Updates on and Clarification of Criteria for T Cell- and Antibody-Mediated Rejection. *Am J Transplant* (2020) 20:2318–31. doi: 10.1111/ajt.15898
5. Schinstock CA, Mannon RB, Budde K, Chong AS, Haas M, Knechtle S, et al. Recommended Treatment for Antibody-Mediated Rejection After Kidney Transplantation: The 2019 Expert Consensus From the Transplantion Society Working Group. *Transplantation* (2020) 104:911–22. doi: 10.1097/TP.0000000000003095
6. Casiraghi F, Perico N, Cortinovis M, Remuzzi G. Mesenchymal Stromal Cells in Renal Transplantation: Opportunities and Challenges. *Nat Rev Nephrol* (2016) 12:241–53. doi: 10.1038/nrneph.2016.7
7. Le Blanc K, Rasmusson I, Sundberg B, Gotherstrom C, Hassan M, Uzunel M, et al. Treatment of Severe Acute Graft-Versus-Host Disease With Third Party Haploidentical Mesenchymal Stem Cells. *Lancet* (2004) 363:1439–41. doi: 10.1016/S0140-6736(04)16104-7
8. Galipeau J, Sensebe L. Mesenchymal Stromal Cells: Clinical Challenges and Therapeutic Opportunities. *Cell Stem Cell* (2018) 22:824–33. doi: 10.1016/j.stem.2018.05.004
9. Tan J, Wu W, Xu X, Liao L, Zheng F, Messinger S, et al. Induction Therapy With Autologous Mesenchymal Stem Cells in Living-Related Kidney Transplants: A Randomized Controlled Trial. *JAMA* (2012) 307:1169–77. doi: 10.1001/jama.2012.316
10. Sun Q, Huang Z, Han F, Zhao M, Cao R, Zhao D, et al. Allogeneic Mesenchymal Stem Cells as Induction Therapy Are Safe and Feasible in Renal Allografts: Pilot Results of a Multicenter Randomized Controlled Trial. *J Transl Med* (2018) 16:52. doi: 10.1186/s12967-018-1422-x
11. Peng Y, Ke M, Xu L, Liu L, Chen X, Xia W, et al. Donor-Derived Mesenchymal Stem Cells Combined With Low-Dose Tacrolimus Prevent Acute Rejection After Renal Transplantation: A Clinical Pilot Study. *Transplantation* (2013) 95:161–8. doi: 10.1097/TP.0b013e3182754c53
12. Reinders ME, Dreyer GJ, Bank JR, Roelofs H, Heidt S, Roelen DL, et al. Safety of Allogeneic Bone Marrow Derived Mesenchymal Stromal Cell Therapy in Renal Transplant Recipients: The Neptune Study. *J Transl Med* (2015) 13:344. doi: 10.1186/s12967-015-0700-0
13. Casiraghi F, Perico N, Gotti E, Todeschini M, Mister M, Cortinovis M, et al. Kidney Transplant Tolerance Associated With Remote Autologous Mesenchymal Stromal Cell Administration. *Stem Cells Transl Med* (2020) 9:427–32. doi: 10.1002/sctm.19-0185
14. Podesta MA, Remuzzi G, Casiraghi F. Mesenchymal Stromal Cells for Transplant Tolerance. *Front Immunol* (2019) 10:1287. doi: 10.3389/fimmu.2019.01287

15. Ramirez-Bajo MJ, Rovira J, Lazo-Rodriguez M, Banon-Maneus E, Tubita V, Moya-Rull D, et al. Impact of Mesenchymal Stromal Cells and Their Extracellular Vesicles in a Rat Model of Kidney Rejection. *Front Cell Dev Biol* (2020) 8:10. doi: 10.3389/fcell.2020.00010
16. Erpicum P, Weekers L, Detry O, Bonvoisin C, Delbouille MH, Gregoire C, et al. Infusion of Third-Party Mesenchymal Stromal Cells After Kidney Transplantation: A Phase I-II, Open-Label, Clinical Study. *Kidney Int* (2019) 95:693–707. doi: 10.1016/j.kint.2018.08.046
17. Franquesa M, Herrero E, Torras J, Ripoll E, Flaquer M, Goma M, et al. Mesenchymal Stem Cell Therapy Prevents Interstitial Fibrosis and Tubular Atrophy in a Rat Kidney Allograft Model. *Stem Cells Dev* (2012) 21:3125–35. doi: 10.1089/scd.2012.0096
18. Reinders ME, de Fijter JW, Roelofs H, Bajema IM, de Vries DK, Schaapherder AF, et al. Autologous Bone Marrow-Derived Mesenchymal Stromal Cells for the Treatment of Allograft Rejection After Renal Transplantation: Results of a Phase I Study. *Stem Cells Transl Med* (2013) 2:107–11. doi: 10.5966/sctm.2012-0114
19. Perico N, Casiraghi F, Introna M, Gotti E, Todeschini M, Cavinato RA, et al. Autologous Mesenchymal Stromal Cells and Kidney Transplantation: A Pilot Study of Safety and Clinical Feasibility. *Clin J Am Soc Nephrol* (2011) 6:412–22. doi: 10.2215/CJN.04950610
20. Molenberghs G, Fitzmaurice G, Kenward MG, Tsiatis A, Verbeke G. *Handbook of Missing Data Methodology*. CRC Press (2014).
21. Irish W, Nickerson P, Astor BC, Chong E, Wiebe C, Moreso F, et al. Change in Estimated GFR and Risk of Allograft Failure in Patients Diagnosed With Late Active Antibody-Mediated Rejection Following Kidney Transplantation. *Transplantation* (2021) 105:648–59. doi: 10.1097/TP.0000000000003274
22. Griffin MD, Ryan AE, Alagesan S, Lohan P, Treacy O, Ritter T. Anti-Donor Immune Responses Elicited by Allogeneic Mesenchymal Stem Cells: What Have We Learned So Far? *Immunol Cell Biol* (2013) 91:40–51. doi: 10.1038/icb.2012.67
23. Alagesan S, Griffin MD. Autologous and Allogeneic Mesenchymal Stem Cells in Organ Transplantation: What do We Know About Their Safety and Efficacy? *Curr Opin Organ Transplant* (2014) 19:65–72. doi: 10.1097/MOT.0000000000000043
24. Wang D, Li J, Zhang Y, Zhang M, Chen J, Li X, et al. Umbilical Cord Mesenchymal Stem Cell Transplantation in Active and Refractory Systemic Lupus Erythematosus: A Multicenter Clinical Study. *Arthritis Res Ther* (2014) 16:R79. doi: 10.1186/ar4520
25. Barbado J, Tabera S, Sanchez A, Garcia-Sancho J. Therapeutic Potential of Allogeneic Mesenchymal Stromal Cells Transplantation for Lupus Nephritis. *Lupus* (2018) 27:2161–5. doi: 10.1177/0961203318804922
26. Ban TH, Lee S, Kim HD, Ko EJ, Kim BM, Kim KW, et al. Clinical Trial of Allogeneic Mesenchymal Stem Cell Therapy for Chronic Active Antibody-Mediated Rejection in Kidney Transplant Recipients Unresponsive to Rituximab and Intravenous Immunoglobulin. *Stem Cells Int* (2021) 2021:6672644. doi: 10.1155/2021/6672644
27. Khare D, Or R, Resnick I, Barkatz C, Almogi-Hazan O, Avni B. Mesenchymal Stromal Cell-Derived Exosomes Affect mRNA Expression and Function of B-Lymphocytes. *Front Immunol* (2018) 9:3053. doi: 10.3389/fimmu.2018.03053
28. Carreras-Planella L, Monguio-Tortajada M, Borras FE, Franquesa M. Immunomodulatory Effect of MSC on B Cells Is Independent of Secreted Extracellular Vesicles. *Front Immunol* (2019) 10:1288. doi: 10.3389/fimmu.2019.01288
29. Chen X, Cai C, Xu D, Liu Q, Zheng S, Liu L, et al. Human Mesenchymal Stem Cell-Treated Regulatory CD23(+) CD43(+) B Cells Alleviate Intestinal Inflammation. *Theranostics* (2019) 9:4633–47. doi: 10.7150/thno.32260
30. Rosado MM, Bernardo ME, Scarsella M, Conforti A, Giorda E, Biagini S, et al. Inhibition of B-Cell Proliferation and Antibody Production by Mesenchymal Stromal Cells Is Mediated by T Cells. *Stem Cells Dev* (2015) 24:93–103. doi: 10.1089/scd.2014.0155
31. Wang H, Qi F, Dai X, Tian W, Liu T, Han H, et al. Requirement of B7-H1 in Mesenchymal Stem Cells for Immune Tolerance to Cardiac Allografts in Combination Therapy With Rapamycin. *Transpl Immunol* (2014) 31:65–74. doi: 10.1016/j.trim.2014.06.005
32. Peng Y, Chen X, Liu Q, Zhang X, Huang K, Liu L, et al. Mesenchymal Stromal Cells Infusions Improve Refractory Chronic Graft Versus Host Disease Through an Increase of CD5+ Regulatory B Cells Producing Interleukin 10. *Leukemia* (2015) 29:636–46. doi: 10.1038/leu.2014.225
33. Streitz M, Miloud T, Kapinsky M, Reed MR, Magari R, Geissler EK, et al. Standardization of Whole Blood Immune Phenotype Monitoring for Clinical Trials: Panels and Methods From the ONE Study. *Transplant Res* (2013) 2:17. doi: 10.1186/2047-1440-2-17
34. Wei C, Anolik J, Cappione A, Zheng B, Pugh-Bernard A, Brooks J, et al. A New Population of Cells Lacking Expression of CD27 Represents a Notable Component of the B Cell Memory Compartment in Systemic Lupus Erythematosus. *J Immunol* (2007) 178:6624–33. doi: 10.4049/jimmunol.178.10.6624
35. Klein U, Rajewsky K, Kuppers R. Human Immunoglobulin (Ig)M+IgD+ Peripheral Blood B Cells Expressing the CD27 Cell Surface Antigen Carry Somatically Mutated Variable Region Genes: CD27 as a General Marker for Somatically Mutated (Memory) B Cells. *J Exp Med* (1998) 188:1679–89. doi: 10.1084/jem.188.9.1679
36. Jenks SA, Cashman KS, Zumaquero E, Marigorta UM, Patel AV, Wang X, et al. Distinct Effector B Cells Induced by Unregulated Toll-Like Receptor 7 Contribute to Pathogenic Responses in Systemic Lupus Erythematosus. *Immunity* (2018) 49:725–39. doi: 10.1016/j.immuni.2018.08.015
37. Wang S, Wang J, Kumar V, Karnell JL, Naiman B, Gross PS, et al. IL-21 Drives Expansion and Plasma Cell Differentiation of Autoreactive CD11c(Hi)T-Bet (+) B Cells in SLE. *Nat Commun* (2018) 9:1758. doi: 10.1038/s41467-018-03750-7
38. You X, Zhang R, Shao M, He J, Chen J, Liu J, et al. Double Negative B Cell Is Associated With Renal Impairment in Systemic Lupus Erythematosus and Acts as a Marker for Nephritis Remission. *Front Med (Lausanne)* (2020) 7:85. doi: 10.3389/fmed.2020.00085
39. Mahmood Z, Muhammad K, Schmalzing M, Roll P, Dorner T, Tony HP. CD27-IgD- Memory B Cells Are Modulated by In Vivo Interleukin-6 Receptor (IL-6R) Blockade in Rheumatoid Arthritis. *Arthritis Res Ther* (2015) 17:61. doi: 10.1186/s13075-015-0580-y
40. Centuori SM, Gomes CJ, Kim SS, Putnam CW, Larsen BT, Garland LL, et al. Double-Negative (CD27(-)Igd(-)) B Cells Are Expanded in NSCLC and Inversely Correlate With Affinity-Matured B Cell Populations. *J Transl Med* (2018) 16:30. doi: 10.1186/s12967-018-1404-z
41. Sosa-Hernandez VA, Torres-Ruiz J, Cervantes-Diaz R, Romero-Ramirez S, Paez-Franco JC, Meza-Sanchez DE, et al. B Cell Subsets as Severity-Associated Signatures in COVID-19 Patients. *Front Immunol* (2020) 11:611004. doi: 10.3389/fimmu.2020.611004
42. Zarkhin V, Lovelace PA, Li L, Hsieh SC, Sarwal MM. Phenotypic Evaluation of B-Cell Subsets After Rituximab for Treatment of Acute Renal Allograft Rejection in Pediatric Recipients. *Transplantation* (2011) 91:1010–8. doi: 10.1097/TP.0b013e318213df29
43. Santilli V, Cagigi A, Guzzo I, Rinaldi S, Mora N, Zotta F, et al. Cellular Immune Profile of Kidney Transplant Patients Developing Anti-HLA Antibodies During Childhood. *Pediatr Nephrol* (2016) 31:1001–10. doi: 10.1007/s00467-015-3274-4
44. Nicholas MW, Dooley MA, Hogan SL, Anolik J, Looney J, Sanz I, et al. A Novel Subset of Memory B Cells Is Enriched in Autoreactivity and Correlates With Adverse Outcomes in SLE. *Clin Immunol* (2008) 126:189–201. doi: 10.1016/j.clim.2007.10.004
45. Sanz I, Wei C, Jenks SA, Cashman KS, Tipton C, Woodruff MC, et al. Challenges and Opportunities for Consistent Classification of Human B Cell and Plasma Cell Populations. *Front Immunol* (2019) 10:2458. doi: 10.3389/fimmu.2019.02458
46. Sharpe AH, Pauken KE. The Diverse Functions of the PD1 Inhibitory Pathway. *Nat Rev Immunol* (2018) 18:153–67. doi: 10.1038/nri.2017.108
47. Sen DR, Kaminski J, Barnitz RA, Kurachi M, Gerdemann U, Yates KB, et al. The Epigenetic Landscape of T Cell Exhaustion. *Science* (2016) 354:1165–9. doi: 10.1126/science.aae0491
48. De Biasi S, Meschiari M, Gibellini L, Bellinazzi C, Borella R, Fidanza L, et al. Marked T Cell Activation, Senescence, Exhaustion and Skewing Towards TH17 in Patients With COVID-19 Pneumonia. *Nat Commun* (2020) 11:3434. doi: 10.1038/s41467-020-17292-4
49. Shi Y, Wang Y, Li Q, Liu K, Hou J, Shao C, et al. Immunoregulatory Mechanisms of Mesenchymal Stem and Stromal Cells in Inflammatory

Diseases. *Nat Rev Nephrol* (2018) 14:493–507. doi: 10.1038/s41581-018-0023-5

50. Rafei M, Campeau PM, Aguilar-Mahecha A, Buchanan M, Williams P, Birman E, et al. Mesenchymal Stromal Cells Ameliorate Experimental Autoimmune Encephalomyelitis by Inhibiting CD4 Th17 T Cells in a CC Chemokine Ligand 2-Dependent Manner. *J Immunol* (2009) 182:5994–6002. doi: 10.4049/jimmunol.0803962
51. Ren G, Zhang L, Zhao X, Xu G, Zhang Y, Roberts AI, et al. Mesenchymal Stem Cell-Mediated Immunosuppression Occurs Via Concerted Action of Chemokines and Nitric Oxide. *Cell Stem Cell* (2008) 2:141–50. doi: 10.1016/j.stem.2007.11.014
52. Haas M, Loupy A, Lefaucheur C, Roufosse C, Glotz D, Seron D, et al. The Banff 2017 Kidney Meeting Report: Revised Diagnostic Criteria for Chronic Active T Cell-Mediated Rejection, Antibody-Mediated Rejection, and Prospects for Integrative Endpoints for Next-Generation Clinical Trials. *Am J Transplant* (2018) 18:293–307. doi: 10.1111/ajt.14625

Conflict of Interest: The authors declare this study was conducted in the absence of any commercial or financial relationships that could be construed as a potential conflict of interest.

Advantages of publishing in Frontiers

OPEN ACCESS
Articles are free to read for greatest visibility and readership

FAST PUBLICATION
Around 90 days from submission to decision

HIGH QUALITY PEER-REVIEW
Rigorous, collaborative, and constructive peer-review

TRANSPARENT PEER-REVIEW
Editors and reviewers acknowledged by name on published articles

Frontiers
Avenue du Tribunal-Fédéral 34
1005 Lausanne | Switzerland

Visit us: www.frontiersin.org
Contact us: frontiersin.org/about/contact

REPRODUCIBILITY OF RESEARCH
Support open data and methods to enhance research reproducibility

DIGITAL PUBLISHING
Articles designed for optimal readership across devices

FOLLOW US
@frontiersin

IMPACT METRICS
Advanced article metrics track visibility across digital media

EXTENSIVE PROMOTION
Marketing and promotion of impactful research

LOOP RESEARCH NETWORK
Our network increases your article's readership